

**THE SYNTHESIS & DERIVATISATION OF AMINO ACIDS
INTO CONFORMATIONALLY RESTRICTED UNNATURAL
AMINO ACID & SPIROCYCLIC SCAFFOLDS**

Khadijah Anwar



This thesis is submitted for the degree of PhD
at the
University of Wuppertal

10 July 2024

This page intentionally left blank

Candidate's Declaration

This dissertation is submitted in fulfilment of the requirements for the degree of Doctor of Philosophy in Chemistry. It constitutes the record of work carried out in the Department of Chemistry at the Faculty of Mathematics and Natural Sciences under the supervision of Dr. Adrián Gómez Suárez and Prof. Stefan Kirsch. I, Khadijah Anwar, hereby declare that this thesis has been written by me. Unless specifically indicated in the text, the research described has been carried out by me.

Date.....Signature of Candidate.....

List of publications

This work was carried out under the direction of Dr Adrián Gómez Suárez between August 2020 and October 2023 at the University of Wuppertal.

† Denotes equal contribution.

Parts of this work have been published:

1. **K. Anwar**, L. Capaldo, T. Wan, T. Noël, A. Gómez-Suárez* *Chem. Commun.*, **2024**, 60, 1456–1459.
2. **K. Anwar**, F. J. Aguilar Troyano,[†] A. H. Abazid,[†] O. El Yarroudi, I. Funes-Ardoiz, A. Gómez-Suárez* *Org. Lett.* **2023**, 25, 3216–3221.

Other publications by the author:

3. F. J. Aguilar Troyano,[†] **K. Anwar**,[†] F. Mohr, G. Robert, A. Gómez-Suárez* *Eur. J. Org. Chem.* **2022**, 26, e202201176.
4. **K. Anwar**,[†] K. Merkens,[†] F. J. Aguilar Troyano,[†] A. Gómez-Suárez* *Eur. J. Org. Chem.* **2022**, 26, e202200330.
5. K. Merkens,[†] F.J. Aguilar Troyano,[†] **K. Anwar**, A. Gómez-Suárez* *J. Org. Chem.* **2021**, 12, 8448–8456.
6. F.J. Aguilar Troyano[†], K. Merkens[†], **K. Anwar**, A. Gómez-Suárez* *Angew. Chem. Int. Ed.* **2021**, 60, 1098–1115.

Acknowledgements

Completing a doctoral thesis is a significant milestone, and it would not have been possible without the support and guidance of many individuals.

First and foremost, I would like to thank my advisor, Dr Adrián Gómez Suárez, for his unwavering support, insightful guidance, and continuous encouragement. Your patience – which was definitely tested at times – and dedication have been instrumental in shaping not only this research, but also me as an academic and person. I am deeply grateful for the many hours you spent mentoring me, providing feedback, and helping me navigate the challenges of a PhD and life. I hope that our relationship will continue even once I have left, at least for the kids. I would also like to extend my appreciation to Prof. Stefan Kirsch for allowing me the opportunity to conduct my doctoral studies within the group.

I am grateful to the faculty and staff of the Kirsch group at for providing endless support and kindness. Special thanks to Dr Hülya Aldemir for your help and for always being a cheerful face despite when things are frustrating.

To the students of the Kirsch group, thank you for your friendship, intellectual discussions, and moral support. The shared experiences, challenges, and triumphs have made this journey memorable and enjoyable. To Fran and Kay, I would not be the chemist I was today without the both of you putting up with nonstop questions, so I am beyond thankful for your patience.

A special thank you to my fellow tea drinkers – Kathrin and Timo. I am going to miss spending hours – whoops – bonding over a cup of Yorkshire so much, and I hope there are many tea breaks in our future. Kathrin, I genuinely do not know how I would have survived this PhD without you. You were literally my support rock, and I will miss you so much. To Seb, for the constant encouragement, care, and support – I will continue voicing my gratitude until you inevitably get sick of me.

To Mum, Papa, Qasim, thank you for your unconditional love, sacrifices, and belief in my abilities. Zo, my other half, I cannot say it has been easy not seeing you 24/7, but I am grateful for you always being there when I need you most.

Abbreviations

2,2-DMP	2,2-Dimethoxypropane
3 Å MS	3 Å Molecular sieves
4CzIPN	1,2,3,5-Tetrakis(carbazol-9-yl)-4,6-dicyanobenzene
9-BBN	9-Borabicyclo[3.3.1]nonane
AAs	Amino acids
Ac	acetyl
AIBN	azobisisobutyronitrile
Ala	Alanine
Ar	aryl
Arg	Arginine
Asn	Asparagine
Asp	Aspartic acid
BDE	bond-dissociation energy
BINAP	2,2'-bis(diphenylphosphino)-1,1'-binaphthyl
BMS	Bristol-Myers Squibb
Bn	benzyl
Boc	<i>tert</i> -butyloxycarbonyl
bpy	2,2'-bipyridine
Bu	butyl
Bz	benzoyl
Cbz	benzyloxycarbonyl
COD	Cycloocta-1,5-diene
CT	charge transfer
CyHex	Cyclohexane
Cys	Cysteine
DABCO	1,4-diazabicyclo[2.2.2]octane
DAT	Dopamine transporter receptor
DBU	1,8-Diazabicyclo[5.4.0]undec-7-ene
DCC	dicyclohexyl carbodiimide
DCE	1,2-dichloroethane
dF(CF₃)ppy	2-(2,4-difluorophenyl)-5-(trifluoromethyl)pyridine

dF(CH₃)ppy	2-(2,4-difluorophenyl)-5-methylpyridine
dFppy	2-(2,4-difluorophenyl)pyridine
Dha	Dehydroalanine
DIBAL	diisobutylaluminium
Dig	diagonal
DIPEA	N,N-Diisopropylethylamine
DMA	Dimethylacetamide
DME	1,2-dimethoxyethane
DMF	<i>N,N'</i> -dimethylformamide
DMSO	dimethylsulfoxide
DMPU	N,N'-Dimethylpropyleneurea
DOPA	3,4-dihydroxyphenylalanine
d.r.	diastereomeric ratio
dtbbpy	4,4'-di- <i>tert</i> -butyl-2,2'-bipyridine
EDA	electron donor-acceptor
EDCI	1-Ethyl-3-(3-dimethylaminopropyl)carbodiimide
e.e.	enantiomeric excess
EPR	electron paramagnetic resonance spectroscopy
equiv.	molar equivalents
Et	ethyl
<i>fac</i>	facial isomer of (octahedral) complex
FDA	United States Food and Drug Administration
FG	functional group
GABA	γ-Aminobutyric acid
GE	General Electric
Gln	glutamine
Glu	glutamate
GSK	GlaxoSmithKline
Gly	Glycine
HAT	hydrogen-atom transfer
His	Histidine
HOMO	Highest occupied molecular orbital

HOPO	2-Hydroxypyridine N-Oxide
Hyp	hydroxyproline
IBX	2-iodoxybenzoic acid
IC	Internal conversion
Ile	Isoleucine
<i>i</i>Pr	isopropyl
IrF	[Ir(dF(CF ₃)ppy) ₂ (dtbbpy)] ⁺
ISC	inter-system crossing
JAK	Janus Kinase
KB	Karady-Beckwith
KRAS	Kirsten rat sarcoma virus
LDA	lithium diisopropylamide
LED	Light-emitting diode
Leu	Leucine
LiDBB	lithium di- <i>tert</i> -butyl biphenylide
LMCT	ligand-to-metal charge transfer
LUMO	Lowest unoccupied molecular orbital
Lys	Lysine
<i>m</i>	<i>meta</i> , substituent orientation in phenyl ring
<i>m</i>CPBA	<i>meta</i> -chloroperbenzoic acid
Me	methyl
MEK	methyl ethyl ketone
Mes-Acr	9-mesityl-10-methylacridinium
MesBA	2,4,6-trimethylphenyl boronic acid
Met	Methionine
MLCT	metal-to-ligand charge transfer
MOA	mode of action
Ms	mesyl, methanesulfonyl
MSD	Merck, Sharp & Dohme
MTBE	Methyl <i>tert</i> -butyl ether
MW	microwave
NBS	<i>N</i> -bromosuccinimide

NCS	<i>N</i> -chlorosuccinimide
NFSI	<i>N</i> -fluorobenzenesulfonimide
NMDA	<i>N</i> -methyl- <i>D</i> -aspartic acid
NMR	nuclear magnetic resonance spectroscopy
NSAID	non-steroidal anti-inflammatory drug
<i>o</i>	<i>ortho</i> , substituent orientation in phenyl ring
OCD	Obsessive compulsive disorder
<i>p</i>	<i>para</i> , substituent orientation in phenyl ring
PC	photocatalyst
PCSK9	proprotein convertase subtilisin/kexin type 9
Pd/C	Palladium on carcoal
PG	protecting group
Ph	phenyl
Phe	Phenylalanine
phen	1,10-phenanthroline
Phth	phthaloyl
PIDA	phenyl iodoacetate
PIFA	(bis(trifluoroacetoxy)iodo)benzene
ppy	2-phenylpyridine
Pro	proline
rt	room temperature
SARS-CoV-2	Severe acute respiratory syndrome coronavirus 2
SCE	saturated calomel electrode
SDS	Sodium dodecylsulfate
Sec	Selenocysteine
Ser	Serine
SET	single-electron transfer
S_H2	bimolecular radical substitution (group transfer)
S_N2	bimolecular nucleophilic substitution
S_NAr	nucleophilic aromatic substitution
SPECT	Single-photon emission computed tomography
TBA	tetrabutylammonium

TBADT	tetrabutylammonium decatungstate
TBAP	Tetrabutylammonium phosphate
<i>t</i>Bu	<i>tert</i> -butyl
TEMPO	2,2,6,6-tetramethylpiperidinyloxy
TES	triethylsilyl
Tf	triflyl
TFA	trifluoroacetic acid
TFE	2,2,2-trifluoroethanol
THF	tetrahydrofuran
Thr	Threonine
Tle	L- <i>tert</i> -leucine
TMS	trimethylsilyl
trig	trigonal (sp ²)
TRIP	(2,4,6-triisopropyl)phenyl
Trp	tryptophan
Ts	tosyl, <i>p</i> -toluenesulfonyl
TS	transition state
TTET	triplet-triplet energy transfer
Tyr	Tyrosine
UAAs	Unnatural amino acids
Val	Valine
XAT	halogen-atom transfer

Table of contents

Candidate's Declaration	2
Acknowledgements	4
Abstract	12
I General introduction	14
1.1 Amino Acids	14
II Accessing Sterically Congested β -Amino Acids & Spirocyclic Dihydropyrroles	80
IIA. Synthesis of Sterically Congested $\beta^{2,2}$ -Amino Acids	87
A.1 Introduction	87
A.1.1 $\beta^{2,2}$ -Amino Acids	88
A.2 Objectives	92
A.3 Results & discussion	94
A.3.1 Reaction Optimisation	94
A.3.1.1 <i>Photo-mediated Giese-Type Reaction</i>	94
A.3.1.2 <i>Oxidative Esterification & Amidation</i>	95
A.3.2 Scope & Limitations	96
A.3.2.1 <i>Oxidative Esterification/Amidation in Flow</i>	101
A.3.2.2 <i>Alternative Approaches to the Oxidative Esterification</i>	103
A.3.3 Deprotection & Derivatisation Attempts	104
A.3.4 Mechanistic Studies	105
A.4 Outlook & Future Aspirations	108
IIB. Modular Construction of Polar Spirocycles	109
B.1 Introduction	109
B.1.1 Synthesis of Spirocyclic Pyrrolidines	120
B.1.1.1 <i>Radical Methods</i>	125
B.2 Objectives	131
B.3 Results & discussion	133
B.3.1 Reaction Optimisation	133
B.3.2 Scope & Limitations	135
B.3.3 Scale-up & Derivatisation Attempts	137
B.3.4 Mechanistic Studies	138
B.4 Outlook & Future Aspirations	140
III. Synthesis of Spirocyclic (α -Amino- γ -)Butyrolactones	141
3.1 Introduction	141

3.2 Objectives	161
3.3 Results & discussion	165
3.3.1 Initial Reaction Optimisation	165
3.3.2 Scope & Limitations	169
3.3.3 Mechanistic Studies & Investigation into Decomposition	170
4 Experimental Section	174
4.1 General Remarks	174
4.1.1 Analytical Techniques	174
4.1.2 Photocatalytic Setup	175
Chapter IIA: Synthesis of Sterically Congested $\beta^{2,2}$-Amino Acids	176
<i>Oxidative esterification:</i>	177
Conversion of Malononitrile Intermediate 110 into Spirocyclic Species 111	213
Chapter IIA: Synthesis of Sterically Congested $\beta^{2,2}$-Amino Acids	243
Alkylidenemalononitriles	243
β-Amino Acids	286
Product Derivatisations	296
Alkylidenemalononitriles	298
Products	328
References	337

Word count: 60,975

Abstract

The synthesis and derivatisation of amino acids to create molecules with enhanced three-dimensionality is of paramount importance in advancing pharmaceutical and agrochemical research. The thesis focusses on highlighting the importance of enhancing molecular three-dimensionality in drug design, aligning with concepts like "escape from the flatland" and "conformational restriction." The developed radical-based methods provide versatile and efficient routes to synthesise complex, 3D amino acid derivatives, thereby broadening the methods available for medicinal chemists and facilitating the discovery of novel, bioactive molecules with improved pharmacological profiles.

β -Amino acids, particularly $\beta^{2,2}$ -amino acids, play a crucial role in modifying peptide secondary structures, leading to increased resistance to proteolytic degradation and providing intermediates for various biologically relevant compounds. However, the synthesis of these derivatives poses significant challenges due to the complexity of constructing quaternary centres. This thesis presents a novel two-step protocol for the modular synthesis of β^2 - and $\beta^{2,2}$ -amino acid derivatives. The key steps involve a photocatalytic Giese-type reaction followed by oxidative functionalisation to access *N*-protected β -amino acids, esters, and amides. This approach leverages radical chemistry to overcome steric hindrance, facilitating the formation of quaternary centres and enhancing the three-dimensional character of the resulting molecules. The method is further optimised for scalability through continuous-flow technology, ensuring its practical application in large-scale synthesis.

In addition to the two-step protocol, this work explores the synthesis of spirocyclic scaffolds from abundant starting materials such as cyclic ketones and α -amino acids. The sequence employs a straightforward Knoevenagel condensation followed by a domino Giese-type reaction and base-mediated cyclisation, yielding a broad scope of polar spirocyclic scaffolds with high efficiency. These spirocycles exhibit increased three-dimensionality and structural novelty, which are critical for interacting with three-dimensional binding pockets and accessing unclaimed chemical space.

Finally, despite advancements in synthetic methods for lactones, challenges remain, particularly in constructing spirocyclic lactones due to the difficulty in forming quaternary centres. Traditional intramolecular esterification from hydroxy acid precursors often falls short for spirocyclic systems. Chapter III focuses on a novel approach using vinylogous

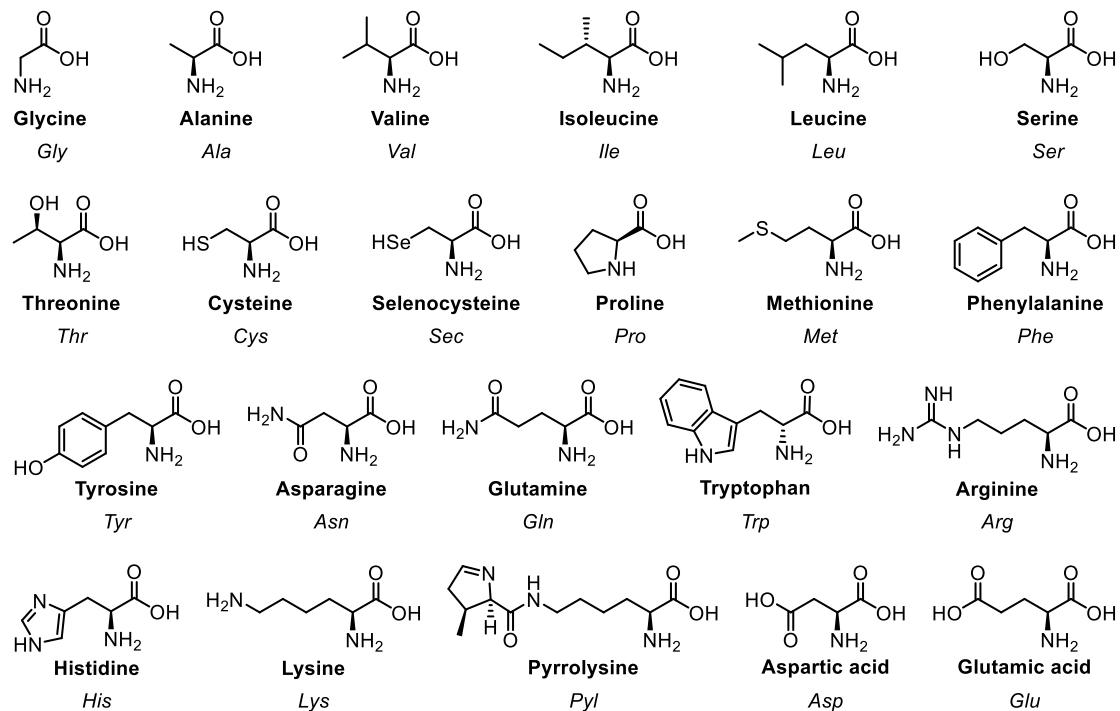
Michael acceptors and cyclic aliphatic alcohols to synthesise spirocyclic α -amino γ -butyrolactones in a single operation from simple precursors, without the need for pre-existing quaternary centres. Inspired by MacMillan's methodology, boronate activation of alcohols to preferentially abstract α -hydroxy C–H bonds was utilised, forming α -carbamoyl ketyl radicals for subsequent Michael addition and cyclisation. Optimisation studies identified effective conditions using boronic acids as activators, Ir-F photocatalyst, and quinuclidine as a HAT catalyst. Challenges remain in achieving high yields and addressing decomposition issues, suggesting the need for further mechanistic studies and refinements in the presented approach.

I General introduction

1.1 Amino Acids

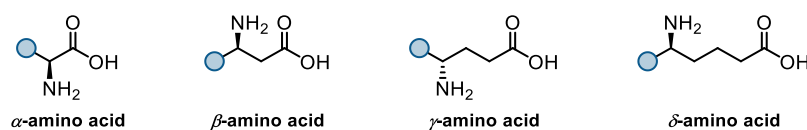
Amino acids are not simple compounds; as they are intricately tailored structures with distinct stereochemistry, functional groups, and diverse side chains. Their synthesis within living organisms is evidence to the attractive accuracy of enzyme-catalysed reactions and elaborate metabolic pathways. Understanding the difficulties of amino acid synthesis not only sheds light on the interplay of organic reactions but also uncovers the remarkable enzymatic strategies that orchestrate these processes. The stepwise assembly of amino acids involves a symphony of chemical transformations, including coupling reactions, protecting group manipulations, and chiral induction. These reactions showcase the ingenuity of organic chemists and the complexity that nature employs in constructing even the most fundamental molecules of life.

In the simplest form of the α -amino acids, these functional groups are separated by a single carbon atom, such as the methylene group in glycine (Gly), the simplest of the canonical AAs. Depending on the substitution pattern at the α -position (C-2), many different variations are possible, including the group of twenty canonical or proteinogenic AAs, which are synonymously known as the natural amino acids, plus an additional two (selenocysteine and pyrrolysine) that are incorporated by special translation mechanisms (**Scheme 1**). Many naturally occurring amino acids which are not part of the canonical group are known (around 800 examples), e.g., the mammalian neurotransmitter GABA – the simplest γ -amino acid (*vide infra*).¹



Scheme 1: structure of the 20 proteinogenic AAs plus two additional, with 3 letter codes.

Amino acids which do not belong to the canonical twenty are generally known as non-canonical or unnatural amino acids, despite their occurrence in nature as secondary metabolites. Their designation as unnatural stems from the fact that they generally do not occur as part of natural polypeptide chains. Hence, the term unnatural AA is often synonymous with the term non-proteinogenic (non-protein forming) AAs. Apart from the α -amino acids subclass, variations with different length exist, separated by two (β), three (γ), or even four carbon atoms (δ -amino acids) (**Scheme 2**).

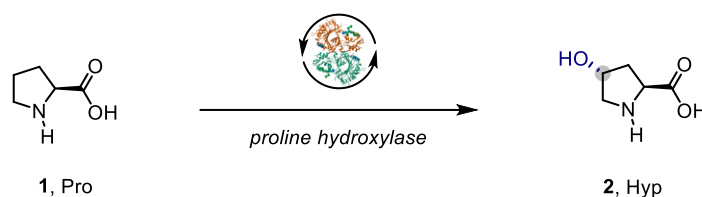


Scheme 2: subclasses of amino acids.

Amino acids are one of the fundamental building blocks of life. Linking two amino acids via an amide bond leads to the formation of a (di)peptide. All the structural units in a peptide are AA residues, although the existence of amino acids such as lysine (Lys) and glutamic acid (Glu) implies the possibility to form (sidechain) isopeptide bonds. Short peptides of less than 10 residues are known as oligopeptides, and larger assemblies are called polypeptides. Although the term is not exactly defined, large polypeptides with a molecular weight above 10 kDa are known as proteins, a major family of biological (macro)molecules and prime

focus of the study of biochemistry, along with the carbohydrates (saccharides) and the nucleic acids.

The canonical amino acids are encoded by triplet codons in the nucleic acids for biological protein synthesis by ribosomes (translation). Other amino acids are not encoded in the genetic code but can be formed by cellular processes such as post-translational modifications (by enzymes), e.g., the conversion of proline (Pro) **1** to hydroxyproline (Hyp) **2** – a component of the structural protein collagen (**Scheme 3**).²



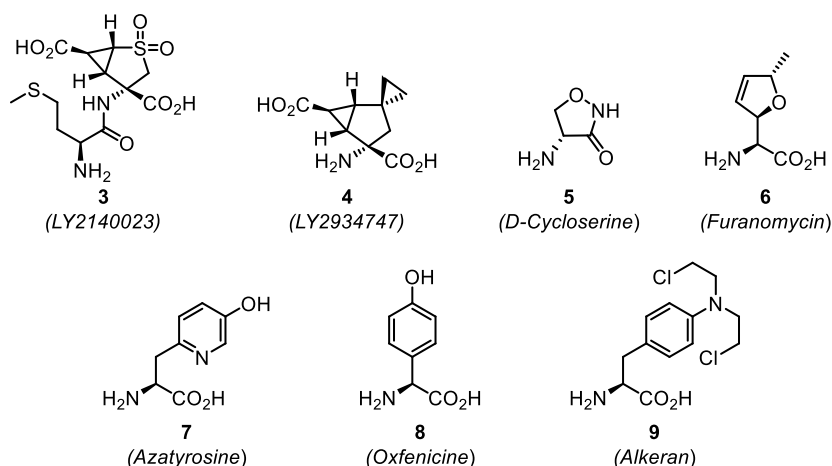
Scheme 3: Conversion of canonical Pro to non-canonical Hyp by a post-translational enzymatic hydroxylation.

Interest in non-canonical or unnatural amino acids (UAAs) stems from their ability to influence the structure and function of the aforementioned (macro)molecular family of peptides. Other than the number of carbon atoms between the amino and carboxylic acid functionalities of the amino acid, UAAs can be classified into two groups: analogues of the canonical AAs (e.g., 4-amino-Phe, *vide infra*), and surrogates. Analogues are generally more focused on closely mimicking the structure of natural amino acids, often with slight modifications. The term surrogates typically implies that the UAAs are being used to substitute natural amino acids with a purpose of imparting new properties or functionalities.

1.1.1 Medicinal chemistry

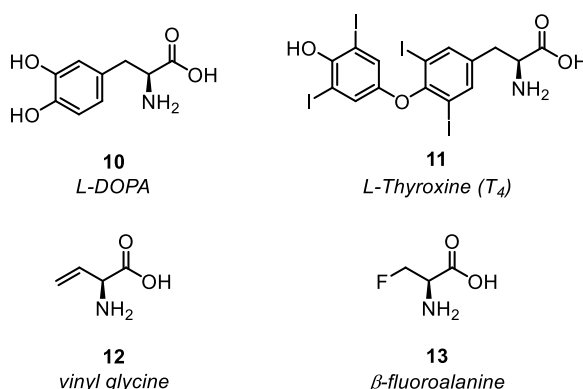
UAAs are extremely important in medicinal chemistry as they often display interesting biological activity. They can occur as structural components of small molecule drugs, peptides, or as free amino acids. For example, Eli Lilly and Company, Ltd. has developed a range of constrained, bicyclic UAAs as Glu receptor (mGlu2/3) antagonists (**Scheme 4**), as possible treatments for schizophrenia, such as dipeptide **3** (LY2140023) and **4** (LY2934747).³⁻⁵ Another example is cycloserine, a naturally occurring antibiotic which acts as a GABA transaminase inhibitor and inhibits bacterial cell wall synthesis relying on the incorporation of the amino acid D-alanine, of which cycloserine is an analogue. It was originally isolated from a *Streptomyces* strain and is used as a second-line treatment for tuberculosis infections.⁶ Additionally, it has also shown activity as an NMDA agonist to treat

OCD. Several other non-canonical AAs are known for their antibiotic activity, e.g., (+)-furanomycin **6** and L-azatyrosine **7**. Oxfenicine **8** is an experimental drug which inhibits fatty acid oxidation in the heart, while alkeran **9** is an approved chemotherapeutic agent used to treat several types of cancers known as Melaphan (**Scheme 4**).^{7,8,9}



Scheme 4: Selected biologically active amino acids.

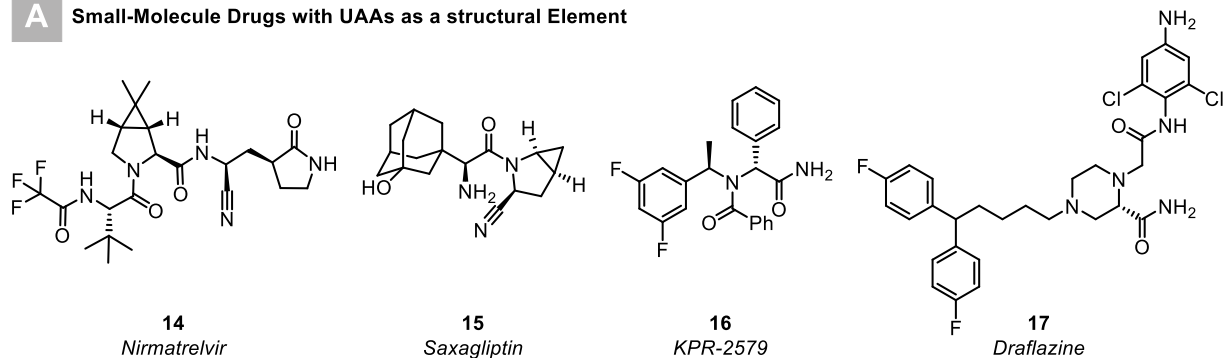
L-DOPA **10** is a Phe/Tyr analogue and a metabolic precursor (by decarboxylation) to the neurotransmitter dopamine, used as treatment for Parkinson's disease (**Scheme 5**).¹⁰ The thyroid hormone thyroxine (T_4 , **11**) is also a noncanonical, iodinated Tyr analogue, and is given to patients with hypothyroidism as levothyroxine (Synthroid).¹¹ Unsaturated amino acids, such as vinyl glycine **12**, show biological activity by acting as Michael acceptors and completely inhibiting the activity of certain enzymes.¹² Additionally, fluorinated AAs such as β -fluoroalanine **13** function as precursors for these Michael acceptors *in vivo* and also show protein inhibitory activity (**Scheme 5**).¹³



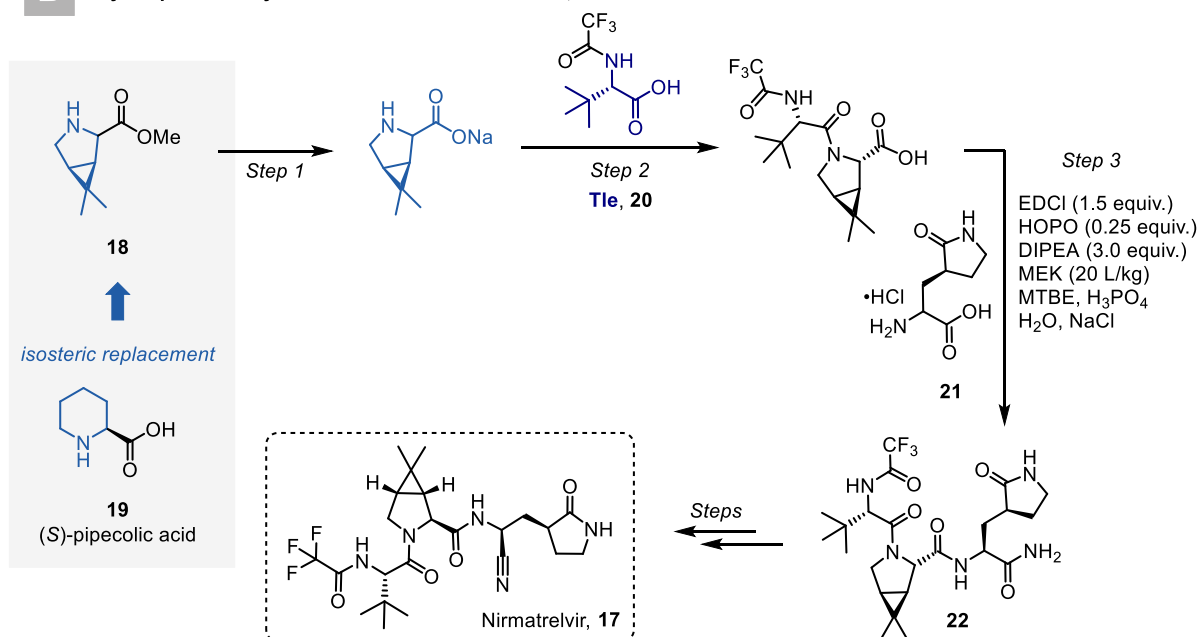
Scheme 5: structures of L-DOPA, Thyroxine, vinyl glycine, and β -fluoroalanine.

Many small-molecule drugs contain UAAs as a structural element. Arguably the most relevant example is the recently approved (FDA) nirmatrelvir **14** (Paxlovid, marketed as a combination drug with ritonavir), as treatment for covid-19 caused by the coronavirus SARS-CoV-2.¹⁴ Saxagliptin **15**, a drug developed by Bristol-Myers Squibb (BMS) for the treatment of type 2 diabetes, contains a bulky side chain based on adamantanol.¹⁵ KPR-2579 (**16**), a Kissei Pharmaceutical Co., Ltd. investigational drug for bladder dysfunction, is formally derived from α -phenylglycine.¹⁶ Draflazine (R-75231), developed by Roche, contains piperazine-2-carboxylic acid as a structural unit (**Scheme 6A**).¹⁷

A Small-Molecule Drugs with UAAs as a structural Element



B Key Steps in the Synthesis of Nirmatrelvir – Pfizer, 2023



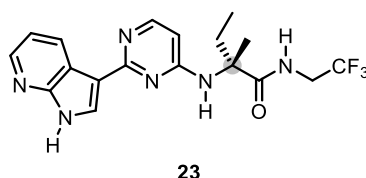
Scheme 6: A) selected examples of small molecule drugs containing an UAA subunit; B) key steps in the synthesis of Nirmatrelvir using UAAs.

Nirmatrelvir notably contains two UAAs, a bicyclic analogue (**18**) of pipercolic acid (**19**), and L-*tert*-leucine (Tle, **20**). Additionally, its preparation involves an amide coupling between

these fragments and what can be considered another UAA derivative (**21**), which is then dehydrated to install the nitrile group used for covalent inhibition of the cysteine protease (**Scheme 6B**). The latter is used by the virus to cleave the proteins required for assembly of new viral particles.

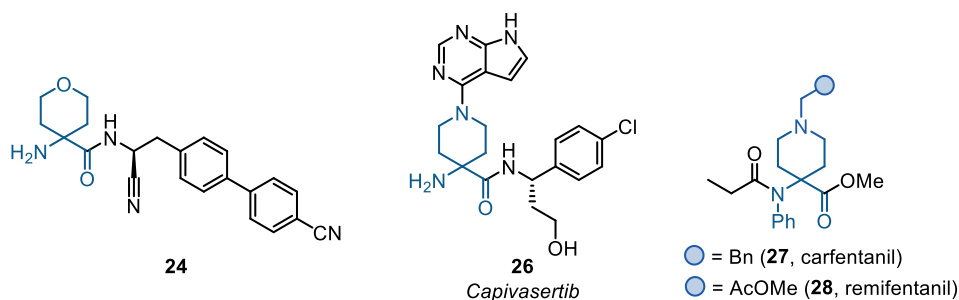
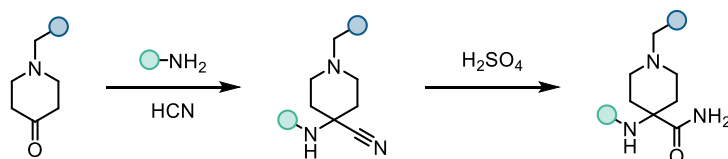
α,α -Disubstituted AAs are even more sterically congested than the aforementioned examples, including Tle (**20**). This substitution pattern carries several advantages as it prevents the occurrence of racemisation, locks conformation and improves the metabolic stability against proteolysis when incorporated in small molecules and peptides (see chapter II for further reading).

Decernotinib **23**, developed by Vertex (VX-509) as an experimental JAK3 inhibitor, contains a disubstituted residue (2-amino-3-methylbutyric acid) as a central component (**Scheme 7**).¹⁸



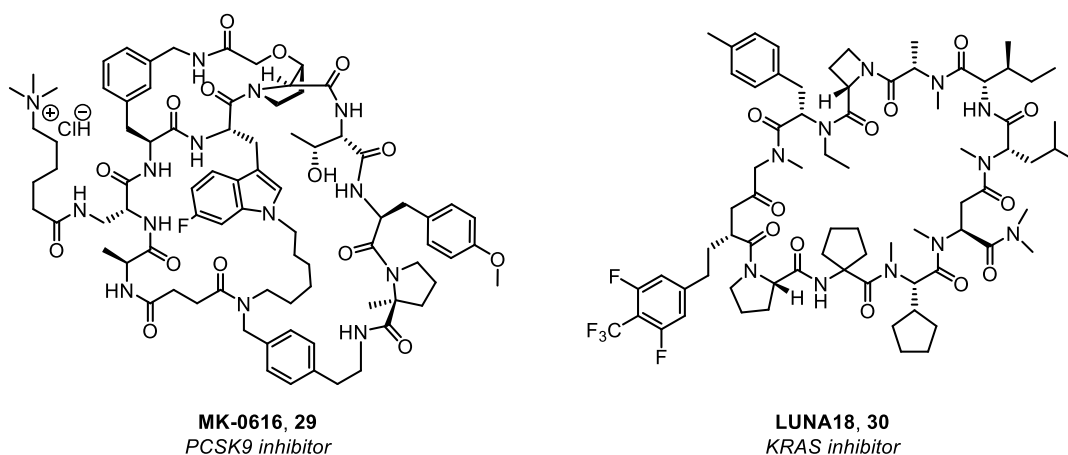
Scheme 7: Experimental JAK3 inhibitor decernotinib (VX-509).

Cyclic amino acids are even more conformationally constrained than their non-cyclic counterparts.¹⁹ Compound **24** was developed by AstraZeneca as part of a SAR program on covalent inhibitors of the cysteine protease cathepsin C, which is implicated in inflammatory and auto-immune diseases (**Scheme 8A**).²⁰ Similar to intermediate **22** in the synthesis of nirmatrelvir (**Scheme 6B**), the medicinal chemistry route involves amide coupling of two UAA fragments and dehydration of an amino amide to the nitrile through the use of Burgess' reagent.²¹ Similar amino acids, in which the THP unit is exchanged for a piperidine, occur as structural elements of the oncology drug capivasertib **25** (AZD5363, approved by the FDA in late 2023) and several analogues of the fentanyl analgesic developed by Janssen.²² Although only carfentanil **26**, used exclusively in veterinary medicine due to its potency, and remifentanil **27**, which is used in human anaesthesia due to its short half-life, contain the 4-substituted piperidine amino acid fragment shared with capivasertib, several other fentanyl analogues feature the amino acids as an intermediate in their preparation. Synthetically, these structures are accessed through the Strecker AA synthesis, where the quaternary centre is created through addition of cyanide to a carbonyl compound (or derivative) followed by hydrolysis (**Scheme 8B**).²³

A Small-molecule drugs containing cyclic α,α -disubstituted UAAs

B Key Step to Access Constrained Fentanyl Analogues – *Strecker Condensation*


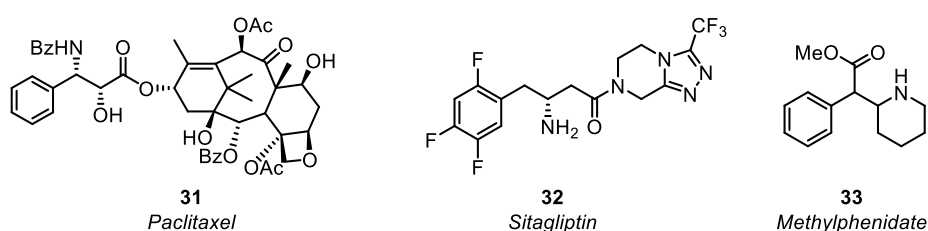
Scheme 8: A) selected small molecules containing cyclic α,α -disubstituted amino acid structures; B) Strecker route to assemble fentanyl analogues.

As shown before, UAAs have been successfully applied to improve the properties of peptidomimetic drugs such as nirmatrelvir **17**. Another area of application which is also particularly relevant for the more elongated β -AAs is the use of UAAs as components of cyclic peptide drugs, which are currently experiencing a wave of interest from medicinal chemists for their attractive pharmacokinetic properties including increased oral bioavailability.²⁴ MK-0616 (**29**, MSD) is a macrocyclic peptide of considerable complexity, acting as a PCSK9 inhibitor for oral treatment of atherosclerosis which is currently undergoing phase III clinical trials (**Scheme 9**).^{25,26} It contains several non-canonical UAAs, both analogues and surrogates of canonical AAs. LUNA18, which is developed by Chugai Pharmaceutical Co., Ltd. is a cyclic peptide inhibitor of KRAS.²⁷ RAS genes, of which KRAS is one, encode for proteins in the RAS/MAPK signalling pathway (such as K-Ras) involved in, e.g., cell division and differentiation. These genes are regulated and remain unexpressed until activated by extracellular signals. RAS mutations frequently lead to improper regulation of this signalling pathway with uncontrolled cellular growth as a potential consequence (oncogenesis).²⁸ These mutations are linked to poor clinical outcomes in several types of cancer including non-small cell lung cancer, which accounts for 80% of lung cancer cases.



Scheme 9: novel macrocyclic peptide drugs containing unnatural amino acid residues.

β -AAs and their derivatives are represented as structural units in a number of compounds with biological activity, such as the commercial drugs paclitaxel **31** (Taxol®), sitagliptin **32** (Januvia, MSD) and dopamine re-uptake inhibitors, such as methylphenidate **33**, (Ritalin, GSK) can formally be considered β -AA derivatives (**Scheme 10**). Like non-canonical α -AAs, one of the therapeutic areas in which β -AAs show particular potential is in the development of macrocyclic peptide drugs.²⁹



Scheme 10: small molecule drugs derived from β -AAs.

β -AAs can be classified in several categories, one type being the elongated, flexible analogue of an α -AA containing an extra methylene group (depending on whether this is in the α - or the β -position, this would, respectively, be a β^2 or β^3 -AA) and a side-chain analogous to a canonical (or non-canonical) AA, and the other the category of the so-called alicyclic β -AAs, which are constrained β -AAs containing a ring fusion at the α - and β -position, which are $\beta^{2,3}$ -AAs (additional information can be found in Chapter II).

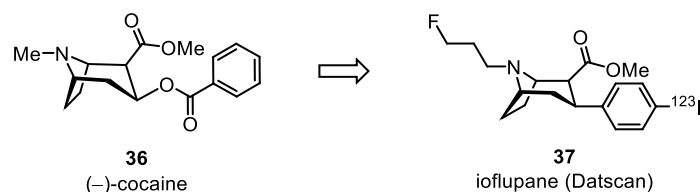
Interest in these compounds was sparked by the discovery of the potent antifungal properties of the culture broth of the foodborne pathogen *Bacillus cereus*. This is due to the presence of (–)-cispentacin **34**, an alicyclic β -AA formally containing a cyclopentyl group in α,β -fusion as the side chain with antifungal activity against *Candida albicans* (**Scheme 11**).³⁰

This yeast can commonly lead to pathogenesis (known as candidiasis) in, for example, immunocompromised individuals in a hospital setting. SAR studies have shown that other analogues can also show antifungal activity, including cyclobutyl and cyclohexyl-substituted varieties. This led to the development of icofungipen **35** (BAY-10-8888) by Bayer, as an experimental oral treatment for yeast infections caused by *C. albicans*.³¹



Scheme 11: alicyclic β -amino acids with antifungal activity.

(-)-Cocaine, **36**, can also be considered an alicyclic β -AA derivative. Its abuse potential is a consequence of its strong properties as a dopamine reuptake inhibitor (a similar MOA as **33**), which it exerts by competitively binding to the dopamine transporter protein which is responsible for returning dopamine from the synaptic cleft.³² The benzoyl group is responsible for fitting cocaine into a hydrophobic pocket of the dopamine transporter protein. Improvements in binding affinity are observed by introducing lipophilic halide functionalities onto the aromatic group, such as iodine. Ioflupane **37** (Datscan) is one such compound, marketed by GE Healthcare Technologies, Inc., which includes an iodine-123 (¹²³I) label (**Scheme 12**). It is used as a ligand to visualise the dopamine transporter in the brain as it decays through electron capture, leading to proton annihilation in the atomic nucleus, decreasing Z from 53 (I) to 52 (Te). In the annihilation process, a proton is converted to a neutron with emission of a γ -ray, which can be visualised using crystalline scintillation (SPECT). As patients with certain neurodegenerative diseases show a marked decrease in the number of dopamine transporters in the brain, this compound can be used as a diagnostic tool for Parkinson's disease.³³



Scheme 12: Design of a diagnostic dopamine transport receptor (DAT) radioligand using the (-)-cocaine natural product as a template.

Various other substitution patterns are possible, including the presence of a quaternary centre at the α or β -position, which are the less commonly investigated $\beta^{2,2}$ - and $\beta^{3,3}$ -AAs.

The potential of these building blocks likely remains mostly untapped as a consequence of their difficult preparation, which is the focus of chapter II, detailing a straightforward route to access constrained $\beta^{2,2}$ -AAs.

1.2 Synthesis of UAAs

Thus far, approximately 800 naturally occurring non-proteogenic AAs have been documented in the literature, while thousands of synthetic amino acids have also been reported.³⁴ UAAs can be generated from their natural analogues *via* modifications such as amine alkylation, side-chain substitution and backbone modification, or through the use of ligands and transition metal-based catalysts (e.g., palladium, rhodium or nickel).^{35,36} Additionally, employing biocatalysts in the synthesis of UAAs has become a successful strategy for their preparation.³⁷ Among the various types of AAs, α - and β -amino acids are the most common, thus the focus will be on these.

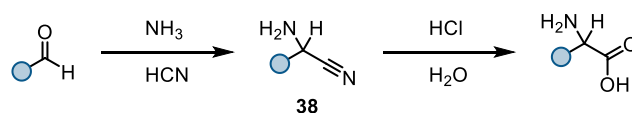
1.2.1 α -AAs

Since the publication of the Strecker reaction in the mid-nineteenth century, a prominent focus has been on developing a diverse array of catalytic technologies and sophisticated asymmetric catalyst designs for the synthesis of enantiopure α -AAs. Notable advancements include the Strecker reaction and its asymmetric variants, development of chiral auxiliaries, and asymmetric hydrogenation reactions.^{38,39} These methodologies, among many others, have significantly expanded the toolkit available for the synthesis of α -AAs, enabling the production of complex and highly functionalised amino acids for various applications.

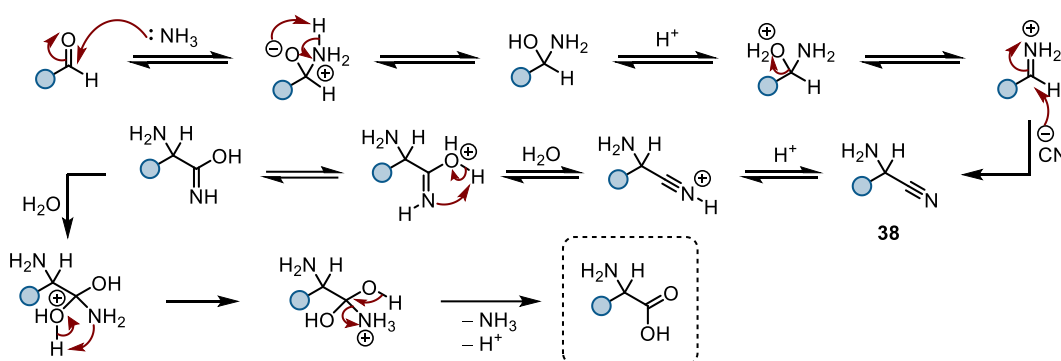
The efficient synthesis of α -amino acids was first identified as a challenge with the introduction of the Strecker condensation (**Scheme 13**).⁴⁰ The reaction, also known as the Strecker synthesis, is a seminal reaction in organic chemistry, first reported by Adolph Strecker in 1850, and serves as a foundational method for synthesising α -AAs from aldehydes or ketones, significantly influencing the field of amino acid chemistry. First, the condensation of an aldehyde or ketone with an amine (typically NH_3) occurs, forming an imine which undergoes nucleophilic addition of hydrogen cyanide to create the key α -amino nitrile species **38**. The addition of cyanide is facilitated by the nucleophilicity of the cyanide ion, which effectively attacks the electrophilic carbon of the imine. The final step in the Strecker synthesis involves the hydrolysis of the α -amino nitrile in the presence of an acid, such as hydrochloric acid, to yield the desired α -amino acid. In the initial report, a high yield

of the amino nitrile adduct was achieved by mixing easily accessible acetaldehyde, ammonia, and hydrogen cyanide for a fixed amount of time, followed by hydrolysis to obtain alanine. This simple synthesis resulted in the first laboratory-based production of an amino acid, even preceding its isolation from natural sources.

Strecker Condensation



Mechanism



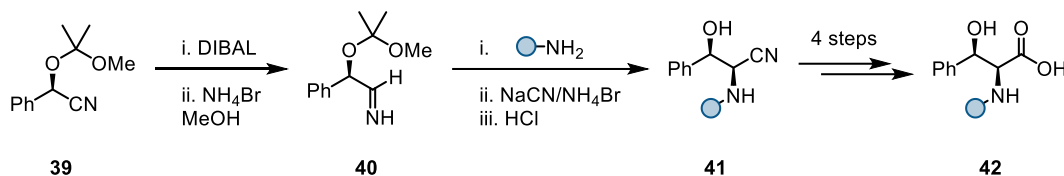
Scheme 13: mechanism of the Strecker condensation.

One of the most important criteria in the synthesis of AAs is gaining high optical purity. Driven by the growing demand for enantioenriched α -amino acids across various fields such as life sciences, chemistry, and industry, asymmetric Strecker condensations have emerged as a prominent area of research in organic chemistry.³⁸ While the reaction was initially led to the formation of racemates, advancements in chiral mediators have substantially enhanced the versatility of this method, establishing its status as the primary approach for amino acid synthesis.

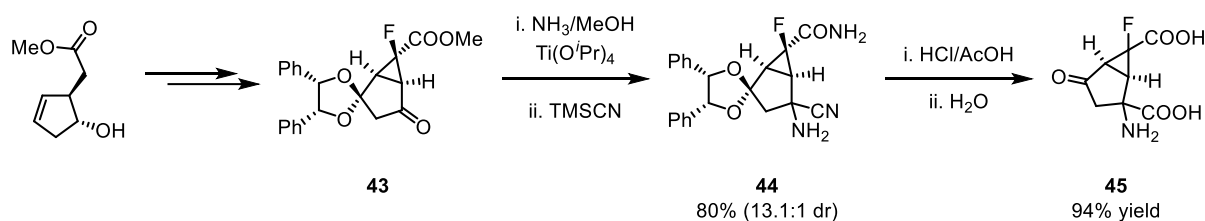
One of the earliest examples utilising the Strecker reaction was reported in 1992 by Brussee *et al.*, comprising of a one-pot reduction–transamination–hydrocyanation protocol to convert optically active *O*-protected cyanohydrins to β -hydroxy- α -cyanoamines (**Scheme 14A**).⁴¹ First, DIBAL reduction of cyanohydrin **39** forms primary imine **40** which is subsequently converted to a more stable *N*-alkyl imine **41** *via* transamination with methylamine/benzylamine. Hydrocyanation then provides the desired β -hydroxy- α -cyanoamine product **42** after deprotection with remarkable diastereoselectivity. Four further steps are then required to convert the cyano group into the carboxylic acid. In 2005, Tan, Yasuda, and co-workers reported a Strecker reaction of the ketimine derived from

enantiopure bicyclic ketone **43**, forming the α -aminonitrile **44** in high yield and diastereoselectivity (d.r. 13.1:1) (**Scheme 14B**).⁴² Global hydrolysis of **44** using mixture of AcOH and 8 M HCl provided the corresponding enantiopure α -amino acid **45**, also in good yield.

A One-pot Reduction–Transamination–Hydrocyanation

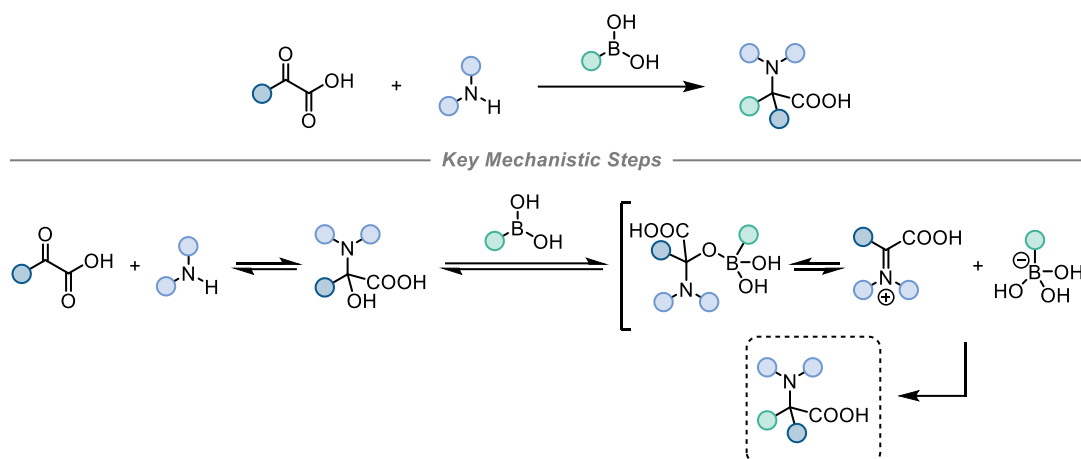


B Stereoselective Strecker Synthesis of a Cyclic α -Amino Acid



Scheme 14: A) one-pot reduction–transamination–hydrocyanation sequence to access β -hydroxy- α -cyanoamines; B) stereoselective Strecker reaction in the synthesis of **45**.

Since the initial report on the Strecker condensation, similar methods have been reported, such as the Petasis reaction, also known as the Petasis borono-Mannich reaction (**Scheme 15**).⁴³ This multicomponent reaction involves the coupling of an amine, a boronic acid, and a carbonyl compound, typically an aldehyde or glyoxylic acid, to form α -amino acids or their derivatives, and is noted for its mild conditions, high functional group tolerance, and the ability to generate products with high stereoselectivity.

Petasis Borono-Mannich Reaction


Scheme 15: Petasis borono-Mannich reaction with key mechanistic steps.

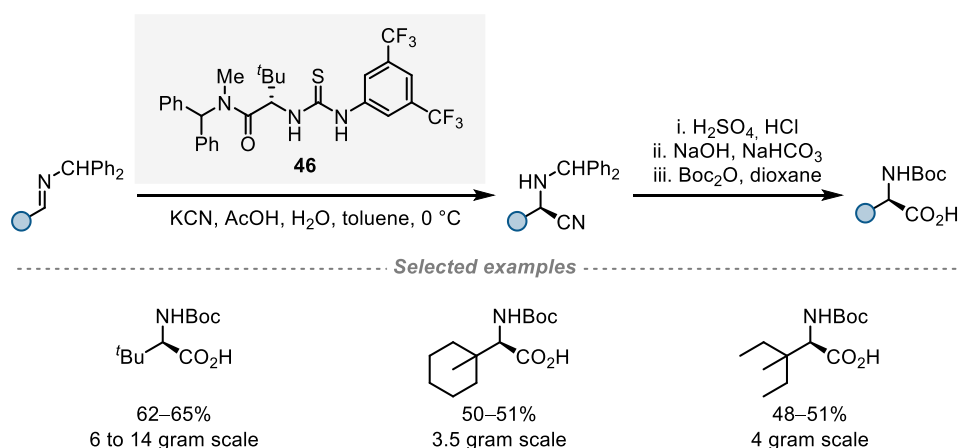
The reaction proceeds *via* an imine with the organic group of the boronic acid which acts as the nucleophile. Typically, numerous interdependent equilibrium steps are involved – some identical to those in the Mannich reaction – however, the key step involving nucleophilic addition of the organic ligand from the boronate to the imine still remains elusive. Notably, the use of glyoxylic acid in the Petasis reaction is particularly beneficial as it leads to the construction of α -AAs and derivatives in a single step, whilst avoiding forming toxic byproducts such as HCN in the Strecker reaction. Since the stereochemical outcome of the Petasis reaction is strongly correlated to the chirality of the amine, using bulky chiral amines as nucleophiles (*e.g.*, chiral benzyl amines, 2-substituted pyrrolidines, and 5-substituted 2-morpholinones) can induce good to excellent diastereomeric excess.^{44–47}

Auxiliary-based approaches for the synthesis of α -AAs involve the use of chiral auxiliaries to induce stereoselectivity in chemical reactions, leading to the formation of enantiomerically pure products. These methods are pivotal in asymmetric synthesis, allowing chemists to precisely control the configuration of newly formed chiral centres. The choice of auxiliary and the method of attachment are crucial as they define the steric and electronic environment of the substrate. Once attached, the chiral auxiliary controls the stereochemistry of the reaction by creating a chiral environment around the reaction site, and after removal, the auxiliary is removed under conditions that do not affect the newly formed chiral centre. This steric and electronic influence can guide the addition of reagents in a stereoselective manner. This method was particularly utilised for the construction of amino acids in the 1980s.

The use of chiral, optically pure amines as chiral auxiliaries has developed into a widely applicable and robust method for achieving highly diastereoselective Strecker reactions, providing access to various enantiomerically pure α -amino acids. This strategy necessitates the use of stoichiometric amounts of chiral auxiliaries, which must be cleaved from the products post-reaction, although in some instances they can be recycled. The first instance of such a chiral auxiliary-assisted Strecker reaction was reported by Harada in 1963, over 110 years after the original Strecker reaction was discovered.⁴⁸ In this modification, enantiopure (*S*)- α -phenylethylamine replaced ammonia, leading to the formation of the corresponding α -aminonitrile in a diastereoselective ratio of 3.3:1. Subsequent transformations yielded chiral alanine with an overall yield of 17% and 90% ee. This significant breakthrough paved the way for the successful preparation of more optically active α -amino acids using similar methods.

More recently, Jacobsen and co-workers published a catalytic asymmetric method for synthesising highly enantiomerically α -AAs, utilising potassium cyanide and a chiral amidothiourea catalyst to control the crucial hydrocyanation step (**Scheme 16**).⁴⁹ The highly enantiomerically enriched, sterically demanding protected α -AAs – including substrates bearing quaternary alkyl substituents – were isolated by recrystallisation, i.e., no chromatographic purification. This robust catalyst (**46**) contains a single stereogenic centre and is prepared in three steps from commercially available reagents (74% overall yield on a 5-gram scale) and is compatible with aqueous cyanide salts, offering a safer and more manageable alternative to other cyanide sources previously reported. This compatibility is highlighted by its adaptability for large-scale (25–100 mmol) synthesis.

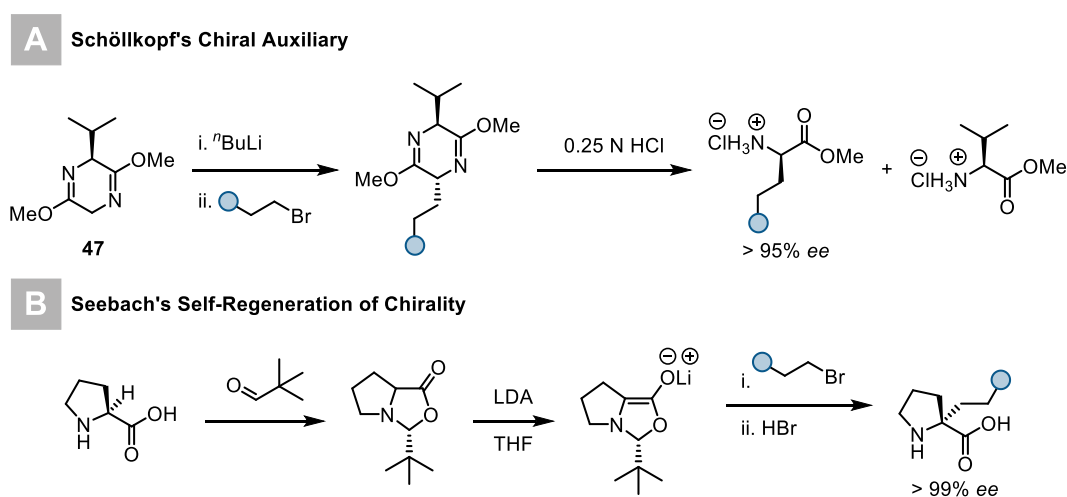
Jacobsen, 2009



Scheme 16: Organocatalytic asymmetric Strecker reaction using KCN.

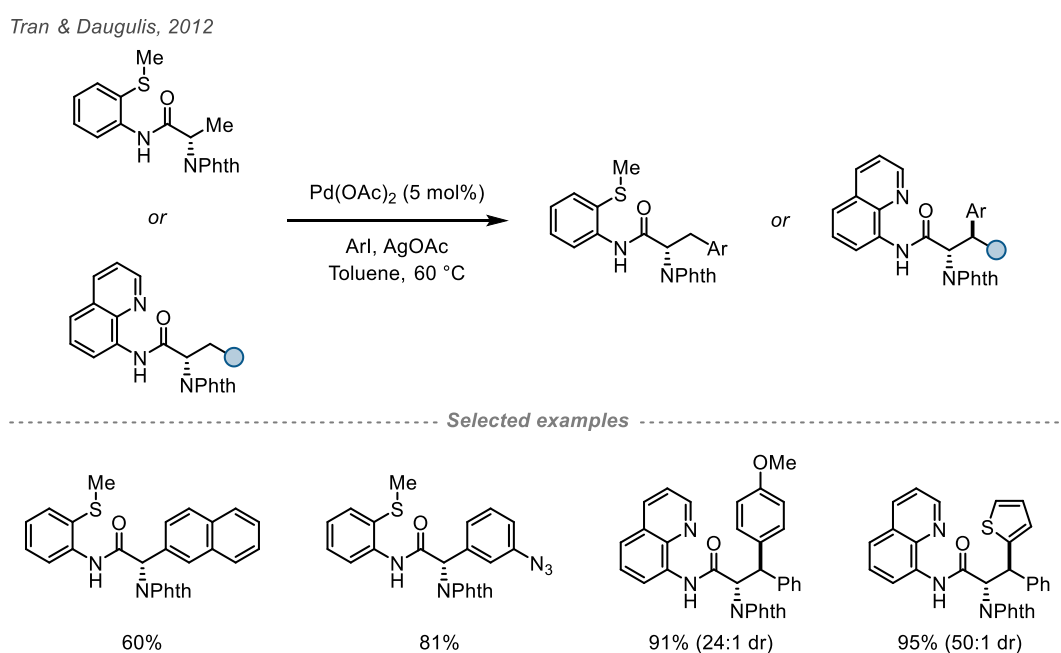
The synthesis of unnatural amino acids often involves the derivatisation of natural AAs, utilising them as starting materials for further chemical modifications. This approach, while conceptually straightforward and advantageous in leveraging the inherent stereochemistry of natural AAs, remains relatively underdeveloped in the field. This method harnesses the pre-existing chiral centres and side chain functionalities to facilitate the creation of structurally complex molecules, however, limitations of this strategy can be attributed to challenges in achieving selective functionalisation without compromising the pre-existing structure and bioactivity. The precision required for such derivatisations often necessitates advanced catalytic systems and regioselective methodologies or the use of chiral auxiliaries.

In 1981, Schöllkopf developed an auxiliary based on a diketopiperazine (a cyclic dipeptide derived from glycine and L-valine) framework modified to form a bis-lactim ether (**47**) and is highly effective for the diastereoselective alkylation of glycine derivatives (**Scheme 17A**).⁵⁰ The bis-lactim ether is first alkylated in a stereoselective manner, then cleaved to release the α -amino acid with high enantiomeric purity. Only two years later, Seebach described the self-regeneration of chirality using proline – a pioneering approach in asymmetric synthesis which leverages the inherent chirality of proline to facilitate enantioselective reactions (**Scheme 17B**).⁵¹ In this method, proline forms an iminium ion intermediate with an aldehyde or ketone, which then undergoes an enantioselective nucleophilic addition, creating a new chiral centre with high enantiomeric excess, while proline remains intact and chiral. This method is particularly useful for synthesising cyclic quaternary α -amino acids.



Scheme 17: chiral auxiliaries developed in the 1980s for the synthesis of amino acids.

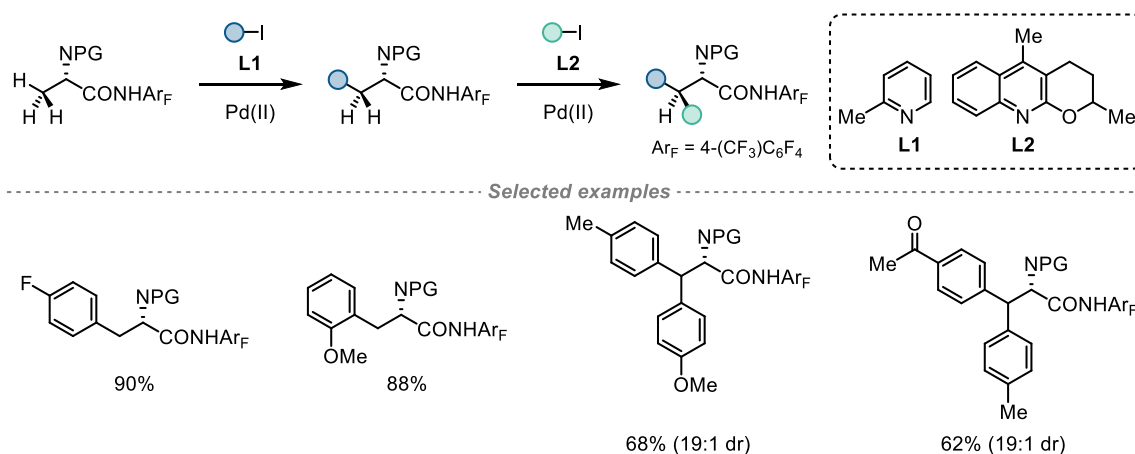
Recent advancements in catalytic processes, such as the development of ligand-controlled Pd-catalysed reactions, have shown promise in overcoming certain challenges. Innovative approaches allow for selective C–H activation/functionalisation, providing a more efficient and controlled means of modifying AAs to access a wide array of UAA derivatives. In 2012, Tran and Daugulis developed the Pd-catalysed synthesis of UAAs *via* C–H bond functionalisation (**Scheme 18**).⁵² By leveraging directing groups – installed by treating phthaloylamino acid chlorides with 8-aminoquinoline or 2-thiomethylaniline – the approach facilitated the diarylation of methyl groups and diastereoselective monoarylation of methylene groups in AAs. Using phenyl iodide and a Pd catalyst in the presence of a base, a diverse array of substituted phenylalanine derivatives was obtained, as the methodology is tolerable with various iodinated arenes, including those bearing functional groups such as methoxy and azido groups, and removal of the directing group post-arylation is also facile. Preliminary results of the acetoxylation and alkylation of C–H bonds in the AA derivatives were also shown.



Scheme 18: the Pd-catalysed synthesis of substituted phenylalanine derivatives by employing *N*-phthaloylalanine with 2-thiomethylaniline as a directing group.

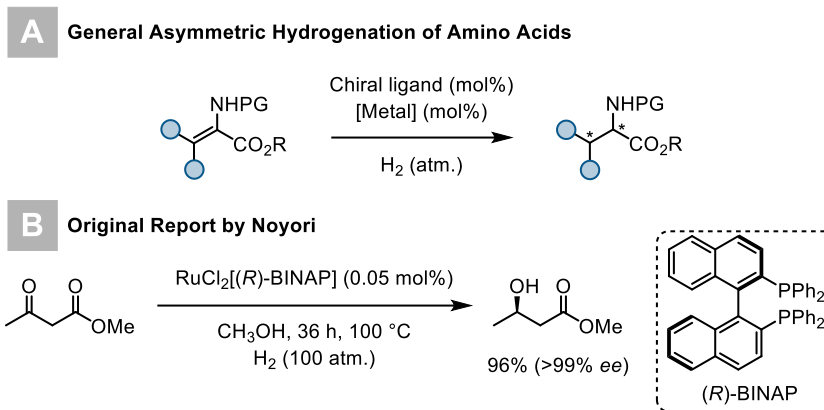
In 2014, He, Lie and colleagues made significant strides in the field by developing a method to synthesise chiral α -amino acids from alanine *via* C(sp³)–H arylation and olefination that leverages ligand-controlled reactivity for selective functionalisation of C(sp³)–H bonds (**Scheme 19**).⁵³ Alanine derivatives are first protected and modified to incorporate an amide directing group which coordinates with the Pd catalyst, allowing for selective

activation of the β -C(sp³)-H bonds. This catalyst-controlled arylation process utilises pyridine (e.g., 2-picoline, **L1**) and quinoline derivatives, where the former promotes exclusive monoarylation. When combined with ligand **L2**, the latter activates the catalyst further to achieve diarylation, forming β -aryl- β -aryl'- α -amino acids with two different aryl iodides in high diastereoselectivity. After the arylation reactions, the amide auxiliary is easily removed using NaNO₂ in AcOH/Ac₂O.



Scheme 19: ligand-controlled synthesis of α -AAs from alanine *via* Pd-catalysed C(sp³)-H arylation.

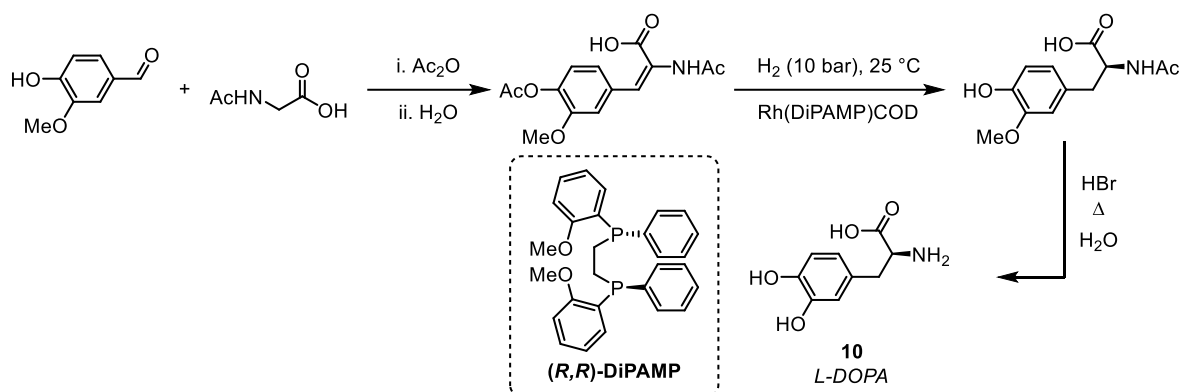
Asymmetric hydrogenation is one of the most valuable and well-explored methods for synthesising α -AAs, renowned for its ability to produce enantiomerically pure compounds with high precision. This catalytic process involves the selective hydrogenation of prochiral or racemic substrates using chiral catalysts, leading to the formation of optically active amino acids. In 1987, the first examples of asymmetric hydrogenation using a homogeneous catalysts were reported.⁵⁴ This approach gained significant recognition when Noyori and Knowles were awarded the Nobel Prize in 2001 for their pioneering work in developing asymmetric hydrogenation reactions (**Scheme 20**).^{55,56}



Scheme 20: A) asymmetric hydrogenation of amino acids using chiral ligands; B) Noyori's original report developing asymmetric hydrogenation reactions using the ligand (*R*)-BINAP.

Since the initial discovery, the reaction has become a standard technique in both laboratory and industrial-scale organic chemistry and has continued to achieve numerous significant advancements. Over the years, thousands of mono- and bidentate phosphine ligands have been studied, some of which, such as those highlighted by Nájera in the 2007 *Chem. Rev.* article “*Catalytic Asymmetric Synthesis of α -Amino Acids*”, work efficiently at just 1.0 atm. of hydrogen pressure.⁵⁷ Among the various metals used, rhodium and ruthenium complexes are the most versatile, though Rh-complexes typically exhibit a narrower substrate scope compared to Ru-complexes due to fundamental differences in their catalytic mechanisms.

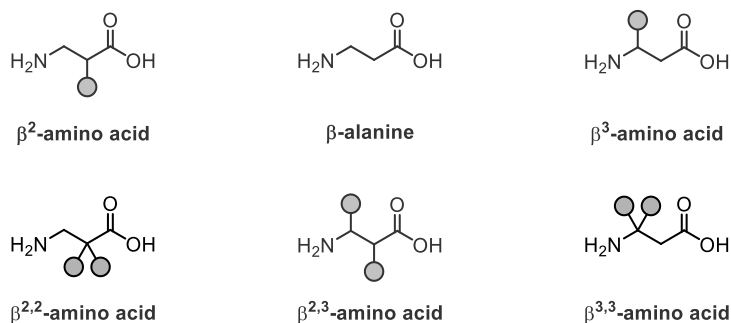
One notable industrial application of this method is the synthesis of (*S*)-3',4'-dihydroxyphenylalanine (L-DOPA, **10**), a crucial drug for treating Parkinson's disease, which is produced on a multi-ton scale annually (**Scheme 21**).⁵⁸ While working at Monsanto in the late 1970s, Knowles developed a protocol for synthesising L-DOPA featuring a Rh-catalysed enantioselective hydrogenation using (*R,R*)-DiPAMP as a chiral ligand.⁵⁹ This was the first successful industrial application of a homogeneous catalytic asymmetric hydrogenation, which awarded him the 2001 Nobel Prize in Chemistry for this discovery.⁵⁵



Scheme 21: Knowles' protocol for the industrial synthesis of *L*-DOPA via Rh-catalysed enantioselective hydrogenation with the ligand (R,R) -DiPAMP.

1.2.2 β -AAs

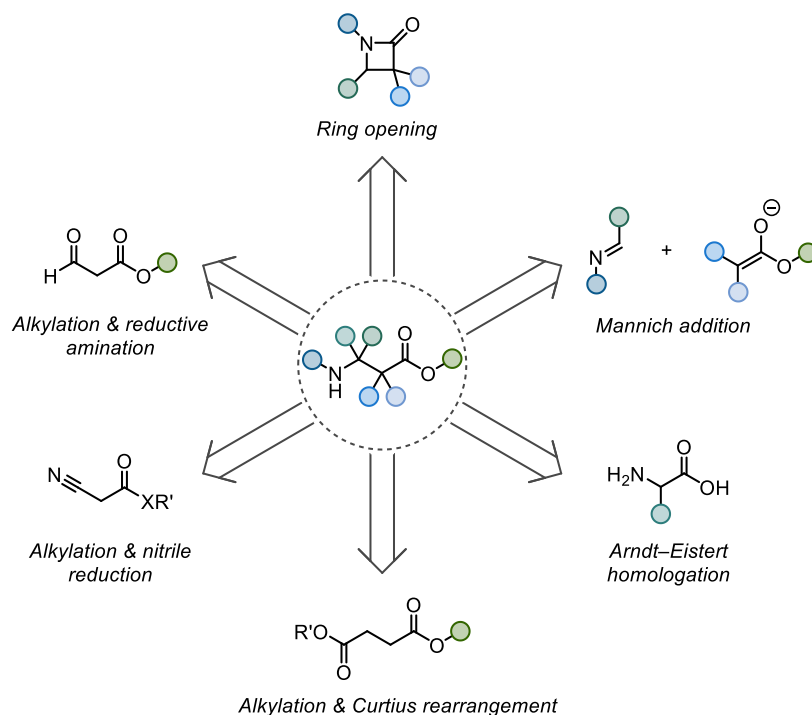
Depending on the substitution pattern, β -amino acids can be split into further classifications, as there are two carbons available for substitution, leading to four sites. The superscripts seen in **Scheme 22** denote the position where substituents are present. Two primary classes of β -amino acids exist, distinguished by the carbon atom to which the residue attaches: those with the residue adjacent to the amine are known as β^3 , while those with it next to the carbonyl group are termed β^2 . β -peptides may comprise solely one variety of these amino acids (either β^2 -peptides or β^3 -peptides), or they may exhibit a combination of the two.



Scheme 22: subcategories of β -amino acids depending on substitution pattern.

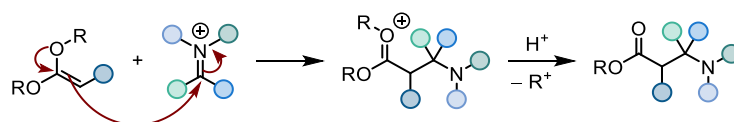
Over the years, a number of synthetic approaches to access β -amino acid derivatives have emerged (**Scheme 23**). Classically, they can be obtained in several different methods: the Mannich addition, the Arndt-Eistert homologation, the Curtius rearrangement, the conjugate addition of nitrogen nucleophiles to unsaturated esters, the addition of carbon nucleophiles to imines, or ring-opening reactions. Several methodologies involving alkylation

reactions followed by reduction/reductive aminations have also been developed, as well as numerous transition metal-catalysed procedures.



Scheme 23: synthetic routes to access β -amino acid derivatives.

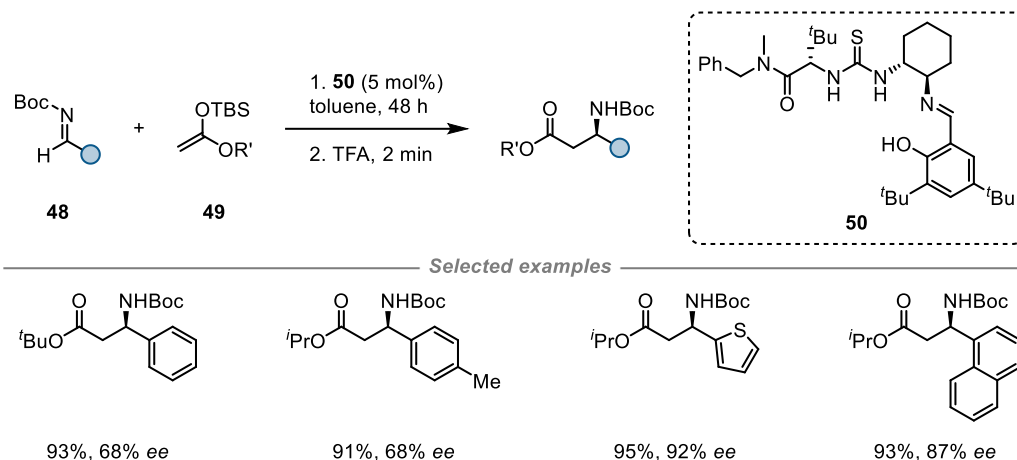
The most prominent strategy in literature to prepare β -amino carbonyl compounds is the Mannich-type addition. Classically, Mannich reactions of enolisable carbonyl compounds to yield β -aminoketones have involved treatment of an acidic mixture of formaldehyde and a simple secondary amine such as dimethylamine with the ketone in ethanol under reflux for several days. Alternatively, the reaction of more nucleophilic enolates or softer silyl enol ethers with imines can be used. **Scheme 24** shows the mechanism of the reaction consisting of a condensation between an enolate equivalent (e.g., silyl enol ethers) and an activated imine *i.e.*, an iminium ion.⁶⁰



Scheme 24: general mechanism of the Mannich addition between an enol and iminium species.

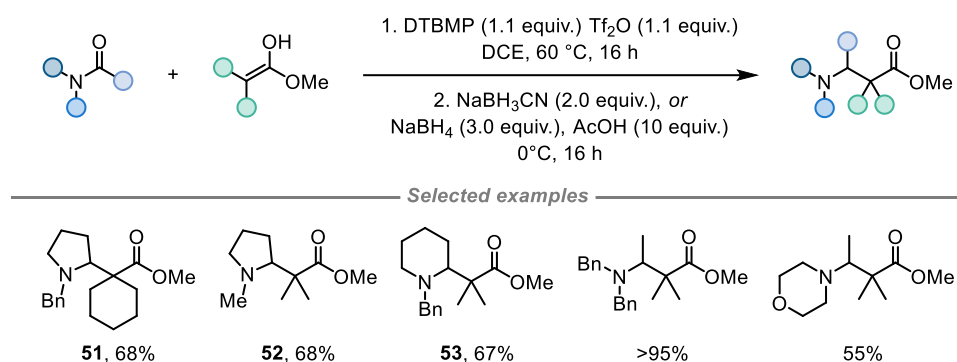
In 2002, Jacobsen published a highly efficient route to *N*-Boc protected β^3 -amino acids (*i.e.*, β -aryl- β -amino acids) in an asymmetric catalytic Mannich reaction (**Scheme 25**).⁶¹ The method proceeds *via* the enantioselective addition of silyl ketene acetals (**49**) to *N*-Boc-aldimines (**48**, imines where one substituent is a H), catalysed by a thiourea derivative.

While the yield and e.e. of isolated products are excellent, the use of aldimines is limited to aryl aldimines.



Scheme 25: synthesis of *N*-Boc-protected β -amino acids *via* Mannich reaction.

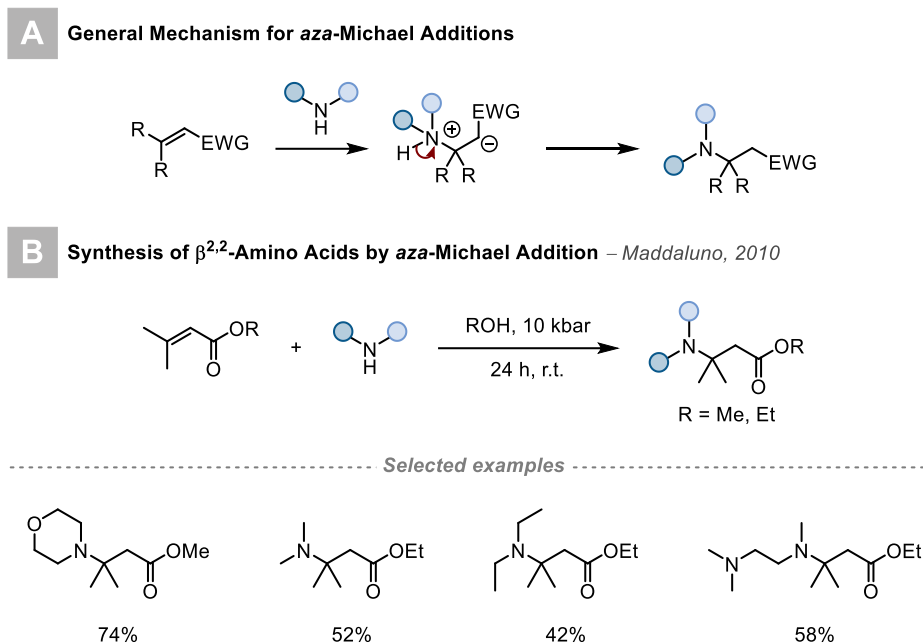
A notable drawback to the Mannich addition is the limited reactivity of the imine which can restrict the type of substitution pattern accessible. This can be circumvented through activation of the imine to an iminium cation with either a Lewis acid or alkylating reagent. This can be seen in a report by Bélanger in 2015 on the preparation of highly substituted β -amino acids utilising a Vilsmeier-Haack-type addition of non-aromatic carbon nucleophiles on to activated amides, followed by *in situ* reduction of the iminium ion to amine (**Scheme 26**).⁶² The reaction gave rise to several $\beta^{2,2,3}$ -amino esters, including derivatives of homoproline (**51 & 52**), and homopipicolic esters (**53**) bearing quaternary centres.



Scheme 26: synthesis of $\beta^{2,2,3}$ -amino esters using a Vilsmeier reagent.

In addition to the Mannich, another common strategy for the synthesis of β -AA derivatives is based on *aza*-Michael addition reactions. This involves a 1,4-addition (conjugate addition) of a nitrogen nucleophile to a Michael acceptor (**Scheme 27A**). This is

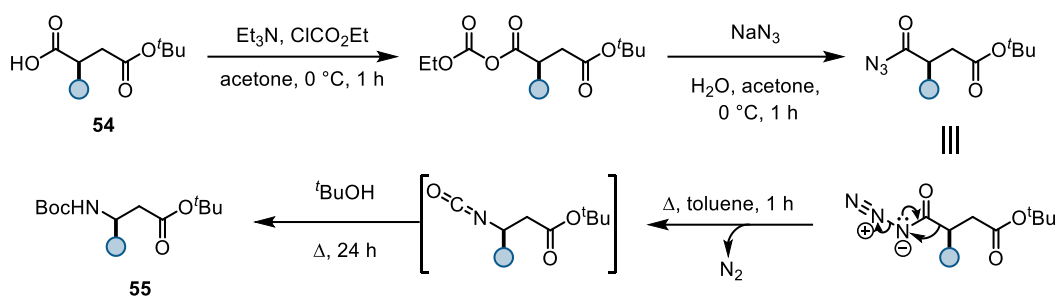
demonstrated by the work of Maddaluno and co-workers in the synthesis of $\beta^{3,3}$ -amino acid derivatives from α,β -unsaturated esters and tertiary amines (**Scheme 27B**).⁶³



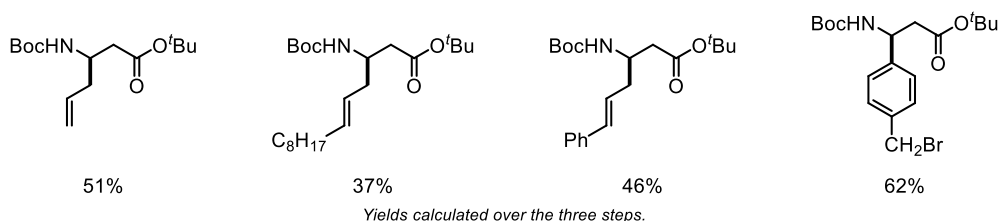
Scheme 27: A) general mechanism of an aza-Michael addition; B) Maddaluno's work synthesising $\beta^{3,3}$ -amino acid derivatives from α,β -unsaturated esters under hyperbaric conditions.

The use of rearrangements has been applied for the construction of β -AAs. In 2000, the group of Deshpande reported the synthesis of β^3 -AA derivatives in a regio- and stereoselective manner (**Scheme 28**).⁶⁴ The key step of the method is a one-pot conversion of the carboxyl group in **54** to the Boc-protected amine (**55**) *via* a Curtius rearrangement. While the reaction provides moderate to good yields with retention of stereochemistry, a lengthy synthetic process is required, often with harsh conditions.

Deshpande, 2000



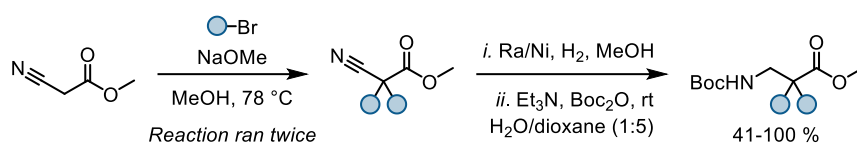
----- Selected examples -----



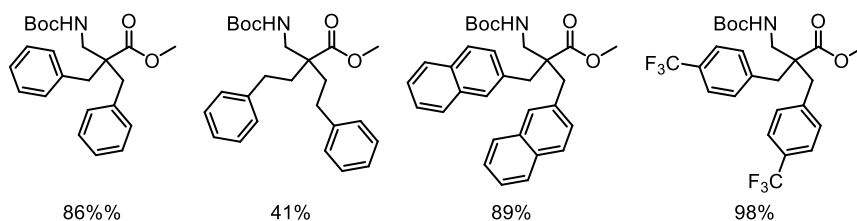
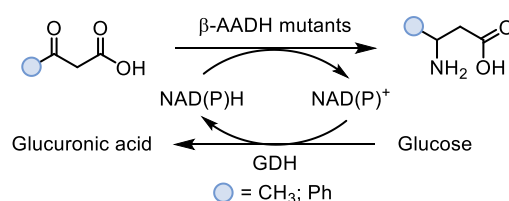
Scheme 28: one-pot conversion of a carboxyl group to a protected amino group *via* Curtius rearrangement.

Alkylative processes can also be combined with reductive amination reactions or nitrile reduction (e.g., reduction of cyanoesters or cyanoamides). In 2010, Strøm and co-workers reported the synthesis of antimicrobial β -peptidomimetics based on lipophilic $\beta^{2,2}$ -amino acid methyl esters through an alkylative/nitrile reduction process (**Scheme 29A**).⁶⁵ Various amino esters were obtained through firstly a dialkylation, followed by nitrile reduction and amine protection. Yields ranged from moderate to high, however the process requires two alkylations with exclusively primary and/or activated electrophiles, to form the α,α -substituted cyanoacetate derivatives.

More recently, Zhu *et al.* developed the first biocatalytic method for direct reductive amination of aromatic and aliphatic β -keto esters *via* β -amino acid dehydrogenase (β -AADH) (**Scheme 29B**).⁶⁶ Initially, due to their instability in aqueous solution, the β -keto esters had to be hydrolysed to the corresponding acid prior to the reaction. Reductive amination of selected keto acids in the presence of the biocatalyst and D-glucose dehydrogenase (GDH) for the NADPH regeneration provided various β -amino acids, albeit in low yields (12–22%).

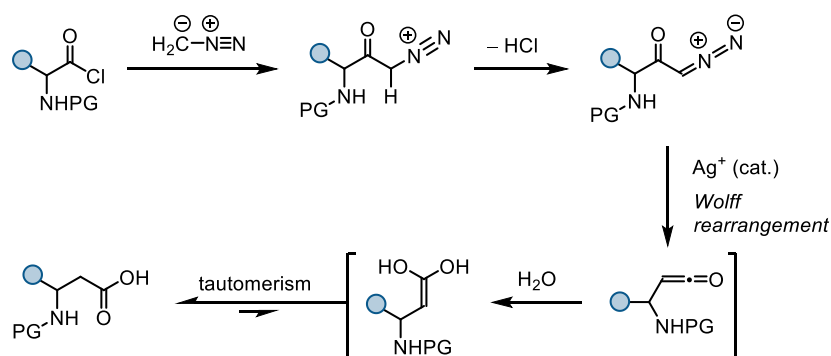
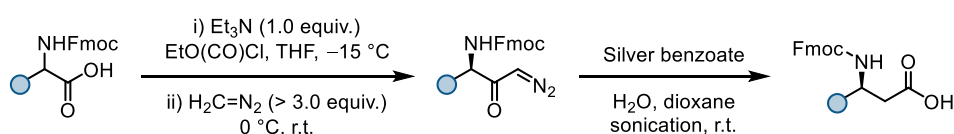
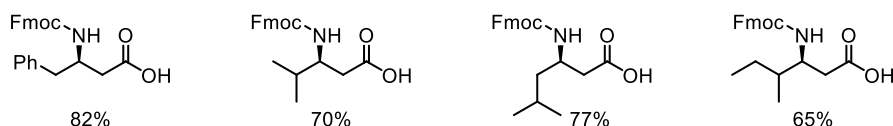
A Synthesis of $\beta^{2,2}$ -amino Acids via Nitrile Reduction – Strøm, 2010


Selected examples


B Biocatalytic Synthesis of β -amino Acids via Reductive Amination – Zhu, 2015


Scheme 29: A) synthesis of $\beta^{2,2}$ -AA esters via nitrile reduction; B) biocatalytic synthesis of β -AAs via reductive amination.

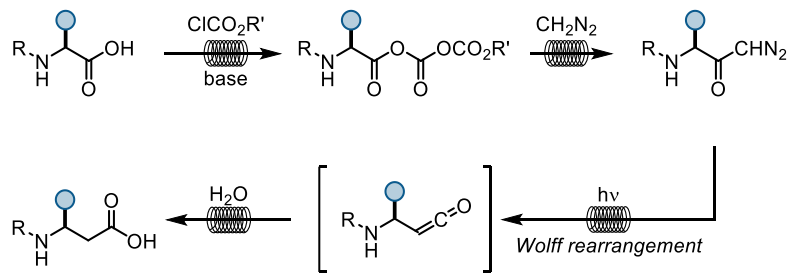
An important and popular method to construct β -AAs is the Arndt-Eistert homologation which involves treatment of an acid chloride (formed from an α -amino acid) with diazomethane in the presence of water and a metal catalyst.⁶⁷ Mechanistically, the acid chloride undergoes an attack by diazomethane with loss of HCl, forming an α -diazoketone species (**Scheme 30A**). This species then undergoes the key step of the reaction – a Wolff rearrangement of the diazoketone to a ketene – either thermally, photochemically or by silver(I) catalysis. One of the first examples utilising the reaction for β -AA synthesis was in 1997 by Sewald and co-workers (**Scheme 30B**).⁶⁸ The reaction uses a silver catalyst to promote a Wolff rearrangement of Fmoc-protected α -amino acids activated as mixed anhydrides using ethyl chloroformate, forming Fmoc-protected β -amino acids.

A General Mechanism for Arndt-Eistert Homologation

B Synthesis of Fmoc- β -AAs by Wolff Rearrangement – Sewald, 1997

Selected examples


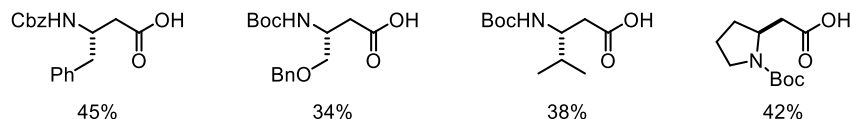
Scheme 30: A) general mechanism of the Arndt Eistert homologation to construct β -AAs; B) synthesis of Fmoc- β -AAs by ultrasound-promoted Wolff rearrangement.

The primary limitation of the Arndt-Eistert homologation process stems from safety issues linked to the use of diazomethane (CH_2N_2), a volatile, irritating, toxic, and carcinogenic compound. Additionally, diazomethane is highly sensitive to heat, light, and shock, thus being prone to explosive decomposition. To avoid this, in 2014 the group of Kappe proposed a four-step continuous-flow process for the preparation of β -amino acids from the corresponding α -amino acids *via* an Arndt–Eistert homologation approach (**Scheme 31**).⁶⁹ The method comprises of first an activation of the α -amino acid to an anhydride, followed by acylation of diazomethane to form an α -diazoketone, and finally a photo-Wolff rearrangement, providing the β -amino acids in overall moderate yields.⁷⁰ By using flow technology, the on-demand generation and consumption of diazomethane avoids exposure to the hazardous and explosive nature of the reagent.

Kappe, 2014



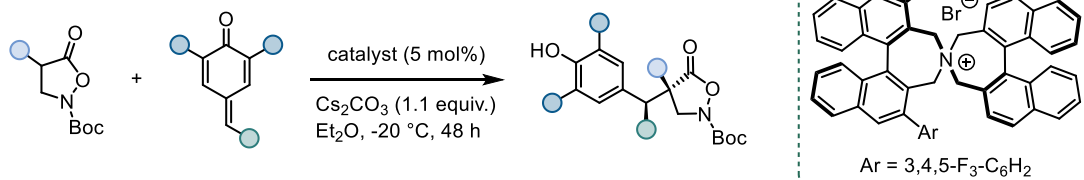
----- Selected examples -----



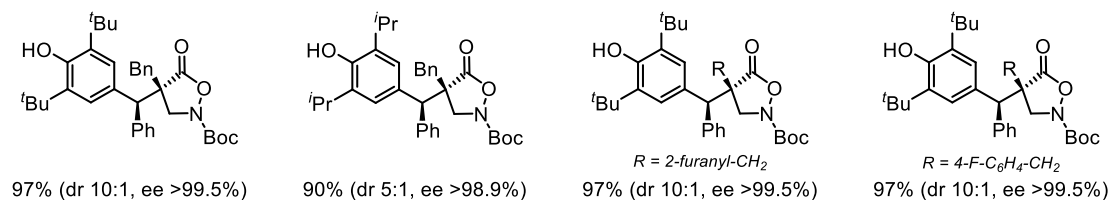
Scheme 31: β -amino acid synthesis via an Arndt–Eistert homologation sequence.

Recently, the group of Waser reported a highly enantioselective synthesis of densely functionalized $\beta^{2,2}$ -amino acid derivatives through the reaction of isoxazolidin-5-ones with *para*-quinone methides, catalysed by chiral ammonium salt phase-transfer species (**Scheme 32**).⁷¹ While the method requires a low catalyst loading and tolerates a large variety of functional groups, it also requires the use of lower temperatures and extended reaction times.

Waser, 2020



----- Selected examples -----

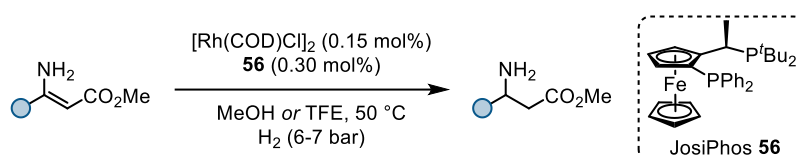


Scheme 32: enantioselective synthesis of $\beta^{2,2}$ -AA syntheses from isoxazolidin-5-ones.

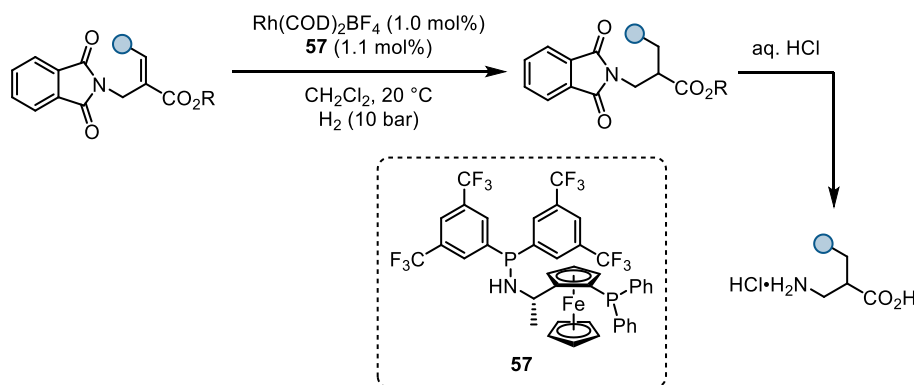
A number of transition metal-based methods have also been reported over the years for the synthesis of β -amino acids, some of which also utilise chiral ligands for enantioselective syntheses. A commonly implemented strategy involves catalytic asymmetric hydrogenation of (*E*)- and (*Z*)- β -dehydroamino acid derivatives, typically via rhodium catalysis.⁷² Hsiao and co-workers made a significant breakthrough Rh-catalysed

hydrogenations by using chiral ferrocenylphosphine (Josiphos) ligand **56** in the hydrogenation of (*Z*)-enamine esters, which contain an unprotected amine group, in MeOH or trifluoroethanol (TFE) as the solvent (**Scheme 33A**).⁷³ This process yielded the corresponding amino esters with excellent enantiomeric excess (*ee*), reaching up to 97%. This work represents the first instance of a high-yield enantioselective hydrogenation of unprotected β -enamine esters without requiring either a directing or protecting group. Additionally, a chiral BoPhoz-type ligand **57** was used in the Rh-catalysed hydrogenation of alkyl-(*E*)- β -phenyl- α -(phthalimidomethyl)acrylates (**Scheme 33B**).⁷⁴ The products were obtained in high yields and with excellent *ee*. In one example, the corresponding β -amino acid was obtained in good yield following the cleavage of the phthalimide protecting group and hydrolysis of the ester group.

A Rh-catalysed hydrogenation of Unprotected Enamines – Hsiao, 2004



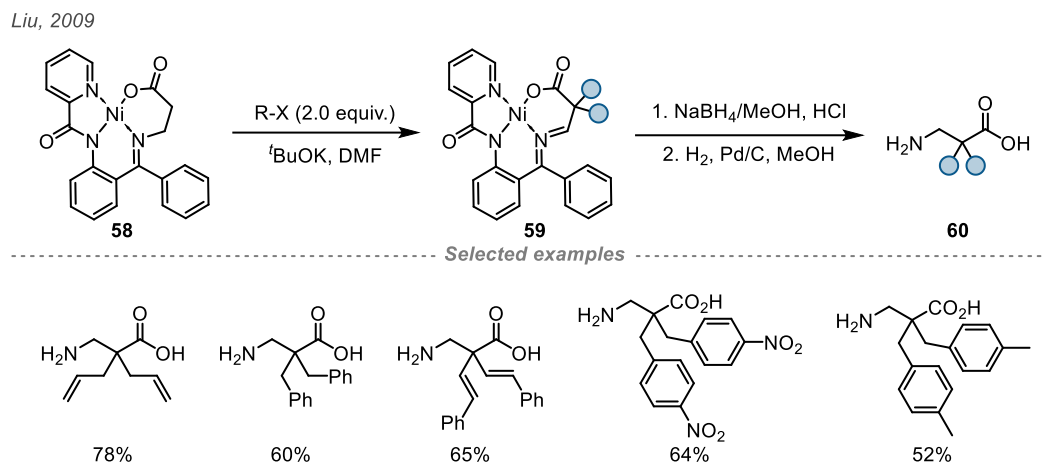
B Rh-BoPhoz-catalysed Hydrogenation of Phthalimide-protected Enamines – Zheng, 2008



Scheme 33: A) Rh-catalysed hydrogenation of unprotected enamines; B) Rh-BoPhoz-catalysed hydrogenation of phthalimide-protected enamines.

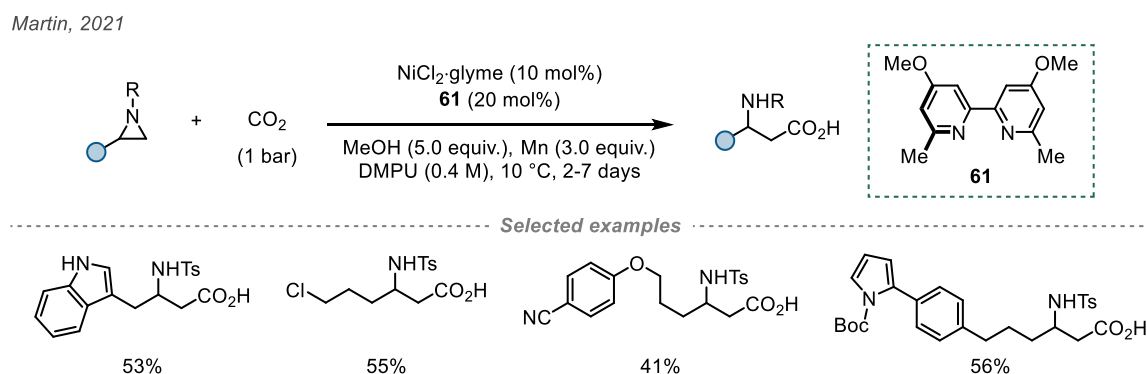
In 2010, the group of Liu reported the synthesis of symmetrical $\beta^{2,2}$ -amino acids *via* a nucleophilic β -alanine Ni(II) complex (**Scheme 34**).⁷⁵ The method proceeds through the alkyl halide alkylation of Ni(II) complex **58** to produce dialkylated species **59**, which can be hydrolysed to then provide the desired disubstituted amino acid **60**. While the reaction does not necessitate inert conditions and can be ran at room temperature, several steps are needed, including the two-step synthesis of precursor **58**. Additionally, due to the harsh

conditions needed for the hydrogenation of the C–N bond, functional group tolerance is notably low.



Scheme 34: synthesis of disubstituted β -amino acids via Ni(II) complex.

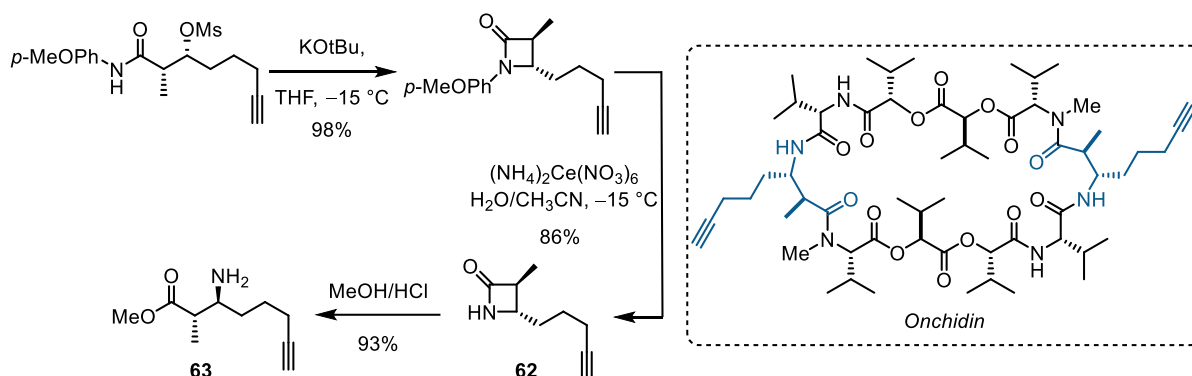
Cyclic precursors such as aziridines or β -lactams are often used to synthesize β -AAs. In 2021, Martin reported the Ni-catalysed carboxylation of *N*-substituted aziridines with CO_2 to form β^3 -AAs (**Scheme 35**).⁷⁶ While the mild and selective conditions allow for a wide substrate scope in a chemo- and regioselective manner, diminished yields for more hindered substrate combinations, along with extensive reaction times (2-7 days) could be improved upon.



Scheme 35: Ni-catalysed carboxylation of *N*-substituted aziridines.

Recently, the use of β -lactam rings has been prominent in the synthesis of β -AAs and derivatives.⁷⁷ In one example, Muñoz and co-workers carried out an asymmetric synthesis of the $\beta^{2,3}$ -amino acid methyl ester fragment of Onchidin, a dimeric depsipeptide from the marine mollusc *Onchidium* spp. (**Scheme 36**). After synthesis and deprotection, ring opening of β -lactam **62** under acidic conditions afforded β -amino ester **63** in close to quantitative

yield. For many similar procedures involving the cleavage of the β -lactam C–N bond via hydrolysis and alcoholysis, harsh acidic or basic reactions are required.



Scheme 36: Synthesis and acid methanolysis of β -lactam forming key β -AA unit of Onchidin.

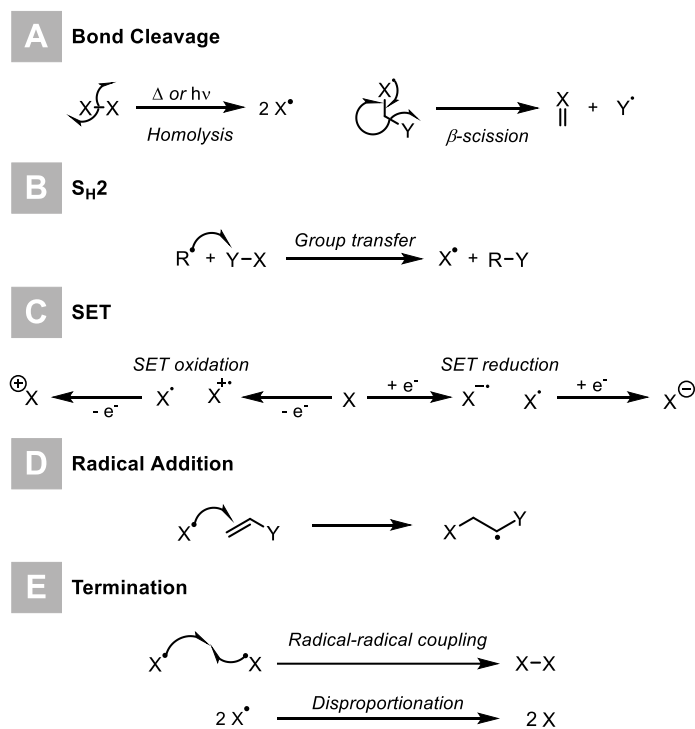
1.3 Radical Chemistry

Radical chemistry is an important area of study within the field of chemistry, characterised by species that contain an unpaired electron, also known as open-shell species. Despite their significant roles in various redox processes, the application of radicals in synthesis has been historically limited due to their perceived uncontrollable reactivity. This reputation, however, is evolving as a deeper understanding of radical behaviour, and control mechanisms, emerges.^{78,79}

Radicals participate in a variety of reactions, all of which can be categorised into a few elementary processes.⁸⁰ These include bond cleavages (homolysis, α - and β -scission), bimolecular radical substitution (S_{H2}) reactions – *i.e.*, group transfers, of which hydrogen atom transfer (HAT) and halogen atom transfer (XAT) are specific examples – single-electron transfer (SET), radical additions (π -addition), and termination reactions, *e.g.*, radical-radical coupling and disproportionation. An overview of the common type of radical reactions can be seen in **Scheme 37**. These processes form the basis of radical chemistry and illustrate the versatility of radicals in both synthetic and natural contexts.

The formation of radicals occurs primarily through two mechanisms. The first involves the thermal or photochemical homolysis of weak bonds in neutral, closed-shell species, leading to the formation of two radicals. This bond cleavage process is a key step (initiation) in many radical reactions. The second mechanism involves SET reactions between neutral species and existing radicals (more appropriately, open-shell species, as this includes many transition metals) producing radical cations and anions. Neutral radicals can be terminated

through oxidation to cations or reduction to anions *via* SET, thereby completing various redox cycles. Additionally, some transition metals – along with some organic compounds in their excited states – exist as radical species. Although less common, several molecules such as molecular oxygen (O₂) and nitric oxide (NO) are open-shell species in their ground state, showcasing the diversity of radical species in different chemical environments.⁸¹



Scheme 37: Elementary radical reactions.

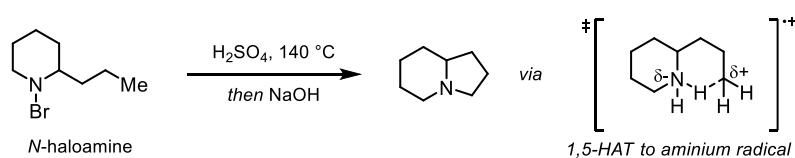
Single electron transfer (SET) reactions are fundamental in redox or electron-relay catalysis, where catalytic cycles typically involve alternating SET oxidation and reduction steps. The redox behaviour of a species is quantified by its reduction potential (E) and is key to determine how readily the species undergoes oxidation or reduction. While standard redox potentials (E^\ominus) for many inorganic redox couples are well-documented – owing to the multiple stable oxidation states of many transition metals and their ability to undergo reversible SET – the redox behaviour of organic molecules is more complex.⁸² This is because SET often produces highly reactive radicals that do not often show reversible redox characteristics.

To evaluate the redox properties of organic molecules, researchers often refer to the half-wave potential ($E_{1/2}$), defined as the applied potential at which the current reaches half of its maximum value (I_{max}) during an irreversible oxidation wave in cyclic voltammetry. These values are typically measured against a reference electrode such as the Saturated

Calomel Electrode (SCE) and provide crucial insights into the redox behaviour of organic radicals.

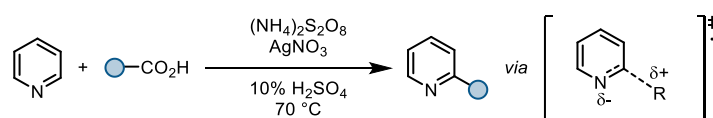
1.3.1 Notable Radical-Based Reactions

Several radical reactions have played significant roles in the history of chemistry, both in theoretical understanding and practical applications. One of the oldest examples of a radical reaction is the Hofmann-Löffler-Freytag reaction which was described in 1883 (**Scheme 38**).⁸³ The reaction is used to construct pyrrolidines from *N*-haloamines *via* a 1,5-HAT process with nitrogen radicals. Initially, the haloamine undergoes light-induced homolytic cleavage of the N–Cl bond, generating Cl and N radicals. The reaction proceeds through a selective HAT *via* a six-membered ring transition state, converting the nitrogen radical into a stable secondary carbon radical which reacts with the Cl radical to form a 1,4-chloroamine. An intramolecular S_N2 reaction then produces the pyrrolidine ring. To this day, this remains an important method for pyrrolidine synthesis.



Scheme 38: Hofmann-Löffler-Freytag reaction.

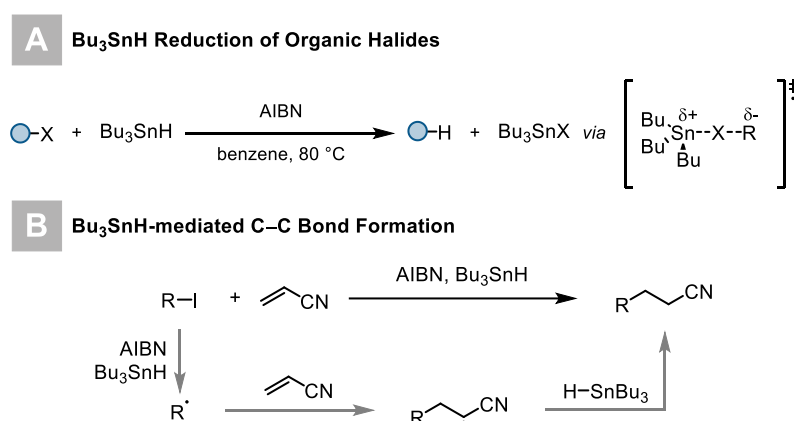
The Minisci reaction, developed in 1971, is significant due to its application of one of the fundamental reactions of radicals: addition to π -systems (**Scheme 39**).⁸⁴ This reaction is especially valuable in medicinal chemistry because it provides a versatile method for functionalizing pyridine scaffolds, which are commonly found in many pharmaceuticals. By enabling the direct addition of various alkyl radicals to heteroaromatic compounds like pyridine, the Minisci reaction allows for the modification and diversification of these structures, facilitating the development of new drugs.



Scheme 39: The Minisci reaction.

Tin hydride radical chemistry, established by Noltes and Van der Kerk, originated in 1957 when they observed that the reaction of Ph₃SnH with allyl bromide unexpectedly produced Ph₃SnBr and propene (**Scheme 40A**).⁸⁵ This XAT reaction was later studied in greater detail by Kuivila and Menapace, who expanded the method and exchanged the

reagent for Bu_3SnH , using AIBN as the initiator. Additionally, radical chain reactions mediated by Bu_3SnH can facilitate the formation of C–C bonds (**Scheme 40B**).⁸⁶ A crucial element in these reactions is a C–X (often C–I) bond, which reacts with the chain-propagating Bu_3Sn radical to generate a carbon radical, which then combines with an alkene/alkyne to form the new C–C bond. These reactions can occur both inter- and intramolecularly, with the latter more preferential for higher yields and better regioselectivity. Since radical reactions are kinetically controlled, they offer an effective strategy for synthesising 5-membered rings.

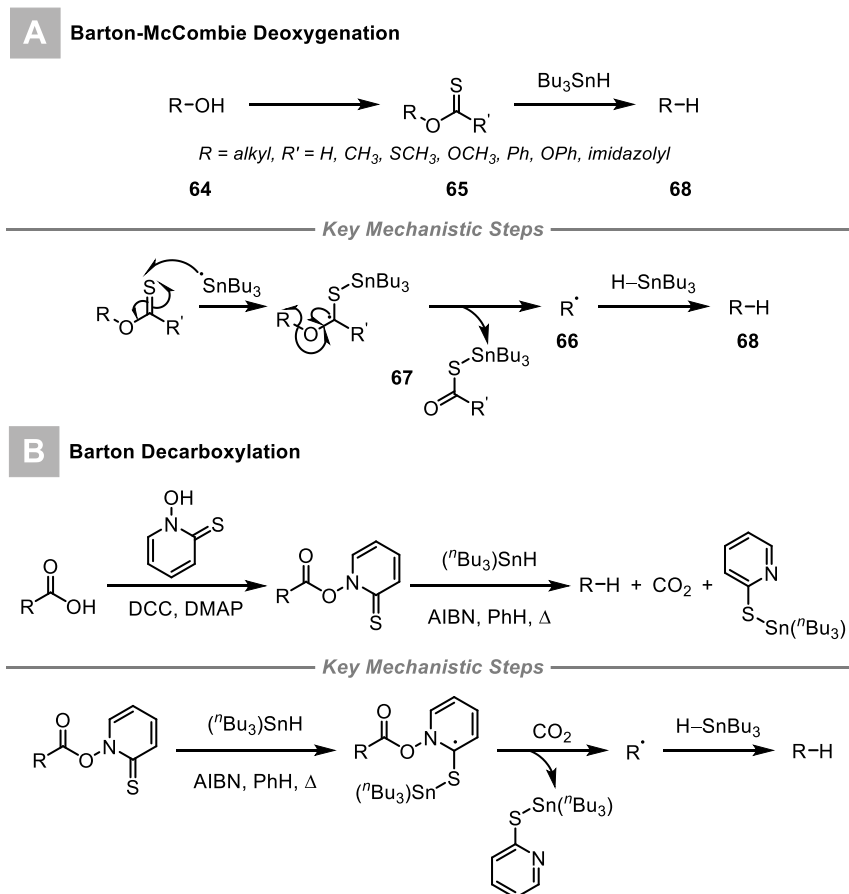


Scheme 40: A) tin hydride reduction of organic halides; B) C–C bond-forming reaction mediated by Bu_3SnH .

Named after British chemists Sir Derek Harold Richard Barton and Stuart W. McCombie, the Barton-McCombie deoxygenation is a radical-mediated process used to cleave alcohol groups from molecules, effectively reducing them (**Scheme 41A**).^{87,88} Initially, the alcohol (**64**) is converted into a reactive carbonothioyl intermediate (e.g., thionoester or xanthate **65**). Heating a radical initiator such as AIBN causes it to undergo homolytic cleavage, forming two radicals, which each abstract a hydrogen atom from Bu_3SnH , generating Bu_3Sn radicals and inactive byproducts. The Bu_3Sn radical then attacks the sulfur atom in the xanthate group of **65**, resulting in homolytic cleavage of the C–S π -bond and a C-centred radical. The latter forms a C–O π -bond through α -scission, producing alkyl radical **66**, and **67** which is thought to drive the reaction through the high stability of the S–Sn bond. The alkyl radical (**66**) then abstracts a hydrogen atom from a new molecule of Bu_3SnH , forming the desired deoxygenated product (**68**) and regenerating a new radical species for the chain propagation.

Similarly, the Barton decarboxylation is a valuable radical-based method for removing carboxylic acids from molecules without the need for a β -carbonyl group (**Scheme 41**).^{89,90}

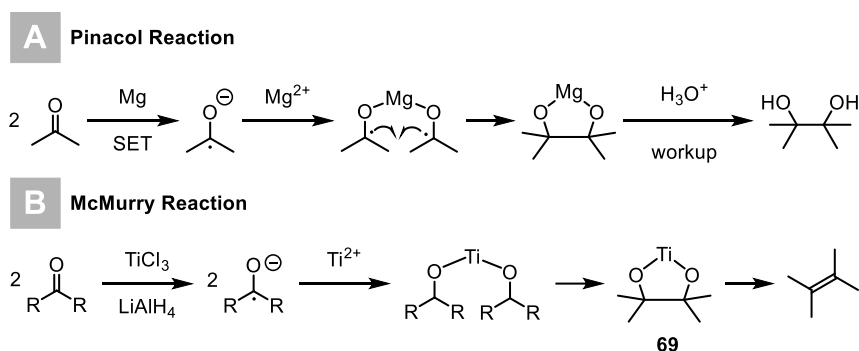
Initially, the carboxylic acid is converted into a thiocarbonyl intermediate using thiocarbonyl derivatives which then reacts with Bu_3Sn radicals (generated similarly to the Barton-McCombie reaction). The radicals abstract a sulfur atom, creating a C-centred radical that undergoes decarboxylation, releasing CO_2 and forming a carbon radical which abstracts a hydrogen atom from Bu_3SnH , yielding the decarboxylated product and regenerating the Bu_3Sn radical to continue the chain reaction.



Scheme 41: Barton-McCombie deoxygenation & Barton decarboxylation.

Named after the compound pinacol, the Pinacol coupling reaction involves C–C bond formation between the carbonyl groups of aldehydes/ ketones in the presence of an electron donor *via* a radical process (**Scheme 42A**).⁹¹ Two equivalents of acetone react with Mg metal through SET, producing two ketyl radical anions, which then couple to form a vicinal diol and are protonated by water. When Mg is used, the initial product is a 5-membered ring complex with the oxidised Mg^{2+} ion, which collapses in the presence of water, forming pinacol and $\text{Mg}(\text{OH})_2$. The pinacol reaction is well-studied and compatible with various reductants, including electrochemical methods.⁹² A related reaction, the McMurry reaction, uses TiCl_3 and a reducing agent to form a metal-diol complex, followed by deoxygenation to

yield an alkene (**Scheme 42B**).⁹³ The reaction is similar to the pinacol reaction, with the exception of the final step. TiCl_3 and LiAlH_4 are used to generate titanium metal *in situ*, which then reacts with two ketones to form the ketyl radical anions as previously described. Unlike in the pinacol reaction, a 5-membered titanacycle **69** forms which then undergoes deoxygenation, essentially combining two ketones into an alkene.



Scheme 42: Pinacol Reaction & McMurry Reaction.

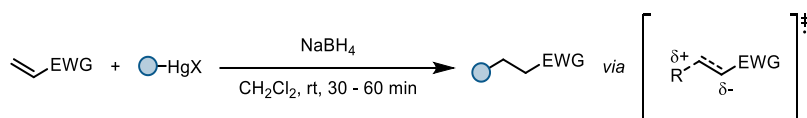
1.3.1.1 Giese Reaction

The Giese reaction, named after chemist Bernd Giese, is a notable radical-mediated process in organic chemistry, first reported in the late 1970s (**Scheme 43**).⁹⁴ This reaction involves the addition of carbon-centred radicals from a precursor to a π -bond in conjugation with an electron-withdrawing group (EWG), resulting in the formation of new C–C bonds. It is particularly valued for its ability to generate complex molecules under relatively mild conditions, making it an essential tool in synthetic organic chemistry.

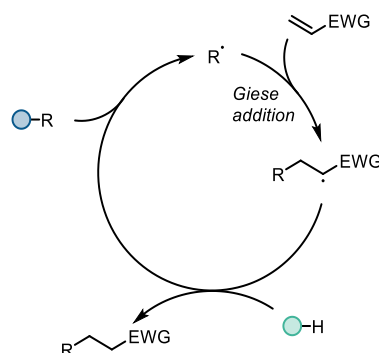
The Giese reaction typically employs radical initiators such as Bu_3SnH or related tin-based compounds, which facilitate the generation of carbon radicals which then add to alkenes/alkynes, forming versatile intermediates that can be further functionalised. The reaction's utility in forming C–C bonds efficiently and selectively has led to its widespread application in the synthesis of pharmaceuticals, natural products, and advanced materials.

The reaction is also one of the first steps in numerous radical polymerisations (e.g., free-radical polymerisation of vinyl acetate/methyl acrylate).⁹⁵ It is typically regarded as a radical hydrofunctionalisation reaction involving nucleophilic (alkyl) radicals. In the original publication, organomercury(II) halides were combined with a stoichiometric reductant (NaBH_4) to generate alkyl radicals through a radical chain process. Like the Minisci reaction, the Giese reaction's range has broadened to encompass numerous, milder catalytic methods for radical generation from a variety of precursors.

Original Giese Reaction Conditions



General Mechanism



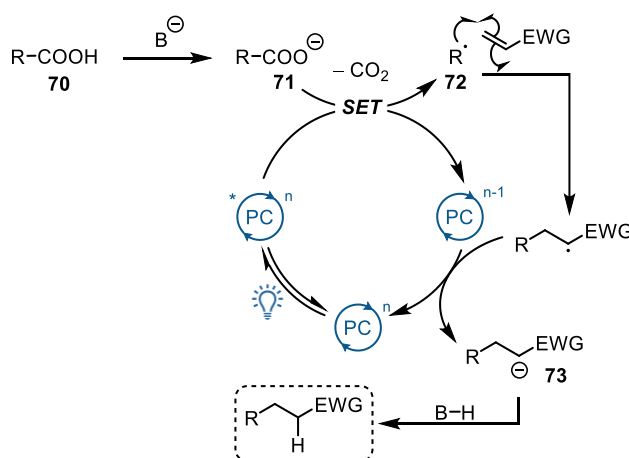
Scheme 43: Giese's original reported reaction in the 1970s, and a general mechanism for the Giese reaction.

All Giese reactions share some common mechanistic steps; the first of which is the formation of an alkyl radical from a suitable precursor. This can be an alkane, carboxylic acid, alkyl halide, an alkyl group with a redox auxiliary group (*i.e.*, a group that can be removed by SET, either oxidation as in the case of carboxylic acids, or reduction when using alkyl iodides), or bimolecular radical substitution (*e.g.*, HAT with an alkane or XAT with an alkyl halide). The resulting radical then carries out a π -addition to the electron-poor olefin – typically an acrylate or any olefin conjugated with an electron-withdrawing group, *e.g.*, alkylidene malononitriles (seen in chapter II). The Giese adduct then must accept a hydrogen, either through SET reduction and protonation, or HAT. In some cases, the latter occurs between the radical precursor and the Giese adduct, thus leading to the typical chain process (*e.g.*, as seen with Bu_3SnH).

Since Giese's initial report, the search for a more mild and sustainable approach to produce highly reactive carbon-centred intermediates has renewed interest in radical chemistry.⁹⁶ Carboxylic acids, in particular, are appealing radical precursors because of their abundance, affordability, diversity, and low environmental cost. Radical decarboxylation reactions have been well-established, with research conducted by Kolbe, Hunsdiecker, and Barton as early as 1848.^{89,97–100} However, their protocols are limited by a narrow substrate scope and harsh conditions such as high temperatures and ultraviolet (UV) irradiation. Moreover, the Barton decarboxylation was arguably the most widely used method, but the required esters frequently proved unstable and necessitated toxic reducing agents. Only in

the past 30 years have more benign decarboxylation methods been developed, allowing for a broader range of substrates.

More specifically, the use of visible-light photosensitisers/photocatalysts as electron-transfer 'reagents' has permitted the production of highly reactive intermediates under mild conditions, providing a plethora of valuable transformations.^{101–103} Photocatalytic decarboxylative Giese reactions usually proceed *via* a reductive quenching pathway, shown in **Scheme 44**. Visible-light photoexcitation of the photocatalyst forms an oxidising species ($^*PC_{ox}$) which initiates the decarboxylation. The carboxylic acid (**70**) is normally deprotonated to the more easily oxidised carboxylate (**71**) ($E^{ed}_{1/2} = +1.25$ to $+1.31$ V vs. SCE) before decarboxylation, so the use of a stoichiometric base is common.¹⁰⁴ Without a base, the acid is more challenging to oxidise ($E^{ed}_{1/2} = +2.51$ V vs. SCE for 2-phenylacetic acid). Oxidative SET between $^*PC_{ox}$ and the carboxylate **71** generates the reducing species (PC_{red}) and the corresponding carboxyl radical.¹⁰⁵ Subsequent decarboxylation yields the carbon-centred radical **72**, which undergoes conjugate addition with a Michael acceptor. The resulting secondary radical intermediate is reduced to the carbanion species **73** *via* SET with PC_{red} , regenerating PC and closing the cycle. The desired Giese product is then obtained after protonation of the carbanion.

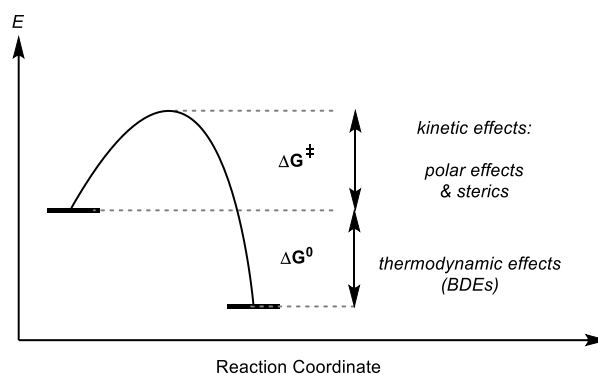


Scheme 44: General mechanism for direct decarboxylative Giese additions via photocatalysis. Mechanisms are consistent with a reductive quenching pathway.

1.3.2 Kinetics & Thermodynamics of Radical Reactions

Generally, the selectivity of radical processes is influenced by both thermodynamic and kinetic factors (**Scheme 45**): the relative stability of substrates/products, *i.e.*, reaction enthalpy (ΔG°) is what determines the thermodynamics of a reaction – also known as bond strengths, expressed using bond-dissociation energies (BDE). Conversely, kinetics of the

reaction are determined by the reaction barrier (ΔG^\ddagger) and are influenced by steric and polar effects (radical philicity), the latter of which were depicted by Roberts as the impact of charge transfer in the transition state on the reaction barrier.¹⁰⁶ While both thermodynamics and kinetics contribute to the reaction outcome, the dominant factor is dependent on the transition state structure and how strong of a bond is being created.



Scheme 45: energy profile depicting kinetic and thermodynamic factors concerned in the selectivity of radical reactions.

To determine the thermodynamic viability of a radical reaction, the BDE and the half-wave oxidation potential ($E_{1/2}$) for a SET process is typically used to provide an insight. Beyond kinetic considerations, understanding the thermodynamics is crucial for determining whether certain reactions (e.g., HAT or XAT) will transpire spontaneously, and as earlier, fundamental bimolecular processes are typically (thermodynamically) driven by the formation of stronger bonds or the generation of more stable radicals.

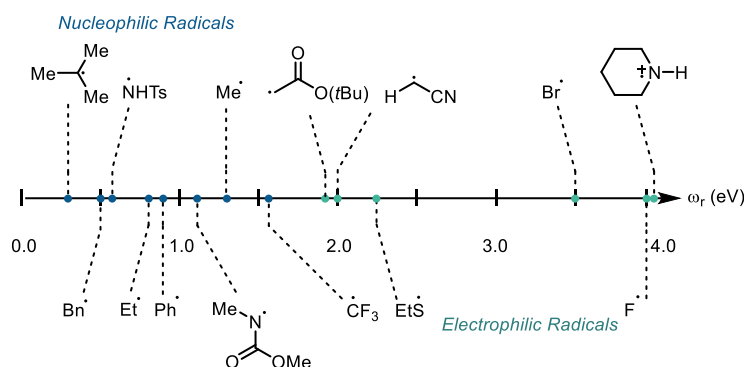
Moreover, radical philicity influences the selectivity and reactivity of radical processes. For example, an electrophilic radical will more readily react with a nucleophilic site, while a nucleophilic radical will target electrophilic sites. This concept is crucial in understanding and predicting the outcomes of radical reactions, and to evaluate the philicity of radicals, Parr and co-workers developed the global electrophilicity index, ω , which is determined based on the chemical potential (μ) and chemical hardness (η):

$$\omega = \frac{\mu^2}{2\eta}$$

which are derived from the vertical ionization energy (I) and electron affinity (A).¹⁰⁷ The local electrophilicity index, ω_r , is the product of the global electrophilicity index and the Fukui function for nucleophilic attack at the radical centre ($f^+(r)$):

$$\omega_r = \omega f^+(r)$$

De Proft and colleagues first used these parameters to calculate the electrophilicities of 35 radicals, and subsequent calculations have determined local electrophilicity indices for nitrogen-based radicals.¹⁰⁸ **Scheme 46** depicts an overview of the calculated electrophilicities of several radical species, based on numerous sources.¹⁰⁹



Scheme 46: electrophilicity scale for frequent radicals based on local electrophilicity index ω_r .

Free radical C–H halogenation processes are a straightforward example of how these factors influence the result of a reaction. This involves a HAT to the halogen atom (X), followed by the construction of a C–X bond through an S_H2 reaction with the molecular halogen (X₂). In C–H chlorination reactions, thermodynamic effects are predominant because they form strongly polarised bonds with chlorine, which have high bond dissociation energies (BDEs) exceeding 100 kcal mol⁻¹. Conversely, in C–H bromination, polar effects are more significant due to the more polarizable and weaker C–Br bond, which has a BDE of approximately 80 kcal mol⁻¹.¹¹⁰ For substrates with multiple C–H bonds exhibiting small differences in BDE, polar effects significantly influence selectivity. Polarity-matched reactions that encompass the interaction of radicals and acceptors with opposing philicity are typically kinetically favoured. Consequently, philicity is a major factor determining the regioselectivity of radical reactions.

1.2.2 Photoredox Catalysis

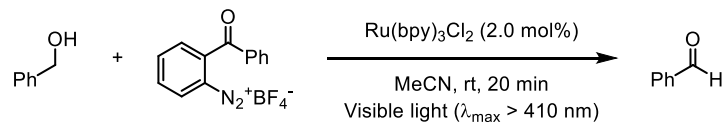
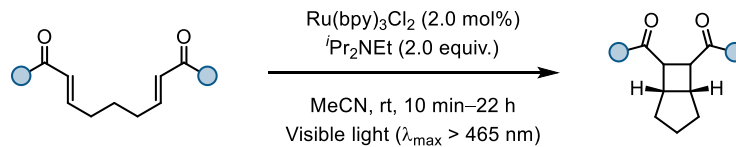
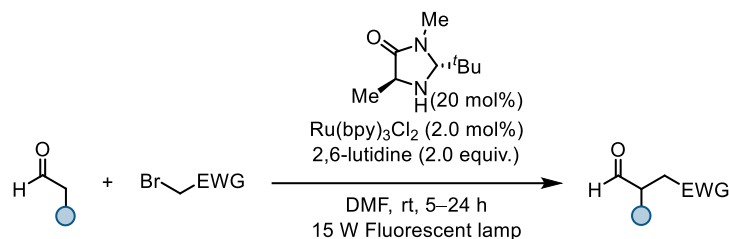
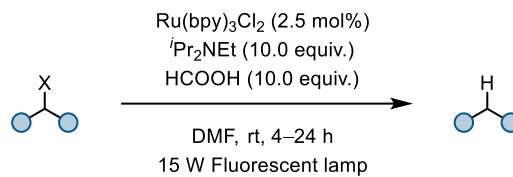
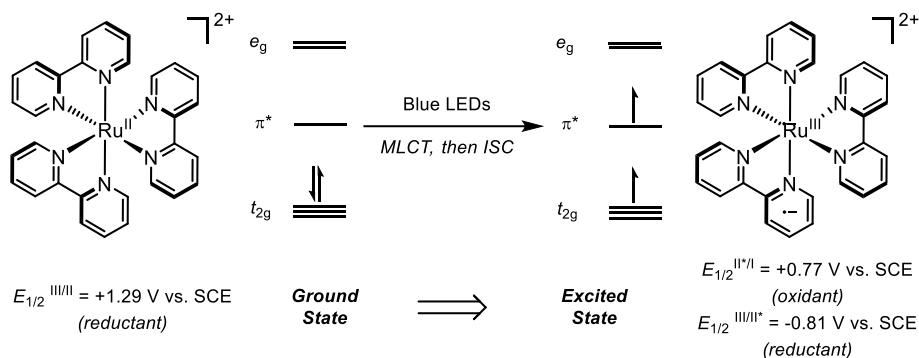
Light has played a pivotal role in human history, and consequently, harnessing this abundant energy source for chemical energy has become a paramount goal for scientists in the past century. In 1912, Ciamician initially proposed the concept of artificial photosynthesis as a potential solution for the escalating problem of the reliance on fossil fuels by developing the first photochemical organic transformation using ultra-violet (UV) light as main energy source.¹¹¹ Although efficient artificial photosynthetic systems to convert highly oxidised

products into reduced species remain elusive, numerous examples have demonstrated that photons can supply the necessary energy to either make or break chemical bonds and facilitate endothermal processes.

These constraints prompted scientists to explore a different segment of sunlight: the visible light range (365-750 nm). Unlike UV light, visible light accounts for approximately 44% of solar irradiation and encompasses energies (about 70-115 kcal mol⁻¹) suitable for breaking various chemical bonds. Harnessing the right wavelength and energy level should offer a solution to the selectivity issue. However, the difficulty lies in leveraging this portion of sunlight effectively, given that most organic molecules absorb UV light. To overcome this, the use of chromophores or sensitizers capable of absorbing in the visible spectrum is essential, as they are able to capture energy from visible light and direct it towards desired chemical transformations.

Photoredox catalysis, a groundbreaking field in organic chemistry, leverages light to initiate and drive chemical reactions. By using visible light, photoredox catalysts facilitate electron transfer processes, thereby activating typically inert organic molecules. This approach has become a versatile tool for constructing complex molecular structures, offering mild reaction conditions, high efficiency, and broad substrate compatibility. It enables the formation of C–C bonds and the modification of functional groups, revolutionising synthetic methodologies and leading to innovative strategies in chemical synthesis. Redox (or electron-transfer) catalysis involves a catalytic cycle characterised by both oxidation and reduction reactions within the same species. These processes occur through transition metals with two accessible oxidation states that differ by a single electron, such as Ir(III)/Ir(II).

Photoredox catalysts are extensively utilised due to their long-lived excited states, enabling quenching processes. For example, the commonly exploited Ru(bpy)₃Cl₂ was first described in 1984 by Deronzier and later used in the pioneering works by Yoon, MacMillan and Stephenson (**Scheme 47**).^{112–114} The complex exhibits three oxidation states, based on the Ru(III)/Ru(II) and Ru(II)/Ru(I) redox couples.

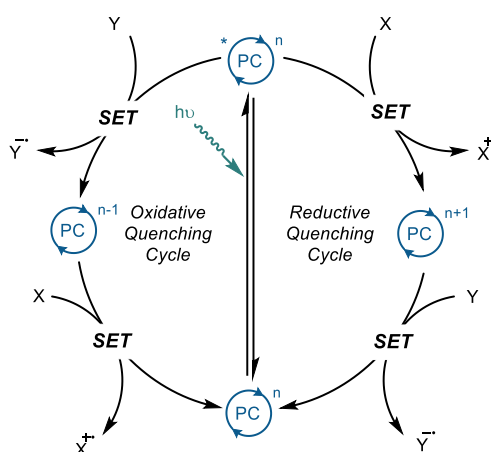
A Ru(II)-Catalysed Photo-oxidation of Carbinols – Deronzier, 1984

B Photocatalytic [2+2] Cycloaddition of Enones – Yoon, 2008

C Enantioselective Intermolecular α -Alkylation of Aldehydes – MacMillan, 2008

D Photocatalytic Reductive Dehalogenation – Stephenson, 2009

Oxidation States of Ru


Scheme 47: pioneering work carried out using Ru-based photocatalysts and properties of $\text{Ru}(\text{bpy})_3^{2+}$ in the ground state and excited state.

Since it is a d^6 complex with octahedral symmetry (O_h), the five 4d orbitals experience ligand splitting with the bpy ligands, resulting in three degenerate occupied t_{2g} orbitals and two degenerate unoccupied e_g orbitals. The unoccupied π^* orbital centred on the ligands occupies an intermediate energy level between the metal-centred t_{2g} and e_g orbitals. The

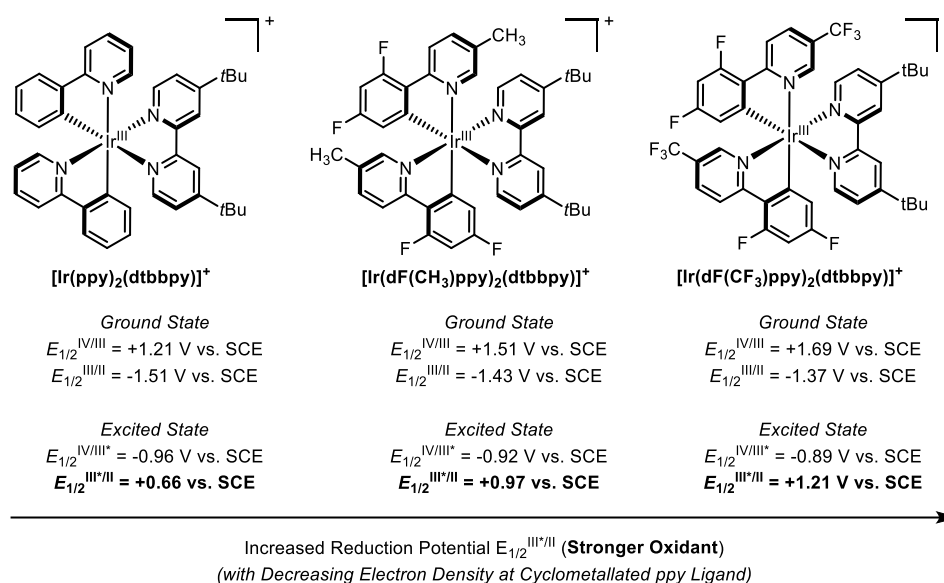
ground state complex first absorbs a quantum of blue light to undergo metal-to-ligand charge transfer (MLCT) which occurs *via* excitation of an electron from the t_{2g} orbitals to the π^* of the bpy ligands. The singlet excited state then endures intersystem crossing to a long-lived triplet state which is lower in energy, i.e., the key excited state facilitating photochemical reactions which is a greater oxidant and a more effective reductant compared to its ground state.

A general diagram in **Scheme 48** depicts the two possible distinct catalytic quenching cycles of a photocatalyst: depending on if the metal undergoes oxidation or reduction after excitation, they are known as oxidative or reductive quenching cycles. In an oxidative quenching cycle, the photoredox catalyst (PC) absorbs a photon, promoting it from its ground state to an excited state. The excited state of the catalyst (*PC) donates an electron to an electron acceptor (oxidant), generating an oxidised form of the catalyst. The oxidised catalyst (PC^{n+1}) is then reduced back to its original state by accepting an electron from a sacrificial electron donor. The reductive quenching cycle is similar to the oxidative cycle; after excitation, PC^* accepts an electron from an electron donor, generating a reduced form of the catalyst. The reduced catalyst (PC^{n-1}) is then oxidised back to its original state by transferring an electron to an electron acceptor. The decision to use oxidative or reductive quenching is influenced by the redox potentials of the species involved and the specific needs of the reaction. Besides the oxidative and reductive quenching cycles that rely on single electron transfer (SET), there exists a third productive pathway known as triplet-triplet energy transfer (TTET). In this process, energy is transferred from the triplet (T_1) excited state of the photocatalyst to another molecule, elevating that molecule from its ground state (S_0) to its T_1 .



Scheme 48: general cycle for the oxidative and reductive quenching steps in photoredox catalysis.

Iridium-based photocatalysts are gaining significant attention for their exceptional efficiency and adjustable reactivity, making them vital in advancing sustainable and efficient photochemical methodologies. Predominantly, heteroleptic complexes, where a metal ion is coordinated by more than one type of ligand, are employed. Notable examples include $[\text{Ir}(\text{dF}(\text{CF}_3)\text{ppy})_2(\text{dtbbpy})]^+$ (Ir-F) and $[\text{Ir}(\text{ppy})_2(\text{dtbbpy})]^+$, along with other commercially available complexes that have slight structural and redox potential variations (**Scheme 49**). Compared to ppy, the ligand dtbbpy reduces the excited photocatalyst's reducing power, while the incorporation of electronegative groups such as F and CF_3 creates a more electron-deficient Ir(III) centre, thus enhancing the complex's oxidising capability.



Scheme 49: heteroleptic Ir complexes (as PF_6 salts) used in photoredox catalysis.

1.3 Radical Synthesis & Functionalisation of UAAs

Radical intermediates are exceptionally well-suited for the selective synthesis/functionalisation of amino acids as they can be readily formed in the presence of sensitive functional groups, while still maintaining sufficient reactivity at room temperature. Given the variety of photocatalysts available and the promising synthetic pathways that have been investigated using radical chemistry/photoredox catalysis, a comprehensive overview of the applications of visible light photocatalysis in the synthesis and functionalisation of amino acids is presented.

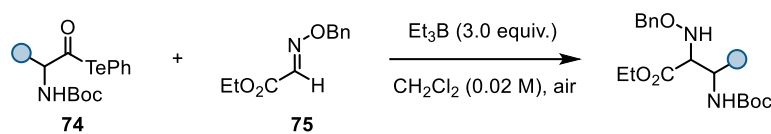
Despite the number of methodologies established for the preparation of unnatural amino acid derivatives, many of these require metal-mediated multistep manipulations or pre-functionalised substrates. Although effective, two-electron methods often require harsh

conditions or have limitations with the substituents that can be incorporated into the final product. In contrast, radical chemistry presents certain advantages to classic methods. The comparatively high energy of radicals can be used to overcome kinetic barriers associated with steric hindrance, which may be more difficult to accomplish with a two-electron approach.

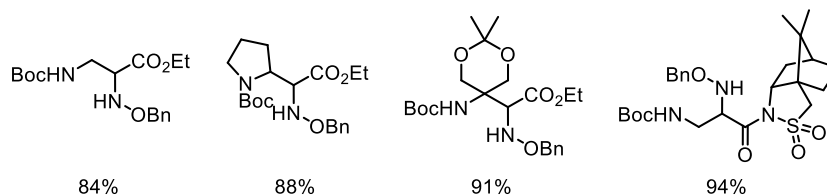
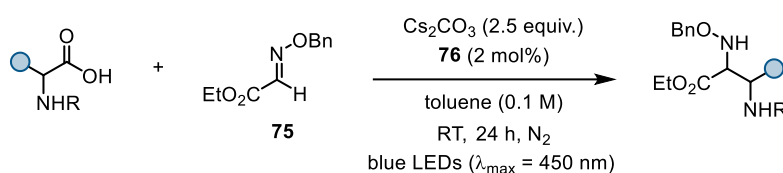
1.3.1 α -AAs

Radical-based methods for synthesising α -AAs can be broadly categorised into three main types: the addition of an open-shell species to an imine, C(sp³)-H aminations, and the utilization of carbon dioxide (CO₂) as a building block.

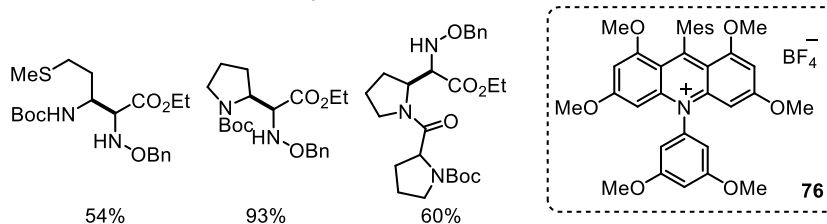
The addition of radical species to imines is a prominent method that allows for the formation of either racemic or enantioenriched α -AAs, as the nature of the *N*-substituents on the imine plays a critical role in determining the stereochemical outcome of the reaction. This approach leverages the inherent reactivity of radicals and the electrophilicity of imines, facilitating the formation of C–N bonds under mild conditions. For example, in 2015, Inoue and co-workers reported a Et₃B-mediated method for synthesising α,β -diamino acid derivatives starting from α -aminoacyl tellurides **74**, which are easily prepared from the corresponding α -amino acids and diphenyl telluride, along with ethyl glyoxylate oxime **75** (**Scheme 50A**).¹¹⁵ The crucial step involves cleavage of the C–Te bond in **74**, forming an acyl radical intermediate that undergoes decarbonylation to produce a highly stabilised α -amino radical species.¹¹⁶ This species then adds to **75**, and subsequent protonation yields the desired α,β -diamino acid. More recently, Ye reported a visible-light photoredox catalysed method for the same α,β -diamino esters from amino acids and glyoxylic oxime ethers (**Scheme 50B**).¹¹⁷ The mechanism involves the photoexcitation of an acridinium-based photocatalyst (**76**), which oxidises the deprotonated carboxylic acid to form an alkyl radical via decarboxylation. This radical adds to the glyoxylic oxime ether, forming a stabilised nitrogen radical that undergoes further electron transfer and protonation to yield the α,β -diamino ester.

A Synthesis of α,β -diamino acid derivatives from acyl tellurides – Inoue 2015


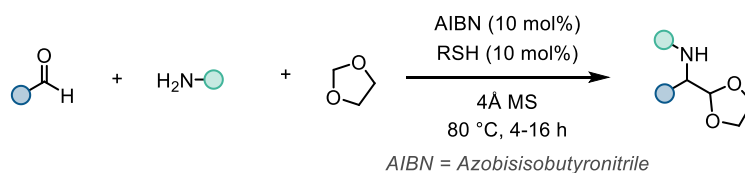
Selected examples


B Synthesis of α,β -diamino acid derivatives via decarboxylation – Ye 2019


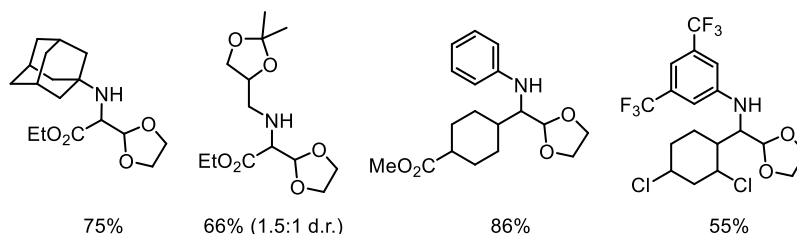
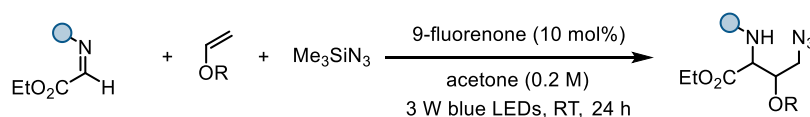
Selected examples


Scheme 50: syntheses of α,β -diamino esters, A) from acyl tellurides; B) from carboxylic acids.

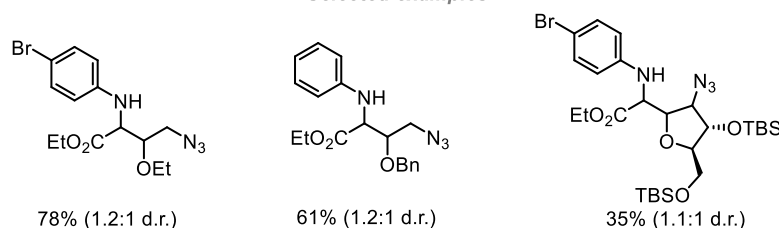
Due to the ability to generate imines *in situ* from a combination of amines and carbonyl motifs, multicomponent reactions have also been devised for constructing α -amino acids. In 2018, Lu, Gong, and co-workers introduced a three-component, one-pot reaction for synthesising masked α -amino aldehydes (**Scheme 51A**).¹¹⁸ This reaction proceeds *via* an AIBN-initiated radical chain mechanism, resulting in the desired α -amino aldehydes after the addition of an α -oxo radical generated from 1,3-dioxolane to the *in situ* generated imine. Later, the same group developed a light-mediated, redox-neutral strategy to synthesise γ -azide- α -amino acids (**Scheme 51B**).¹¹⁹ This three-component, one-pot reaction involves the addition of electrophilic azidyl radical **77** – formed from TMSN_3 – to an enol ether, forming nucleophilic radical intermediate **78** that subsequently reacts with the imine to yield the targeted product.

A AIBN-Mediated Synthesis of Masked Amino Aldehydes – Lu & Gong 2018


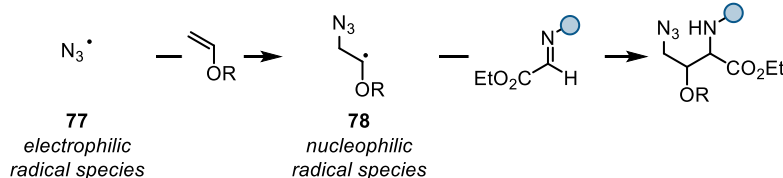
Selected examples


B Light-Mediated Polarity-Reversed Addition of Enol Ethers to Imines – Lu 2019


Selected examples

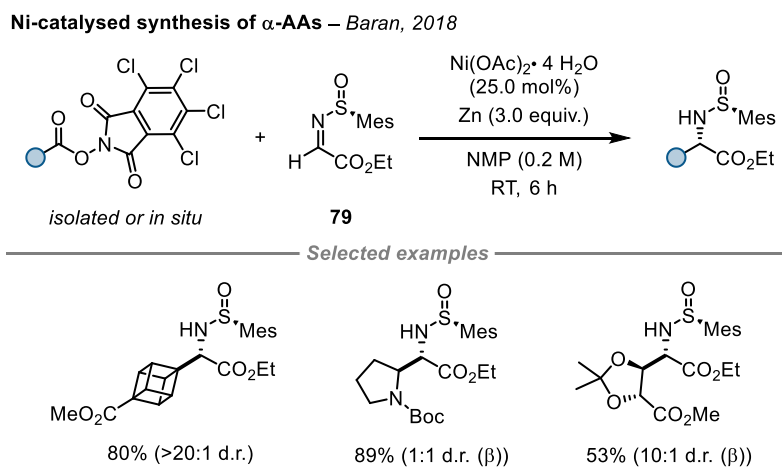


Key Mechanistic Step


Scheme 51: three-component syntheses of α -AAs.

For achieving high levels of diastereoselectivity during the key radical-addition step, chiral auxiliaries, such as the mesitylsulfinyl group, are commonly employed on the *N*-substituent of the imine. In 2018, this strategy was utilised by Baran and co-workers in a Ni-catalysed approach for diastereoselectively synthesising α -amino acids *via* NHP-derived redox-active esters (RAEs) as radical precursors (**Scheme 52**).¹²⁰ These RAEs readily undergo SET with Ni(I) species, yielding alkyl radicals that add to the imine with chiral auxiliary (**79**), resulting in the desired α -amino acids. This mild and scalable method demonstrates extensive versatility – providing 85 examples of enantiomerically pure α -amino

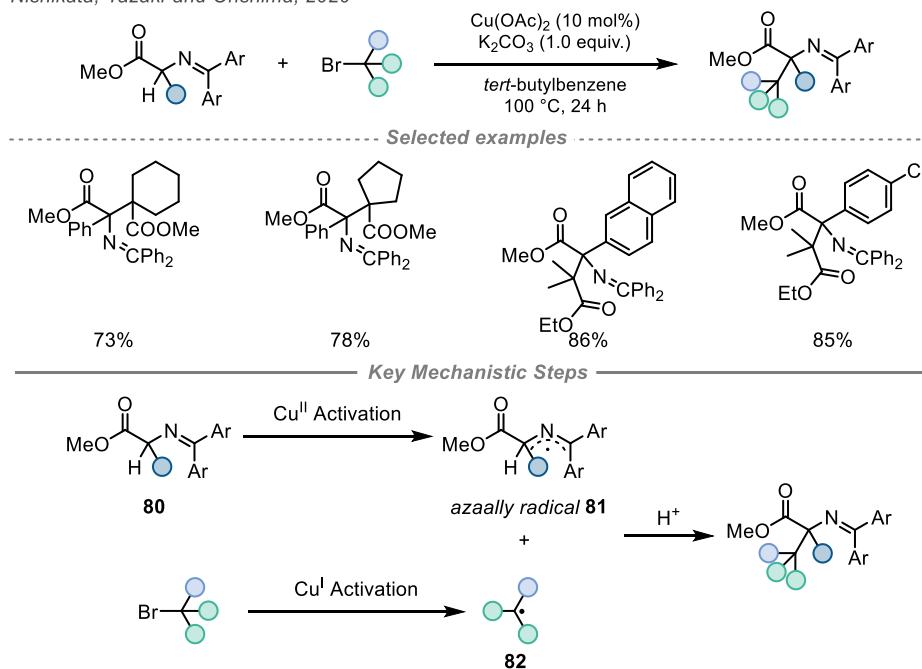
acids – and displaying broad functional group tolerance, including the derivatisation of natural products and pharmaceuticals.



Scheme 52: nickel-catalysed method to obtain α -AAs NHP-derived redox-active esters (RAEs) as radical precursors.

In 2020, Nishikata, Yazaki and Ohshima developed an efficient cross-coupling method for the synthesis of unnatural α -amino acids *via* a novel catalytic activation strategy using amino acid Schiff bases which serve as crucial intermediates (**Scheme 53**).¹²¹ This redox active copper-catalysed α -alkylation process was applied to obtain enantiomerically enriched α -tetrasubstituted α -amino acids in a diastereoselective manner by using menthol derivatives as a chiral auxiliary. The authors propose that Cu(II) is able to assist in the formation of key aza-allyl radical species **81** *via* a SET with α -monosubstituted amino acid Schiff base **80**. This radical can then couple with tertiary alkyl radical **82**, providing the highly substituted α -AA derivatives.

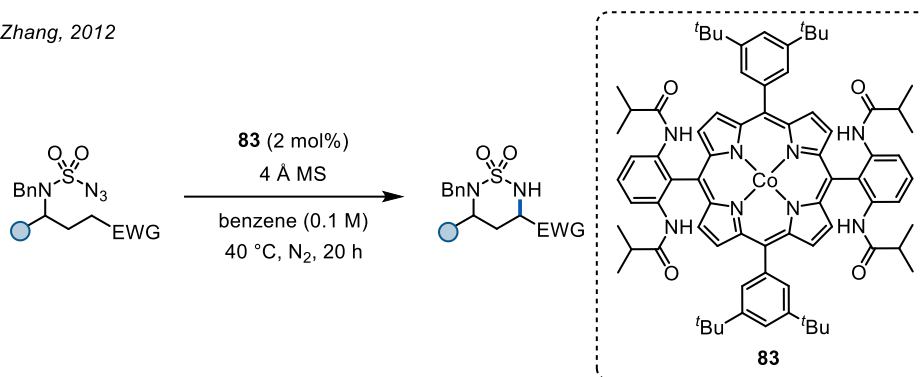
Nishikata, Yazaki and Ohshima, 2020



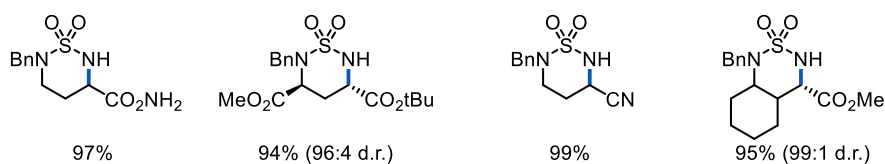
Scheme 53: Cu-catalysed diastereoselective synthesis of tetrasubstituted α -amino acids.

$\text{C}(\text{sp}^3)\text{-H}$ aminations represent another significant class of radical reactions used in α -AA synthesis. These transformations involve the direct functionalisation of $\text{C}(\text{sp}^3)\text{-H}$ bonds adjacent to nitrogen, enabling the formation of α -AAs without the need for pre-functionalised substrates. An early example comes from Zhang and co-workers who disclosed a method employing cobalt catalysis for the synthesis of α -amino acids *via* intramolecular radical $\text{C}(\text{sp}^3)\text{-H}$ aminations (**Scheme 54**).¹²² Here, a Co(II)-porphyrin complex (**83**) was utilised to generate an *N*-centred radical, which, through a 1,6-HAT process, forms a *C*-centred radical. Subsequent intramolecular α -amination leads to the formation of the desired cyclic AA derivative. Selectivity towards the less hydridic C-H bond is achieved by the formation of a nucleophilic Co(III)-nitrene radical intermediate, as well as the bulky sulfamide favouring a six-membered transition state. The use of enantiopure starting materials enables high levels of diastereoselectivity in the reaction.

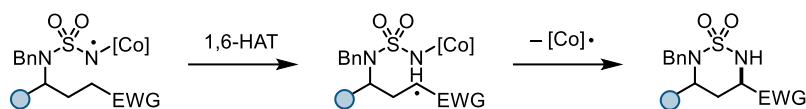
Zhang, 2012



Selected examples



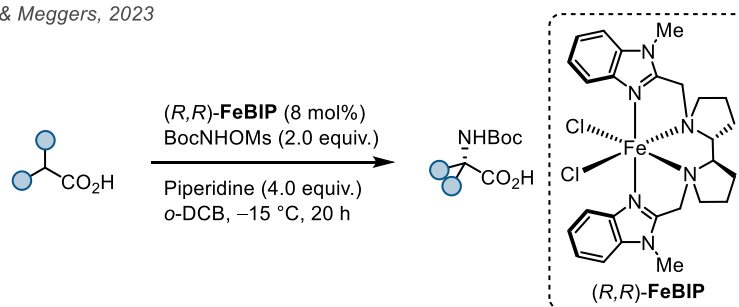
Key Mechanistic Step



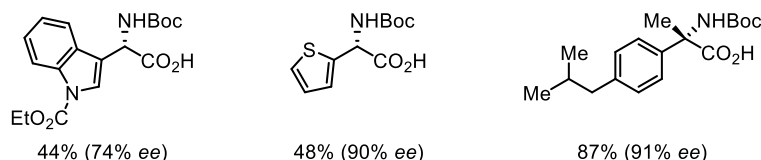
Scheme 54: synthesis of α -AAs via Co-catalysed C(sp³)-H amination.

More recently, Chen, Meggers, and co-workers developed an Ir-catalysed, single-step asymmetric intermolecular C(sp³)-H amination (**Scheme 55**).¹²³ The authors leverage directed nitrene-mediated C-H insertion, facilitated by a metal-coordinating functional group, to achieve stereocontrol in the α -amination process. The mechanism proposed initially involves a base-induced reaction of the Fe catalyst with amination reagent **84**, forming [Fe]-nitrene intermediate **85**. This intermediate then coordinates with the deprotonated carboxylic acid substrate to promote a 1,5-HAT process, leading to the formation of diradical **86**, which undergoes bond rotation to a preferred conformation. The subsequent radical-radical coupling step that forms the new C-N bond is proposed to determine the stereochemistry of the product.

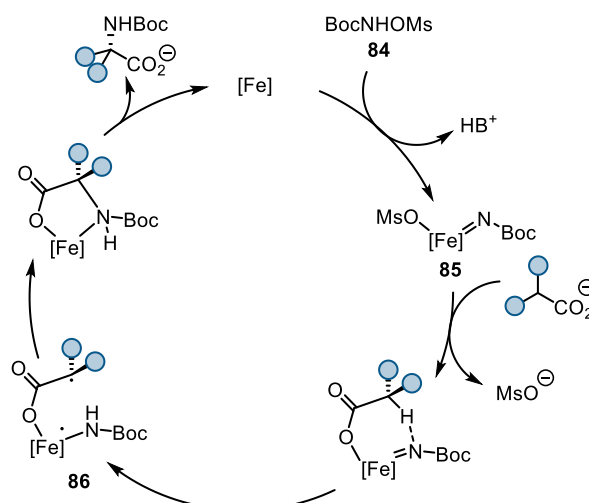
Chen & Meggers, 2023



Selected examples

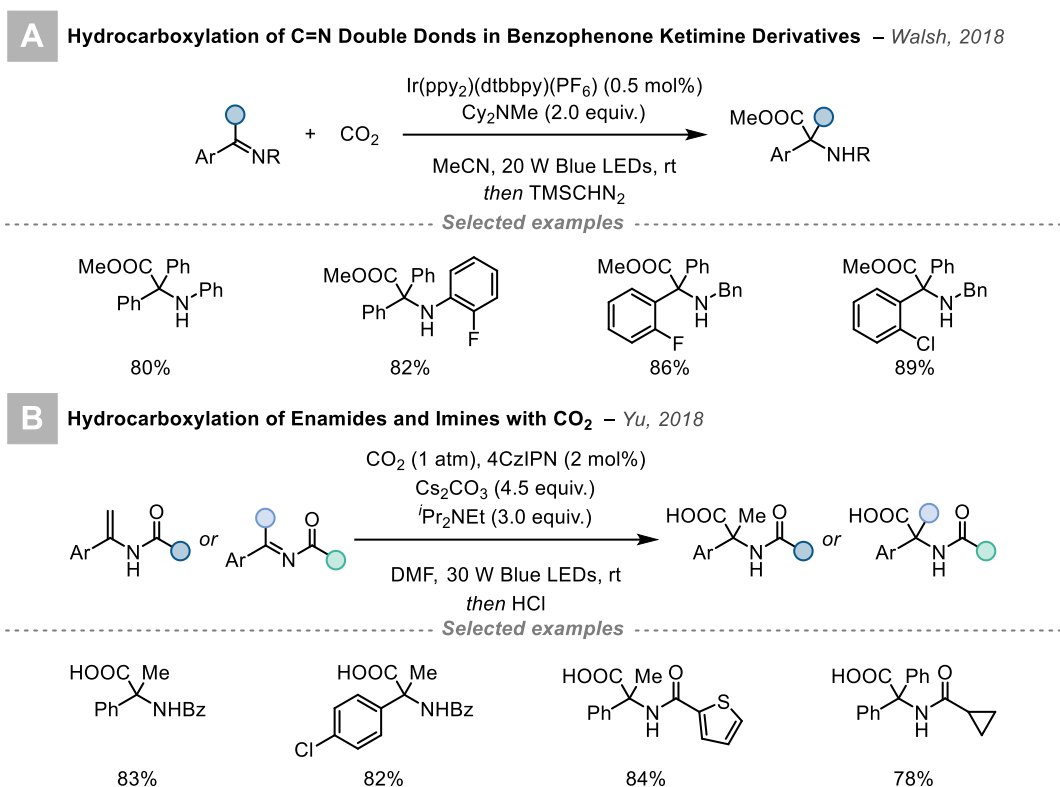


Mechanism


Scheme 55: Ir-catalysed asymmetric, intermolecular C(sp³)-H amination.

Another method to access α -AAs involves the use of carbon dioxide (CO₂) as a building block to not only incorporate a sustainable carbon source but also enable the construction of α -AAs through carboxylation reactions. Radical intermediates involved typically facilitate the activation and incorporation of CO₂. Independent reports by Prikhod'ko, Walter, Py, Radosevich, and Mita and Sata relied on forming α -amino radicals – typically derived from imine substrates – with (super)stoichiometric reductants, such as Sml₂, Mg or Mn, which would subsequently couple with CO₂. Similarly, in 2018 the groups of Walsh and Lu published visible light-promoted CO₂ incorporation methodologies for the construction of α -AAs.^{124,125} These radicals are further reduced to the corresponding carbanion, which is then trapped by the CO₂. Walsh's process utilises benzophenone ketimine derivatives and an Ir-based photocatalyst to achieve CO₂ fixation through hydrocarboxylation of C=N double bonds, yielding α,α -disubstituted α -AA derivatives in good to excellent yields under mild

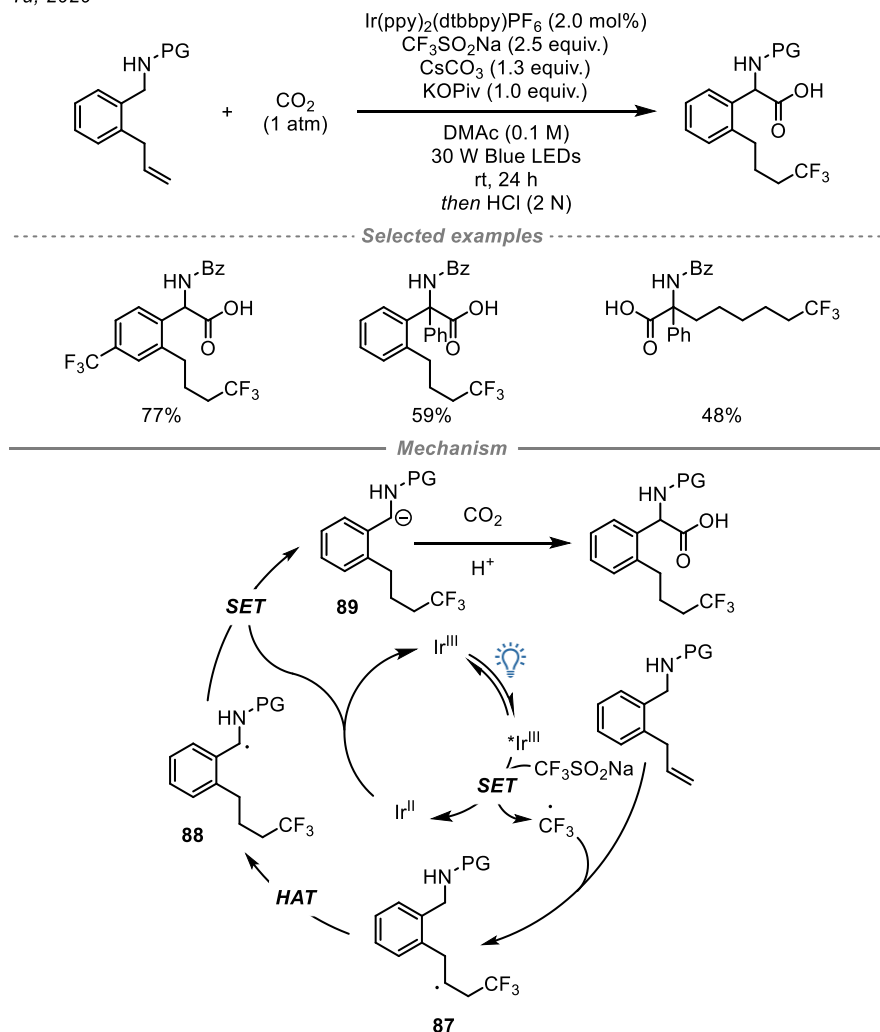
conditions (**Scheme 56A**). In the paper of Yu, a transition-metal-free, catalytic method for the hydrocarboxylation of enamides and imines with CO₂ was developed, yielding valuable α,α -disubstituted α -amino acids (**Scheme 56B**). Both strategies rely on the generation of α -amino radicals by single-electron reduction of imine precursors.



Scheme 56: A) Ir-catalysed hydrocarboxylation benzophenone ketimine derivatives; B) hydrocarboxylation of enamides and imines with CO₂ to form α,α -disubstituted α -amino acids.

More recently, Yu also proposed an innovative method for the remote difunctionalisation carboxylation of alkenes with CO₂ using visible-light photoredox catalysis (**Scheme 57**).¹²⁶ This process comprises of a 1,5-HAT to access the key α -amino radical followed by reduction and remote C–H functionalisation (CO₂ trapping). The following mechanism is proposed: first, the excited Ir(III) photocatalyst is reductively quenched by CF₃SO₂Na, yielding a CF₃ radical and an Ir(II) species. The CF₃ radical then adds to the C=C bond, forming alkyl radical **87**. A rate-limiting 1,5-HAT process occurs regioselectively to form the more stable benzylic radical **88**. Reduction of **88** by Ir(II) generates the α -amino benzylic anionic species **89** and re-forms the ground-state photocatalyst. Nucleophilic attack by **89** on CO₂, followed by protonation, yields the desired AAs. A similar α -C–H functionalisation protocol reported in the same year by Jamison and co-workers implemented a photoredox catalytic α -carboxylation of amines with CO₂ in continuous flow.¹²⁷

Yu, 2020

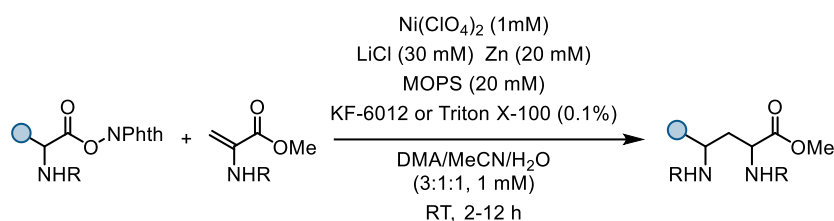
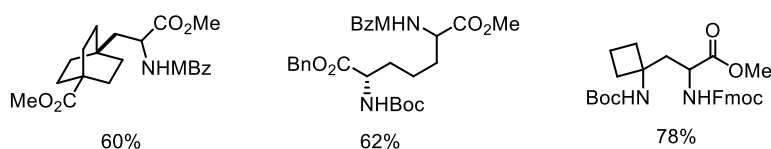
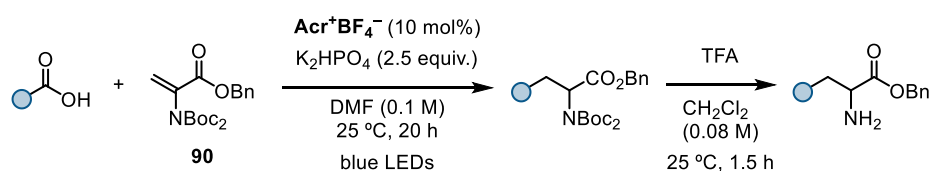
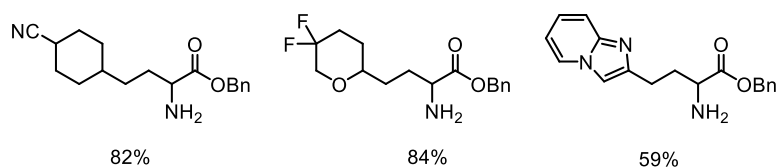


Scheme 57: difunctionalisation carboxylation of alkenes with CO_2 using visible-light photoredox catalysis.

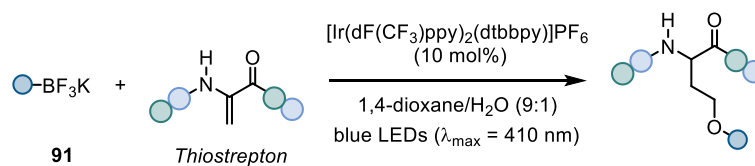
1.3.1.1 Dehydroalanine

Dehydroalanine (Dha) derivatives are highly versatile synthons, typically acting as Michael acceptors. Radical pathways for Dha modifications can be broadly classified based on whether the reaction yields racemic or enantioenriched α -AAs. Various methodologies for Giese-type reactions with Dha using radical precursors (RAEs, carboxylic acids, imines, ketals, trifluoroborates, alkyl halides, thioesters, etc.) have been reported.^{128–134}

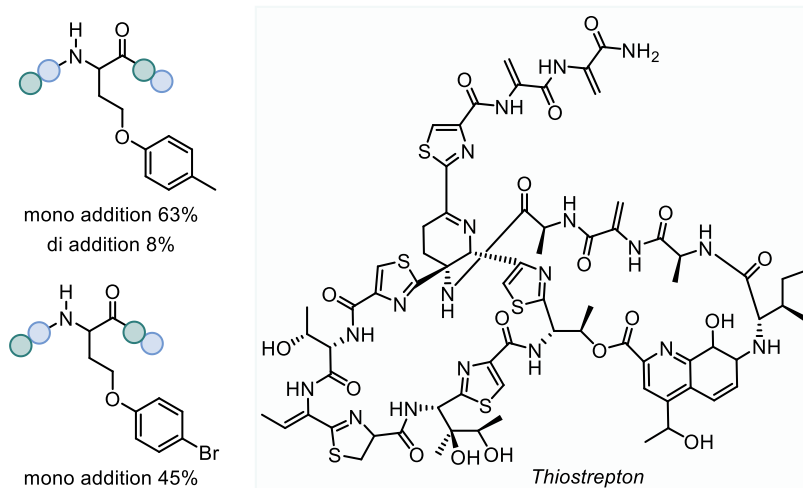
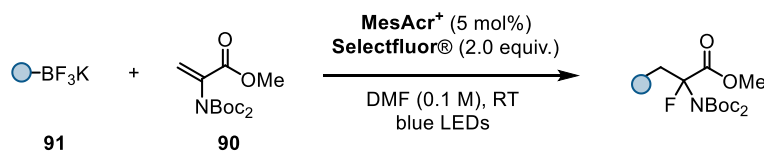
In 2018, Baran adapted his Ni-catalysed Giese reaction to use NHP-derived RAEs to acquire DNA-encoded libraries, requiring highly diluted conditions due to DNA's poor solubility in water (**Scheme 58A**).¹³⁵ More recently, Shah introduced a one-pot, light-mediated, metal-free decarboxylative method for synthesising unprotected UAAs using carboxylic acids (1° , 2° , or 3°) and *N*-Boc₂-Dha **90** derivatives (**Scheme 58B**).¹²⁹

A Synthesis of UAA under DNA-Compatible Reaction Conditions – Baran & Blackmond, 2018

Selected examples

B Light-Mediated, Metal-Free Decarboxylative Synthesis of UAAs – Shah 2020

Selected examples

Scheme 58: modifications of Dha *via* decarboxylative strategies.

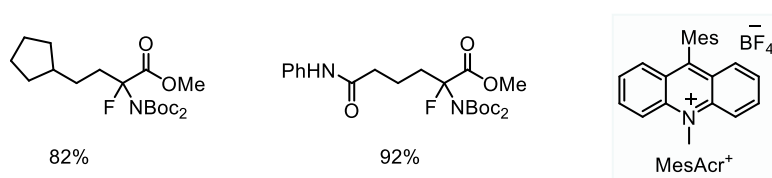
Trifluoroborate salts **91** are versatile radical precursors in photoredox chemistry and are often utilised for Dha modifications. For example, Roelfes reported a light-mediated alkylation of Dha residues in antimicrobial peptides using an Ir-photocatalyst and trifluoroborate derivatives (**Scheme 59A**).¹³² Additionally, Molander developed a photoredox-mediated three-component (alkyltrifluoroborates **91**, and Selectfluor®) reaction for α -fluorinated UAAs synthesis (**Scheme 59B**).¹³⁶ Crucial to the reaction is the importance of the *N*-protecting group's electron-withdrawing character, which facilitates nucleophilic attack of the alkyl radical on **90** over a competing fluorination reaction with Selectfluor®.

A Light-mediated alkylation of Dha residues in peptides – Roelfes, 2018


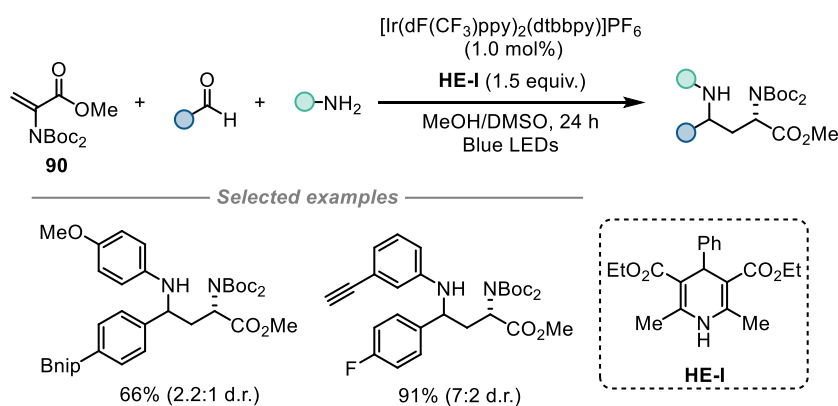
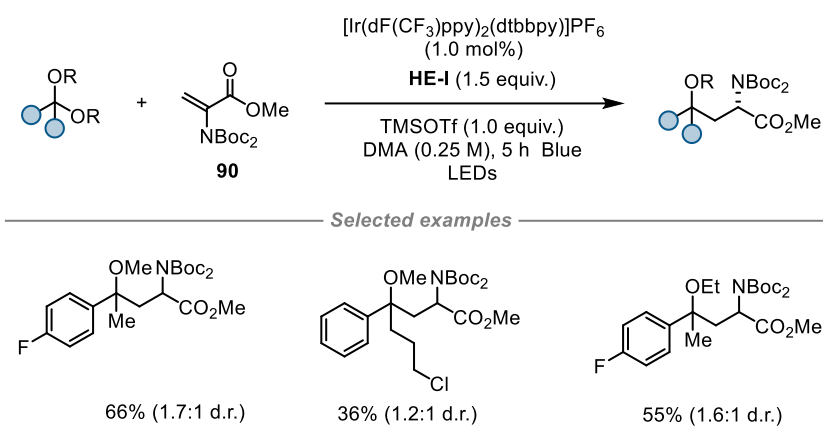
Selected examples


B Synthesis of α -fluorinated UAAs – Molander, 2019


Selected examples

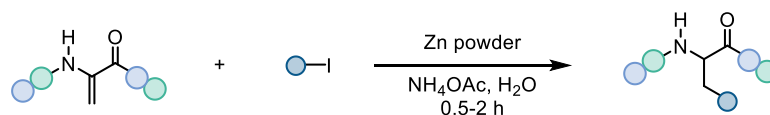

Scheme 59: derivatisations of Dha using organoborates.

Dixon and co-workers have contributed greatly to the modification of Dha. Recently, the group introduced light-mediated method for modifying Dha derivatives in a three-component umpolung method to construct 1,3-diamines, where *in situ* generated imines are reduced by an Ir-based PC, forming α -amino radicals which add to **90** (**Scheme 60A**).¹³⁰ Later, they developed a method exploiting Lewis acids for the *in situ* formation of oxocarbenium species from ketals, which are then reduced by a Ir-based PC to provide α -alkoxy radicals (**Scheme 60B**).¹³¹

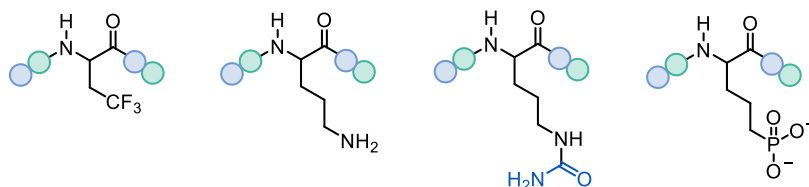
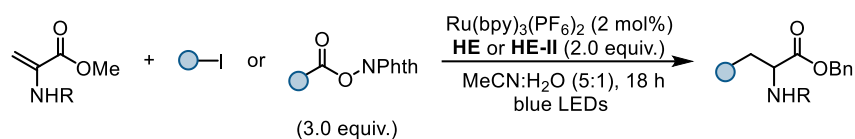
A Photocatalytic Three-Component Umpolung Synthesis of 1,3-Diamines – Dixon, 2018

B Light-Mediated Synthesis of α -Tertiary Ethers - Dixon, 2019


Scheme 60: Dha modifications by reduction of *in situ* generated oxocarbeniums.

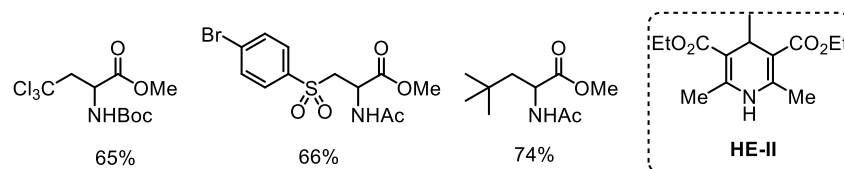
Over the years, several methodologies for Dha modification with alkyl halides have been reported. This includes a report by Davis on the side-chain modification of proteins via selective addition of alkyl radicals (created *via* the reaction of alkyl bromides/iodides and NaBH_4) to Dha residues (**Scheme 61A**).¹³⁷ Later, García-Mancheño and co-workers developed a light-mediated strategy for the Ru-catalysed functionalisation of Dha and peptides using fluorinated alkyl halides, arylsulfonyl chlorides or NHP-derived RAEs (**Scheme 61B**).¹³³

A Bio-Orthogonal Side-Chain Modification of Proteins – Davis, 2016


Selected examples

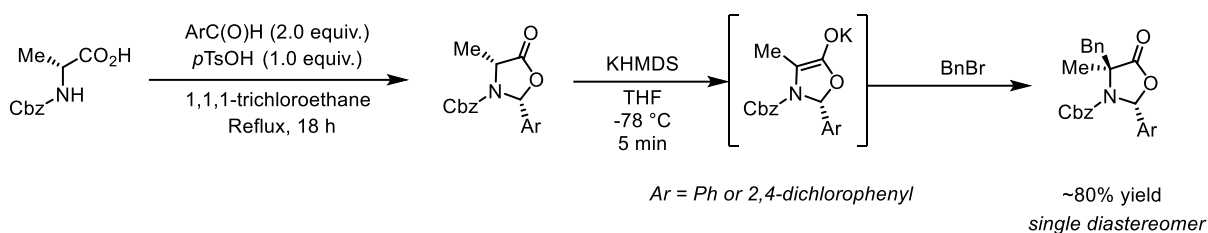
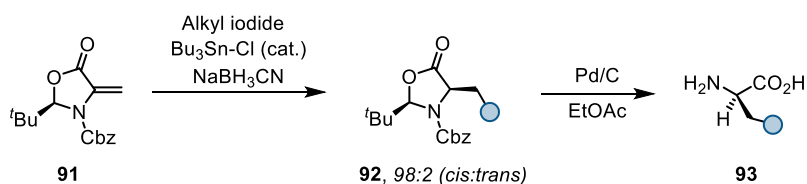

B Light-Mediated Functionalisation of Dha Derivatives – García Mancheño, 2019


Selected examples


Scheme 61: Modifications of Dha using alkyl halides.

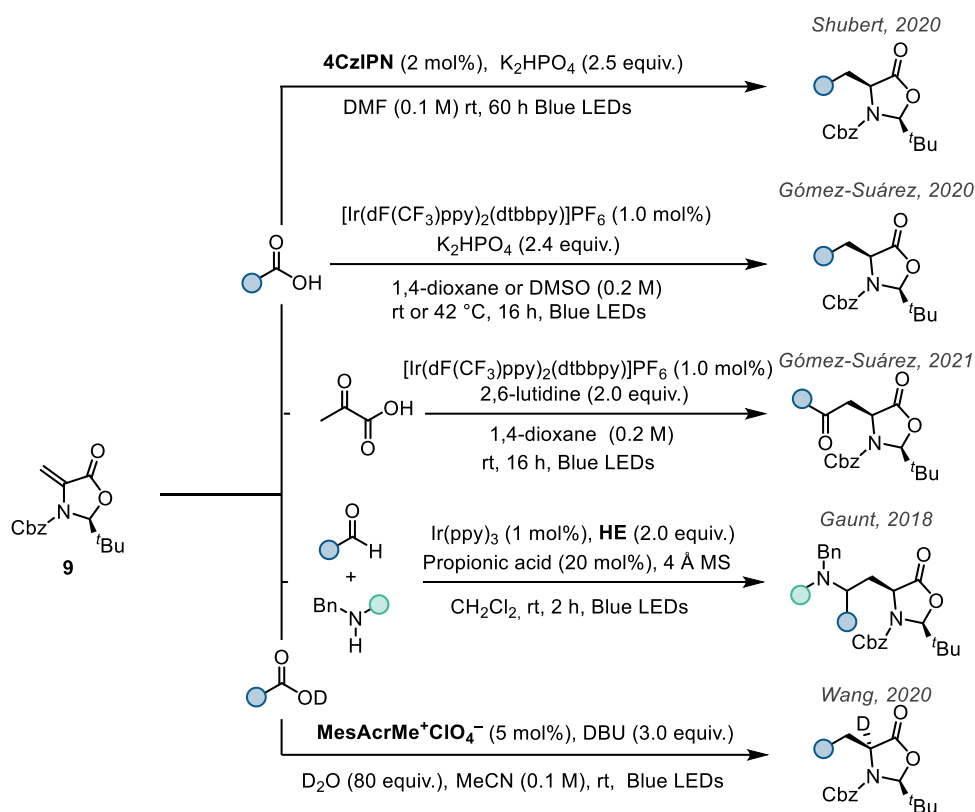
While Dha is a promising candidate for radical side-chain modifications due to its ability to accept nucleophiles and nucleophilic radicals, radical additions to the Michael system of Dha typically result in racemic product mixtures. This challenge can be addressed using asymmetric catalysis, i.e., developing chiral catalysts or ligands which can be time- and labour-intensive, or by using a chiral auxiliary, i.e., converting dehydroalanine into a cyclic, chiral derivative, providing the desired stereochemical control without costly chiral catalyst development. In 1984,

Karady and colleagues reported alkylation of amino acid-derived oxazolidinones with enantio-retention (**Scheme 62A**).¹³⁸ Later, Beckwith and colleagues extended this concept using a dehydroalanine-derived oxazolidinone system (**91**) for diastereoselective radical additions (**Scheme 62B**).¹³⁹ This Dha derivative undergoes radical addition with alkyl iodides in the presence of catalytic ⁿBu₃SnH and NaBH₃CN, forming α -amino alkylated species **92** in a diastereoselective manner. Subsequent hydrogenation of **92** with Pd/C provided (*R*)-configured UAA **93** as a single enantiomer.

A Diastereoselectivity of Radical Addition to Oxazolidinones – Karady, 1984

B Diastereoselective Radical Addition to a Dha Derivative – Beckwith, 1995


Scheme 62: seminal work by Karady and Beckwith on Dha-derived oxazolidinone systems for enantioselective synthesis of AAs.

Since then, **91** is known as the Karady-Beckwith (KB) alkene and has been widely used for highly diastereoselective UAA synthesis. Recent photoredox methods using various radical precursors, such as alcohols, heteroaryl halides, amines, and acids, have expanded its application. In 2017, Jui introduced a practical and scalable light-mediated synthesis of heteroaryl α -AAs (**Scheme 63A**).¹⁴⁰ The central step in this photoredox-mediated protocol is the single electron reduction of heteroaryl halides by a highly reducing Ir(II) species, formed from the excited state quenching of an Ir(III)-based PC with HE. The methodology showcases broad functional group tolerance and scope, making it suitable for large-scale synthesis. The following year, the same group reported the synthesis of UAAs and peptides via a light-mediated aminoalkylation method where the crucial step in this transformation is the generation of an amine radical cation, produced by the oxidation of tertiary amines by an excited Ir-based photocatalyst (**Scheme 63B**).¹⁴¹

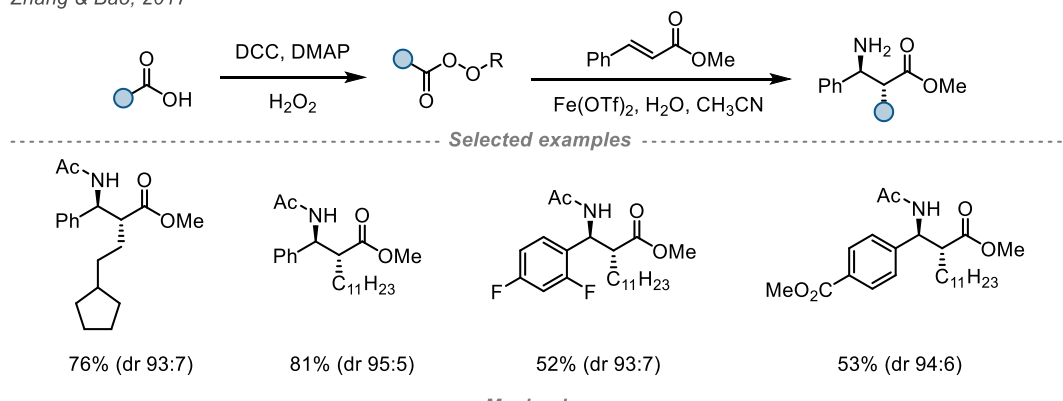


Scheme 64: decarboxylative strategies for the functionalisation of **91**.

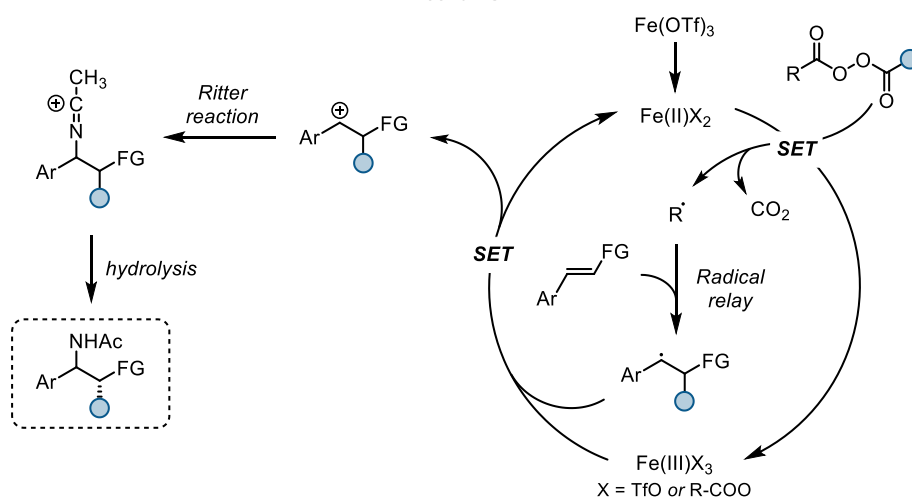
1.3.2 β -AAs

In 2017, Zhang and Bao reported the rapid construction of α -alkyl- β -aryl- β -amino acids ($\beta^{2,3}$ -AAs) (**Scheme 65**).¹⁴⁶ The method proceeds *via* intermolecular alkyl amination of vinylarenes, enabled by an iron catalyst and alkyl diacyl peroxides (synthesized from aliphatic carboxylic acids) that work as both the alkylating reagents as well as internal oxidising agents. The authors propose a possible radical–polar crossover mechanism where the Fe(II) catalyst transfers an electron to the diacyl peroxide, generating the Fe(III) complex and an alkyl acyloxy radical. Decarboxylation forms an alkyl radical which reacts with the vinylarene to produce a benzylic radical containing a stereogenic centre. A carbocation forms after oxidation by Fe(III) which undergoes a Ritter reaction (addition to the nitrile nitrogen to give a nitrilium ion intermediate) and the desired product after hydrolysis.

Zhang & Bao, 2017



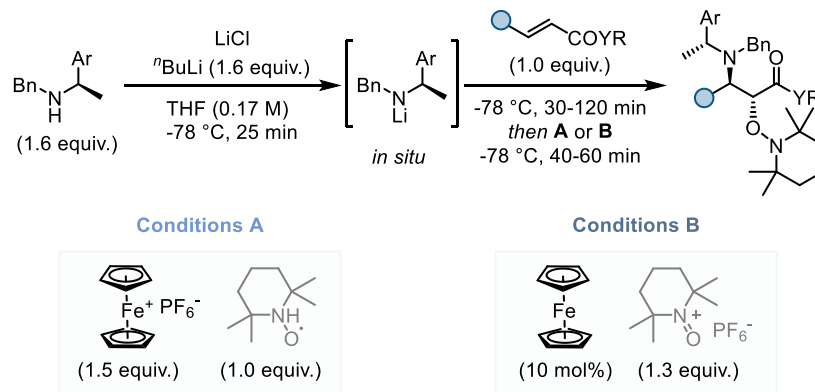
----- *Mechanism* -----



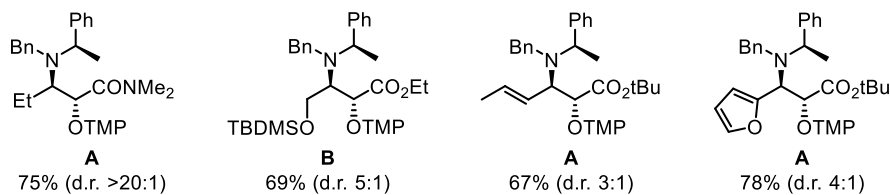
Scheme 65: iron-catalysed carboamination of olefins.

In 2018, the group of Jahn described a method for the asymmetric synthesis of *anti*- β -amino- α -(aminoxy) esters and amides in a diastereoselective manner (**Scheme 66**).¹⁴⁷ The process involves a polar, asymmetric *aza*-Michael addition of lithium amides onto α,β -unsaturated carboxylic acid derivatives, which is followed by a diastereoselective radical recombination with the persistent free radical TEMPO, *i.e.*, the oxygen source. With TMP now acting as the oxygen protecting group, deprotection can only be carried out using zinc and acetic acid. Additionally, the methodology tolerated a good range of functional groups (TBDMS, amides, furan, etc.), despite the relatively harsh conditions.

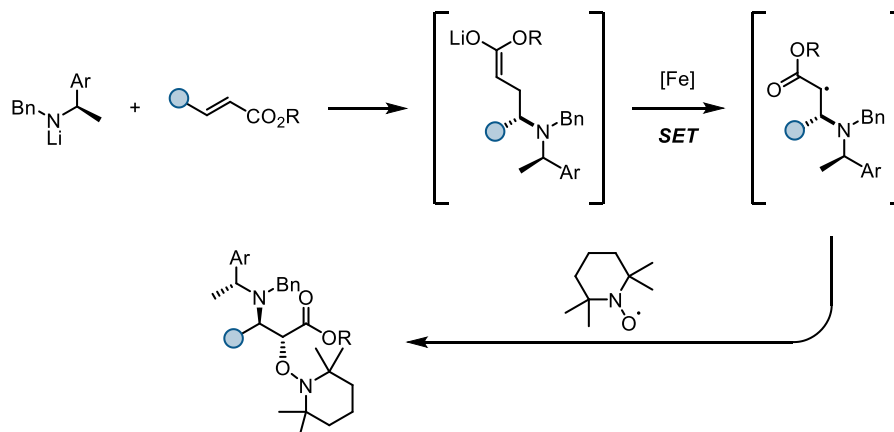
Jahn, 2018



----- Selected examples -----



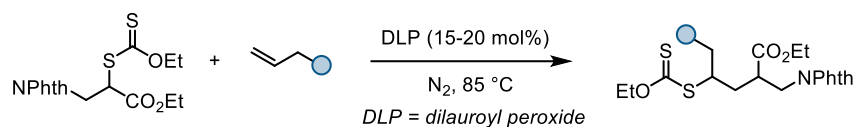
----- Mechanism -----



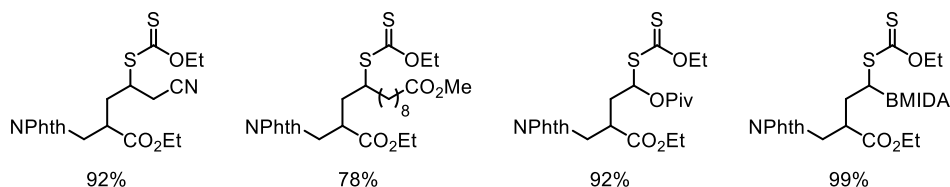
Scheme 66: Jahn's asymmetric synthesis of β -amino- α -(aminoxyl) esters and amides.

Two years later in 2020, Zard and co-workers used xanthates as radical precursors for the construction of β^2 -AAs (**Scheme 67**).¹⁴⁸ The reaction proceeds *via* radical addition of β -phthalimido- α -xanthyl propionic acid derivatives to vinylic olefins or heteroaromatic molecules, promoted by dilauroyl peroxide (DLP). When using the free acid however, spontaneous decarboxylation of the intermediate can occur which leads to the formation of β -heteroarylethylamines instead.

Zard, 2020

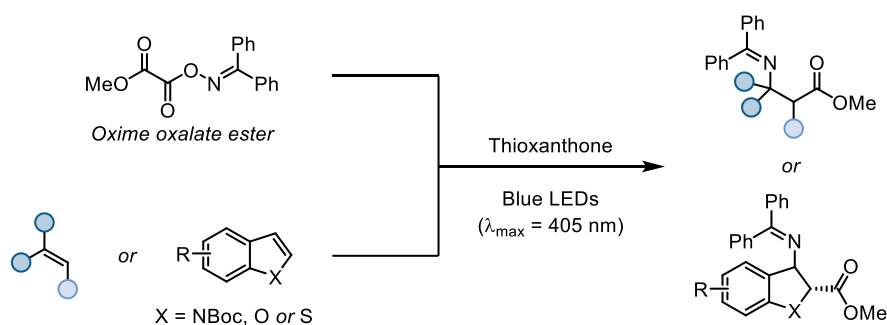


Selected examples



Scheme 67: radical addition of β -phthalimido- α -xanthyl propionic acids to vinylic olefins.

Recently in 2022, Glorius reported a photochemical synthesis of β -AA derivatives from alkenes and (hetero)arenes (**Scheme 68**).¹⁴⁹ The reaction proceeds via an energy-transfer enabled intermolecular aminocarboxylation to install both the amine and ester groups, derived from the *N,O*-cleavage of an oxime oxalate ester. The mild, metal-free conditions allowed for a broad scope and exceptional functional group tolerance.



Scheme 68: metal-free photosensitized aminocarboxylation for the synthesis of β -AA derivatives.

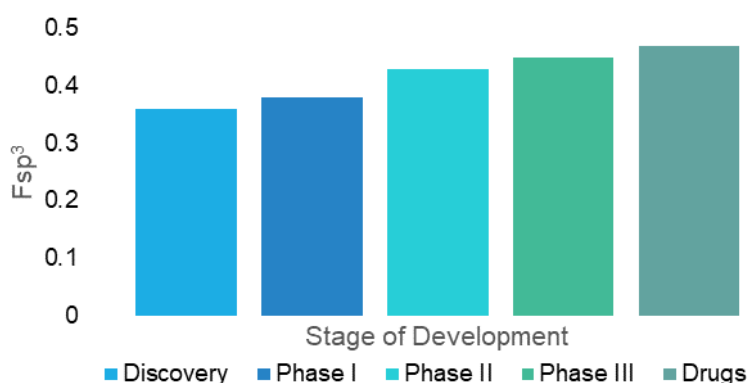
1.4 Spirocycles in Medicinal Chemistry

Spirocycles have become increasingly prevalent in medicinal chemistry since the late 1990s. This trend occurred in parallel with the introduction of a new paradigm in medicinal chemistry known as “*Escape from Flatland*”, derived from the 1884 novel by Edwin A. Abbott, *Flatland: a romance of many dimensions*.¹⁵⁰ In the novel, the characters inhabit a two-dimensional world (i.e., Flatland), and are visited by a three-dimensional character (a sphere), who convinces one inhabitant of the existence of a third dimension. In a similar manner, in 2009 Lovering, Bikker, and Humblet influenced the medicinal chemistry community of the need to escape the chemical space they were exploring, which was dominated by flat, two-dimensional structures (i.e., aromatic moieties) by showing that

increasing the fraction of C(sp³)-hybridised carbon atoms, F_{sp³}, a molecular descriptor calculated as:

$$F_{sp^3} = \frac{\# \text{ } sp^3 \text{ hybridised carbon atoms}}{\text{total carbon count}}$$

was associated with improved clinical success rates in all stages of drug development, from discovery to phase III (**Scheme 69**).¹⁵¹ The average F_{sp³} was 0.36 for “discovery compounds” and increased to 0.47 for drugs, showing a 31% increase in the saturated fraction.



Scheme 69: Mean F_{sp³} for compounds in different development stages.

Data from Lovering *et al.* (2009).¹⁵¹

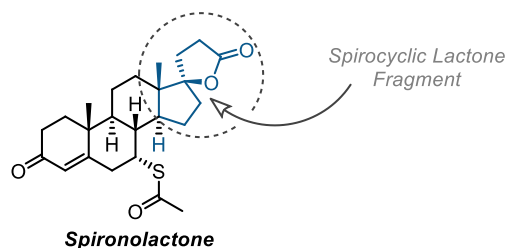
The findings were published in an article called *Escape From Flatland*, which has since become eponymous with the medicinal chemistry strategy of increasing saturation. Additional findings from the paper were that: a) the number of chiral centres increases throughout the discovery process; b) based on 1202 compounds derived from a solubility dataset reported by Hou *et al*, an increase in F_{sp³} is associated with increased solubility – a desirable property for drug bioavailability; and c) a lower melting point, based on 4432 compounds from a melting point data set from Karthikeyan *et al.*, which is also positively associated with oral bioavailability.^{152,153}

The proposed rationale behind the improved success rates observed for clinical candidates with a higher F_{sp³} was that increasing saturation offers the possibility to rationally adjust molecular shape, which in turn allows for better binding between the drug and its target, leading to more selective and potent drugs. Moving from two to three dimensions is also associated with an increase in molecular complexity, as there are naturally more opportunities for functionalisation in the latter sp³-hybridised carbon scaffolds

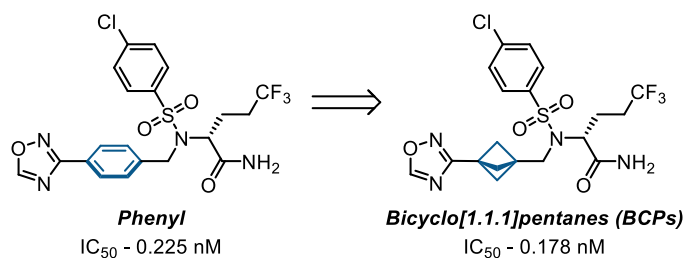
can simply be more densely functionalised. A larger chemical space is then accessible for exploration. The popularity of spirocycles in medicinal chemistry is directly related to these observations and the concept of isosterism. Isosteres are atoms or functional groups which can be replaced in a bioactive molecule without (significant) negative effects on its bioactivity.¹⁵⁴ IP considerations relating to the patentability of clinical candidates which have gone an isosteric replacement are another driver for the further development and use of bioisosteres.¹⁵⁵

Although somewhat of a modern trend, spironolactone, which contains a spirocyclic γ -lactone and is the first spirocyclic drug, was discovered as early as 1957, although the spirocyclic lactone fragment was introduced to address other concerns (**Scheme 70A**).¹⁵⁶ Similarly to arenes, spirocycles – particularly those containing small rings such as cyclobutane or its four-membered heterocyclic analogues – are rigid scaffolds with defined exit vectors, allowing for careful optimisation of the molecular shape and accompanying improvements in potency and selectivity.¹⁵⁷ Arenes are now frequently replaced with saturated isosteres with defined exit vectors, with the most well-known example being the bicyclo[1.1.1]pentanes (BCPs, **Scheme 70B**). Other saturated isosteres are also being explored.¹⁵⁵ Publications on the synthesis of saturated benzene isosteres appear regularly in current literature, with examples such as cubanes, [2]-ladderanes, cuneanes, (3-aza)bicyclo[3.1.1]heptanes, (2-oxa)bicyclo[2.1.1]hexanes and (2-oxa)bicyclo[2.2.2]octanes, and others (**Scheme 70C**).^{158–164}

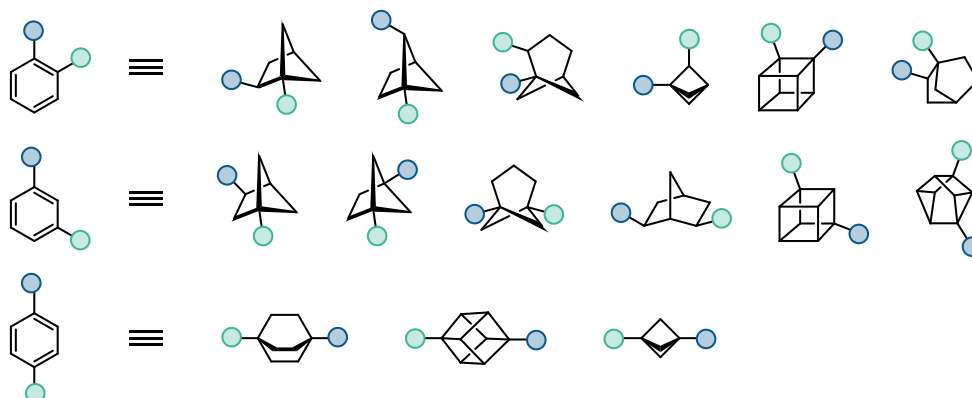
A Spirolactone as the First Spirocyclic Drug – 1957



B Bicyclo[1.1.1]pentanes as Isosteres for Phenyl – Stepan, 2012

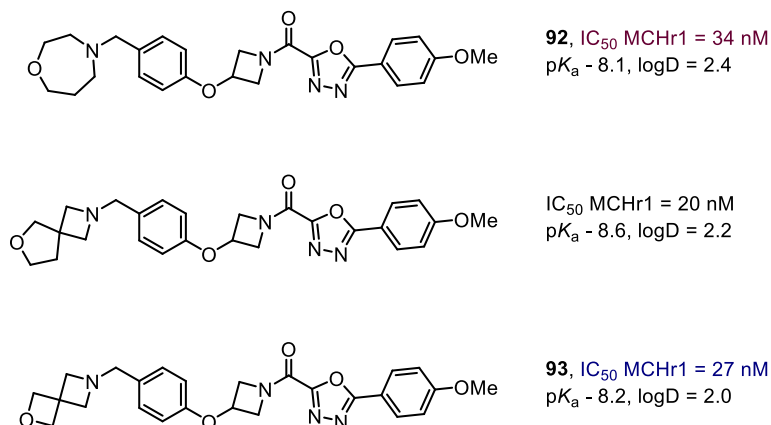


C Other Common Isosteres



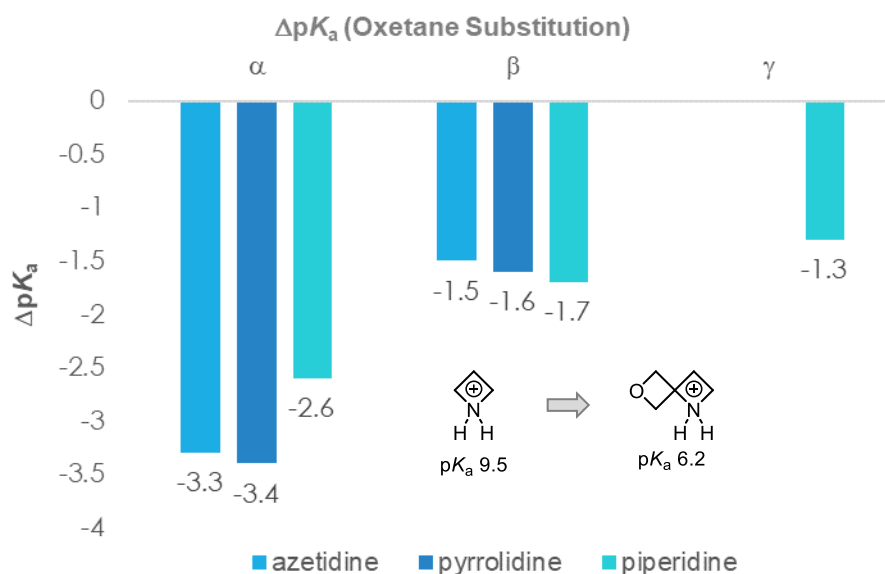
Scheme 70: overview of common isosteres for arenes currently used in synthesis.

More relevant to the topic of spirocycles is arguably the isosteric replacement of the cyclic secondary amine fragments which are commonly used in medicinal chemistry.¹⁶⁵ As with the isosteric replacements above, this can alter a drug's physicochemical properties, including its solubility, metabolic stability, and basicity. As a more polar heterocycle, morpholine is frequently used to increase a drug's water solubility but can be sensitive to oxidation.¹⁶⁶ Isosteric replacement of morpholine with 2-oxa-6-azaspiro[3.3]heptane is one strategy that used to deal with this issue.¹⁶⁷ Johansson and co-workers discovered compound **92** during their efforts in developing melanin concentrating hormone receptor 1 (MCHR1) antagonists (**Scheme 71**).¹⁶⁸ It comprises of an uncommon homomorpholine fragment which proved highly sensitive to oxidation. Substitution with 2-oxa-6-azaspiro[3.3]heptane by isosteric replacement in **93** led to only a marginal increase in the basicity (pK_a increase of 0.1) but a considerable improvement in metabolic stability.



Scheme 71: comparison of IC_{50} values and pK_a when exchanging homomorpholine to spirocyclic isosteres.

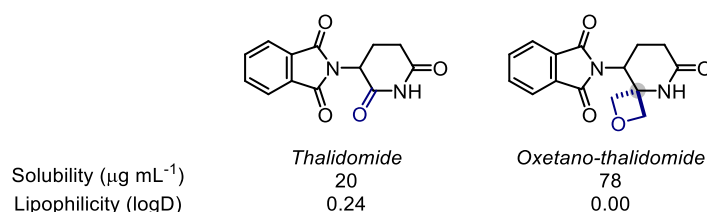
As a relatively small fragment, formally fusing oxetanes and various cyclic amines such as piperidine through a spiro centre can be used to modulate basicity and water solubility without increasing the molecular weight (MW) immensely (MW < 500 Da is one of Lipinski's rules). In the γ -position, spiro-fusion with an oxetane fragment can decrease the basicity of piperidine tenfold, or up to a 100-fold when the oxetane is placed in the α -position (**Scheme 72**).¹⁶⁹



Scheme 72: difference in pK_a for oxetane-fused derivative of azetidine, pyrrolidine and piperidine versus the parent amines.

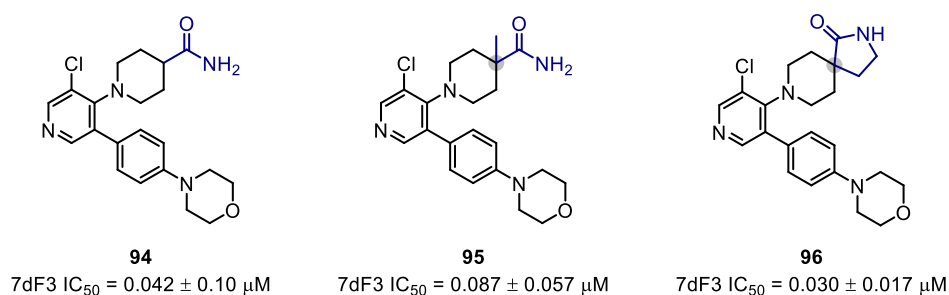
Spiro-fusion at the α -position with oxetane also functions as an isosteric replacement of the amide functionality, but with higher stability. This was demonstrated by Carreira and co-workers using the drug thalidomide, which is well-known for the teratogenic effects of (S)-

thalidomide, formed through *in vivo* racemisation of its (*R*)-enantiomer (**Scheme 73**). The spiro-fused analogue was resistant to racemisation in human blood plasma after 5 hours and had more favourable aqueous solubility and lipophilicity than the imide. Isosteric replacement of the piperazine ring with 2-oxa-6-azaspiro[3.3]heptane in the antibiotic ciprofloxacin was also demonstrated without any loss of activity and improved metabolic stability.



Scheme 73: comparison of physicochemical properties of thalidomide and oxetano-thalidomide.

Although not strictly an isosteric replacement, Mallinger and co-workers optimised the structure of the piperidine carboxamide in compound **94**, which was studied as an inhibitor of the WNT signalling pathway.¹⁷⁰ Methylation at the α -position (**95**) was carried out to optimise the geometry and improve the metabolic stability against amidases, but led to a decrease in potency which was restored by introducing a γ -lactam at the piperidine C-4 position (**96**).



Scheme 74: Spirofusion with γ -butyrolactam improves the stability and activity of a carboxamide.

Despite these advances, the synthesis of spirocycles is often laborious and complicated as a quaternary centre must be constructed. For this reason, medicinal chemists mostly avoid synthesising spirocycles and rely on chemical suppliers for their preparation. From this point of view, the development of novel synthetic strategies for the construction of compounds containing quaternary centres (and by extension, spirocycles) from simple starting materials is currently of interest.

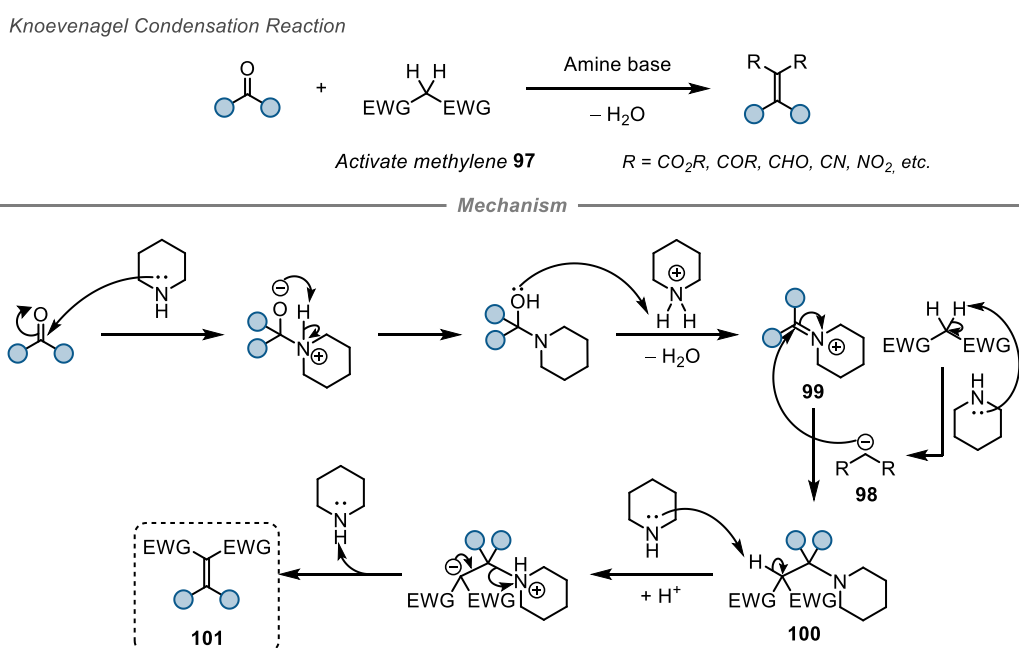
II Accessing Sterically Congested β -Amino Acids & Spirocyclic Dihydropyrroles

2.1 General introduction

2.1.1 Knoevenagel condensation

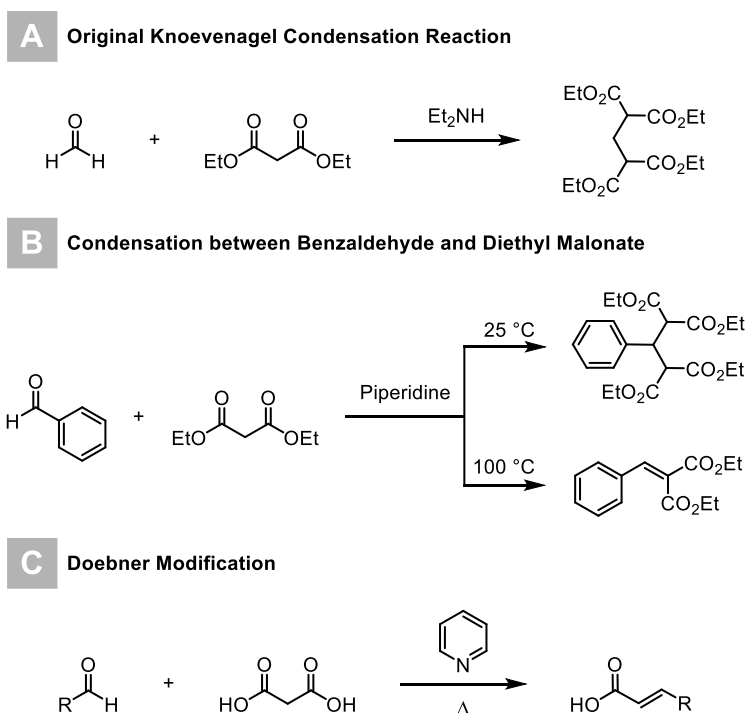
Named after German chemist Emil Albert Knoevenagel during in the late 19th century, the Knoevenagel reaction represents a nucleophilic addition between ketones/aldehydes and an activated (methylene) hydrogen compound (e.g., diethyl malonate, Meldrum's acid, malononitrile, or ethyl cyanoacetate, **Scheme 75**).¹⁷¹ Knoevenagel demonstrated that primary and secondary amines could act as catalysts in the condensation of β -ketoesters or malonates with carbonyls, thus distinguishing the method from a traditional aldol mechanism. To this day, the reaction remains a highly significant and dependable technique for forming C–C bonds and has been extensively utilised in industry.¹⁷²

Mechanistically, the reaction involves the deprotonation of the active methylene compound (**97**) by the amine catalyst (typically piperidine), generating a stabilised carbanion (**98**). The amine catalyst also condensates with the aldehyde or ketone to form iminium ion intermediate **99**, which is then attacked by the carbanion **98**. The resulting intermediate **100** is deprotonated by the base, reforming a carbanion. A rearrangement then occurs releasing the amine base, regenerating the catalyst, and providing the olefin product **101**.



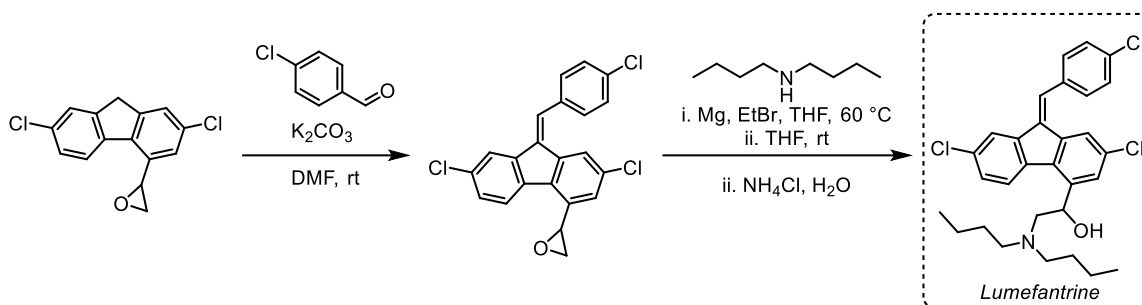
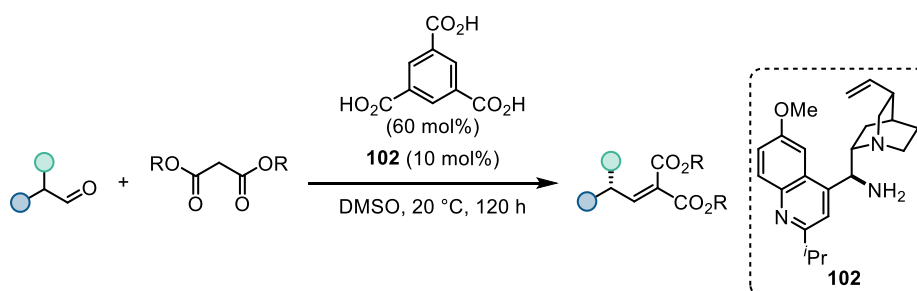
Scheme 75: mechanism of the Knoevenagel condensation reaction.

The original Knoevenagel reaction was conducted using aliphatic formaldehyde and diethyl malonate under alkaline conditions (**Scheme 76A**), and later was expanded to incorporate a range of aromatic aldehydes (**Scheme 76B**).¹⁷² Since then, many modifications have emerged, notably the Doebner modification (**Scheme 76C**), which is based on the piperidine-catalysed conversion of aromatic aldehydes using organic di-acids (e.g., malonic acid) instead of diethyl malonate. The reaction is conducted in pyridine under reflux, which leads to decarboxylation of the di-acid.



Scheme 76: A) original Knoevenagel reaction of formaldehyde and diethyl malonate; B) expanding to benzaldehyde to give the disubstituted or unsaturated mono product depending on temperature; C) Doebner modification.

Since its discovery, the Knoevenagel reaction has been implemented in numerous syntheses, such as in the commercial manufacturing of lumefantrine, an antimalarial medication (**Scheme 77A**).¹⁷³ Some have noted that Knoevenagel's seminal discovery more than 100 years ago established the historical groundwork for the evolution of contemporary aminocatalysis.¹⁷⁴ This has led to numerous developments, such as a report by List and co-workers in 2011 on a catalytic asymmetric Knoevenagel condensation using a *Cinchona* alkaloid **102** as a base (**Scheme 77B**).¹⁷⁵

A Key Steps in the Synthesis of Lumefantrine

B Catalytic Asymmetric Knoevenagel Condensation – List, 2011


Scheme 77: A) structure of lumefantrine; B) List's catalytic Knoevenagel condensation protocol.

2.1.2 Photoredox-mediated Giese-type reaction

The substituted olefins formed in the Knoevenagel reaction have been used in numerous methodologies and shows a wide range of versatility.¹⁷⁶ For example, as substituted electron-deficient alkenes (*i.e.*, alkylidene/benzylidene malononitriles or alkylidene malonic acid dimethyl esters) they have a well-established precedent for undergoing conjugate addition or reduction, as well as serving as dipolarophiles in cycloaddition reactions, given that the olefin is extensively polarised by the presence of two electron-withdrawing groups. These adducts have been extensively exploited in radical addition reactions as radical coupling partners, *i.e.*, in Giese-type additions.^{177–180}

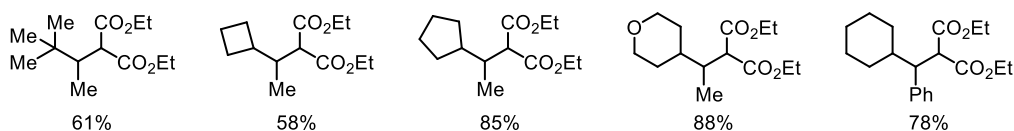
One of the earliest examples utilising these compounds was described in 2015 by Akita which illustrated the generation of carbon radicals via photoredox catalysis from organoborates and carboxylic acids, enabling radical C–C bond formation with electron-deficient olefins (**Scheme 78A**).¹⁸¹ The paper illustrated how the photocatalyst [Acr-Mes]⁺ can prompt a decarboxylative Giese-type reaction with the activated olefins as the radical acceptor, though it was observed that the scope is somewhat limited. This methodology was expanded to allow for the direct use of carboxylic acids in the presence of a base, and later using cycloalkanol.^{177,178}

More recently, Pu and Deng developed pyridine *N*-oxide derivatives as effective catalysts for site-selective functionalization of aliphatic C–H bonds, including unactivated alkanes (**Scheme 78B**).¹⁸² These *N*-oxides, when activated by photoredox catalysis, generate pyridine *N*-oxide radicals that facilitate HAT, enabling various C–H functionalisation reactions such as alkylation, amination, azidation, allylation, and cyanation.

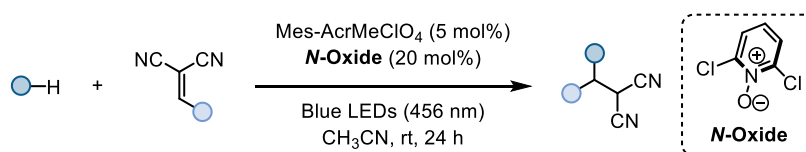
A Photocatalytic Generation of Carbon Radicals *via* Ethylidenemalonic Acid Dimethyl Esters – Akita, 2015



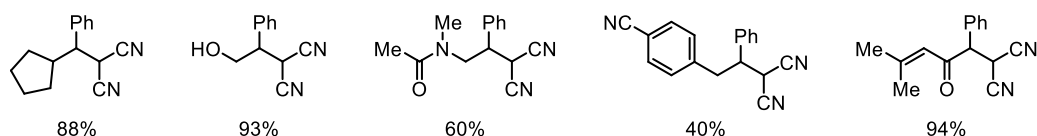
Selected examples



B 2,6-Dichloropyridine *N*-Oxide/Mes-Acr-MeClO₄ Catalysed C–H Functionalisation – Pu & Deng, 2022



Selected examples

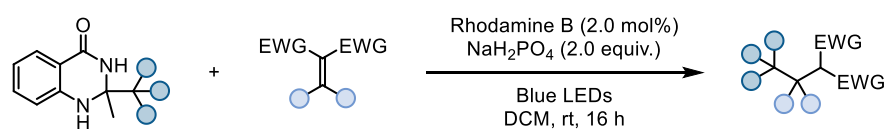


Scheme 78: Giese-type addition reactions exploiting electron-deficient alkenes as radical acceptors in photocatalytic methodologies.

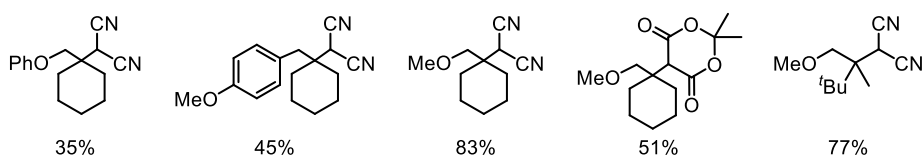
Alkylidene malononitrile have also been shown to facilitate the construction of quaternary centres, as demonstrated in a report by Zhu and co-workers where a method for constructing vicinal quaternary carbon centres using visible-light-driven organophotoredox catalysis is described (**Scheme 79**).¹⁸³ Alkyl radicals, derived from 2,2-disubstituted dihydroquinazolinones, undergo intermolecular conjugate addition to alkylidene malononitriles under blue light irradiation and rhodamine B catalysis. Typically, radical additions to tetrasubstituted alkenes are strenuous, due to a combination of stereo-electronic factors, leading to slow rates of radical addition. However, the highly nucleophilic

methoxymethyl radical (**103**) undergoes a polarity-matched addition to the electron-poor alkylidene malononitrile (**104**), which is highly electrophilic, due to the strong electron-withdrawing nature of the two nitrile groups. The increased stability of the resulting tertiary radical intermediate facilitates this alkylation step. Although the steric hindrance associated with creating a quaternary centre increases the reaction barrier, stabilisation of the partial charges in the transition state by the presence of the electron-withdrawing alkyl groups leads to the formation of difficult-to-access quaternary centres at acceptable rates and under mild conditions.

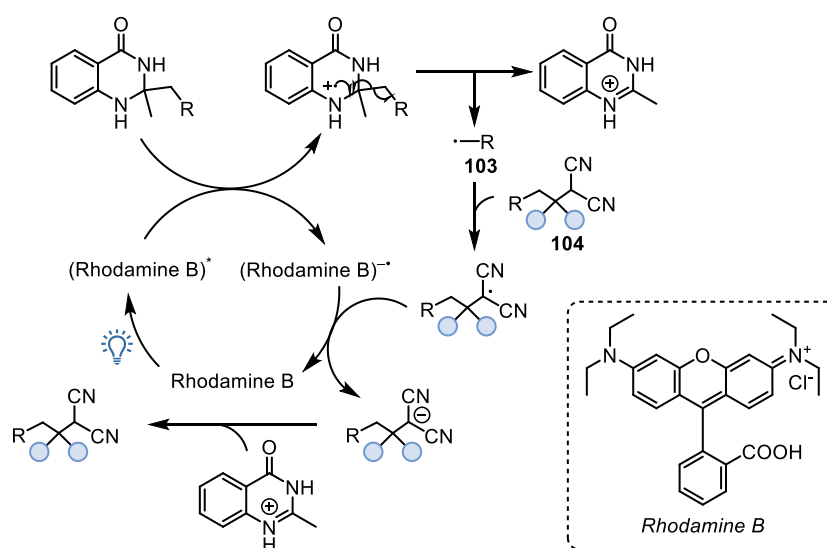
Zhu, 2020



----- Selected examples -----



----- Mechanism -----

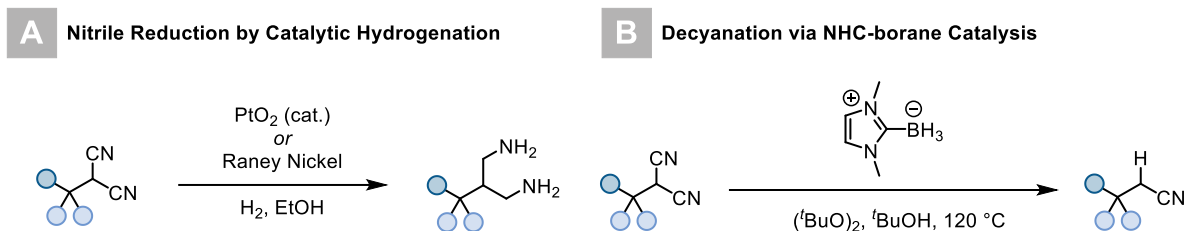


Scheme 79: Rhodium-catalysed intermolecular conjugate addition of alkyl radicals to malononitriles.

2.1.3 Oxidative Functionalisation

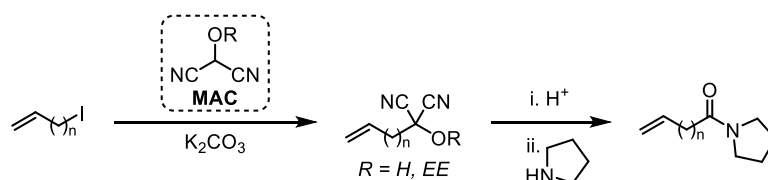
Alkylidene malononitriles provide a notable advantage in their versatility, facilitating the conversion of the nitrile groups into alternative functional groups. For example, nitrile reduction by catalytic hydrogenation, or partial reduction to the corresponding aldehyde. One

cyano group can be directly eliminated using 1,3-dimethylimidazol-2-ylideneborane (NHC-BH₃) and di-tert-butyl peroxide (^tBuO)₂ as the initiator (**Scheme 80B**).^{183–185}



Scheme 80: A) nitrile reduction via catalytic hydrogenation, either by PtO₂ (cat.) or Raney Nickel; B) decyanation of one cyano group using NHC-trihydroborane reagents.

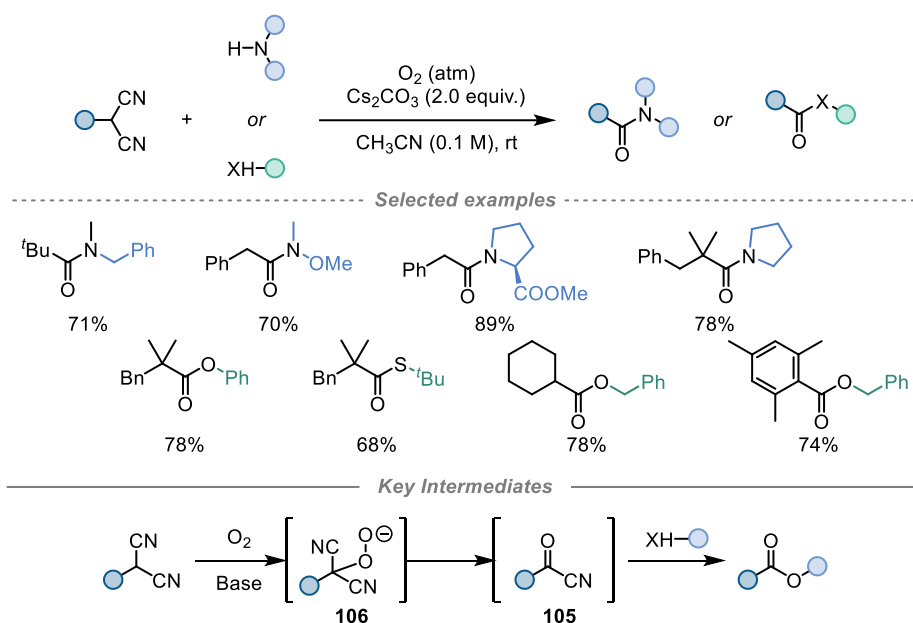
In 1990, Yamamoto and co-workers first introduced the concept of a masked acyl cyanide (MAC) in the formation of amides (**Scheme 81**).¹⁸⁶ A MAC is a species where the acyl cyanide functional group is temporarily blocked or "masked" by another chemical moiety. This masking group prevents the acyl cyanide from reacting or exhibiting its typical properties until it is unmasked or removed under specific conditions, revealing the acyl cyanide reactivity. In Yamamoto's seminal report, the MAC refer to protected hydroxyl malononitriles. The strategy involved the reaction of the malononitrile with an electrophile to produce an intermediate that undergoes elimination of a cyano group, resulting in the formation of an acyl cyanide (see **106**). Treatment with a nucleophile then yields the desired product. Furthermore, they demonstrated the synthesis of a dipeptide via an α -amino acid with the masked activated functionality using this acyl anion equivalent.



Scheme 81: seminal work by Yamamoto and co-workers describing the use of MACs to form amides.

Since the initial introduction of MACs, the oxidation of substituted malononitriles using strong oxidation reagents such as *m*CPBA or H₂O₂ has been widely used to access the acyl cyanide.^{187,188} In 2016, Lear and Hayashi reported a protocol for the oxidative amidation of sterically demanding substrates using 1,1-dicyanoalkanes and amines, facilitated by O₂ and a carbonate base (**Scheme 82**).¹⁸⁹ The process is highly efficient, chemoselective, and practical, allowing for the formation of amides in good yields and stereochemical retention. A mechanistic pathway is proposed involving firstly the deprotonation of the α -substituted malononitrile, which reacts with molecular oxygen to form a peroxide adduct (**106**). This then

fragments into acylating species (**105**), which is intercepted by the amine, forming the amide product. This methodology was later expanded to include the use of alcohols as nucleophiles, providing ester products from substituted malononitriles.¹⁹⁰



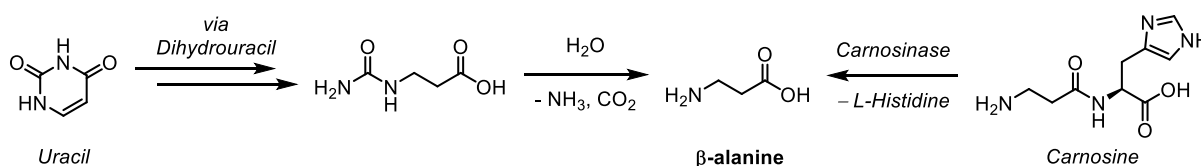
Scheme 82: Lear and Hayashi's oxidative amidation/esterification of α -substituted malononitriles using molecular oxygen.

IIA. Synthesis of Sterically Congested $\beta^{2,2}$ -Amino Acids

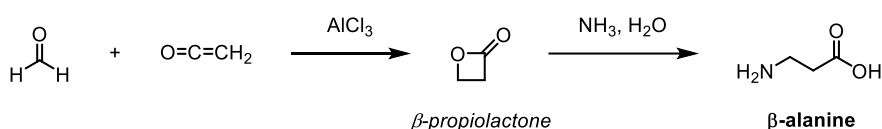
A.1 Introduction

β -amino acids (β -AAs) are key components in a wide range of biologically active molecules. In addition, their incorporation into peptides results in strong modifications to their secondary structure, often leading to increased resistance to proteases and peptidases.^{191,192} The simplest example of a β -amino acid is β -alanine, which is frequently used as a performance enhancer for high-intensity exercise.¹⁹³ It also has purpose in pharmaceuticals, e.g., as a precursor to vitamin B₅, coenzyme A, as well as in synthetic materials such as nylon-3 (polyalanine).^{194–196} Biosynthetically, it is formed *via* the degradation of uracil or the dipeptide carnosine. In the body, β -alanine ethyl ester is hydrolysed to form the amino acid.¹⁹⁷ The industrial production involves the reaction of ammonia with β -propiolactone, the latter of which requires a multistep preparation and the use of harsh reaction conditions (**Scheme 83**).¹⁹⁸

A Biosynthesis of β -alanine – *via* Degradation of Uracil or Carnosine



B Industrial Synthesis of β -alanine – *via* Reaction of Ammonia with β -propiolactone



Scheme 83: biosynthesis and industrial route to β -alanine.

Synthetic derivatives of biologically relevant peptides incorporating β -AAs often display interesting pharmacological activity, with increased potency and enzymatic stability. A notable advantage of β -AAs over α -AAs is the former's ability for greater diversity. The difference of three tuneable positions versus five is a significant advantage, as the additional C–C bond increases diversity and provides new opportunities to modify the substituent pattern on the C–2 and C–3 positions. Thus, the synthesis of these derivatives has evoked

widespread interest. Among the several types of β -amino acids, β^2 - and β^3 -amino acids represent the most abundant in the Life Sciences.

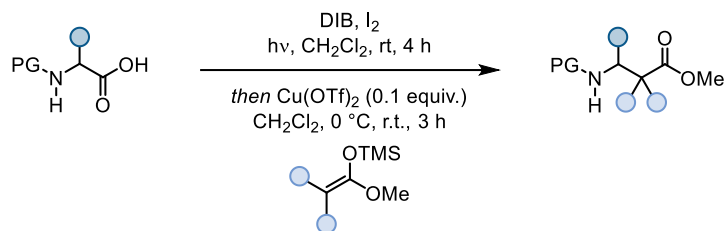
A.1.1 $\beta^{2,2}$ -Amino Acids

Sterically congested $\beta^{2,2}$ -amino acids are particularly effective at affecting a peptide's conformation by inducing the formation of more rigid secondary structures, and thus enhancing the stability towards proteolytic degradation and resistance to all kinds of proteases and peptidases.¹⁹¹ This has led to an increased motivation of several research groups in the use of these congested peptides for the rational design of novel, defined nanoscopic patterns, such as helical secondary structures and foldamers.^{199,200}

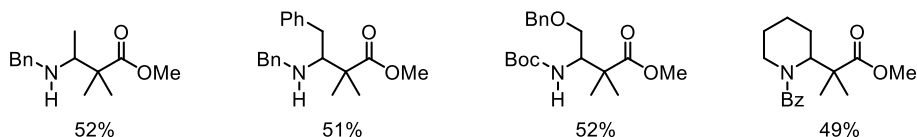
One difficulty associated with synthesising these highly substituted amino acids is the formation of a quaternary centre. The barriers associated with the construction of these centres are higher due to steric hindrance, e.g., the addition of amines to trisubstituted Michael acceptors as in the aza-Michael addition, or carbon nucleophiles to imines in the Mannich reaction. This in general results in reactions that are slow and low-yielding. Radical-based approaches are often used to construct these as radical species are already high in energy and typically less sensitive to steric effects. This is demonstrated by the many examples of radical reactions used to synthesize natural products containing quaternary centres.²⁰¹

An early example on the synthesis of $\beta^{2,2}$ -AAs was reported in 2009 by Hernández and Boto (**Scheme 84**).²⁰² The method involves a one-pot conversion of α -amino acids to β -amino acids through a PIDA-mediated decarboxylation. The resulting α -amino-alkyl radical is then converted to an iminium ion, either through a second oxidation, or via trapping with iodine and subsequent elimination of the unstable, putative α -iodo-amine intermediate. Iminium alkylation with silyl enol ether nucleophiles then gives the β -amino acid derivatives in a net homologation.

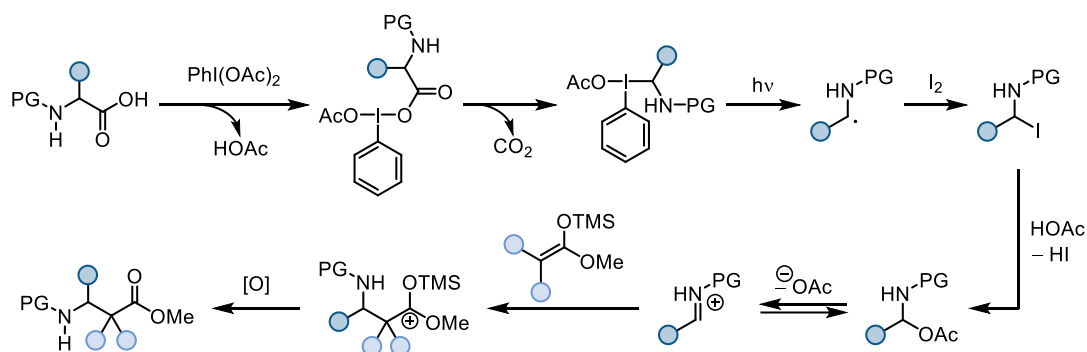
Boto, 2009



Selected examples



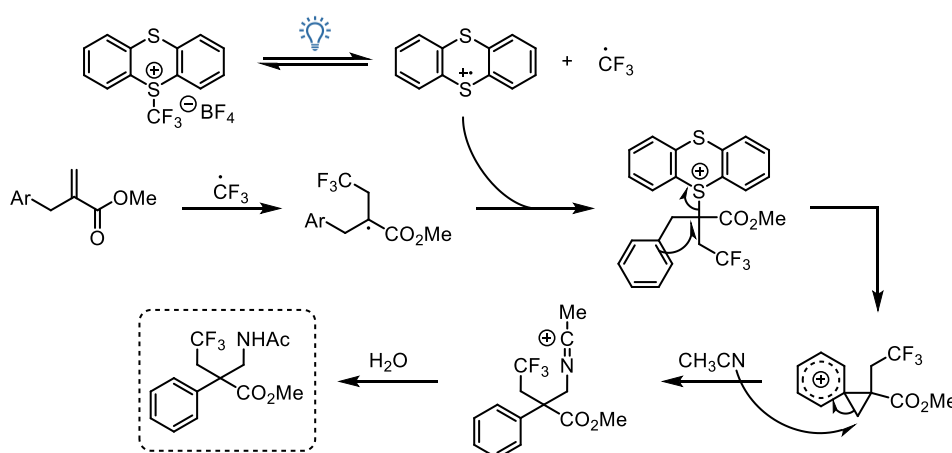
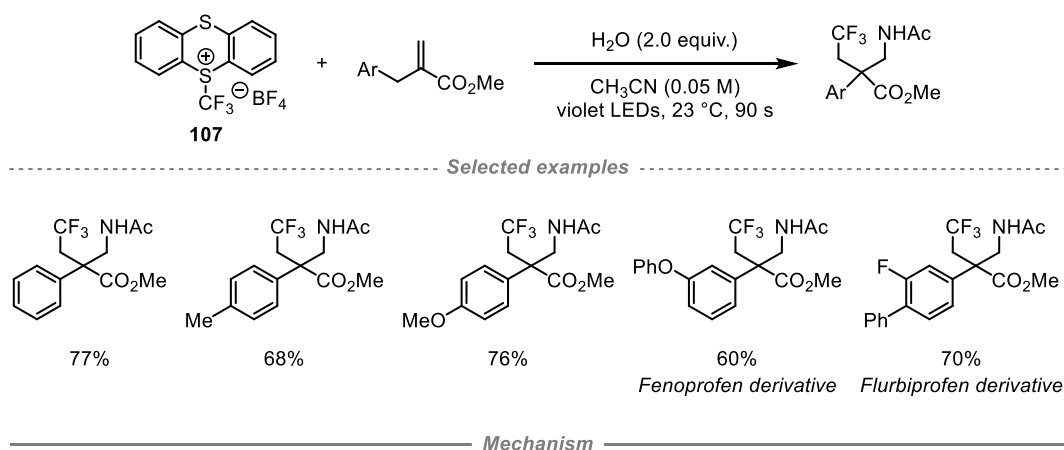
Mechanism



Scheme 84: one-pot conversion of α -amino acids to β -amino acids through a PIDA-mediated decarboxylation.

In 2022, Ritter and co-workers proposed a new photochemical approach to access $\beta^{2,2}$ trifluoromethyl substituted amino acids through a combination of Michael addition and Ritter-type amination with the CF_3 α -thianthrenium reagent **107** (Scheme 85).²⁰³ Homolysis of the weak S- CF_3 bond in the thianthrenium reagent **107** (similar to Umemoto's reagent) leads to the formation of the ambiphilic CF_3 radical which undergoes a Giese-type addition to *gem*-disubstituted Michael acceptors in which one group is electron-withdrawing and the other is either phenyl (for α -amino acids) or benzyl (for β -amino acids). This is necessary in order to render the radical thermodynamically stable as the next step of the mechanism involves radical-radical coupling between the Giese adduct and the persistent thianthrenium radical cation. The resulting sulfonium salt is a strong electrophile which can be displaced by CH_3CN used as the solvent (Ritter reaction). A nitrilium ion is formed which is subsequently hydrolysed to the corresponding acetylamide.

Ritter, 2022

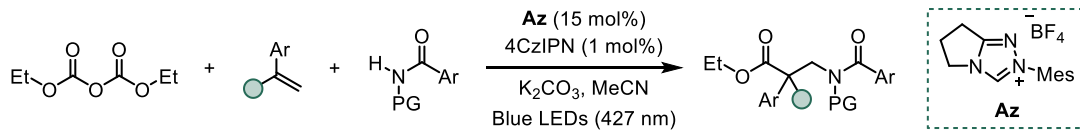


Scheme 85: access to $\beta^{2,2}$ -AA analogues via radical addition of trifluoromethyl-thianthrenium **107** to 2-substituted acrylates.

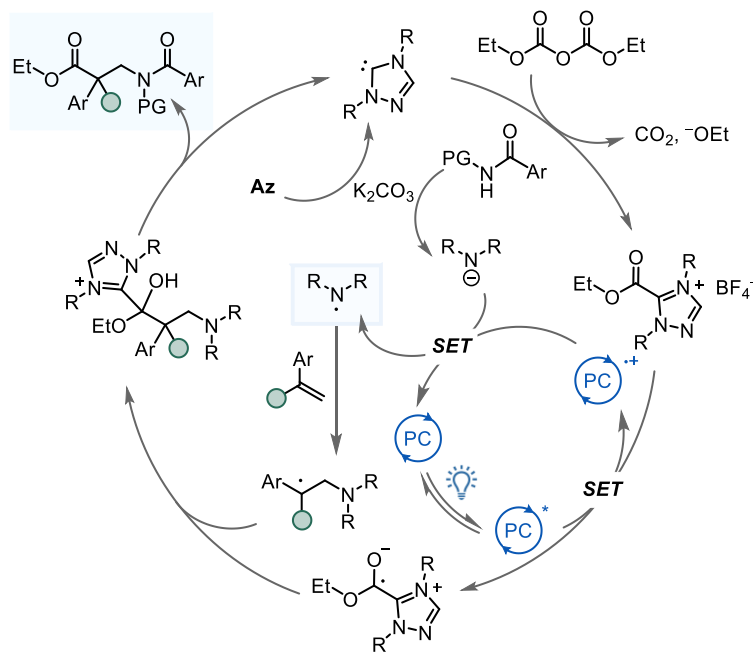
Very recently, the group of Scheidt developed a dual N-heterocyclic carbene/photocatalysed synthesis of β -amino esters (**Scheme 86**).²⁰⁴ The method utilises olefins, imides, and pyrocarbonates to give sterically congested $\beta^{2,2}$ -amino esters in moderate to excellent yields. The method relies on an oxidative quenching cycle with 4CzIPN as the catalyst. Stern-Volmer fluorescence quenching studies indicate that the excited NHC amide **Az** (formed *in situ* through reaction of the carbonate with the NHC) is reduced to the persistent ketyl radical equivalent. The oxidised photocatalyst oxidises the deprotonated imide to the electrophilic, N-centred radical which can add in an *anti*-Markovnikov fashion to the *gem*-disubstituted olefin, thus creating a tertiary radical in the process. The latter is then intercepted by the ketyl radical, creating the quaternary centre (*via* radical-radical coupling). While the reaction can successfully provide α,α -disubstituted β -AAs, the olefin scope is limited to α -alkyl styrenes as a consequence of the radical recombination step, which works best when the species involved has longer lifetimes (i.e.,

persistent radicals). This necessity entails that one of the α -substituents in the final $\beta^{2,2}$ -AA is an aryl group.

A β -Amino Ester Synthesis via Cooperative Carbene Photocatalysis – Scheidt, 2023



B Proposed Mechanism



Scheme 86: Dual NHC/photocatalysis for $\beta^{2,2}$ -amino ester synthesis.

A.2 Objectives

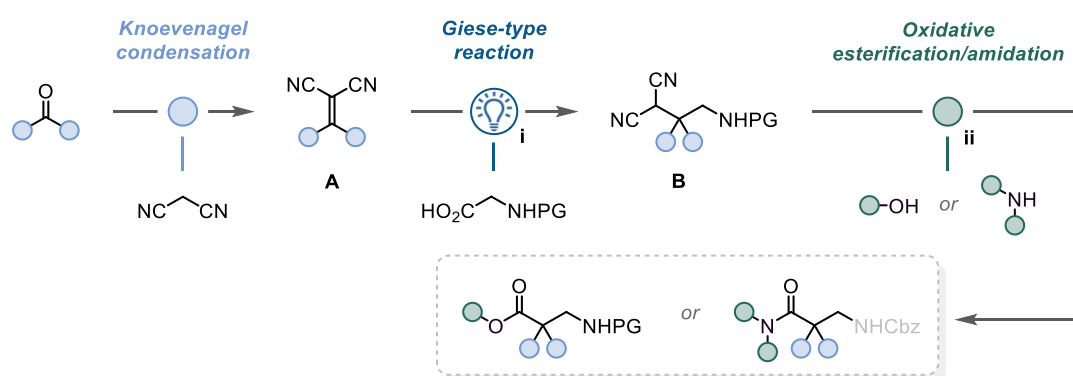
The aim of this project was to develop an innovative and simple method to synthesise highly congested $\beta^{2,2}$ -amino acid derivatives. As previously noted, their pharmacological effects and ability to induce the development of more inflexible peptide structures highlight their significance as a valuable class of compounds.²⁰⁵ Additionally, with the increasing popularity of peptide-based drugs, as well as the urgent need for new antibiotics, there is an imminent interest in these molecules in the medicinal chemistry field.²⁰⁶ The syntheses of these moieties however tend to pose a challenge. The quaternary centre motif signifies a challenge in modern organic synthesis, owing to the intrinsic steric issues related to the formation of these $C(sp^3)-C(sp^3)$ bonds.²⁰¹

Traditional methods such as the Mannich addition are limited by the reactivity of the imine, which can restrict the type of substitution pattern accessible, e.g., $\beta^{3,3}$ -substituted compounds. Steric hindrance due to bulky substituents at the C-2 position of an enolate (as in Mannich-type additions) or equivalent nucleophile significantly slow down the reaction, and thus cannot be used to prepare highly congested moieties such as $\beta^{2,2}$ -AAs. This also leads to limitations in the type of nucleophile that can be used. As result, activation of the imine to an iminium cation with either a Lewis acid or alkylating reagent is typically required. This activation addresses kinetic issues by increasing the electrophilicity of the imine acceptor, e.g., by converting formamides into highly reactive iminium ions, as in the Vilsmeier-Haack-type approach. However, this strategy typically requires toxic reagents such as triflic anhydride and phosphoryl chloride. This often leads to restrictions in the type of substituents/functional groups that can be featured into the final products.

Similarly, while some methods based on *aza*-Michael additions have been highly effective, the reaction has several limitations, e.g., restrictions in the steric bulk of the substituents on the acceptor double bond. The addition of certain amines to more densely substituted Michael acceptors requires the use of higher pressures and can take multiple days to produce even low yields.^{207,208} Additionally, alkylative methods typically are restricted to substrates lacking key substituents at the β -position due to frequent complications when attempting to construct quaternary centres, leading to a serious absence of versatility.

Therefore, the development of more versatile, general, and straightforward synthetic strategies for the synthesis of sterically congested $\beta^{2,2}$ -amino acids from readily available precursors is of significant worth.

Here, a three-step radical-based process is proposed whereby easily accessible ketones and α -amino acids are converted into $\beta^{2,2}$ -amino acids/esters (**Scheme 87**). Inspired by the seminal work of Lear and Hayashi, the ketones are first converted into highly electrophilic alkyldiene malononitriles *via* a Knoevenagel condensation reaction.^{189,190} Facilitated by photoredox catalysis, α -carbamoyl radicals (formed from the α -amino acid) undergo a Giese-type addition to the alkyldiene malononitrile which acts as a Michael-type acceptor. This step forms the key quaternary centre. Typically, radical additions to tetrasubstituted alkenes are strenuous, due to a combination of stereo-electronic factors, leading to slow rates of radical addition, however the polarity match of the two reacting species results in a facile addition.



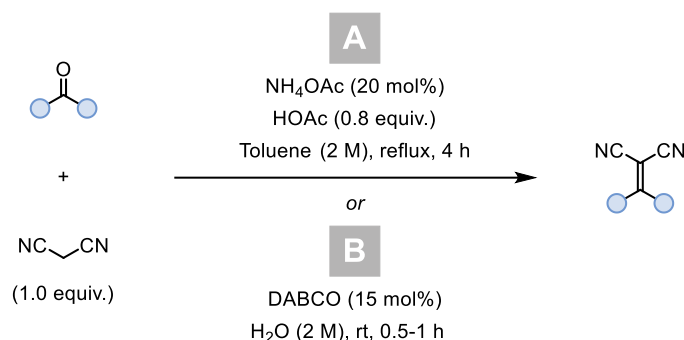
Scheme 87: Proposed strategy for the synthesis of congested $\beta^{2,2}$ -amino acid derivatives.

These α -substituted malononitriles can then either be converted to the corresponding $\beta^{2,2}$ -amino ester *via* an oxidative esterification, or to the free carboxylic acid after oxidation. The cyano groups present in the alkyldiene malononitriles therefore serve a dual purpose: the strong electron-withdrawing nature of the two nitrile groups aids in stabilisation of transient radicals and anions, and act as leaving groups for the final oxidation/oxidative esterification step.

A.3 Results & discussion

A.3.1 Reaction Optimisation

Alkylidenemalononitrile derivatives could be synthesised *via* two methods (**Scheme 88**). For classical Knoevenagel conditions, a procedure adapted from Grenning *et al.* was used; refluxing the desired ketone/aldehyde and malononitrile with catalytic amounts of NH₄OAc in a mixture of acetic acid and toluene provided a number of compounds with varying functional groups.²⁰⁹ Alternatively, several substrates could be converted into the desired compounds using DABCO as the catalyst.²¹⁰ This method uses exceedingly mild conditions to rapidly provide substrates in excellent yields, however several ketones and aldehydes were unable to be successfully converted with these conditions, resulting in decomposition, therefore method A was preferred.



Scheme 88: methods to access alkylidenemalononitrile derivatives. A) the classical Knoevenagel condensation approach; B) DABCO-catalysed condensation method.

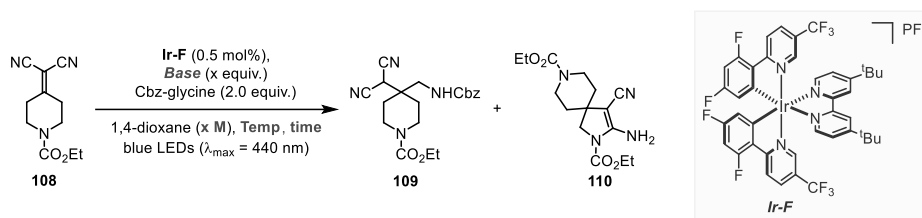
A.3.1.1 Photo-mediated Giese-Type Reaction

Optimisation of the light-mediated Giese-type reaction was then carried out (**Table 1**). Reaction temperature, time and concentration were investigated along with the solvent, base, and scale, using standard alkylidenemalononitrile substrate **108** and *N*-Cbz-glycine, in the presence of a photocatalyst.

The use of elevated temperatures (40 °C for 24 h) resulted in a substantial increase in yield compared to room temperature, and a further increase to 60 °C led to full conversion to the desired product **109** in half the time (**entries 5 and 8**). 1,4-Dioxane (0.2 M) proved to be superior to other solvents tested, however, an increase in concentration led to substantially diminished yields. Additionally, the use of *sym*-collidine (2.0 equiv.) as the base was crucial, as other bases – both organic and inorganic – led to a decrease or trace amounts of the desired product, or the formation of an undesired spirocycle side-product (**110**). The final

optimised conditions are as follows: irradiation (blue LEDs, 2 x 32 W, $\lambda_{\text{max}} = 440 \text{ nm}$) of a mixture of **108** (1.0 equiv.) and Cbz-glycine (2.0 equiv.) in the presence of Ir-F (Ir[(dF(CF₃)ppy)₂(dtbpy)]PF₆, 0.5 mol%) and *sym*-collidine (2.0 equiv.), in 1,4-dioxane (0.2 M) at 60 °C, afforded the targeted malononitrile **109** in 95% isolated yield.

Table 1: Optimization studies of the Giese-type reaction.



Entry	Base (equiv.)	Conc. (M)	Photocat. (mol%)	Temp. (°C)	Time (h)	109 (%) [*]	110 (%) [*]
1	K ₂ HPO ₄ (2.4)	0.1	Ir-F (1)	42	16	<5	84
2	2,6-Lutidine (2.4)	0.1	Ir-F (1)	42	16	43	58
3	Collidine (2.4)	0.1	Ir-F (1)	42	16	59	44
4	Collidine (2.4)	0.1	Ir-F (1)	24	16	24	76
5	Collidine (2.4)	0.1	Ir-F (1)	42	24	73	39
6	Collidine (2)	0.1	Ir-F (1)	60	16	>99	-
7	Collidine (2)	0.2	Ir-F (1)	60	16	>99	-
8	Collidine (2)	0.2	Ir-F (0.5)	60	16	>99	-
9	Collidine (2.4)	0.2	Ir-F (1)	42	16	46	21
10	Collidine (2.4)	0.4	Ir-F (1)	42	16	59	41
11	Collidine (2)	0.2	4CzIPN (1)	60	16	0	-
12	Collidine (2)	0.2	-	60	16	0	-
13 ^{**}	Collidine (2)	0.2	Ir-F (1)	60	16	0	-

^{*}Calculated by ¹H NMR using TCl (trichloroethylene) as internal standard. ^{**}Ran in the dark.

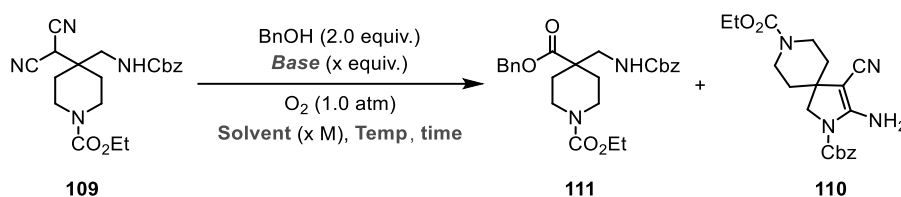
The use of alternative photocatalysts such as 4CzIPN (entry 11) resulted in decomposition of the reaction mixture, which is arguably expected, as photo-organocatalysts are often unstable at elevated temperatures. Control experiments (entries 12 & 13) revealed that Ir-F, in addition to light irradiation, are vital for the reaction to ensue.

A.3.1.2 Oxidative Esterification & Amidation

Next, a procedure to access the desired β -AA derivatives from malononitriles was investigated (Table 2). Recently, Lear and Hayashi reported a straightforward method for the oxidative esterification and amidation of α -substituted malononitriles.^{189,190} The reaction employs molecular oxygen, a base, and the respective alcohol or amine as nucleophilic reagents. For 24 h, malononitrile **109** (1.0 equiv.) was reacted under 1.0 bar of O₂ in the presence of EtOH (10.0 equiv.) as the nucleophile and Cs₂CO₃ (2.0 equiv.) as the base in CH₃CN (0.1 M). With these conditions, optimal yields of product **111** were obtained. An increase in temperature resulted in a mixture of products, while longer reaction times proved to be beneficial in increasing the yield. Additionally, a number of bases were screened;

K_2CO_3 exhibited similar results to Cs_2CO_3 , as did DBU, however the latter was disregarded, due to the potential hazard of cyanide when using organic bases. Notably, the use of inorganic bases produces cyanide salts which can be safely filtered off, compared to organic bases which are more cumbersome and require more care to dispose of safely. Other bases such as Et_3N and DIPEA gave a mixture of product **111** and **110**, while *sym*-collidine failed to deliver any product. The latter can be rationalised by its high pK_{aH} value (7.3) compared to malononitrile (10).

Table 2: Optimization studies of the oxidative esterification reaction.



Entry	Base (equiv.)	Nucleophile (equiv.)	Solvent (M)	Temp. (°C)	Time (h)	109 (%) [*]	111 (%) [*]	110 (%) [*]
1	Cs_2CO_3 (2)	BnOH (2)	MeCN (0.1)	RT	16	30	26	34
2	Cs_2CO_3 (2)	BnOH (2)	MeCN (0.1)	RT	24	0	72	3
3	Cs_2CO_3 (2)	BnOH (2)	MeCN (0.1)	RT	72	0	74	22
4	Cs_2CO_3 (2)	BnOH (2)	MeCN (0.1)	0	16	0	24	35
5	Cs_2CO_3 (2)	BnOH (2)	MeCN (0.1)	50	24	0	52	19
6	Cs_2CO_3 (2)	BnOH (2)	MeCN/ C_6HF_5 (9:1)	RT	16	0	42	55
7	Cs_2CO_3 (1)	BnOH (2)	MeCN (0.1)	RT	24	0	50	45
8	DIPEA (2)	BnOH (2)	MeCN (0.1)	RT	24	0	32	37
9	Collidine (2)	BnOH (2)	MeCN (0.1)	RT	24	99	0	0
10	Et_3N (2)	BnOH (2)	MeCN (0.1)	RT	24	0	13	16
11	DBU (2)	BnOH (2)	MeCN (0.1)	RT	24	0	82	0
12	Cs_2CO_3 (2)	EtOH (10)	MeCN (0.1)	RT	24	0	60	10

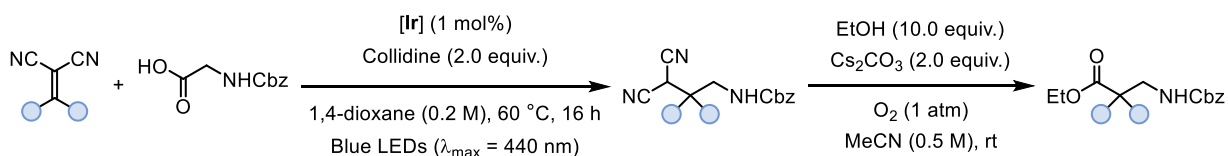
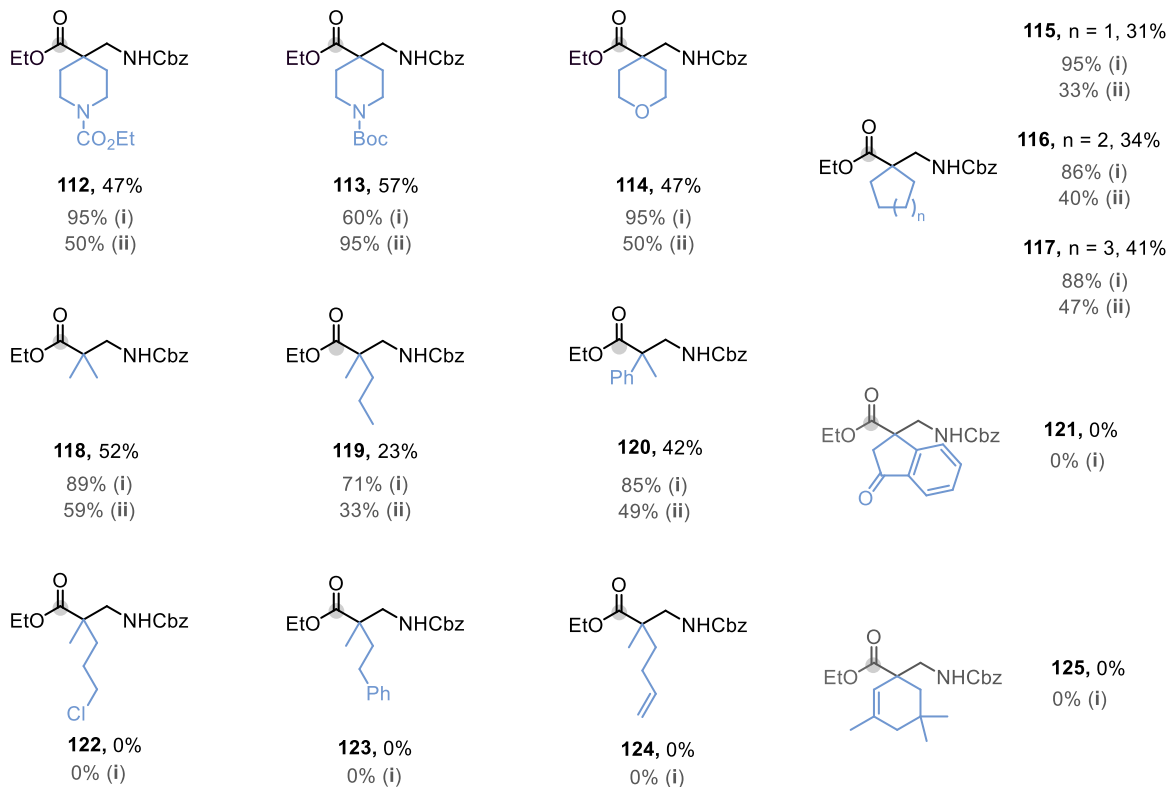
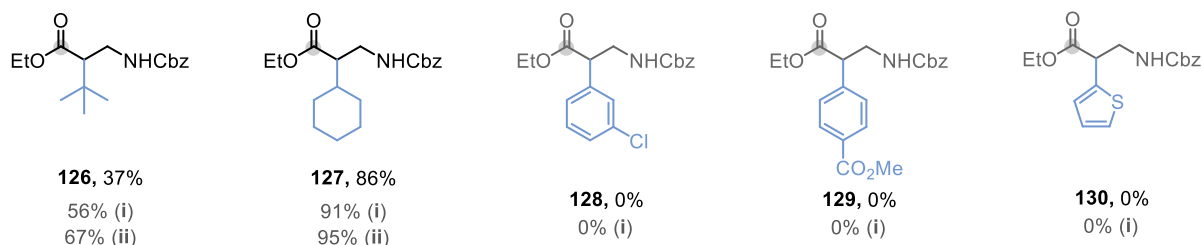
^{*}Calculated by 1H NMR using TCI (trichloroethylene) as internal standard.

Crucial to the success of the reaction was sufficient oxygen saturation in the solvent. In an anaerobic environment, the formation of **111** dominates, forming either a mixture, or exclusively the undesired side product. Furthermore, deviations from CH_3CN to other solvents with high oxygen solubility, such as CH_2Cl_2 , MTBE and C_6HF_5 (pentafluorobenzene), resulted in decreased yields. Cooling the reaction to 0 °C to maximise oxygen saturation also proved to be ineffective, as did the addition of molecular sieves. Therefore, to ensure adequate saturation, the solvent was pre-bubbled with oxygen for a minimum of 4 h.

A.3.2 Scope & Limitations

With the optimised conditions acquired, the substrate scope was investigated. First, the malononitrile scope was explored (**Scheme 89**). (Hetero)cyclic precursors proved to be highly effective, as seen in the quaternary $\beta^{2,2}$ -amino ester products bearing piperidine (**112**

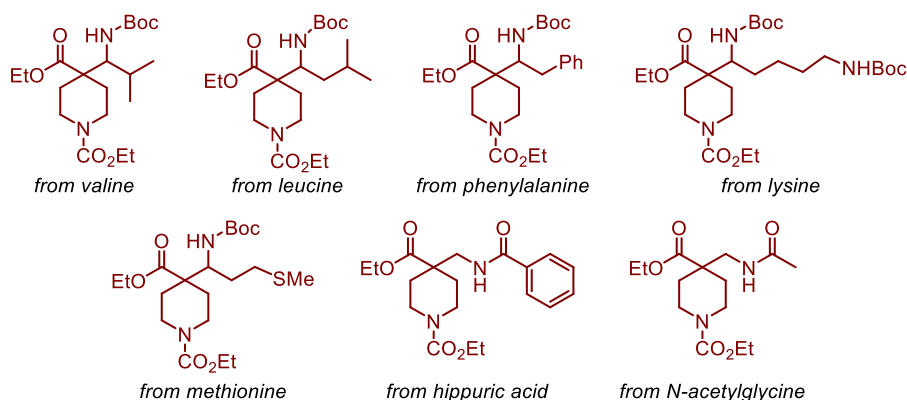
and **113**), and tetrahydropyran (**114**), which were isolated in two steps from the corresponding alkylidenemalononitrile in good or moderate yield (47%, 57%, and 47%, respectively). The Giese-type reaction of compound **110** could also be scaled up and out, providing the substituted malononitrile derivative in an isolated yield of 88% (2 × 5.0 mmol, 3.38 g) without the need for purification. Additionally, modification of the ring size at the α -position was tolerated, exhibited in the use of cyclopentanone **115**, cyclohexanone **116** and cycloheptanone **117** (31%, 34%, and 41%, respectively, over two steps). Furthermore, the use of linear ketones was possible, giving access to $\beta^{2,2}$ -amino esters **118-120** in good yields (52%, 23%, and 42%, respectively). Unfortunately, for highly bulky substrates, including a dihydroindenone-derived (**121**), several other linear examples (**122-124**), as well as the isophorone-derived alkylidenemalononitrile (**125**), were unsuccessful.


Ketone scope

Aldehyde scope


Scheme 89: ketone and aldehyde scope of synthesised $\beta^{2,2}$ -amino esters.

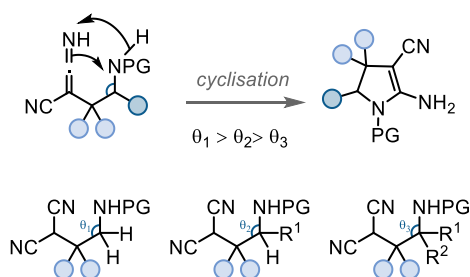
As the Knoevenagel condensation is not limited to ketones, aldehydes could be used for the synthesis of monosubstituted β^2 -amino esters bearing sterically demanding substituents, such as *tert*-butyl (**126**) or cyclohexyl (**127**), in 37% and 86% yield, respectively. Substrates bearing benzyl motifs, such as **128**, led to a complex mixture of products during the Giese-type reaction. Additionally, analysis of attempts to obtain **129** exclusively showed the presence of starting material, while decomposition was observed in the case of **130**.

Numerous *N*-protected amino acids were investigated in the Giese-type reaction (**Scheme 90**). Substrates assessed, including phenylalanine, lysine, leucine, methionine, and valine, all resulted in the formation of the undesired spirocyclic side product. Hippuric acid and *N*-acetylglycine were also explored, however both resulted in the decomposition of the malononitrile.



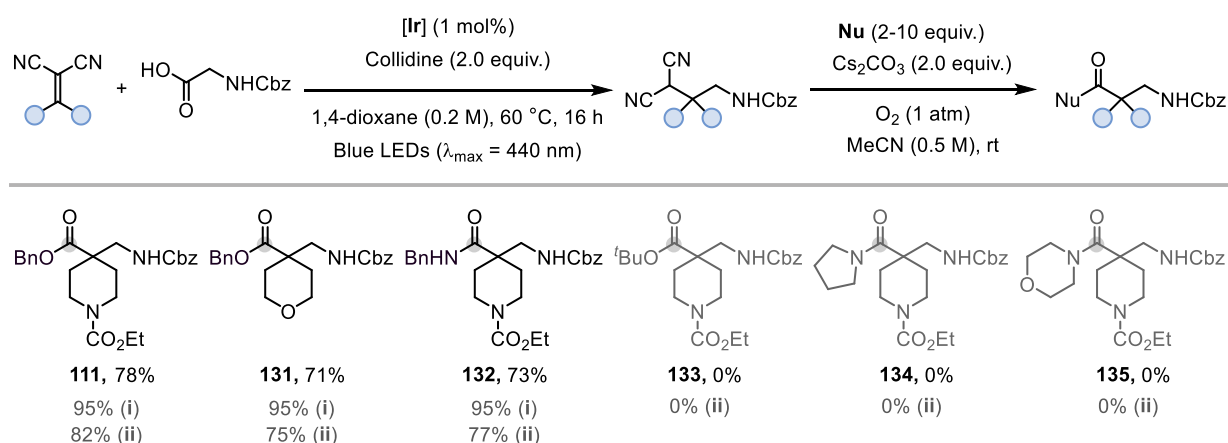
Scheme 90: $\beta^{2,2}$ -amino esters derived from other *N*-protected amino acids that were isolated as the corresponding spirocyclic side product.

When using amino acids with greater substitution compared to Cbz-glycine, the increased steric hinderance of the additional groups was hypothesized to further entropically drive the reaction towards the intramolecular, 5-*exo-dig* cyclisation, forming the dihydropyrroles. This can be rationalised *via* the Thorpe-Ingold effect exerted by the *gem*-dialkyl groups; substitution of methylene hydrogens with more sterically demanding alkyl groups compresses the bond angle θ between the two reacting groups to be narrower than the typical tetrahedral angle of 109.5° , bringing them closer together (**Scheme 91**).²¹¹ Coupled with the decreased conformational freedom caused by steric repulsion of the substituents, the probability of entering a conformation favouring intramolecular cyclisation significantly increases.



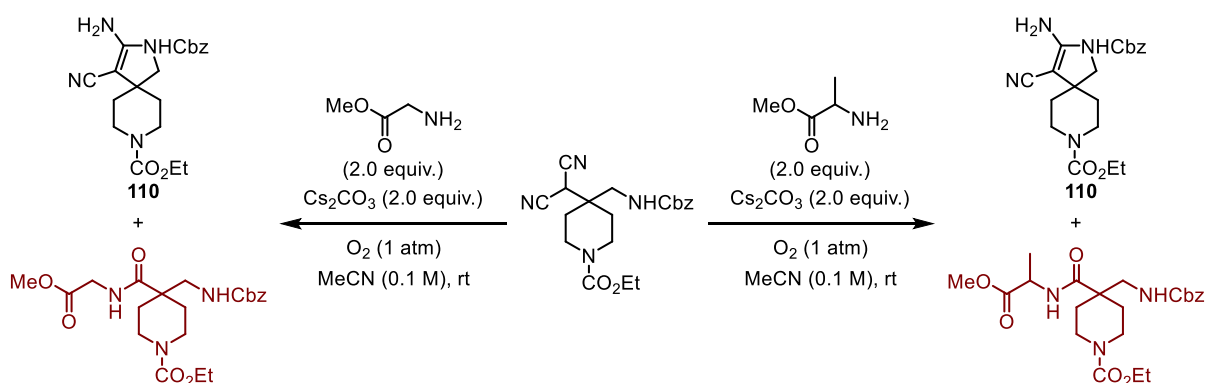
Scheme 91: rationalisation of spirocycle side product *via* the Thorpe-Ingold effect.

Next, the scope of suitable nucleophiles was explored (**Scheme 92**). The use of benzyl alcohol worked well, allowing for the synthesis of corresponding benzyl-protected esters **111** and **131** in good yields (78% and 71%, respectively). Notably, the use of a benzyl protected ester in conjunction with a Cbz-protected amine is complementary, as both groups can be deprotected simultaneously by catalytic hydrogenation, giving the free β -amino acid. The use of benzyl amine provided the corresponding amide (**132**) in good yield (73%). While larger nucleophiles, such as *tert*-butanol, failed to deliver the desired *tert*-butyl esters (**133**), Numerous other nucleophiles were tested, including pyrrolidine (**134**) and morpholine (**135**), however no product could be isolated.



Scheme 92: scope of nucleophiles tried in the oxidative esterification/amidation.

Furthermore, attempts to use amino acids or dipeptides in the oxidative amidation resulted in the formation of **110**, as seen in **Scheme 93**.



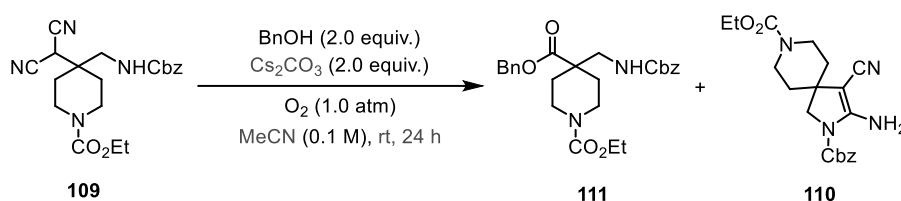
Scheme 93: failed attempts at obtaining hindered dipeptides; both reactions (left, using glycine methyl ester, right, using alanine methyl ester) resulted in the formation of spirocycle **110**.

A.3.2.1 Oxidative Esterification/Amidation in Flow

The following work was conducted in a collaboration with Dr Luca Capaldo, Ting Wan, and Prof. Timothy Noël at the Van't Hoff Institute for Molecular Sciences (HIMS), University of Amsterdam. For more information, see the experimental section.

The low solubility of gases in organic media often necessitates the use of high pressures, with the concentration of dissolved gas also dramatically decreasing with an increase in temperature.²¹² As mentioned earlier, a major drawback arises from the low oxygen solubility in organic solvents, which slows down formation of the desired acyl cyanide intermediates. While this could be tolerated for some substrates, many others resulted in either low yield, or exclusive formation of the spirocyclic dihydropyrrole by-product (e.g., **110**), which is able to outcompete the oxidation. Moreover, when scaling-up the oxidative esterification step (from 0.2 mmol to 0.5 mmol), the effectiveness of the reaction drops considerably, due to this competitive side product formation (**Table 3**). To circumvent this issue and increase O₂ content in batch scale, operating at elevated O₂ pressures would be necessary, leading to heightened safety risks, and constraining the versatility of the approach.

Table 3: scale-up of the oxidative esterification reaction.



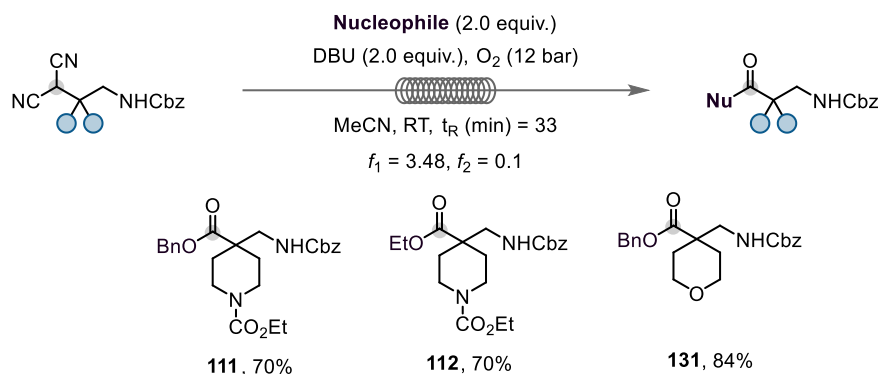
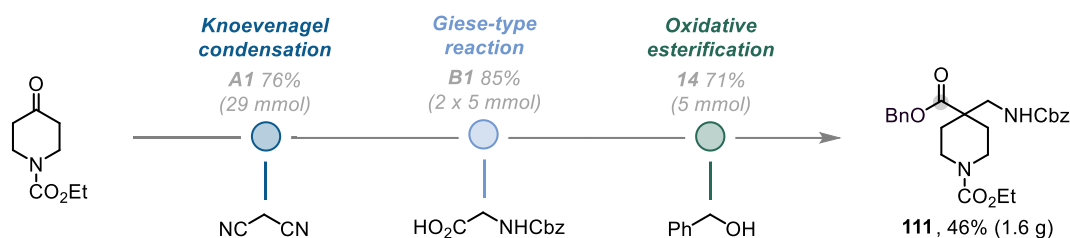
Entry	Scale (mmol)	111 (%) [*]	110 (%) [*]
1	0.1	72	<5
2	0.2	78	<5
3	0.5	50	50

^{*}Isolated yields.

Over the last few years, flow chemistry has developed into a formidable alternative to conventional batch procedures. This offers numerous benefits, such as increased efficiency, shorter reaction times, scalability, and improved reproducibility. Moreover, there are numerous benefits to using flow chemistry in conjunction with gases.²¹³ The application of gases in continuous flow has expanded the possibilities for conducting various chemical processes that were previously considered too hazardous for large-scale batch chemistry, or simply inefficient due to high pressure constraints. Generally, gases are more straightforward to operate in flow even at elevated pressures, due to the small reactor volumes.²¹⁴ Additionally, a substantial increase in the interfacial contact area in biphasic gas-

liquid systems can allow for reactions unsuccessful in batch synthesis to be accelerated in flow, and as a result of this large gas-liquid interfacial area, mass transfer is enhanced.²¹⁵ Furthermore, the use of a mass flow controller allows for precise control over reaction stoichiometry, while efficient mixing can be reached due to the creation of vortices, which also increases the interfacial area.

With this in mind, a collaborative investigation with the Noël group into adapting the oxidative esterification step from batch to flow conditions was conducted. To avoid potential clogging complications, an adjustment in reaction conditions was required. Encouragingly, in batch, DBU was identified as a suitable substitute for insoluble Cs_2CO_3 , delivering comparable yields in a homogeneous mixture, as required for flow. The Noël group conducted extensive optimisation studies before reaching the final conditions. A liquid feed containing the desired malononitrile, nucleophile, and DBU, was mixed with an O_2 feed by means of a T-mixer, and with a residence time (t_R) of 33 min, access to esters **111**, **112**, and **131** was possible in high yields (**Scheme 94**). Using these conditions, the crucial oxidative esterification step could be easily scaled up to 5 mmol scale, giving **111** in 71% yield (1.6 g, 46% yield over three steps).

A Oxidative esterification/amidation in flow – scope

B Scale-up synthesis of $\beta^{2,2}$ -amino ester – 5 mmol scale


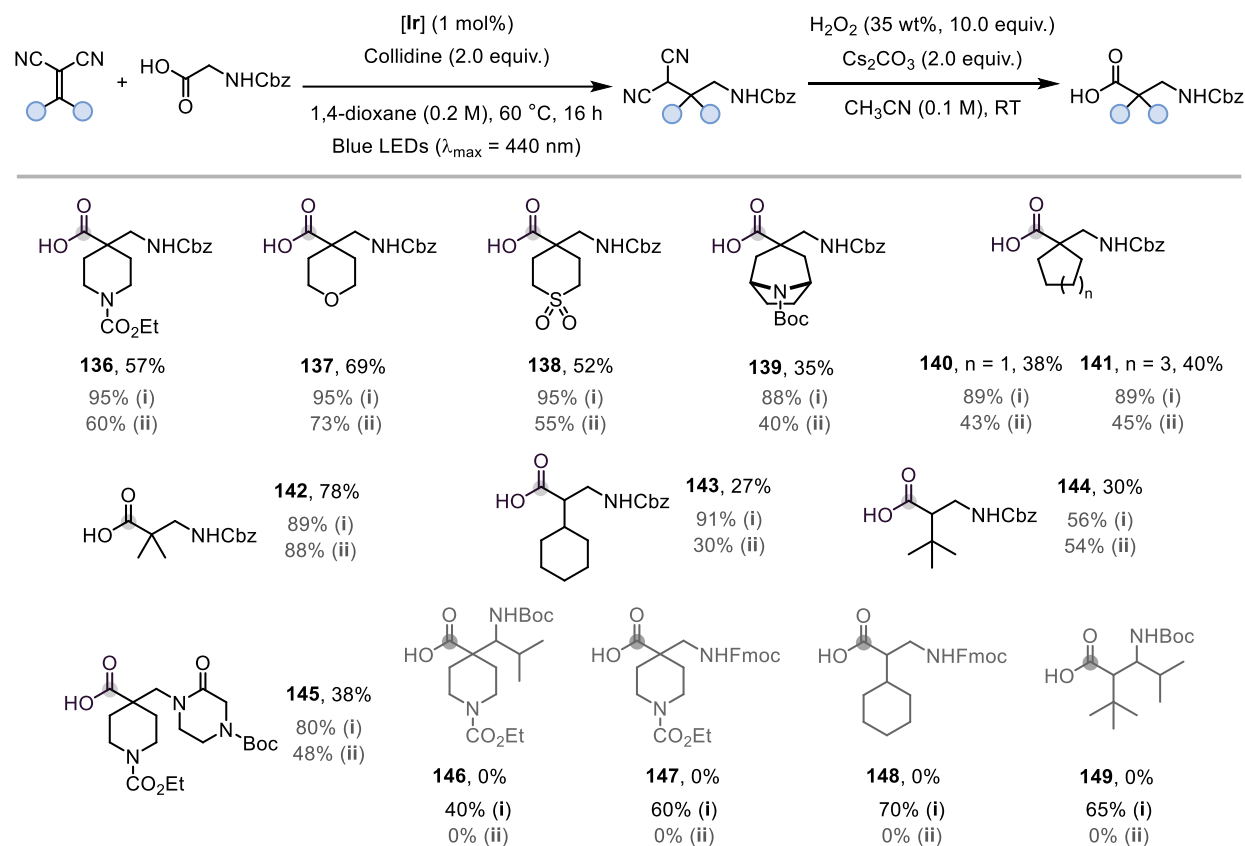
Scheme 94: work by the Noël group; scope & scale-up of oxidative esterification using flow conditions.

A.3.2.2 Alternative Approaches to the Oxidative Esterification

To broaden the range of applications for the approach and to provide an alternative batch procedure, a method to directly access *N*-protected β -amino acids was explored. Recently, Sun and co-workers reported the oxidative hydrolysis of sugar-based α -substituted propanedinitriles *via* an acyl cyanide intermediate.²¹⁶

Using aqueous H₂O₂ (35% (w/w) in H₂O (10.0 equiv.)) as a mild oxidant in the presence of Cs₂CO₃ (2.0 equiv.), it was possible to obtain various $\beta^{2,2}$ -amino acids with (hetero)cyclic motifs in varying yields (**136-141**) (**Scheme 95**). Interestingly, for compound **138**, derived from 4-thianone, the oxidative conditions were sufficient to transform it into the corresponding sulfone product. Furthermore, the method tolerates the use of acyclic ketones like **142** as malononitrile precursors, in addition to aldehydes (**143** and **144**), which were formed in good yields. In an effort to increase further the molecular complexity, Cbz-glycine was exchanged in the Giese-type reaction for an unnatural amino acid containing a piperazinone core. After oxidative hydrolysis, the highly polar amino acid **145** was obtained in 38% yield. Notably, substrates containing Fmoc protecting groups could not be tolerated,

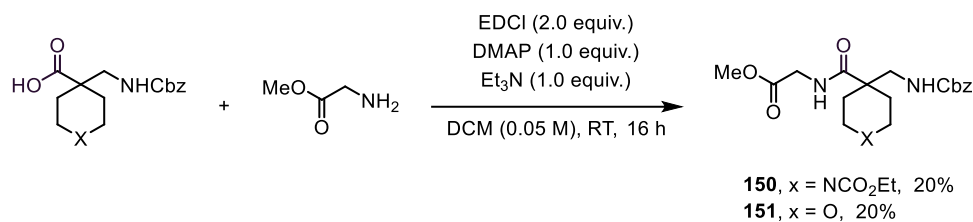
resulting in partial cleavage of the group as seen in **147**, or decomposition of the product (**148**). Compound **149** could not be isolated and showed signs of epimerization.



Scheme 95: synthesis of β -amino acids.

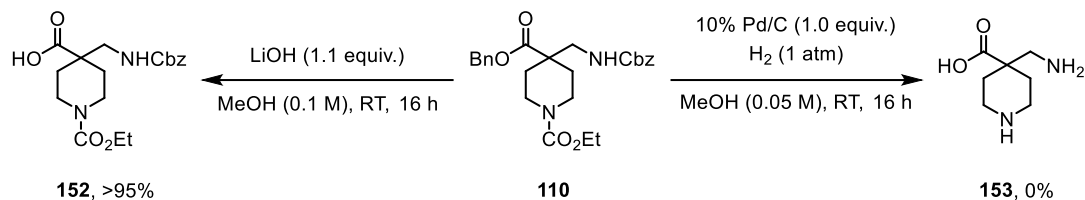
A.3.3 Deprotection & Derivatisation Attempts

Incorporation of these hindered $\beta^{2,2}$ -amino acids in peptides is known to impact and modulate peptide conformation by forcing the end groups together and inducing the formation of more rigid secondary structures. To obtain sterically hindered small peptides, amide couplings of the β -amino acids were tested with several free amino acid esters, using either EDCI or HATU as the coupling reagent (**Scheme 96**). While *L*-phenylalanine methyl ester could not be successfully incorporated, dipeptides **150** and **151** were formed in a coupling with glycine methyl ester, though in low yields. Further experiments are required to explore the potential application of this methodology for the synthesis of small peptides.



Scheme 96: amide bond formation in hindered $\beta^{2,2}$ -amino acids to form peptides.

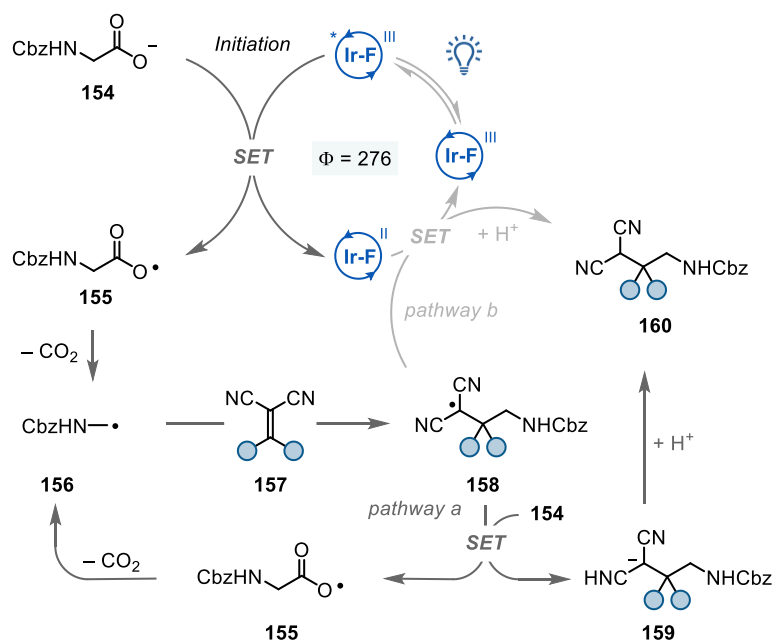
Several attempts to deprotect the carbamate-protected amino acid esters were conducted (**Scheme 97**). Selective deprotection of the benzyl ester in **110** could be carried out using lithium hydroxide, quantitatively forming **152**. A total deprotection using Pd/C and H₂ to form **153** was initially unsuccessful and resulted in decomposition, however, more experiments are required for better insight.



Scheme 97: deprotection of $\beta^{2,2}$ -amino ester **110** to form either **152** or **153**.

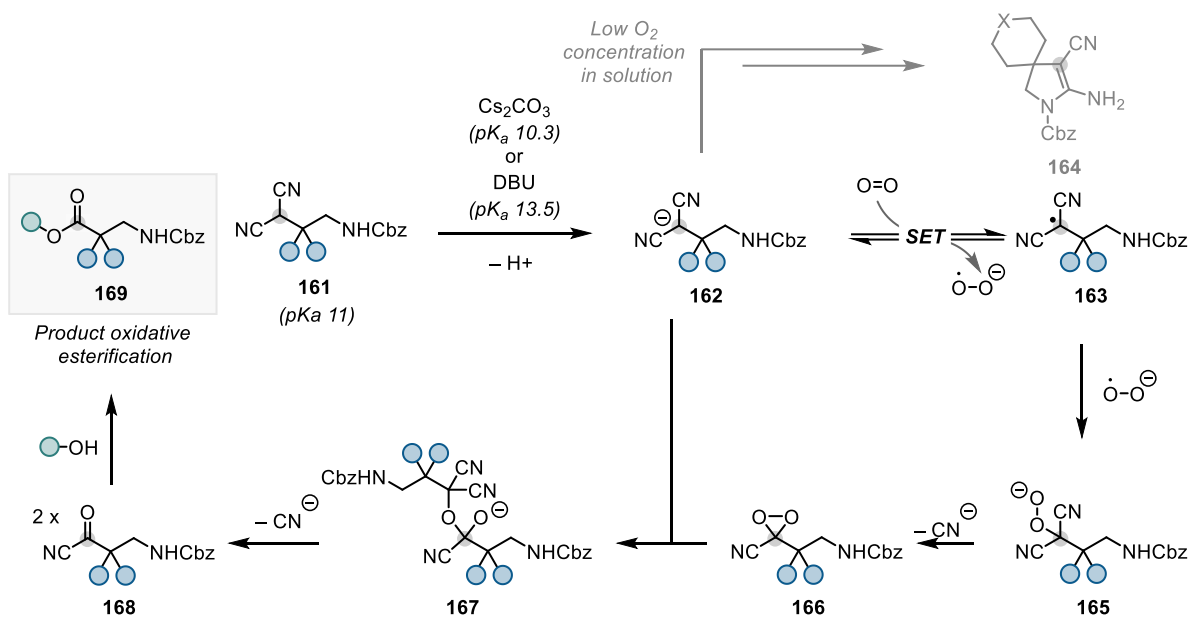
A.3.4 Mechanistic Studies

A plausible mechanism for both steps is as follows (**Scheme 98**). Based on the measured quantum yield ($\Phi = 276$), the Giese-type reaction should proceed *via* a light-initiated radical-chain mechanism. The process begins with the reductive quenching of the excited photocatalyst ($^*\text{Ir-F}^{\text{III}}$, $^*E_{1/2} = +1.21 \text{ V vs SCE in CH}_3\text{CN}$) by the corresponding α -amino carboxylate species **154** ($E_{1/2} = +0.95 \text{ V versus SCE in CH}_3\text{CN}$) generating an acyloxy radical (**155**).^{217,218} This swiftly undergoes decarboxylation to give a nucleophilic α -amino radical (**156**). Addition of this to a highly electrophilic alkylidenemalononitrile (**157**) delivers stabilised tertiary radical intermediate **158**. The latter can react *via* two pathways: either **158** undergoes a SET with α -amino carboxylate **154**, providing species **155** and anion **159**, thus propagating the radical chain, or **158** can undergo SET with the reduced photocatalyst (Ir-F^{II} , $E_{1/2} = -1.37 \text{ V vs SCE in CH}_3\text{CN}$), to close the photocatalytic cycle and form anion **159**. Lastly, protonation of **159** results in the formation of β -quaternary malononitrile species **160**.



Scheme 98: proposed mechanism for the photo-mediated Giese-type reaction.

A possible mechanism for the oxidative esterification/amidation can be described as follows, based on the work of Lear and Hayashi (**Scheme 99**). First, deprotonation of malononitrile **161** facilitated by either Cs₂CO₃ (pK_a = 10.3 in H₂O) or DBU (pK_a = 13.5 ± 1.5 in H₂O) gives stabilised anion **162**.²¹⁹ Here, an insufficient concentration of oxygen will lead to the preferential formation of spirocycle **164**. With sufficient O₂ saturation, **162** undergoes SET with triplet oxygen (³O₂), forming a superoxide anion and radical **163** which react together in a radical-radical coupling to give peroxide **165**. The latter undergoes a 3-exo-tet intramolecular cyclisation with expulsion of cyanide, providing dioxirane **166** which, in turn, can react with another molecule of carbanion **162**, yielding tetrahedral intermediate **167**. This then collapses, leading to the formation of two equivalents of acyl cyanide **168**. This then functions as an activated ester which undergoes nucleophilic substitution at the carbonyl via addition-elimination with the desired nucleophile, providing the targeted β^{2,2}-amino ester **169**.



Scheme 99: proposed mechanism for the oxidative esterification/amidation.

A.4 Outlook & Future Aspirations

In summary, a straightforward, two-step approach was realised for the construction of quaternary $\beta^{2,2}$ -amino acid derivatives, using easily accessible ketones, malononitrile, and α -amino acids as reagents. This methodology accommodates the incorporation of bulky (hetero)cyclic and acyclic substituents at the β -position and facilitates the formation of monosubstituted β^2 -amino acids when ketones are replaced with aldehydes. Furthermore, with adjustments to the final step of the approach, selective formation of β -amino esters, β -amino amides, or *N*-protected β -amino acids is possible. To address challenges in adapting the oxidative esterification step to higher scales, a collaboration was conducted to develop a continuous-flow process, ensuring dependable and scalable access to α -quaternary $\beta^{2,2}$ -amino esters on gram scale.

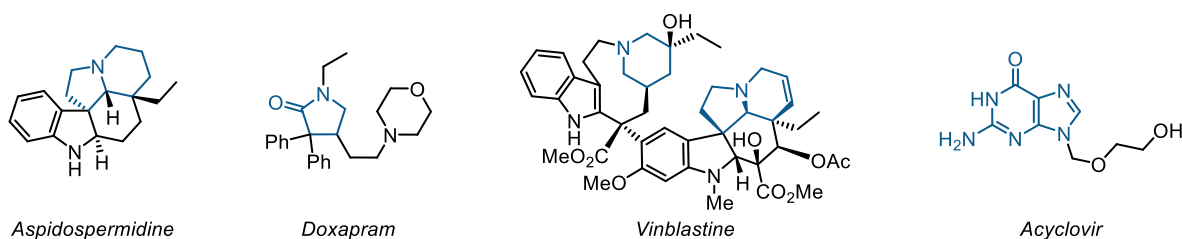
Moving forward, future aspirations concerning the project are to optimise the method to tolerate the use of amino acids bearing more functionality. Additionally, implementing the photoreaction into a continuous flow process would be beneficial as this would allow for a telescoped strategy of the two key reactions. Furthermore, initial investigation into synthesizing dipeptides containing the $\beta^{2,2}$ -amino acid derivatives resulted in poor yields. Therefore, it would be highly beneficial to continue searching for the optimal conditions to construct these sterically hindered di- or tripeptides. This could be simply achieved by screening additional amide bond-forming conditions.

Ultimately, the addition of nucleophilic radicals to electron-poor Michael acceptors (Giese reaction) is a promising approach to synthesize nitrogen-containing compounds bearing quaternary centres. Leveraging the high electrophilicity of the malononitrile component (or other activated methylene compounds) in Giese-type reactions then using derivatisations – such as oxidation – to convert it into a more useful synthetic handle is likely to yield more interesting results in the future. Moreover, the radical reaction partners could be derived from something other than amino (or carboxylic) acids, which could further expand the scope of the reaction. The exceptional electrophilicity of active methylene-derived Michael acceptors could even be exploited further, e.g., by combining the *aza*-Michael addition with oxidation.

IIB. Modular Construction of Polar Spirocycles

B.1 Introduction

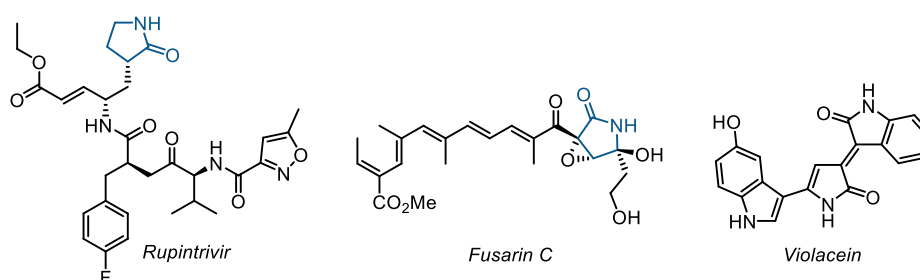
Azaheterocycles, a class of organic compounds that contain one or more nitrogen atoms within a heterocyclic ring, have garnered significant attention within the field of medicinal chemistry and drug development. These structures are widely found in nature and play a crucial role in many biological processes, serving as prominent scaffolds in bioactive molecules due to their diverse properties and applications. This is demonstrated by the prevalence of *N*-heterocycles in most pharmaceuticals and agrochemicals (**Scheme 100**). Biologically active compounds often feature *N*-heterocycles that can mimic the structure of key biomolecules such as nucleic acids or amino acids. This can enable them to interact with biological targets in a similar manner to endogenous molecules, facilitating binding and biological activity. *N*-heterocycles typically contain various functional groups, e.g., amines, amides, ethers, and carbonyls. These functional groups contribute to the compound's ability to readily form hydrogen bonds, e.g., with DNA, which is in part why azaheterocyclic agents exhibit anti-cancer properties.²²⁰ Additionally, they can facilitate coordination to metal ions, or engagement in other types of interactions with biological targets.



Scheme 100: Bioactive compounds containing azaheterocycles.

Many *N*-heterocycles display favourable pharmacokinetic properties, such as good oral bioavailability and metabolic stability, making them appropriate candidates for drug development. In 2014, Njardarson and co-workers presented the first comprehensive investigation on the occurrence of nitrogen heterocycles in FDA-approved drugs.¹⁶⁵ Of the 1086 small molecule drugs studied, 84% contained at least one nitrogen atom, with 59% of those containing a nitrogen heterocycle. Additionally, in the 640 unique drugs studied containing a nitrogen heterocycle, the most common structure is piperidine (found in 72 drugs), followed by pyridine and piperazine (62 and 59, respectively). The fourth and fifth most common are cephem, a β -lactam core (41 total) and pyrrolidine (37 total, and the only non-aromatic five-membered ring in the top 10).

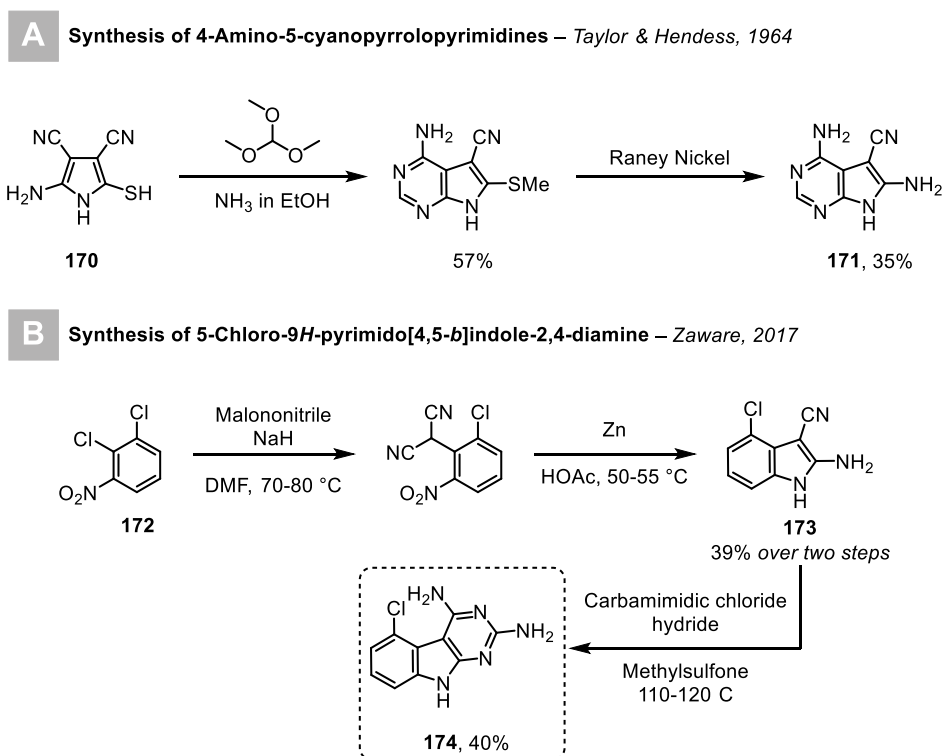
In particular, polar molecules containing pyrrole or pyrrolidine scaffolds frequently function as pivotal pharmacophores, with extensively documented biological activities, including antibacterial, antiviral, anti-inflammatory, and anti-cancer. The presence of a pyrrolidine/pyrrole motif in a drug has the potential to boost aqueous solubility and enhance other physiochemical properties, while also serving as an integral part of the pharmacophore. The NH group can act as a hydrogen bond donor, and when its NH is blocked, the nitrogen atom can function as a hydrogen bond acceptor with a target protein. For example, the peptidomimetic antiviral drug Rupintrivir, initially developed as a rhinovirus protease inhibitor for the most common viral infection causing the common cold, was investigated for the 2019 coronavirus SARS-CoV-2 (**Scheme 101**).²²¹ The drug works by targeting and inhibiting a viral enzyme called 3C protease, preventing the virus from replicating and spreading within the host cells. Substituted pyrrolidone scaffolds have been found extensively in natural products and biologically active compounds. For example, the naturally occurring bis-indole pigment Violacein exhibits antibiotic properties, and fusarin C is a potential HIV integrase inhibitor candidate.^{222–224} Additionally, 2-pyrrolidones, which are γ -lactams, have been used as to access substituted γ -lactams, as well as pyrrole and pyrrolidine derivatives.



Scheme 101: bioactive molecules containing the pyrrolidine/pyrrolidone/pyrrolinone scaffold.

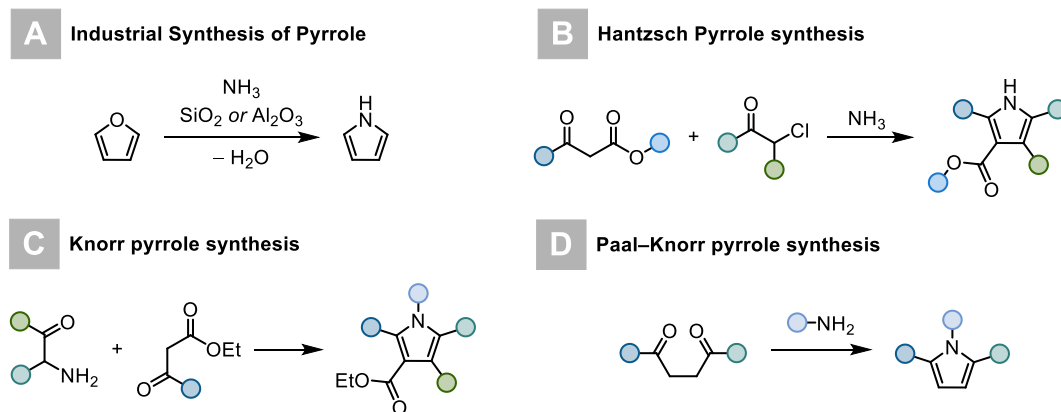
Pyrrole derivatives are also often used as building blocks to access complex fused ring systems. For example, 2-amino-3-cyanopyrroles are recognized for their extensive versatility as precursors to various heterocycles, such as pyrrolopyrimidines, pyrrolopyridines, and pyrrolopyrimidinones. As early as 1964, Taylor and co-workers described the synthesis 4-amino-5-cyanopyrrolo[2,3-*d*]pyrimidines, reported to be structurally related to bioactive molecules Tubercidin and Toyocamycin (**Scheme 102A**).²²⁵ This was accomplished through the treatment of pyrrole derivative **170** with trimethyl orthoformate and a solution of ammonia in EtOH, followed by desulfurization with Raney Ni, providing the desired pyrrolopyrimidine **171** product in moderate yield. More recently, Zaware *et al.* reported the synthesis of intermediate 5-chloro-9*H*-pyrimido[4,5-*b*]indole-2,4-diamine **174** from 2,3-

dichloronitrobenzene (**172**).²²⁶ Interest of this class of molecules grew after a seminal paper by Traxler *et al.* reported a series of *N*-substituted phenyl-9*H*-pyrimido[4,5-*b*]indoles as inhibitors of tumour growth receptors.^{227,228} **Scheme 102B** shows the synthetic route: **172** undergoes NaH-induced nucleophilic aromatic substitution with malononitrile, followed by Clemmensen reduction and a 5-*exo*-dig cyclisation to give the 2-amino-3-cyanopyrrole **173**. The desired pyrimidine ring is formed by condensation with carbamimidic chloride hydride.



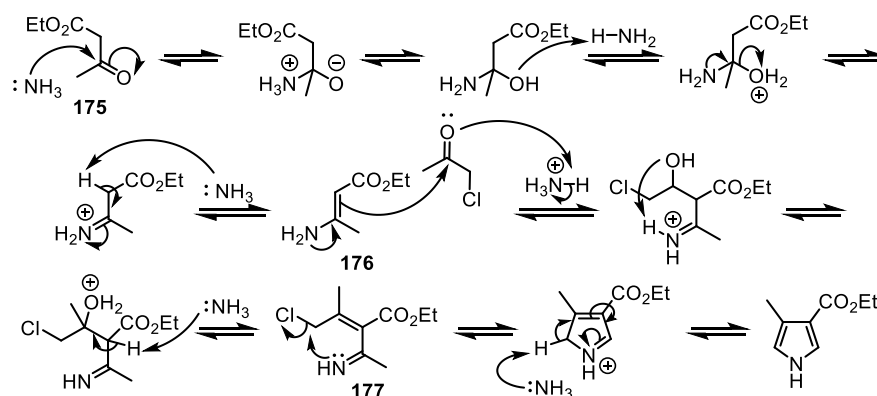
Scheme 102: synthesis of cyanopyrrolo[2,3-*d*]pyrimidine derivatives: A) *via* cyclisation with trimethyl orthoformate and ammonia; B) *via* condensation with carbamimidic chloride.

Many synthetic methods have been established for the construction of pyrroles (**Scheme 103**). Industrially, pyrrole is prepared by treating furan with ammonia in the presence of solid acid catalysts SiO_2 and Al_2O_3 (A). The most common methods used include the classical Hantzsch pyrrole synthesis (B), Knorr (C) and Paal-Knorr synthesis (D).



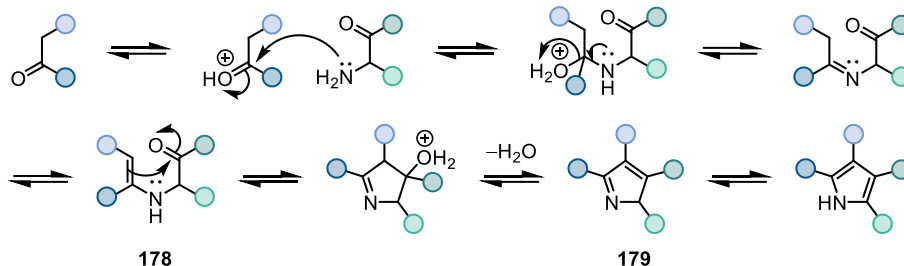
Scheme 103: typical methods to synthesize pyrroles.

In the Hantzsch pyrrole synthesis, named after Arthur Rudolf Hantzsch, an β -ketoester reacts a primary amine, typically ammonia, and an α -haloketone. In the mechanism, the β -ketoester **175** is attacked by the amine to form enaminone **176**, which subsequently attacks the carbonyl carbon of the α -haloketone (**Scheme 104**). After the elimination of H_2O , the resulting imine species **177** undergoes an intramolecular nucleophilic attack, and after elimination of hydrogen then rearrangement, the substituted pyrrole is formed.



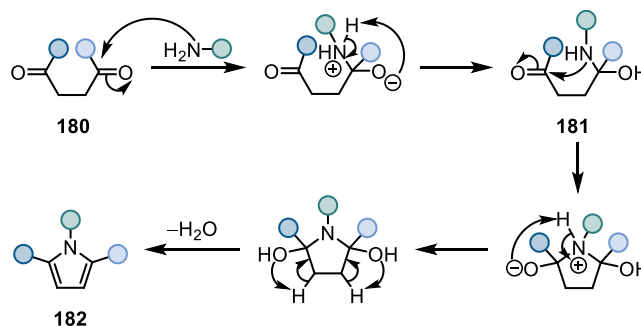
Scheme 104: mechanism of the Hantzsch pyrrole synthesis.

The Knorr method involves the condensation of an α -aminoketone or α -amino- β -ketoester with a ketone or ketoester.²²⁹ The reaction requires the presence of an acid or base catalyst to facilitate the condensation and cyclization steps, typically zinc and acetic acid. The mechanism involves first the condensation of the amine and ketone, producing an imine which subsequently tautomerizes to enamine **178** (**Scheme 105**). Then, this enamine intermediate undergoes cyclisation onto the adjacent carbonyl, and water is removed. The desired pyrrole is obtained after isomerisation of **179**.



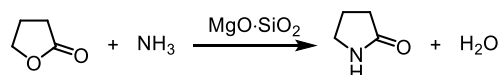
Scheme 105: mechanism of Knorr pyrrole synthesis.

Similarly, the Paal-Knorr synthesis, originally reported as a method to obtain furans, has been adapted for the preparation of pyrroles and has been widely used because of its straightforwardness and effectiveness. The reaction involves an acid-catalysed condensation of alkyl amines with 1,6-dicarbonyl compounds, however various modifications have been reported since.²³⁰ A decade after Paal and Knorr individually published their routes, V. Amarnath *et al.* investigated a possible mechanism (**Scheme 106**): The carbonyl of **180** is attacked by the amine, forming hemiaminal **181**.^{231,232} This hemi-aminal intermediate then undergoes cyclisation in the rate-determining step via attack of the amine to the carbonyl, followed by dehydration to give the desire pyrrole product **182**. In the classical Paal-Knorr pyrrole synthesis, reaction times can be excessive (a minimum of 12 hours), however this can be drastically shortened using microwave irradiation.^{233]}



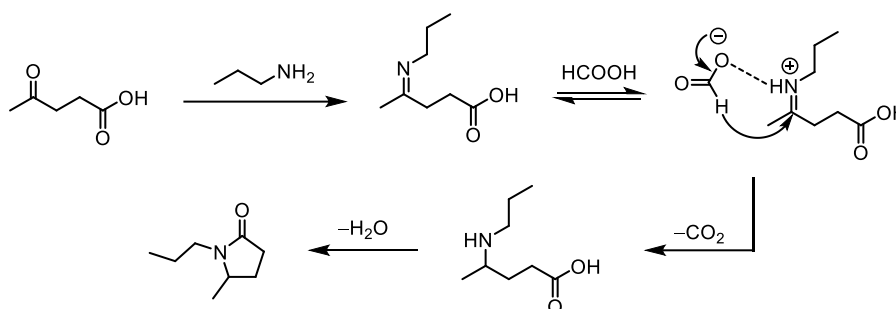
Scheme 106: mechanism of Paal-Knorr pyrrole synthesis.

Similarly to pyrroles, pyrrolidone (or pyrrolidinone) scaffolds are prominently featured in bioactive molecules, therefore synthetic methods to obtain these structures have been well-documented. The simplest form, 2-pyrrolidone, is industrially formed through the treatment of aqueous gamma-butyrolactone with ammonia in the presence of magnesium silicate catalysts (**Scheme 107**).²³⁴ Typically, high temperatures of approx. 270 °C and a pressure range of 0.4–1.4 MPa are required.



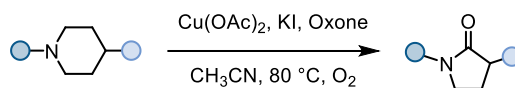
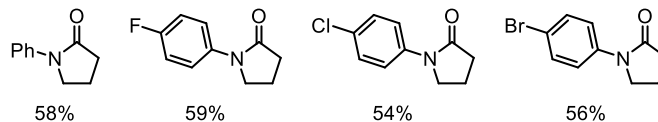
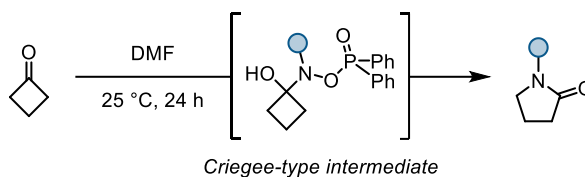
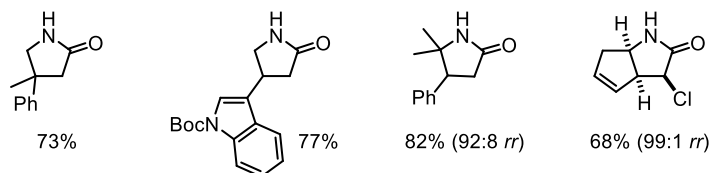
Scheme 107: Industrial synthesis of 2-pyrrolidone using magnesium silicate catalysts.

It is also possible to access *N*-substituted-5-methyl-pyrrolidones from levulinic acid, formic acid and a primary amine by reductive amination and cyclisation.^{235,236} This reaction proceeding via the Leuckart-Wallach mechanism – depicted in **Scheme 108** – is well documented. First, the amine undergoes a nucleophilic attack on the carbonyl group of levulinic acid, and after elimination of H₂O, an imine is formed. Hydrogenation of this intermediate then occurs in the presence of formic acid, forming CO₂ and H₂O as by-products and the desired lactam after cyclisation.



Scheme 108: mechanism of the Leuckart-Wallach reaction.

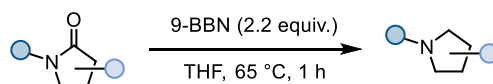
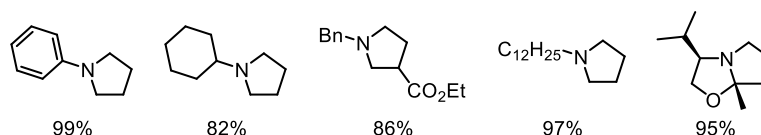
In 2019, Fan and co-workers reported the selective synthesis of pyrrolidin-2-ones via the oxidative ring contraction and deformylative functionalisation of piperidine derivatives (**Scheme 109A**).²³⁷ Using Cu(OAc)₂ and Oxone as the oxidant, the group could convert thirteen piperidine structures to the corresponding functionalised pyrrolidinones in moderate yields. Conversely, ring expansion has also been implemented for the construction of pyrrolidinones. For example, Wahl and co-workers developed a method for the stereospecific nitrogen insertion of cyclobutanones using amino diphenylphosphinates (**Scheme 109B**).²³⁸ Mechanistic studies suggest that the reaction proceeds *via* an aza-Baeyer-Villiger pathway, involving addition of the hydroxylamine phosphinate at the carbonyl and collapse of the tetrahedral intermediate, leading to ring expansion and expulsion of the phosphinate.

A Synthesis of Pyrrolidin-2-ones via Oxidative Ring Contraction – Fan, 2019

Selected examples

B Stereospecific Nitrogen Insertion of Cyclobutanones – Wahl, 2022

Selected examples


Scheme 109: A) oxidative ring contraction of piperidine derivatives; B) ring expansion of cyclobutanones *via* an aza-Baeyer–Villiger mechanism.

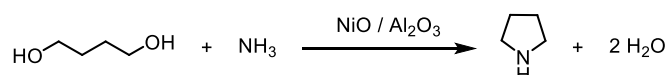
Pyrrolidones also play an important role in the synthesis of another 5-membered cycle: pyrrolidines. Pyrrolidines can be obtained through the reduction of the former using mild reducing agents, such as organoboranes.²³⁹ In 1999, Singaram and co-workers reported the chemoselective reduction of 5-membered lactams using 9-BBN, converting them to the corresponding pyrrolidine motif, while preserving the presence of other functional groups such as esters (**Scheme 110**).²⁴⁰

Singaram, 1999


Selected examples


Scheme 110: synthesis of pyrrolidines through the reduction of pyrrolidones.

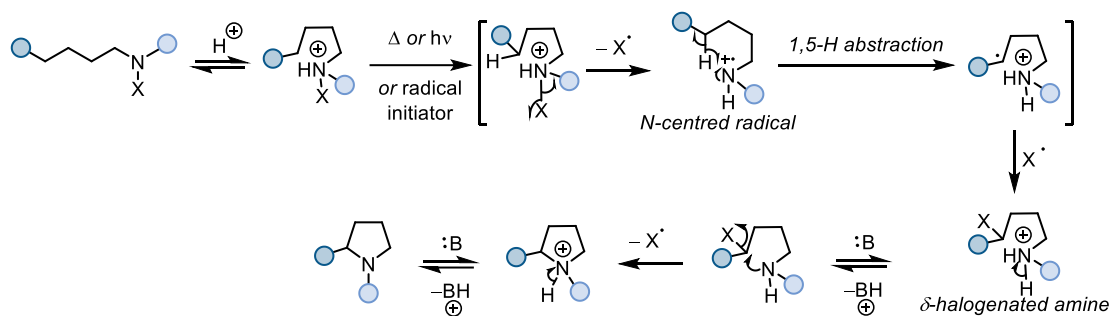
Additional methods to form pyrrolidines include the Hofmann–Löffler–Freitag (HLF) reaction, [3+2] cycloadditions, hydrogenation reactions, and reductive amination. Industrially, pyrrolidine is made by reacting 1,4-butanediol and ammonia in the presence of a nickel oxide catalyst supported on alumina (**Scheme 111**). High temperatures (165–200 °C) and a pressure of approximately 20 MPa are also required. It is also possible to form pyrrolidine from pyrrolidone via amide reduction or transition metal-mediated deoxygenative hydrogenation.^{241,242}



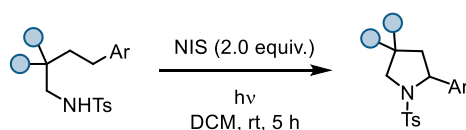
Scheme 111: industrial synthesis of pyrrolidine using a nickel oxide catalyst on alumina.

The HLF reaction is frequently used to obtain pyrrolidines.^{243–245} The method involves the thermal or photochemical decomposition of an *N*-halogenated amine in the presence of a strong acid, typically concentrated sulfuric acid or TFA. Mechanistically, it proceeds *via* a radical chain reaction (**Scheme 112A**): first, the *N*-halogenated amine is protonated to give the corresponding ammonium salt. Using either light irradiation, heat or an initiator, a nitrogen-centred radical is formed through homolytic cleavage of the N-X bond. This forms a δ -halogenated amine, which cyclises in the presence of a base to form the desired pyrrolidine. In 2016, the HLF reaction was utilised by Muñiz *et al.* where *N*-Iodosuccinimide was exploited to promote the site-selective intramolecular C-H amination of aliphatic sulfonamides (**Scheme 112B**).²⁴⁶ The reaction is initiated by visible light in the absence of a photocatalyst, providing 17 pyrrolidine products in good yields.

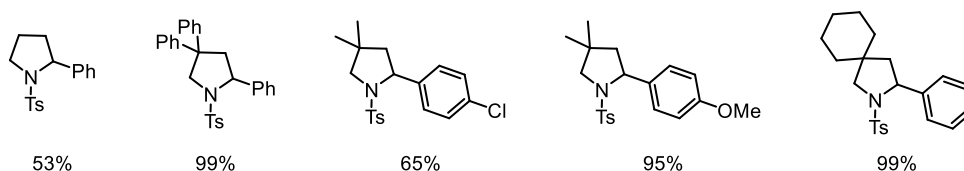
A Hofmann–Löffler–Freitag Reaction – General mechanism



A Intramolecular C-H Amination of Aliphatic Sulfonamides – Muñiz, 2016

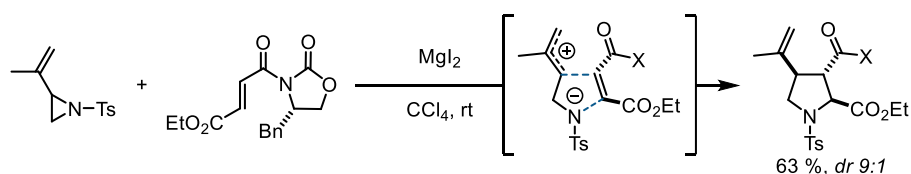


Selected examples



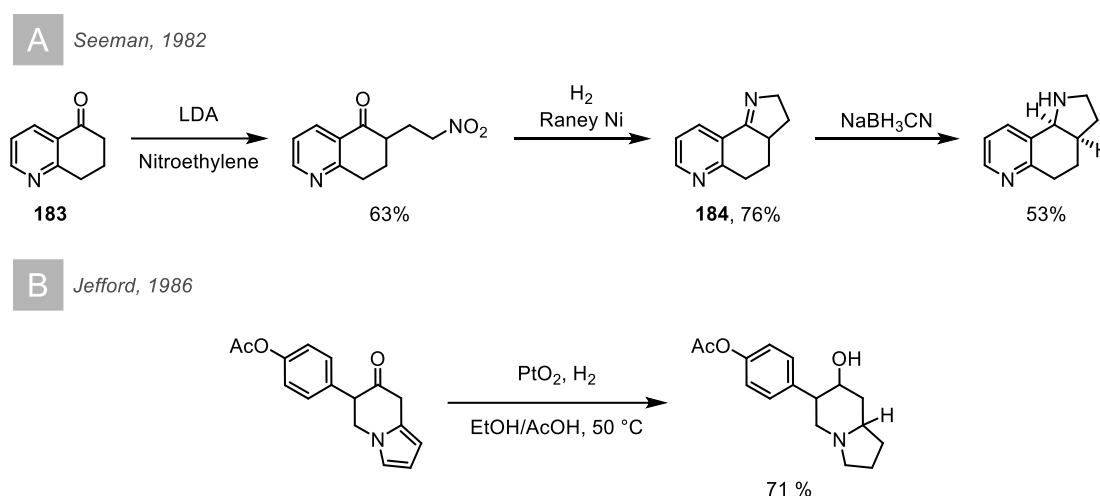
Scheme 112: A) general mechanism of the HLF reaction; B) visible light-catalysed, iodosuccinimide-promoted HLF reaction of sulfonimides.

Another method to synthesize pyrrolidines is by cycloaddition reactions. For example, in 2013 Aggarwal and co-workers proposed the total synthesis of (+)-*allo*-kainic acid via MgI_2 -promoted S_N2' aziridine ring opening/[3+2] cycloaddition (**Scheme 113**).²⁴⁷ The procedure successfully synthesized the desired natural product in 6 steps with an overall yield of 24%. The key ring-opening/ S_N2' cyclisation sequence to form the 2,3,4-trisubstituted pyrrolidine product (63% yield, 9:1 dr), can be seen in **Scheme 113**, with the stereochemistry rationalised based on attack of the ring-opened aziridine on the more accessible *Si* face.



Scheme 113: key MgI_2 -mediated aziridine ring-opening followed by [3+2] cycloaddition for the synthesis of pyrrolidines using vinyl aziridines with Evans' fumarates.

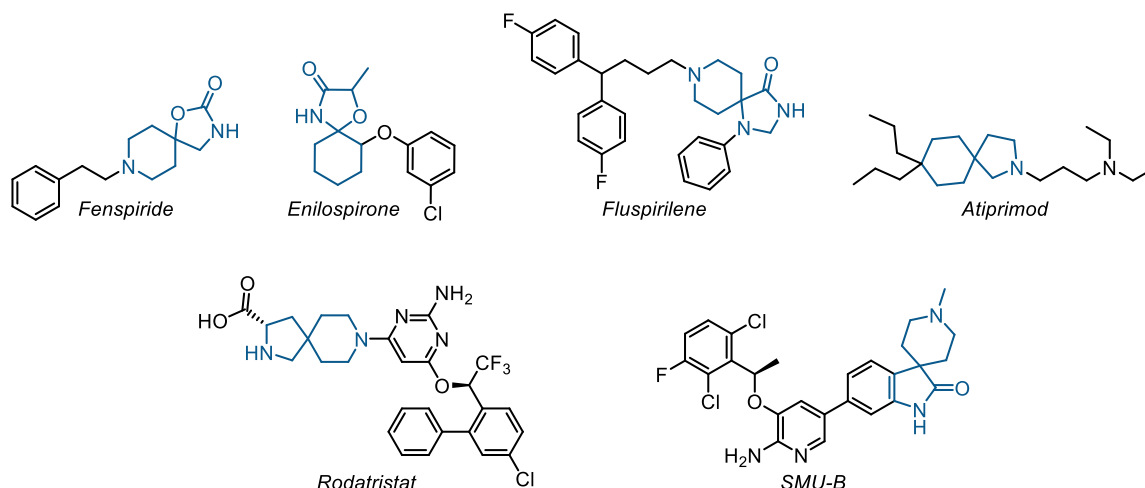
Pyrrolidines can also be formed by catalytic hydrogenation reactions. In 1983, Seeman and co-workers reported the synthesis of a 2,3-annulated tricyclic conformationally constrained nicotine analogue.²⁴⁸ To make the 5-membered heterocycle, an LDA-mediated Michael-type addition of **183** to nitroethylene occurs (**Scheme 114A**). Then, reduction of the nitro group is carried out by catalytic hydrogenation using Raney nickel, and the resulting amine undergoes an intramolecular condensation with the carbonyl group to form imine **184**. Reductive amination of **184** by NaBH₃CN provides the desired pyrrolidine derivative. The direct hydrogenation of pyrrole derivatives has also been reported. For example, in a 1986 publication on the total synthesis of (\pm)-*ipalbidine* by Jefford *et al.*, the reduction of a bicyclic pyrrole system was carried out via PtO₂-catalysed hydrogenation (**Scheme 114B**).²⁴⁹



Scheme 114: A) synthesis of a nicotine analogue developed in Seeman and co-workers *via* catalytic hydrogenation then reductive amination; B) PtO₂-catalysed reduction of a pyrrole derivative.

Typically, these pyrrole/pyrrolidine cores are rigid and planar unsaturated structures, which facilitate control over the molecule's conformation and spatial orientation. However, as mentioned earlier, with the increased popularity of concepts such as "escape from the flatland", or "conformational restriction", the advantages of isosteric analogues that lead to higher F_{sp^3} and enhanced three-dimensionality have been widely reviewed.^{250,251} Increasing saturation has been linked to an increase in metabolic stability, as well as improvements in physicochemical properties, e.g., increased solubility with a higher fraction of sp^3 carbons. In drug discovery, this breakthrough has led to improved success of compounds selected for clinical development. Additionally, with an increase of bonds that can be formed with sp^3 carbons, there is a larger chemical space available to explore – a concept known as increased vectorial functionalisation.

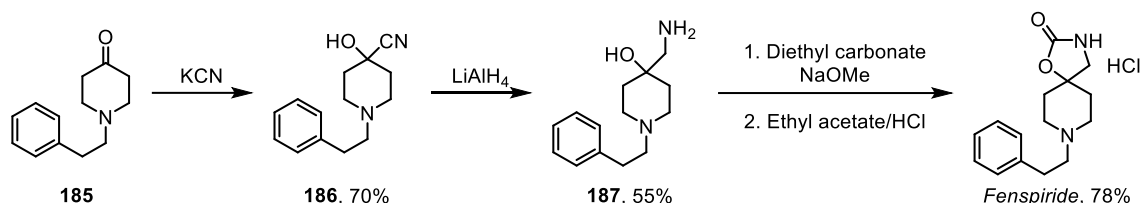
As a consequence of the surge of interest in bioactive compounds with less planarity, the development and preparation of spirocyclic pyrrolidine(s) and derivatives are among the most popular spirocyclic cores.^{252,253} These molecules with increased 3D character serve as sp^3 -rich analogues of 2D aromatics while retaining the pharmacological activities of the aromatic azaheterocycles. Their well-defined spatial orientation enables control over conformation, often resulting in enhanced binding affinities as they can interact with 3D binding pockets more effectively compared to their planar, unsaturated counterparts. Recent development on the isolation and characterisation of these novel structures from natural products, as well as new synthetic methods to obtain spirocyclic motifs have led to their incorporation into molecules for pharmacological applications and in some scenarios, their successful development as commercial drugs (**Scheme 115**). This can be seen in numerous compounds such as Rodatristat – a potent, peripheral inhibitor of TPH1 containing the spirocyclic pyrrolidine motif.²⁵⁴



Scheme 115: bioactive molecules containing pyrrolo-based spirocyclic scaffolds.

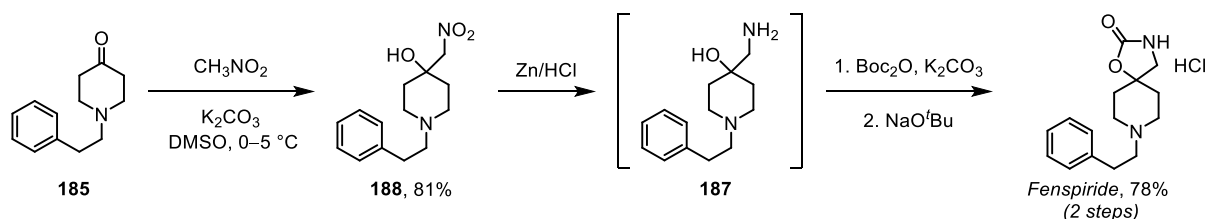
Typically, construction of these spirocycles is exceedingly difficult due to construction of the key quaternary centre – a concept itself considered a challenging task in synthetic organic chemistry.²⁵⁵ Their synthesis often involves two-electron disconnections, with the requirement of multistep and complex strategies. For example, Fenspiride, an anti-inflammatory, anti-allergic and antioxidant drug used to treat bronchial asthma, allergic rhinitis, and other allergy symptoms, was first obtained by Gilbert *et al.* in four steps for the use of bronchodilators, analgesics, and anti-inflammatory agents (**Scheme 116**).^{110,256} Here, harsh conditions were required to construct the key quaternary centre. Treatment of piperidone **185** with KCN gave cyanohydrin species **186**, followed by reduction of the nitrile

group with LiAlH_4 , providing amino alcohol **187**. Cyclisation of **187** is then achieved with diethyl carbonate under reflux, in the presence of freshly prepared sodium methoxide.



Scheme 116: first successful synthesis of Fenspiride by Gilbert in four steps.

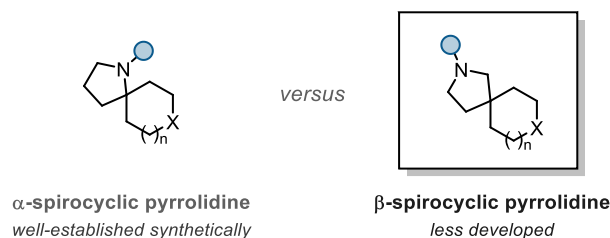
Since the initial synthetic route was proposed, numerous other approaches were published, usually varying in the construction of the amino alcohol, however the majority still comprised of toxic reagents and/or harsh conditions – a detrimental obstacle for commercial success.²⁵⁷ In 2019, a new 4-step route avoiding the use of such materials was proposed by Emcure Pharmaceuticals in collaboration with the University of Pune (**Scheme 117**).²⁵⁷ Nitro-aldol addition (Henry reaction) of **185** with nitromethane was followed by a Clemmensen reduction of the nitro group with Zn in HCl. To avoid purification issues of the free amine after aqueous work-up, a Boc protection was carried out, and the final cyclisation of *N*-Boc-protected **187** could be promoted using NaO^tBu via intramolecular displacement of the *tert*-butoxy group in the carbamate and ring closure, providing fenspiride hydrochloride after treatment with HCl. Using this route, the group were able to synthesise fenspiride on a large scale in relatively mild conditions, starting from 1 kg of **188**, 78% of the product was obtained.



Scheme 117: novel protocol for the large-scale production of Fenspiride in 4 steps.

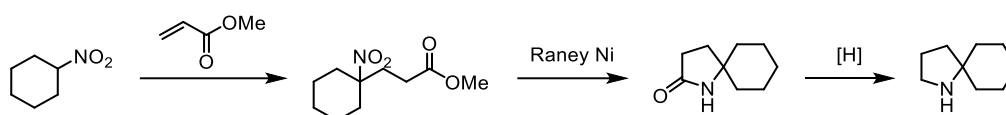
B.1.1 Synthesis of Spirocyclic Pyrrolidines

Over the years, many methods have been developed to construct spirocyclic pyrrolidine/pyrrole derivatives. Generally, these strategies lead to the formation of either α - or β -spirocyclic motifs (**Scheme 118**).



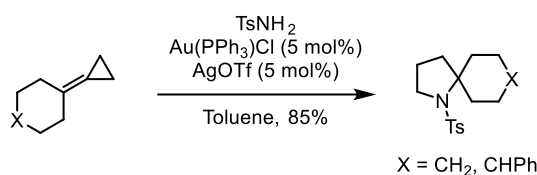
Scheme 118: α - versus β -spirocyclic pyrrolidine structures.

In 1957, the first example and relatively simple method for synthesising an α -spirocyclic pyrrolidine structure was outlined by Moffet, starting with cyclic nitro compounds in a three-step process (**Scheme 119**).²⁵⁸ The first step is a conjugate addition of an alkyl nitro compound with methyl acrylate, followed by reduction of the nitro group to a primary amine, triggering the cyclisation. The resulting amide can be subsequently reduced to the corresponding amine. While straightforward, multigram synthesis of such nitro compounds – which are typically not commercially available – is not safe due to potential explosion hazard.



Scheme 119: seminal work by Moffet on the construction of α -spirocyclic pyrrolidines.

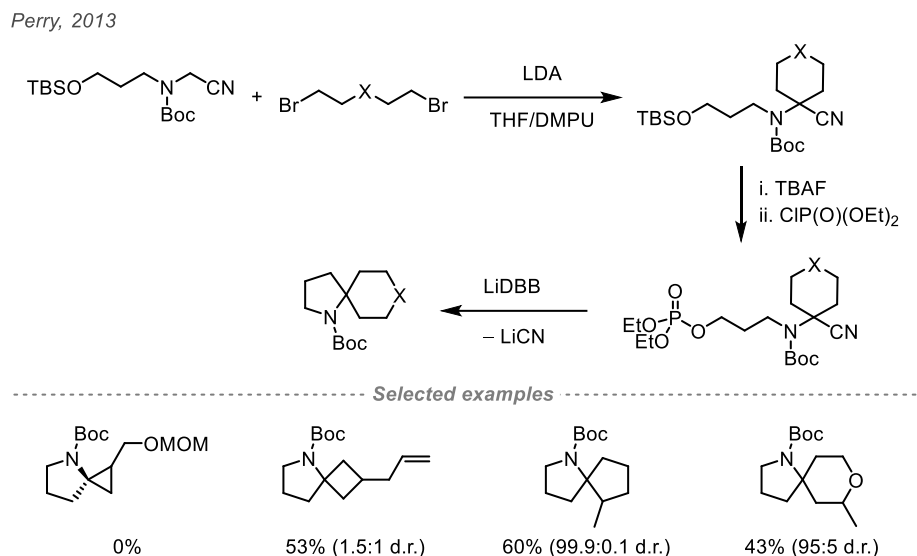
Since then, numerous procedures to construct α -spirocyclic pyrrolidines have emerged. In 2006, Shi and co-workers reported an Au(I)-catalysed reaction of methylene cyclopropanes with sulfonamides (**Scheme 120**).²⁵⁹ The method proceeds *via* a domino ring-opening/ring-closing hydroamination sequence, leading to the formation of two examples of Ts-protected spiropyrrolidines. Limitations, however, arise from the high loading of expensive and not easily accessible Ag(I) and Au(I) catalysts.



Scheme 120: Au(I)-catalysed ring-opening/closing hydroamination of methylene cyclopropanes.

Later, in 2013 Perry *et al.* published a method that allowed for the synthesis of α -spirocyclic pyrrolidines in a reductive cyclisation of *N*-Boc α -amino nitrile derivatives (**Scheme 121**).²⁶⁰ The reaction is mediated by LiDBB (lithium di-*tert*-butyl biphenylide) which is constructed via a double alkylation of aminoacetonitrile derivatives. While reported yields

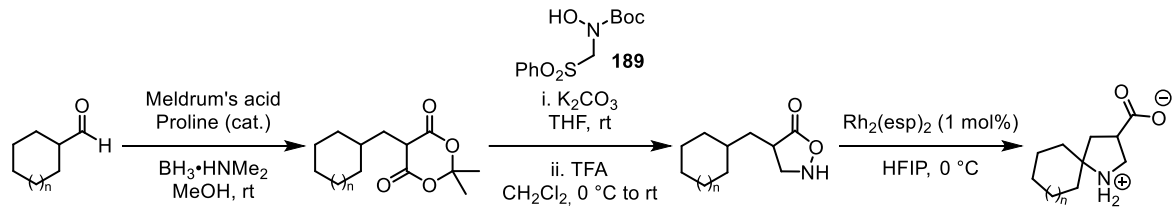
are moderate and diastereoselectivity is very high, strategy is notably lengthy, uses harsh conditions and results in the formation of toxic cyanide waste that requires careful disposal.



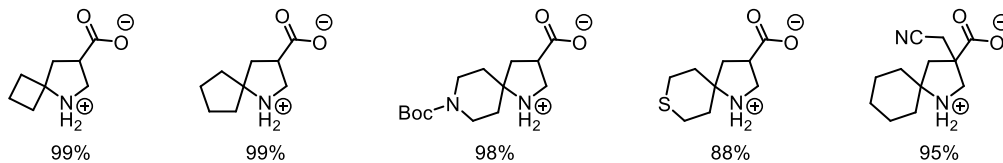
Scheme 121: LiDBB-mediated reductive cyclisation of *N*-Boc α -amino nitrile derivatives.

More recently, in 2019 Shibasaki reported a Rh-catalysed synthesis of unprotected spirocyclic β -prolines and β -homoprolines (**Scheme 122**).²⁶¹ The authors propose the formation of a Rh nitrenoid generated by the N–O bond cleavage of substituted isoxazolidin-5-ones which then undergoes intramolecular C–H insertion into the latter. The required 4-substituted isoxazolidin-5-one substrates are synthesised from cyclic aldehydes in three steps: activation of the aldehyde with Meldrum's acid, followed by a decarboxylative [3+2] cycloaddition with sulfone-amide **189** which was previously developed by the Brière group.²⁶² This is followed by a TFA-mediated deprotection of the Boc group, providing the desired unprotected isoxazolidinone.

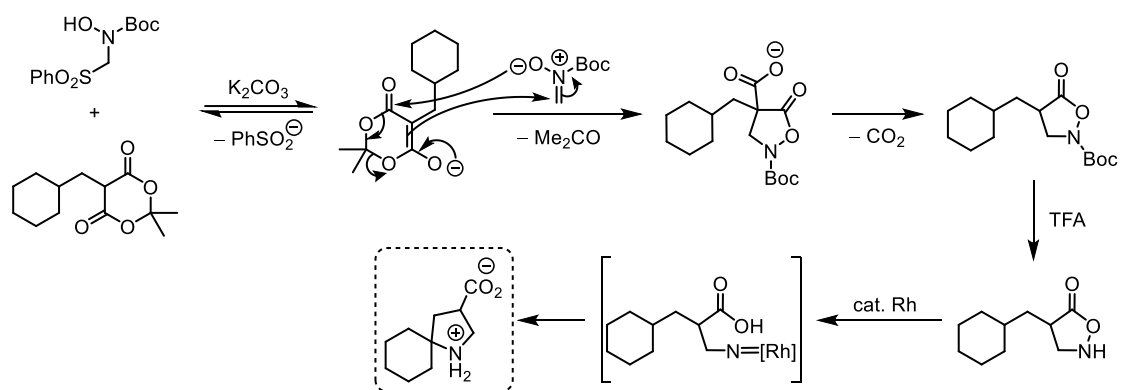
Shibasaki, 2019



Selected examples



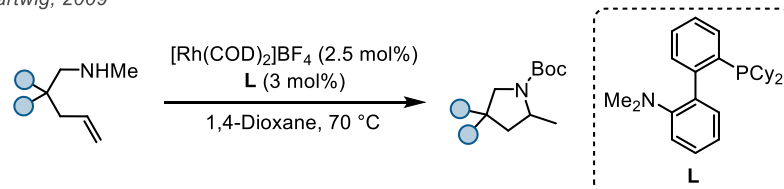
Mechanism



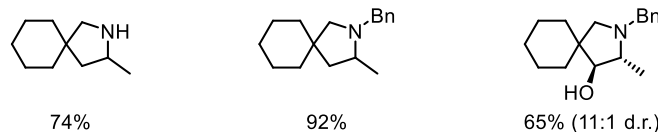
Scheme 122: Rh-catalysed synthesis of unprotected spirocyclic β -prolines and β -homoprolines.

Literature examples on methods to construct β -spirocyclic pyrrolidines are sparse in comparison to α -spirocyclic pyrrolidines. The most typical procedures available centre around hydroamination reactions of terminal alkenes, as demonstrated in 2009 by Hartwig and co-workers where a rhodium complex is utilised to catalyse the intramolecular cyclisation of aminoalkenes (**Scheme 123**).²⁶³

Hartwig, 2009

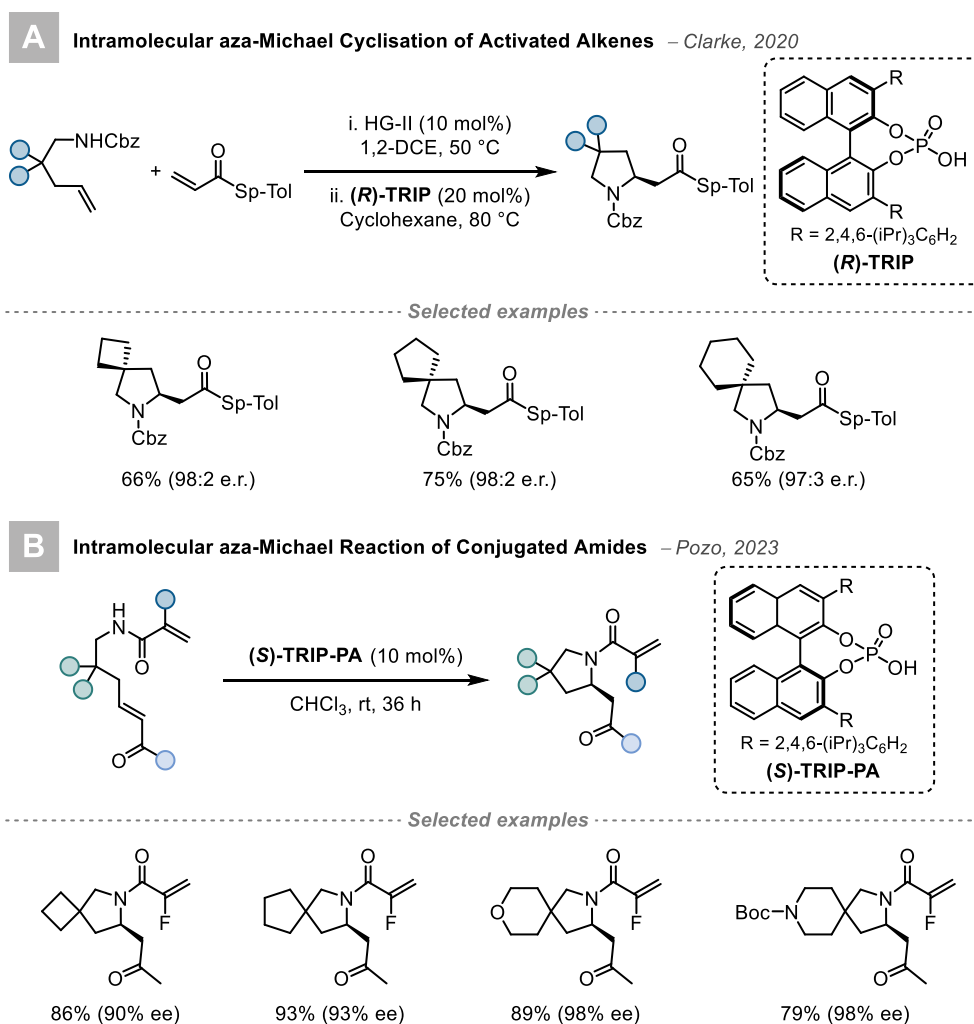


Selected examples



Scheme 123: β -spirocyclic pyrrolidines *via* Rh-catalysed intramolecular cyclisation of aminoalkenes.

More recently in 2020, Clarke and co-workers reported an asymmetric cyclisation of activated alkenes, catalysed by a chiral phosphoric acid, to synthesise spirocyclic pyrrolidine derivatives (**Scheme 124A**).²⁶⁴ The alkenes are prepared by coupling bis-homoallylic amines and a thioacrylate *via* an alkene metathesis reaction with Hoveyda-Grubbs second-generation catalyst (HG-II), to create amines with a pendant olefin. These substrates are ideally poised to undergo intramolecular aza-Michael cyclisation. In order to form the desired spirocycle, however, the linear precursor must already contain a quaternary centre. Similarly, del Pozo and co-workers developed an enantioselective intramolecular aza-Michael reaction of conjugated amides which feature a remote α,β -unsaturated ketone (**Scheme 124B**).²⁶⁵ The aza-Michael addition is catalysed by the chiral phosphoric acid (PA) (*S*)-TRIP, which delivers the chiral pyrrolidine.

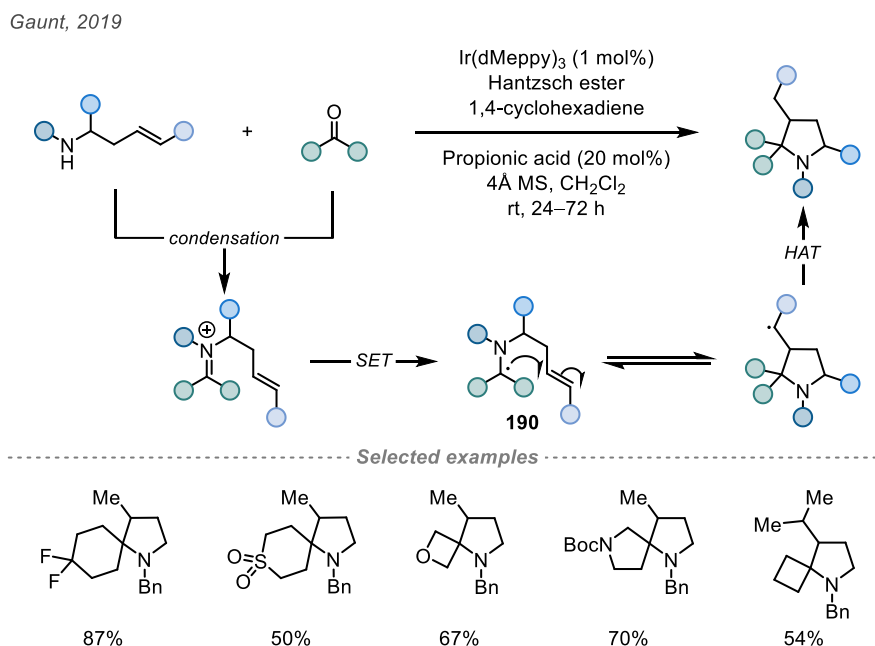


Scheme 124: intramolecular aza-Michael cyclisations to construct β -spirocyclic pyrrolidines.

B.1.1.1 Radical Methods

In recent years, there has been a notable development of mild and versatile radical-based methodologies in organic synthesis, enabling access to a wide array of otherwise difficult to construct structural motifs. While this has also been reflected in numerous reports focusing on single electron disconnection strategies for spirocyclic pyrrolidine synthesis, the predominant emphasis remains on α - over β - derivatives.

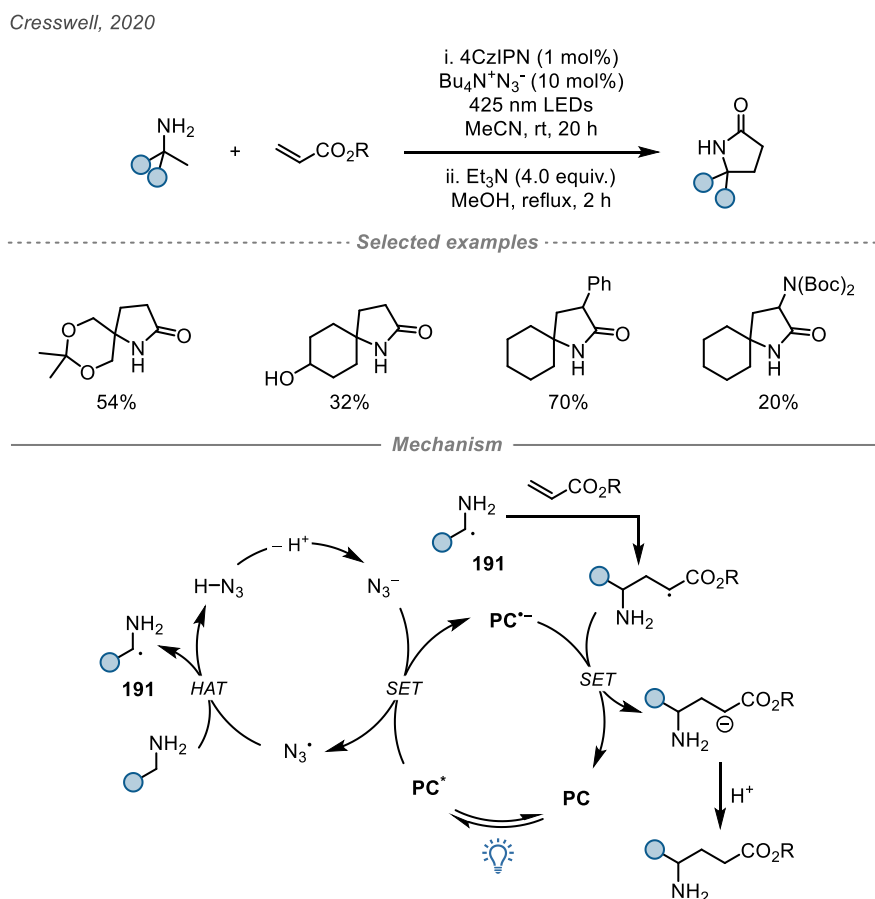
In 2019, Gaunt and co-workers describes a novel method for synthesising complex C(sp³)-rich *N*-heterospirocycles from common aliphatic ketones and aldehydes, as well as alkene-containing secondary amines, *via* visible-light-mediated photocatalysis (**Scheme 125**).²⁶⁶ A highly reducing iridium-based photocatalyst is utilised for the photocatalytic reduction of alkyl iminium ions, forming cyclic tertiary α -amino radicals (**190**). A 5-*exo*-trig cyclisation between the amine and alkene moiety occurs, leading to the substituted pyrrolidine-based spirocyclic scaffold after HAT from 1,4-cyclohexadiene (1,4-CHD). The reduced photocatalyst is regenerated after reduction by the Hantzsch ester.



Scheme 125: visible-light-mediated reduction of alkyl iminiumions and 5-*exo*-trig cyclisation.

One year later, Cresswell and co-workers presented a practical and scalable method for synthesising α,α,α -trisubstituted (α -tertiary) primary amines from unprotected amines and electrophilic Michael acceptors *via* C-H functionalisation (**Scheme 126**).²⁶⁷ These α -tertiary amines are then converted to the corresponding γ -lactam. The authors propose the generation of an azidyl radical *via* oxidation of azide ions (from tetrabutylammonium azide,

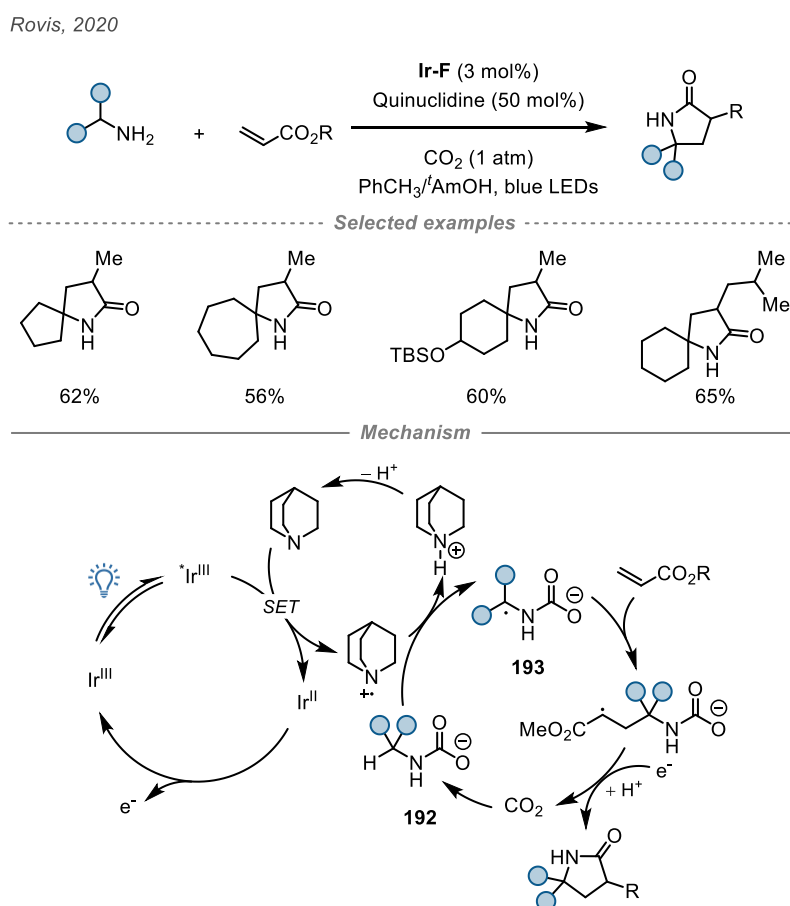
$\text{Bu}_4\text{N}^+\text{N}_3^-$) by the excited photocatalyst. This highly oxidising species undergoes HAT with the $\alpha\text{-C-H}$ bond of the primary amine, forming α -amino radical **191** which undergoes a polarity-matched addition to the Michael acceptor. SET and protonation of the resulting radical species forms the α -tertiary primary amine, which cyclises to the γ -lactam upon exposure to Et_3N . A wide range of synthetically diverse spirocyclic pyrrolidinones could be obtained, and the scalability of the reaction was demonstrated through continuous flow synthesis, highlighting its applicability for large-scale production.



Scheme 126: synthesis of α,α,α -trisubstituted (α -tertiary) primary amines from unprotected amines and electrophilic Michael acceptors *via* C-H functionalisation.

Similarly, in the same year, the group of Rovis proposed a CO_2 -promoted α -alkylation/lactamization of primary aliphatic amines and electron-deficient acrylates (**Scheme 127**).²⁶⁸ The authors describe *in situ* formation of alkylammonium carbamates (**192**) from CO_2 and the primary amine, where CO_2 acts as a temporary protecting group to decrease the nucleophilicity of the NH_2 group, providing an opportunity for functionalisation of less reactive C-H bonds. Central to their approach is the use of electrostatic interactions between the alkylammonium carbamate and a cationic hydrogen atom transfer (HAT)

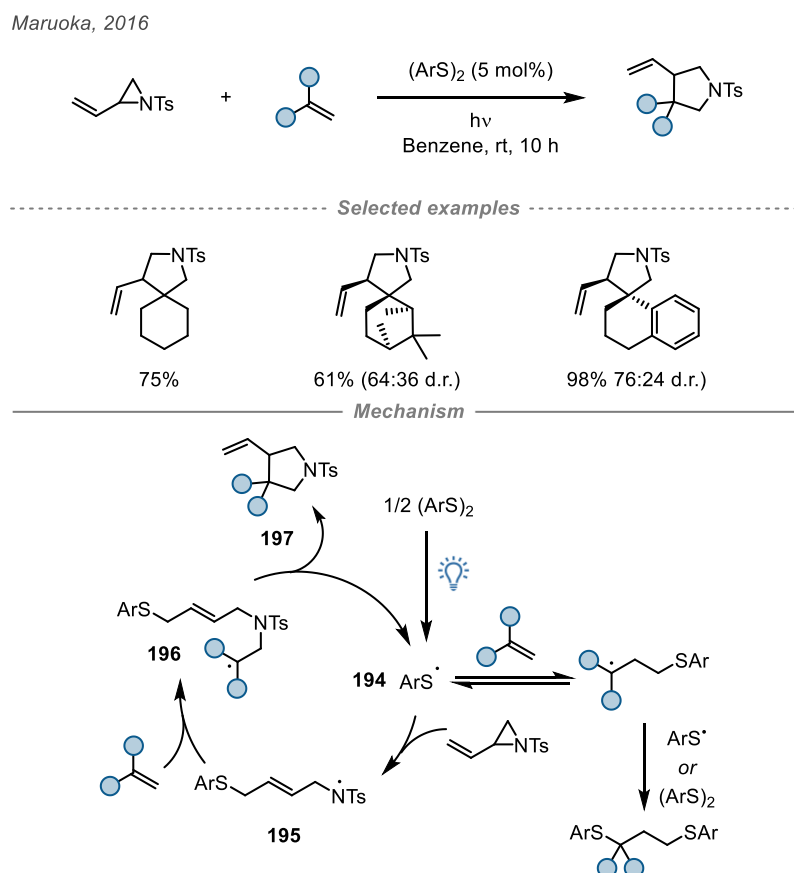
catalyst – the electrostatic attraction between the negatively charged carbamate and the positively charged HAT catalyst (formed *via* SET by the photocatalyst) is hypothesised to facilitate selective α -alkylation/lactamization of the amine (i.e., selectively abstracting the α -C–H bond of the alkylammonium carbamate), forming radical **193**. This species undergoes addition into the Michael acceptor, and after reduction and protonation the desired spirocyclic lactam is formed.



Scheme 127: CO₂-promoted α -alkylation/lactamization of primary aliphatic amines and electron-deficient acrylates.

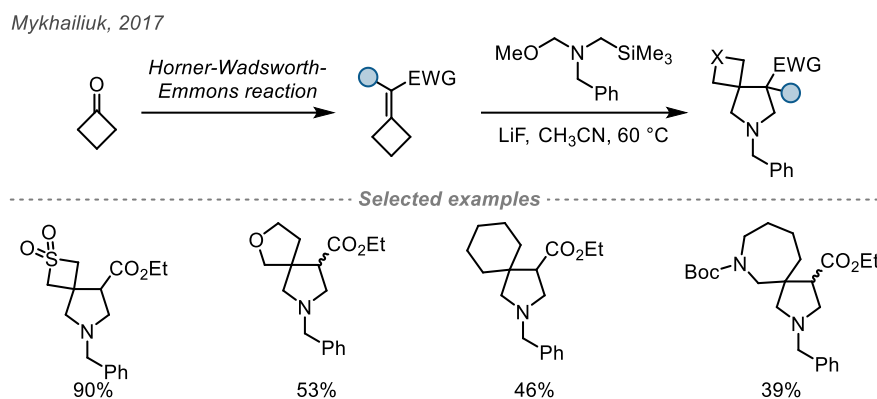
Conversely, the number of radical-based protocols published to synthesise β -spirocyclic pyrrolidines is limited. One example comes from Maruoka and co-workers in 2016 where they developed a novel chiral thiyl photocatalyst for a [3+2]-cyclisation of *N*-tosylvinylaziridines and alkenes (**Scheme 128**).²⁶⁹ The reaction faces challenges due to catalyst degradation, but can be overcome through the use of a sterically demanding thiyl radical catalyst, and unlike transition metal- or Lewis acid-catalysed [3+2] cyclisation reactions, is not limited to electron-deficient alkenes.^{165,270} Mechanistically, after photo-mediated generation of the active thiyl radical catalyst, radical **194** reacts with the

vinylaziridine, forming aminyl radical **195** which reacts with the alkene to give alkyl radical **196**. Cyclisation of **196** then occurs, providing the desired product **197** and regenerating the thiyl radical catalyst. Three examples using cyclic alkene substrates resulted in the formation of spirocyclic pyrrolidines in high yields.



Scheme 128: [3+2]-cycloaddition of *N*-tosylvinylaziridines and alkenes using a novel thiyl catalyst.

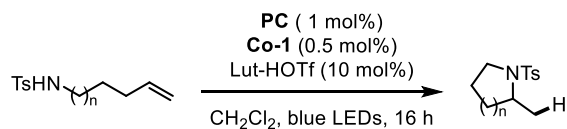
In 2017, Mykhailiuk reported a method for synthesising β -spirocyclic pyrrolidines in a two-step process from (hetero)aliphatic cyclic alkenes (**Scheme 129**).²⁵² Key to the transformation is a [3+2]-cycloaddition between the electron-deficient exocyclic alkene – synthesised by a Horner-Wadsworth-Emmons reaction – and an *N*-benzyl azomethine ylide generated *in situ*. While cyclopentane-containing alkenes did not yield the desired products, other three-to-seven-membered ring alkenes provided the desired spirocyclic products in good to excellent yields.



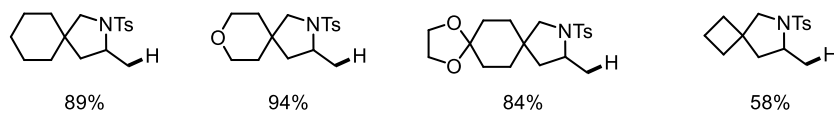
Scheme 129: two-step process from cyclic ketones to synthesise β -spirocyclic pyrrolidines: Horner-Wadsworth-Emmons reaction, followed by [3+2]-cycloaddition.

Very recently, Carreira and co-workers developed a procedure to synthesise heterocycles *via* a photo- and cobalt-catalysed cycloisomerisation of unactivated olefins with pendant nucleophiles (**Scheme 130**).²⁷¹ A benzothiazinoquinoxaline organophotocatalyst is utilised and in its excited state it can interact with the Co(II)-salen catalyst *via* SET, forming an anionic Co(I) species (**198**) which can be reversibly protonated to give **199**. This then undergoes HAT with the olefin, followed by oxidation by the photocatalyst to form Co(IV) species **200**. Nucleophilic attack of the activated olefinic carbon by the pendant nucleophile triggers the cyclisation, providing the desired product and releases the initial Co(II) species. The method is Markovnikov-selective and the use of a photocatalyst in conjunction with a Co-salen catalyst eliminates the need for stoichiometric oxidants/reductants which were previously reported in similar procedures.^{272–274} While a number of β -spirocyclic pyrrolidine derivatives were obtained in high yields, the compounds are limited to tosylated pyrrolidines, as the amine functionality is susceptible to oxidation under these conditions.

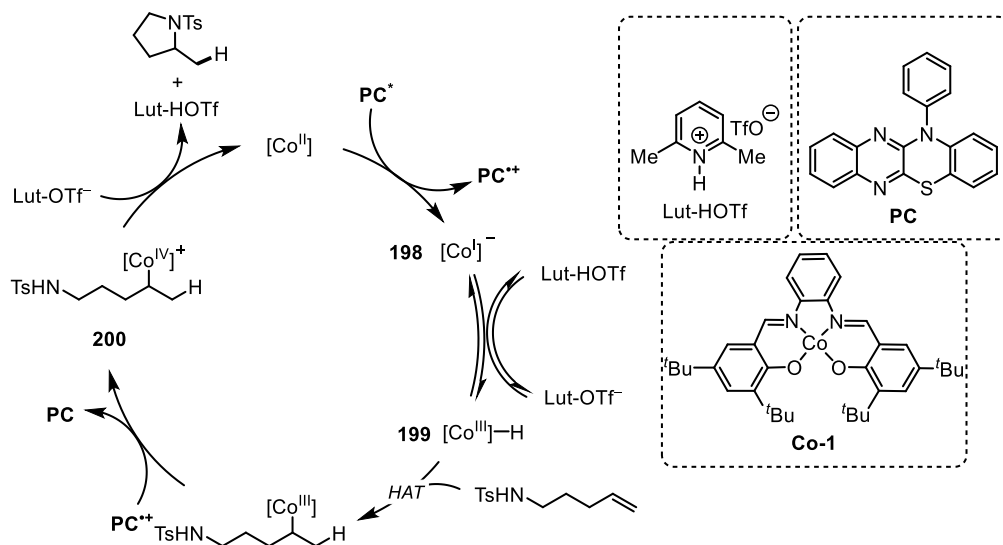
Carreira, 2024



----- *Selected examples* -----



----- *Mechanism* -----



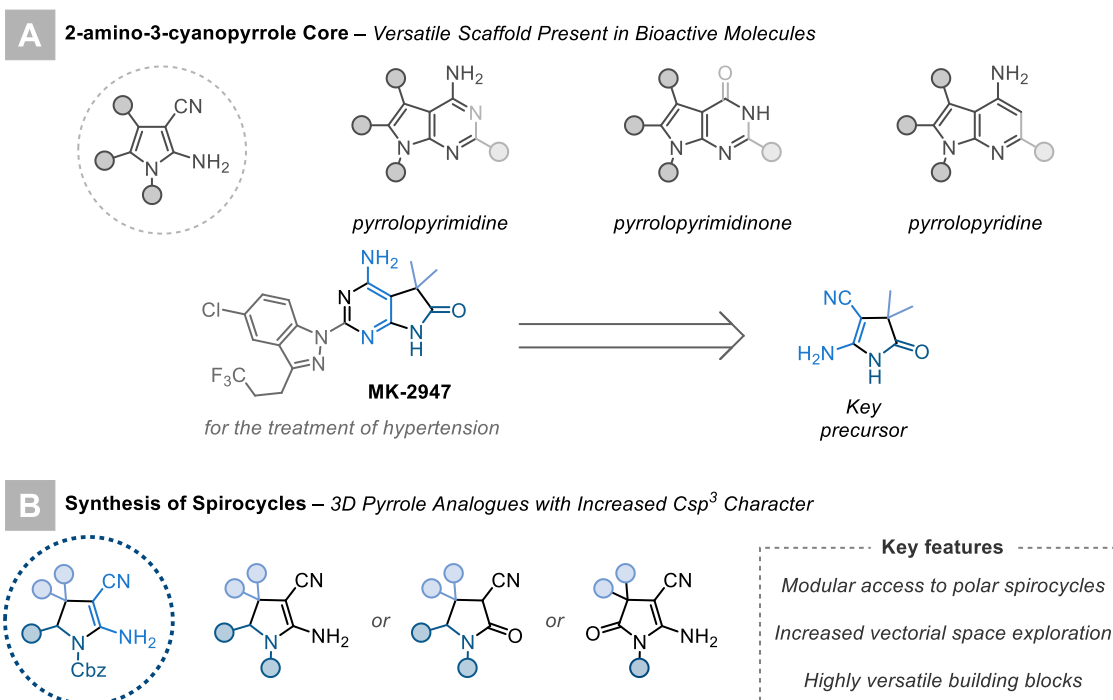
Scheme 130: synthesis of (spirocyclic) heterocycles via a photo- and cobalt-catalysed cycloisomerisation of unactivated olefins with pendant nucleophiles.

B.2 Objectives

Despite the apparent importance of this class of molecules, the majority of current synthetic processes to access substituted pyrrolo scaffolds are limited by harsh reaction conditions and multistep reactions, leading to limited substrate scope and modest yields.

As mentioned in the previous section, optimisation of the Giese-type reaction unexpectedly led to the formation of spirocyclic scaffold **110**. This alkylidenemalononitrile derivative bears a large resemblance to 2-amino-3-cyanopyrroles, which are considered as highly versatile building blocks and can be used to construct a wide range of heterocycles, e.g., pyrrolopyrimidines, pyrrolopyrimidinones and pyrrolopyridine.

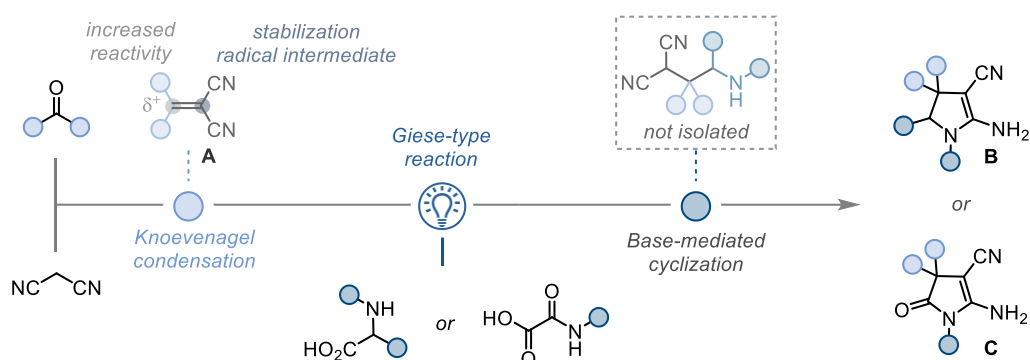
Moreover, spirocyclic pyrrolidine derivatives are among the most popular spirocyclic cores (**Scheme 131**). Typical two electron disconnection strategies mainly focus on the synthesis of α -spirocyclic pyrrolidines, whereas exploration of β -spirocyclic pyrrolidine derivatives is still relatively limited, despite their appearance as drug-like molecules.



Scheme 131: the use of pyrrolo scaffolds as bioactive molecules and the desired spirocyclic pyrrole analogues.

Motivated by the prospect of accessing a wide range of polar β -spirocyclic pyrrolidine derivatives that enable access to *N*-heterocycles with increased 3D and Csp³ character, a two-step process was envisioned.

The method seen in **Scheme 132** proposes a straightforward Knoevenagel condensation from readily available cyclic ketones to form malononitrile substrates. These compounds could be used with α -amino or oxamic acids to synthesize the 3-aminomalononitriles via a domino Giese-type reaction/base-mediated intramolecular cyclisation process, providing a wide variety of polar spirocyclic scaffolds. Diversifying the products could be attempted in numerous methods, thereby enhancing the adaptability of the approach and enabling the rapid creation of libraries containing potential drug-like molecules.



Scheme 132: concept and synthetic strategy.

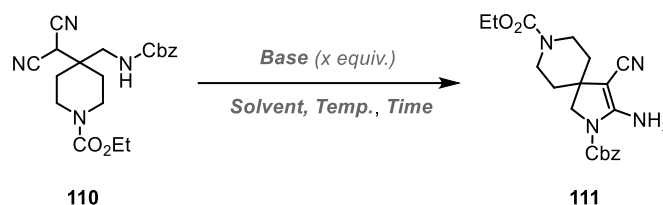
B.3 Results & discussion

This project was carried out in a collaborative manner with the following people: Dr Francisco José Aguilar Troyano, Dr Ayham H. Abazid, and Oumayma El Yarroudi, with computational experiments conducted by Dr Ignacio Funes-Ardoiz. Reactions carried out or compounds synthesized by co-workers are highlighted in schemes with the colour red.

B.3.1 Reaction Optimisation

Initially, optimisation began using **110** which is obtained in the Giese-type photoreaction. To investigate the cyclisation step, a series of bases (entries 2-3) and solvents (entries 4-6) were tested as seen in **Table 4**. Initial studies using deuterated acetonitrile (CD₃CN) gave a promising quantitative yield after 16 h at 50 °C (entry 2). As seen in entry 1, decreasing the temperature or reaction time dramatically diminishes the yield. Several polar solvents were tried, with high yields formed in all with the exception of ethanol, which led to an undistinguishable mixture. Moreover, Cs₂CO₃ was able to be exchanged for the less expensive and more stable K₂CO₃.

Table 4: initial investigation into conditions for the cyclisation step



Entry	Solvent (M)	Base (equiv.)	Temp. (°C)	Time (h)	111 (%)	110 left (%)
1	CD ₃ CN (0.1)	Cs ₂ CO ₃ (2)	24	16	<20	60
2	CD ₃ CN (0.1)	Cs ₂ CO ₃ (2)	50	16	>95	0
3	CH ₃ CN (0.1)	K ₂ CO ₃ (2)	50	16	75	0
4	EtOH (0.1)	K ₂ CO ₃ (2)	50	16	0	-
5	EtOAc (0.1)	K ₂ CO ₃ (2)	50	16	82	0
6	1,4-dioxane (0.1)	K ₂ CO ₃ (2)	50	16	87	0
7	1,4-dioxane (0.1)	K ₂ CO ₃ (2)	50	4	<20	80

When running the reaction in 1,4-dioxane, a promising yield of 87% was achieved. Since the previous photochemical reaction was carried out using this solvent, a one-pot system was considered, whereby the Giese-type photoreaction could be combined with the base-mediated cyclisation. An investigation into this design showed that for full conversion of **110**, a reaction temperature of 60 °C, generated by the lack of external cooling of the two blue LEDs (32 W, λ_{max} = 440 nm), was of great importance (**Figure 1**). This could be rationalised by the need for additional energy to allow for the molecule to be present in the

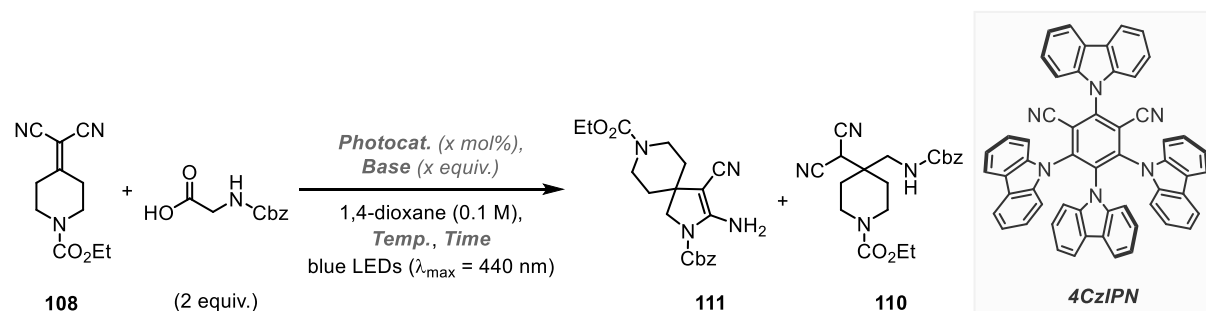
optimal conformation where the reacting groups are aligned, promoting the cyclisation. Additionally, *sym*-collidine could be exchanged for a large excess of K_2CO_3 .



Figure 1: set-up using two blue LEDs (32 W, $\lambda_{\max} = 440$ nm) for reaction at 60 °C.

The final optimised conditions (**Table 4**, entry 7) – irradiation with blue LEDs of a 1:2 mixture of the corresponding alkylidenemalononitrile and α -amino acid in the presence of Ir-F (1.0 mol%) and K_2CO_3 (5.0 equiv.), in 1,4-dioxane (0.1 M) at 60 °C – provided the desired spirocyclic compound in exceptional yields.

Table 5: optimisation studies of the Giese-type reaction and cyclisation in one pot.



Entry	Base (equiv.)	Photocatalyst (mol%)	Temp. (°C)	Time (h)	111 (%)	110 (%)	108 left (%)
1	K_2CO_3 (3)	Ir-F (1)	42	24	15	-	85
2	Cs_2CO_3 (3)	Ir-F (1)	42	24	25	75	-
3	K_2CO_3 (5)	Ir-F (1)	42	24	8	92	-
4	Cs_2CO_3 (5)	Ir-F (1)	42	24	11	-	89
5	K_2CO_3 (5)	Ir-F (1)	50	4	-	>99	-
6	K_2CO_3 (5)	Ir-F (1)	50	18	94	6	-
7	K_2CO_3 (5)	Ir-F (1)	60	18	>99	-	-
8	K_2CO_3 (5)	Ir-F (1)	60	24	>99	-	-
9 ^[a]	K_2CO_3 (5)	4CzIPN (5)	60	18	-	-	-
10	K_2CO_3 (5)	-	60	18	-	-	24
11 ^[b]	K_2CO_3 (5)	Ir-F (1)	60	18	-	-	>99
12	KOAc (5)	Ir-F (1)	60	18	>99	-	-

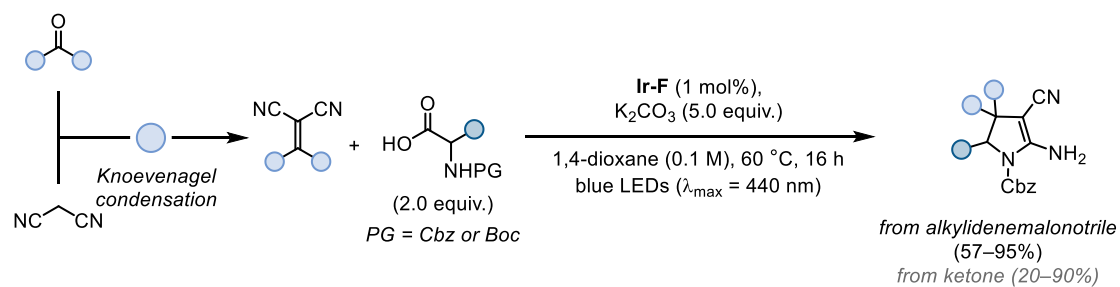
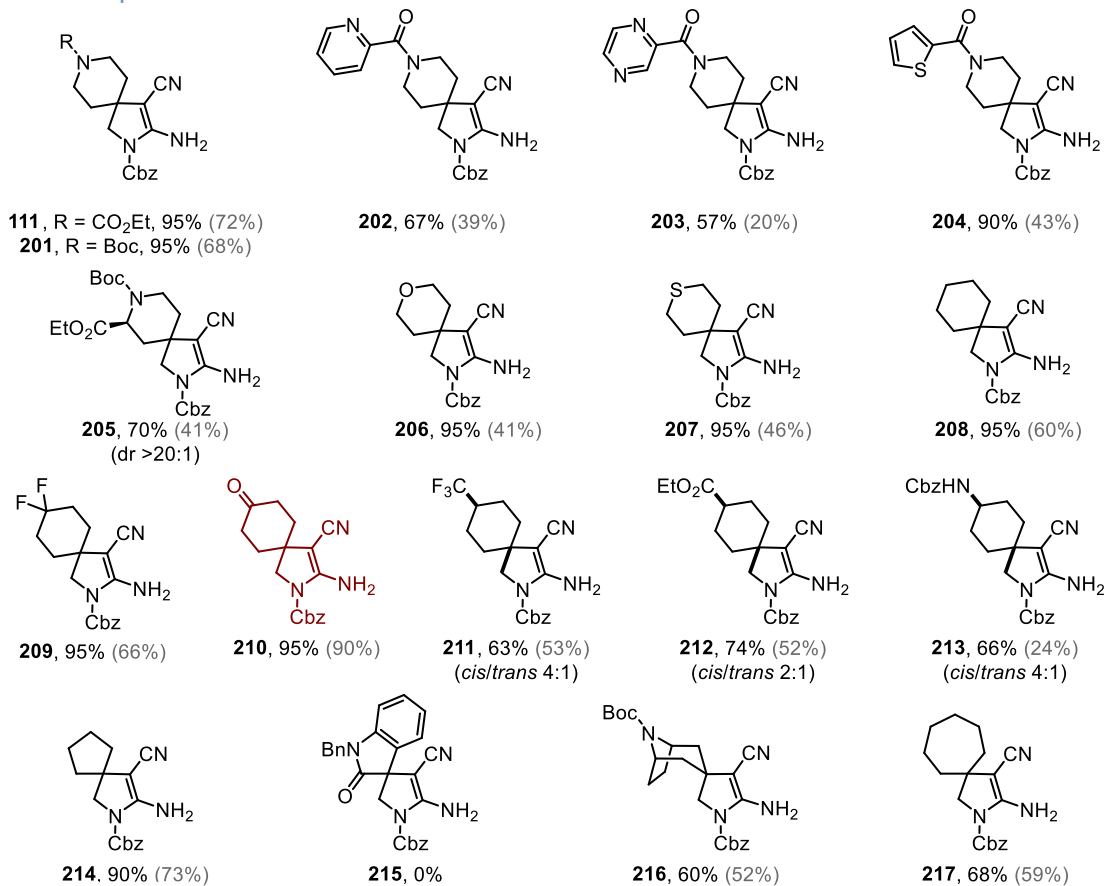
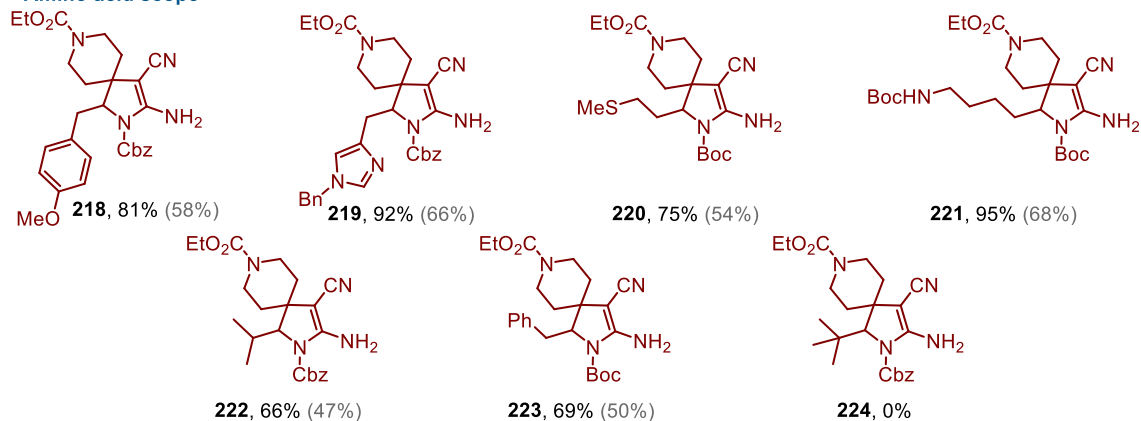
^[a] Only decomposition of **108** was observed; ^[b] No irradiation.

B.3.2 Scope & Limitations

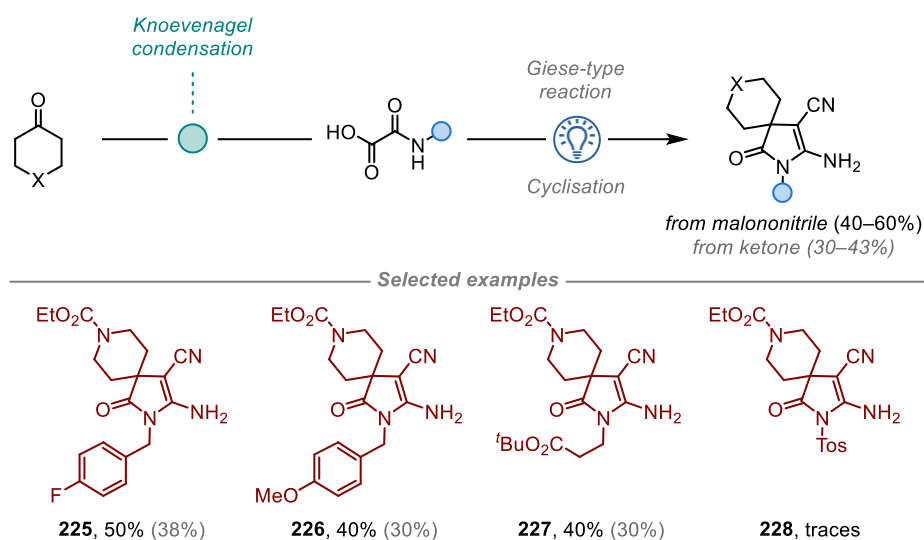
With the optimised conditions acquired, the substrate scope was explored. Investigation into the ketone scope shown in **Scheme 133** led to the synthesis of piperidine-derived spirocycles with Boc-protecting groups (**201**), heterocycles such as pyridines (**202**) and pyrazines (**203**), as well as thiophenes (**204**), all in high yields. Compound **205** could be obtained from an *L*-pipecolic ester derivative in excellent yield (70%) and diastereoselectivity (*d.r.* > 20:1), while other saturated ring systems such as tetrahydropyran and thiane-derived products **206** and **207** were attained in quantitative yields. Using cyclohexanone alkylidene malononitriles with different functionalities attached – such as *gem*-difluoro (**209**), ketones (**210**), esters (**212**) or protected primary amines (**213**) – provided numerous high-yielding polar spirocyclic scaffolds with varying *cis/trans* selectivity, highlighting the method's broad functional group tolerance.

Additionally, modification of the ring size could be achieved, as seen in cyclopentanone-derived product **214**, along with spirocycles **216** and **217** which stemmed from Boc-protected nortropinone and heptanone, respectively.

The next step consisted of exploring the amino acid scope. Protected α -amino acids with benzylic or aliphatic side chains, such as phenylalanine, methylated tyrosine, benzyl protected histidine, methionine, and lysine provided the desired products (**218-221**) in exceptional yields (69–95%). The use of more sterically hindered amino acids such as Cbz-protected valine (**222**) resulted in slightly diminished yields, while even more hindered *tert*-leucine derived compound **224** could not be synthesised.


Ketone scope

Amino acid scope

Scheme 133: ketone and α -amino acid scope of the described methodology.

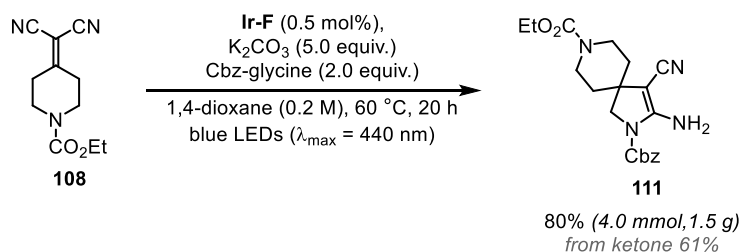
Additionally, it is possible to replace α -amino acids with oxamic acids (**Scheme 134**). This exchange allows for access to a wide range of potential 5,5-substituted spirocyclic pyrrolopyrimidinone precursors with increased 3D and Fsp³ character. Using the standard optimised conditions, a new class of spirocyclic scaffolds were readily accessed. *This work was conducted by Oumayma El Yarroudi (MSc) under my mentorship.*



Scheme 134: oxamic acid scope, conducted by Oumayma El Yarroudi, MSc.

B.3.3 Scale-up & Derivatisation Attempts

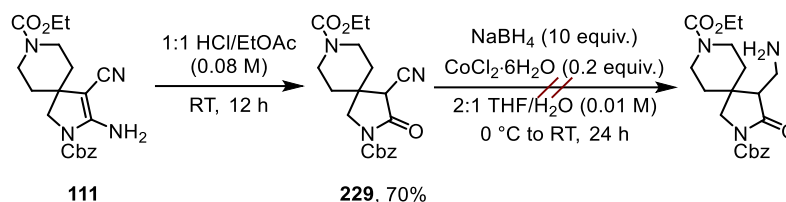
To demonstrate the scalability of the procedure, a gram-scale reaction using alkylidenemalononitrile **108** was conducted (**Scheme 135**). In this instance, the catalyst loading could be reduced (Ir-F, 0.5 mol%), and the concentration was increased to 0.2 M. Encouragingly, this led to the formation of targeted polar spirocyclic species **111** with a remarkable yield after the photochemical step and cyclisation (80%, 4.0 mmol, 1.5 g), resulting in an overall yield of 61% from **108**.



Scheme 135: scale-up synthesis of polar spirocycle **111** from **108** in 5 mmol, with reduced catalyst loading and increased concentration.

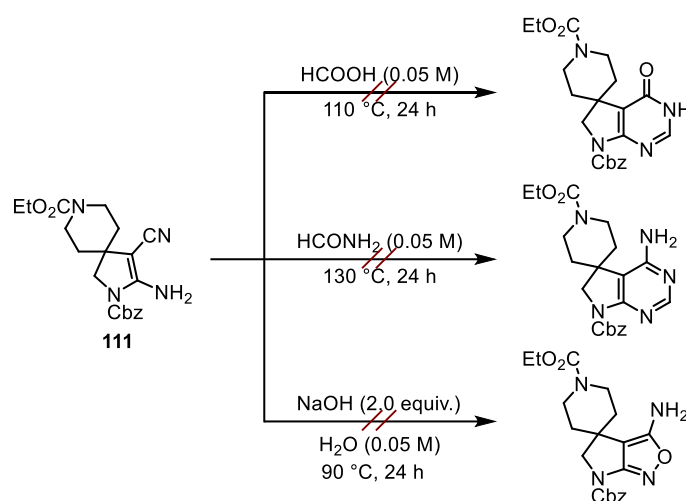
Next, an investigation into derivatisation of the dihydropyrrole compounds was carried out. Functionalisation was attempted on the free amino group, as well as the nitrile group.

Under acidic conditions, hydrolysis of the amine could be accomplished in 70% to provide the desired lactam (**Scheme 136**). Similarly, access to the succinimide was achieved when utilising a spirocycle derived from an oxamic acid. Subsequent attempts to selectively reduce the nitrile group using NaBH_4 catalysed with a Co^{II} species, were unsuccessful, however more experiments are required for a conclusive result.



Scheme 136: Hydrolysis of NH_2 , followed by reduction of nitrile.

Using conditions from literature, several cyclisation attempts shown in **Scheme 137** were conducted to access pyrrolopyridinone-, aminopyrimidine-, isoxazole-type scaffolds.²⁷⁵ All reactions were unsuccessful and resulted in re-isolation of starting material. This could be rationalised by the steric hindrance of the spirocyclic substrate. Therefore, it could be hypothesised that there is a need for harsher conditions such as in **Scheme 137**, or longer reaction times, however further experiments are required.



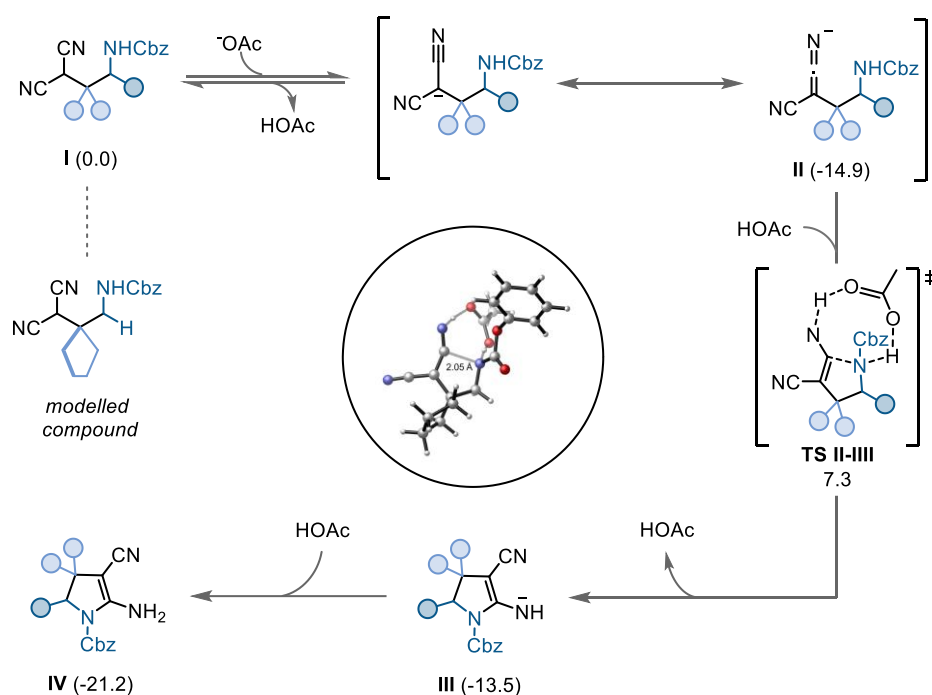
Scheme 137: failed cyclisation attempts of **111**.

B.3.4 Mechanistic Studies

DFT calculations were carried out by Dr Ignacio Funes-Ardoiz, Centro de Investigación en Síntesis Química (CISQ), Universidad de La Rioja, 26004 Logroño, Spain.

The proposed mechanism can be viewed in **Scheme 138**. The first step of this domino process – the light-mediated Giese-type reaction - can be viewed in detail in the previous

chapter. Typically, intramolecular cyclisations involving malononitrile derivatives occur under an acidic environment, unlike the proposed base-mediated reaction here. Hence, *in silico* studies (DFT calculations) were conducted to shed some light on the cyclisation step. Experimentally, the use of KOAc instead of K_2CO_3 did not lead to diminished yields, therefore calculations conducted were modelled using the former for simplicity (since carbonate is a dianion, computational methods usually provide large errors for poly-charged systems). Deprotonated species **I** can undergo a series of proton transfers, leading to the formation of anionic ketenimine species **II**, with delocalisation of the charge. Then, an intramolecular 5-*exo-dig* cyclisation facilitated by the base *via* a concerted proton transfer leads to the construction of intermediate **III** through a free energy barrier of 22.2 kcal mol⁻¹. After re-protonation, the desired dihydropyrrole scaffold **IV** is obtained exergonically (-21.2 kcal mol⁻¹).

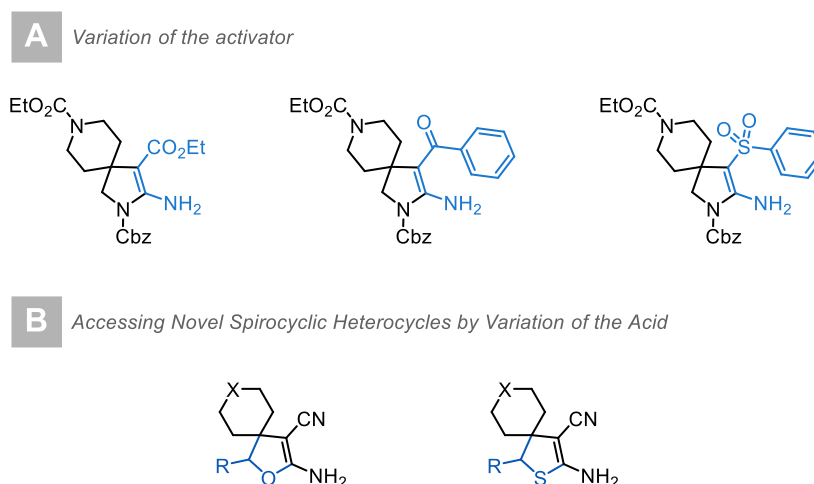


Scheme 138: DFT-calculated base-mediated spirocyclisation reaction mechanism (kcal/mol).

B.4 Outlook & Future Aspirations

In summary, a highly effective method to synthesize a range of polar β -spirocyclic pyrrolidine derivatives from abundant cyclic ketones and α -amino acids was established. Modification of conditions based on results attained from the previous project led to the development a one-pot, cascade procedure to prepare β -spirocyclic pyrrolidine derivatives in high yields. The method tolerates a range of functional groups such as fluorides, heterocycles, and protected amines, and can be modified by using oxamic acid as radical precursors, accessing potential 5,5-substituted pyrrolopyrimidinone precursors with increased 3D and Fsp³ character. Moreover, the reaction can be scaled up with ease even with reduced catalyst loading. Furthermore, hydrolysis of the enamine could be accomplished to provide β -spirocyclic γ -lactams. DFT calculations were also conducted *in silico* to support the proposed mechanism for the base-mediated cyclisation step.

Further derivatisation and cyclisation attempts of the products were as of yet unsuccessful, however additional experiments investigating alternative conditions are required for sufficient analysis. Additionally, in order to make the method more general, exploration into altering the activator used to synthesise the starting material could result in the incorporation of several interesting functionalities, as seen in **Scheme 139**. Furthermore, the use of alternative acids in the Giese-type reaction could form new classes of spirocyclic heterocycles, such as oxaspiro and thiaspiro derivatives.



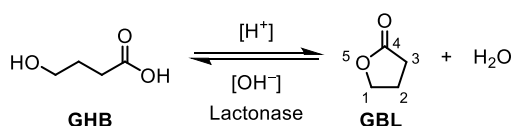
Scheme 139: future aspirations: A) varying the activator of the starting material for added functionality; B) using alternative carboxylic acids to access attractive spirocyclic heterocyclic scaffolds.

III. Synthesis of Spirocyclic (α -Amino- γ -)Butyrolactones

3.1 Introduction

3.1.1 Importance of (α -Amino- γ -)butyrolactones

γ -Butyrolactones are 5-membered cyclic esters of hydroxy carboxylic acids, containing a 1-oxacycloalkan-2-one group. The simplest example of a 5-membered lactone is γ -butyrolactone (GBL), which acts as a prodrug for γ -hydroxybutyric acid (GHB), a naturally occurring neurotransmitter and recreational depressant drug. GBL is rapidly metabolised into GHB by lactonase enzymes present in the blood (**Scheme 140**). Most of its pharmacological and toxicological effects are mediated through GHB; GBL's heightened bioavailability and elevated lipophilicity are influential factors contributing to the faster onset of action of GBL compared to GHB, ultimately lending it a greater potency and longer duration of activity.²⁷⁶⁻²⁷⁸

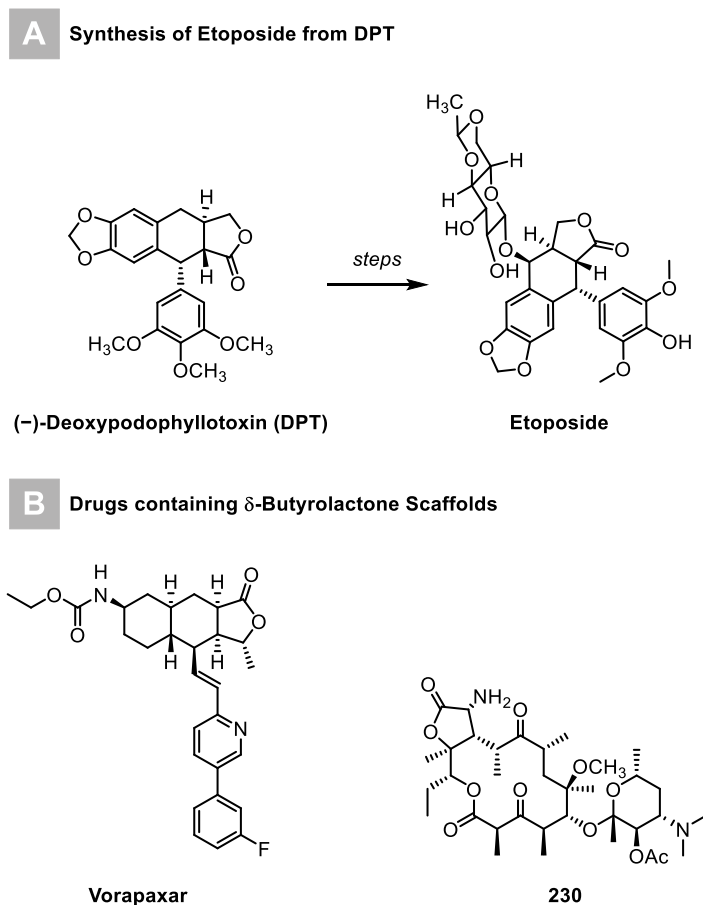


Scheme 140: GBL to GHB via lactonase enzymes.

The broad biological and pharmacological activity of butyrolactones has been extensively explored in the field of drug discovery. This has been demonstrated by the vast number of FDA-approved γ -butyrolactone-containing drugs, such as the podophyllotoxin derivative Etoposide, a chemotherapy plant-derived drug used for the treatment of numerous types of cancer (**Scheme 141**).²⁷⁹ The compound specifically targets and inhibits DNA topoisomerase II, which belongs to a class of enzymes responsible for managing the winding and unwinding of DNA during replication/repair. When etoposide binds to the enzyme while it is in the process of breaking and rejoining DNA strands, a complex subsequently forms between the three, preventing the enzyme from resealing the DNA strands. By disrupting DNA replication and repair, etoposide inhibits the growth and division of cancer cells, ultimately leading to their death. Currently, etoposide is produced semi-synthetically from (–)-podophyllotoxin extracted from the plant *Sinopodophyllum hexandrum*, however, due to a shortage of the drug, several (bio)synthetic procedures to access its intermediates have been developed.²⁸⁰

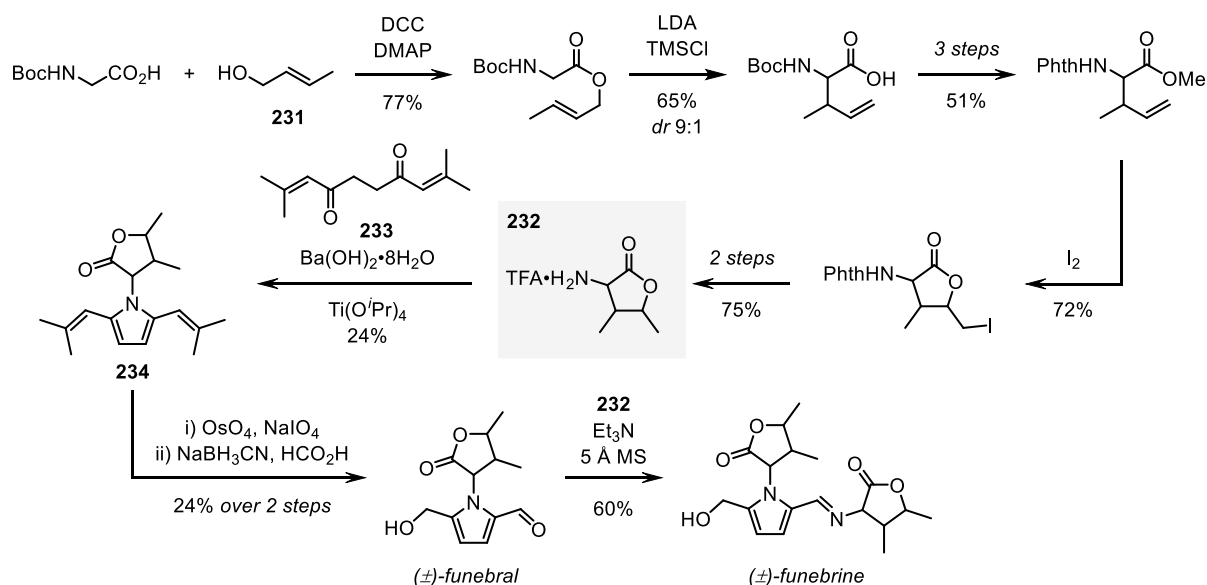
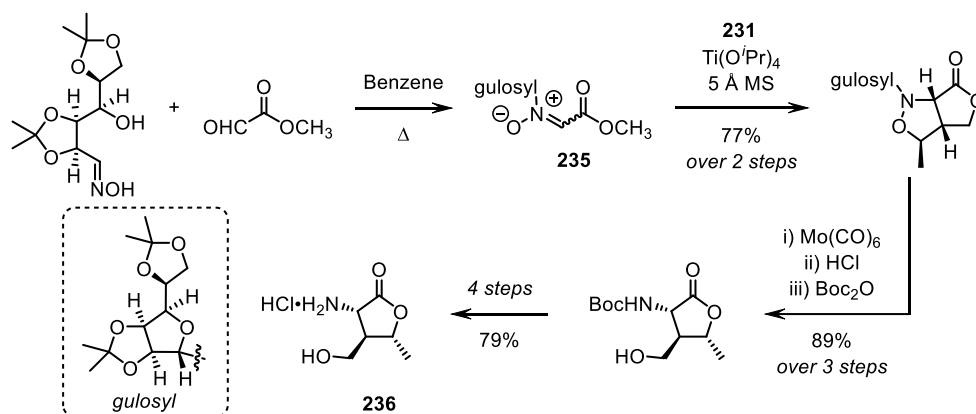
Vorapaxar, developed by MSD, has been used to reduce the risk of heart attacks and stroke in high-risk patients (**Scheme 141A**).²⁸¹ This antiplatelet medication operates by inhibiting the protease-activated receptor-1 (PAR-1) on platelets.²⁸² This receptor is involved in the activation process that leads to platelet aggregation and blood clot formation. Vorapaxar specifically targets thrombin, a vital enzyme in blood clotting, averting its interaction with PAR-1. By blocking this pathway, vorapaxar reduces platelet activation and aggregation, thus lowering the risk of cardiovascular incidents such as heart attacks and strokes. Commonly prescribed alongside other antiplatelet drugs, vorapaxar is used for individuals with a high risk of blood clot-related complications.

α -Amino- γ -butyrolactones are derivatives of γ -butyrolactone containing an amino group at the carbonyl α -position and are components in many biologically active natural compounds. In 2014, the group of Pavlović collaborated with GSK to synthesize substituted γ -lactone ketolides, including α -amino lactone derivative of clarithromycin **230**, which was suspected to possess potential as a macrolide antibiotic (**Scheme 141B**).²⁸³



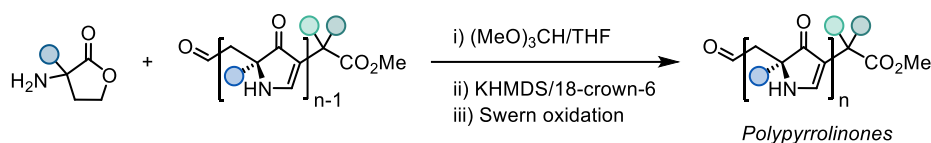
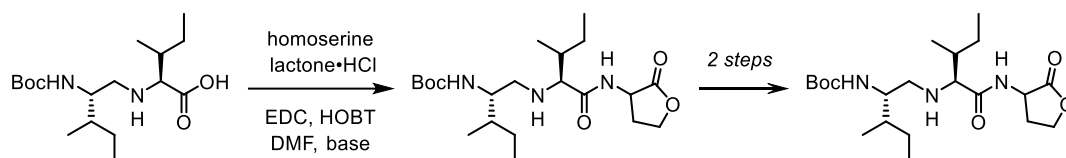
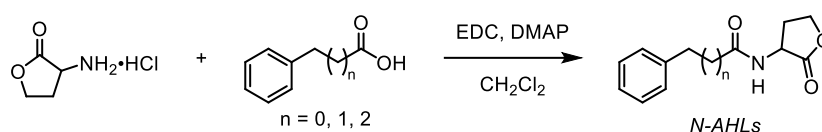
Scheme 141: a) structure of etoposide and its precursor, DPT; b) Vorapaxar and **230**.

α -Amino- γ -butyrolactones are also important intermediates in the preparation of natural products, e.g., in the total synthesis of funebral, a sterically hindered, rotationally restricted pyrrole alkaloid. Although the molecule lacks any biological activity, the presence of three consecutive stereocentres and a sterically congested pyrrole ring has spurred numerous attempts at its challenging synthesis. In 1995, Le Quesne and co-workers first reported the total synthesis of (\pm)-funebral (**3**) and its derivative, (\pm)-funebrine (**Scheme 142A**).^{284–286} Synthesis of racemic α -amino- γ -butyrolactone **232** was conducted in 8 steps in an overall yield of 18%, *via* a diastereoselective Claisen rearrangement and iodolactonization. Compound **232** can then undergo a Paal–Knorr condensation with dione **233** using titanium(IV)isopropoxide, forming pyrrole **234**. Treatment with osmium tetroxide catalyses an oxidative olefin cleavage and monoreduction, providing (\pm)-funebral. Condensation with **232** leads to (\pm)-funebrine. Subsequently, Ishibashi and colleagues reported the enantioselective synthesis of both compounds in 2003, employing a comparable approach, with the exception of (–)- α -amino- γ -lactone **236** which was constructed *via* a [3+2]-cycloaddition of (*E*)-crotyl alcohol **231** with nitrene **235** (**Scheme 142B**).²⁸⁷

A Racemic Synthesis of Funebral & Funebrine – Le Quesne, 1995

B Ring-forming Steps in the Enantioselective Synthesis Funebral & Funebrine – Ishibashi, 2003


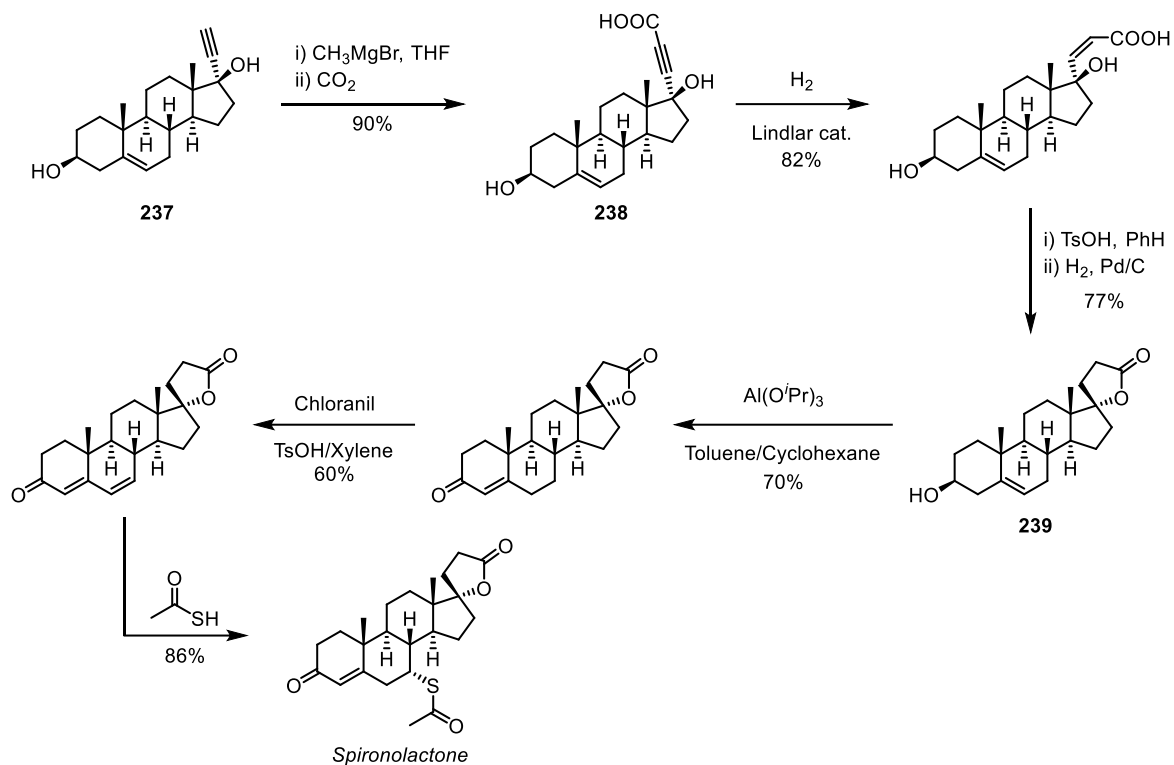
Scheme 142: a) key steps in the racemic synthesis of funebral and funebrine by Le Quesne and co-workers; b) enantioselective synthesis of **236** by Ishibashi and co-workers.

α -Amino- γ -butyrolactones have also been utilised as building blocks for the construction of peptidomimetics, as seen in the three-step asymmetric synthesis of polypyrrolinones (**Scheme 143A**), as well as in the synthesis of farnesyltransferase inhibitors, a class of experimental cancer drugs (**Scheme 143B**).^{288,289} Additionally, derivatives known as *N*-acyl homoserine lactones (*N*-AHLs), which consist of a homoserine lactone group connected to an acyl side chain, are a class of signalling molecules involved in bacterial quorum sensing – a mechanism used by some bacteria to communicate and coordinate with one another (**Scheme 143C**).²⁹⁰

A Asymmetric Synthesis of Polypyrrolinones

B Synthesis of Novel Farnesyltransferase Inhibitors

C General Synthesis of N-acyl homoserine lactones (N-AHLs)


Scheme 143: (a), synthesis of polypyrrolinone; (b) farnesyltransferase; (c) N-AHLs.

Spirocyclic butyrolactones are featured in numerous pharmaceutical compounds. As mentioned in Chapter I, the presence of the spirocyclic quaternary centre results in a rigid three-dimensional structure that directly influences the molecule's biological properties. For example, the steroidal prodrug spironolactone, a mineralocorticoid inhibitor, and derivative of progesterone, is primarily used to treat heart failure and hypertension. The structural differences between spironolactone and progesterone, including the former's inclusion of a spirocyclic centre, results in increased oral bioavailability and potency, leading to potent anti-androgenic and strongly reduced progestogenic activity.²⁹¹ Since its initial synthesis in 1957, numerous synthetic methodologies have been documented over the years, including multiple industrial syntheses.²⁹² The first industrial synthesis of spironolactone was reported in 1957 by G. D. Searle and Co., a subsidiary of Pfizer (**Scheme 144**).²⁹³ Deprotonation of building block **237** at the alkyne terminus, followed by quenching with CO_2 , provided alkyne **238**. Hydrogenation of propargylic acid **238** with Lindlar's catalyst, followed by lactonization by *p*-toluenesulfonic acid and another catalytic hydrogenation yielded spirocycle **239**. A series of oxidations and conjugate addition then leads to the desired spiro lactone in an overall yield of 21%.

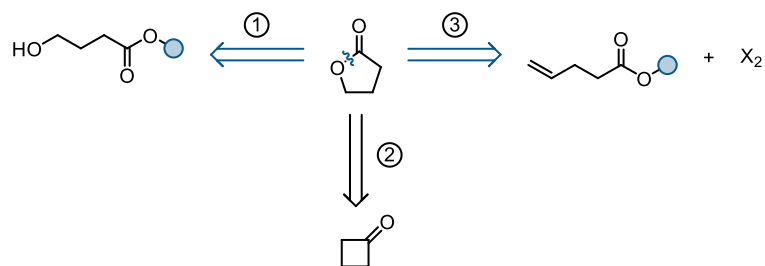


Scheme 144: first industrial synthesis of spironolactone by G. D. Searle and Co.

3.1.2 Synthesis of Lactones

3.1.2.1 Ionic Methods

As seen in **Scheme 145**, a number of methods exist for the construction of (butyro)lactones. The most common methods are: 1) intramolecular esterification (of hydroxy acids and derivatives); 2) Baeyer-Villiger oxidation of cyclic ketones; and 3) halolactonization i.e., forming halolactones from olefinic carboxylic acids *via* addition of an oxygen and halogen to a double bond.

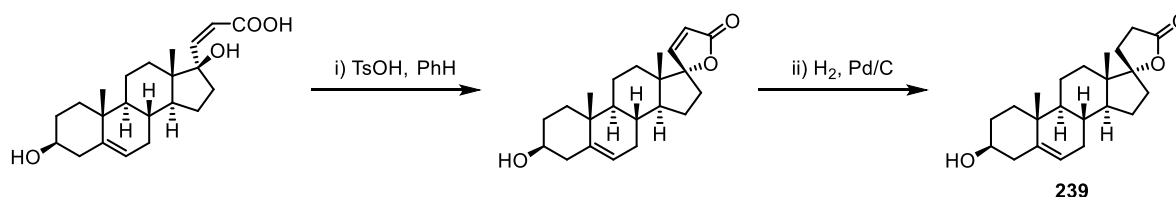


Scheme 145: most common disconnection strategies for the construction of (butyro)lactones.

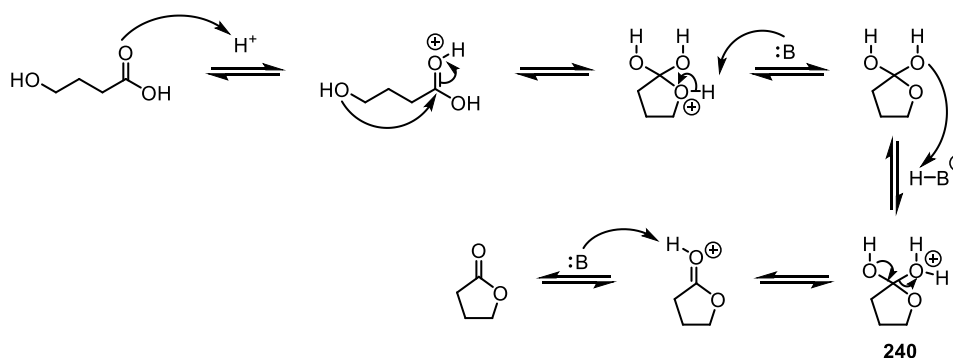
Lactonization of hydroxy acids and esters (intramolecular Fischer esterification) is typically the most straightforward and therefore most utilised method of lactone formation. This is especially true for butyrolactones, which are typically strain-free and among the

easiest to form. This is usually conducted in an acidic medium, however, basic conditions have also been reported. For example, in the total synthesis of spironolactone **239** described earlier, the key step to form the butyrolactone is an acid-mediated lactonization (**Scheme 146**). In the mechanism, after the carbonyl oxygen is protonated, nucleophilic attack of the alcohol forms oxonium species **240** with two hydroxyl groups. After elimination of water followed by a proton transfer, the desired lactone is formed.

Intramolecular Lactonization of Spironolactone Precursor – G. D. Searle and Co, 1957



Mechanism of Lactonization

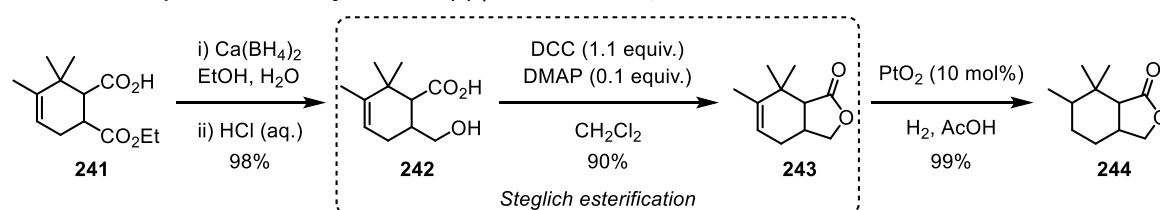


Scheme 146: acid-mediated lactonization step in Searle's synthesis of spironolactone.

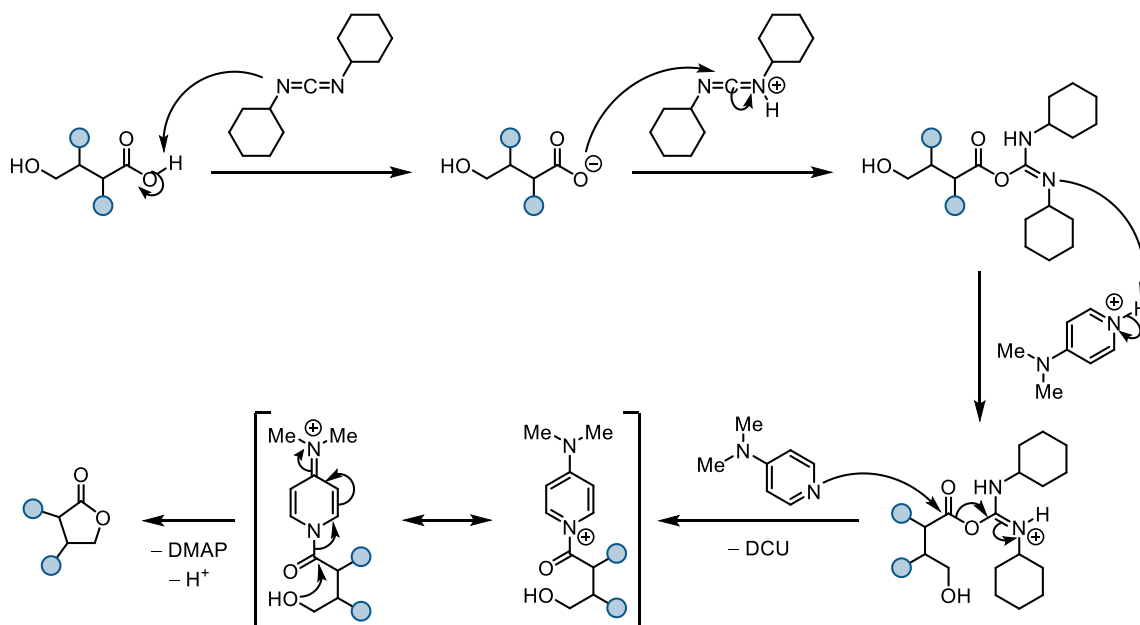
Similarly, the (intramolecular) Steglich esterification has been used to construct lactones. First described by Neises and Steglich in 1978, the mildly basic conditions of the reaction allow for the use of acid-labile substrates less compatible with the acidic conditions of the Fischer esterification.²⁹⁴ The first step of the mechanism is the formation of a more nucleophilic *O*-acylurea intermediate from the carboxylic acid by a carbodiimide coupling reagent (often DCC, dicyclohexylcarbodiimide). Attack of the alcohol to the activated carboxylic acid forms dicyclohexylurea (DCU) as a by-product and the desired lactone after deprotonation. When using a poor nucleophile, side reactions can occur, leading to the formation of unreactive *N*-acylurea. The use of catalytic quantities of DMAP prevents this by acting as an acyl transfer-reagent, forming an intermediate that cannot form intramolecular side products but reacts rapidly with alcohols. In 2001, Gosselin and co-workers used the Steglich esterification to synthesise intermediate **243** in their formal synthesis of the fragrance component (\pm)- γ -irone (**Scheme 147**).²⁹⁵ Starting from intermediate **241** which was

prepared by Diels-Alder cycloaddition of 3,4-dimethylpenta-1,3-diene with maleic anhydride, reduction and hydrolysis gave the cyclic γ -hydroxycarboxylic acid **242**. This intermediate then underwent Steglich esterification to the lactone **243** in 90% yield, followed by hydrogenation to access fragment **244** (four steps, 64% overall yield). Four further steps are then required for the synthesis of γ -irone (27% overall yield).²⁹⁶

Lactonization step in the Formal Synthesis of (\pm)- γ -Irone – Gosselin, 2001



Mechanism of Steglich Lactonization

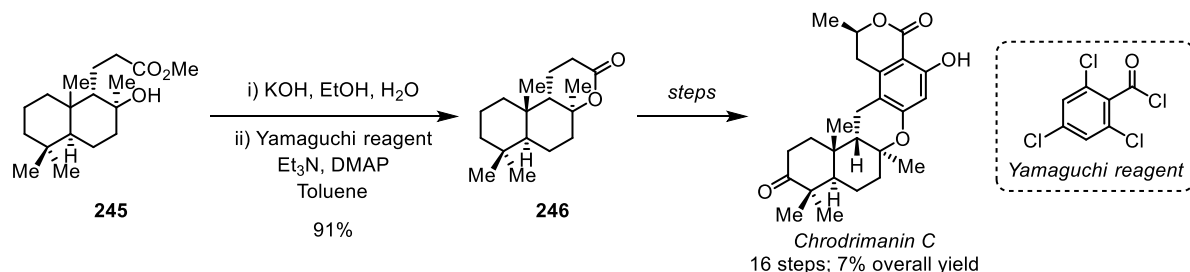


Scheme 147: ring-forming step in the synthesis of (\pm)- γ -irone via Steglich esterification and mechanism.

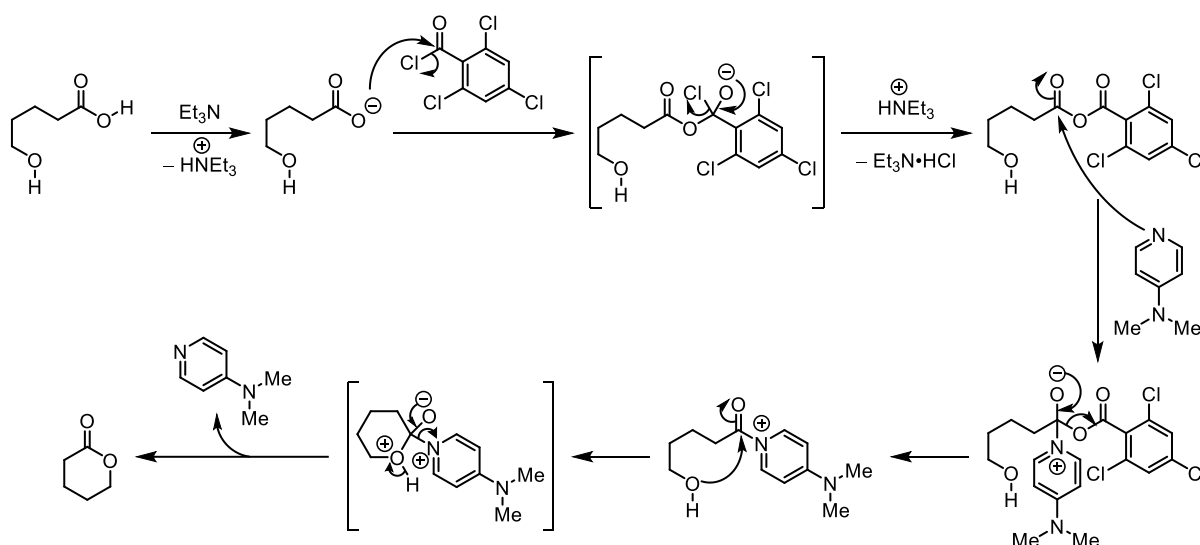
Primarily used to form macro-lactones, the Yamaguchi lactonization is also conducted in the presence of carboxylic acids and alcohols, using 2,4,6-trichlorobenzoyl chloride (TCBC, known as the Yamaguchi reagent) as an activation reagent for carboxylic acids and a stoichiometric amount of DMAP.²⁹⁷ The reaction involves converting hydroxycarboxylic acids into reactive acid anhydrides, which are then regioselectively attacked by DMAP at the less hindered carbon (**Scheme 148**). As in the Steglich esterification, this forms acyl-substituted DMAP which is highly electrophilic in nature and is subsequently attacked by the alcohol to form the lactone. Recently, Renata and co-workers utilised the Yamaguchi

reagent in a 16-step synthesis of chrodrimanin C.²⁹⁸ **Scheme 148** shows the relevant steps: tertiary alcohol **245** was first saponified using KOH and then converted to the lactone **246**, in 91% over two steps.

Lactonization of Chrodrimanin C Precursor via Yamaguchi Reagent – Renata, 2021



Mechanism of Yamaguchi Lactonization

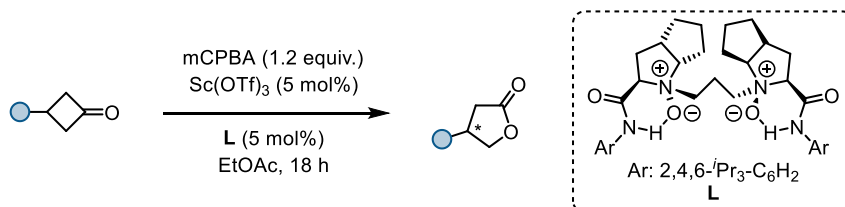


Scheme 148: the lactonization step in Renata's total synthesis of chrodrimanin C.

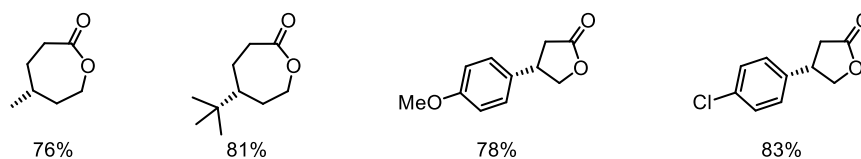
Arguably one of the most recognisable methods for the construction of lactones is the Baeyer–Villiger oxidation, where the oxidative cleavage of a carbon-carbon bond adjacent to a carbonyl results in the conversion of cyclic ketones to lactones, using peroxyacids such as *m*CBPA. Since the initial report by Baeyer and Villiger in 1899, dozens of modifications have been published, including Feng's work on the Baeyer-Villiger oxidations of both *meso* and racemic cyclic ketones in the presence of chiral *N,N*-dioxide-Sc^{III} complex catalysts (**Scheme 149A**).^{299,300} Additionally, the discovery of Baeyer-Villiger monooxygenases (BVMOs) – enzymes containing a flavin co-factor that catalyse the Baeyer-Villiger oxidation reaction in biological systems – has led to their widespread investigation as biocatalysts.³⁰¹ BVMOs have also inspired biomimetic approaches, such as the work of Murahashi and Imada (2002). The authors developed a planar-chiral bisflavin catalyst to catalyse the

asymmetric Baeyer-Villiger reaction of cyclobutanones with hydrogen peroxide allowing the preparation of chiral γ -butyrolactones (**Scheme 149B**).³⁰²

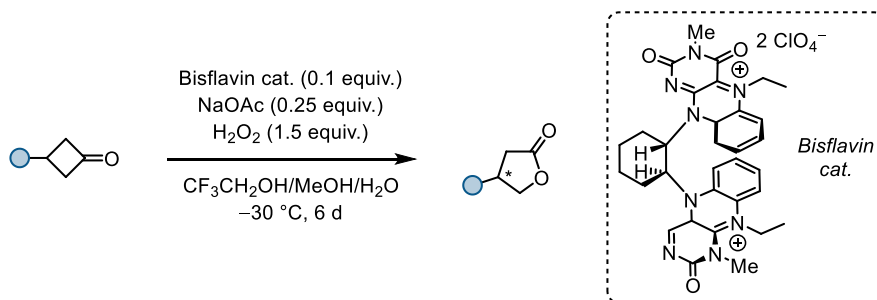
A Baeyer-Villiger Oxidations of Meso & Racemic Cyclic Ketones – Feng, 2012



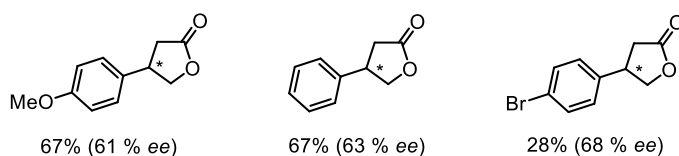
Selected examples



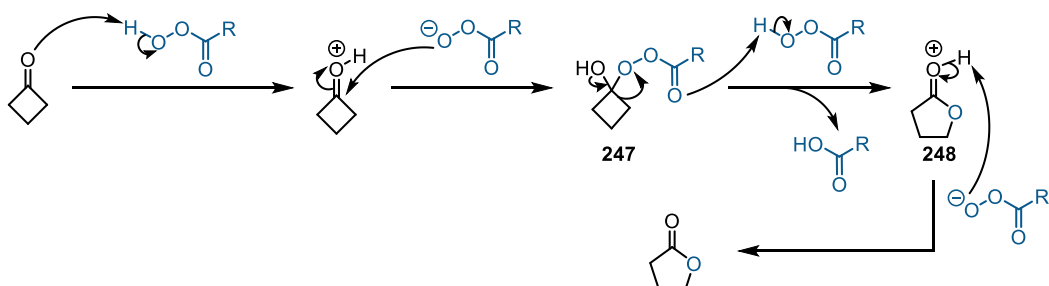
B Bisflavin-catalysed Asymmetric Baeyer-Villiger of Cyclobutanones – Murahashi & Imada, 2002



Selected examples



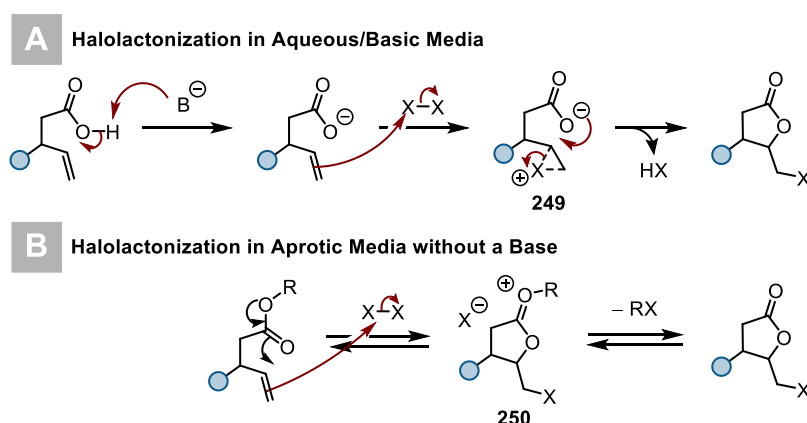
Mechanism of Baeyer-Villiger Oxidation



Scheme 149: selected examples utilising the Baeyer-Villiger oxidation of cyclic ketones.

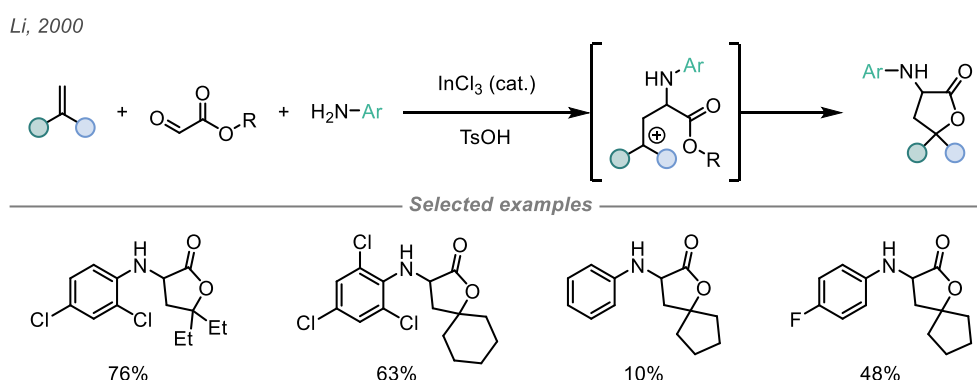
In the mechanism of the reaction shown in **Scheme 149**, the first step is protonation of the oxygen of the carbonyl group by the peroxyacid, rendering the carbonyl group more susceptible to attack by the latter. The transformation begins with the formation of a peroxycarboxylic acid from a carboxylic acid and peroxide, typically catalysed by a Lewis acid or base. The ketone substrate then undergoes nucleophilic attack by the peroxycarboxylic acid at the carbonyl carbon, resulting in the formation of a tetrahedral intermediate **247**. Next, a rearrangement occurs facilitated by the release of a carboxylate anion or a proton, leading to migration of an alkyl/aryl group from the carbonyl carbon to the adjacent oxygen atom of the peroxycarboxylic acid. Migration of one substituent on the ketone to oxygen of the peroxide group occurs along with the elimination of the carboxylic acid, in a concerted manner which also the rate-determining step. Deprotonation of oxonium ion species **248** then provides the desired lactone.

In 1904, Bougault reported a reaction – now referred to as halolactonization – that involves the formation of a lactone ring from an olefinic ester or acid precursor in the presence of a molecular halogen (**Scheme 150**).³⁰³ The reaction involves electrophilic halogenation of the olefin double bond to form a cyclic halonium ion (**249**), which undergoes ring-opening with the carboxylate (formed from the corresponding acid in the presence of a base). In the latter case, a lactone is obtained. In the case of acids/esters without a base in aprotic neutral solvents, halogen and the carboxyl oxygen add to the double bond in a concerted fashion to form the oxonium ion (**250**). This can then be deprotonated/dealkylated by addition of the halide counterion at carbon, releasing the lactone and an alkyl halide (generally CH₃I).



Scheme 150: mechanism of halolactonization in A) basic, aqueous and B) non-basic, aprotic conditions.

Since the initial discovery, halolactonization has proven to be one of the most proficient means of synthesizing lactones. For example, in the total synthesis of funebral mentioned earlier, the key step to form the (–)- α -amino- γ -lactone is *via* an iodolactonization. One of the characteristics of this method is that the product is necessarily a halogenated compound, which may not always be desirable. An alternative that does not require any halogenation is through the use of iminium ion intermediates. This is exhibited by the seminal work of Li and co-workers, who developed an InCl_3 -mediated three-component tandem cyclisation to generate α -amino- γ -lactones (**Scheme 151**).³⁰⁴ Starting from glyoxylates as substrates, addition of an amine leads to the formation of an imine-iminium equilibrium under Lewis acidic conditions. The iminium ion is highly electrophilic and, in a similar fashion to the halolactonization, can act as the electrophilic acceptor in a 5-*exo*-trig cyclisation with the alkoxy group of the ester, leading directly to the formation of α -amino γ -butyrolactones. Unfortunately, the methodology is limited to highly electron-deficient polychlorinated/fluorinated primary anilines, as well as the requirement of stoichiometric amounts of a Lewis acid and Brønsted acid.



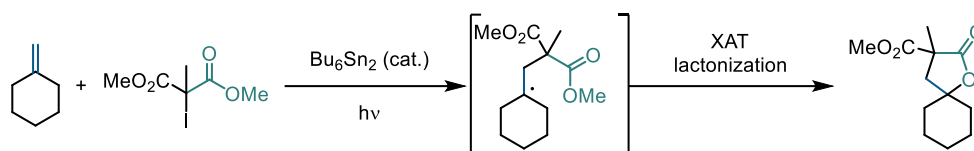
Scheme 151: Li's cationic tandem, three-component synthesis of α -amino γ -lactones.

3.1.2.2 Radical Methods

Many radical reactions use α -halo carbonyls to perform atom transfer radical reactions on alkenes (ATRA). The resulting γ -halo esters are ideally poised for intramolecular 5-*exo*-tet cyclisation to form lactones.

One of the first reports of this reaction was by the group of Curran in 1989, using dimeric Sn_2Bu_6 as a halogen atom transfer (XAT) agent. It can be fragmented homolytically under UV-light irradiation, forming a pair of nucleophilic Sn radicals. Sn radicals are ideal for halogen-atom transfer chemistry, as they are both highly nucleophilic and able to form strong Sn–X bonds which leads to an exergonic XAT step. XAT from α -halocarbonyls can be used

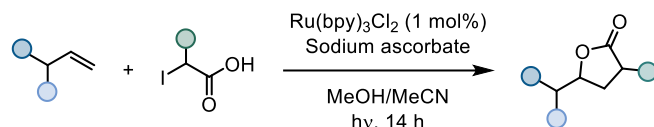
to create a stabilised and electrophilic radical in the carbonyl α -position (**Scheme 152**).³⁰⁵ This can undergo a polar-matched addition to the (electron rich) alkene. The carbon radical formed after the initial addition is nucleophilic and can react with another equivalent of α -halo carbonyl, leading to a second XAT step. This is yet another thermodynamically favourable step as the C–X bond will be stronger in the γ -halo carbonyl compared to the α -halocarbonyl. As another electrophilic radical **251** is then formed, it can act as a chain carrier in a radical chain propagation mechanism. The Sn_2Bu_6 is therefore only necessary in sub-stoichiometric amounts to initiate the chain. This process is comparable to what occurs during the halolactonization; the alkoxy group of the ester attacks the carbon bearing the halide which then subsequently attacks the methyl group of the ester, leading to the formation of the methyl halide and lactone.



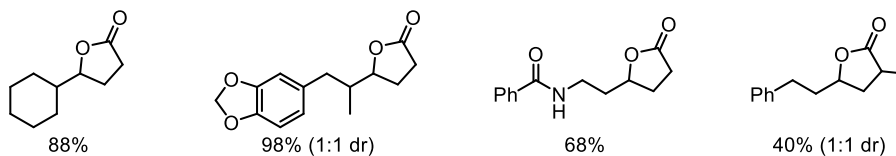
Scheme 152: seminal work by the Curran group utilising XAT chemistry.

Many variations on this reaction have since been developed using milder conditions for the initial radical generation, thereby avoiding the use of organostannanes. For example, Kokotos used $\text{Ru}(\text{bpy})_3^{2+}$ to initiate the reaction *via* an initial SET reduction of the weak C–I bond, i.e., initiation through an oxidative quenching cycle (**Scheme 153**).³⁰⁶

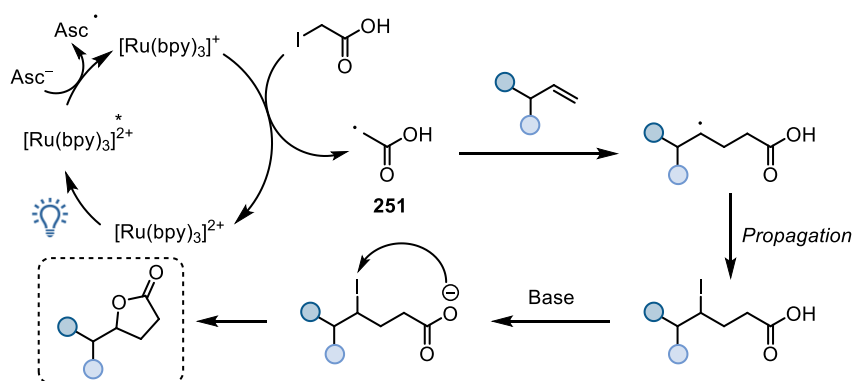
Kokotos, 2017



Selected examples



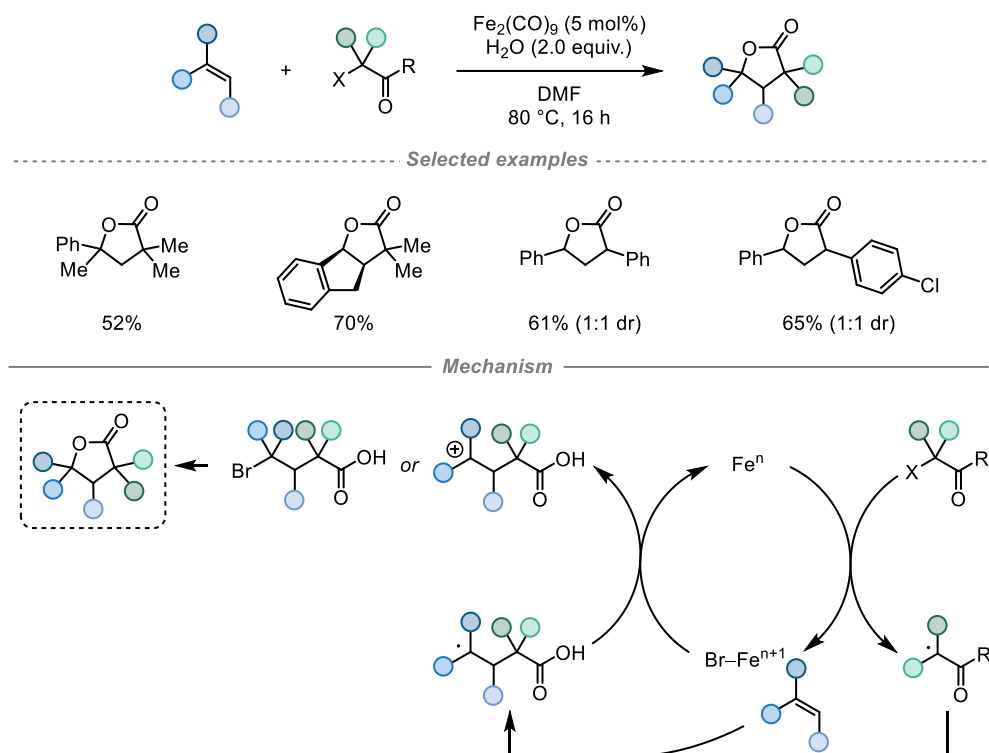
Mechanism



Scheme 153: Kokotos' photocatalytic lactonization *via* addition of iodoacetic acid to olefins.

Another example was reported in 2018 by Nishihara using $\text{Fe}_2(\text{CO})_9$ where a SET is also proposed as the initial step (**Scheme 154**).³⁰⁷ The mechanism likely occurs through a similar chain pathway, although transfer of the halide from an intermediate Fe–Br complex is possible.

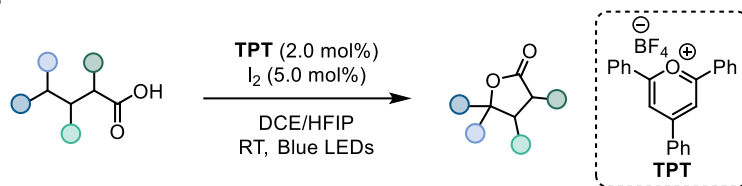
Nishihara, 2018



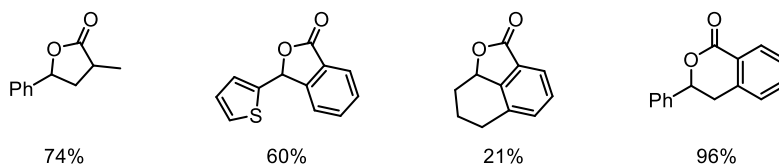
Scheme 154: Nishihara's iron-catalysed radical annulation of alkenes with α -halocarboxylic acids.

To avoid the use of α -halo carbonyls, Muñiz and co-workers developed a process using catalytic iodination, albeit the reaction is limited to the use of esters with a phenyl group at the γ -position, as it is required as an electrophore (**Scheme 155**).³⁰⁸ TPT (2,4,6-triphenylpyrylium tetrafluoroborate) acts as the photocatalyst, oxidising the phenyl group to an aryl radical cation, subsequently forming either the benzylic cation (after another oxidation step) or it can react with iodine forming a γ -halo carbonyl. Either intermediate can again cyclise in a 5-*exo-trig* (benzylic cation) or 5-*exo-tet* cyclisation (γ -halocarbonyl), forming the lactone. The authors propose that molecular oxygen is responsible for turnover of the reduced photocatalyst and acts as the terminal reductant in the reaction. The iodide which is formed after the substitution is then oxidised again to an electrophilic iodine species (I_2 or HOI) and turnover via O_2 reduction is again proposed for to be responsible for catalyst regeneration.

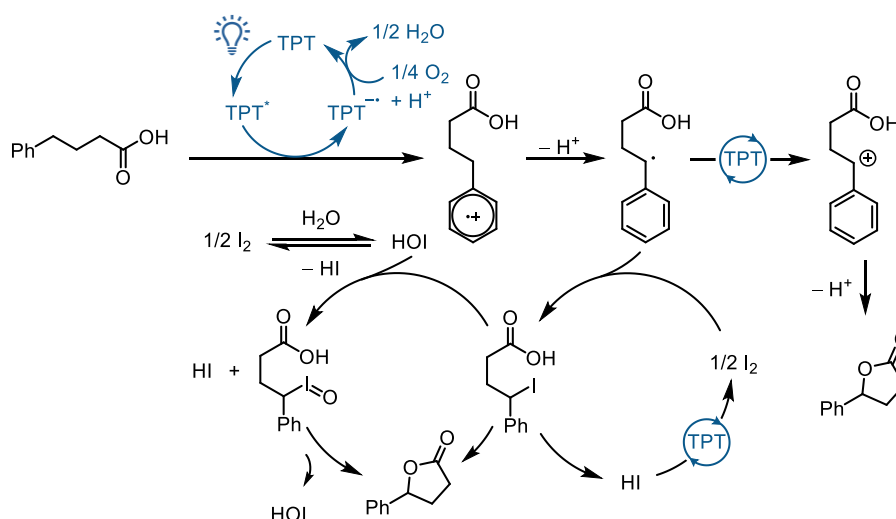
Muñiz, 2018



Selected examples



Mechanism

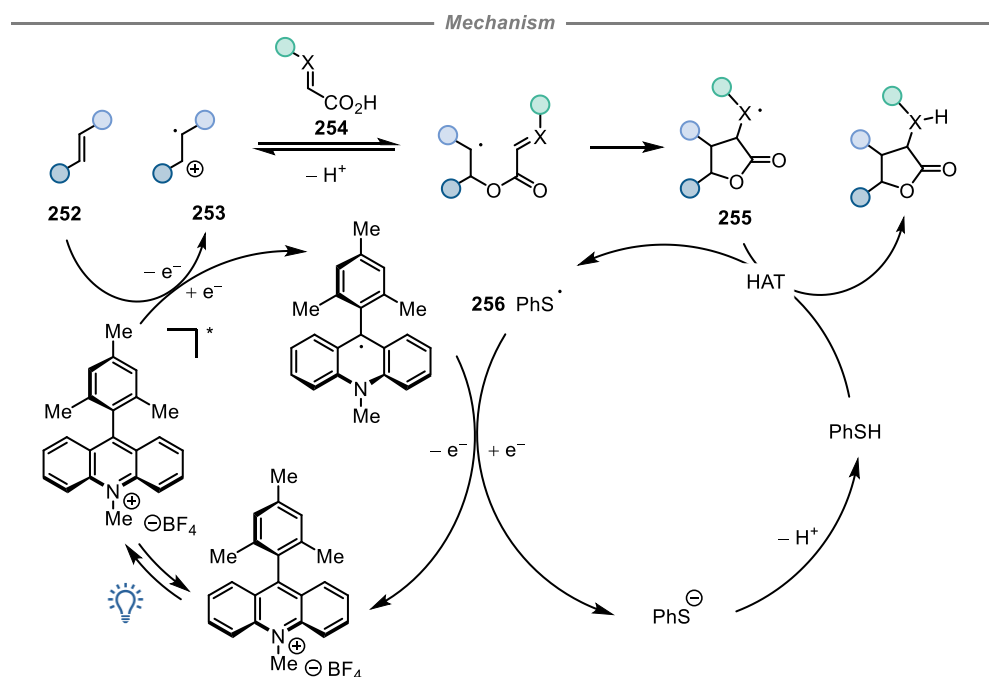
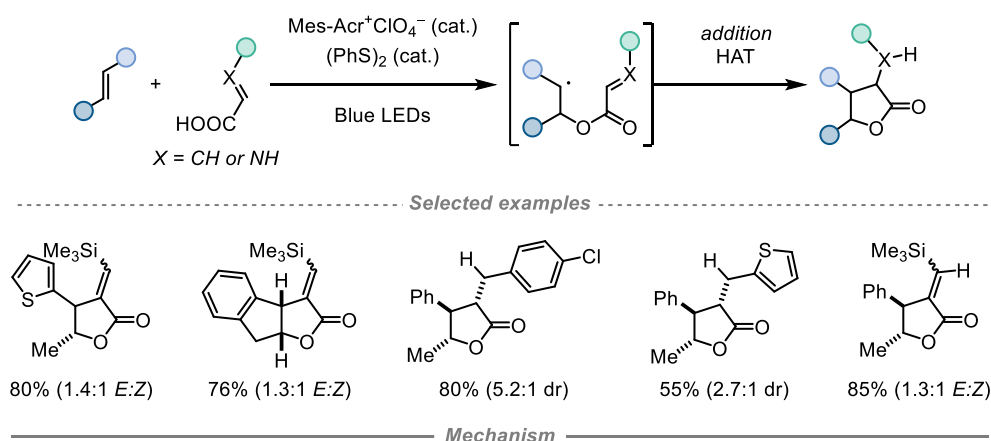


Scheme 155: co-operative iodine and photoredox catalysis for the formation of γ - and δ -lactones from carboxylic acids via direct conversion of OH to C–O bonds.

In 2014, Nicewicz reported an oxidative photocatalytic lactonization method based on a radical cycloaddition between electron-rich olefins and α,β -unsaturated acids (**Scheme 156**).³⁰⁹ The reaction is based on an oxidative quenching cycle using a strongly oxidising Fukuzumi-type acridinium photocatalyst ([Mes-Acr]ClO₄). After excitation with blue light, the excited state of the photocatalyst is quenched by electron-rich olefin **252**, forming the reduced catalyst and carbon radical cation **253**. α,β -unsaturated acid **254** can react through its nucleophilic carboxylate functionality, leading to a neutral radical adduct, which can undergo 5-*exo*-trig cyclisation onto the pendent olefin, forming the exocyclic β -carbon radical of γ -lactone **255**. This species then abstracts a proton in a polar-matched HAT step with the catalytic hydrogen donor thiophenol (formed *in situ* from the diphenyl disulfide). The resulting thiyl radical **256** which is then formed (initially through the homolysis or SET reduction of the disulfide) is also responsible for the turnover of the photocatalyst. After it is reduced, the resulting thiolate acts as a base, essentially transferring a proton from the carboxylic acid

(ionic) to **255** (radical, HAT). As this methodology relies on alkene oxidation, it is limited to alkenes whose oxidation potentials are within the redox window of the PC which means the reaction is limited to easily oxidisable alkenes, such as methyl styrenes and certain trisubstituted olefins. An additional limitation on the Michael acceptor side is that radical **255** formed after the intramolecular cyclisation, has to be stabilised for the reaction to occur. Hence, there are also limitations on the α,β -unsaturated olefin scope, which is mainly composed of cinnamates (and similar systems) and maleates, with a few exceptions.

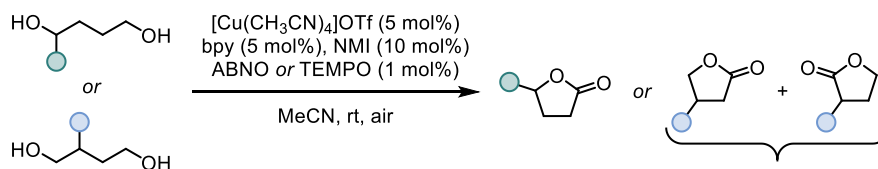
Nicewicz, 2014



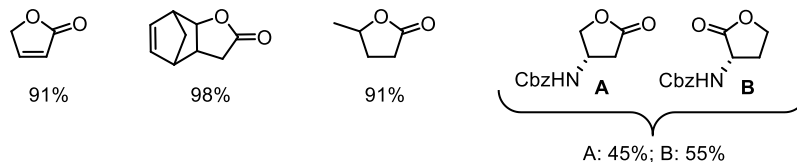
Scheme 156: Nicewicz' catalytic synthesis of γ -butyrolactones from olefins and unsaturated acids using an acridinium photo-oxidant and substoichiometric a redox-active co-catalyst.

A unique strategy based on the oxidation of linear diol precursors was reported by Stahl and co-workers in 2015 (**Scheme 157**).³¹⁰ The nitroxyl radical/ Cu^{I} catalyst system is

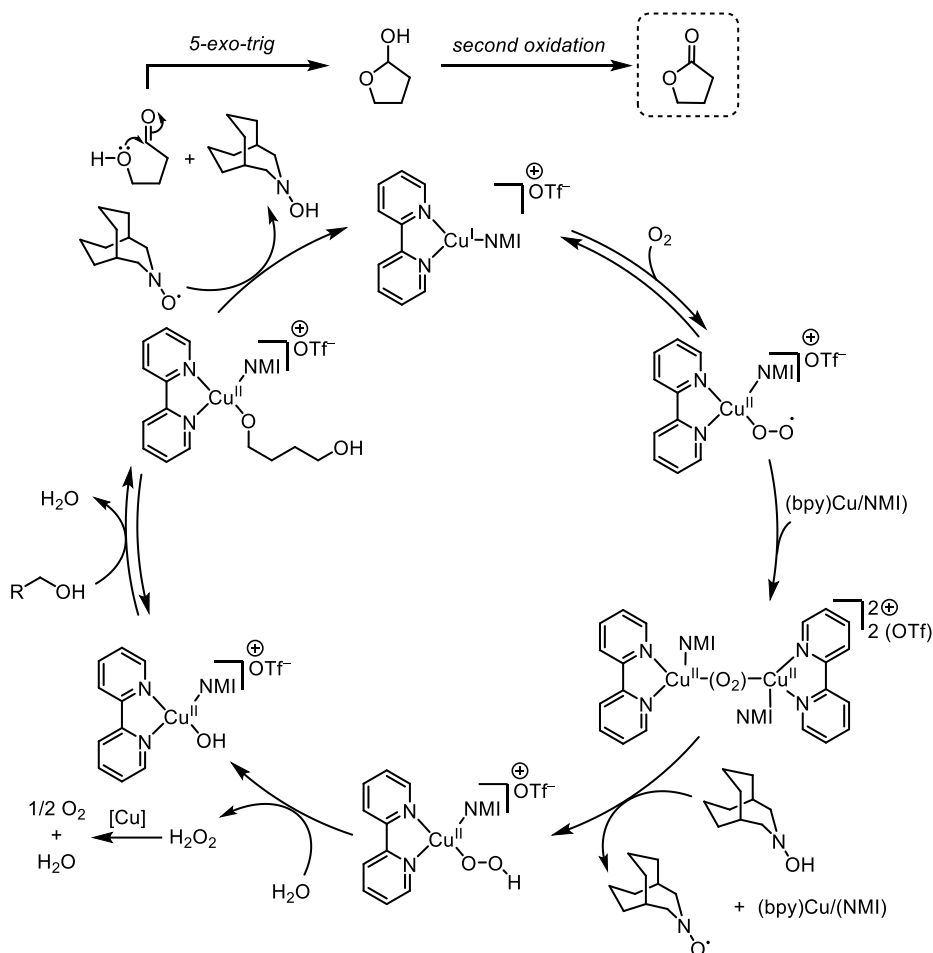
used under aerobic conditions to oxidise one of the alcohol groups to an aldehyde. An intramolecular 5-exo-trig cyclisation forms a lactol, and a second oxidation of the hemiacetal alcohol group furnishes the lactone. The reaction works with symmetrical diols, but surprisingly, non-symmetrical diols could also be used as substrates with the less hindered (in comparison to TEMPO) ANBO, which shows good kinetic selectivity for the least hindered alcohol. This means that the bulkiest side of the diol will be incorporated on the alkoxy side of the γ -lactone.



Selected examples



Mechanism



Scheme 157: Stahl's Cu/nitroxyl-catalysed aerobic oxidative lactonization of diols. NB: the mechanism is shown with ABNO as the nitroxyl co-catalyst, however this can be exchanged for TEMPO.

Mechanistically, the redox properties of copper(I) as a reductant are enhanced through addition of the bpy ligand (a sigma donor) which allows for the reduction of oxygen to superoxide and subsequent coordination to copper(II). The copper(II)-peroxo complex then reacts with the copper(I) catalyst, forming a bridged peroxo dimer through the same

mechanism. This then oxidises ANBO-H to ANBO[•], regenerating the copper(I) catalyst and forming a copper(II) hydroperoxide. The latter can react with the alcohol or water, releasing hydrogen peroxide and forming a copper(II) alkoxide complex which allows the nitroxyl radical species to engage in a HAT step with the coordinated alkoxide. The aldehyde (or ketone in the case of secondary alcohols) is then released along with copper(I) and the hydroxylamine (*i.e.*, ANBO-H). Despite the very benign reaction conditions, the scope of the method was demonstrated mostly on very simple diols with no other functional groups.

3.2 Objectives

Despite the widespread availability of synthetic methods to construct lactones, several challenges still exist. The most common method to synthesize lactones is intramolecular esterification from linear hydroxy acid precursors. When spirocyclic lactones are the target, this method falls short, as the difficulty in synthesising these molecules lies in the construction of the quaternary centre. When choosing an acyclic precursor for the Fischer-type lactonization, this quaternary centre must already be incorporated in the linear precursor, which is challenging in itself. Moreover, the presence of amine functionalities can be problematic in certain cases (e.g., Steglich esterification) as amines are more nucleophilic than alcohols, potentially leading to chemoselectivity issues. Additionally, the Baeyer-Villiger oxidation is typically not ideal to synthesize spirocyclic γ -lactones as the required spirocyclobutanone starting materials are more difficult to synthesize than the corresponding butyrolactones.

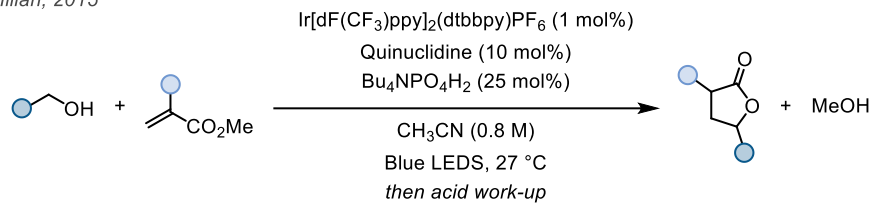
The other common strategy is halolactonization and its variations, and while a versatile method, the use of molecular halogens also limits the scope. Combined with the required formation of a very electrophilic halonium ion in order for the reaction to succeed, these factors preclude the use of precursors containing nucleophilic functional groups. Similar issues arise when using methods based on oxidation (e.g., Nicewicz's or Stahl's work) as they are not always compatible with nucleophilic functionalities which are prone to oxidation due to their electron-rich nature. They can also be limited to certain substitution patterns, such as electron-rich and stabilised olefin coupling partners. Unlike many of the others, the Lewis acid-catalysed methodology reported by Li and co-workers can be used to synthesize α -amino spirocyclic γ -lactones – the compound class targeted in this chapter – but it is not compatible with alkyl amines and is limited to the use of very electron-poor anilines.

Moreover, ATRA-cyclisation of α -halo carbonyls and olefins is a useful method for the construction of spirocyclic lactones as demonstrated by Curran and co-workers, but the use of electrophilic α -halo carbonyls again introduces limitations, as they are not compatible with nucleophiles. Furthermore, the required substitution pattern at the carbonyl α -position (*i.e.*, stabilisation with a second electron-withdrawing group) signifies that it is impossible to have an amine substituent at the desired carbonyl α -position.

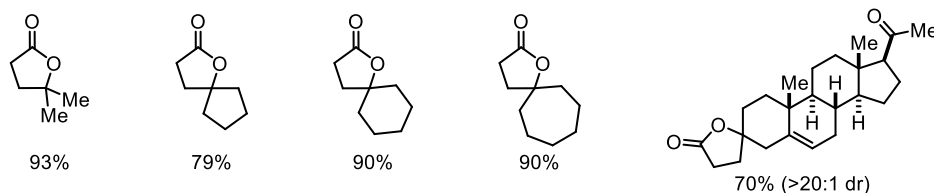
A method which can be used to construct spirocyclic α -amino γ -butyrolactones in a single operation from simple (*i.e.*, not containing any quaternary centres) precursors, such

as vinylogous Michael acceptors and cyclic aliphatic alcohols, would be highly desirable. In fact, such a strategy to access spirocyclic γ -butyrolactones was reported in 2015 by the group of MacMillan (**Scheme 158**).³¹¹ By using a hydrogen-bond acceptor to coordinate to the alcohol, the α -C–H bond is sufficiently weakened so that it can engage in a thermodynamically driven hydrogen atom transfer step with quinuclidine radical cation. The latter is generated *via* photo-induced SET with excited Ir(III) and acts as a HAT catalyst. As the α -hydroxy radical is strongly nucleophilic due to electron donation from the oxygen lone pair into its 2p SOMO, it can react in a polarity-matched, kinetically favourable π -addition with a Michael acceptor such as methyl acrylate (*i.e.*, a Giese-type addition). It is therefore possible to use α,α -disubstituted alcohols, as not only is the C–H bond weakened with increasing substitution, lowering of the barrier associated with polarity-matched additions compensates for the increase of the barrier caused by sterics. Addition of an α -hydroxy radical to an acrylate yields a hydroxy ester precursor (in the case of α,α -disubstituted alcohols, this will contain the required quaternary centre) which can then cyclise, forming the spirocyclic lactone.

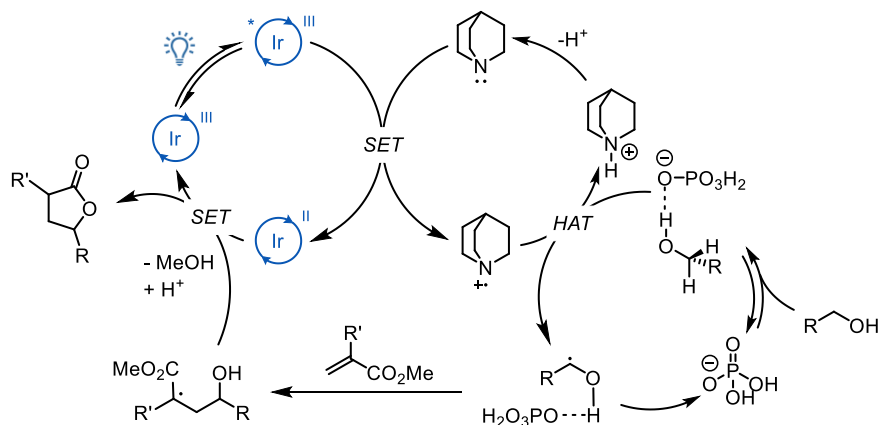
MacMillan, 2015



Selected examples



Mechanism

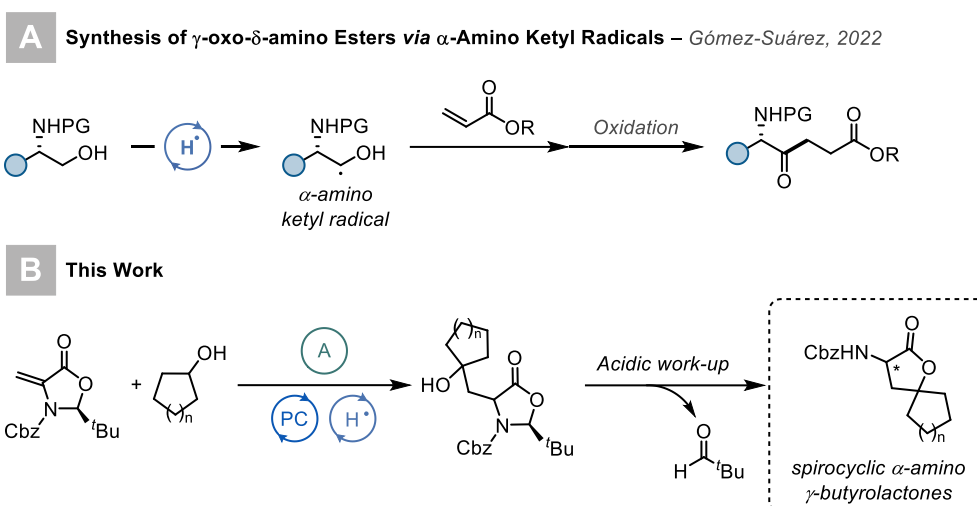


Scheme 158: highly selective photoredox α -alkylation/lactonization of alcohols with methyl acrylate via a hydrogen atom transfer mechanism.

The reaction is based on a reductive quenching cycle where the excited state of the photocatalyst $[\text{Ir}(\text{dF}(\text{CF}_3)\text{ppy})_2(\text{dtbbpy})]\text{PF}_6$, is quenched by sub-stoichiometric quinuclidine which forms protonated quinuclidinium after the spontaneous HAT with the alcohol. Turnover of the photocatalyst is achieved by reduction of the Giese adduct and proton transfer, regenerating ground state Ir(III) and quinuclidine. The hydroxy ester then undergoes a cyclisation (essentially a transesterification) with the pendent alcohol introduced during the Giese step, which is achieved by adding Amberlyst 15 and heating at 50 °C for 3 h.

Recently in our group, we have found that covalent activation of an alcohol as a boronate allows the hydrogen in the α -hydroxy C–H bond to be preferentially abstracted over an H atom in an α -carbamoyl C–H bond, thus leading to the formation of α -carbamoyl ketyl radicals.³¹² These can be trapped by a Michael acceptor (e.g., acrylate) which was applied to the synthesis of γ -oxo- δ -amino acid derivatives (**Scheme 159A**). This led to speculation into whether using the Karady-Beckwith alkene as the vinylogous Michael acceptor would allow us to access spirocyclic α -amino γ -butyrolactones (**Scheme 159B**).

Firstly, an initial Giese-type addition would introduce the quaternary hydroxy precursor in a 1,5-relationship with the carbonyl group. A 5-*exo-trig* cyclisation (transesterification), followed by elimination of pivaldehyde, would then furnish the desired spirocyclic aminolactone.



Scheme 159: A) previous work in the group concerning covalent activation of alcohols to synthesize γ -oxo- δ -amino acid esters; B) this work on accessing spirocyclic α -amino spirocyclic γ -butyrolactones.

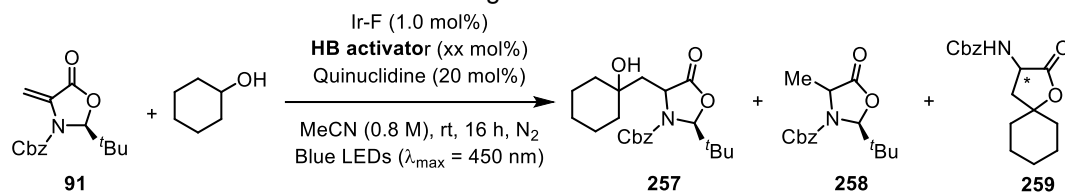
3.3 Results & discussion

3.3.1 Initial Reaction Optimisation

For the optimisation, using the Karady-Beckwith alkene (A) and cyclohexanol as the substrates, the photocatalyst, HAT catalyst, hydrogen bond activator, solvent, and time were investigated. Each parameter can be seen in the following tables, with the parameters kept constant shown in the scheme above the table.

The key ketyl radical species needed to be accessed *via* HAT from the alcohol substrate requires the use of a hydrogen bond (HB) or Lewis acid activator, therefore the most suitable additive was determined first. In **Table 6**, all of the activators tested can be seen.

Table 6: initial investigation into a suitable activator.



Entry	Additive	Equiv. (mol%)	91 (%)	257 (%)	258 (%)	259 (%)
1	Tetrabutylammonium acetate	25	40	25	0	5
2	Tetrabutylammonium monophosphate	25	80	5	2	11
3	Tetrabutylammonium monophosphate	50	31	0	10	31
4	Tetrabutylammonium tetrafluoroborate	25	0	65	1	16
5	Tetrabutylammonium tetrafluoroborate	50	0	43	0	43
6	Tetrabutylammonium tetrafluoroborate	100	0	0	0	69
7	Tetrabutylammonium perchlorate	25	0	38	0	34
8	Boric acid	25	0	50	0	23
9	Phenylboronic acid	25	0	18	6	45
10	Bis(3,4-dimethylphenyl)(hydroxy)borane	25	0	20	14	31
11	2,4-Difluorophenylboronic acid	25	0	44	0	26
12	2,4,6-Trimethylphenyl boronic acid	25	0	0	5	66
13	2,4,6-Trimethylphenyl boronic acid	50	0	7	2	67
14	3,5-Bis(trifluoromethyl)benzeneboronic acid	25	97	0	0	0
15	(2,4,6-Triisopropylphenyl)boronic acid	25	0	31	0	41
16	4-Fluorophenylboronic acid	25	100	0	0	0
17	4-Methoxyphenylboronic acid	25	90	1	0	0
18	4-tert-Butylphenylboronic acid	25	40	40	0	0

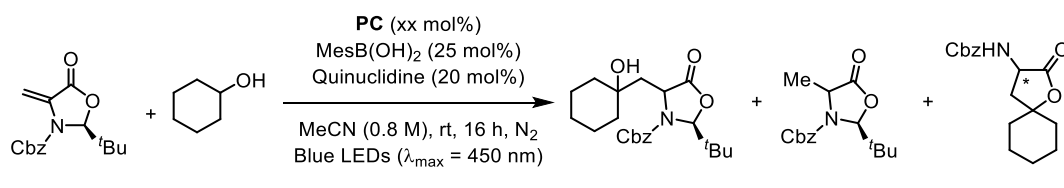
Inspired by MacMillan's seminal work, tetrabutylammonium (TBA) salts were initially tested. TBA acetate provided **257** in 25% and trace amounts of the desired spirocyclic butyrolactone **259** (**Table 6**, entry 1), while TBA monophosphate formed trace amounts of **257** and 31% of **259**, without the need for any work-up (entry 2). In an attempt to convert

more of **91** to product, the concentration of additive was increased to 50 mol%, however, this unexpectedly led to the formation of the reduced starting material, **258** (entry 3). TBA tetrafluoroborate provided a moderate yield of uncyclized product, however, increasing the concentration to 50 mol% gave a 1:1 ratio of **257** and **259**, with stoichiometric amounts of the additive providing **259** in 69% (**Table 6**, entries 4-6). Finally, TBA perchlorate also resulted in a 1:1 ratio of **257** and **259**, albeit with a poor mass balance (**Table 6**, entry 7).

Overall, the best performing additives were the boronic acids, with 2,4,6-trimethylphenyl/mesityl boronic acid (MesBA) providing the highest yield and best mass balance (entry 12). An increase of MesBA (25 to 50 mol%, entry 13, **Table 6**) did not provide a higher yield. Additional boronic acids were also tested, including both electron rich systems such as triisopropylphenyl boronic acid, methoxyphenylboronic acid and *tert*-butylphenylboronic acid (**Table 6**, entries 15, 17 and 18), as well as electron poor additives such as difluorinated, trifluoromethylated and monofluorinated (**Table 6**, entries 11, 14 and 16). Surprisingly, no trend was observed, as the only additives that provided any yield were difluorophenyl boronic acid (26%) and triisopropylphenyl boronic acid (41%), which also resulted in 31% of the uncyclised product **257**. Additionally, boric acid and dimethylphenylhydroxy borane (**Table 6**, entries 8 and 10) were examined, however only moderate yields were observed (23% and 31%, respectively) as well as significant percentage of uncyclized product.

Next, the photocatalyst was investigated (**Table 7**). Overall, the best result was achieved using 1 mol% of Ir-F (entry 1). A small increase was observed with a loading of 2.5 mol% (entry 2). Ir-F(Me), which exhibits a similar potential as Ir-F, performed slightly worse (entry 2). The use of organo-photocatalyst 4-CzIPN (entries 4-6) resulted in the formation of only **D**, however a high loading of 5.0 mol% was required to gain a similar yield as Ir-F.

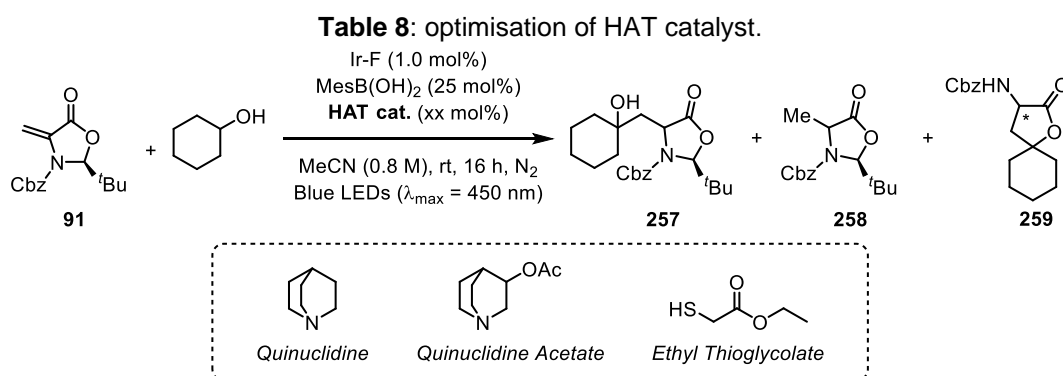
Table 7: optimisation of photocatalyst.



Entry	Photocatalyst	Loading (mol%)	91 (%)	257 (%)	258 (%)	259 (%)
1	Ir-F	1.0	0	17	6	66
2	Ir-F	2.5	0	5	0	70
3	Ir-F(Me)	1.0	0	0	0	60
4	4-CzIPN	1.0	0	0	0	50

5	4-CzIPN	2.5	0	16	0	42
6	4-CzIPN	5.0	0	0	0	68

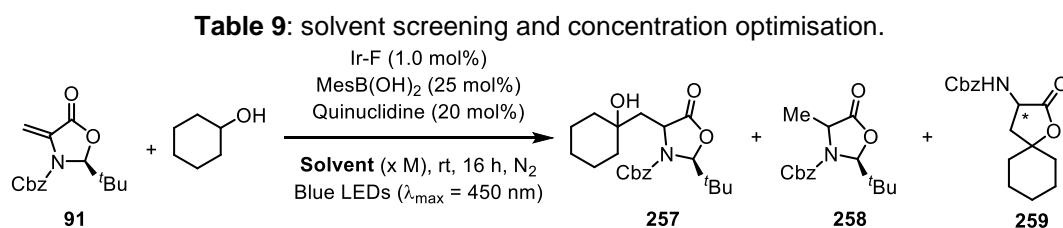
Numerous HAT catalysts were tested (**Table 8**). The highest yield was achieved when using 20 mol% of quinuclidine (**Table 8**, entry 1). Any increase in catalyst loading did not provide an increase in yield (**Table 8**, entries 2 and 3). Its acetate derivative gave a significantly lower yield of 23% (**Table 8**, entry 5), while both TBADT (tetrabutylammonium decatungstate, used without an additional photocatalyst as it can perform the HAT directly under irradiation with 365 nm LEDs) and ethyl thioglycolate failed to provide any product (entries 4 and 6).



Entry	HAT Catalyst	HAT Catalyst Loading (mol%)	259 (%)
1	Quinuclidine	20	66
2	Quinuclidine	25	64
3	Quinuclidine	50	64
4 ^x	TBADT	25	0
5	Quinuclidine Acetate	25	23
6	Ethyl thioglycolate	25	0

^x using a 365 nm light source and no external catalyst.

Next, the optimal solvent was investigated (**Table 9**). Although acetone and DMF (**Table 9**, entries 7 and 9) performed similarly to CH₃CN (**Table 9**, entry 4), the latter was chosen as it is more broadly applicable as a solvent compared to acetone, as well as more green and less toxic compared to DMF. The apolar solvent CH₂Cl₂ gave a low yield of 36% (**Table 9**, entry 5), and similar results were also observed with dioxane, THF and DMSO (**Table 9**, entries 6, 8 and 10).

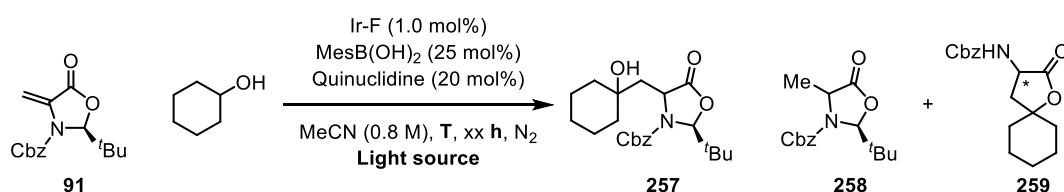


Entry	Solvent	Concentration (M)	91 (%)	257 (%)	258 (%)	259 (%)
1	CH ₃ CN	0.1	0	60	0	0
2	CH ₃ CN	0.2	0	41	0	27
3	CH ₃ CN	0.4	0	0	0	50
4	CH ₃ CN	0.8	0	0	5	66
5	CH ₂ Cl ₂	0.8	0	0	0	36
6	1,4-Dioxane	0.8	0	10	0	44
7	DMF	0.8	0	0	0	68
8	THF	0.8	0	0	0	15
9	Acetone	0.8	0	3	0	65
10	DMSO	0.8	0	0	0	36

An imperative factor observed was the importance of concentration. At a concentration of 0.2 M, 41% of **257** is present and 27% of the desired spirocycle (**Table 9**, entry 2). Under less concentrated conditions, only the open form is observable (**Table 9**, entry 1), contrasting with a significantly more concentrated setting where **259** emerges as the sole product (**Table 9**, entry 4).

Finally, the light source, temperature, and reaction time were investigated (**Table 10**). Overall, using a LED lamp with wavelengths of 405 nm and 425 nm provided similar results, but gave a decreased yield compared to a wavelength of 450 nm (**Table 10**, entries 1-3). Decreasing the reaction time resulted in a slight decrease in yield, while running the reaction for 24 hours gains a slightly higher yield (**Table 10**, entries 4 and 5). An elevated reaction temperature also led to a decrease in the formation of **259** (**Table 10**, entry 6).

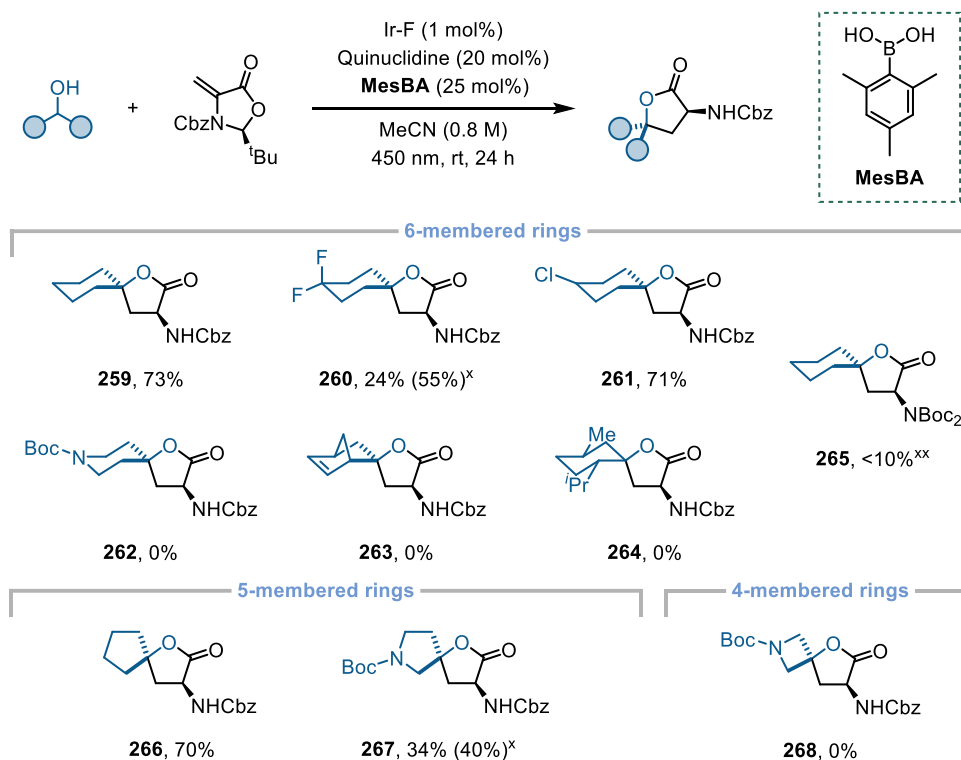
Table 10: optimisation of light source, temperature, and time.



Entry	Light source (nm)	Temperature (°C)	Time (hours)	259 (%)
1	405	25	16	57
2	425	25	16	57
3	450	25	16	66
4	450	25	8	60
5	450	25	24	75
6	450	40	16	57

3.3.2 Scope & Limitations

Thus, with the optimised conditions in hand, a number of substrates were investigated for the scope of the method. Initially, a selected number of substrates were tried to investigate the tolerance of the methodology, and a full scope was to be envisioned later.



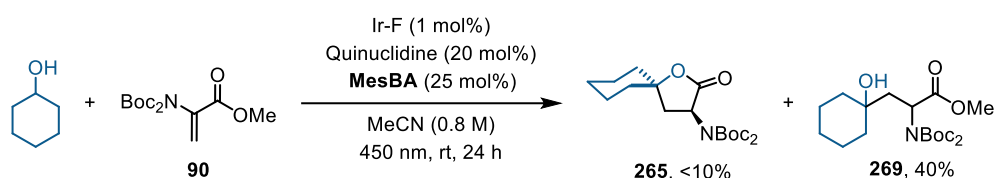
Scheme 160: scope of alcohols tested. ^xNMR yield calculated using TCI as the internal standard; ^{xx}reaction carried out using **161** (0.5 mmol, 1.0 equiv.) instead of **91**.

Spirocyclic **259** could be accessed to provide an isolated yield of 73%. Similarly, 4-chlorocyclohexanol was successfully converted to the corresponding butyrolactone **261** in high yield. In comparison to the 55% yield detected by NMR analysis, fluorinated product **260** was isolated in a lower yield of 24%. This could be attributed to product loss occurring in the purification process. No starting material or other side products were isolated or detected *via* NMR spectroscopy. This led to speculation into the cause of poor mass balance with certain substrates. Attempts to obtain compounds **263** and **264** derived from 5-norbornen-2-ol and (-)-menthol, respectively, failed, resulting in the re-isolation of **91**. The lack of reactivity of these two substrates could be attributed to presence of bulky groups which ultimately lead to steric repulsion, hindering the reaction.

Exploration into additional ring sizes was also conducted. Both cyclopentanol and Boc-protected pyrrolidinol were successfully converted into the corresponding products **266** and

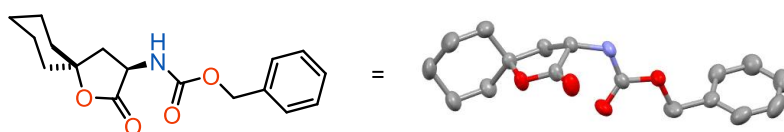
267 in 70% and 34%, respectively. Notably, the isolated yield of **267** was also lower in comparison to the calculated NMR yield, which could have occurred during the purification process. Next, an investigation into 4-membered rings was conducted. Compound **268**, derived from Boc-protected azetidinol, however, was not isolated. Instead, **258**, the reduced form of **91**, was isolated, as well as the recovery of unreacted alcohol starting material.

Furthermore, the use of other Dha derivatives as radical acceptors, instead of **91**, was investigated. **Scheme 161** shows the reaction of cyclohexanol with protected Dha derivative **90**, where the desired product **265** was isolated in less than 10%. Instead, the open, uncyclized form (**269**) was obtained as the major product in 40% yield. No other products or starting material were detected/isolated, therefore the mass balance of the reaction appeared to be notably poor – approximately 50%.



Scheme 161: reaction of **90** with cyclohexanol. Yields shown are of isolated product.

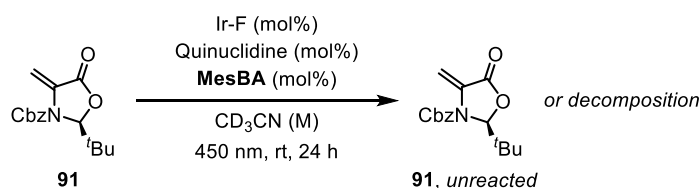
To further elucidate the structure of these novel spirocyclic γ -butyrolactones, crystals were grown to use for single-crystal X-ray diffraction. **Scheme 162** shows the X-ray crystal structure of compound **259**. Unfortunately, despite the tendency of these compounds to crystallise, suitable crystals of any of the other spirocycle could not be obtained as of yet. *Note:* additional information can be found in the experimental section.



Scheme 162: X-ray crystal structure of spirocyclic γ -butyrolactone **259**.

3.3.3 Mechanistic Studies & Investigation into Decomposition

Due to the inconsistencies experienced during the exploration of the substrate scope, an examination into the possible cause of the low yields and poor mass balance was conducted. Initially, to investigate the possibility of decomposition of **91** occurring under the optimised conditions, a series of test reactions were conducted in the absence of an alcohol substrate (**Table 11**), where reaction components were systematically omitted.

Table 11: investigation into the decomposition of **91**.


Entry	Ir-F (mol%)	Quinuclidine (mol%)	MesBA (mol%)	CD ₃ CN (M)	91 left (%)
1 ^x	-	100	-	0.1	>95
2 ^x	-	-	100	0.1	>95
3 ^x	-	100	100	0.1	>95
4	1.0	20	-	0.8	>95
5	1.0	-	25	0.8	>95
6	-	20	25	0.8	>95
7	1.0	20	25	0.8	<20

^xRan in the absence of photocatalyst, under air and no LED light source. **91** left was calculated by NMR analysis using TCI as the internal standard.

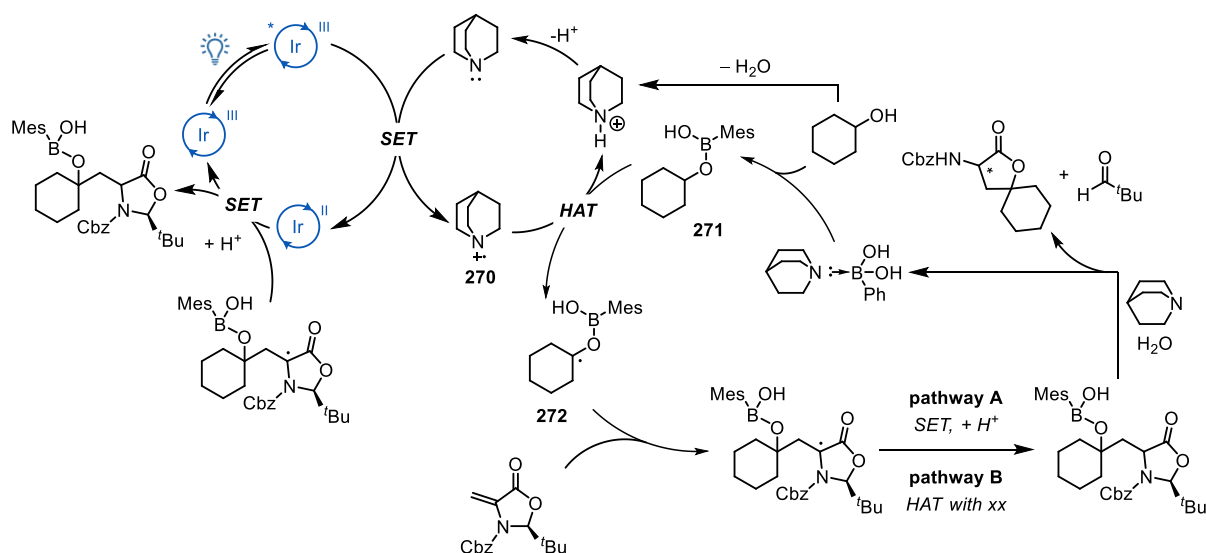
Each reaction was run in a 0.1 mmol scale under the conditions shown above, using deuterated solvent in order to analyse the outcome prior to any work-up. To detect whether decomposition was occurring exclusively under irradiative conditions, test reactions were also carried out in air without the presence of a photocatalyst or LED light source (**Table 11**, entries 1-3). **91** was reacted with stoichiometric quantities of quinuclidine and MesBA, both individually and together. No decomposition was observed in any of these reactions, and the presence of unreacted alkene was confirmed by ¹H NMR using an internal standard.

Under the optimised photoreaction conditions, no decomposition was discovered when using quinuclidine and MesBA individually in the presence of the photocatalyst (**Table 11**, entries 4 and 5). Additionally, when using both additives in the absence of Ir-F, the alkene remained unaltered (**Table 11**, entry 6). The only entry in **Table 11** that resulted in decomposition was entry 7 – the optimised conditions in the absence of any alcohol substrate. No starting material or other products could be detected *via* NMR.

From the results above it is apparent that in the absence of the alcohol substrate, both the photocatalyst, HAT catalyst as well as the activator are necessary for alkene decomposition. Additional experiments are required to establish whether the alkene is decomposed by sensitization-polymerisation (*i.e.*, by the photocatalyst itself), or whether radicals resulting from quenching of photocatalyst by the boronate are responsible.

An initial mechanism is shown below (**Scheme 163**), however mechanistic studies should be carried out to support the proposal. Initially, after irradiation, the excited

photocatalyst undergoes a SET with quinuclidine, forming the reduced photocatalyst and radical cation **270**. This species can react with boronic ester species **271** in a HAT to form ketyl radical **272**. This is followed by the addition of the ketyl radical to the Michael acceptor i.e., the KB alkene **91**, which can theoretically undergo two pathways: SET followed by protonation, or a HAT. An intramolecular cyclisation then occurs to provide the desired spirocyclic γ -butyrolactone, and pivaldehyde as the by-product, the latter of which was detected by running the reaction in deuterated solvent. From the optimisation studies, it can be deduced that the additive also plays multiple roles; it is needed for the activation of the alcohol towards HAT, as well as to promote the final cyclisation step. Further experiments must be carried out, including radical trapping experiments and quantum yield calculations. Furthermore, Stern-Volmer experiments would shed light on the species that is quenching the excited state of the photocatalyst.



Scheme 163: proposed mechanism of the methodology.

3.4 Outlook & Future Aspirations

In summary, based on previous research on the synthesis of enantioenriched α -amino acids using the Beckwith-Karady alkene, a method to synthesis of enantioenriched spirocyclic α -amino butyrolactones was developed. The protocol uses readily available starting materials, such as cyclic alcohols, and converts them into biologically relevant three-dimensional spirocycles, without the need for stoichiometric amounts of strong acids/bases. Although high yields were obtained during the optimisation of the reaction, complications arose when investigating the alcohol scope, such as poor mass balance and difficulties during purification, leading to low yields. Additionally, a significant dispute of decomposition of the alkene was observed.

Additional experiments are required to address these concerns, depending on the results of the reactions suggested in the previous section. If the boronate species derived from quinuclidine and the boronic acid is quenching the photocatalyst, switching to an alternative Lewis acid may be necessary. Although high concentrations seem to be beneficial for the cyclisation, similar conversions of the starting material were also obtained at higher dilutions. If polymerisation is the issue, diluting the reaction mixture and carrying out the cyclisation in an additional step, e.g., with an acidic work-up, is recommended.

Although there are notable concerns that demand resolution, with some work this method holds significant promise and could offer direct access to libraries of remarkably attractive enantioenriched building blocks.

4 Experimental Section

In this section, experimental and synthetic work carried out by collaborators (as detailed above in the appropriate entries of the thesis) is not reported and can be found in the supporting information of the corresponding publications.

4.1 General Remarks

All reactions were performed in oven-dried glassware under argon, unless otherwise stated. Reaction temperatures are referred to the ones of the heating/cooling media (heating block, cryogenic bath), unless otherwise stated. Reactions were stirred using PTFE-coated magnetic stirring bars at ~ 1000 rpm, unless otherwise stated. Commercially available chemicals were purchased from Sigma-Aldrich, ABCR, Acros Organics, Alfa Aesar, TCI Europe, Fluorochem, Chempur, Carbolution Chemicals, Combi Blocks and used as received, unless otherwise noted. Low boiling solvents (<110 °C) were removed by rotary evaporation under reduced pressure, heating the solution with a water bath at 40 °C. High boiling solvents (>110 °C) were removed in vacuo (< 1 mbar) at room temperature or under mild heating (< 50 °C), unless otherwise stated. Yields refer to chromatographically and spectroscopically (¹H, ¹³C, ¹⁹F) homogeneous material, unless otherwise stated. The identity of literature-known compounds was assessed by comparison of ¹H NMR spectra and therefore reported. New compounds were characterised using ¹H NMR, ¹³C NMR, ¹⁹F NMR (when applicable), HRMS, retention factor on thin layer chromatography.

4.1.1 Analytical Techniques

TLC were conducted with precoated glass-backed plates (silica gel 60 F254) and visualized by exposure to UV light (254 nm) or stained with basic potassium permanganate (KMnO₄), Ninhydrin or p-anisaldehyde solutions, and subsequent heating. Flash column chromatography was performed on silica gel (40-60 μm) or on neutral aluminum oxide (Brockmann Grade I, 58 Å), the eluent used is reported in the respective experiments. ¹H NMR spectra were recorded at 400 MHz or 600 MHz, ¹³C NMR spectra at 101 MHz or 151 MHz, using Bruker Avance III 600 and Bruker Avance 400. Chemical shifts are reported in ppm relative to the solvent signal, coupling constants J in Hz. Multiplicities were defined by standard abbreviations. High-resolution mass spectra (HRMS) were obtained using ESI ionization (positive) on a Bruker micrOTOF. IR spectra were measured on a Bruker ALPHA spectrometer using attenuated total reflexion (ATR). OPUS 7.5 was used to analyse the measured spectra. The recorded peaks were defined as weak (w), medium (m) or strong (s).

Determination of enantiomeric excess was performed using a HPLC system from Agilent Technologies (1260 Infinity II) employing chiral prepacked columns (CHIRALPAK IA and CHIRALCEL OJ-H) from Daicel Chemical Industries Ltd.

4.1.2 Photocatalytic Setup

Kessil PR160-440nm or EvoluChem HCK1012-01-008 blue LEDs (32 W, $\lambda_{\text{max}} = 440 \text{ nm}$, **Figure S1A**) were used for irradiation, in combination with an EvoluChem™ PhotoRedOx Box (**Figure S1B**). The reaction temperature was kept at 27 °C by the fans incorporated in the reactor. With the fans switched off, reactions could be conducted at a constant temperature of 42 °C. For reactions carried out at 60 °C, two 32 W LED lamps were placed at 2.5 cm from the reaction vessel (**Figure S1C**). The heat produced by the LEDs was sufficient to maintain a constant temperature.

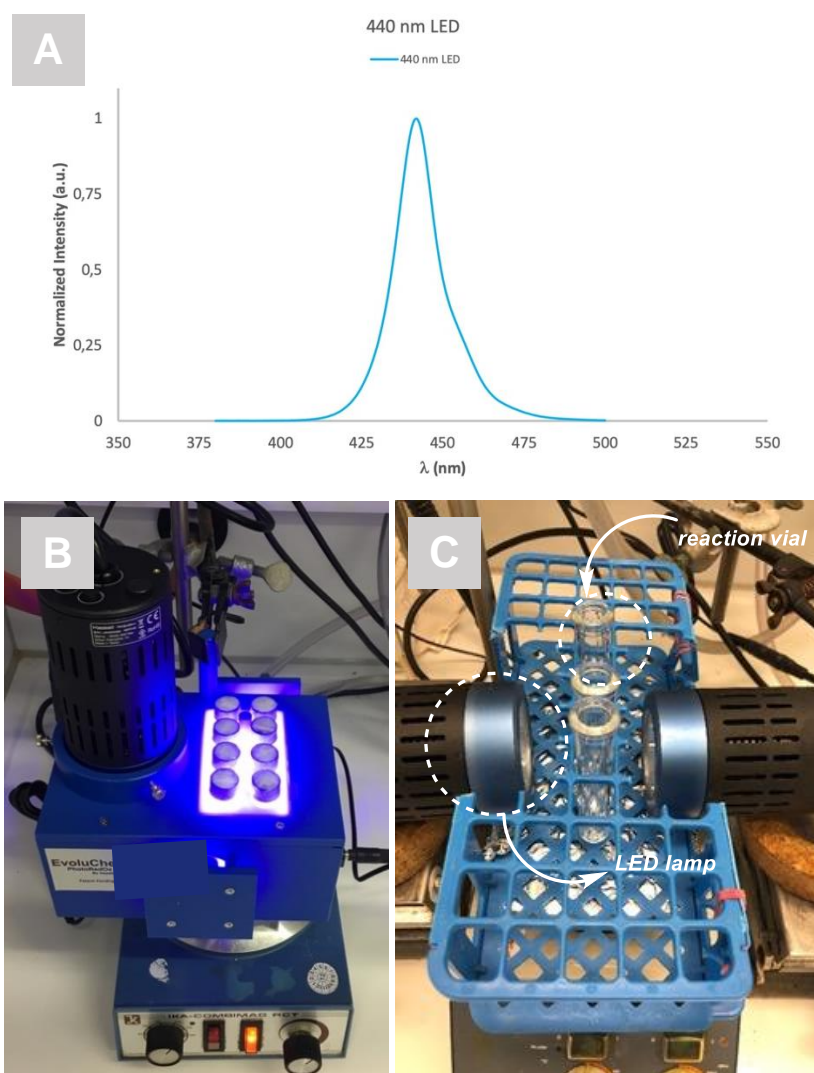


Figure S1. A) LED lamp emission spectrum. B) Reaction set-up for reactions at 27 °C or 42 °C. C) Reaction set-up for reactions at 60 °C.

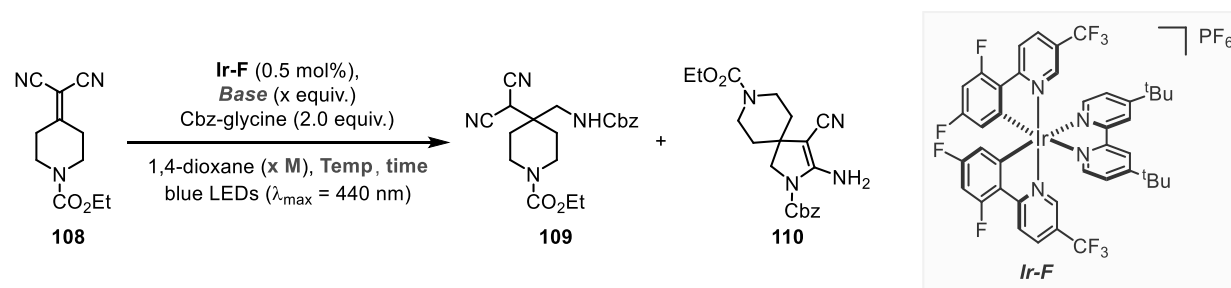
Chapter IIA: Synthesis of Sterically Congested $\beta^{2,2}$ -Amino Acids

Optimisation of Reaction Conditions

Giese-type Reaction:

General protocol: **A1** (21.9 mg, 1.0 equiv. 0.1 mmol), **Ir-F** (0.5-1.0 mol%), base (1.0 – 2.0 equiv.) and Cbz-glycine (41.8 mg, 0.2 mmol, 2.0 equiv.) were added to an 8 mL microwave vial and purged with N₂ (10 minutes under vacuum then open to N₂, repeated three times). 1,4-dioxane was added and the reaction bubbled with N₂ for 15 minutes. Bubbling was stopped and the vial was sealed and wrapped with parafilm, then irradiated at 440 nm, 60 °C for 16 hours. After removal of the solvent, the yields of the product and remaining starting material were calculated by ¹H NMR using trichloroethylene (9.0 μ l, 0.1 mmol, 1.0 equiv.) as internal standard.

Table S1. Optimisation studies of the Giese-type reaction.



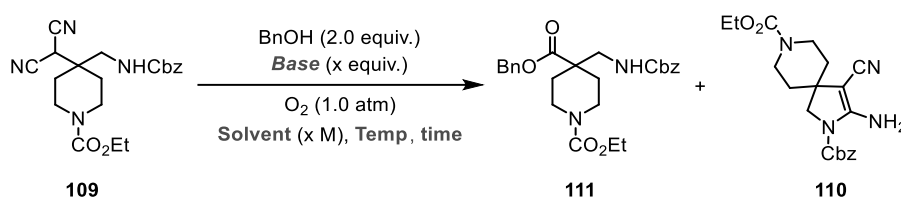
Entry	Base (equiv.)	Conc. (M)	Photocat. (mol%)	Temp. (°C)	Time (h)	109 (%) [*]	110 (%) [*]
1	K ₂ HPO ₄ (2.4)	0.1	Ir-F (1)	42	16	<5	84
2	2,6-Lutidine (2.4)	0.1	Ir-F (1)	42	16	43	58
3	Collidine (2.4)	0.1	Ir-F (1)	42	16	59	44
4	Collidine (2.4)	0.1	Ir-F (1)	24	16	24	76
5	Collidine (2.4)	0.1	Ir-F (1)	42	24	73	39
6	Collidine (2)	0.1	Ir-F (1)	60	16	>99	-
7	Collidine (2)	0.2	Ir-F (1)	60	16	>99	-
8	Collidine (2)	0.2	Ir-F (0.5)	60	16	>99	-
9	Collidine (2.4)	0.2	Ir-F (1)	42	16	46	21
10	Collidine (2.4)	0.4	Ir-F (1)	42	16	59	41
11	Collidine (2)	0.2	4CzIPN (1)	60	16	0	-
12	Collidine (2)	0.2	-	60	16	0	-
13 ^{**}	Collidine (2)	0.2	Ir-F (1)	60	16	0	-

^{*}Calculated by ¹H NMR using TCl (trichloroethylene) as internal standard. ^{**}Ran in the dark.

Oxidative esterification:

General protocol: The following procedure was adapted from Hayashi and co-workers. **109** (39 mg, 0.1 mmol, 1.0 equiv.) and Cs₂CO₃ (65 mg, 0.2 mmol, 2.0 equiv.) were purged with O₂. The solvent (0.1 M, pre-bubbled with O₂ for at least 4 h) was added. Then, benzyl alcohol (22 mg, 0.2 mmol, 2.0 equiv.) was added, and the reaction was bubbled for 2 min. The reaction was stirred with an O₂ balloon inserted. After removal of the solvent and solids, the yields of the product (**109**), spirocyclic by-product (**110**), and remaining starting material were calculated by ¹H NMR using trichloroethylene (9.0 μl, 0.1 mmol, 1.0 equiv.) as internal standard.

Table S2: Optimisation studies of the oxidative esterification reaction.



Entry	Base (equiv.)	Nucleophile (equiv.)	Solvent (M)	Temp. (°C)	Time (h)	109 (%) [*]	111 (%) [*]	110 (%) [*]
1	Cs ₂ CO ₃ (2)	BnOH (2)	MeCN (0.1)	RT	16	30	26	34
2*	Cs ₂ CO ₃ (2)	BnOH (2)	MeCN (0.1)	RT	24	0	72	3
3	Cs ₂ CO ₃ (2)	BnOH (2)	MeCN (0.1)	RT	72	0	74	22
4	Cs ₂ CO ₃ (2)	BnOH (2)	MeCN (0.1)	0	16	0	24	35
5	Cs ₂ CO ₃ (2)	BnOH (2)	MeCN (0.1)	50	24	0	52	19
6	Cs ₂ CO ₃ (2)	BnOH (2)	MeCN/C ₆ HF ₅ (9:1)	RT	16	0	42	55
7	Cs ₂ CO ₃ (1)	BnOH (2)	MeCN (0.1)	RT	24	0	50	45
8	DIPEA (2)	BnOH (2)	MeCN (0.1)	RT	24	0	32	37
9	Collidine (2)	BnOH (2)	MeCN (0.1)	RT	24	99	0	0
10	Et ₃ N (2)	BnOH (2)	MeCN (0.1)	RT	24	0	13	16
11**	DBU (2)	BnOH (2)	MeCN (0.1)	RT	24	0	82	0
12	Cs ₂ CO ₃ (2)	EtOH (10)	MeCN (0.1)	RT	24	0	60	10

^{*}Calculated by ¹H NMR using TCI (trichloroethylene) as internal standard.

*While results using BnOH as the nucleophile performed slightly better, it was decided to use EtOH for the scope, due to practicality in purification, as well as the utility of the EtO-protected amino esters. Additionally, to avoid evaporation of the volatile substrate, a large excess of 10 equiv. of the nucleophile was used.

**Although DBU provided slightly higher NMR yields than C₂CO₃, work-up and isolation of the targeted product in small scale was easier with the latter. Therefore, C₂CO₃ was selected as the optimal base for the reaction.

Synthesis & Characterisation of Starting Materials

Alkylidenemalononitriles:

General procedure 1 (GP1): Adapted from a procedure reported by Grenning and co-workers.³¹³ The corresponding cyclic ketone (1.0 equiv.) was dissolved in toluene (1.0 M). Malononitrile (1.0 equiv.), ammonium acetate (0.1 equiv.), and toluene/glacial acetic acid (3:1 v/v, 1.0 M total) were added. The reaction was heated at reflux (110-120 °C) with a Dean-Stark apparatus until completion (monitored by TLC). The reaction was then concentrated and quenched with 2N aq. HCl. The aqueous layer was extracted with ethyl acetate and the combined organic phases were washed with NaHCO₃, dried over anhydrous Na₂SO₄, filtered, and concentrated. The residue was purified by flash chromatography to afford the targeted product. Alkylidenemalononitriles **A12** (CAS 13166-10-4), and **A14** (CAS 2972-73-8) are commercially available and were purchased from Fluorochem.

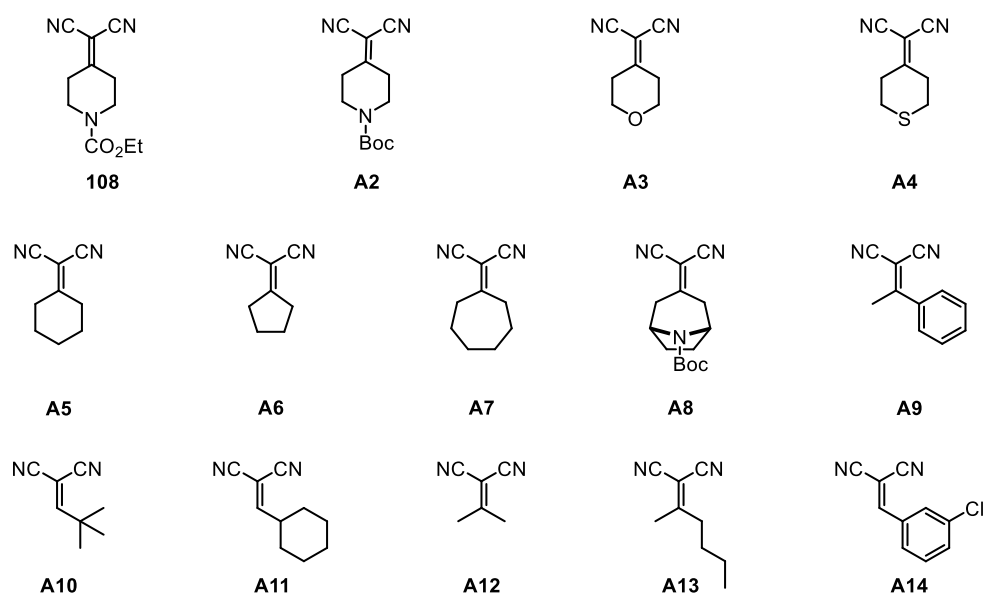
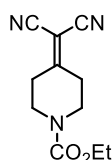


Figure S2. Synthesised alkylidenemalononitriles.

108



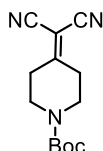
Synthesised following **GP1** using ethyl 4-oxopiperidine-1-carboxylate (5.0 g, 29.2 mmol, 1.0 equiv.). Purification via flash chromatography using silica gel (cyclohexane/EtOAc 3:1)

afforded **108** as an off-white solid in 76% yield (4.85 g, 22.2 mmol). Characterisation data matches the literature.³¹⁴

¹H NMR (600 MHz, CDCl₃) δ 4.19 (q, *J* = 7.1 Hz, 2H), 3.66 (t, *J* = 5.9 Hz, 4H), 2.75 (t, *J* = 5.9 Hz, 4H), 1.29 (t, *J* = 7.1 Hz, 3H).

¹³C NMR (151 MHz, CDCl₃) δ 179.0, 155.0, 111.2, 85.1, 62.4, 43.8, 34.1, 14.7.

A2



Synthesized following **GP1** using tert-butyl 4-oxopiperidine-1-carboxylate (1.0 g, 5.0 mmol, 1.0 equiv.). Purification via flash chromatography using silica gel (cyclohexane/EtOAc 3:1) afforded **A2** as a white solid in 76% yield (0.94 g, 3.8 mmol).³¹³

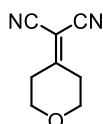
¹H NMR (400 MHz, CDCl₃) δ 3.60 (t, *J* = 5.8 Hz, 4H), 2.72 (t, *J* = 5.8 Hz, 4H), 1.47 (s, 9H).

¹³C{¹H} NMR (101 MHz, CDCl₃) δ 179.5, 154.1, 111.2, 84.8, 81.2, 43.8, 34.1, 28.4.

HRMS (ESI): [*m/z*] calculated for C₁₃H₁₆N₃O₂ ([M-H]): 246.1249; Found: 246.1248.

R_f (cyHex/EtOAc, 4:1) = 0.4 [Ninhydrin]

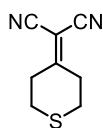
A3



Synthesized following **GP1** using tetrahydro-4H-pyran-4-one (0.6 mL g, 6.6 mmol, 1.0 equiv.). During the extraction a white precipitate formed which was filtered and washed to afford **A3** as a white solid in 43% yield (417 g, 2.8 mmol). Characterization data matches the literature.³¹³

¹H NMR (400 MHz, CDCl₃): δ 3.86 (t, *J* = 5.56, 4H), 2.80 (t, *J* = 5.56, 8 4H) ppm.

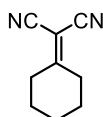
¹³C{¹H} NMR (101 MHz, CDCl₃): δ 178.5, 111.1, 84.2, 67.8, 35.1 ppm.

A4


Synthesized following **GP1** using tetrahydro-4H-thiopyran-4-one (0.582 g, 5.0 mmol, 1.0 equiv.). **A4** was isolated as a white solid in 48% yield (393 mg, 2.4 mmol). Characterization data matches the literature.³¹³

¹H NMR (400 MHz, CDCl₃): 3.04-2.99 (m, 4H), 2.91-2.86 (m, 4H) ppm.

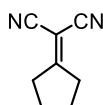
¹³C{¹H} NMR (101 MHz, CDCl₃) δ 180.8, 111.2, 85.2, 36.4, 30.8 ppm.

A5


Synthesized following **GP1** using cyclohexanone (0.68 mL, 6.6 mmol, 1.0 equiv.). Purification via flash chromatography using silica gel (cyclohexane/EtOAc 4:1) afforded **A5** as a colorless oil in 63% yield (4.85 g, 4.2 mmol). Characterization data matches the literature.³¹³

¹H NMR (400 MHz, CDCl₃) δ 2.67-2.64 (m, 4H), 1.83-1.77 (m, 4H), 1.71-1.66 (m, 2H)

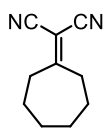
¹³C{¹H} NMR (101 MHz, CDCl₃) δ 185.0, 111.7, 82.6, 34.7, 28.0, 25.0.

A6


Synthesized following **GP1** using cyclopentanone (750 mg, 8.9 mmol, 1.0 equiv.). Purification via flash chromatography using silica gel (cyclohexane/EtOAc 7:1 → 5:1) afforded **A6** as a yellow oil in 81% yield (952 mg, 7.2 mmol). Characterization data matches the literature.³¹³

¹H NMR (600 MHz, CDCl₃) δ 2.82 – 2.72 (m, 4H), 1.94 – 1.86 (m, 4H).

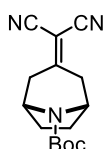
¹³C{¹H} NMR (101 MHz, CDCl₃) δ 192.6, 111.8, 81.3, 36.2, 26.0.

A7


Synthesized following **GP1** using cycloheptanone 2.5 g, 22.3 mmol, 1.0 equiv.). Purification via flash chromatography using silica gel (cyclohexane/EtOAc 1:1) afforded **A7** as a yellow solid in 87% yield (3.1 g, 19.4 mmol). Characterization data matches the literature.³¹³

¹H NMR (600 MHz, CDCl₃) δ 2.79 (t, 4H), 1.76 (dt, *J* = 9.47, 4.52 Hz, 4H), 1.58 (dt, *J* = 6.15, 2.83 Hz, 4H).

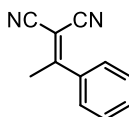
¹³C{¹H} NMR (151 MHz, CDCl₃) δ 188.6, 111.9, 85.0, 36.3, 29.1, 26.2.

A8


Synthesized following **GP1** using tert-butyl 3-oxo-8-azabicyclo[3.2.1]octane-8-carboxylate (500 mg, 2.22 mmol, 1.0 equiv.). Purification via flash chromatography using silica gel (cyclohexane/EtOAc 4:1 → 2:1) afforded **A8** as a pink solid in 87% yield (428 mg, 1.93 mmol). Characterization data matches the literature.³¹³

¹H NMR (600 MHz, CDCl₃) δ 4.45 (s, 2H), 2.91 (d, *J* = 15.62 Hz, 2H), 2.72 (d, *J* = 58.40 Hz, 2H), 2.16 – 1.97 (m, 2H), 1.55 (d, *J* = 8.19 Hz, 2H), 1.48 (s, 9H).

¹³C{¹H} NMR (151 MHz, CDCl₃) δ 178.9, 153.2, 111.3, 87.9, 81.0, 53.8, 40.1, 28.5.

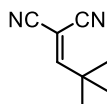
A9


Synthesized following **GP1** using cycloheptanone 2.5 g, 22.3 mmol, 1.0 equiv.). Purification via flash chromatography using silica gel (cyclohexane/EtOAc 1:1) afforded **A9** as a yellow solid in 87% yield (3.1 g, 19.4 mmol). Characterization data matches the literature.³¹⁵

$^1\text{H NMR}$ (600 MHz, CDCl_3) δ 7.55 (dt, $J = 7.68, 2.84$ Hz, 3H), 7.53 – 7.49 (m, 2H), 2.64 (s, 3H).

$^{13}\text{C}\{^1\text{H}\}$ NMR (151 MHz, CDCl_3) δ 175.6, 136.0, 132.4, 129.2, 127.5, 112.9, 112.8, 84.9, 24.4.

A10

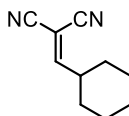


Synthesized following **GP1** using cycloheptanone 2.5 g, 22.3 mmol, 1.0 equiv.). Purification via flash chromatography using silica gel (cyclohexane/EtOAc 1:1) afforded **A10** as a yellow solid in 87% yield (3.1 g, 19.4 mmol). Characterization data matches the literature.³¹⁵

$^1\text{H NMR}$ (600 MHz, CDCl_3) δ 7.21 (s, 1H), 1.31 (s, 9H).

$^{13}\text{C}\{^1\text{H}\}$ NMR (151 MHz, CDCl_3) δ 177.6, 113.2, 111.2, 87.0, 37.1, 28.7.

A11

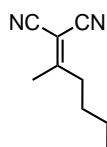


Synthesized following **GP1** using cycloheptanone 2.5 g, 22.3 mmol, 1.0 equiv.). Purification via flash chromatography using silica gel (cyclohexane/EtOAc 1:1) afforded **A11** as a yellow solid in 87% yield (3.1 g, 19.4 mmol). Characterization data matches the literature.³¹⁵

$^1\text{H NMR}$ (600 MHz, CDCl_3) δ 7.15 (d, $J = 10.49$ Hz, 1H), 2.82 – 2.62 (m, 1H), 1.83 – 1.70 (m, 5H), 1.42 – 1.31 (m, 2H), 1.25 (qd, $J = 12.59, 11.93, 3.21$ Hz, 3H).

$^{13}\text{C}\{^1\text{H}\}$ NMR (151 MHz, CDCl_3) δ 173.8, 112.4, 110.7, 88.0, 42.3, 31.0, 25.2, 24.7.

A13



Synthesized following **GP1** using 2-hexanone (0.45 g, 4.5 mmol, 1.0 equiv.). Purification via flash chromatography using silica gel (cyclohexane/EtOAc 1:1) afforded **A13** as an orange oil in 66% yield (0.36 g, 2.9 mmol). Characterization data matches the literature.³¹⁵

¹H NMR (600 MHz, CDCl₃) δ 2.58 (m, 2H), 2.27 (s, 3H), 1.55 (p, *J* = 7.6 Hz, 2H), 1.43 – 1.35 (m, 2H), 0.95 (t, *J* = 7.4 Hz, 3H).

Synthesis & Characterisation of Substituted Malononitrile Derivatives

General procedure 2 (GP2): The malononitrile derivative (1.0 mmol, 1.0 equiv.), **Ir-F** (5.5 mg, 1.0 mol%) and Cbz-glycine (209.2 mg, 1.0 mmol, 2.0 equiv.) were added to an 8 mL microwave vial and purged with N₂ (5 minutes under vacuum then open to N₂, repeating three times). 1,4-dioxane (5 mL, 0.2 M) was added and the reaction was bubbled with N₂ for 10 minutes. Bubbling was stopped and *sym*-collidine (264 μL, 2.0 mmol, 2.0 equiv.) was added, and the solution was bubbled for an additional 30 seconds. The vial was sealed and wrapped with parafilm, then irradiated at 440 nm, 60 °C (fan off) for 16 hours. Afterwards, the solvent was removed in vacuo and EtOAc was added. Citric acid (10 wt%) was added and the aqueous phase was washed with EtOAc. The organic phases were then washed with sat. NaHCO₃ (aq.), dried over anhydrous Na₂SO₄, filtered, and concentrated. The residue was purified to afford the desired product.

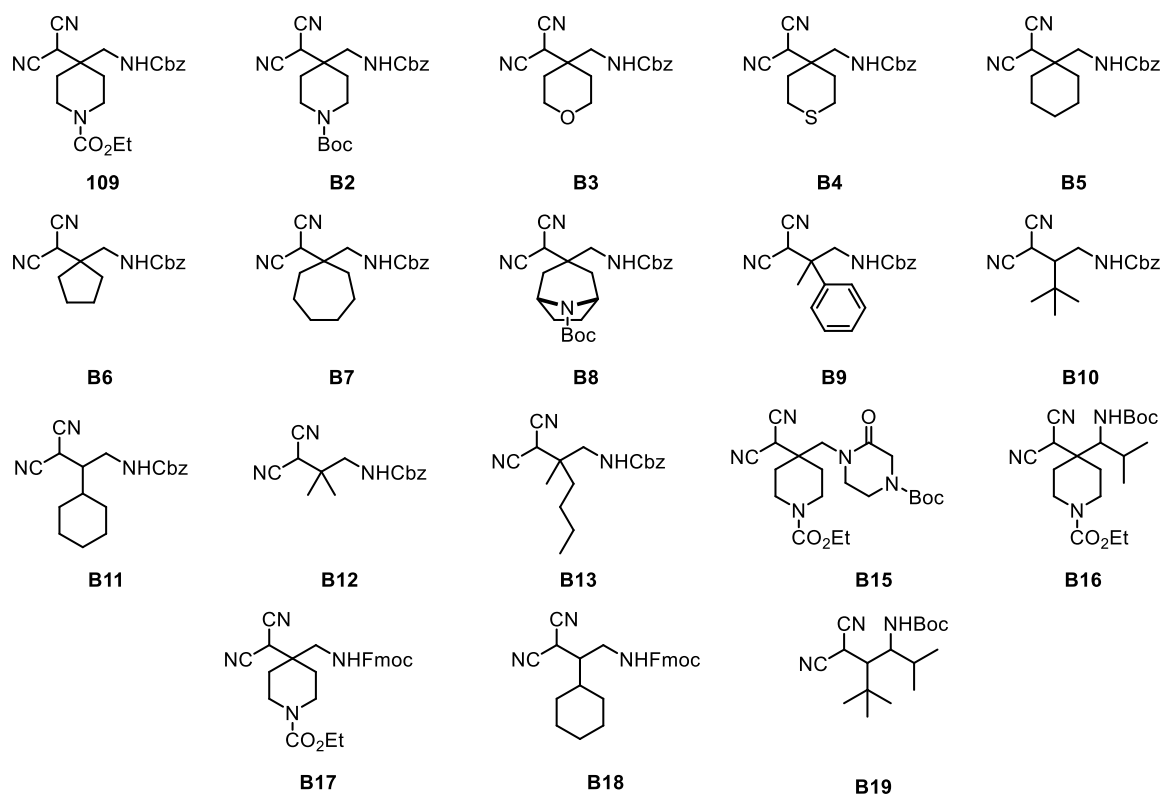
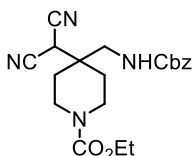


Figure S3. Synthesised substituted malononitrile derivatives.

109



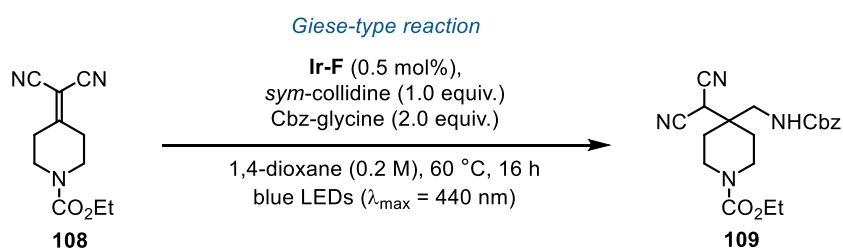
Synthesized following **GP2** using **108** (0.22 g, 1.0 mmol, 1.0 equiv.) and Z-glycine (418.4 mg, 2.0 mmol, 2.0 equiv.). **109** was isolated as a yellowish solid in 95% yield (0.37 g, 0.95 mmol).

¹H NMR (400 MHz, CDCl₃) δ 7.43 – 7.28 (m, 5H), 5.37 (s, 1H), 5.11 (s, 2H), 4.13 (q, *J* = 7.13 Hz, 2H), 3.96 (s, 2H), 3.87 (s, 1H), 3.51 (s, 2H), 3.16 (s, 2H), 1.69 (dt, *J* = 17.43, 8.61 Hz, 4H), 1.25 (t, *J* = 7.12 Hz, 3H).

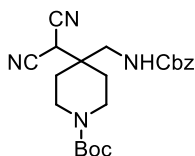
¹³C{¹H} NMR (101 MHz, CDCl₃) δ 157.3, 155.4, 135.9, 128.8, 128.6, 128.4, 111.3, 67.7, 61.9, 42.5, 41.4, 39.1, 32.2, 29.9, 14.7.

HRMS (ESI): [*m/z*] calculated for C₂₀H₂₄N₄NaO₄ ([*M*+Na]⁺): 407.1693; Found: 407.1690.

Scale-up synthesis of **109** – 2 x 5.0 mmol



The following reaction was performed in duplicate and combined for purification. **108** (1.1 g, 5.0 mmol, 1.0 equiv.), Ir-F (27.5 mg, 0.5 mol%) and Cbz-glycine (2.09 g, 10.0 mmol, 2.0 equiv.) were added to a 50 mL Schlenk flask (external ø = 3.0 cm, internal ø = 2.2 cm) and purged with N₂ (10 minutes under vacuum then open to N₂, repeated three times). Dry and degassed 1,4-dioxane (25 mL, 0.2 M) was added and the reaction was bubbled with N₂ for 5 minutes. Bubbling was stopped and *sym*-collidine (264 µL, 2.0 mmol, 2.0 equiv.) was added, and the solution was bubbled for an additional 30 seconds. The vial was sealed and wrapped with parafilm, then irradiated at 440 nm, 60 °C (fan off) for 16 hours. Afterwards, the solvent was removed in vacuo and EtOAc was added. Citric acid (10 wt%) was added and the aqueous phase was washed with EtOAc. The organic phases were then washed with sat. NaHCO₃ (aq.), dried over anhydrous Na₂SO₄, filtered, and concentrated. No further purification was necessary, and **109** was isolated in a combined yield of 88% (3.38 g).

B2


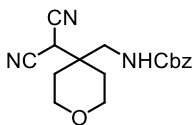
Synthesized following **GP2** using **A2** (247.3 mg, 1.0 mmol, 1.0 equiv.) and *Z*-glycine (418.4 mg, 2.0 mmol, 2.0 equiv.). Purification via flash chromatography using silica gel (cyclohexane/EtOAc, 4:1) afforded **B2** as a yellowish solid in 60% yield (247.5 mg, 0.60 mmol).

¹H NMR (600 MHz, CDCl₃) δ 7.35 (dp, *J* = 12.96, 6.62, 5.90 Hz, 5H), 5.25 (s, 1H), 5.11 (s, 2H), 4.00 – 3.73 (m, 3H), 3.50 (s, 2H), 3.12 (s, 2H), 1.83 – 1.58 (m, 4H), 1.45 (s, 9H).

¹³C{¹H} NMR (151 MHz, CDCl₃) δ 157.3, 154.6, 135.9, 128.8, 128.6, 128.4, 111.3, 80.5, 67.7, 42.7, 41.4, 32.2, 30.0, 28.5.

HRMS (ESI): [*m/z*] calculated for C₂₂H₂₈N₄NaO₄ ([*M*+Na]⁺): 435.2007; Found: 435.2003.

R_f (cyHex/EtOAc, 1:1) = 0.50 [Ninhydrin].

B3


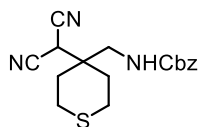
Synthesized following **GP2** using **A3** (148.2 mg, 1.0 mmol, 1.0 equiv.) and *Z*-glycine (418.4 mg, 2.0 mmol, 2.0 equiv.). Purification via flash chromatography using silica gel (cyclohexane/EtOAc, 4:1) afforded **B3** as a white solid in 95% yield (266.4 mg, 0.95 mmol).

¹H NMR (600 MHz, CDCl₃) δ 7.35 (q, *J* = 6.59 Hz, 5H), 5.22 (t, *J* = 7.61 Hz, 1H), 5.12 (s, 2H), 3.84 (d, *J* = 11.46 Hz, 3H), 3.69 (q, *J* = 9.28, 8.38 Hz, 2H), 3.57 (d, *J* = 6.83 Hz, 2H), 1.84 (d, *J* = 10.26 Hz, 2H), 1.64 (d, *J* = 13.84 Hz, 2H).

¹³C{¹H} NMR (151 MHz, CDCl₃) δ 157.3, 135.9, 128.8, 128.6, 128.3, 111.3, 67.7, 63.0, 42.9, 40.6, 32.6, 30.6.

HRMS (ESI): [*m/z*] calculated for C₁₇H₁₉N₃NaO₃ ([*M*+Na]⁺): 336.1320; Found: 336.1319.

R_f (cyHex/EtOAc, 1:1) = 0.55 [Ninhydrin].

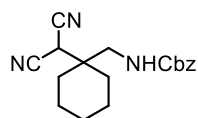
B4


Synthesized following **GP2** using **A4** (164.04 mg, 1.0 mmol, 1.0 equiv.) and *Z*-glycine (418.4 mg, 2.0 mmol, 2.0 equiv.). Purification via flash chromatography using silica gel (CyHex/EtOAc, 4:1) afforded **B4** as a yellow solid in 95% yield (312.9 mg, 0.95 mmol).

¹H NMR (600 MHz, CDCl₃) δ 7.40 – 7.31 (m, 5H), 5.22 – 4.99 (m, 3H), 3.81 (s, 1H), 3.48 (d, *J* = 6.88 Hz, 2H), 2.89 (d, *J* = 12.45 Hz, 2H), 2.54 (d, *J* = 14.05 Hz, 2H), 2.04 – 1.91 (m, 4H).
¹³C{¹H} NMR (151 MHz, CDCl₃) δ 157.2, 135.9, 128.8, 128.7, 128.4, 111.2, 67.8, 43.4, 41.8, 32.5, 32.0, 23.1.

HRMS (ESI): [*m/z*] calculated for C₁₇H₁₉N₃NaO₂S ([*M*+Na]⁺): 352.1088; Found: 352.1090.

R_f (cyHex/EtOAc, 1:1) = 0.46 [Ninhydrin].

B5


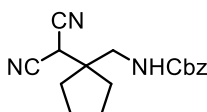
Synthesized following **GP2** using **A5** (146.2 mg, 1.0 mmol, 1.0 equiv.) and *Z*-glycine (418.4 mg, 2.0 mmol, 2.0 equiv.). Purification via flash chromatography using silica gel (CyHex/EtOAc, 4:1) afforded **B5** as a yellowish solid in 86% yield (267.8 mg, 0.86 mmol).

¹H NMR (600 MHz, CDCl₃) δ 7.35 (q, *J* = 8.46, 7.27 Hz, 5H), 5.12 (s, 2H), 5.06 (s, 1H), 3.83 (s, 1H), 3.46 (d, *J* = 6.97 Hz, 2H), 1.77 – 1.47 (m, 9H), 1.37 – 1.27 (m, 1H).

¹³C{¹H} NMR (151 MHz, CDCl₃) δ 157.2, 136.1, 128.7, 128.5, 128.3, 111.8, 67.5, 43.9, 42.3, 32.3, 30.8, 24.9, 21.3.

HRMS (ESI): [*m/z*] calculated for C₁₈H₂₁N₃NaO₂ ([*M*+Na]⁺): 334.1523; Found: 334.1526.

R_f (cyHex/EtOAc, 1:1) = 0.35 [Ninhydrin].

B6


Synthesized following **GP2** using **A6** (132.2 mg, 1.0 mmol, 1.0 equiv.) and *Z*-glycine (418.4 mg, 2.0 mmol, 2.0 equiv.). Purification via flash chromatography using silica gel (CyHex/EtOAc, 4:1) afforded **B6** as a yellowish oil in 95% yield (282.5 mg, 0.95 mmol).

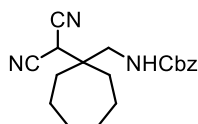
¹H NMR (600 MHz, CDCl₃) δ 7.34 (q, *J* = 7.83, 7.24 Hz, 6H), 5.36 – 5.24 (m, 1H), 5.12 (s, 2H), 3.89 (s, 1H), 3.33 (d, *J* = 6.84 Hz, 2H), 1.81 (s, 2H), 1.73 (s, 6H).

¹³C{¹H} NMR (151 MHz, CDCl₃) δ 157.3, 136.1, 128.7, 128.5, 128.3, 112.5, 67.5, 50.5, 46.7, 33.9, 31.3, 25.1.

HRMS (ESI): [*m/z*] calculated for C₁₇H₁₉N₃NaO₂ ([*M*+Na]⁺): 320.1369; Found: 320.1369.

R_f (cyHex/EtOAc, 1:1) = 0.30 [Ninhydrin].

B7



Synthesized following **GP2** using **A7** (160.2 mg, 1.0 mmol, 1.0 equiv.) and *Z*-glycine (418.4 mg, 2.0 mmol, 2.0 equiv.). Purification via flash chromatography using silica gel (CyHex/EtOAc, 4:1) afforded **B7** as a yellow oil in 88% yield (286.4 mg, 0.88 mmol).

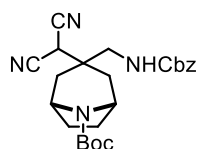
¹H NMR (600 MHz, CDCl₃) δ 7.44 – 7.28 (m, 5H), 5.11 (d, *J* = 17.05 Hz, 3H), 3.71 (s, 1H), 3.35 (d, *J* = 6.94 Hz, 2H), 1.74 – 1.61 (m, 6H), 1.57 (s, 6H).

¹³C{¹H} NMR (151 MHz, CDCl₃) δ 157.2, 136.1, 128.7, 128.5, 128.3, 112.3, 67.5, 47.0, 45.3, 36.4, 34.4, 32.4, 30.2, 29.2, 26.3, 22.8.

HRMS (ESI): [*m/z*] calculated for C₁₉H₂₃N₃NaO₂ ([*M*+Na]⁺): 348.1682; Found: 348.1682.

R_f (cyHex/EtOAc, 1:1) = 0.34 [Ninhydrin].

B8



Synthesized following **GP2** using **A8** (273.3 mg, 1.0 mmol, 1.0 equiv.) and *Z*-glycine (418.4 mg, 2.0 mmol, 2.0 equiv.). Purification via flash chromatography using silica gel (CyHex/EtOAc, 4:1) afforded **B8** as a yellowish solid in 88% yield (385.9 mg, 0.88 mmol).

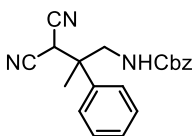
¹H NMR (400 MHz, CDCl₃) δ 7.37 – 7.33 (m, 5H), 5.37 (t, *J* = 6.95 Hz, 1H), 5.15 – 5.07 (m, 2H), 4.28 (s, 2H), 4.19 (s, 1H), 3.30 (d, *J* = 6.69 Hz, 2H), 2.08 (s, 4H), 1.72 (s, 2H), 1.56 (s, 2H), 1.44 (s, 9H).

¹³C{¹H} NMR (101 MHz, CDCl₃) δ 157.2, 153.3, 136.0, 128.7, 128.5, 128.2, 111.8, 80.4, 67.6, 51.8 & 51.1 (rotamer, 1C), 50.0, 39.4, 34.9 & 34.1 (rotamer, 1C), 32.6, 28.5 (4C).

HRMS (ESI): [m/z] calculated for C₂₄H₃₀N₄NaO₄ ([M+Na]⁺): 461.2157; Found: 461.2159.

R_f (cyHex/EtOAc, 1:1) = 0.28 [Ninhydrin].

B9



Synthesized following **GP2** using **A9** (168.2 mg, 1.0 mmol, 1.0 equiv.) and *Z*-glycine (418.4 mg, 2.0 mmol, 2.0 equiv.). Purification via flash chromatography using silica gel (CyHex/EtOAc, 4:1) afforded **B9** as a yellow oil in 85% yield (283.4 mg, 0.85 mmol).

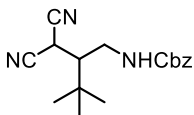
¹H NMR (600 MHz, CDCl₃) δ 7.43 (d, *J* = 7.44 Hz, 2H), 7.41 – 7.30 (m, 8H), 5.13 – 5.05 (m, 2H), 4.79 (t, *J* = 6.73 Hz, 1H), 4.15 (s, 1H), 3.77 (dd, *J* = 14.62, 7.21 Hz, 1H), 3.70 (dd, *J* = 14.20, 6.01 Hz, 1H), 1.71 (s, 3H).

¹³C{¹H} NMR (151 MHz, CDCl₃) δ 156.8, 137.9, 136.0, 129.6, 128.9, 128.7, 128.5, 128.4, 126.3, 111.7, 111.6, 67.6, 48.9, 46.0, 33.4, 20.9.

HRMS (ESI): [m/z] calculated for C₂₀H₁₉N₃NaO₂ ([M+Na]⁺): 356.1376; Found: 356.1369.

R_f (cyHex/EtOAc, 1:1) = 0.35 [Ninhydrin].

B10



Synthesized following **GP2** using **A10** (134.2 mg, 1.0 mmol, 1.0 equiv.) and *Z*-glycine (418.4 mg, 2.0 mmol, 2.0 equiv.). Purification via flash chromatography using silica gel (CyHex/EtOAc, 4:1) afforded **B10** as a pale oil in 56% yield (167.7 mg, 0.56 mmol).

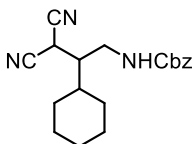
¹H NMR (600 MHz, CDCl₃) δ 7.39 – 7.30 (m, 5H), 5.24 (s, 1H), 5.19 – 5.09 (m, 2H), 3.98 (d, *J* = 1.90 Hz, 1H), 3.84 – 3.73 (m, 1H), 3.21 (ddd, *J* = 14.55, 10.92, 6.58 Hz, 1H), 2.47 – 2.36 (m, 1H), 1.08 (s, 9H).

$^{13}\text{C}\{^1\text{H}\}$ NMR (151 MHz, CDCl_3) δ 156.7, 136.2, 128.7, 128.4, 128.3, 113.3, 112.8, 67.5, 50.0, 40.4, 33.5, 27.8, 21.7.

HRMS (ESI): $[m/z]$ calculated for $\text{C}_{17}\text{H}_{21}\text{N}_3\text{NaO}_2$ ($[\text{M}+\text{Na}]^+$): 322.1527; Found: 322.1526.

R_f (cyHex/EtOAc, 1:1) = 0.44 [Ninhydrin].

B11



Synthesized following **GP2** using **A11** (160.2 mg, 1.0 mmol, 1.0 equiv.) and *Z*-glycine (418.4 mg, 2.0 mmol, 2.0 equiv.). Purification via flash chromatography using silica gel (CyHex/EtOAc, 4:1) afforded **B11** as a yellow oil in 91% yield (296.1 mg, 0.91 mmol).

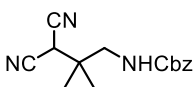
^1H NMR (600 MHz, CDCl_3) δ 7.38 – 7.31 (m, 5H), 5.13 (d, J = 5.73 Hz, 3H), 4.01 (d, J = 3.99 Hz, 1H), 3.68 – 3.57 (m, 1H), 3.24 (dt, J = 15.27, 7.62 Hz, 1H), 2.19 (s, 1H), 1.87 – 1.59 (m, 6H), 1.32 – 1.07 (m, 5H).

$^{13}\text{C}\{^1\text{H}\}$ NMR (151 MHz, CDCl_3) δ 156.8, 136.1, 128.7, 128.5, 128.4, 112.7, 112.5, 67.5, 46.2, 41.0, 38.5, 30.9, 29.7, 26.3, 26.1, 26.0, 23.7.

HRMS (ESI): $[m/z]$ calculated for $\text{C}_{19}\text{H}_{23}\text{N}_3\text{NaO}_2$ ($[\text{M}+\text{Na}]^+$): 348.1682; Found: 348.1682.

R_f (cyHex/EtOAc, 1:1) = 0.30 [Ninhydrin].

B12



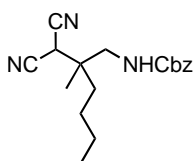
Synthesized following **GP2** using **A12** (106.1 mg, 1.0 mmol, 1.0 equiv.) and *Z*-glycine (418.4 mg, 2.0 mmol, 2.0 equiv.). Purification via flash chromatography using silica gel (CyHex/EtOAc, 4:1) afforded **B12** as a yellowish oil in 89% yield (241.5 mg, 0.89 mmol).

^1H NMR (400 MHz, CDCl_3) δ 7.36 (d, J = 2.58 Hz, 6H), 5.12 (s, 2H), 5.05 (s, 1H), 3.71 (s, 1H), 3.30 (d, J = 6.90 Hz, 2H), 1.23 (s, 5H).

$^{13}\text{C}\{^1\text{H}\}$ NMR (101 MHz, CDCl_3) δ 157.1, 136.0, 128.8, 128.6, 128.5, 111.8, 67.7, 48.9, 40.1, 32.5, 23.0.

HRMS (ESI): $[m/z]$ calculated for $\text{C}_{15}\text{H}_{17}\text{N}_3\text{NaO}_2$ ($[\text{M}+\text{Na}]^+$): 294.1210; Found: 294.1213.

R_f (cyHex/EtOAc, 1:1) = 0.40 [Ninhydrin].

B13


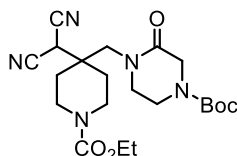
Synthesized following **GP2** using **A13** (148.2 mg, 1.0 mmol, 1.0 equiv.) and *Z*-glycine (418.4 mg, 2.0 mmol, 2.0 equiv.). Purification via flash chromatography using silica gel (CyHex/EtOAc, 4:1) afforded **B13** as a yellowish oil in 71% yield 222.5 mg, 0.71 mmol).

¹H NMR (400 MHz, CDCl₃) δ 7.45 – 7.28 (m, 5H), 5.12 (s, 2H), 5.01 (s, 1H), 3.74 (s, 1H), 3.31 (q, *J* = 7.85 Hz, 2H), 1.63 – 1.42 (m, 2H), 1.39 – 1.26 (m, 4H), 1.18 (s, 3H), 0.93 (t, *J* = 6.90 Hz, 3H).

¹³C{¹H} NMR (101 MHz, CDCl₃) δ 157.1, 136.0, 128.8, 128.6, 128.4, 112.0, 111.9, 67.6, 46.7, 42.4, 35.4, 31.9, 25.7, 23.2, 20.4, 14.0.

HRMS (ESI): [*m/z*] calculated for C₁₈H₂₃N₃NaO₂ ([*M*+Na]⁺): 336.1681; Found: 336.1682.

R_f (cyHex/EtOAc, 1:1) = 0.41 [Ninhydrin].

B15


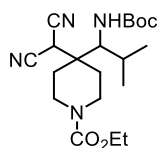
Synthesized following **GP2** using **A1** (219 .2 mg, 1.0 mmol, 1.0 equiv.) and 2-(4-(tert-butoxycarbonyl)-2-oxopiperazin-1-yl)acetic acid (387.5 mg, 1.5 mmol, 1.5 equiv.). Purification via flash chromatography using silica gel (CyHex/EtOAc, 4:1) afforded **B15** as a white solid in 80% yield (346.8 mg, 0.80 mmol).

¹H NMR (600 MHz, CDCl₃) δ 4.16 (q, *J* = 7.07 Hz, 4H), 4.13 (d, *J* = 4.09 Hz, 3H), 3.87 (dt, *J* = 14.19, 4.76 Hz, 2H), 3.69 (dd, *J* = 9.48, 3.99 Hz, 4H), 3.50 (t, *J* = 5.35 Hz, 2H), 3.33 (ddd, *J* = 13.89, 8.07, 5.36 Hz, 2H), 1.87 – 1.75 (m, 4H), 1.47 (s, 9H), 1.27 (t, *J* = 7.11 Hz, 3H).

¹³C{¹H} NMR (151 MHz, CDCl₃) δ 169.1, 155.4, 153.9, 111.6, 81.3, 61.9, 51.7, 50.7, 48.2, 41.7, 39.5, 32.4, 31.6, 28.5, 28.5, 14.7.

HRMS (ESI): [*m/z*] calculated for C₂₁H₃₁N₅NaO₅ ([*M*+Na]⁺): 456.2217; Found: 456.2217.

R_f (cyHex/EtOAc, 1:1) = 0.25 [Ninhydrin].

B16


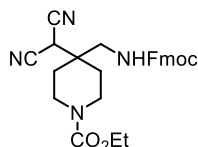
Synthesized following **GP2** using **A1** (219 .2 mg, 1.0 mmol, 1.0 equiv.) and (tert-butoxycarbonyl)valine (326.0 mg, 1.5 mmol, 1.5 equiv.). Purification via flash chromatography using silica gel (CyHex/EtOAc, 4:1) afforded **B16** as a white solid in 80% yield (346.8 mg, 0.80 mmol).

¹H NMR (600 MHz, CDCl₃) δ 4.77 (d, *J* = 11.0 Hz, 1H), 4.18 – 4.05 (m, 3H), 3.98 (d, *J* = 11.0 Hz, 1H), 3.87 – 3.73 (m, 1H), 3.69 (dt, *J* = 11.6, 5.1 Hz, 1H), 3.45 – 2.96 (m, 2H), 2.15 (hept, *J* = 6.7 Hz, 1H), 1.91 (ddt, *J* = 18.7, 14.2, 7.1 Hz, 1H), 1.85 – 1.68 (m, 3H), 1.44 (s, 9H), 1.24 (t, *J* = 7.1 Hz, 3H), 1.02 (d, *J* = 6.8 Hz, 3H), 0.97 (d, *J* = 6.7 Hz, 3H).

¹³C{¹H} NMR (151 MHz, CDCl₃) δ 156.2, 155.4, 111.8, 80.4, 61.8, 44.2, 38.9, 30.4, 28.4, 27.9, 27.0, 23.6, 17.9, 14.7.

HRMS (ESI): [m/z] calculated for C₂₀H₃₂N₄NaO₄ ([M+Na]⁺): 415.2317; Found: 415.2316.

R_f (cyHex/EtOAc, 1:1) = 0.30 [Ninhydrin].

B17


Synthesized following **GP2** using **A1** (219 .2 mg, 1.0 mmol, 1.0 equiv.) and (((9H-fluoren-9-yl)methoxy)carbonyl)glycine (446.0 mg, 1.5 mmol, 1.5 equiv.). Purification via flash chromatography using silica gel (CyHex/EtOAc, 4:1) afforded **B17** as a white solid in 80% yield (346.8 mg, 0.80 mmol).

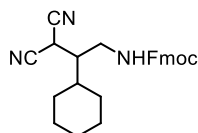
¹H NMR (400 MHz, CDCl₃) δ 7.76 (d, *J* = 7.5 Hz, 2H), 7.57 (d, *J* = 7.4 Hz, 2H), 7.41 (t, *J* = 7.5 Hz, 2H), 7.32 (td, *J* = 7.7, 1.2 Hz, 2H), 5.17 – 5.04 (m, 1H), 4.55 (d, *J* = 6.0 Hz, 2H), 4.14 (q, *J* = 7.1 Hz, 3H), 3.96 (s, 2H), 3.67 (s, 1H), 3.45 (s, 2H), 3.11 (s, 2H), 1.70 (d, *J* = 11.9 Hz, 2H), 1.59 (d, *J* = 13.6 Hz, 2H), 1.26 (t, *J* = 6.6 Hz, 3H).

¹³C{¹H} NMR (101 MHz, CDCl₃) δ 157.3, 155.4, 143.6, 141.5, 128.0, 127.2, 125.0, 120.2, 111.3, 66.8, 61.9, 47.5, 42.3, 41.4, 39.1, 32.3, 29.9, 14.7.

HRMS (ESI): [m/z] calculated for C₂₇H₂₈N₄NaO₄ ([M+Na]⁺): 495.2002; Found: 495.2003.

R_f (cyHex/EtOAc, 1:1) = 0.25 [Ninhydrin].

B18



Synthesized following **GP2** using **A11** (160.2 mg, 1.0 mmol, 1.0 equiv.) and (((9H-fluoren-9-yl)methoxy)carbonyl)glycine (446.0 mg, 1.5 mmol, 1.5 equiv.). Purification via flash chromatography using silica gel (CyHex/EtOAc, 4:1) afforded **B18** as a white solid in 80% yield (346.8 mg, 0.80 mmol).

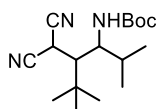
¹H NMR (400 MHz, CDCl₃) δ 7.77 (d, *J* = 7.5 Hz, 2H), 7.59 (d, *J* = 7.4 Hz, 2H), 7.42 (t, *J* = 7.5 Hz, 2H), 7.33 (t, *J* = 7.3 Hz, 2H), 5.00 (s, 1H), 4.50 (t, *J* = 5.8 Hz, 2H), 4.21 (t, *J* = 6.0 Hz, 1H), 3.87 (d, *J* = 3.8 Hz, 1H), 3.59 (d, *J* = 14.3 Hz, 1H), 3.31 – 3.11 (m, 1H), 2.15 (s, 1H), 1.86 – 1.58 (m, 6H), 1.32 – 1.03 (m, 5H).

¹³C{¹H} NMR (101 MHz, CDCl₃) δ 156.8, 143.9, 141.5, 127.9, 127.2, 125.1, 120.2, 112.7, 112.4, 67.0, 47.5, 46.1, 40.9, 38.6, 30.9, 29.6, 26.3, 26.1, 26.0, 23.6.

HRMS (ESI): [m/z] calculated for C₂₆H₂₇N₃NaO₂ ([M+Na]⁺): 436.1997; Found: 436.1995.

R_f (cyHex/EtOAc, 1:1) = 0.25 [Ninhydrin].

B19



Synthesized following **GP2** using **A10** (219.2 mg, 1.0 mmol, 1.0 equiv.) and (tert-butoxycarbonyl)valine (326.0 mg, 1.5 mmol, 1.5 equiv.). Purification via flash chromatography using silica gel (CyHex/EtOAc, 4:1) afforded **B19** as a white solid in 80% yield (346.8 mg, 0.80 mmol).

¹H NMR (400 MHz, CDCl₃) δ 4.82 (d, *J* = 10.7 Hz, 1H), 4.01 (d, *J* = 3.0 Hz, 1H), 3.89 (ddd, *J* = 10.5, 6.3, 3.7 Hz, 1H), 1.98 (t, *J* = 3.4 Hz, 1H), 1.88 (q, *J* = 6.6 Hz, 1H), 1.45 (s, 9H), 1.13 (s, 9H), 0.98 (dd, *J* = 8.9, 6.7 Hz, 6H).

¹³C{¹H} NMR (101 MHz, CDCl₃, rotamers) δ 156.1, 114.5, 113.4, 80.2, 54.0, 52.0, 34.9, 33.4, 28.4, 28.2, 21.0, 20.4, 16.9.

HRMS (ESI): [m/z] calculated for $C_{17}H_{29}N_3NaO_2$ ($[M+Na]^+$): 330.2155; Found: 330.2152.

R_f (cyHex/EtOAc, 1:1) = 0.25 [Ninhydrin].

Synthesis & Characterisation of β -Amino Esters/Amides

General procedure for oxidative esterification/amidation (GP3): In an 8 mL glass vial, the desired malononitrile derivative **B** (0.2 mmol, 2.0 equiv.) and Cs_2CO_3 (130.4 mg, 0.4 mmol, 2.0 equiv.) were purged with O_2 . MeCN (0.1 M, pre-bubbled with O_2 for at least 4h) was added. The nucleophile (2.0–10.0 equiv.) was added, and the reaction was bubbled for 2 min. The reaction was stirred for 18 hours with an O_2 balloon inserted. Then, the solvent was removed, and the resulting residue was purified to afford the desired product.

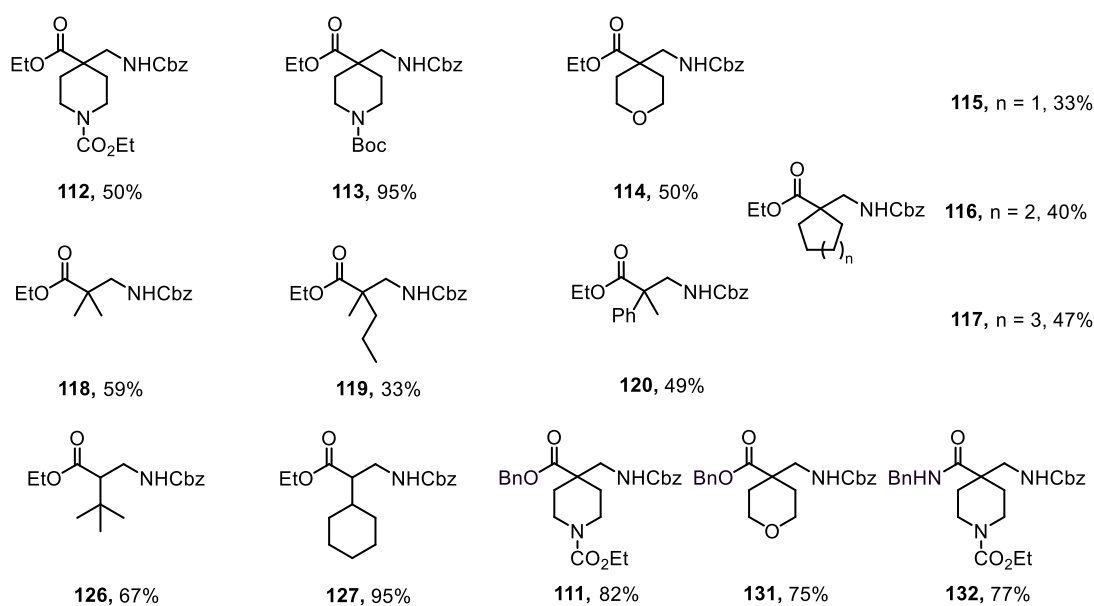
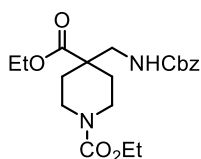


Figure S4. Synthesised substituted β -amino esters.

112



Synthesized following **GP3** using **109** (76.9 mg, 0.2 mmol, 1.0 equiv.) and EtOH (113 μL , 2.0 mmol, 10.0 equiv.). Purification via flash chromatography using silica gel (CyHex/EtOAc, 4:1) afforded **112** as a yellow oil in 50% yield (39.2 mg, 0.10 mmol).

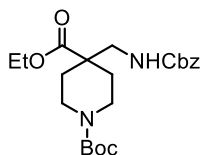
$^1\text{H NMR}$ (400 MHz, CDCl_3) δ 7.37 – 7.26 (m, 5H), 5.13 (t, $J = 6.57$ Hz, 1H), 5.06 (s, 2H), 4.12 (dq, $J = 19.46, 7.10$ Hz, 4H), 3.84 – 3.70 (m, 2H), 3.35 (d, $J = 6.52$ Hz, 2H), 3.20 – 3.05 (m, 2H), 2.02 (dt, $J = 13.61, 4.33$ Hz, 2H), 1.41 (ddd, $J = 13.83, 9.82, 4.11$ Hz, 2H), 1.23 (td, $J = 7.09, 3.92$ Hz, 6H).

$^{13}\text{C}\{^1\text{H}\}$ NMR (101 MHz, CDCl_3) δ 174.6, 156.6, 155.5, 136.4, 128.6, 128.2, 128.2, 66.9, 61.4, 61.2, 47.5, 46.6, 40.7, 30.6, 14.7, 14.2.

HRMS (ESI): [m/z] calculated for $\text{C}_{20}\text{H}_{28}\text{N}_2\text{O}_6$ ([M-H] $^-$): 393.2025; Found: 393.2026.

R_f (cyHex/EtOAc, 1:1) = 0.33 [Ninhydrin].

113



Synthesized following **GP3** using **B2** (82.5 mg, 0.2 mmol, 1.0 equiv.) and EtOH (113 μL , 2.0 mmol, 10.0 equiv.). Purification via flash chromatography using silica gel (CyHex/EtOAc, 4:1) afforded **113** as a yellow oil in 95% yield (79.9 mg, 0.19 mmol).

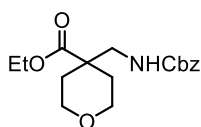
^1H NMR (400 MHz, CDCl_3) δ 7.40 – 7.26 (m, 5H), 5.08 (s, 2H), 5.02 (d, J = 6.46 Hz, 1H), 4.16 (q, J = 7.10 Hz, 2H), 3.72 (dt, J = 13.77, 4.87 Hz, 2H), 3.37 (d, J = 6.48 Hz, 2H), 3.11 (ddd, J = 13.52, 9.69, 3.28 Hz, 2H), 2.08 – 1.98 (m, 2H), 1.44 (s, 11H), 1.25 (t, J = 7.11 Hz, 3H).

$^{13}\text{C}\{^1\text{H}\}$ NMR (101 MHz, CDCl_3) δ 174.8, 156.6, 154.9, 136.5, 128.7, 128.3, 128.3, 79.7, 67.0, 61.3, 47.4, 46.6, 40.6, 30.8, 28.5, 14.3.

HRMS (ESI): [m/z] calculated for $\text{C}_{22}\text{H}_{32}\text{N}_2\text{NaO}_6$ ([M+Na] $^+$): 443.2153; Found: 443.2153.

R_f (cyHex/EtOAc, 1:1) = 0.25 [Ninhydrin].

114



Synthesized following **GP3** using **B3** (62.7 mg, 0.2 mmol, 1.0 equiv.) and EtOH (113 μL , 2.0 mmol, 10.0 equiv.). Purification via flash chromatography using silica gel (CyHex/EtOAc, 4:1) afforded **114** as a yellow oil in 50% yield (32.1 mg, 0.10 mmol).

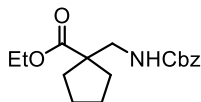
^1H NMR (600 MHz, CDCl_3) δ 7.38 – 7.29 (m, 5H), 5.08 (s, 2H), 5.01 (s, 1H), 4.18 (q, J = 7.13 Hz, 2H), 3.82 (dt, J = 12.13, 4.50 Hz, 2H), 3.52 (ddd, J = 12.21, 9.51, 2.86 Hz, 2H), 3.40 (d, J = 6.48 Hz, 2H), 2.09 – 2.02 (m, 2H), 1.54 (ddd, J = 13.88, 9.58, 4.16 Hz, 2H), 1.27 – 1.24 (m, 4H).

$^{13}\text{C}\{^1\text{H}\}$ NMR (101 MHz, CDCl_3) δ 174.9, 156.6, 136.5, 128.7, 128.3, 128.3, 67.0, 64.8, 61.3, 47.9, 45.8, 31.5, 14.3.

HRMS (ESI): [m/z] calculated for $\text{C}_{17}\text{H}_{23}\text{NNaO}_5$ ($[\text{M}+\text{Na}]^+$): 344.1469; Found: 344.1468.

R_f (cyHex/EtOAc, 1:1) = 0.30 [Ninhydrin].

115



Synthesized following **GP3** using **B6** (59.5 mg, 0.2 mmol, 1.0 equiv.) and EtOH (113 μL , 2.0 mmol, 10.0 equiv.). Purification via flash chromatography using silica gel (CyHex/EtOAc, 4:1) afforded **115** as a yellow oil in 33% yield (20.2 mg, 0.07 mmol).

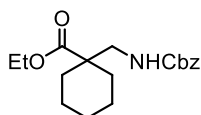
^1H NMR (400 MHz, CDCl_3) δ 7.41 – 7.27 (m, 5H), 5.32 (t, J = 6.46 Hz, 1H), 5.09 (s, 2H), 4.13 (q, J = 7.11 Hz, 2H), 3.34 (d, J = 6.41 Hz, 2H), 2.03 – 1.90 (m, 2H), 1.73 (qd, J = 7.43, 6.77, 3.43 Hz, 5H), 1.62 (dt, J = 10.80, 3.40 Hz, 3H), 1.25 (t, J = 7.12 Hz, 4H).

$^{13}\text{C}\{^1\text{H}\}$ NMR (101 MHz, CDCl_3) δ 177.8, 157.0, 136.7, 128.7, 128.2, 128.2, 66.8, 60.9, 54.3, 46.7, 34.6, 25.7, 14.3.

HRMS (ESI): [m/z] calculated for $\text{C}_{17}\text{H}_{23}\text{NNaO}_4$ ($[\text{M}+\text{Na}]^+$): 328.1518; Found: 328.1519.

R_f (cyHex/EtOAc, 1:1) = 0.22 [Ninhydrin].

116



Synthesized following **GP3** using **B5** (62.3 mg, 0.2 mmol, 1.0 equiv.) and EtOH (113 μL , 2.0 mmol, 10.0 equiv.). Purification via flash chromatography using silica gel (CyHex/EtOAc, 4:1) afforded **116** as a yellow oil in 40% yield (25.6 mg, 0.08 mmol).

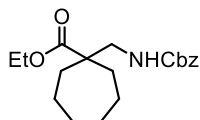
^1H NMR (400 MHz, CDCl_3) δ 7.41 – 7.27 (m, 5H), 5.08 (s, 2H), 5.03 (s, 1H), 4.14 (q, J = 7.10 Hz, 2H), 3.35 (d, J = 6.36 Hz, 2H), 2.04 – 1.90 (m, 2H), 1.65 – 1.46 (m, 3H), 1.36 (tdd, J = 21.86, 10.67, 3.41 Hz, 5H), 1.25 (t, J = 7.11 Hz, 4H).

$^{13}\text{C}\{^1\text{H}\}$ NMR (101 MHz, CDCl_3) δ 176.1, 156.6, 136.7, 128.6, 128.2, 66.8, 60.8, 47.7, 47.6, 31.5, 25.7, 22.5, 14.3.

HRMS (ESI): [m/z] calculated for $\text{C}_{18}\text{H}_{25}\text{NNaO}_4$ ($[\text{M}+\text{Na}]^+$): 342.1675; Found: 342.1676.

R_f (cyHex/EtOAc, 1:1) = 0.34 [Ninhydrin].

117



Synthesized following **GP3** using **B7** (65.1 mg, 0.2 mmol, 1.0 equiv.) and EtOH (113 μ L, 2.0 mmol, 10.0 equiv.). Purification via flash chromatography using silica gel (CyHex/EtOAc, 4:1) afforded **117** as a yellow oil in 47% yield (31.3 mg, 0.09 mmol).

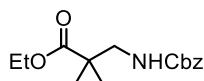
$^1\text{H NMR}$ (400 MHz, CDCl_3) δ 7.39 – 7.27 (m, 5H), 5.19 – 5.11 (m, 1H), 5.08 (s, 2H), 4.13 (q, $J = 7.12$ Hz, 2H), 3.31 (d, $J = 6.45$ Hz, 2H), 2.02 – 1.88 (m, 2H), 1.62 – 1.45 (m, 10H), 1.25 (t, $J = 7.14$ Hz, 4H).

$^{13}\text{C}\{^1\text{H}\}$ NMR (101 MHz, CDCl_3) δ 177.4, 156.8, 136.7, 128.6, 128.4, 128.2, 66.8, 60.9, 50.4, 47.9, 33.9, 30.7, 23.6, 14.3.

HRMS (ESI): $[m/z]$ calculated for $\text{C}_{19}\text{H}_{27}\text{NNaO}_4$ ($[\text{M}+\text{Na}]^+$): 356.1829; Found: 356.1832.

R_f (cyHex/EtOAc, 1:1) = 0.25 [Ninhydrin].

118



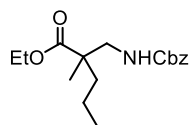
Synthesized following **GP3** using **B12** (54.3 mg, 0.2 mmol, 1.0 equiv.) and EtOH (113 μ L, 2.0 mmol, 10.0 equiv.). Purification via flash chromatography using silica gel (CyHex/EtOAc, 4:1) afforded **118** as a yellow oil in 59% yield (33.0 mg, 0.12 mmol).

$^1\text{H NMR}$ (400 MHz, CDCl_3) δ 7.40 – 7.28 (m, 5H), 5.25 (s, 1H), 5.09 (s, 2H), 4.12 (q, $J = 7.16$ Hz, 2H), 3.31 (d, $J = 6.57$ Hz, 2H), 1.24 (t, $J = 7.13$ Hz, 4H), 1.19 (s, 6H).

$^{13}\text{C}\{^1\text{H}\}$ NMR (101 MHz, CDCl_3) δ 177.2, 156.8, 136.7, 128.6, 128.2, 128.2, 66.8, 60.9, 48.9, 43.6, 23.1, 14.2.

HRMS (ESI): $[m/z]$ calculated for $\text{C}_{15}\text{H}_{21}\text{NNaO}_4$ ($[\text{M}+\text{Na}]^+$): 302.1471; Found: 302.1394.

R_f (cyHex/EtOAc, 1:1) = 0.33 [Ninhydrin].

119


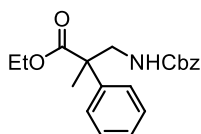
Synthesized following **GP3** using **B13** (62.7 mg, 0.2 mmol, 1.0 equiv.) and EtOH (113 μ L, 2.0 mmol, 10.0 equiv.). Purification via flash chromatography using silica gel (CyHex/EtOAc, 4:1) afforded **119** as a yellow oil in 33% yield (21.2 mg, 0.07 mmol).

^1H NMR (400 MHz, CDCl_3) δ 7.35 (d, $J = 4.59$ Hz, 5H), 5.19 – 5.11 (m, 1H), 5.09 (d, $J = 3.77$ Hz, 2H), 4.13 (q, $J = 7.13$ Hz, 2H), 3.45 – 3.20 (m, 2H), 1.62 – 1.43 (m, 2H), 1.29 – 1.18 (m, 7H), 1.16 (s, 3H), 0.87 (t, $J = 7.03$ Hz, 3H).

$^{13}\text{C}\{^1\text{H}\}$ NMR (101 MHz, CDCl_3) δ 176.8, 156.8, 136.8, 128.6, 128.5, 128.2, 66.8, 60.8, 47.5, 47.1, 36.9, 26.5, 23.2, 20.5, 14.3, 14.0.

HRMS (ESI): $[m/z]$ calculated for $\text{C}_{18}\text{H}_{27}\text{NNaO}_4$ ($[\text{M}+\text{Na}]^+$): 344.1940; Found: 344.1928.

R_f (cyHex/EtOAc, 1:1) = 0.28 [Ninhydrin].

120


Synthesized following **GP3** using **B9** (66.7 mg, 0.2 mmol, 1.0 equiv.) and EtOH (113 μ L, 2.0 mmol, 10.0 equiv.). Purification via flash chromatography using silica gel (CyHex/EtOAc, 4:1) afforded **120** as a yellow oil in 49% yield (33.5 mg, 0.10 mmol).

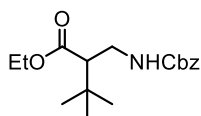
^1H NMR (400 MHz, CDCl_3) δ 7.40 – 7.25 (m, 10H), 5.23 (t, $J = 6.58$ Hz, 1H), 5.07 (s, 2H), 4.17 (qd, $J = 7.11, 4.48$ Hz, 2H), 3.75 – 3.51 (m, 2H), 1.63 (s, 3H), 1.21 (t, $J = 7.12$ Hz, 3H).

$^{13}\text{C}\{^1\text{H}\}$ NMR (101 MHz, CDCl_3) δ 175.7, 156.7, 140.9, 136.7, 128.8, 128.6, 128.2, 128.2, 127.4, 126.1, 66.8, 61.3, 52.0, 49.3, 20.6, 14.1.

HRMS (ESI): $[m/z]$ calculated for $\text{C}_{20}\text{H}_{23}\text{NNaO}_4$ ($[\text{M}+\text{Na}]^+$): 364.1519; Found: 364.1519.

R_f (cyHex/EtOAc, 1:1) = 0.45 [Ninhydrin].

126



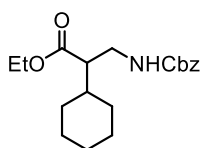
Synthesized following **GP3** using **B10** (59.9 mg, 0.2 mmol, 1.0 equiv.) and EtOH (113 μ L, 2.0 mmol, 10.0 equiv.). Purification via flash chromatography using silica gel (CyHex/EtOAc, 4:1) afforded **126** as a yellow oil in 67% yield (41.2 mg, 0.13 mmol).

$^1\text{H NMR}$ (400 MHz, CDCl_3) δ 7.42 – 7.26 (m, 5H), 5.08 (d, $J = 5.80$ Hz, 2H), 4.94 (t, $J = 6.22$ Hz, 1H), 4.20 – 4.07 (m, 2H), 3.56 (ddd, $J = 13.39, 7.05, 3.73$ Hz, 1H), 3.30 (ddd, $J = 13.46, 11.27, 5.43$ Hz, 1H), 2.51 (dd, $J = 11.23, 3.75$ Hz, 1H), 1.24 (t, $J = 7.15$ Hz, 3H), 1.00 (s, 9H).
 $^{13}\text{C}\{^1\text{H}\}$ NMR (101 MHz, CDCl_3) δ 174.1, 156.4, 136.6, 128.6, 128.2, 128.2, 66.8, 60.4, 56.0, 39.9, 32.6, 28.1, 14.4.

HRMS (ESI): [m/z] calculated for $\text{C}_{17}\text{H}_{25}\text{NNaO}_4$ ($[\text{M}+\text{Na}]^+$): 330.1672; Found: 330.1676.

R_f (cyHex/EtOAc, 1:1) = 0.22 [Ninhydrin].

127



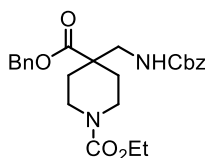
Synthesized following **GP3** using **B11** (65.0 mg, 0.2 mmol, 1.0 equiv.) and EtOH (113 μ L, 2.0 mmol, 10.0 equiv.). Purification via flash chromatography using silica gel (CyHex/EtOAc, 4:1) afforded **127** as a yellow oil in 95% yield (63.3 mg, 0.19 mmol).

$^1\text{H NMR}$ (400 MHz, CDCl_3) δ 7.40 – 7.28 (m, 5H), 5.18 – 5.04 (m, 3H), 4.25 – 4.01 (m, 2H), 3.48 (ddd, $J = 13.64, 6.60, 3.98$ Hz, 1H), 3.34 (ddd, $J = 13.67, 9.31, 5.73$ Hz, 1H), 2.51 – 2.37 (m, 1H), 1.78 – 1.57 (m, 6H), 1.25 (t, $J = 7.13$ Hz, 3H), 1.22 – 0.92 (m, 5H).
 $^{13}\text{C}\{^1\text{H}\}$ NMR (101 MHz, CDCl_3) δ 174.7, 156.4, 136.7, 128.6, 128.2, 128.2, 66.8, 60.6, 51.5, 40.2, 38.4, 30.8, 30.4, 26.3, 14.4.

HRMS (ESI): [m/z] calculated for $\text{C}_{19}\text{H}_{27}\text{NNaO}_4$ ($[\text{M}+\text{Na}]^+$): 356.1840; Found: 356.1832.

R_f (cyHex/EtOAc, 1:1) = 0.20 [Ninhydrin].

111



Synthesized following **GP3** using **109** (76.9 mg, 0.2 mmol, 1.0 equiv.) and benzyl alcohol (41.3 μ L, 0.4 mmol, 2.0 equiv.). Purification via flash chromatography using silica gel (CyHex/EtOAc, 4:1) afforded **111** as a yellowish oil in 82% yield (74.5 mg, 0.16 mmol).

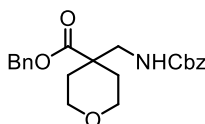
$^1\text{H NMR}$ (400 MHz, CDCl_3) δ 7.41 – 7.28 (m, 10H), 5.14 (s, 2H), 5.06 (s, 2H), 4.98 (t, $J = 6.59$ Hz, 1H), 4.10 (q, $J = 7.12$ Hz, 2H), 3.78 (d, $J = 13.73$ Hz, 2H), 3.38 (d, $J = 6.31$ Hz, 2H), 3.12 (t, $J = 11.08$ Hz, 2H), 2.07 (dd, $J = 10.53, 6.49$ Hz, 2H), 1.45 (ddd, $J = 13.88, 9.82, 4.14$ Hz, 2H), 1.23 (t, $J = 7.16$ Hz, 4H).

$^{13}\text{C}\{^1\text{H}\}$ NMR (101 MHz, CDCl_3) δ 174.5, 156.6, 155.5, 136.4, 135.7, 128.8, 128.6, 128.6, 128.3, 128.3, 128.2, 67.1, 67.0, 61.4, 47.6, 46.9, 40.7, 30.7, 14.8.

HRMS (ESI): [m/z] calculated for $\text{C}_{25}\text{H}_{30}\text{N}_2\text{NaO}_6$ ($[\text{M}+\text{Na}]^+$): 477.1997; Found: 477.1996.

R_f (cyHex/EtOAc, 1:1) = 0.30 [Ninhydrin].

131



Synthesized following **GP3** using **B3** (62.7 mg, 0.2 mmol, 1.0 equiv.) and benzyl alcohol (41.3 μ L, 0.4 mmol, 2.0 equiv.). Purification via flash chromatography using silica gel (CyHex/EtOAc, 4:1) afforded **131** as a yellow oil in 75% yield (57.5 mg, 0.15 mmol).

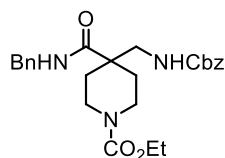
$^1\text{H NMR}$ (400 MHz, CDCl_3) δ 7.40 – 7.28 (m, 10H), 5.15 (s, 2H), 5.07 (s, 2H), 5.04 – 4.92 (m, 1H), 3.81 (dt, $J = 12.00, 4.45$ Hz, 2H), 3.49 (ddd, $J = 12.14, 9.55, 2.79$ Hz, 2H), 3.41 (d, $J = 6.60$ Hz, 2H), 2.08 (dt, $J = 13.80, 3.53$ Hz, 2H), 1.55 (ddd, $J = 13.75, 9.60, 4.11$ Hz, 2H).

$^{13}\text{C}\{^1\text{H}\}$ NMR (101 MHz, CDCl_3) δ 174.6, 156.6, 136.4, 135.7, 128.8, 128.6, 128.5, 128.3, 128.3, 128.2, 67.0, 66.9, 64.7, 48.0, 46.0, 31.4.

HRMS (ESI): [m/z] calculated for $\text{C}_{22}\text{H}_{25}\text{NO}_5$ ($[\text{M}-\text{H}]^-$): 384.1805; Found: 384.1811.

R_f (cyHex/EtOAc, 1:1) = 0.40 [Ninhydrin].

132



Synthesized following **GP3** using **109** (76.9 mg, 0.2 mmol, 1.0 equiv.) and benzyl amine (43.7 μ L, 0.4 mmol, 2.0 equiv.). Purification via flash chromatography using silica gel (CyHex/EtOAc, 4:1) afforded **132** as a yellow oil in 77% yield (69.8 mg, 0.15 mmol).

^1H NMR (300 MHz, CDCl_3) δ 7.49 – 7.12 (m, 11H), 6.49 (t, $J = 5.66$ Hz, 1H), 5.06 (s, 2H), 4.40 (d, $J = 5.64$ Hz, 2H), 4.10 (q, $J = 7.10$ Hz, 2H), 3.76 – 3.49 (m, 2H), 3.39 (d, $J = 5.88$ Hz, 4H), 1.92 (ddd, $J = 13.66, 6.94, 3.69$ Hz, 2H), 1.54 (ddd, $J = 13.14, 8.53, 3.73$ Hz, 2H), 1.24 (t, $J = 7.09$ Hz, 4H).

$^{13}\text{C}\{^1\text{H}\}$ NMR (75 MHz, CDCl_3) δ 174.2, 156.8, 155.5, 138.2, 136.4, 128.8, 128.6, 128.2, 128.1, 127.6, 127.6, 66.9, 61.4, 46.8, 46.0, 43.8, 40.4, 30.9, 14.7.

HRMS (ESI): [m/z] calculated for $\text{C}_{25}\text{H}_{31}\text{N}_3\text{O}_5$ ($[\text{M}-\text{H}]^-$): 454.2354; Found: 454.2342.

R_f (cyHex/EtOAc, 1:1) = 0.40 [Ninhydrin].

Synthesis & Characterisation of β -Amino acids

General procedure 4 (GP4): This procedure was adapted from a report by Sun and co-workers.³¹⁶ Cs_2CO_3 (130.4 mg, 0.4 mmol, 2.0 equiv.) was added to a solution of the desired malononitrile (0.2 mmol, 1.0 equiv.) in MeCN (2.0 mL, 0.1 M), and H_2O_2 (35 wt%, 10.0 equiv.) was added dropwise. The solution was stirred for 16 h at room temperature, then concentrated in vacuo. The reaction was then diluted with CH_2Cl_2 and washed with aqueous sat. NaHCO_3 solution three times. The combined aqueous phases were acidified with 1.0 M HCl until a pH of 2 was reached, and then extracted with EtOAc five times. The combined organic phases were dried over anhydrous Na_2SO_4 , filtered, and concentrated to give the desired product.

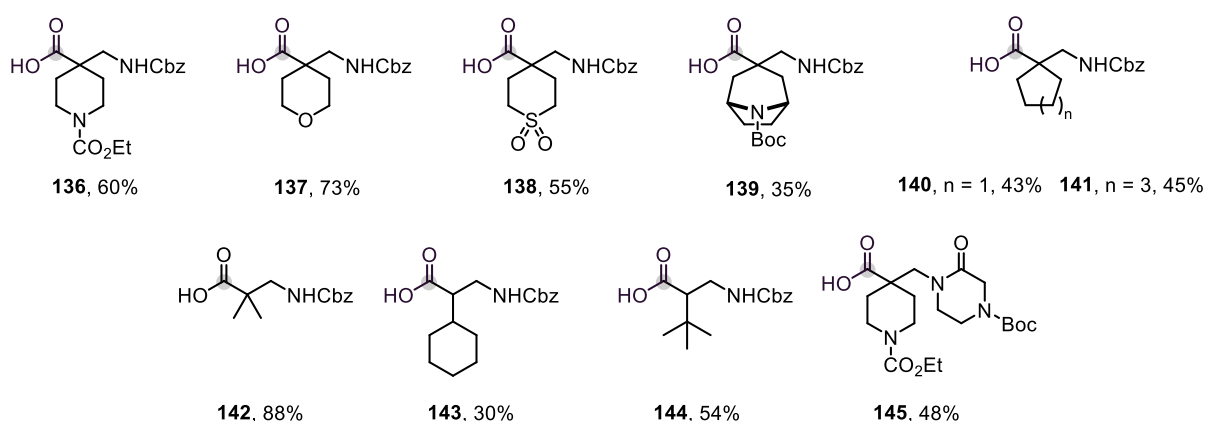
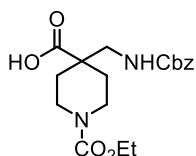


Figure S5. Synthesised β -amino acids.

Product 136



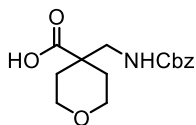
Synthesized following **GP4** using **109** (76.9 mg, 0.2 mmol, 1.0 equiv.). **136** was isolated as a yellowish solid in 60% yield (43.7 mg, 0.12 mmol).

$^1\text{H NMR}$ (600 MHz, CD_3CN) δ 7.66 – 7.34 (m, 5H), 5.98 (d, $J = 7.07$ Hz, 1H), 5.21 (s, 2H), 4.22 (q, $J = 7.09$ Hz, 2H), 3.98 – 3.91 (m, 2H), 3.45 (d, $J = 6.41$ Hz, 2H), 1.57 – 1.48 (m, 2H), 1.37 (t, $J = 7.10$ Hz, 3H).

$^{13}\text{C}\{^1\text{H}\}$ NMR (101 MHz, CD_3CN) δ 176.9, 157.7, 156.2, 138.2, 129.4, 128.8, 128.6, 66.9, 61.9, 48.7, 47.5, 41.7, 31.4, 14.9.

HRMS (ESI): $[m/z]$ calculated for $\text{C}_{18}\text{H}_{24}\text{N}_2\text{NaO}_6$ ($[\text{M}+\text{Na}]^+$): 387.1527; Found: 387.1527.

Product 137



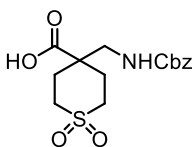
Synthesized following **GP4** using **B3** (62.7 mg, 0.2 mmol, 1.0 equiv.). **137** was isolated as a yellowish solid in 73% yield (42.8 mg, 0.15 mmol).

¹H NMR (400 MHz, CD₃CN) δ 7.58 – 7.16 (m, 5H), 5.84 (s, 1H), 5.07 (s, 2H), 3.79 (dt, *J* = 12.00, 4.19 Hz, 2H), 3.46 (d, *J* = 9.78 Hz, 2H), 3.34 (d, *J* = 6.70 Hz, 2H), 2.00 – 1.89 (m, 2H), 1.50 (ddd, *J* = 14.19, 10.31, 4.26 Hz, 2H).

¹³C{¹H} NMR (101 MHz, CD₃CN) δ 176.7, 157.8, 138.3, 129.5, 128.9, 128.6, 67.0, 65.4, 49.0, 46.7, 32.3.

HRMS (ESI): [*m/z*] calculated for C₁₅H₁₈NO₅ ([*M*-H]⁻): 292.1182; Found: 292.1190.

Product 138



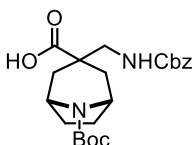
Synthesized following **GP4** using **B4** (65.9 mg, 0.2 mmol, 1.0 equiv.). **138** was isolated as a yellowish solid in 55% yield (37.6 mg, 0.11 mmol).

¹H NMR (400 MHz, CD₃CN) δ 7.45 – 7.26 (m, 3H), 5.93 (s, 0H), 5.06 (s, 1H), 3.35 (d, *J* = 6.72 Hz, 1H), 3.13 – 2.84 (m, 2H), 2.37 (d, *J* = 13.61 Hz, 1H), 1.98 (s, 2H).

¹³C{¹H} NMR (101 MHz, CD₃CN) δ 175.2, 157.8, 138.1, 129.4, 128.8, 128.6, 67.1, 48.7, 48.1, 47.1, 30.2.

HRMS (ESI): [*m/z*] calculated for C₁₅H₁₈NO₆S ([*M*-H]⁻): 340.0860; Found: 340.0860.

Product 139



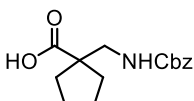
Synthesized following **GP4** using **B8** (87.7 mg, 0.2 mmol, 1.0 equiv.). **139** was isolated as an orange oil in 40% yield (33.5 mg, 0.08 mmol).

^1H NMR (600 MHz, CD_3CN) δ 7.35 (dq, $J = 14.32, 7.37$ Hz, 5H), 5.75 (d, $J = 6.88$ Hz, 1H), 5.03 (s, 2H), 4.07 (s, 2H), 3.12 (d, $J = 6.78$ Hz, 2H), 2.26 (d, $J = 14.12$ Hz, 2H), 1.80 (s, 2H), 1.67 (d, $J = 26.14$ Hz, 4H), 1.42 (s, 9H).

$^{13}\text{C}\{^1\text{H}\}$ NMR (101 MHz, CD_3CN) δ 178.0, 157.7, 154.2, 138.1, 129.4, 128.8, 128.6, 79.7, 66.9, 54.0, 53.2, 52.4, 45.0, 35.8, 35.2, 28.6, 27.7, 26.9.

HRMS (ESI): [m/z] calculated for $\text{C}_{22}\text{H}_{29}\text{N}_2\text{O}_6$ ([M-H] $^-$): 417.2029; Found: 417.2031.

Product 140



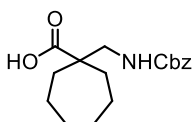
Synthesized following **GP4** using **B6** (59.5 mg, 0.2 mmol, 1.0 equiv.). **140** was isolated as a yellowish oil in 43% yield (23.8 mg, 0.09 mmol).

^1H NMR (400 MHz, CD_3CN) δ 7.50 – 7.18 (m, 5H), 5.71 (s, 1H), 5.05 (s, 2H), 3.30 (d, $J = 6.48$ Hz, 2H), 2.00 – 1.93 (m, 2H), 1.70 – 1.55 (m, 6H).

$^{13}\text{C}\{^1\text{H}\}$ NMR (101 MHz, CD_3CN) δ 178.8, 157.8, 138.4, 129.4, 128.8, 128.6, 66.8, 55.1, 47.4, 34.7, 26.0.

HRMS (ESI): [m/z] calculated for $\text{C}_{15}\text{H}_{18}\text{NO}_4$ ([M-H] $^-$): 276.1236; Found: 276.1241.

Product 141



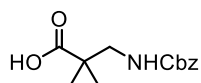
Synthesized following **GP4** using **B7** (65.1 mg, 0.2 mmol, 1.0 equiv.). **141** was isolated as a yellow oil in 45% yield (27.5 mg, 0.09 mmol).

^1H NMR (400 MHz, CD_3CN) δ 7.43 – 7.24 (m, 5H), 5.64 (s, 1H), 5.04 (s, 2H), 3.24 (d, $J = 6.58$ Hz, 2H), 2.00 – 1.91 (m, 2H), 1.51 (s, 10H).

$^{13}\text{C}\{^1\text{H}\}$ NMR (101 MHz, CD_3CN) δ 178.4, 157.7, 138.4, 129.4, 128.8, 128.6, 66.8, 51.2, 49.0, 34.3, 31.0, 24.1.

HRMS (ESI): [m/z] calculated for $\text{C}_{17}\text{H}_{22}\text{NO}_4$ ([M-H] $^-$): 304.1557; Found: 304.1554.

Product 142



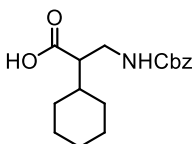
Synthesized following **GP4** using **B12** (54.3 mg, 0.2 mmol, 1.0 equiv.). **142** was isolated as a yellow oil in 88% yield (44.2 mg, 0.18 mmol).

¹H NMR (400 MHz, CD₃CN) δ 7.44 – 7.25 (m, 5H), 5.74 (s, 1H), 5.05 (s, 2H), 3.24 (d, *J* = 6.59 Hz, 3H), 1.12 (s, 6H).

¹³C{¹H} NMR (101 MHz, CD₃CN) δ 179.0, 157.7, 138.4, 129.4, 128.8, 128.6, 66.9, 49.5, 44.0, 23.3.

HRMS (ESI): [*m/z*] calculated for C₁₃H₁₆NO₄ ([*M*-H]⁻): 250.1081; Found: 250.1085.

Product 143



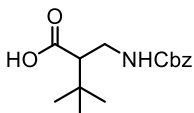
Synthesized following **GP4** using **B11** (65.0 mg, 0.2 mmol, 1.0 equiv.). **143** was isolated as a yellowish oil in 30% yield (18.3 mg, 0.06 mmol).

¹H NMR (400 MHz, CD₃CN) δ 7.52 – 7.17 (m, 5H), 5.70 (s, 1H), 5.04 (s, 2H), 3.43 – 3.16 (m, 2H), 1.79 – 1.49 (m, 7H), 1.27 – 1.01 (m, 5H).

¹³C{¹H} NMR (101 MHz, CD₃CN) δ 175.7, 157.3, 138.4, 129.4, 128.8, 128.6, 66.8, 52.2, 41.2, 38.9, 31.2, 31.2, 30.3, 27.0, 26.9.

HRMS (ESI): [*m/z*] calculated for C₁₇H₂₂NO₄ ([*M*-H]⁻): 304.1555; Found: 304.1554.

Product 144



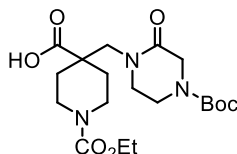
Synthesized following **GP4** using **B10** (59.9 mg, 0.2 mmol, 1.0 equiv.). **144** was isolated as a yellow oil in 54% yield (30.2 mg, 0.11 mmol).

¹H NMR (400 MHz, CD₃CN) δ 7.53 – 7.13 (m, 5H), 5.68 (s, 1H), 5.04 (s, 2H), 3.47 – 3.19 (m, 2H), 2.41 (dd, *J* = 11.01, 3.65 Hz, 1H), 0.98 (s, 9H).

¹³C{¹H} NMR (101 MHz, CD₃CN) δ 175.5, 157.2, 138.4, 129.4, 128.8, 128.6, 66.8, 56.5, 40.7, 32.6, 28.0.

HRMS (ESI): [*m/z*] calculated for C₁₅H₂₀NO₄ ([M-H]⁻): 278.1396; Found: 278.1398.

Product 145



Synthesized following **GP4** using **B15** (86.7 mg, 0.2 mmol, 1.0 equiv.). **145** was isolated as a yellowish oil in 48% yield (39.7 mg, 0.10 mmol).

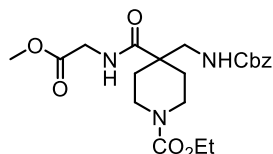
¹H NMR (400 MHz, CDCl₃) δ 4.12 (t, *J* = 7.11 Hz, 2H), 4.08 (d, *J* = 2.62 Hz, 2H), 4.02 (s, 2H), 3.60 (t, *J* = 5.24 Hz, 4H), 3.41 (dd, *J* = 6.40, 4.10 Hz, 2H), 2.91 (s, 2H), 2.12 (d, *J* = 13.28 Hz, 2H), 1.46 (s, 11H), 1.23 (d, *J* = 7.08 Hz, 3H).

¹³C{¹H} NMR (101 MHz, CDCl₃) δ 177.4, 167.6, 155.7, 154.0, 81.4, 61.6, 56.0, 48.9, 47.8, 46.9, 41.2, 40.7 & 40.3 (rotamers, 1C), 31.8, 28.4, 14.8.

HRMS (ESI): [*m/z*] calculated for C₁₉H₃₀N₃O₇ ([M-H]⁻): 412.2085; Found: 412.2089.

Derivatisation & Deprotection Reactions

Dipeptide A



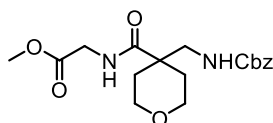
Under N₂, **136** (182.2 mg, 0.5 mmol, 1 equiv.), EDCI (155 mg, 1.0 mmol, 2 equiv.), DMAP (61.3 mg, 0.5 mmol, 1 equiv.), and glycine methyl ester hydrochloride (62.8 mg, 0.5 mmol, 1 equiv.) were dissolved in dry DCM (10 mL, 0.05 M). Et₃N (139.4 μL, 1.0 mmol, 2 equiv.), was added dropwise, and the reaction was stirred at room temperature for 18 hours. Afterwards, the reaction was quenched with 1 M HCl and extracted with DCM. The organic phases were then washed with sat. NaHCO₃ (aq.), dried over anhydrous Na₂SO₄, filtered, and concentrated. Purification via flash chromatography using silica gel (DCM/EtOAc/MeOH, 1:1 + 2%) afforded the product as a yellow oil in 20% yield (43.5 mg, 0.10 mmol).

¹H NMR (600 MHz, CDCl₃) δ 7.33 (s, 3H), 6.34 (t, *J* = 5.78 Hz, 1H), 5.71 (t, *J* = 6.68 Hz, 1H), 5.08 (s, 1H), 4.10 (q, *J* = 7.11 Hz, 1H), 4.06 – 3.93 (m, 1H), 3.74 (s, 3H), 3.38 (d, *J* = 6.65 Hz, 1H), 3.31 – 3.18 (m, 1H), 1.94 (dt, *J* = 14.59, 4.21 Hz, 1H), 1.55 (t, *J* = 11.11 Hz, 1H), 1.23 (t, 3H).

¹³C{¹H} NMR (151 MHz, CDCl₃) δ 174.9, 170.9, 157.0, 155.6, 136.7, 128.6, 128.2, 128.1, 66.9, 61.5, 52.7, 47.8, 46.5, 41.5, 40.7, 30.8, 14.8.

R_f (DCM/EtOAc/MeOH, 1:1 + 2%) = 0.33 [Ninhydrin].

Dipeptide B



Under N₂, **137** (146.7 mg, 0.5 mmol, 1 equiv.), EDCI (155 mg, 1.0 mmol, 2 equiv.), DMAP (61.3 mg, 0.5 mmol, 1 equiv.), and glycine methyl ester hydrochloride (62.8 mg, 0.5 mmol, 1 equiv.) were dissolved in dry DCM (10 mL, 0.05 M). Et₃N (139.4 μL, 1.0 mmol, 2 equiv.), was added dropwise, and the reaction was stirred at room temperature for 18 hours. Afterwards, the reaction was quenched with 1 M HCl and extracted with DCM. The organic phases were then washed with sat. NaHCO₃ (aq.), dried over anhydrous Na₂SO₄, filtered, and

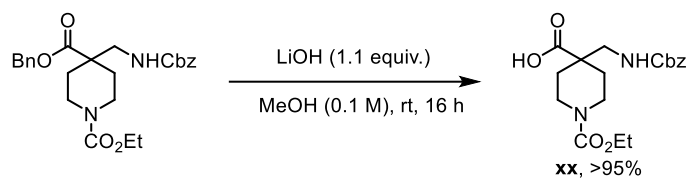
concentrated. Purification via flash chromatography using silica gel (DCM/EtOAc/MeOH, 1:1 + 2%) afforded the product as a yellow oil in 20% yield (29.3 mg, 0.10 mmol).

¹H NMR (400 MHz, CDCl₃) δ 7.39 – 7.26 (m, 5H), 6.31 (t, *J* = 5.19 Hz, 1H), 5.75 (t, *J* = 6.60 Hz, 1H), 5.09 (s, 2H), 4.02 (d, *J* = 5.78 Hz, 2H), 3.80 (ddd, *J* = 11.78, 5.89, 3.93 Hz, 2H), 3.75 (s, 3H), 3.57 (ddd, *J* = 11.77, 8.46, 3.02 Hz, 2H), 3.41 (d, *J* = 6.61 Hz, 2H), 2.00 – 1.89 (m, 2H), 1.64 (ddd, *J* = 13.19, 8.39, 3.67 Hz, 2H).

¹³C{¹H} NMR (101 MHz, CDCl₃) δ 175.2, 171.0, 157.0, 136.6, 128.6, 128.2, 128.1, 66.9, 64.5, 52.7, 47.9, 45.6, 41.5, 31.4.

R_f (DCM/EtOAc/MeOH, 1:1 + 2%) = 0.34 [Ninhydrin].

Deprotection of **111**



To a solution of **111** in MeOH (1 mL, 0.1 M), LiOH (2.6 mg, 0.11 mmol, 1.1 equiv.) was added. The reaction was stirred at room temperature for 16 h. Purification via celite filtration afforded **136** as a white solid in 95% yield (34.6 mg, 0.095 mmol).

Quantum Yield Determination

Determination of the light intensity at 440 nm

Following the procedure of Yoon, the photon flux of the LED ($\lambda_{\max} = 440 \text{ nm}$) was determined by standard ferrioxalate actinometry.³¹⁷ A 0.15 M solution of ferrioxalate was prepared by dissolving potassium ferrioxalate trihydrate (0.73 g) in H_2SO_4 (10 mL of a 0.05 M solution). A buffered solution of 1,10-phenanthroline was prepared by dissolving 1,10-phenanthroline (25 mg) and sodium acetate (5.6 g) in H_2SO_4 (25 mL of a 0.50 M solution). Both solutions were stored in the dark. To determine the photon flux of the LED, the ferrioxalate solution (1.0 mL) was placed in a cuvette and irradiated for 120 seconds at $\lambda_{\max} = 440 \text{ nm}$. After irradiation, the phenanthroline solution (175 μL) was added to the cuvette and the mixture was allowed to stir in the dark for 1 h to allow the ferrous ions to fully coordinate to the phenanthroline. The absorbance of the solution was measured at 510 nm. A non-irradiated sample was also prepared, and the absorbance was measured at 510 nm. Conversion was calculated using eq. S1.

$$\text{mol Fe}^{2+} = \frac{V\Delta A(510\text{nm})}{l\varepsilon} \quad (\text{eq. S1})$$

where V is the total volume (0.001175 L) of the solution after addition of phenanthroline, ΔA is the difference in absorbance at 510 nm between the irradiated and non-irradiated solutions, l is the path length (1.00 cm), and ε is the molar absorptivity of the ferrioxalate actinometer at 510 nm (11,100 $\text{Lmol}^{-1}\text{cm}^{-1}$). With this data, the photon flux was calculated using eq. S2.

$$\text{Photon flux} = \frac{\text{mol Fe}^{2+}}{\Phi t f} \quad (\text{eq. S2})$$

where Φ is the quantum yield for the ferrioxalate actinometer (1.01 at $\lambda_{\text{ex}} = 437 \text{ nm}$), t is the irradiation time (120 s), and f is the fraction of light absorbed at $\lambda_{\text{ex}} = 437 \text{ nm}$ by the ferrioxalate actinometer. This value was calculated using eq. S3 where $A(440 \text{ nm})$ is the absorbance of the ferrioxalate solution at 440 nm. An absorption spectrum gave an $A(440 \text{ nm})$ value of > 3 , indicating that the fraction of absorbed light (f) is > 0.999 .

$$f = 1 - 10^{-A(440 \text{ nm})} \quad (\text{eq. S3})$$

The **photon flux** was thus calculated (as an average of three experiments) to be **8.84367 x 10⁻¹¹ einsteins s⁻¹**.

Determination of the Reaction Quantum Yield

A reaction under the standard conditions using **108** (21.9 mg, 0.1 mmol, 1.0 equiv.) and *Z*-glycine in MeCN (0.1 mL, 0.1 M) was irradiated at 440 nm for 3600 sec. Afterwards, the solvent was removed and CD₃Cl added, followed by the addition of trichloroethylene (8.89 μL, 0.1 mmol, 1.0 equiv.) was added as an internal standard, and an aliquot of the reaction mixture was then analysed by ¹H NMR. The desired product **109** was formed (as an average of three experiments) in 82% yield (8.2 x 10⁻⁵ mol). The reaction quantum yield (Φ) was determined using eq. S4, where the photon flux is 8.84367 x 10⁻¹¹ einsteins s⁻¹ (determined by actinometry as described above), *t* is the reaction time (3600 s) and *f* is the fraction of incident light absorbed by the reaction mixture, determined using eq. S3. An absorption spectrum of the reaction mixture gave an absorbance value of 3.37148 at 437 nm, thus *f* was determined to be a value of 0.9996.

$$\Phi = \frac{\text{mol of product formed}}{\text{Photon flux} \cdot t \cdot f} \quad (\text{eq. S4})$$

Hence, the **reaction quantum yield (Φ)** was thus determined to be **275.67**.

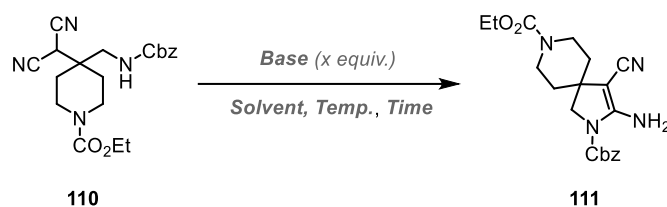
Chapter IIB: Synthesis of Polar Spirocyclic Scaffolds

Optimisation of Reaction Conditions

Giese-type Reaction:

General protocol for optimisation reactions: **109** (21.9 mg, 1.0 equiv. 0.1 mmol) and a base (2.0 equiv.) were added to an 8 mL microwave vial. Solvent (1 mL, 0.1 M) was added and the reaction was heated at varies temperatures for 24 h. The residue was filtered through a plug of celite and washed with EtOAc. After removal of the solvent, the yields of the product and remaining starting material were calculated by ¹H NMR using trichloroethylene (9.0 μl, 0.1 mmol, 1.0 equiv.) as internal standard.

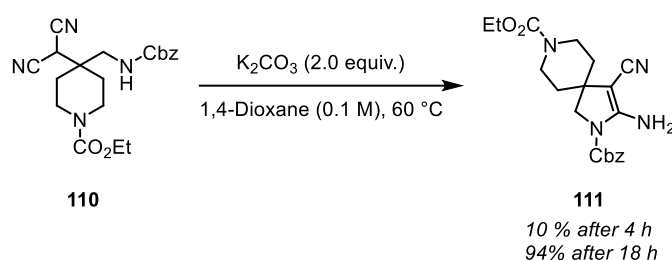
Table S3. Optimisation studies.



Entry	Solvent (M)	Base (equiv.)	Temp. (°C)	Time (h)	111 (%)	110 left (%)
1	CD ₃ CN (0.1)	Cs ₂ CO ₃ (2)	24	16	<20	60
2	CD ₃ CN (0.1)	Cs ₂ CO ₃ (2)	50	16	>95	0
3	CH ₃ CN (0.1)	K ₂ CO ₃ (2)	50	16	75	0

Conversion of Malononitrile Intermediate **110** into Spirocyclic Species **111**

110 (38.4 mg, 1.0 equiv. 0.1 mmol) and K_2CO_3 (27.6 mg, 2.0 equiv., 0.2 mmol) were added to an 8 mL microwave vial and purged with N_2 (10 minutes under vacuum then open to N_2 , repeated three times). Next, 1,4-dioxane (1 mL, 0.1 M) was added and the reaction stirred at 60 °C. After a given time, the residue was filtered through a plug of celite and washed with EtOAc. After removal of the solvent, the yields of the product and remaining starting material were calculated by 1H NMR using trichloroethylene (9.0 μ l, 0.1 mmol, 1.0 equiv.) as internal standard.



Scheme S6. Base-mediated conversion of **110** into spirocycle **111** after 4 h (10%) and 18 h (94%).

Synthesis & Characterisation of Starting materials

Alkylidenemalononitriles

General procedure 1 (GP1): Adapted from a procedure reported by Grenning and co-workers.³¹³ The corresponding cyclic ketone (1.0 equiv.) was dissolved in toluene (1.0 M). Malononitrile (1.0 equiv.), ammonium acetate (0.1 equiv.), and toluene/glacial acetic acid (3:1 v/v, 1.0 M total) were added. The reaction was heated with an oil bath at reflux (110-120 °C) with a Dean-Stark apparatus until completion (monitored by TLC). The reaction was then concentrated and quenched with 2N aq. HCl. The aqueous layer was extracted with ethyl acetate and the combined organic phases were washed with $NaHCO_3$, dried over anhydrous Na_2SO_4 , filtered, and concentrated. The residue was purified by flash chromatography to afford the targeted products.

General procedure 2 (GP2): Adapted from a procedure reported by Wang and co-workers.³¹⁸ A round bottom flask was charged with the cyclic ketone (1.0 equiv.) malononitrile (1.0 equiv.), DABCO (0.99 mmol, 15 mol%) and H_2O (0.66 M). The mixture was stirred at room temperature until a solid precipitated, which was subsequently filtered and dried. If needed, the residue was purified by flash chromatography to afford the targeted products.

General procedure 3 (GP3): A round bottom flask was charged with the ketone (1.0 equiv.), malononitrile (1.0 equiv.), piperidine (0.1 equiv.) and EtOH (0.5 M). The mixture was stirred at room temperature for 0.5–4 h, then the resulting precipitate was filtered, and the residue was recrystallized from ethanol to obtain the targeted product.

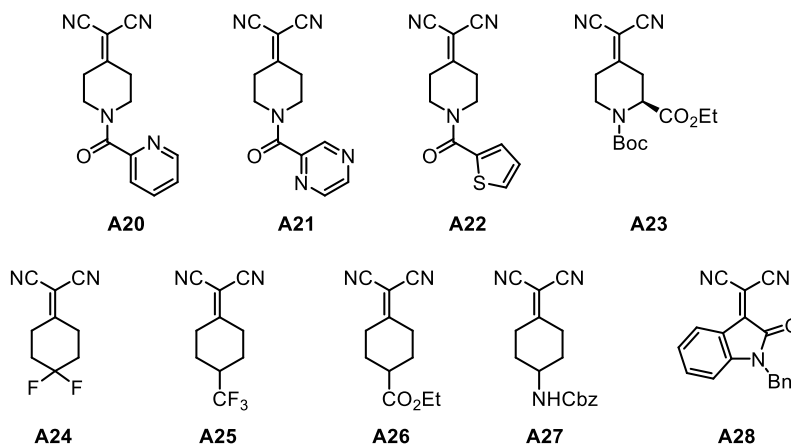
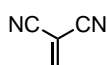


Figure S7. Synthesised alkylidenemalononitriles (overlapping compounds with Project IIA can be found in the section above).

2-(1-nicotinoylpiperidin-4-ylidene)malononitrile (**B20**)



Synthesized following **GP1** using 1-isonicotinoylpiperidin-4-one (380 mg, 1.86 mmol, 1.0 equiv.). Purification via flash chromatography using silica gel (cyclohexane/EtOAc 4:1 → 1:1) afforded **B20** as a pale orange solid in 58% yield (200 mg, 1.08 mmol).

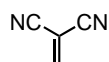
¹H NMR (600 MHz, CDCl₃) δ 8.69 (d, 2H), 7.77 (d, *J* = 7.84 Hz, 1H), 7.39 (d, *J* = 7.86, 4.99 Hz, 1H), 4.06 – 3.49 (m, 4H), 3.06 – 2.54 (m, 4H).

¹³C{¹H} NMR (151 MHz, CDCl₃) δ 177.3, 168.3, 151.7, 148.0, 135.2, 130.5, 123.8, 110.9, 85.8.

HRMS (ESI): [*m/z*] calculated for C₁₄H₁₁N₄O ([M-H]⁺): 251.0938; Found: 251.0938.

R_f (cyHex/EtOAc, 4:1) = 0.28 [CAM]

2-(1-(pyrazine-2-carbonyl)piperidin-4-ylidene)malononitrile (B21)



Synthesized following **GP1** using tert-butyl 4-oxopiperidine-1-carboxylate (0.5 g, 2.4 mmol, 1.0 equiv.). Purification via flash chromatography using silica gel (DCM/EtOAc 2:1) afforded **B21** as a light brown solid in 76% yield (0.48 g, 1.9 mmol).

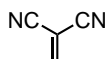
¹H NMR (600 MHz, CDCl₃) δ 9.06 (d, *J* = 1.5 Hz, 1H), 8.71 (d, *J* = 2.5 Hz, 1H), 8.55 (d, *J* = 1.9 Hz, 1H), 3.99 (t, *J* = 6.0 Hz, 2H), 3.88 (t, *J* = 5.8 Hz, 2H), 2.94 (dt, *J* = 9.2, 5.7 Hz, 4H).

¹³C{¹H} NMR (101 MHz, CDCl₃) δ 178.0, 165.2, 148.2, 146.5, 146.3, 142.4, 85.7, 46.6, 42.8, 34.6, 33.7.

HRMS (ESI): [*m/z*] calculated for C₁₃H₁₂N₅O ([M+H]⁺): 254.1040; Found: 254.1036.

R_f (DCM/EtOAc, 1:1) = 0.35 [CAM]

2-(1-(thiophene-2-carbonyl)piperidin-4-ylidene)malononitrile (B22)



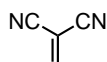
Synthesized following **GP1** using 1-(thiophene-2-carbonyl) piperidine-4-one (500 mg, 2.4 mmol, 1.0 equiv.). Purification via flash chromatography using silica gel (cyclohexane/EtOAc 3:1) afforded **B22** as a yellow solid in 48% yield (308 mg, 1.2 mmol).

¹H NMR (400 MHz, CDCl₃): δ 7.53 (dd, *J* = 5.0, 1.1 Hz, 1H), 7.36 (dd, *J* = 3.7, 1.1 Hz, 1H), 7.10 (dd, *J* = 5.0, 3.7 Hz, 1H), 3.93 (t, 4H), 2.84 (t, 4H).

¹³C{¹H} NMR (101 MHz, CDCl₃): δ 178.1, 164.2, 135.8, 129.9, 129.8f, 127.3, 111.0, 85.5, 34.1, 31.0.

HRMS (ESI): [*m/z*] calculated for C₁₃H₁₁N₃NaOS ([M+Na]⁺): 280.0515; Found: 280.0510.

1-(tert-butyl) 2-ethyl (S)-4-(dicyanomethylene)piperidine-1,2-dicarboxylate (B23)



Synthesized following **GP1** using 1-(tert-butyl) 2-ethyl (S)-4-oxopiperidine-1,2-dicarboxylate (5.0 g, 29.2 mmol, 1.0 equiv.). Purification via flash chromatography using silica gel (cyclohexane/EtOAc 5:1) afforded **B23** as a white solid in 58% yield (100 mg, 16.9 mmol).

¹H NMR (400 MHz, CDCl₃) δ 5.11 (d, *J* = 98.4 Hz, 1H), 4.34 – 4.13 (m, 3H), 3.49 (dd, *J* = 27.5, 14.6 Hz, 1H), 3.14 (d, *J* = 15.1 Hz, 1H), 2.95 (d, *J* = 14.0 Hz, 1H), 2.79 – 2.64 (m, 1H), 2.54 (s, 1H), 1.48 (s, 9H), 1.30 (t, *J* = 7.1 Hz, 3H).

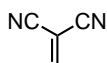
¹³C{¹H} NMR (101 MHz, CDCl₃) δ 176.8, 169.3, 111.0, 111.0, 86.2, 81.9, 62.4, 55.3, 54.6, 41.6, 40.4, 34.9, 33.3, 28.3, 14.2.

HRMS (ESI): [m/z] calculated for C₁₆H₂₁N₃NaO₄ ([M+Na]⁺): 342.1430; Found: 342.1424.

R_f (cyHex/EtOAc, 5:1) = 0.2 [Ninhydrin]

R_f (cyHex/EtOAc, 4:1) = 0.18 [Ninhydrin]

2-(4,4-difluorocyclohexylidene)malononitrile (**B24**)



Synthesized following **GP1** using tert-butyl 4-oxopiperidine-1-carboxylate (0.5 g, 3.73 mmol, 1.0 equiv.). Purification via flash chromatography using silica gel (cyclohexane/EtOAc 3:1) afforded **B24** as a white solid in 70% yield (479 mg, 2.61 mmol).

¹H NMR (600 MHz, CDCl₃) δ 2.90 (dd, *J* = 7.7, 5.9 Hz, 2H), 2.19 (tt, *J* = 13.1, 6.8 Hz, 2H).

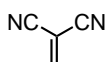
¹³C{¹H} NMR (151 MHz, CDCl₃) δ 177.7, 120.7 (t, *J*_{C-F} = 242.3 Hz), 111.1, 85.9, 33.2 (t, *J*_{C-F} = 25.8 Hz), 30.1 (t, *J*_{C-F} = 5.4 Hz).

¹⁹F NMR -100.0 (p, *J* = 12.68 Hz)

HRMS (ESI): [m/z] calculated for C₉H₇F₂N₂Na ([M-H]⁻): 181.0584; Found: 181.0583.

R_f (cyHex/EtOAc, 4:1) = 0.48 [Ninhydrin]

2-(4-(trifluoromethyl)cyclohexylidene)malononitrile (B25)



Synthesized following **GP1** using 4-(trifluoromethyl)cyclohexan-1-one (0.5 g, 3.01 mmol, 1.0 equiv.). Purification via flash chromatography using silica gel (cyclohexane/EtOAc 4:1) afforded **B25** as a white solid in 85% yield (0.55 g, 2.56 mmol).

¹H NMR (600 MHz, CDCl₃) δ 3.15 (d, *J* = 14.9 Hz, 2H), 2.47 – 2.34 (m, 3H), 2.27 (dd, *J* = 13.5, 3.6 Hz, 2H), 1.65 (qd, *J* = 12.9, 4.2 Hz, 2H).

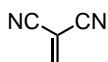
¹³C{¹H} NMR (101 MHz, CDCl₃) δ 180.4, 126.7 (q, *J*_{C-F} = 278.6 Hz), 111.2, 84.6, 40.3 (q, *J*_{C-F} = 27.8 Hz), 32.2, 25.5 (q, *J*_{C-F} = 2.7 Hz).

¹⁹F {¹H} NMR (376 MHz, CDCl₃) δ -73.00.

HRMS (ESI): [*m/z*] calculated for C₁₀H₈F₃N₂ ([M-H]⁻): 213.0646; Found: 213.0645.

R_f (cyHex/EtOAc, 1:1) = 0.5 [CAM]

ethyl 4-(dicyanomethylene)cyclohexane-1-carboxylate (B26)

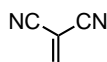


Synthesized following **GP2** using ethyl 4-oxo-cyclohexane-1-carboxylate (0.52 mL, 3.3 mmol, 1.0 equiv.). Purification via flash chromatography using silica gel (cyclohexane/EtOAc 3:1) afforded **B26** as a colorless oil in 71% yield (500 mg, 2.3 mmol). Characterization data matches the literature.

¹H NMR (400 MHz, CDCl₃) δ 4.16 (q, *J* = 7.12 Hz, 2H), 2.94 (dt, *J* = 14.59, 5.22 Hz, 2H), 2.66 (tt, *J* = 8.91, 4.08 Hz, 1H), 2.54 (ddd, *J* = 14.77, 10.05, 4.92 Hz, 2H), 2.15 (dt, *J* = 14.04, 5.06 Hz, 2H), 1.92 (dtd, *J* = 13.91, 9.54, 4.42 Hz, 2H), 1.26 (t, *J* = 7.11 Hz, 3H).

¹³C{¹H} NMR (101 MHz, CDCl₃) δ 182.5, 173.4, 111.5, 83.7, 61.1, 40.6, 32.7, 29.1, 14.3.

Benzyl (4-(dicyanomethylene)cyclohexyl)carbamate (**B27**)



Synthesized following **GP1** using tert-butyl 4-oxopiperidine-1-carboxylate (0.5 g, 2.02 mmol, 1.0 equiv.). Purification via flash chromatography using silica gel (cyclohexane/EtOAc 2:1) afforded **B27** as a white solid in 36% yield (216 mg, 0.73 mmol).

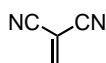
¹H NMR (600 MHz, CDCl₃) δ 7.41 – 7.28 (m, 5H), 5.11 (s, 2H), 4.66 (s, 1H), 3.86 (s, 1H), 3.00 (d, *J* = 15.10 Hz, 2H), 2.59 – 2.44 (m, 2H), 2.26 (d, *J* = 8.82 Hz, 2H), 1.52 (dd, 1H).

¹³C{¹H} NMR (101 MHz, CDCl₃) δ 181.4, 155.7, 136.2, 128.7, 128.5, 128.3, 111.4, 84.2, 67.1, 48.0, 32.8, 32.3.

HRMS (ESI): [*m/z*] calculated for C₁₇H₁₆N₃O₂ ([M-H]⁻): 294.1246; Found: 294.1248.

R_f (cyHex/EtOAc, 1:1) = 0.45 [CAM]

2-(1-benzyl-2-oxoindolin-3-ylidene)malononitrile (**B28**)



Synthesized following **GP3** using 1-benzylindoline-2,3-dione (1.0 g, 4.2 mmol, 1.0 equiv.). **B28** was isolated as a red solid in 83% yield (1.0 g, 3.5 mmol). Characterization data matches the literature.³¹⁹

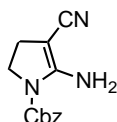
¹H NMR (400 MHz, CDCl₃) δ 8.12 (d, *J* = 6.76 Hz, 1H), 7.47 (td, *J* = 7.85, 1.22 Hz, 1H), 7.39 – 7.28 (m, 5H), 7.11 (td, *J* = 7.75, 0.94 Hz, 1H), 6.79 (d, *J* = 6.43 Hz, 1H), 4.91 (s, 2H).

¹³C{¹H} NMR (101 MHz, CDCl₃) δ 162.7, 149.3, 146.3, 137.8, 134.3, 129.2, 128.5, 127.6, 126.9, 124.0, 118.4, 112.4, 110.8, 110.7, 82.9, 44.3.

Synthesis & Characterisation of Polar Spirocycles

General procedure for reactions with Cbz-glycine (GP6): The corresponding alkylidenemalononitrile derivative (1.0 equiv. 0.50 mmol), **Ir-F** (1 mol%, 5.5 mg), K_2CO_3 (5.0 equiv.) and Cbz-glycine (209.2 mg, 1.00 mmol, 2.0 equiv.) were added to an 8 mL microwave vial and purged with N_2 (5 minutes under vacuum then open to N_2 , repeated three times). 1,4-dioxane (5.0 mL, 0.1 M) was added and the reaction was bubbled with N_2 for 5 minutes. The vial was then sealed, wrapped with parafilm, and irradiated at 440 nm, 60 °C for 12 hours. The residue was either: **a)** filtered through a plug of celite and washed with EtOAc to afford the pure product after solvent evaporation; or **b)** purified by flash chromatography to afford the targeted product.

111



Synthesized following **GP6** using **108** (109.6 mg, 0.50 mmol, 1.0 equiv.). Purification via celite filtration afforded **111** as a white solid in 95% yield (182 mg, 0.47 mmol).

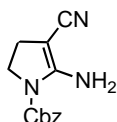
1H NMR (600 MHz, $CDCl_3$) δ 7.42 – 7.34 (m, 5H), 6.07 (s, 2H), 5.20 (s, 2H), 4.12 (q, $J = 7.1$ Hz, 2H), 3.99 (d, $J = 13.6$ Hz, 2H), 3.64 (s, 2H), 3.06 – 2.92 (m, 2H), 1.78 (ddd, $J = 14.8$, 11.1, 4.4 Hz, 2H), 1.53 (d, $J = 13.8$ Hz, 2H), 1.25 (t, $J = 7.1$ Hz, 3H).

$^{13}C\{^1H\}$ NMR (151 MHz, $CDCl_3$) δ 155.5, 153.0, 149.9, 134.9, 129.0, 128.9, 128.6, 118.6, 68.4, 61.8, 61.6, 56.7, 40.8, 40.2, 36.4, 14.8.

HRMS (ESI): [m/z] calculated for $C_{20}H_{24}N_4NaO_4$ ([M+Na] $^+$): 407.1690; Found: 407.1691.

R_f (cyHex/EtOAc, 4:1) = 0.35 [Ninhydrin]

201



Synthesized following **GP6** using **A2** (123.6 mg, 0.50 mmol, 1.0 equiv.). Purification via celite filtration afforded **201** as a light brown solid in 95% yield (231 mg, 0.47 mmol).

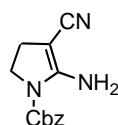
¹H NMR (600 MHz, CDCl₃) δ 7.44 – 7.33 (m, 3H), 6.00 (s, 2H), 5.20 (s, 2H), 3.94 (s, 2H), 3.64 (s, 2H), 3.00 – 2.88 (m, 2H), 1.77 (ddd, *J* = 13.50, 10.98, 4.38 Hz, 2H), 1.52 (d, *J* = 13.79 Hz, 2H), 1.45 (s, 10H).

¹³C{¹H} NMR (151 MHz, CDCl₃) δ 155.6, 154.8, 135.0, 129.0, 128.9, 128.9, 128.6, 118.7, 79.9, 68.4, 67.8, 56.6, 40.3, 36.5, 28.5.

HRMS (ESI): [*m/z*] calculated for C₂₂H₂₉N₄O₄ ([M+H]⁺): 413.2183; Found: 413.2186.

R_f (cyHex/EtOAc, 2:1) = 0.39 [Ninhydrin]

202



Synthesized following **GP6** using **A20** (126 mg, 0.50 mmol, 1.0 equiv.). Purification via flash chromatography using silica gel (CH₂Cl₂/EtOAc 1:4 → 100% EtOAc) afforded **202** as a yellowish solid in 67% yield (140 mg, 0.33 mmol).

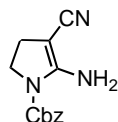
¹H NMR (600 MHz, CDCl₃) δ 8.65 (t, *J* = 4.24 Hz, 2H), 7.76 (d, *J* = 7.87 Hz, 1H), 7.44 – 7.31 (m, 6H), 6.20 (s, 2H), 5.20 (s, 2H), 4.38 (s, 1H), 3.68 (s, 3H), 3.22 (t, *J* = 12.22 Hz, 2H), 1.73 (dd, *J* = 134.20, 57.60 Hz, 4H).

¹³C{¹H} NMR (151 MHz, CDCl₃) δ 167.8, 155.9, 152.9, 150.7, 147.7, 135.3, 134.9, 131.8, 129.1, 128.9, 128.7, 123.7, 118.8, 68.5, 66.6, 57.0, 44.6, 40.4, 37.4.

HRMS (ESI): [*m/z*] calculated for C₂₃H₂₃N₅NaO₃ ([M+Na]⁺): 440.1692; Found: 440.1693.

R_f (cyHex/EtOAc, 1:4) = 0.4 [Ninhydrin]

203



Synthesized following **GP6** using **A21** (126.5 mg, 0.50 mmol, 1.0 equiv.). Purification via flash chromatography using silica gel (EtOAc 100%) afforded **203** as a yellowish solid in 57% yield (120 mg, 0.28 mmol).

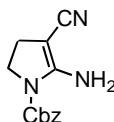
¹H NMR (600 MHz, CDCl₃) δ 8.92 (s, 1H), 8.62 (d, *J* = 2.48 Hz, 1H), 8.52 (d, *J* = 1.93 Hz, 1H), 7.38 (q, *J* = 7.40, 6.43 Hz, 5H), 6.17 (s, 2H), 5.21 (s, 2H), 4.42 (d, *J* = 12.99 Hz, 1H), 3.94 (d, *J* = 14.16 Hz, 1H), 3.76 – 3.60 (m, 2H), 3.34 – 3.18 (m, 2H), 1.91 (dq, *J* = 14.47, 7.41, 4.00 Hz, 2H), 1.78 – 1.55 (m, 2H).

¹³C{¹H} NMR (151 MHz, CDCl₃) δ 165.3, 149.5, 145.7, 145.4, 142.7, 129.0, 128.9, 128.6, 68.5, 57.1, 44.3, 40.4, 39.7, 37.3, 36.5.

HRMS (ESI): [*m/z*] calculated for C₂₂H₂₂N₆NaO₃ ([*M*+Na]⁺): 441.1646; Found: 441.1647.

R_f (cyHex/EtOAc, 1:2) = 0.27 [Ninhydrin]

204



Synthesized following **GP6** using **A22** (128 mg, 0.50 mmol, 1.0 equiv.). Purification via flash chromatography using silica gel (cyclohexane/EtOAc 1:2) afforded **204** as an off-white solid in 90% yield (198 mg, 0.45 mmol).

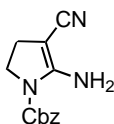
¹H NMR (600 MHz, CDCl₃) δ 7.43 (d, *J* = 5.03 Hz, 1H), 7.38 (t, *J* = 7.13 Hz, 5H), 7.27 (d, *J* = 3.68 Hz, 1H), 7.03 (t, *J* = 4.45 Hz, 1H), 6.12 (s, 2H), 5.21 (s, 2H), 4.23 (d, *J* = 13.83 Hz, 2H), 3.69 (s, 2H), 3.27 (t, *J* = 12.34 Hz, 2H), 1.87 (ddd, *J* = 14.22, 10.45, 4.09 Hz, 2H), 1.67 – 1.59 (m, 2H).

¹³C{¹H} NMR (151 MHz, CDCl₃) δ 163.8, 160.2, 155.9, 153.0, 137.0, 134.9, 129.1, 129.0, 128.8, 128.7, 126.8, 118.7, 68.5, 66.9, 57.1, 40.5, 37.0, 28.5.

HRMS (ESI): [*m/z*] calculated for C₂₂H₂₂N₄NaO₃S ([*M*+Na]⁺): 445.1305; Found: 445.1305.

R_f (cyHex/EtOAc, 1:4) = 0.30 [Ninhydrin]

205



Synthesized following **GP6** using **A23** (110 mg, 0.34 mmol, 1.0 equiv.). Purification via flash chromatography using silica gel (cyclohexane/EtOAc 2:1) afforded **205** as an off-white solid in 70% yield (168 mg, 0.34 mmol).

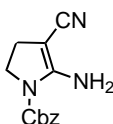
¹H NMR (600 MHz, CDCl₃) δ 7.41 – 7.34 (m, 5H), 6.07 (s, 2H), 5.19 (s, 2H), 4.40 (t, *J* = 7.11 Hz, 1H), 4.29 – 4.16 (m, 2H), 3.68 (dd, *J* = 26.11, 9.34 Hz, 2H), 3.54 (d, *J* = 10.98 Hz, 1H), 3.52 – 3.44 (m, 1H), 2.24 (dd, *J* = 13.88, 7.59 Hz, 1H), 1.87 (td, *J* = 13.06, 12.23, 6.05 Hz, 2H), 1.67 (ddd, *J* = 14.38, 9.37, 5.73 Hz, 1H), 1.43 (s, 9H), 1.26 (t, *J* = 7.18 Hz, 3H).

¹³C{¹H} NMR (151 MHz, CDCl₃) δ 171.6, 156.1, 155.9, 154.8, 152.9, 134.9, 129.0, 128.9, 128.6, 118.6, 80.7, 68.4, 66.5, 61.7, 59.1, 53.6, 39.2, 37.1, 35.8, 28.4, 14.2.

HRMS (ESI): [*m/z*] calculated for C₂₅H₃₂N₄NaO₆ ([*M*+*Na*]⁺): 507.2214; Found: 507.2215.

R_f (cyHex/EtOAc, 1:1) = 0.35 [CAM]

206



Synthesized following **GP6** using **A3** (74 mg, 0.34 mmol, 1.0 equiv.). Purification via celite filtration afforded **206** as a light brown solid in 95% yield (149 mg, 0.47 mmol).

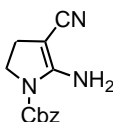
¹H NMR (600 MHz, CDCl₃) δ 7.39 (q, *J* = 7.61, 6.69 Hz, 5H), 6.07 (s, 2H), 5.21 (s, 2H), 3.93 (d, *J* = 12.10 Hz, 2H), 3.69 (s, 2H), 3.44 (td, *J* = 11.55, 2.40 Hz, 2H), 1.91 (ddd, *J* = 14.63, 11.04, 4.41 Hz, 2H), 1.49 (d, *J* = 13.55 Hz, 2H).

¹³C{¹H} NMR (151 MHz, CDCl₃) δ 155.6, 153.1, 135.1, 129.0, 128.9, 128.6, 118.7, 68.3, 68.1, 64.7, 57.1, 39.5, 37.3.

HRMS (ESI): [*m/z*] calculated for C₁₇H₁₉N₃NaO₃ ([*M*+*Na*]⁺): 336.1319; Found: 336.1320.

R_f (cyHex/EtOAc, 1:1) = 0.5 [CAM]

207



Synthesized following **GP6** using **A4** (82 mg, 0.50 mmol, 1.0 equiv.). Purification via celite filtration afforded **207** as an off-white solid in 95% yield (156 mg, 0.47 mmol).

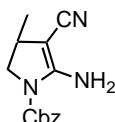
¹H NMR (600 MHz, CDCl₃) δ 7.38 (td, *J* = 8.84, 7.26, 4.67 Hz, 5H), 6.12 (s, 2H), 5.20 (s, 2H), 3.56 (s, 2H), 2.73 – 2.54 (m, 4H), 2.01 – 1.78 (m, 4H).

¹³C{¹H} NMR (151 MHz, CDCl₃) δ 155.6, 153.0, 135.0, 128.9, 128.9, 128.5, 118.9, 68.5, 68.3, 56.6, 40.8, 37.9, 25.0.

HRMS (ESI): [*m/z*] calculated for C₁₇H₁₉N₃NaO₂S ([M+Na]⁺): 352.1087; Found: 352.1090.

R_f (cyHex/EtOAc, 1:1) = 0.45 [CAM]

208



Synthesized following **GP6** using **A5** (71 mg, 0.5 mmol, 1.0 equiv.). Purification via celite filtration afforded **207** as an oil in 95% yield (148 mg, 0.47 mmol).

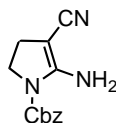
¹H NMR (600 MHz, CDCl₃) δ 7.39 (q, *J* = 7.12, 6.63 Hz, 5H), 5.93 (s, 2H), 5.20 (s, 2H), 3.59 (s, 2H), 1.71 (dt, *J* = 13.67, 3.67 Hz, 2H), 1.56 (tdd, *J* = 17.95, 13.43, 3.99 Hz, 5H), 1.26 (tt, *J* = 19.31, 9.86 Hz, 3H).

¹³C{¹H} NMR (151 MHz, CDCl₃) δ 155.0, 153.3, 135.3, 128.9, 128.5, 119.1, 69.9, 68.1, 57.2, 41.8, 37.2, 32.2, 25.0, 23.0.

HRMS (ESI): [*m/z*] calculated for C₁₈H₂₂N₃O₂ ([M+H]⁺): 312.1707; Found: 312.1707.

R_f (cyHex/EtOAc, 1:1) = 0.54 [CAM]

209



Synthesized following **GP6** using **A24** (91 mg, 0.5 mmol, 1.0 equiv.). Purification via celite filtration afforded **209** as a white solid in 95% yield (165 mg, 0.47 mmol).

¹H NMR (600 MHz, CDCl₃) δ 7.46 – 7.32 (m, 5H), 6.03 (s, 2H), 5.21 (s, 2H), 3.63 (s, 2H), 2.18 (dtt, *J* = 14.35, 10.19, 4.63 Hz, 2H), 1.93 (ddd, *J* = 14.31, 11.25, 4.11 Hz, 2H), 1.80 (dddd, *J* = 25.01, 15.06, 10.80, 5.46 Hz, 2H), 1.68 (dt, *J* = 13.39, 4.95 Hz, 2H).

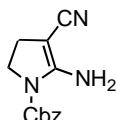
$^{13}\text{C}\{^1\text{H}\}$ NMR (101 MHz, CDCl_3) δ 155.7, 153.0, 134.9, 129.0, 128.9, 128.7, 124.7, 122.3, 118.7, 68.4, 67.2, 66.5, 56.8, 40.5, 33.5 (t), 30.8 (t, $J = 24.65$ Hz).

$^{19}\text{F}\{^1\text{H}\}$ NMR (376 MHz, CDCl_3) δ -94.7, -102.0.

HRMS (ESI): $[m/z]$ calculated for $\text{C}_{18}\text{H}_{20}\text{F}_2\text{N}_3\text{O}_2$ ($[\text{M}+\text{H}]^+$): 348.1518; Found: 348.1517.

R_f (cyHex/EtOAc, 1:1) = 0.33 [CAM]

211



Synthesized following **GP6** using **A25** (107 mg, 0.5 mmol, 1.0 equiv.). ^1H NMR analysis of the crude reaction mixture showed a 4:1 mixture of diastereomers. Purification via flash chromatography using silica gel (cyclohexane/EtOAc 7:1) afforded **211** as a mixture of diastereomers as an off-white solid in 63% yield (118.6 mg, 0.31 mmol).

Major diastereomer

^1H NMR (600 MHz, CDCl_3) δ 7.46 – 7.31 (m, 5H), 6.01 (s, 2H), 5.19 (s, 2H), 3.51 (s, 2H), 2.05 – 2.01 (m, 2H), 1.96 (d, $J = 12.85$ Hz, 2H), 1.90 – 1.78 (m, 2H), 1.44 (td, $J = 12.44, 4.41$ Hz, 2H).

$^{13}\text{C}\{^1\text{H}\}$ NMR (151 MHz, CDCl_3) δ 156.9, 153.0, 135.0, 129.0, 129.0, 128.9, 128.5, 126.8, 125.0, 120.7, 118.2, 68.4, 60.6, 56.2, 40.9 (dd, $J = 53.45, 26.17$ Hz), 37.3, 35.1, 21.7 – 21.3 (m).

$^{19}\text{F}\{^1\text{H}\}$ NMR (376 MHz, CDCl_3) δ -72.97.

HRMS (ESI): $[m/z]$ calculated for $\text{C}_{19}\text{H}_{21}\text{F}_3\text{N}_3\text{O}_2$ ($[\text{M}+\text{H}]^+$): 380.1580; Found: 380.1578.

R_f (cyHex/EtOAc, 4:1) = 0.14 [CAM]

Minor diastereomer

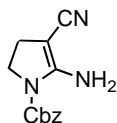
^1H NMR (600 MHz, CDCl_3) δ 7.46 – 7.33 (m, 5H), 5.21 (s, 2H), 3.60 (s, 2H), 2.08 – 2.00 (m, 1H), 1.95 (dd, $J = 19.3, 15.2$ Hz, 2H), 1.70 (d, $J = 13.8$ Hz, 2H), 1.66 – 1.58 (m, 2H), 1.35 – 1.26 (m, 2H).

$^{13}\text{C}\{^1\text{H}\}$ NMR – signals were too weak to be properly assigned. Therefore, there are not reported.

$^{19}\text{F}\{^1\text{H}\}$ NMR ^{19}F NMR (376 MHz, CDCl_3) -73.67.

R_f (cyHex/EtOAc, 4:1) = 0.15 [CAM]

212



Synthesized following **GP6** using **A26** (109 mg, 0.5 mmol, 1.0 equiv.). ¹H NMR analysis of the crude reaction mixture showed a 2:1 mixture of diastereomers. Purification via flash chromatography using silica gel (cyclohexane/EtOAc 2:1) afforded **212** as a mixture of diastereomers as an off-white solid in 74% yield (145 mg, 0.37 mmol).

Major diastereomer

¹H NMR (400 MHz, CDCl₃) δ 7.40 – 7.34 (m, 5H), 6.03 (s, 2H), 5.18 (s, 2H), 4.19 – 4.11 (m, 2H), 3.55 (s, 2H), 2.46 – 2.35 (m, 1H), 2.12 (ddq, *J* = 14.80, 7.75, 3.50 Hz, 2H), 1.81 (ddd, *J* = 12.73, 8.71, 3.52 Hz, 2H), 1.69 (td, *J* = 9.35, 4.45 Hz, 2H), 1.44 (ddd, *J* = 12.34, 8.03, 3.70 Hz, 2H), 1.25 (t, *J* = 7.13 Hz, 3H).

¹³C{¹H} NMR (101 MHz, CDCl₃) δ 174.5, 153.1, 135.1, 128.9, 128.6, 128.5, 119.7, 118.6, 68.2, 60.5, 41.7, 41.0, 35.7, 25.5, 24.5, 23.4, 14.3.

HRMS (ESI): [*m/z*] calculated for C₂₁H₂₅N₃NaO₄ ([*M*+Na]⁺): 406.1737; Found: 406.1736.

R_f (cyHex/EtOAc, 4:1) = 0.11 [CAM]

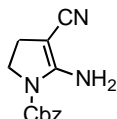
Minor diastereomer

¹H NMR – (400 MHz, CDCl₃) δ 7.39 – 7.33 (m, 5H), 6.03 (s, 2H), 5.18 (s, 2H), 4.12 (q, *J* = 14.44, 7.17 Hz, 2H), 3.60 (s, 2H), 2.24 (tt, *J* = 11.99, 3.54 Hz, 2H), 2.00 – 1.88 (m, 2H), 1.65 – 1.54 (m, 4H), 1.24 (t, *J* = 7.09 Hz, 3H).

¹³C{¹H} NMR – *signals were too weak to be properly assigned. Therefore, there are not reported.*

R_f (cyHex/EtOAc, 1:1) = 0.20 [Ninhydrin]

213



Synthesized following **GP6** using **A27** (147 mg, 0.5 mmol, 1.0 equiv.). ¹H NMR analysis of the crude reaction mixture showed a 4:1 mixture of diastereomers. Purification via celite

filtration afforded **213** as a mixture of diastereomers as an off-white solid in 66% yield (152 mg, 0.33 mmol).

Major diastereomer

¹H NMR (400 MHz, CDCl₃) δ 7.38 – 7.27 (m, 10H), 6.07 (s, 2H), 5.18 (s, 2H), 5.08 (s, 2H), 3.53 (s, 2H), 1.85 – 1.73 (m, 5H), 1.72 – 1.56 (m, 2H), 1.55 – 1.45 (m, 2H).

¹³C{¹H} NMR (101 MHz, CDCl₃) δ 156.4, 155.9, 153.0, 136.7, 135.0, 128.9, 128.8, 128.6, 128.6, 128.5, 128.2, 128.2, 128.1, 120.7, 68.2, 66.6, 59.0, 47.7, 40.7, 35.3, 29.7, 28.5.

HRMS (ESI): [m/z] calculated for C₂₆H₂₉N₄O₄ ([M+H]⁺): 461.2183; Found: 461.2192.

R_f (cyHex/EtOAc, 4:1) = 0.11 [CAM]

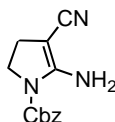
Minor diastereomer

¹H NMR – (600 MHz, CDCl₃) δ 7.36 – 7.33 (m, 10H), 6.06 (s, 2H), 5.10 (s, 2H), 4.99 (s, 2H), 3.59 (s, 2H), 2.02 – 1.97 (m, 2H), 1.94 – 1.88 (m, 2H), 1.87 – 1.81 (m, 5H).

¹³C{¹H} NMR – signals were too weak to be properly assigned. Therefore, there are not reported.

R_f (cyHex/EtOAc, 1:2) = 0.23 [Ninhydrin]

214



Synthesized following **GP6** using **A6** (66 mg, 0.5 mmol, 1.0 equiv.). Purification via celite filtration afforded **214** as a white solid in 90% yield (134.6 mg, 0.45 mmol).

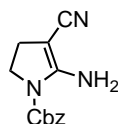
¹H NMR (600 MHz, CDCl₃) δ 7.44 – 7.33 (m, 5H), 5.99 (s, 2H), 5.18 (s, 2H), 3.60 (s, 2H), 1.82 – 1.69 (m, 4H), 1.65 – 1.51 (m, 4H).

¹³C{¹H} NMR (151 MHz, CDCl₃) δ 154.9, 153.1, 135.2, 128.9, 128.6, 128.4, 118.8, 68.1, 67.4, 60.9, 48.8, 39.3, 24.0.

HRMS (ESI): [m/z] calculated for C₁₇H₂₀N₃O₂ ([M+H]⁺): 298.1550; Found: 298.1558.

R_f (cyHex/EtOAc, 1:1) = 0.5 [CAM]

216



Synthesized following **GP6** using **A8** (132 mg, 0.3 mmol, 1.0 equiv.). Purification via flash chromatography using neutral Alox (cyclohexane/EtOAc 2:1) afforded **216** as a yellow solid in 70% yield (92.4 mg, 0.21 mmol).

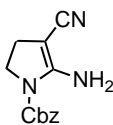
¹H NMR (600 MHz, CDCl₃) δ 7.43 – 7.28 (m, 5H), 6.03 (s, 2H), 5.14 (d, *J* = 16.69 Hz, 2H), 4.49 – 4.07 (m, 2H), 3.88 – 3.44 (m, 2H), 2.17 (s, 2H), 2.02 – 1.88 (m, 2H), 1.64 (dd, *J* = 44.00, 11.63 Hz, 4H), 1.36 (s, 9H).

¹³C{¹H} NMR (151 MHz, CDCl₃) δ 155.5, 153.1, 153.0, 134.9, 128.9, 128.9, 128.8, 119.0, 79.6, 68.3, 63.2, 50.6, 49.4, 44.3, 38.4, 31.1, 28.5.

HRMS (ESI): [*m/z*] calculated for C₂₄H₃₀N₄NaO₄ ([*M*+Na]⁺): 461.2159; Found: 461.2159.

R_f (cyHex/EtOAc, 1:1) = 0.25 [CAM]

217



Synthesized following **GP6** using **A7** (80 mg, 0.5 mmol, 1.0 equiv.). Purification via flash chromatography using silica gel (cyclohexane/EtOAc 2:1) afforded **217** as a yellow oil in 68% yield (111 mg, 0.3 mmol).

¹H NMR (600 MHz, CDCl₃) δ 7.45 – 7.33 (m, 5H), 5.89 (s, 2H), 5.19 (s, 2H), 3.55 (s, 2H), 1.80 (dd, *J* = 13.10, 10.08 Hz, 2H), 1.71 – 1.50 (m, 7H), 1.47 – 1.37 (m, 2H).

¹³C{¹H} NMR (151 MHz, CDCl₃) δ 154.7, 153.3, 135.3, 128.9, 128.8, 128.5, 119.5, 70.8, 68.1, 59.6, 44.8, 40.6, 29.6, 23.1.

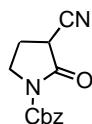
HRMS (ESI): [*m/z*] calculated for C₁₉H₂₄N₃O₂ ([*M*+H]⁺): 326.1863; Found: 326.1865.

R_f (cyHex/EtOAc, 1:1) = 0.35 [CAM]

Derivatisation & Deprotection Reactions

Hydrolysed Products

229



A reaction flask was charged with **111** (96 mg, 0.25 mmol, 1.0 equiv.), and a 1:1 mixture of 1 M HCl/EtOAc (0.1 M) was added. The reaction was stirred at RT for 12 h. The phases were then separated, and the aqueous phase neutralized and extracted with EtOAc. The combined organic phases were washed with brine, dried over Na₂SO₄, and the solvent removed *in vacuo*. Purification via flash chromatography using silica gel (cyclohexane/EtOAc 1:1) afforded **229** as a white solid in 70% yield (89 mg, 0.23 mmol).

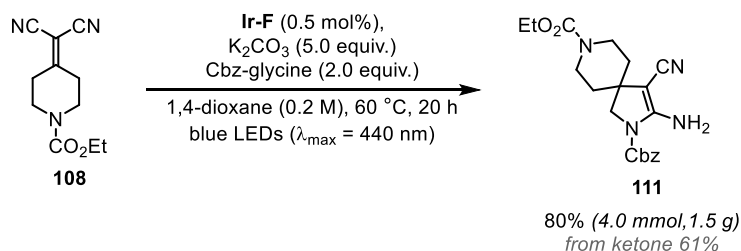
¹H NMR (600 MHz, CDCl₃) δ 7.44 – 7.40 (m, 2H), 7.40 – 7.33 (m, 3H), 5.31 (s, 2H), 4.15 (q, *J* = 7.11 Hz, 2H), 3.93 (d, *J* = 10.61 Hz, 2H), 3.91 – 3.82 (m, 1H), 3.56 (d, *J* = 11.29 Hz, 1H), 3.53 (s, 1H), 3.21 (ddd, *J* = 13.97, 10.35, 3.33 Hz, 1H), 3.09 (t, *J* = 12.58 Hz, 1H), 1.86 (dddd, *J* = 54.98, 14.43, 10.49, 4.36 Hz, 2H), 1.67 (dd, 2H), 1.27 (t, *J* = 7.13 Hz, 3H).

¹³C{¹H} NMR (151 MHz, CDCl₃) δ 163.5, 155.3, 150.9, 134.6, 128.9, 128.9, 128.5, 112.9, 69.3, 61.9, 53.0, 47.4, 40.1, 40.0, 38.0, 34.3, 30.9, 14.8.

HRMS (ESI): [*m/z*] calculated for C₂₀H₂₃N₃NaO₅ ([*M*+Na]⁺): 408.1539; Found: 408.1530.

R_f (cyHex/EtOAc, 1:1) = 0.30 [Ninhydrin]

Scale-up Experiment (5.0 mmol)



108 (1.1 g, 1.0 equiv. 5.0 mmol), **Ir-F** (0.5 mol%, 28 mg), K₂CO₃ (3.4 g, 25.0 mmol, 5.0 equiv.) and Cbz-glycine (2.1 g, 10.0 mmol, 2.0 equiv.) were added to a 50 mL Schlenk flask (external ø = 3.0 cm, internal ø = 2.2 cm) and purged with N₂ (10 minutes under vacuum then open to N₂, repeated three times). Dry and degassed 1,4-dioxane (25 mL, 0.2 M) was added and the reaction was bubbled with N₂ for 5 minutes. The vial was then sealed,

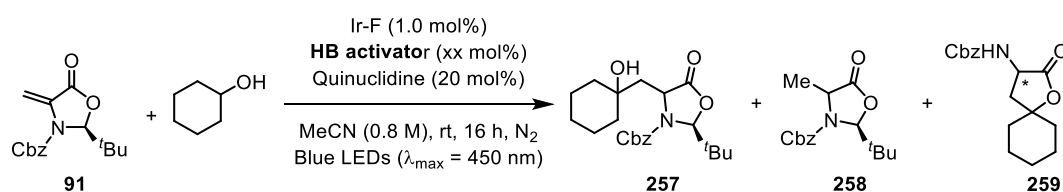
wrapped with parafilm, and irradiated at 440 nm, 60 °C for 12 hours. The residue was purified by flash chromatography using silica gel (cyclohexane/EtOAc 3:1 → 1:2) to afford **111** as a white solid in 81% yield (1.5 g, 4.0 mmol).

Chapter III: Synthesis of α -Amino Spirocyclic γ -Butyrolactones

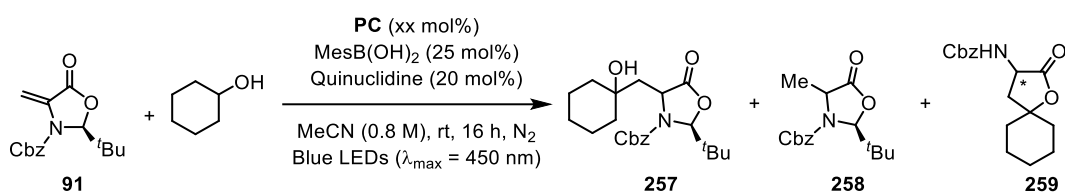
Optimisation of Reaction Conditions

General protocol: **91** (28.0 mg, 1.0 equiv. 0.1 mmol), **PC** (1-5.0 mol%), cyclohexanol (21.1 μ L, 2.0 equiv. 0.2 mmol) **HB activator**, and **HAT catalyst** were added to a 2.0 mL vial and purged with N_2 (10 minutes under vacuum then open to N_2 , repeated three times). MeCN was added and the reaction bubbled with N_2 for 5 minutes. Bubbling was stopped and the vial was sealed and wrapped with parafilm, then irradiated at various wavelengths. After removal of the solvent, the yields of the product(s), side product and remaining starting material were calculated by 1H NMR using trichloroethylene (9.0 μ L, 0.1 mmol, 1.0 equiv.) as internal standard.

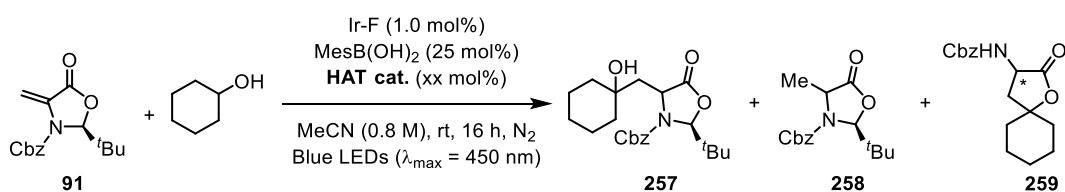
Table S4: initial investigation into a suitable activator.



Entry	Additive	Equiv. (mol%)	91 (%)	257 (%)	258 (%)	259 (%)
1	Tetrabutylammonium acetate	25	40	25	0	5
2	Tetrabutylammonium monophosphate	25	80	5	2	11
3	Tetrabutylammonium monophosphate	50	31	0	10	31
4	Tetrabutylammonium tetrafluoroborate	25	0	65	1	16
5	Tetrabutylammonium tetrafluoroborate	50	0	43	0	43
6	Tetrabutylammonium tetrafluoroborate	100	0	0	0	69
7	Tetrabutylammonium perchlorate	25	0	38	0	34
8	Boric acid	25	0	50	0	23
9	Phenylboronic acid	25	0	18	6	45
10	Bis(3,4-dimethylphenyl)(hydroxy)borane	25	0	20	14	31
11	2,4-Difluorophenylboronic acid	25	0	44	0	26
12	2,4,6-Trimethylphenyl boronic acid (MesBA)	25	0	0	5	66
13	2,4,6-Trimethylphenyl boronic acid	50	0	7	2	67
14	3,5-Bis(trifluoromethyl)benzeneboronic acid	25	97	0	0	0
15	(2,4,6-Triisopropylphenyl)boronic acid	25	0	31	0	41
16	4-Fluorophenylboronic acid	25	100	0	0	0
17	4-Methoxyphenylboronic acid	25	90	1	0	0
18	4-tert-Butylphenylboronic acid	25	40	40	0	0

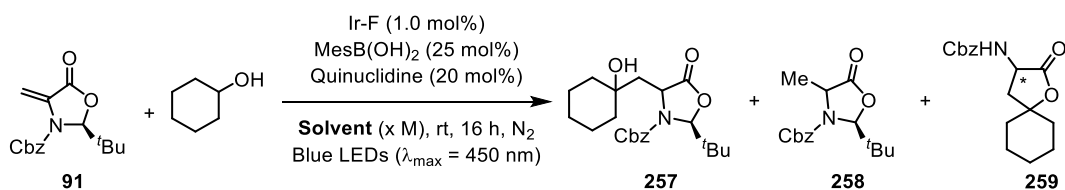
Table S5: optimisation of photocatalyst.


Entry	Photocatalyst	Loading (mol%)	91 (%)	257 (%)	258 (%)	259 (%)
1	Ir-F	1.0	0	17	6	66
2	Ir-F	2.5	0	5	0	70
3	Ir-F(Me)	1.0	0	0	0	60
4	4-CzIPN	1.0	0	0	0	50
5	4-CzIPN	2.5	0	16	0	42
6	4-CzIPN	5.0	0	0	0	68

Table S6: optimisation of HAT catalyst.


Entry	HAT Catalyst	HAT Catalyst Loading (mol%)	259 (%)
1	Quinuclidine	20	66
2	Quinuclidine	25	64
3	Quinuclidine	50	64
4*	TBADT	25	0
5	Quinuclidine Acetate	25	23
6	Ethyl thioglycolate	25	0

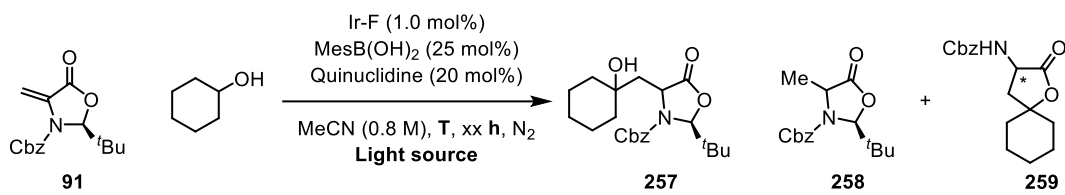
*using a 365 nm light source without a photocatalyst.

Table S7: solvent screening and concentration optimisation.


Entry	Solvent	Concentration (M)	91 (%)	257 (%)	258 (%)	259 (%)
1	CH ₃ CN	0.1	0	60	0	0
2	CH ₃ CN	0.2	0	41	0	27
3	CH ₃ CN	0.4	0	0	0	50
4	CH ₃ CN	0.8	0	0	5	66
5	DCM	0.8	0	0	0	36
6	1,4-Dioxane	0.8	0	10	0	44
7	DMF	0.8	0	0	0	68
8	THF	0.8	0	0	0	15
9	Acetone	0.8	0	3	0	65

10 DMSO 0.8 0 0 0 36

Table S8: optimisation of light source, temperature, and time.

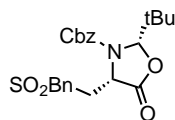


Entry	Light source (nm)	Temperature (°C)	Time (hours)	259 (%)
1	405	25	16	57
2	425	25	16	57
3	450	25	16	66
4	450	25	8	60
5	450	25	24	75
6	450	40	16	57

Synthesis & Characterisation of Starting Materials

Synthesis of 91

Benzyl (2S,4R)-4-((benzylsulfonyl)methyl)-2-(tert-butyl)-5-oxo-oxazolidine-3-carboxylate (A)



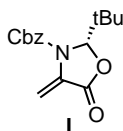
S-benzyl-L-cysteine (10.0 g, 48.0 mmol, 1 eq.) was treated with a solution of sodium hydroxide (1.9 g, 48.0 mmol, 1 equiv.) in water (300 mL) and evaporated until dryness via rotary evaporation leaving a white solid. A solution of pivaldehyde (10.5 mL, 96 mmol, 2 equiv.) in cyclohexane (500 mL) was added to the solid and the mixture stirred and refluxed in presence of a Dean-Stark separator for 5 days (and followed by ^1H NMR). The reaction mixture was then cooled down and evaporated to dryness to achieve the crude imine as a pale yellow gum. The crude was suspended in anh. CH_2Cl_2 (300 mL) and treated with benzyl chloroformate (13.7 mL, 96 mmol, 2 equiv.) at 0°C . After stirring for 2 days, the reaction was quenched with 1 M NaOH (1 x 250 mL), the organic phase was dried over Na_2SO_4 and filtered. Afterward the solvent was removed via rotary evaporation, concentrate was quickly filtered through a silica column (cyclohexane/EtOAc 1:1) to achieve the corresponding diastereomeric mixture of oxazolidinone intermediate (26 g; $R_f = 0.25$, cyclohexane:EtOAc, 4:1) as a brown oil after concentration in vacuo, which was used in the next step without further purification. The crude was dissolved in CH_2Cl_2 (500 mL), treated with *m*CPBA ($\geq 77\%$, 35.2 g, 157.18 mmol, 2.5 equiv.) and stirred for 18 h at room temperature. The reaction was washed with 1M NaOH (3 x 200 mL), then the organic phase was dried over Na_2SO_4 and concentrated in vacuo. Purification via flash column chromatography (cyclohexane:EtOAc, 20:1 – 2.3:1) afforded the desired product as a pale, yellow oil in 43 % yield (9.26 g, 20.78 mmol) over three steps. The spectroscopic data are consistent with those previously reported.¹⁴⁰

^1H NMR (600 MHz, CDCl_3) $\delta = 7.44 - 7.32$ (m, 10H), 5.62 (s, 1H), 5.28 (d, $J = 12.0$, 1H), 5.21 (d, $J = 12.0$, 1H), 5.08 (dd, $J = 8.0, 4.1$, 1H), 4.66 (d, $J = 14.1$, 1H), 4.42 (d, $J = 14.1$, 1H), 3.44 (dd, $J = 15.3, 8.0$, 1H), 3.15 (ddd, $J = 15.3, 4.1, 1.5$, 1H), 0.89 (s, 9H).

$^{13}\text{C}\{^1\text{H}\}$ NMR (151 MHz, CDCl_3) $\delta = 170.8, 155.4, 135.0, 131.1, 129.3, 129.2, 129.0, 128.9, 128.9, 128.1, 97.0, 69.1, 60.6, 53.8, 52.9, 37.3, 24.7$.

R_f (cyclohexane/EtOAc, 4:1) = 0.14 [*p*-Anisaldehyde]

Benzyl (S)-2-(tert-butyl)-4-methylene-5-oxooxazolidine-3-carboxylate (91)



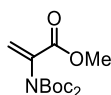
Benzyl (2*S*,4*R*)-4-((benzylsulfonyl)methyl)-2-(tert-butyl)-5-oxo-oxazolidine-3-carboxylate (9.26 g, 20.78 mmol, 1 equiv.) was dissolved in CH₂Cl₂ (260 mL) and cooled in an ice bath, then DBU (6.20 mL, 41.57 mmol, 2 equiv.) was added dropwise via a syringe. The mixture was stirred for 45 min at 0 °C and quenched with sat. aq. NH₄Cl (100 mL) at 0 °C. The organic phase was extracted with sat. aq. NH₄Cl (3 x 200 mL), dried over Na₂SO₄ and concentrated under vacuo. The crude was quickly filtered through a silica column (cyclohexane/EtOAc, 1:1) to provide **91** in 92 % yield (5.54 g, 19.14 mmol) as a white solid after concentration in vacuo. The spectroscopic data are consistent with those previously reported.¹⁴⁰

¹H NMR (600 MHz, CDCl₃) δ = 7.42 – 7.34 (m, 5H), 5.72 (s, 1H), 5.69 (s, 1H), 5.31 - 5.21 (m, 2H), 0.93 (s, 9H).

¹³C{¹H} NMR (151 MHz, CDCl₃) δ = 164.7, 134.9, 130.3, 129.0, 128.9, 128.8, 104.5, 94.2, 77.4, 68.9, 38.8, 24.5.

R_f (cyclohexane /EtOAc, 4:1) = 0.45 [*p*-Anisaldehyde]

Synthesis of Methyl 2-(bis(tert-butoxycarbonyl)amino)acrylate (90)



DL-Serine methyl ester hydrochloride (5 g, 32.1 mmol, 1 equiv.) was dissolved in CH₂Cl₂ (32.5 mL, 1 M) and the mixture cooled down to 0 °C. Then Et₃N (10 mL, 71.7 mmol, 2.2 equiv.) and Boc₂O (9.25 mL, 45.8 mmol, 1.4 equiv.) were added, and the solution was allowed to warm to room temperature overnight. Afterwards, the solvent was concentrated under vacuo and the crude diluted with EtOAc (100 mL). The organic phase was washed with aq. HCl (1 M), a saturated solution of NaHCO₃ (100 mL) and brine (100 mL), dried over Na₂SO₄ and the solvent was concentrated under vacuo to afford methyl 2-((tert-butoxycarbonyl)amino)-3-hydroxypropanoate, which was used in the next step without further purification.

Boc₂O (14.6 mL, 63.6 mmol, 2.0 equiv.) and DMAP (0.78 g, 6.4 mmol, 0.2 equiv.) were added to a solution of 2-((tert-butoxycarbonyl)amino)-3-hydroxypropanoate in acetonitrile (50 mL, 0.6 M) at 0 °C. The reaction was stirred for 1 hour at 0 °C, and then it was slowly warmed to room temperature. After, DBU (0.5 g, 3.3 mmol, 0.1 equiv.) was added dropwise and the reaction mixture stirred at room temperature overnight. Acetonitrile was removed under vacuo and the crude dissolved in EtOAc (100 mL). The organic phase was washed with aq. HCl (1M), a saturated solution of NaHCO₃ (100 mL) and brine (100 mL), dried over Na₂SO₄ and the solvent was removed via rotary evaporation. Compound **90** was isolated as a white solid (6.3 g, 20.9 mmol, 65% over two steps) after column chromatography (cyclohexane:EtOAc, 4:1). The spectroscopic data are consistent with those previously reported.¹³⁴

¹H NMR (600 MHz, CDCl₃) δ = 6.31 (s, 1H), 5.62 (s, 1H), 3.77 (s, 3H), 1.44 (s, 7H).

¹³C NMR (151 MHz, CDCl₃) δ = 164.1, 150.7, 136.2, 124.7, 83.2, 52.4, 28.0.

Synthesis & Characterisation of α -Amino Spirocyclic γ -Butyrolactones

General procedure: Ir-F (5.5 mg, 1.0 mol%), **91** (144.7 mg, 0.5 mmol, 1.0 equiv.), quinuclidine (11.0 mg, 20 mol%), **MesBA** (20.5 mg, 25 mol%) and the desired alcohol (1.0 mmol, 2.0 equiv.) were added to an 8 mL microwave vial and purged with N₂ (5 minutes under vacuum then open to N₂, repeating three times). *NB: if the desired alcohol substrate was volatile, then it was added after purging.* MeCN (125 μ L, 0.8 M) was added and the reaction was bubbled with N₂ for 15 minutes. *NB: volatile alcohol substrates were added at this stage;* bubbling was stopped, the alcohol was added, and the solution was bubbled for an additional 30 seconds. The vial was sealed and wrapped with parafilm, then irradiated at 450 nm, 25 °C (fan on) for 24 hours. Afterwards, the solvent was removed *in vacuo* and the residue was purified by flash column chromatography on silica gel using the indicated solvent system, affording the desired product.

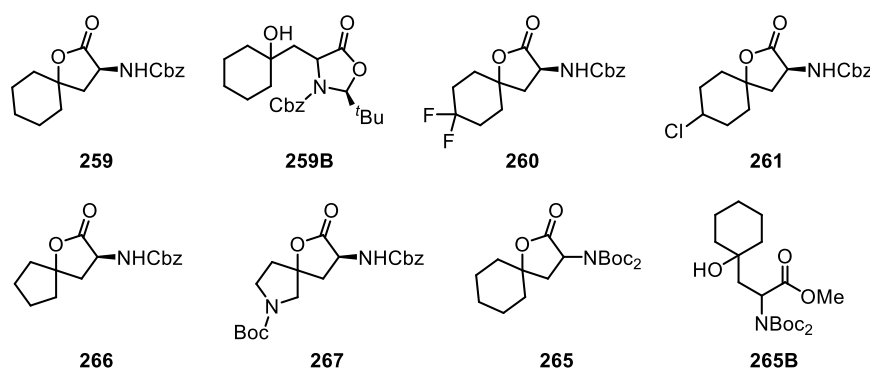
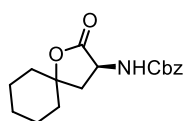


Figure S8. Synthesised α -amino spirocyclic γ -butyrolactones & uncyclised products.

259



Synthesised following the general procedure using hexanol (105.7 μ L, 1.0 mmol, 2.0 equiv.). Purification *via* flash chromatography using silica gel (CyHex/EtOAc, 3:1) afforded **259** as a white crystalline solid in 73% yield (112 mg, 0.37 mmol), as well as the uncyclised product in <5% yield (9.7 mg, 0.025 mmol). The product was also recrystallised in a DCM/Et₂O solvent system.

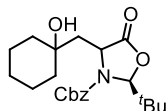
¹H NMR (600 MHz, CDCl₃) δ 7.40 – 7.28 (m, 5H), 5.25 (s, 1H), 5.13 (s, 2H), 4.55 (s, 1H), 2.75 (t, J = 10.90 Hz, 1H), 1.82 – 1.34 (m, 11H).

$^{13}\text{C}\{^1\text{H}\}$ NMR (151 MHz, CDCl_3) δ 156.2, 136.1, 128.7, 128.5, 128.3, 100.1, 67.5, 51.2, 38.4, 36.1, 25.0, 22.7, 22.6.

HRMS (ESI): $[m/z]$ calculated for $\text{C}_{17}\text{H}_{21}\text{NNaO}_4$ ($[\text{M}+\text{Na}]^+$): 326.1363; Found: 326.1363.

R_f (cyHex/EtOAc, 4:1) = 0.40 [*p*-anisaldehyde].

Product 259B



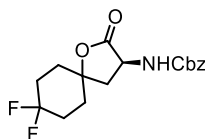
^1H NMR (400 MHz, CDCl_3) δ 7.41 – 7.32 (m, 5H), 5.60 (s, 1H), 5.18 (s, 2H), 4.63 (t, J = 6.2 Hz, 1H), 2.13 – 1.96 (m, 2H), 1.69 – 1.19 (m, 11H), 0.95 (s, 9H).

$^{13}\text{C}\{^1\text{H}\}$ NMR (101 MHz, CDCl_3) δ 174.6, 156.1, 135.0, 129.0, 128.9, 128.7, 96.9, 69.9, 69.1, 54.1, 45.4, 37.2, 25.9, 25.1, 22.2, 22.2.

HRMS (ESI): $[m/z]$ calculated for $\text{C}_{22}\text{H}_{31}\text{NNaO}_5$ ($[\text{M}+\text{Na}]^+$): 412.2094; Found: 412.2094.

R_f (cyHex/EtOAc, 4:1) = 0.45 [*p*-anisaldehyde].

260



Synthesised following the general procedure using 1,1-difluorocyclohexane (136.1 mg, 1.0 mmol, 2.0 equiv.). Purification *via* flash chromatography using silica gel (CyHex/EtOAc, 7:1) afforded **260** as a white crystalline solid in 24% yield (40.7 mg, 0.12 mmol).

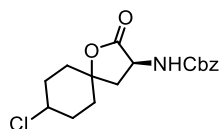
^1H NMR (400 MHz, CDCl_3) δ 7.40 – 7.30 (m, 5H), 5.34 (d, J = 6.0 Hz, 1H), 5.12 (s, 2H), 4.54 (td, J = 9.9, 6.2 Hz, 1H), 2.66 (dd, J = 12.8, 9.1 Hz, 1H), 2.13 – 1.80 (m, 9H).

$^{13}\text{C}\{^1\text{H}\}$ NMR (101 MHz, CDCl_3) δ 173.7, 156.1, 135.9, 128.8, 128.5, 128.4, 122.3 (t, $J_{\text{C-F}}$ = 240 Hz), 81.6, 67.6, 51.0, 40.3, 34.5 (d, $J_{\text{C-F}}$ = 9.4 Hz), 32.9 (d, $J_{\text{C-F}}$ = 4.6 Hz), 30.2 (t, $J_{\text{C-F}}$ = 25.0 Hz), 29.7 (t, $J_{\text{C-F}}$ = 25.0 Hz).

$^{19}\text{F}\{^1\text{H}\}$ NMR (376 MHz, CDCl_3) δ -93.9, -94.5, -103.2, -103.9.

HRMS (ESI): $[m/z]$ calculated for $\text{C}_{17}\text{H}_{19}\text{F}_2\text{NNaO}_4$ ($[\text{M}+\text{Na}]^+$): 362.1176; Found: 362.1174.

R_f (cyHex/EtOAc, 4:1) = 0.30 [*p*-anisaldehyde].

261


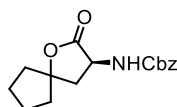
Synthesised following the general procedure using chlorocyclohexane (134.6 mg, 1.0 mmol, 2.0 equiv.). Purification *via* flash chromatography using silica gel (CyHex/EtOAc, 7:1) afforded **261** as a white crystalline solid in 71% yield (119.9 mg, 0.36 mmol).

¹H NMR (400 MHz, CDCl₃) δ 7.40 – 7.30 (m, 5H), 5.31 (d, *J* = 6.2 Hz, 1H), 5.12 (s, 2H), 4.60 – 4.45 (m, 1H), 3.98 (s, 1H), 2.66 (dd, *J* = 12.6, 9.0 Hz, 1H), 2.12 – 1.99 (m, 5H), 1.97 – 1.88 (m, 1H), 1.79 – 1.50 (m, 3H).

¹³C{¹H} NMR (101 MHz, CDCl₃) δ 173.8, 156.1, 135.9, 128.7, 128.5, 128.3, 82.2, 67.6, 57.0, 51.1, 40.6, 32.4, 32.2.

HRMS (ESI): [*m/z*] calculated for C₁₇H₂₀ClNNaO₄ ([M+Na]⁺): 360.0971; Found: 360.0973.

R_f (cyHex/EtOAc, 4:1) = 0.35 [*p*-anisaldehyde].

266


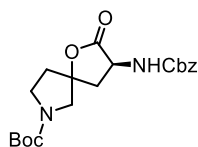
Synthesised following the general procedure using cyclopentanol (86.1 mg, 1.0 mmol, 2.0 equiv.). Purification *via* flash chromatography using silica gel (CyHex/EtOAc, 3:1) afforded **266** as a white crystalline solid in 70% yield (101.3 mg, 0.35 mmol).

¹H NMR (400 MHz, CDCl₃) δ 7.40 – 7.29 (m, 5H), 5.28 (s, 1H), 5.13 (s, 2H), 4.56 (s, 1H), 2.72 (t, *J* = 10.6 Hz, 1H), 2.19 (t, *J* = 12.2 Hz, 1H), 2.07 (s, 1H), 1.96 (t, *J* = 8.2 Hz, 1H), 1.91 – 1.79 (m, 2H), 1.80 – 1.66 (m, 4H), 1.59 (s, 1H).

¹³C{¹H} NMR (101 MHz, CDCl₃) δ 182.1, 174.3, 136.1, 128.7, 128.5, 128.3, 92.8, 67.5, 52.1, 40.7, 39.0, 38.3, 24.4, 23.4.

HRMS (ESI): [*m/z*] calculated for C₁₆H₁₉NNaO₄ ([M+Na]⁺): 312.1212; Found: 312.1269.

R_f (cyHex/EtOAc, 1:1) = 0.40 [*p*-anisaldehyde].

267


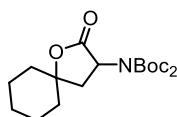
Synthesised following the general procedure using (S)-tert-butyl-3-hydroxypyrrolidine-1-carboxylate (187.2 mg, 1.0 mmol, 2.0 equiv.). Purification *via* flash chromatography using silica gel (DCM/EtOAc, 7:1) afforded **267** as a white crystalline solid in 34% yield (66.4 mg, 0.17 mmol).

¹H NMR (600 MHz, CDCl₃) δ 7.37 (d, *J* = 5.2 Hz, 5H), 5.53 (s, 1H), 5.14 (d, *J* = 2.4 Hz, 2H), 4.40 – 4.03 (m, 2H), 3.60 – 3.17 (m, 2H), 2.57 (d, *J* = 12.5 Hz, 1H), 2.41 – 1.90 (m, 2H), 1.70 (d, *J* = 12.7 Hz, 2H), 1.42 (s, 9H).

¹³C{¹H} NMR (151 MHz, CDCl₃) δ 172.0, 155.7, 154.8, 135.1, 129.0, 128.9, 96.4, 80.0, 68.8, 54.0, 53.1, 39.5, 38.5, 37.2, 28.6, 25.0.

HRMS (ESI): [*m/z*] calculated for C₂₀H₂₆N₂NaO₆ ([M+Na]⁺): 413.1689; Found: 413.2851.

R_f (DCM/EtOAc, 4:1) = 0.20 [*p*-anisaldehyde].

265


Synthesised following the general procedure using **90** (mg, 0.5 mmol, 1.0 equiv.) instead of **91**, and hexanol (105.7 μL, 1.0 mmol, 2.0 equiv.). Purification *via* flash chromatography using silica gel (CyHex/EtOAc, 3:1) afforded **265** as a white crystalline solid in 10% yield (18.5 mg, 0.05 mmol), as well as the uncyclised product in 40% yield (80.2 mg, 0.20 mmol).

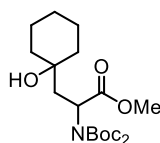
¹H NMR (600 MHz, CDCl₃) δ 5.20 (dd, *J* = 11.0, 9.5 Hz, 1H), 2.40 (dd, *J* = 12.0, 9.5 Hz, 1H), 2.20 (dd, *J* = 12.0, 11.0 Hz, 1H), 1.94 – 1.88 (m, 1H), 1.81 – 1.64 (m, 5H), 1.60 – 1.52 (m, 4H), 1.51 (s, 18H).

¹³C{¹H} NMR (151 MHz, CDCl₃) δ 151.8, 84.1, 83.5, 55.0, 38.1, 37.0, 28.2, 25.0, 22.7, 22.6.

HRMS (ESI): [*m/z*] calculated for C₁₉H₃₁NNaO₆ ([M+Na]⁺): 392.2048; Found: 392.2044.

R_f (cyHex/EtOAc, 1:1) = 0.35 [*p*-anisaldehyde].

269



¹H NMR (600 MHz, CDCl₃) δ 5.10 (t, *J* = 5.4 Hz, 1H), 3.72 (s, 3H), 2.49 (dd, *J* = 15.2, 5.3 Hz, 1H), 1.92 – 1.86 (m, 1H), 1.84 (dd, *J* = 15.2, 5.7 Hz, 1H), 1.77 – 1.67 (m, 1H), 1.68 – 1.53 (m, 5H), 1.50 (s, 18H), 1.44 (s, 4H).

¹³C{¹H} NMR (151 MHz, CDCl₃, rotamers) δ 172.9, 152.3, 83.5, 70.2, 54.6, 52.7, 43.1, 38.9, 37.2, 28.2, 22.4, 22.3.

HRMS (ESI): [*m/z*] calculated for C₂₀H₃₅NNaO₇ ([M+Na]⁺): 424.2305; Found: 424.2306.

R_f (cyHex/EtOAc, 1:1) = 0.40 [*p*-anisaldehyde].

X-Ray Crystallography Data

Compound	259
Identification code	OCKATKB115
Empirical formula	C ₁₇ H ₂₁ NO ₄
Formula weight	303.35
Temperature/K	293
Crystal system	orthorhombic
Space group	P212121
a/Å	5.9759(3)
b/Å	15.8349(6)
c/Å	16.6612(7)
α/°	90
β/°	90
γ/°	90
Volume/Å ³	1576.61(12)
Z	4
ρ _{calc} /cm ³	1.278
μ/mm ⁻¹	0.091
F(000)	648.0
Crystal size/mm ³	0.13 × 0.11 × 0.09
Radiation	Mo Kα (λ = 0.71073)
2θ range for data collection/°	5.146 to 66.53
Index ranges	-8 ≤ h ≤ 7, -14 ≤ k ≤ 23, -25 ≤ l ≤ 20
Reflections collected	13094
Independent reflections	5695 [R _{int} = 0.0214, R _{sigma} = 0.0319]
Data/restraints/parameters	5695/0/199
Goodness-of-fit on F ²	1.024
Final R indexes [I ≥ 2σ (I)]	R ₁ = 0.0430, wR ₂ = 0.0898
Final R indexes [all data]	R ₁ = 0.0697, wR ₂ = 0.1019
Largest diff. peak/hole / e Å ⁻³	0.17/-0.14
Flack parameter	-0.4(4)

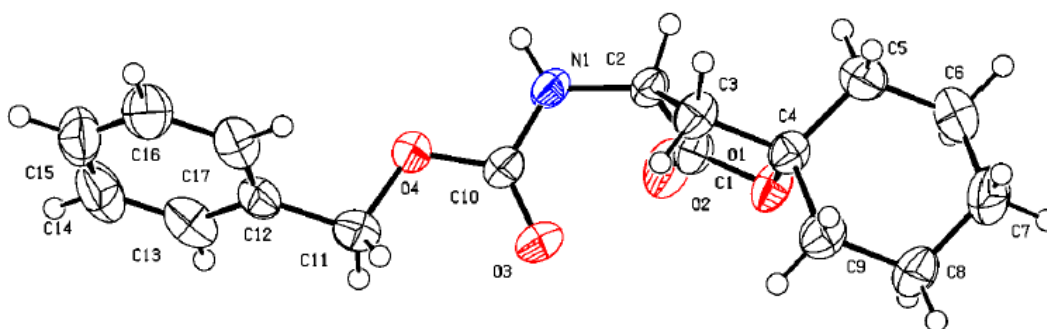
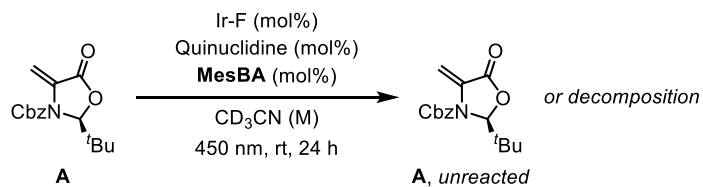


Figure S9. Molecular structure of 259.

Mechanistic Studies & Investigation into Decomposition

General protocol: In a 0.1 mmol scale, the standard reaction conditions were used with KB and cyclohexanol in CDCl_3 . Each component was systematically omitted, once at a time. The amount of **A** left was calculated by ^1H NMR analysis using TCI as the internal standard.

Table S8: investigation into the decomposition of **91**.



Entry	Ir-F (mol%)	Quinuclidine (mol%)	MesBA (mol%)	$\text{CD}_3\text{CN (M)}$	91 left (%)
1*	-	100	-	0.1	>95
2*	-	-	100	0.1	>95
3*	-	100	100	0.1	>95
4	1.0	20	-	0.8	>95
5	1.0	-	25	0.8	>95
6	-	20	25	0.8	>95
7	1.0	20	25	0.8	<20

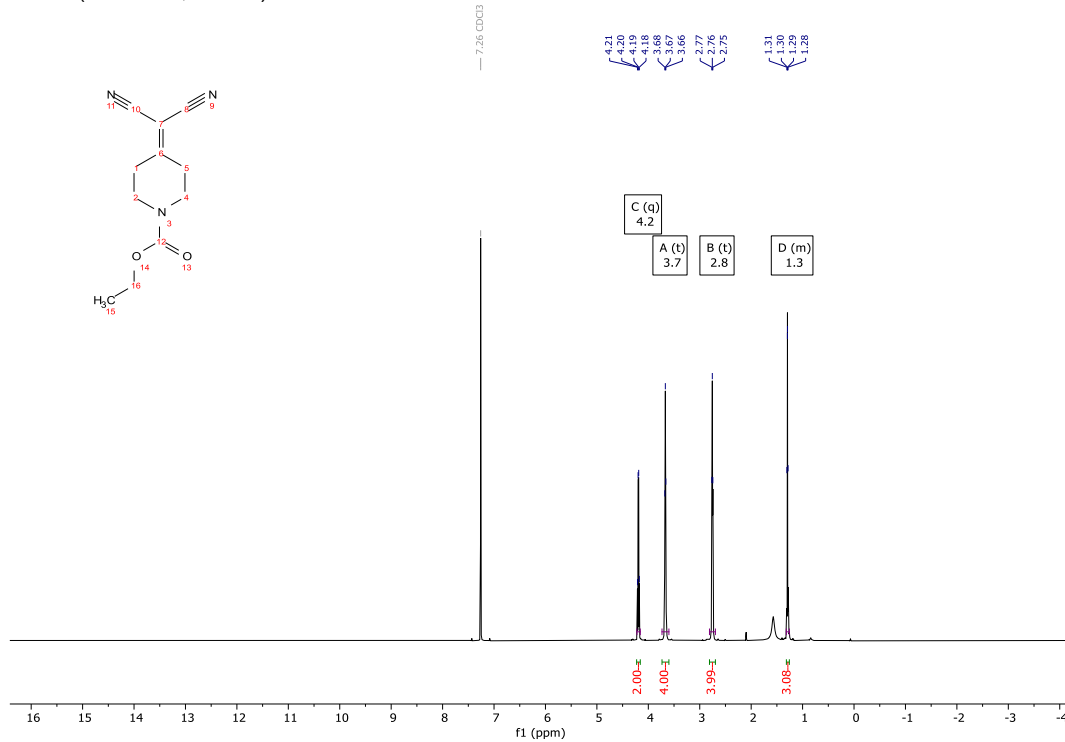
*Ran in the absence of photocatalyst, under air and no LED light source. **91** left was calculated by NMR analysis using TCI as the internal standard.

^1H , ^{13}C NMR Spectra

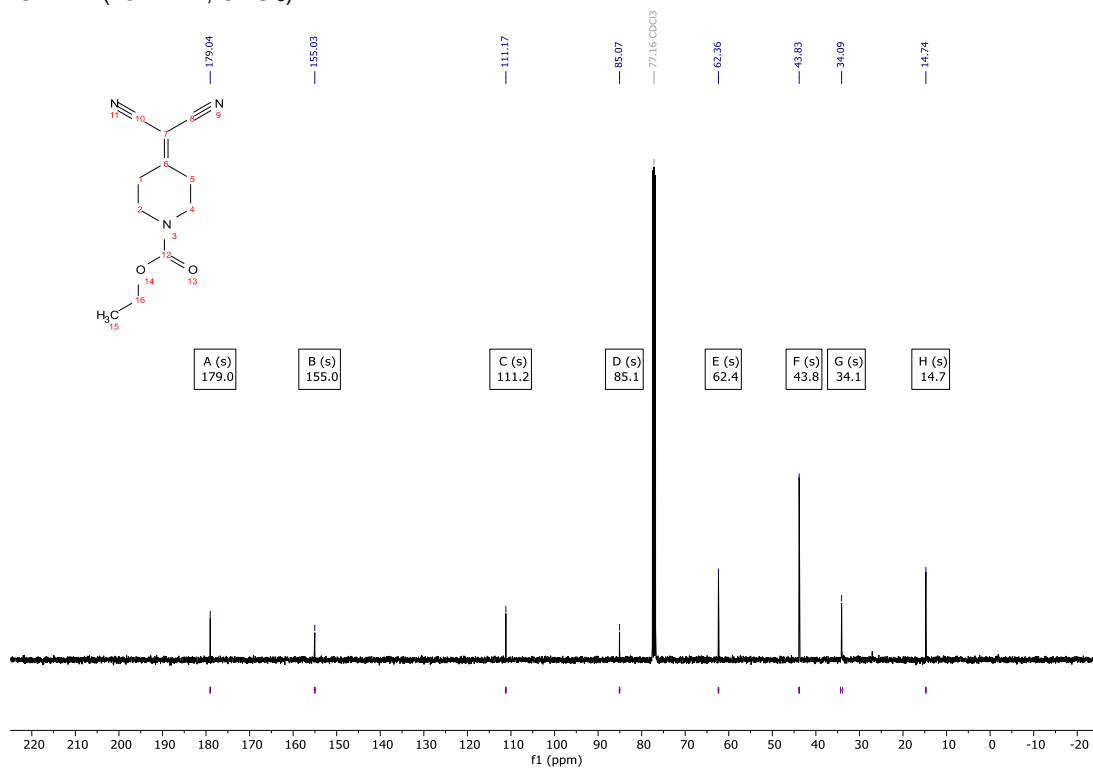
Chapter IIA: Synthesis of Sterically Congested $\beta^{2,2}$ -Amino Acids

Alkylidenemalononitriles

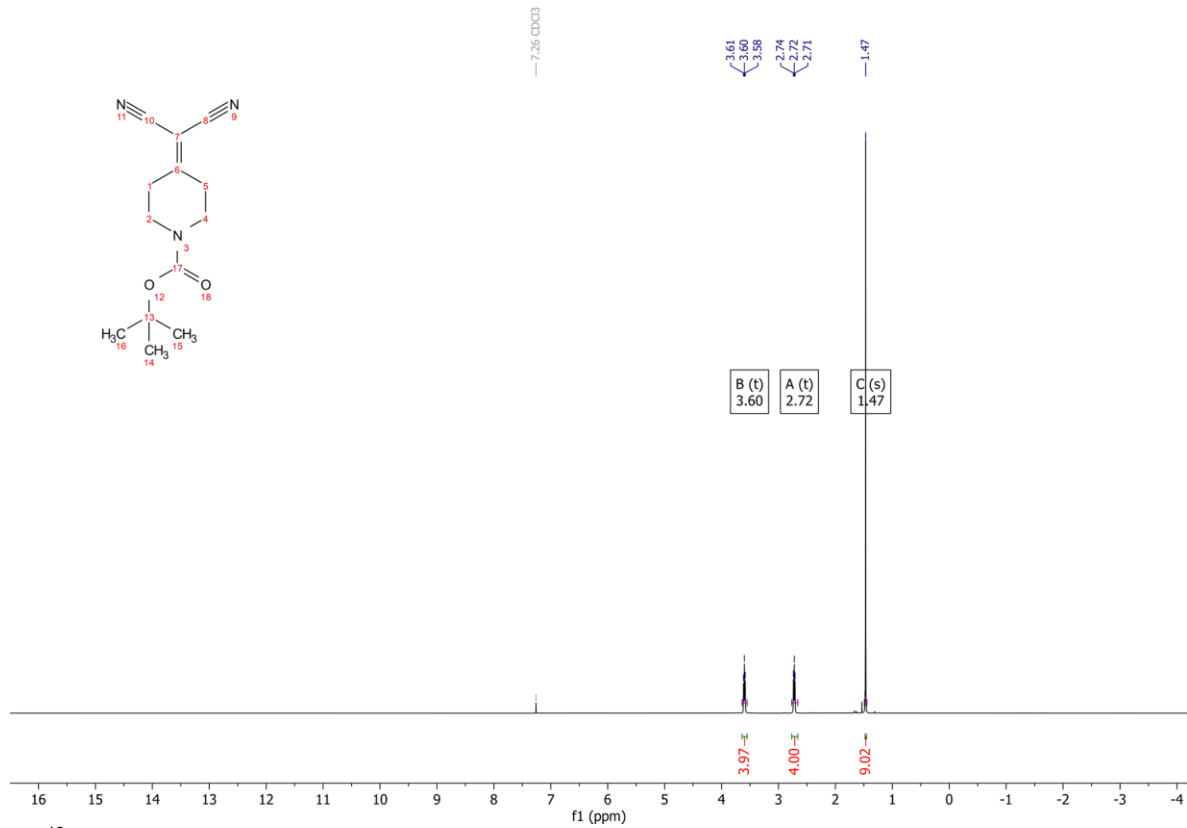
108 ^1H NMR (600 MHz, CDCl_3)



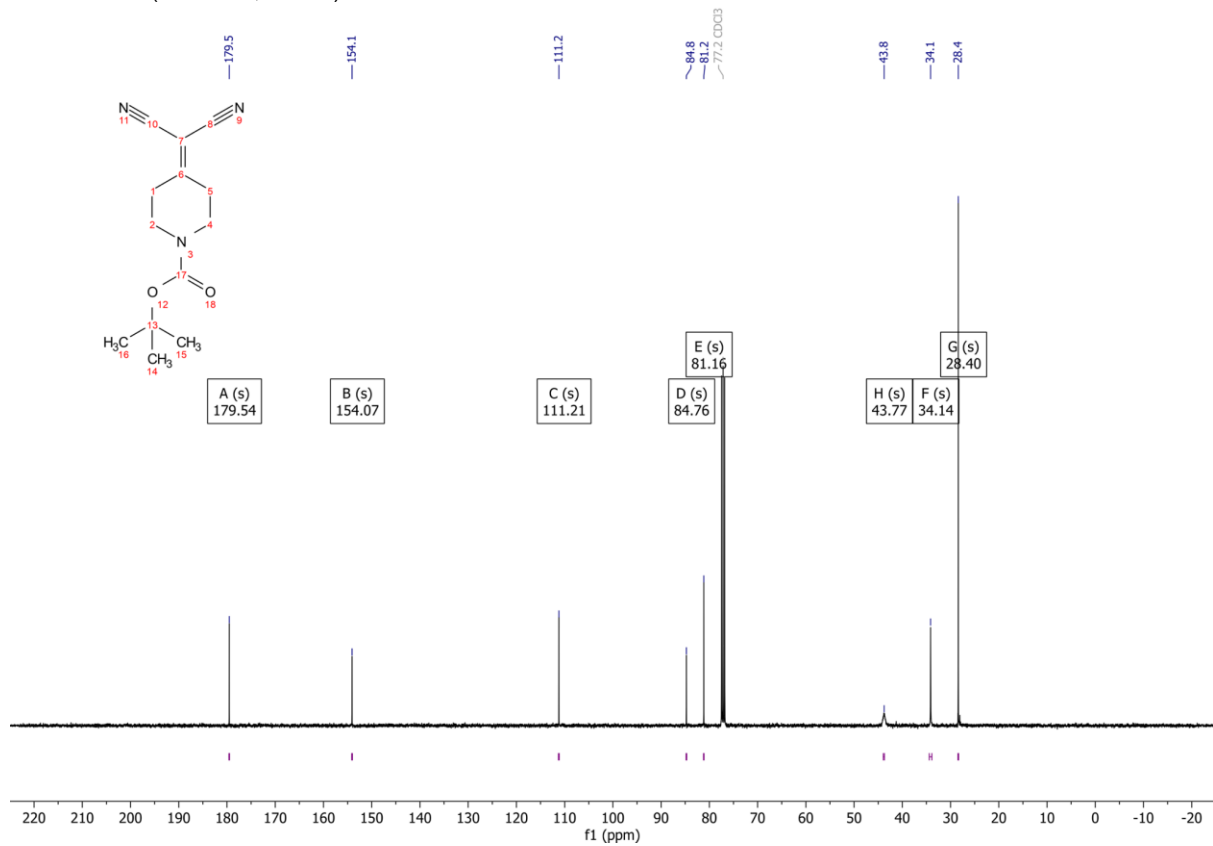
108 ^{13}C NMR (151 MHz, CDCl_3)



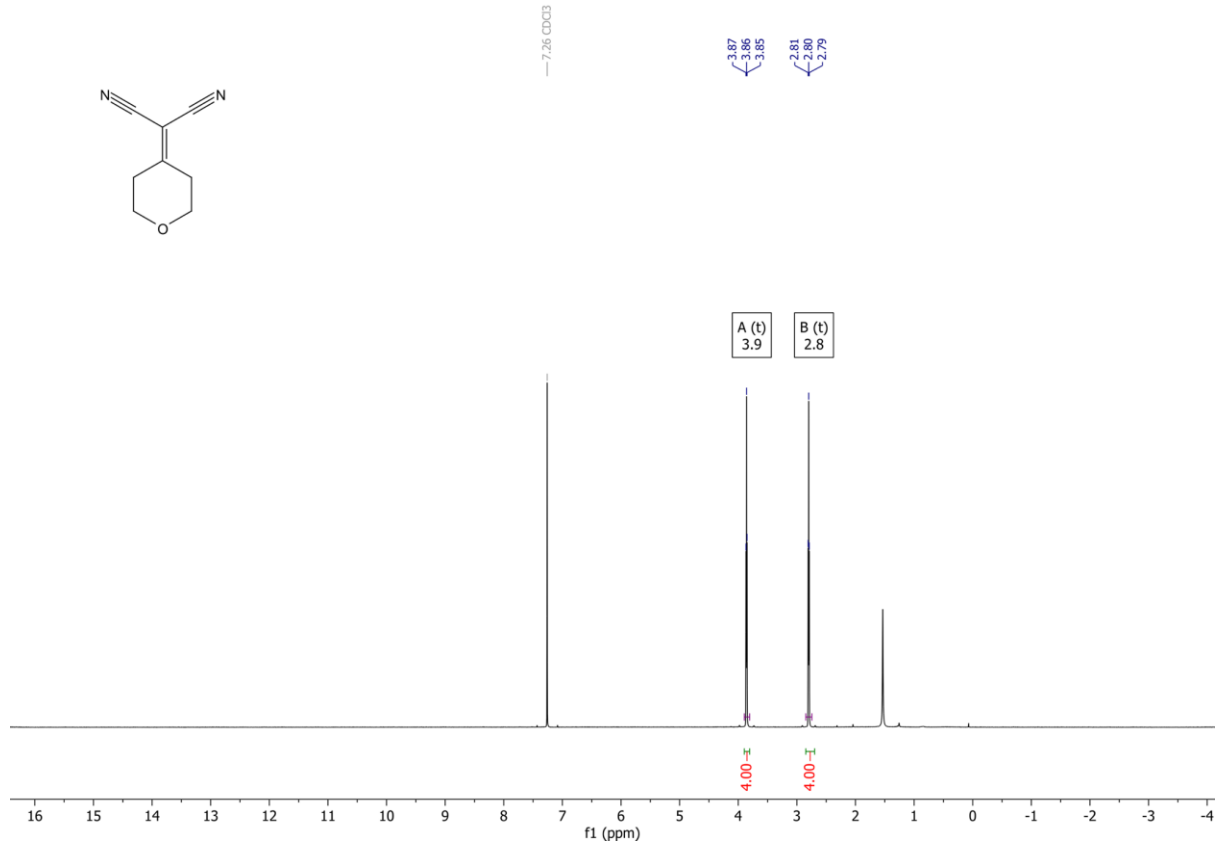
A2 ¹H NMR (400 MHz, CDCl₃)



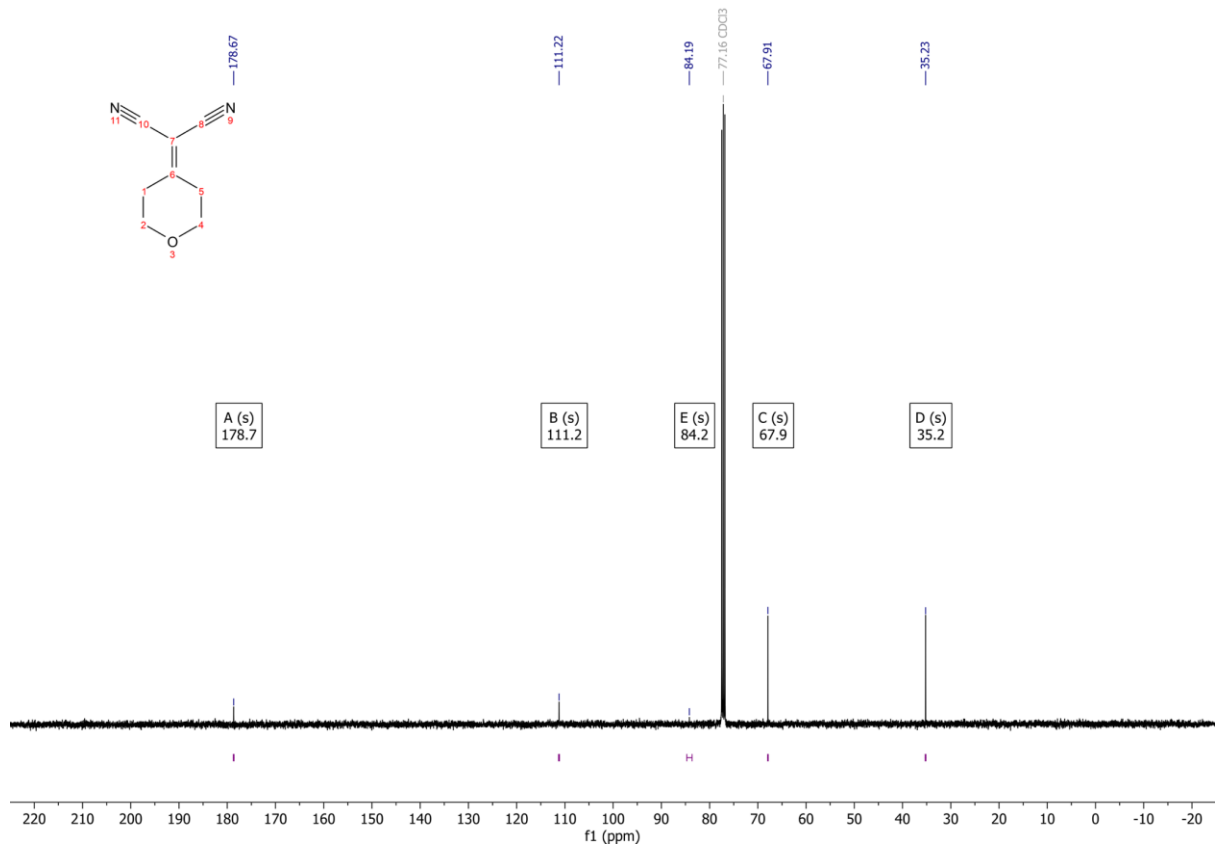
A2 ¹³C NMR (101 MHz, CDCl₃)



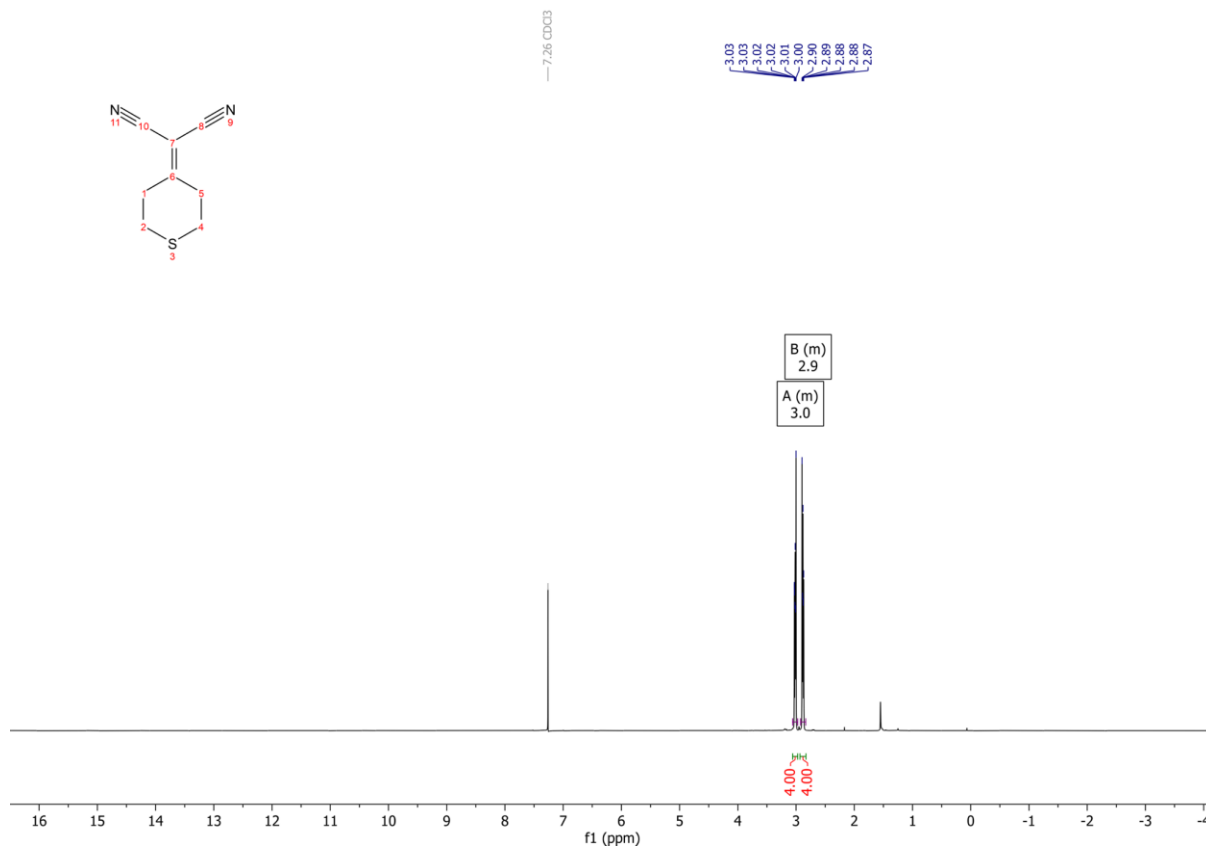
A3 ¹H NMR (400 MHz, CDCl₃)



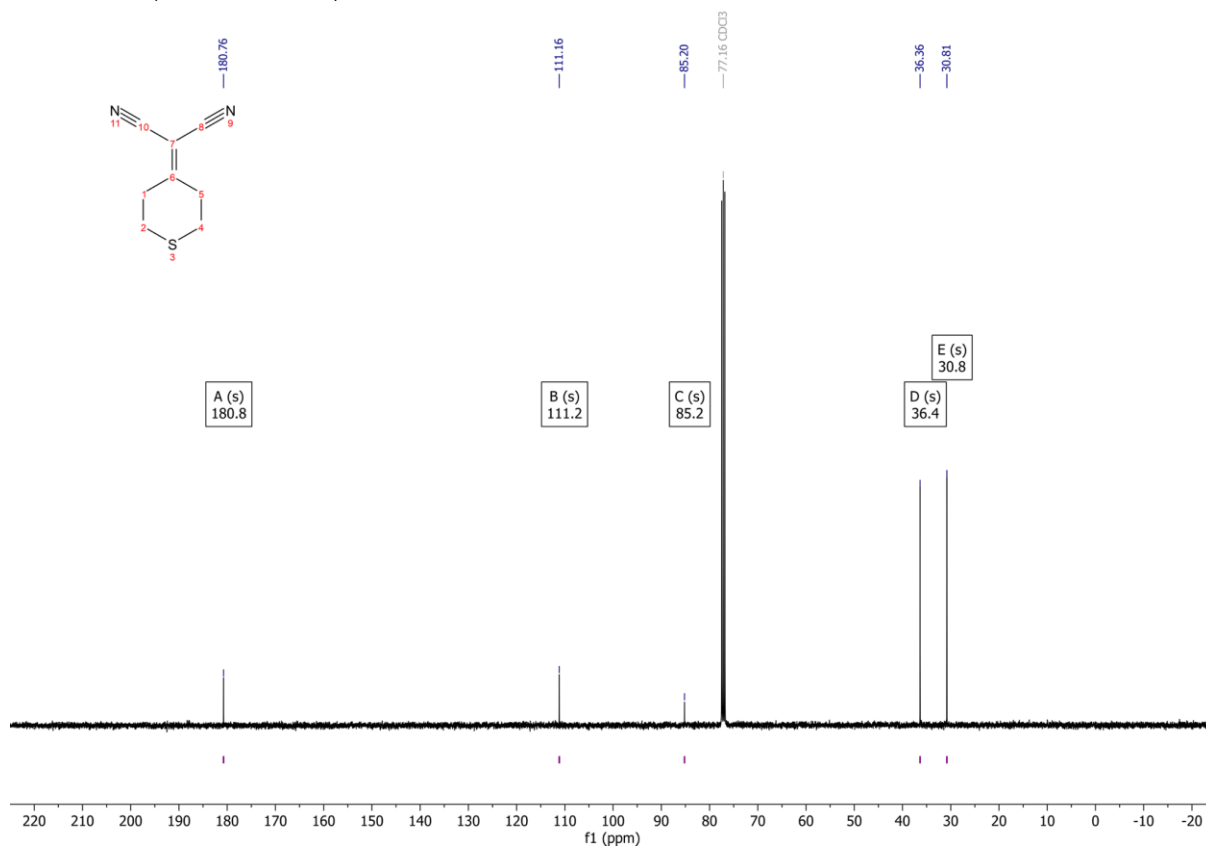
A3 ¹³C NMR (101 MHz, CDCl₃)



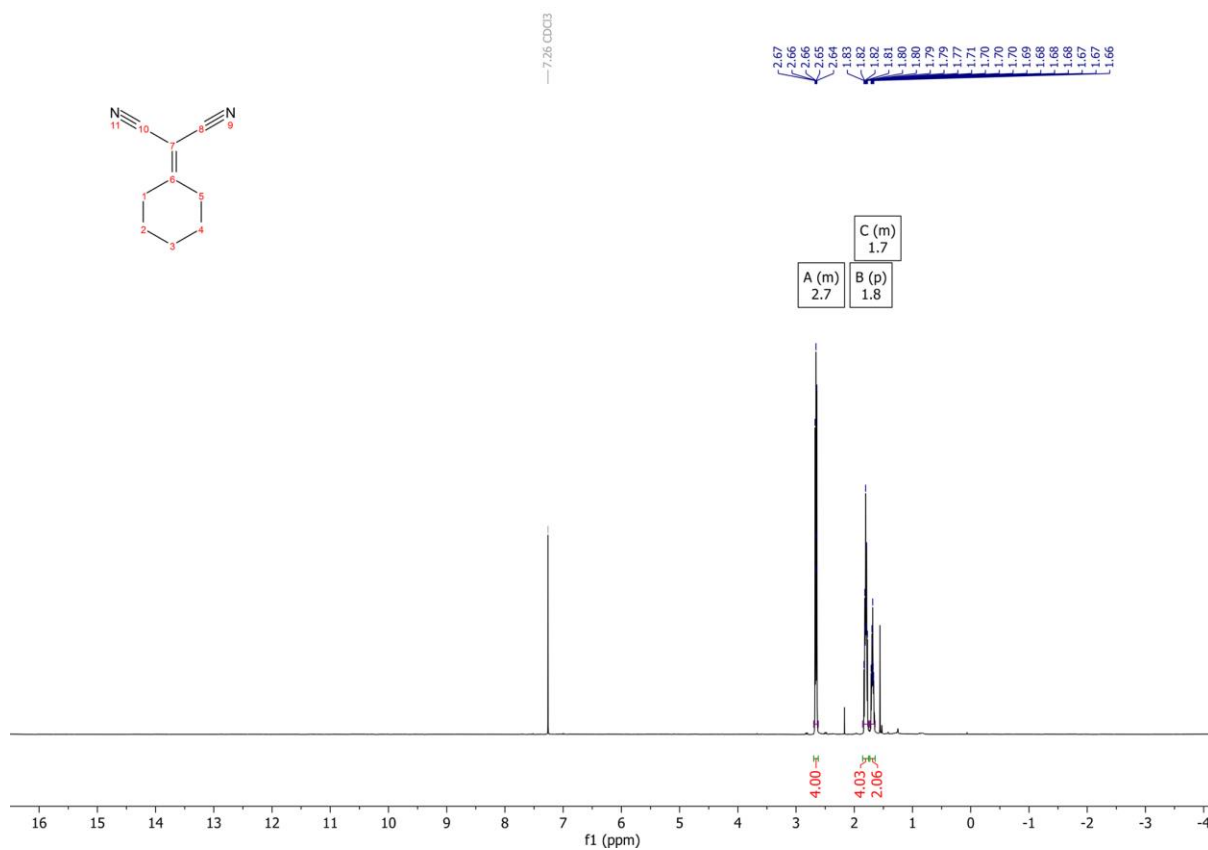
A4 ^1H NMR (400 MHz, CDCl_3)



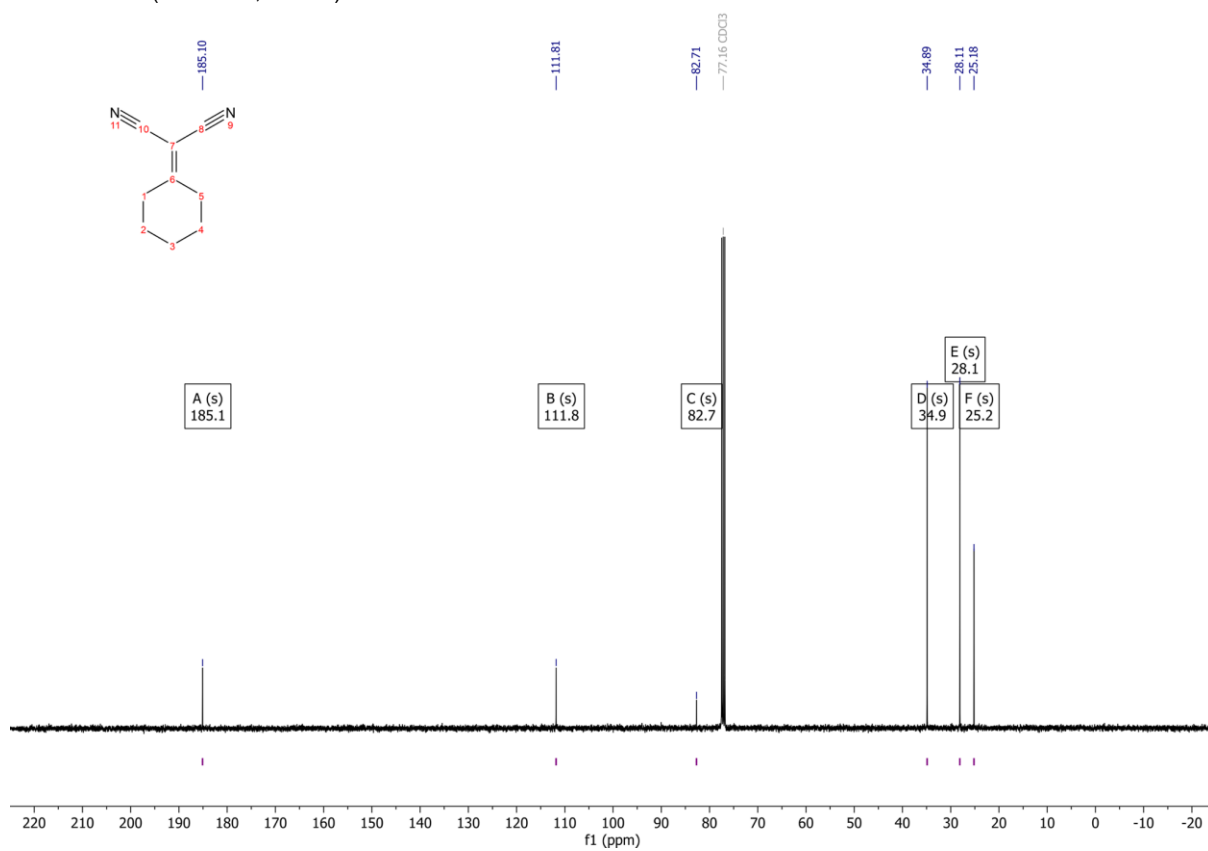
A4 ^{13}C NMR (101 MHz, CDCl_3)



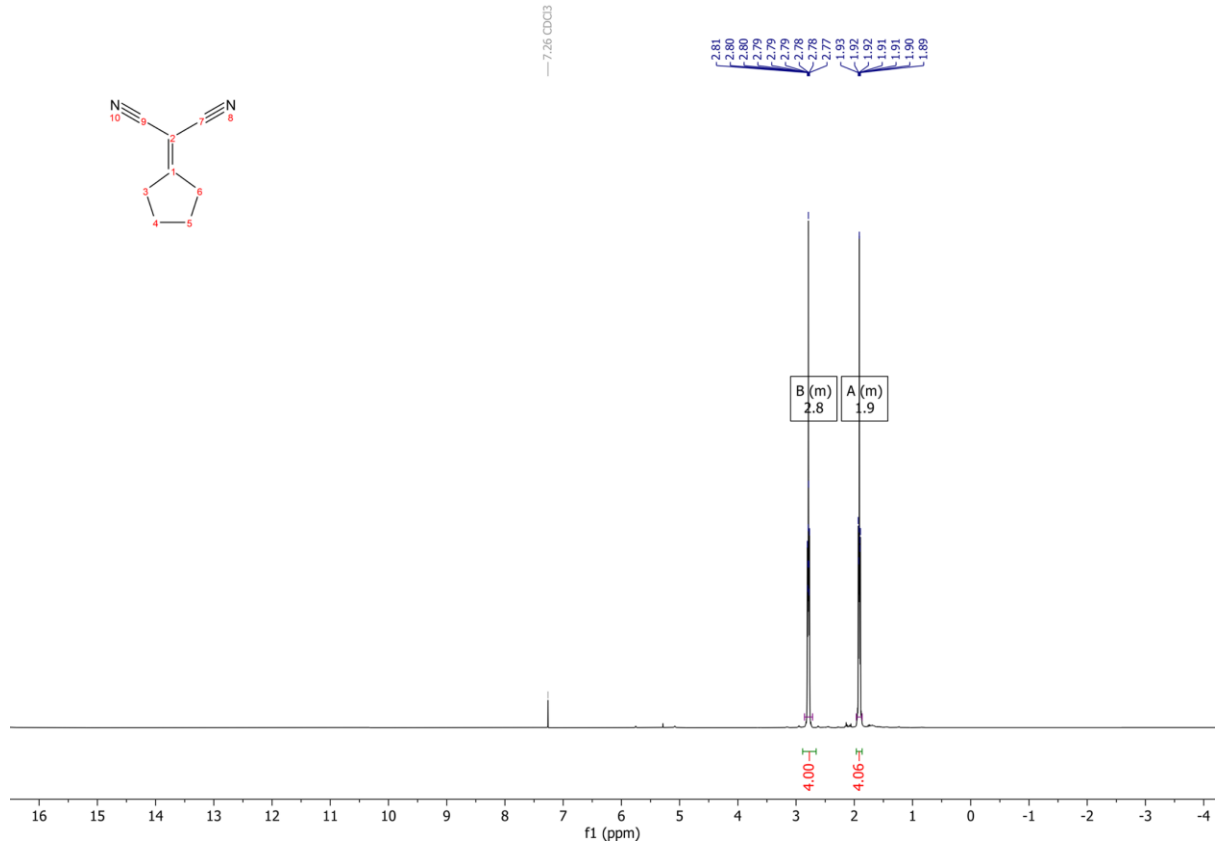
A5 ^1H NMR (400 MHz, CDCl_3)



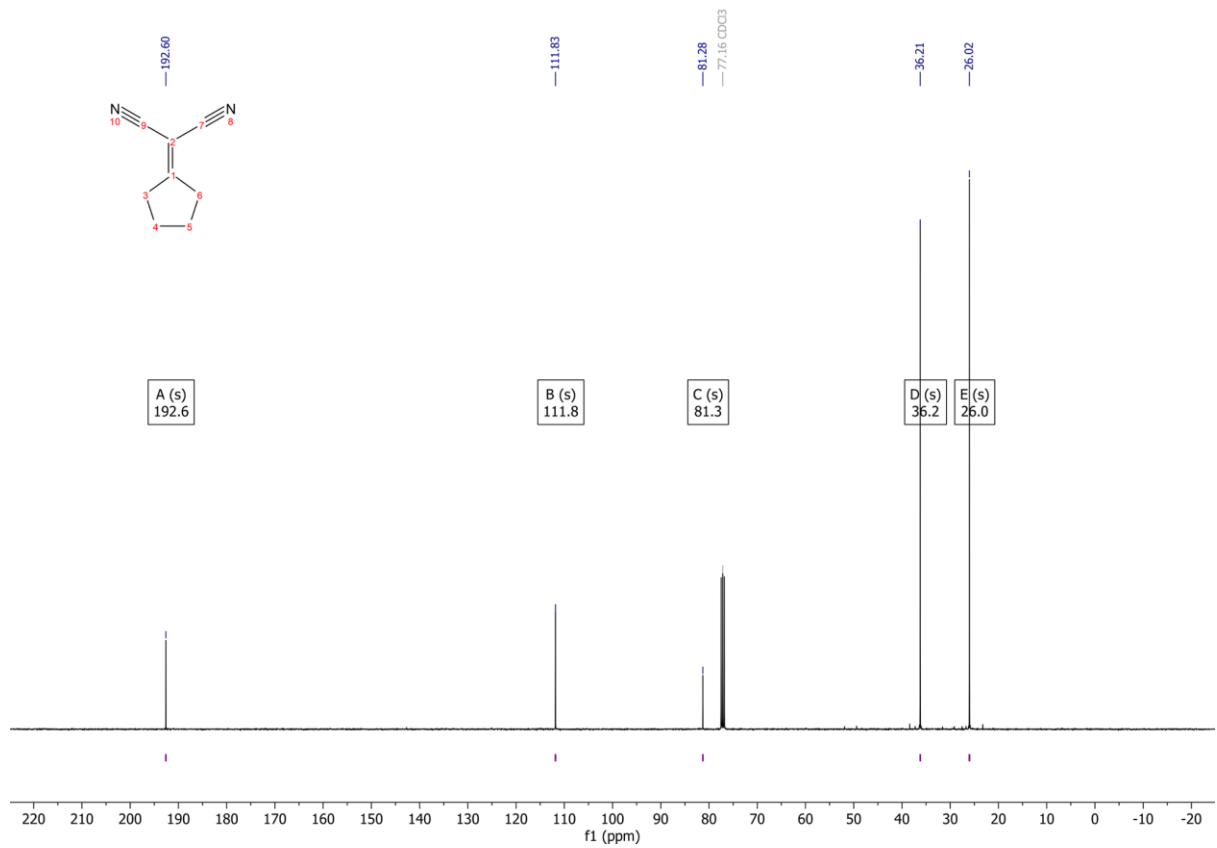
A5 ¹³C NMR (101 MHz, CDCl₃)



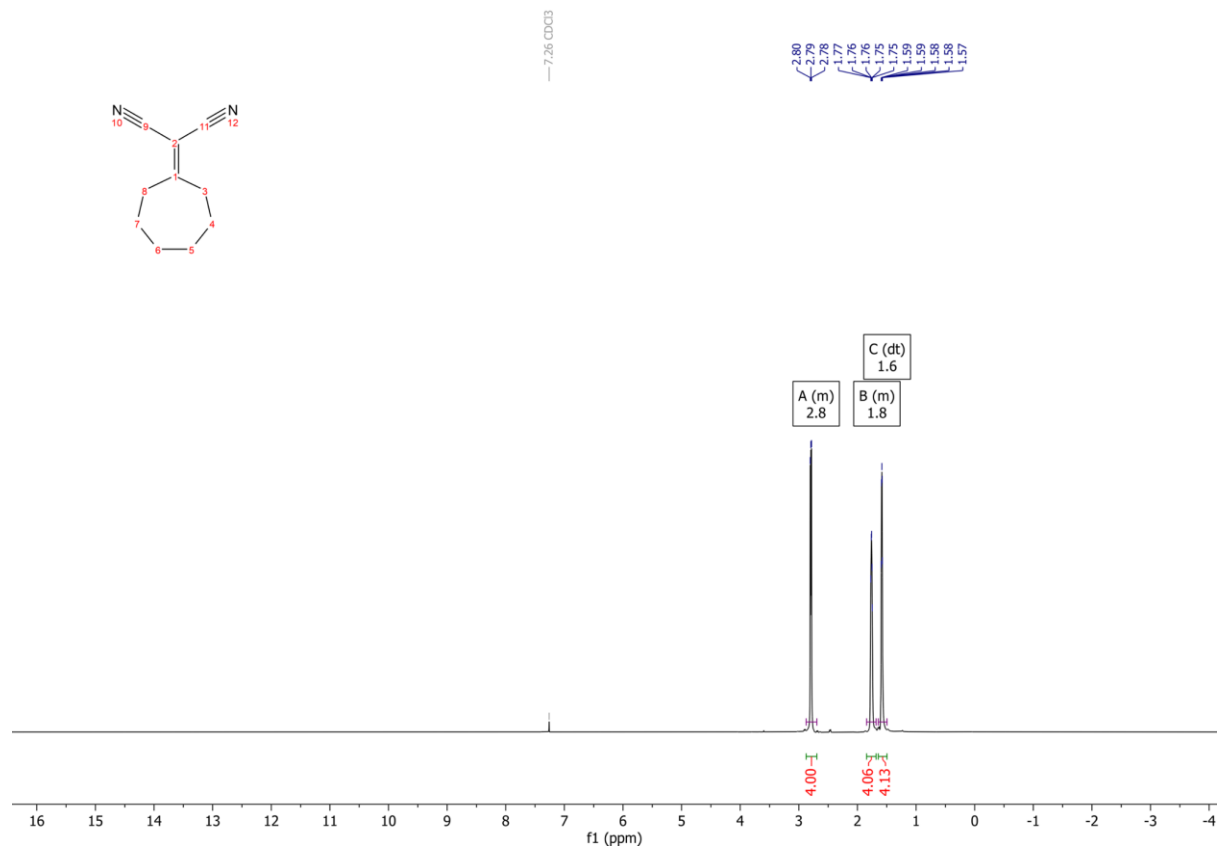
A6 ^1H NMR (600 MHz, CDCl_3)



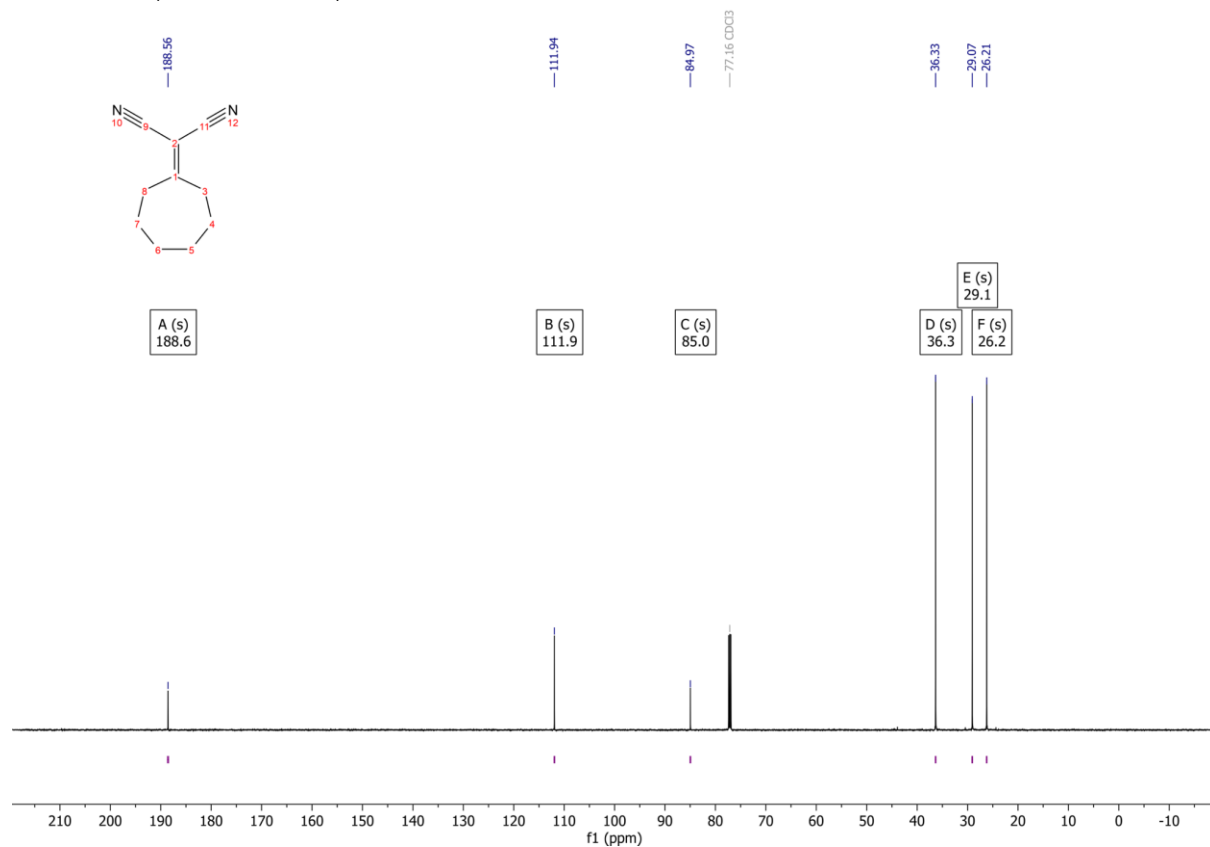
A6 ^{13}C NMR (101 MHz, CDCl_3)



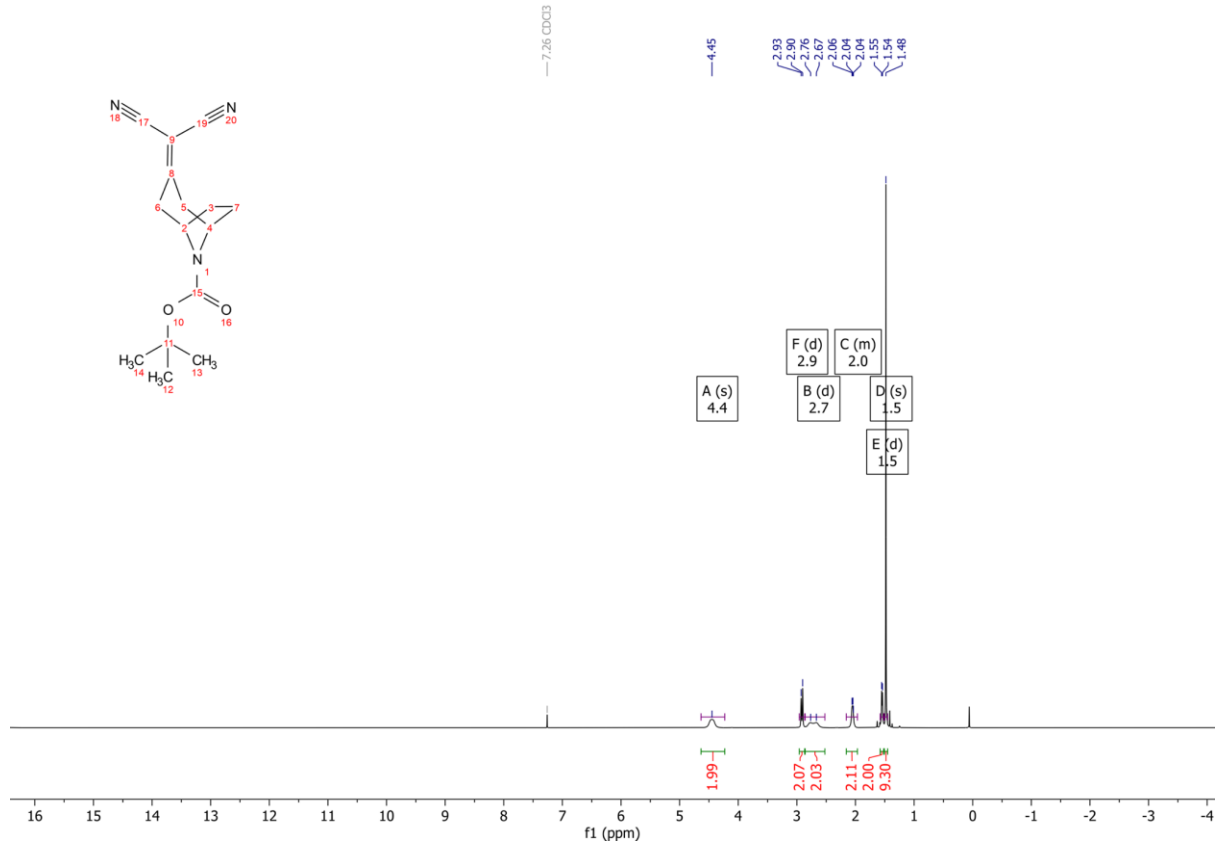
A7 ¹H NMR (600 MHz, CDCl₃)



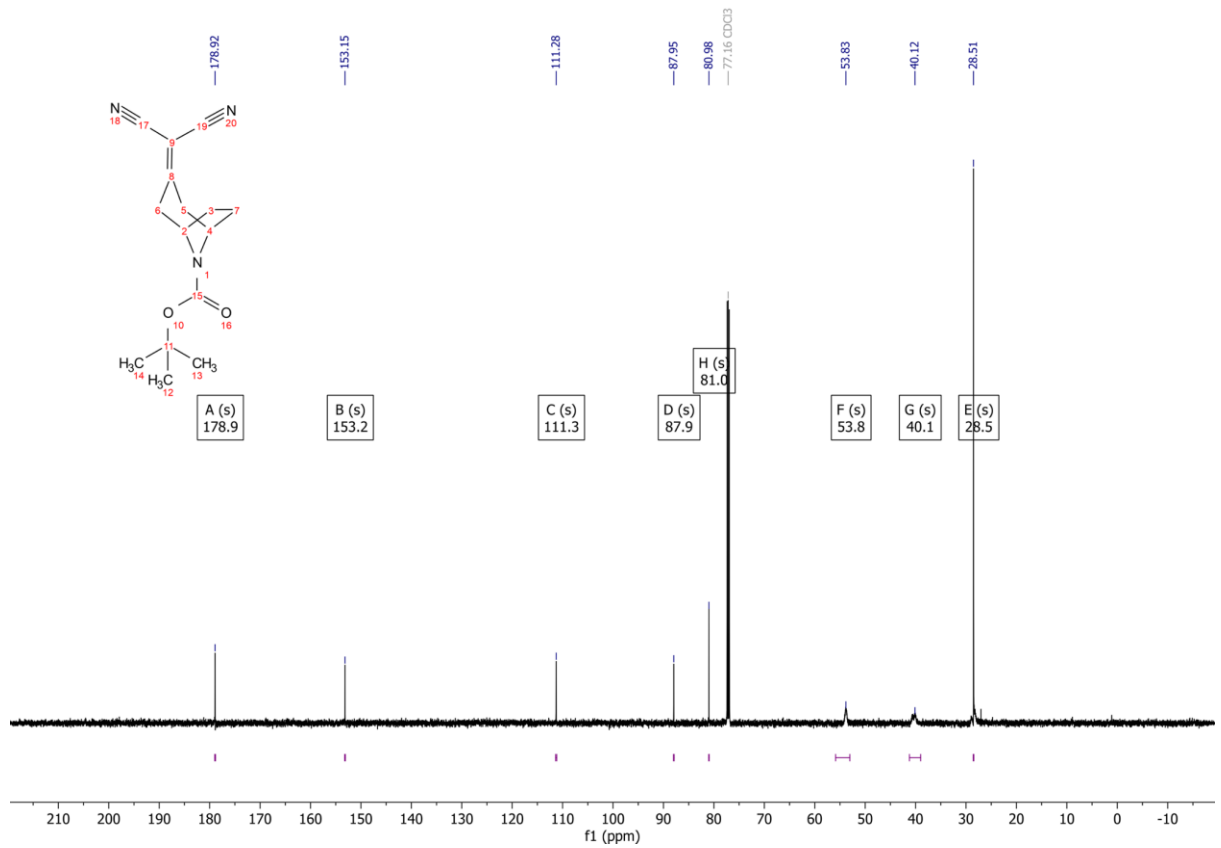
A7 ¹³C NMR (151 MHz, CDCl₃)



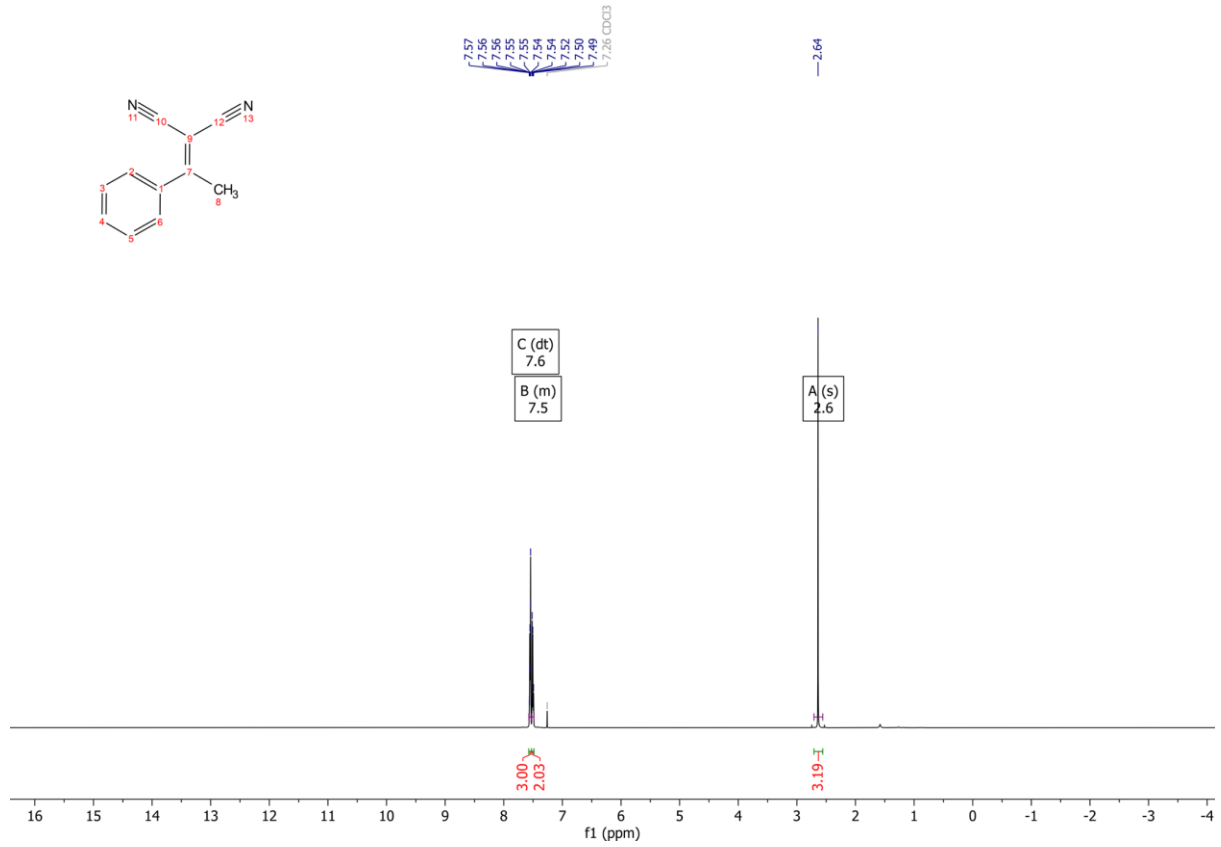
A8 ¹H NMR (600 MHz, CDCl₃)



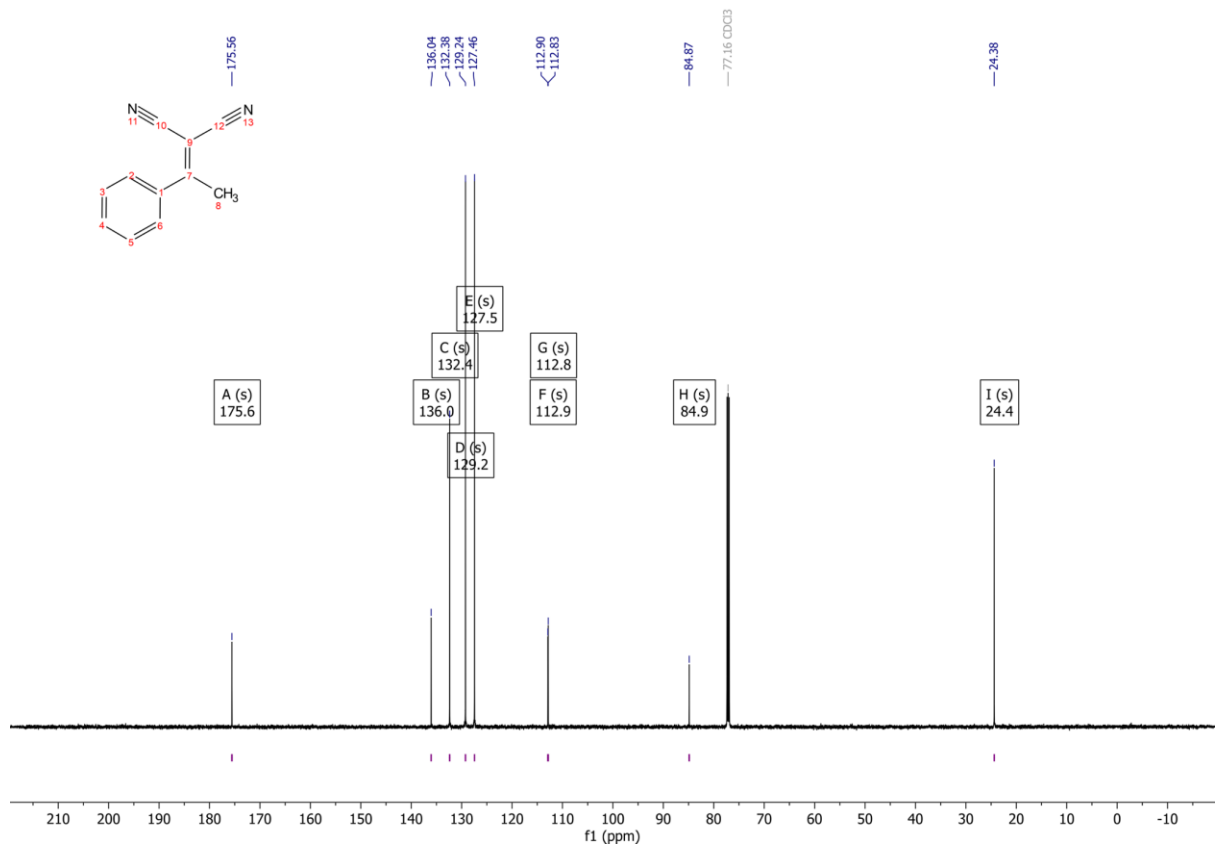
A8 ¹³C NMR (151 MHz, CDCl₃)



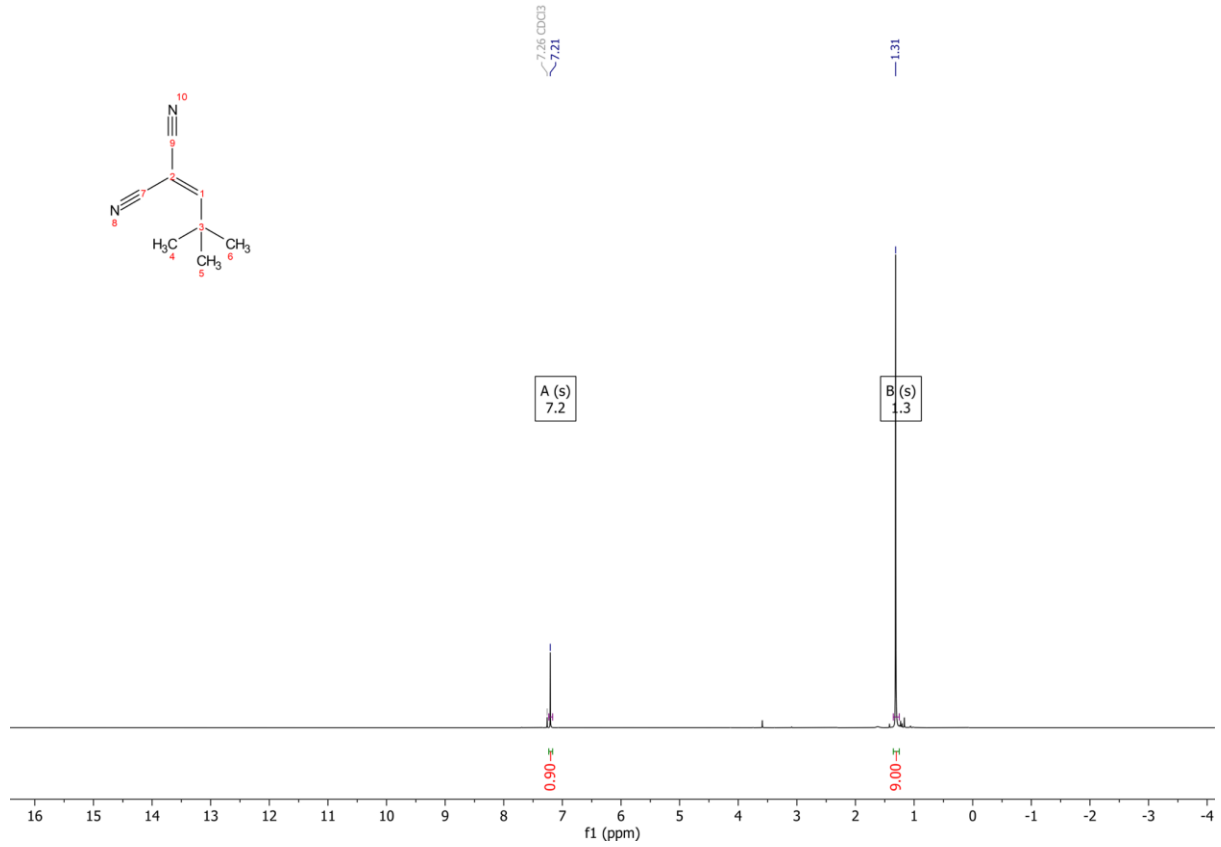
A9 ¹H NMR (600 MHz, CDCl₃)



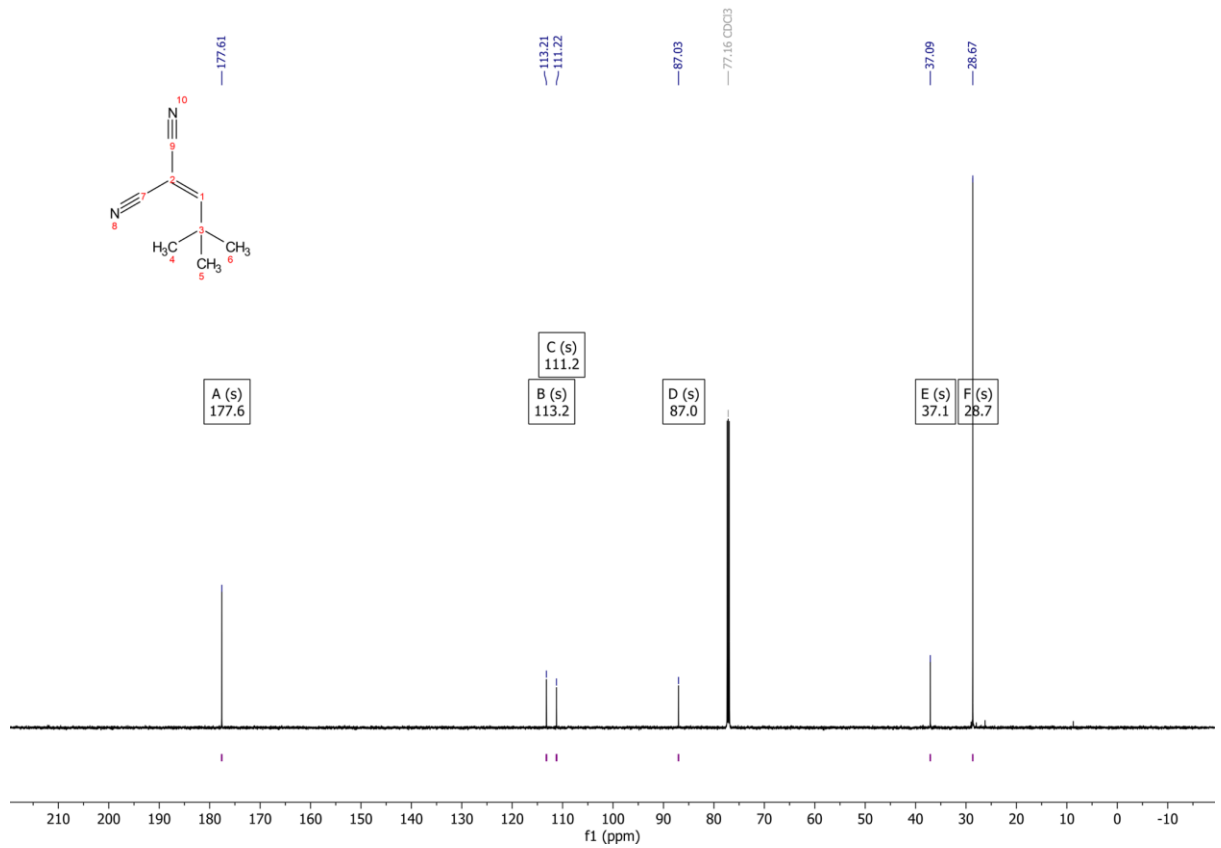
A9 ¹³C NMR (151 MHz, CDCl₃)



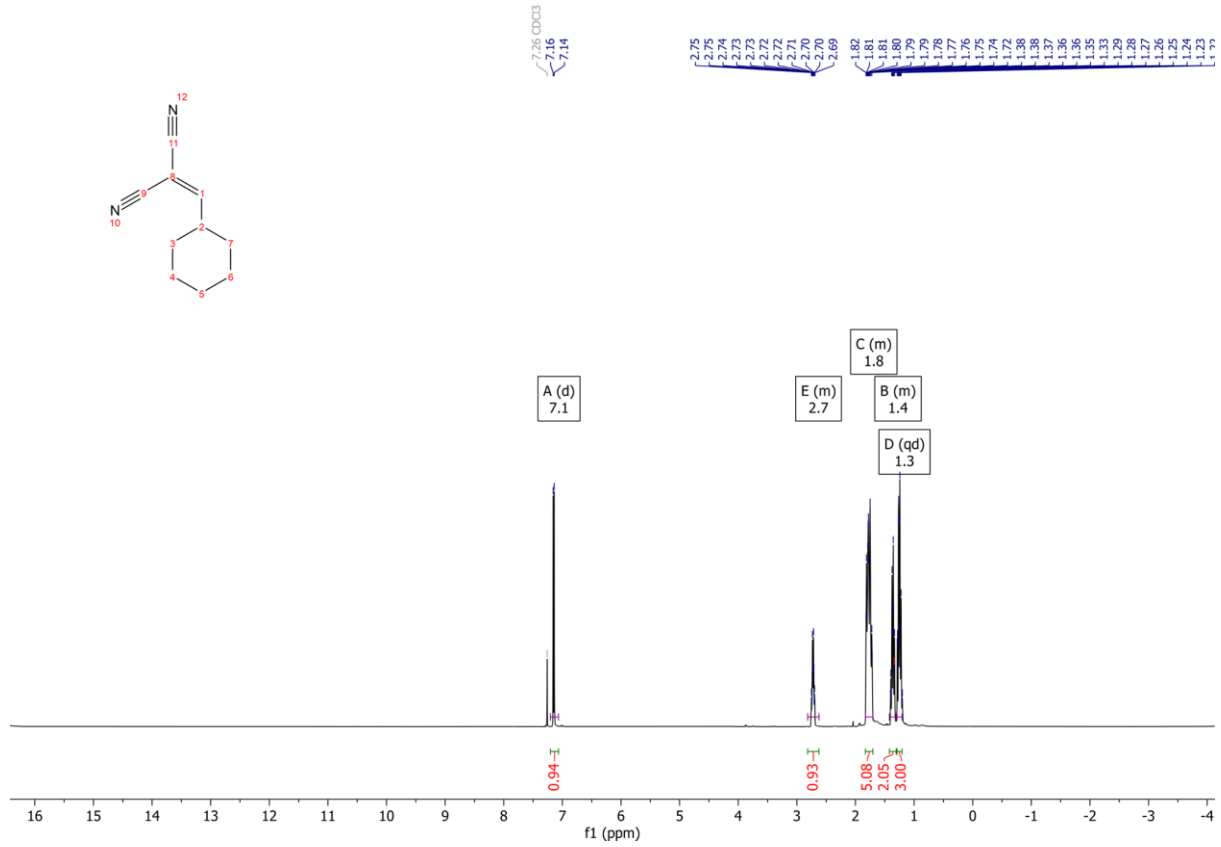
A10 ^1H NMR (600 MHz, CDCl_3)



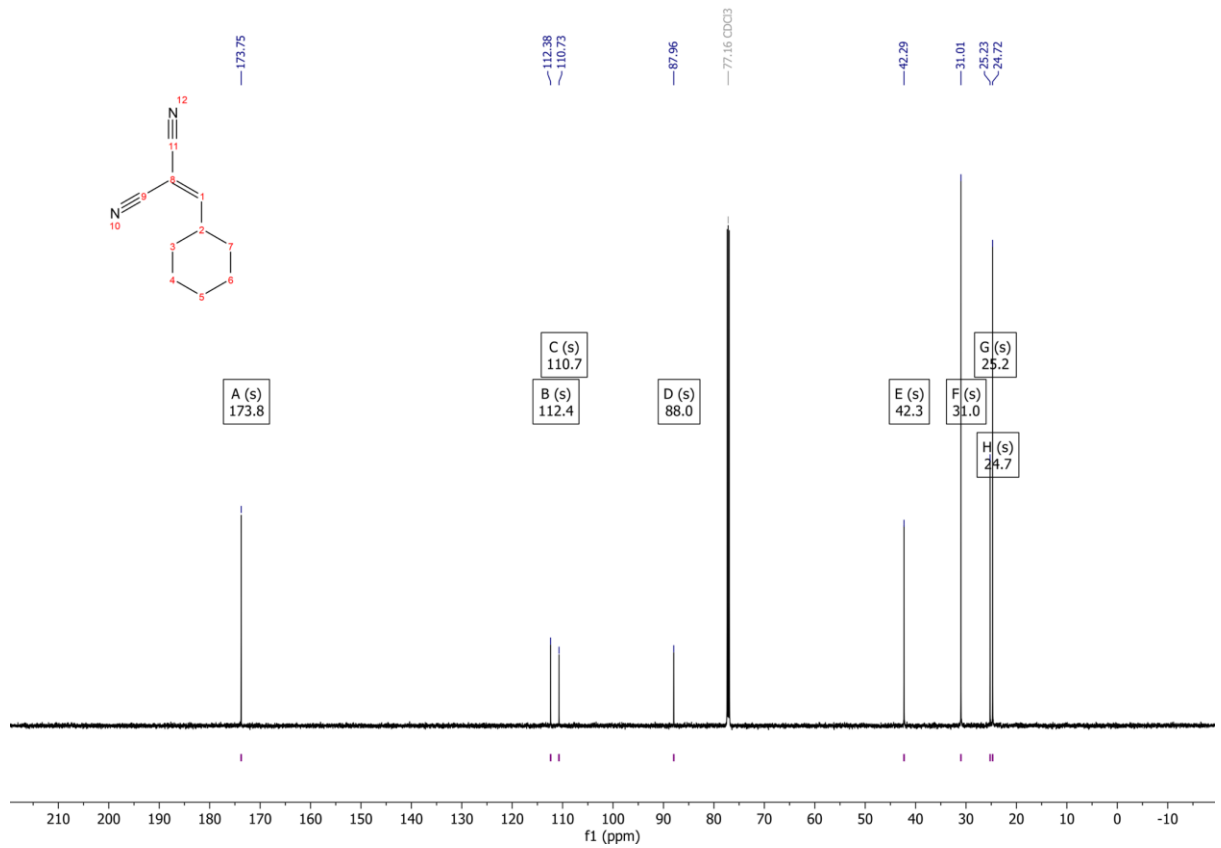
A10 ^{13}C NMR (151 MHz, CDCl_3)



A11 ¹H NMR (600 MHz, CDCl₃)

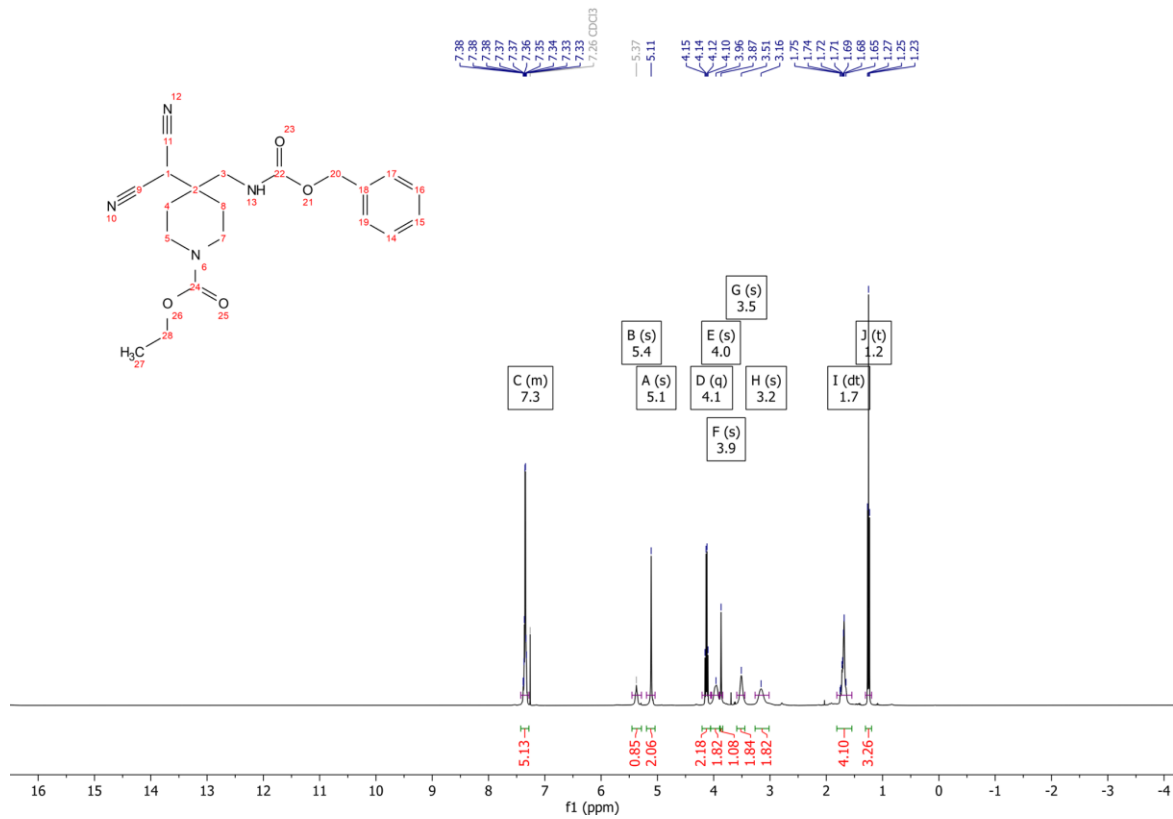


A11 ¹³C NMR (151 MHz, CDCl₃)

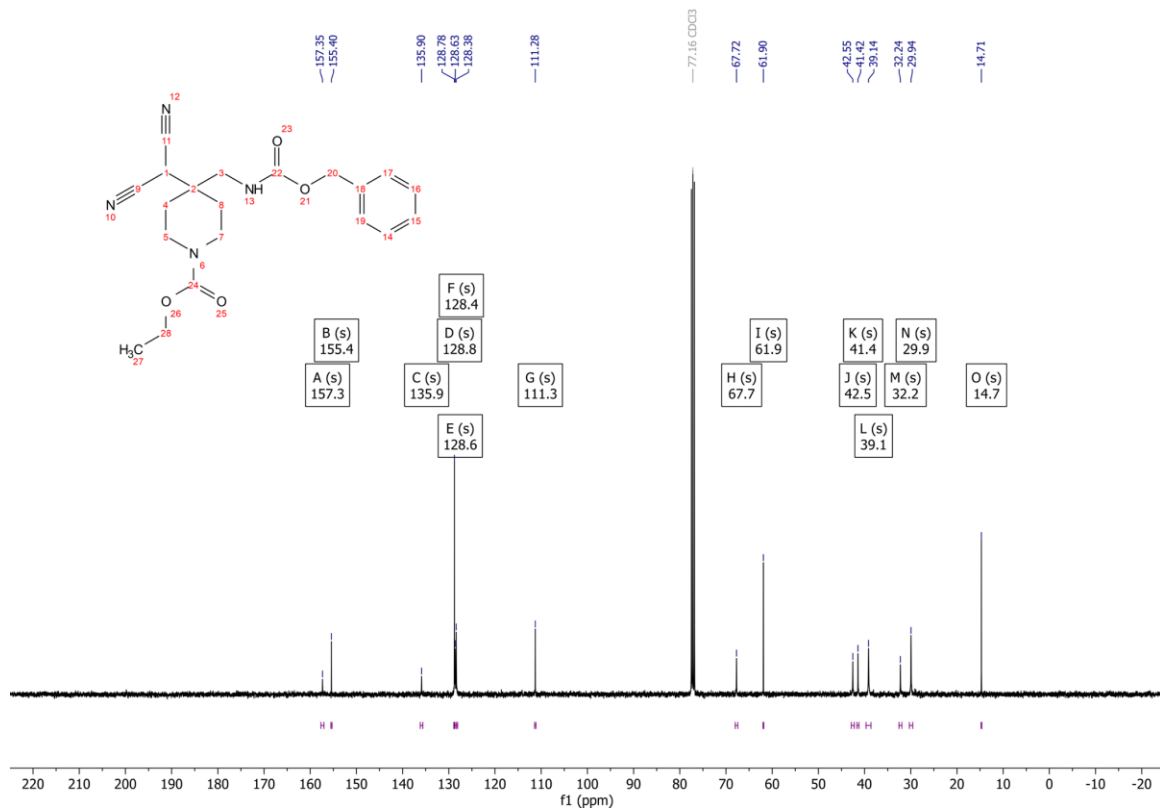


Substituted Malononitrile Derivatives

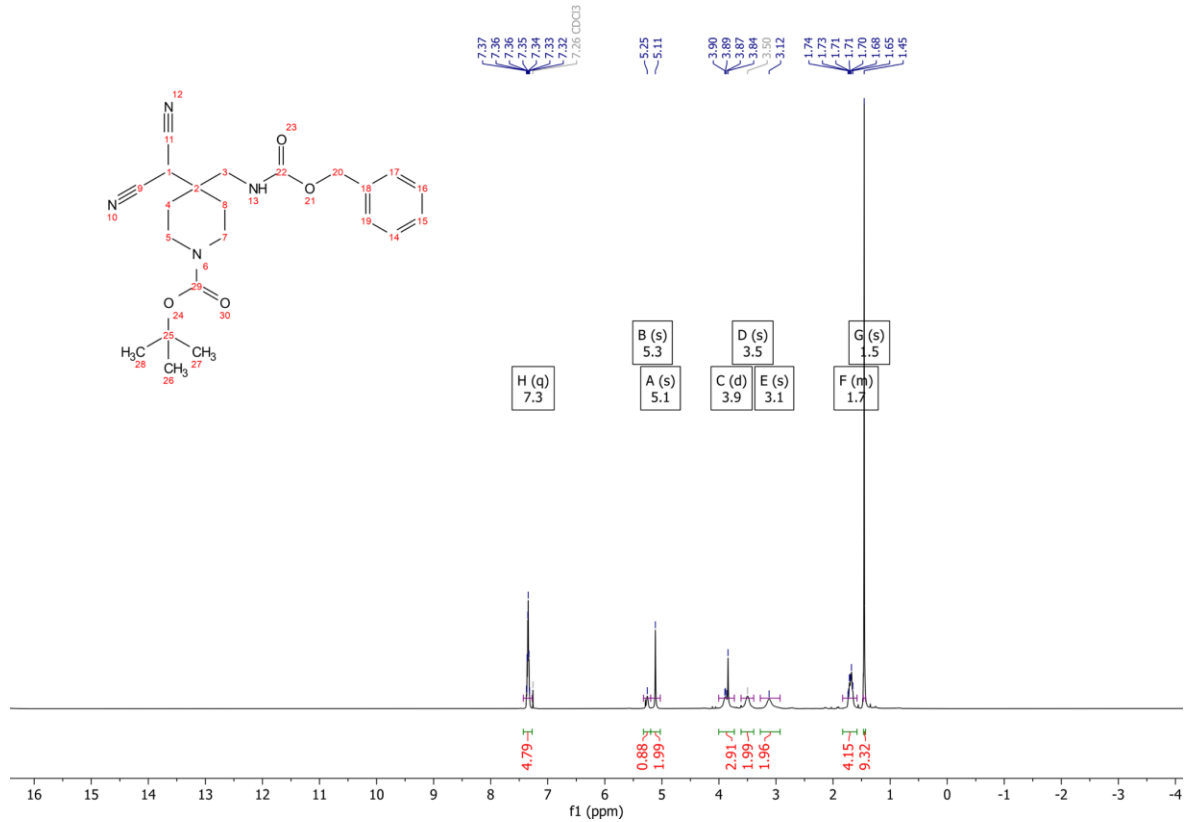
109 ¹H NMR (400 MHz, CDCl₃)



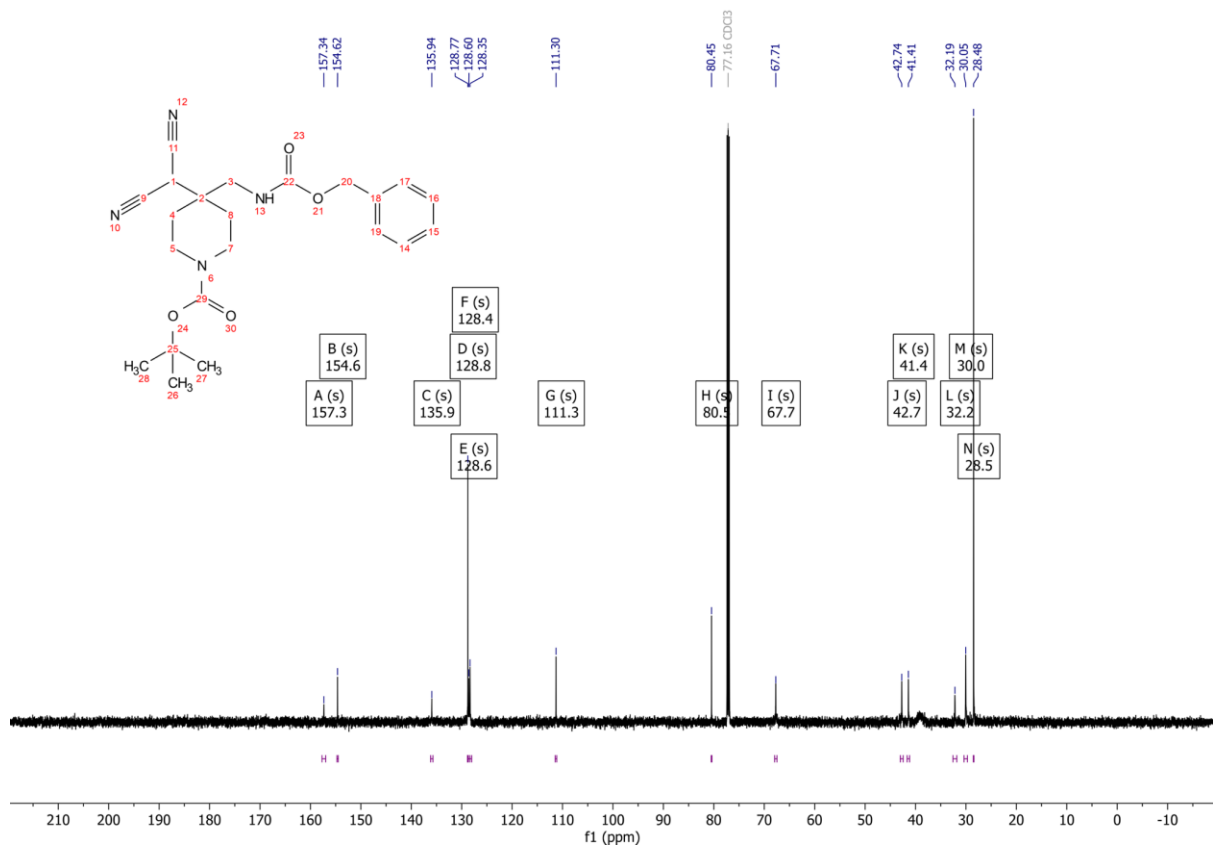
109 ¹³C NMR (101 MHz, CDCl₃)



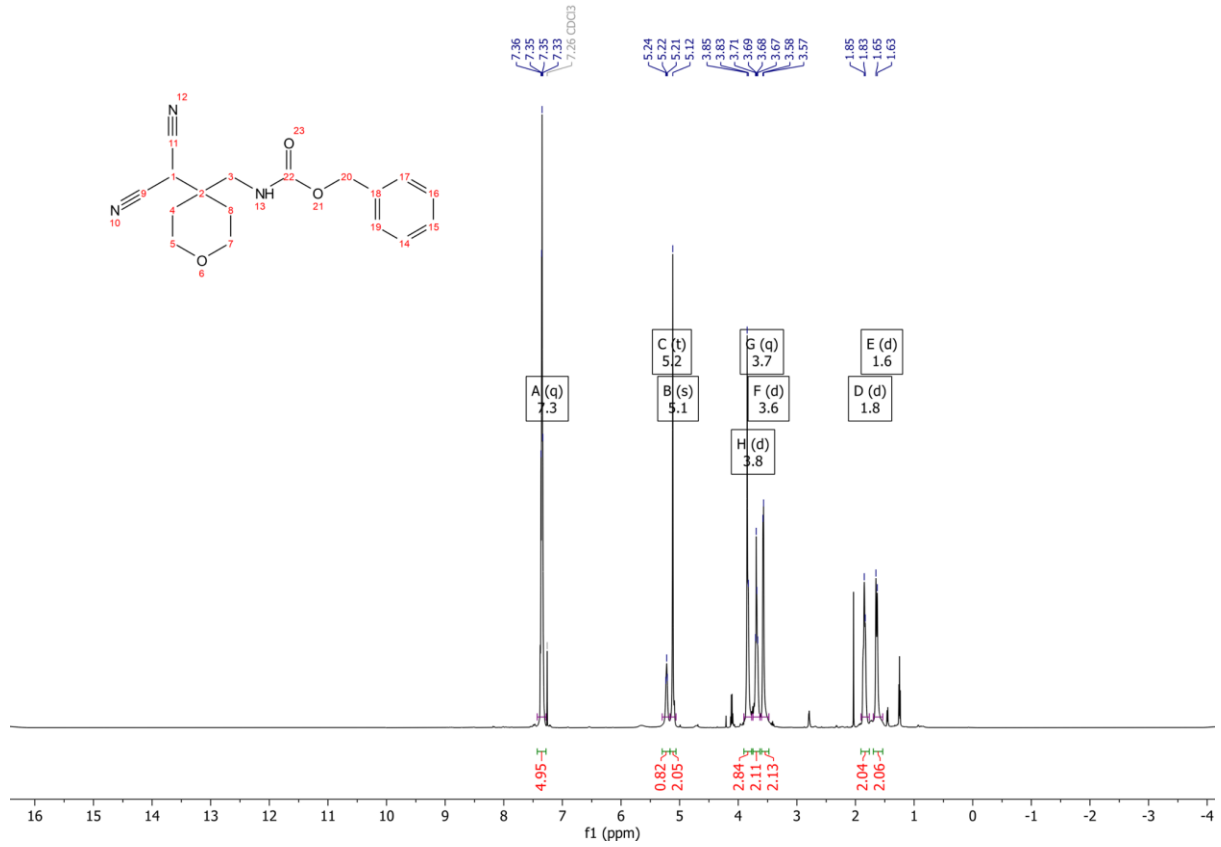
B2 ^1H NMR (600 MHz, CDCl_3)



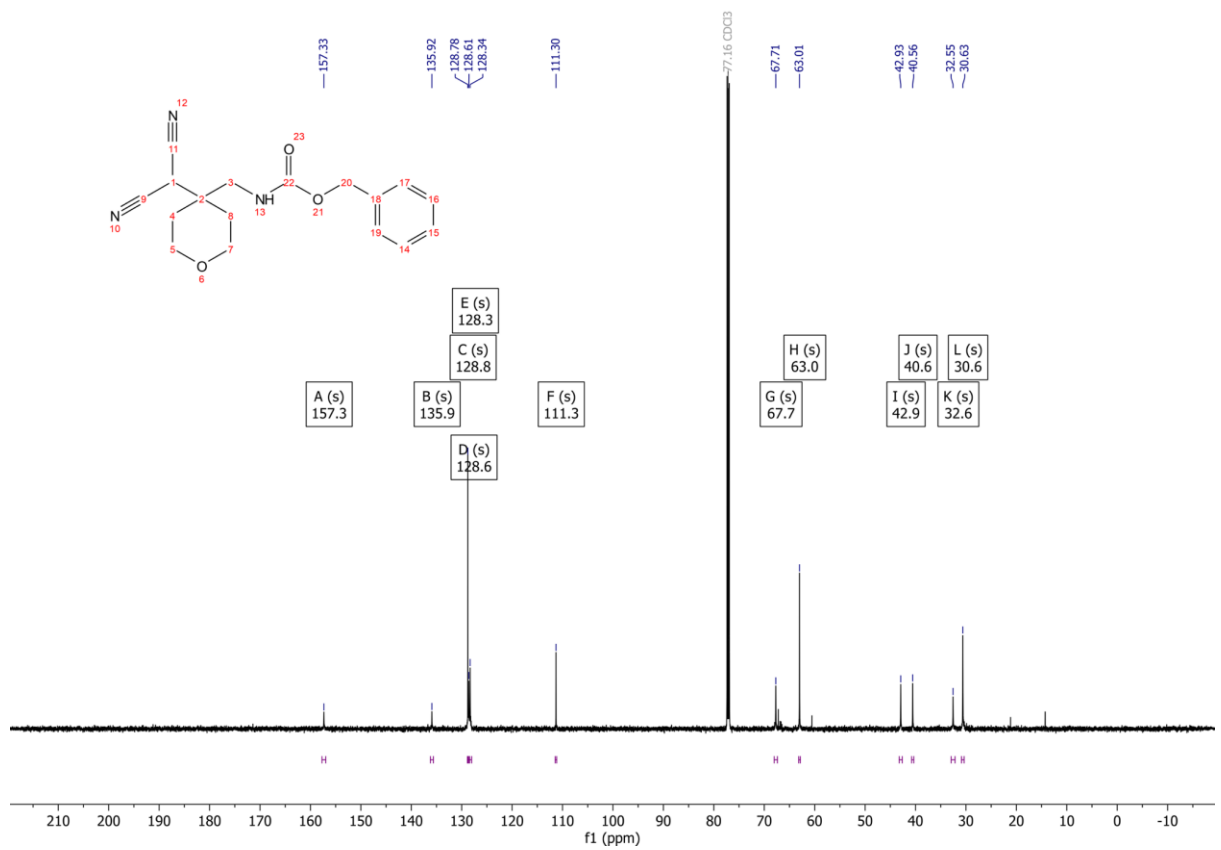
B2 ^{13}C NMR (151 MHz, CDCl_3)



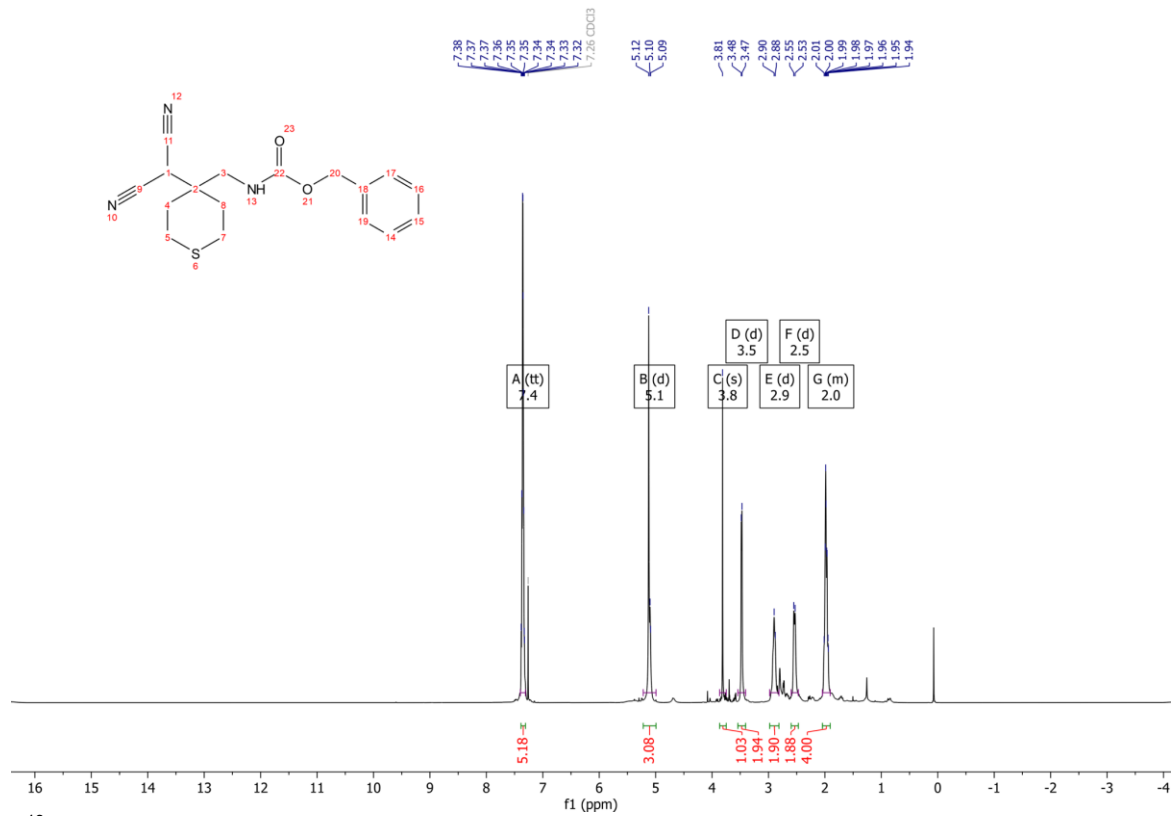
B3 ¹H NMR (600 MHz, CDCl₃)



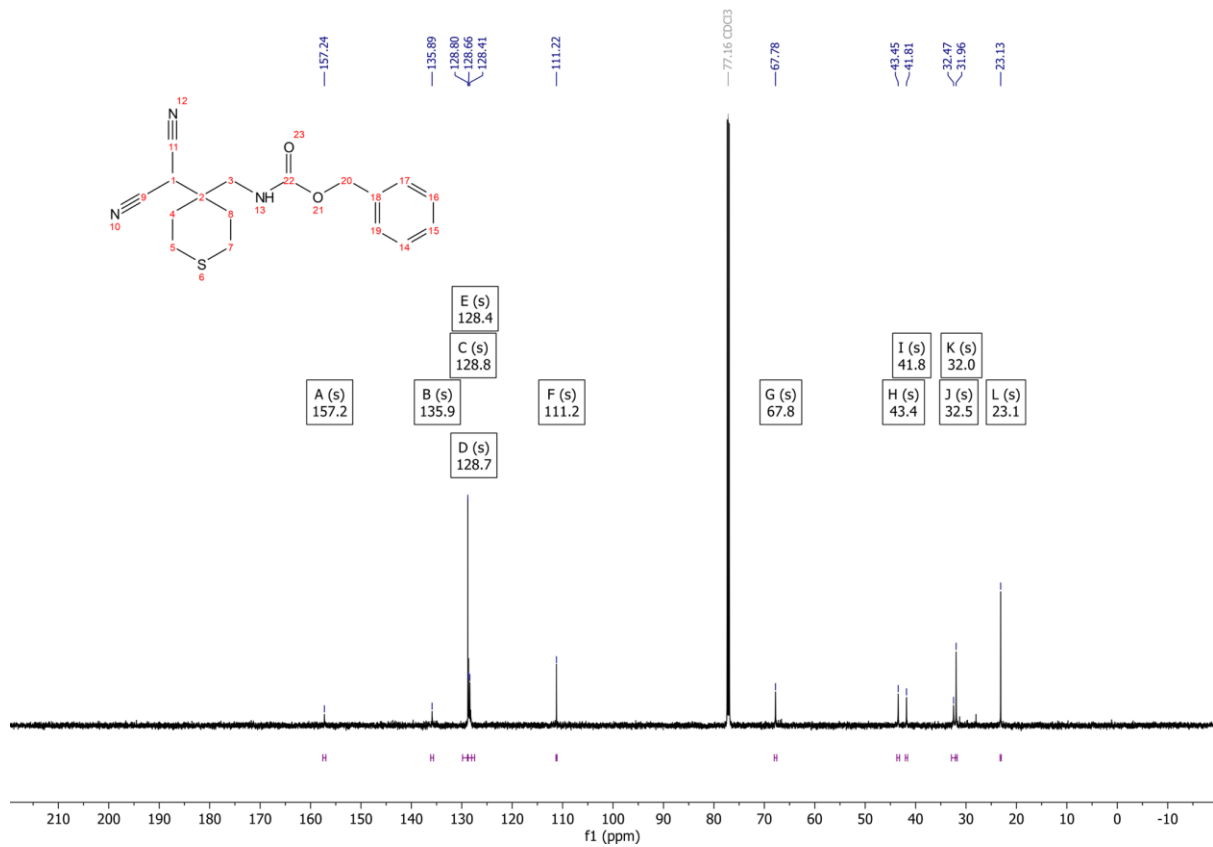
B3 ¹³C NMR (151 MHz, CDCl₃)



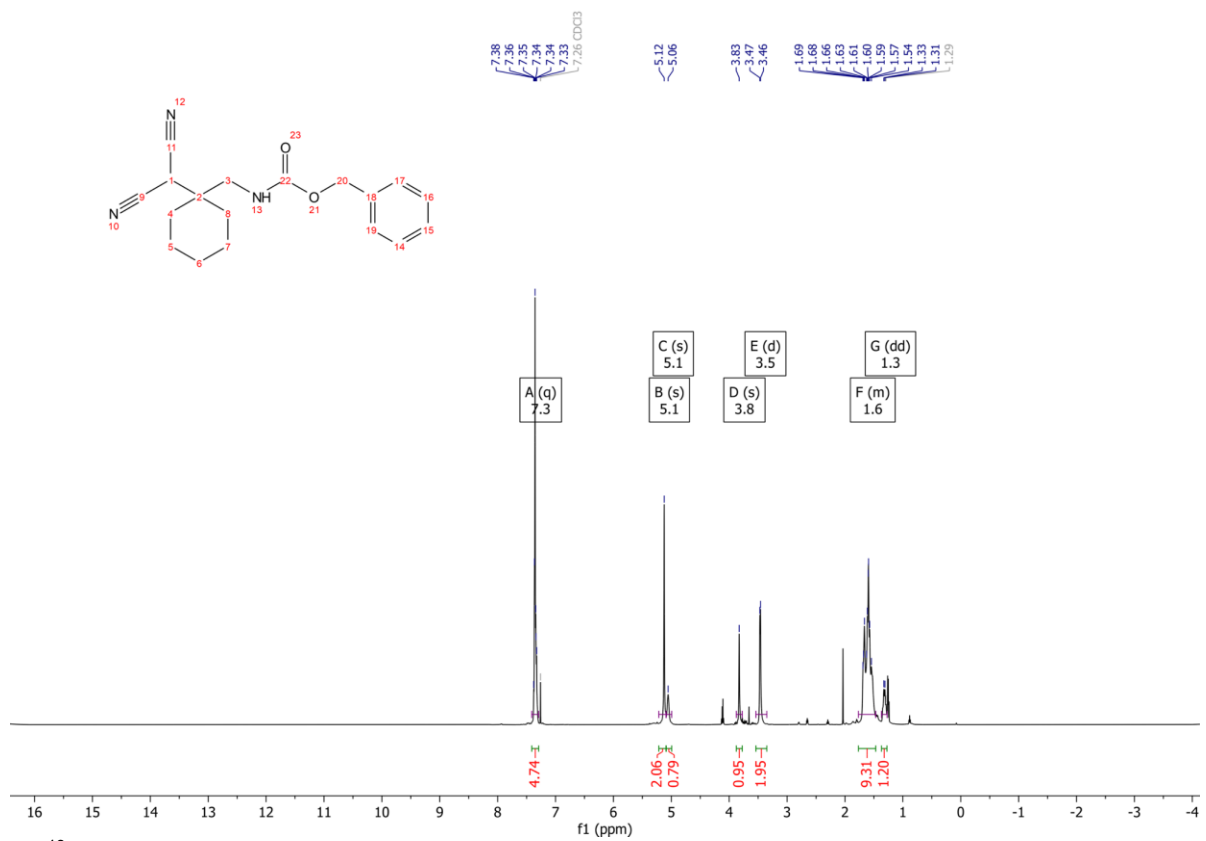
B4 ¹H NMR (600 MHz, CDCl₃)



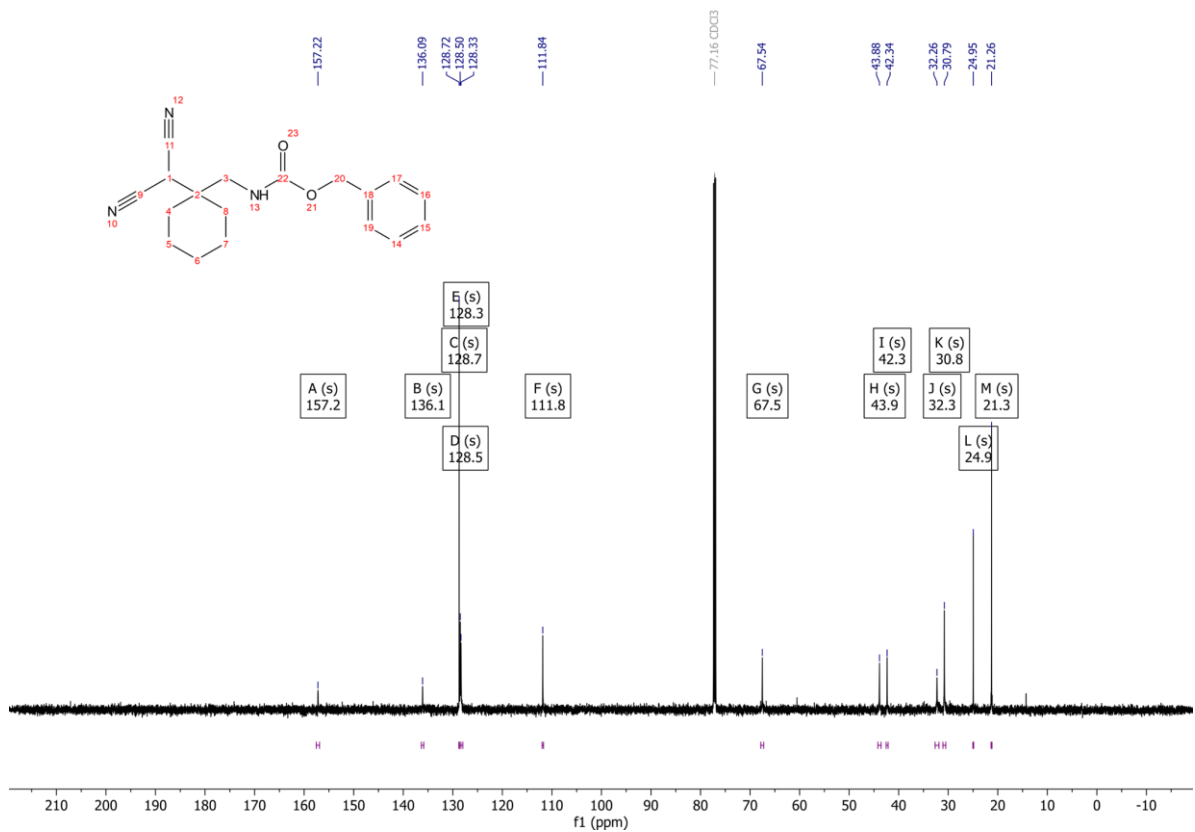
B4 ¹³C NMR (151 MHz, CDCl₃)



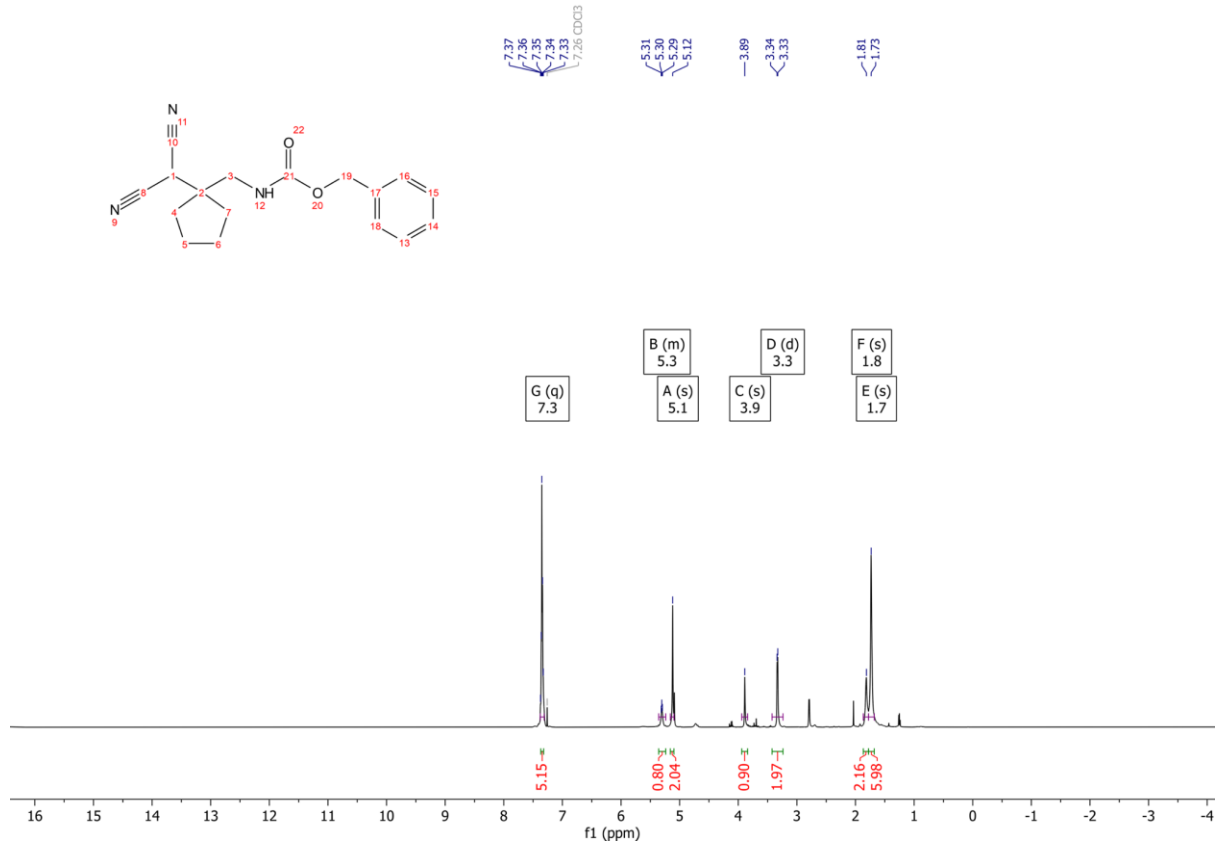
B5 ¹H NMR (600 MHz, CDCl₃)



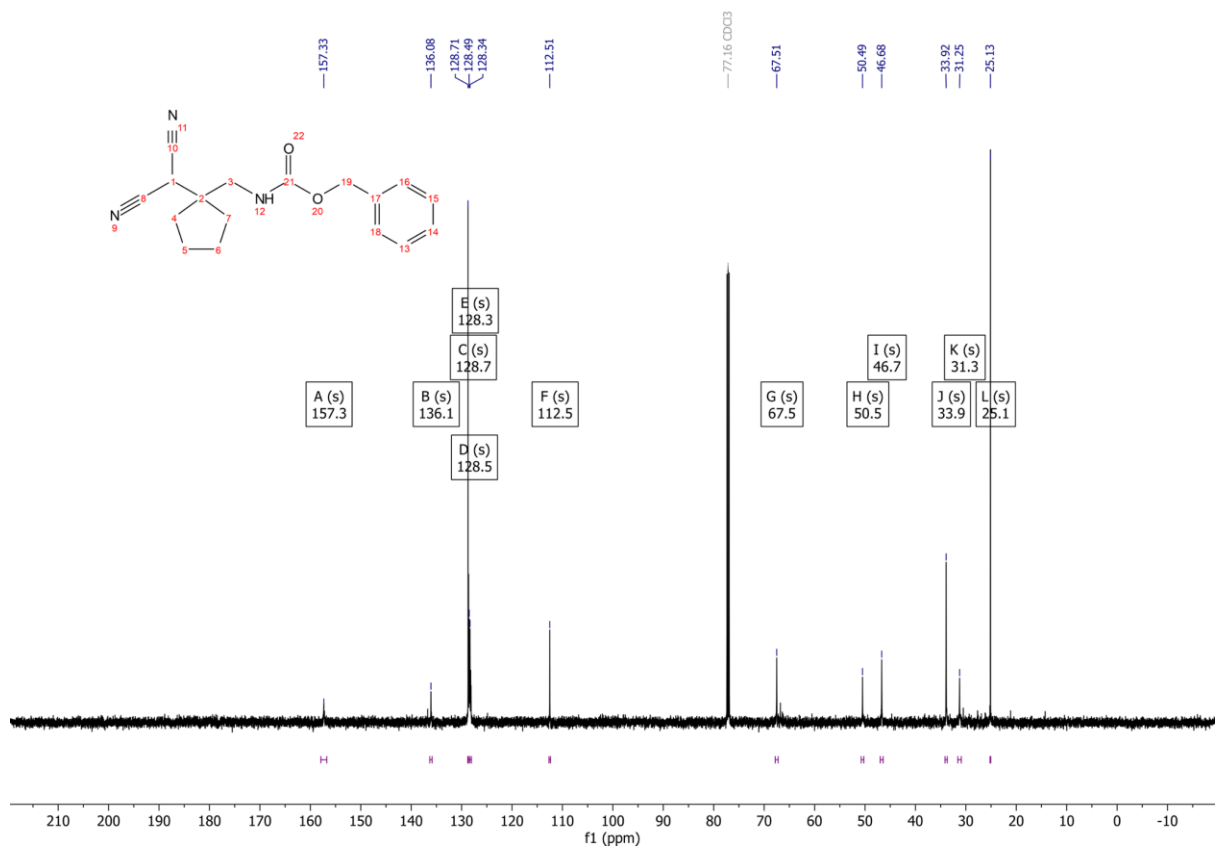
B5 ¹³C NMR (151 MHz, CDCl₃)



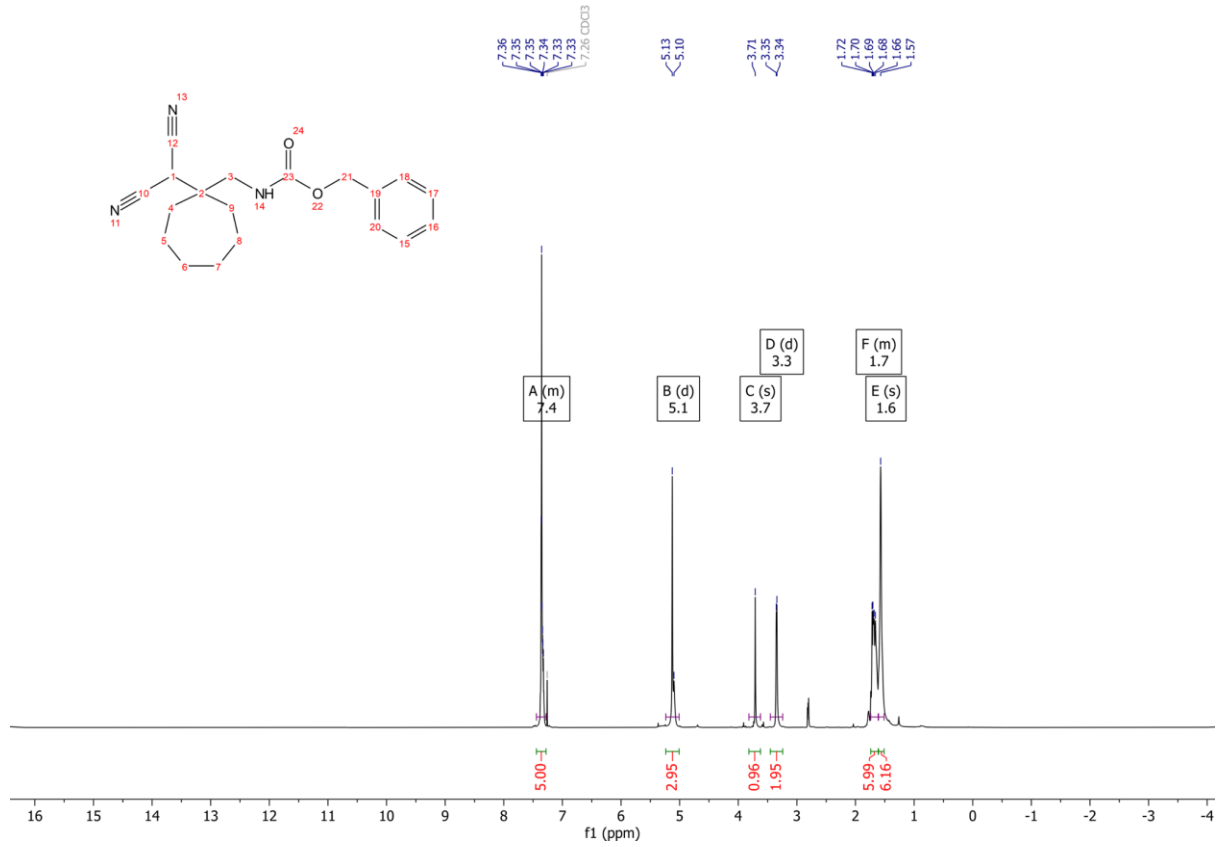
B6 ¹H NMR (600 MHz, CDCl₃)



B6 ¹³C NMR (151 MHz, CDCl₃)



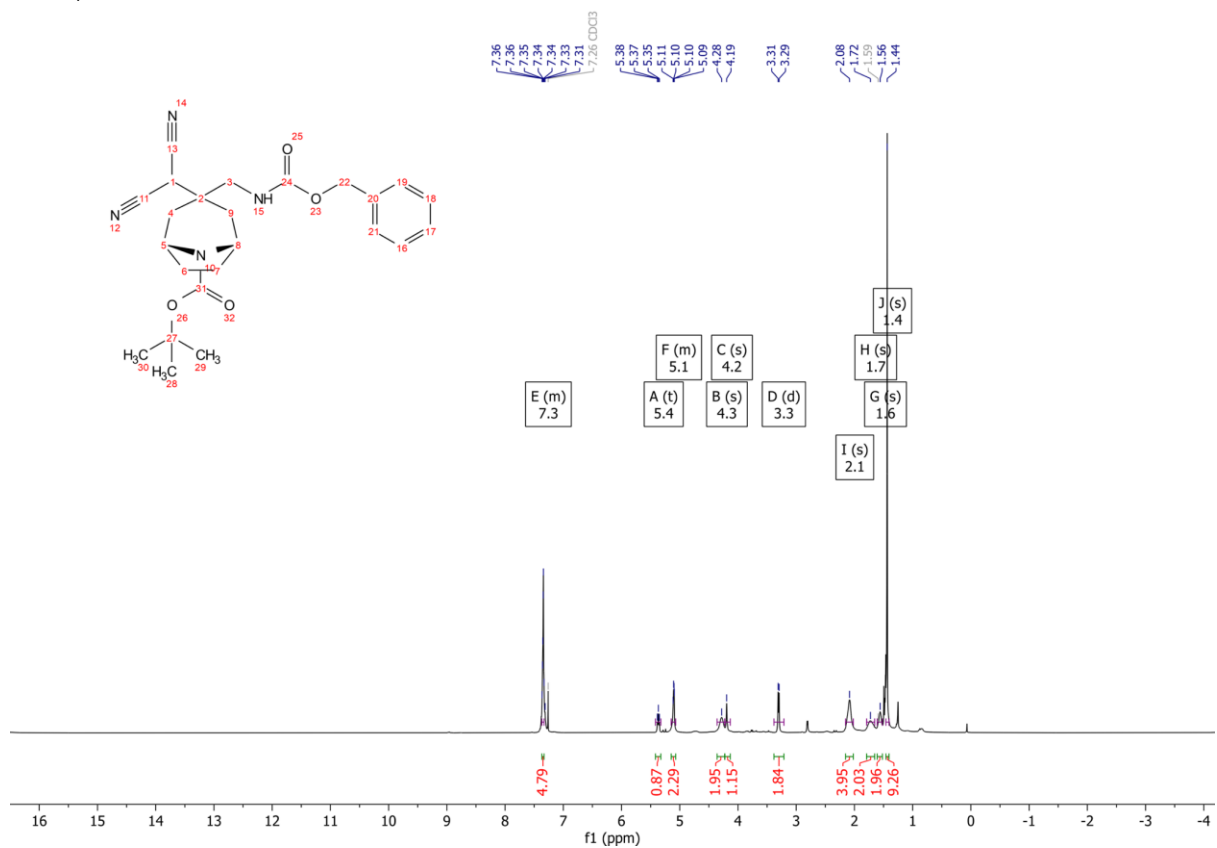
B7 ¹H NMR (600 MHz, CDCl₃)



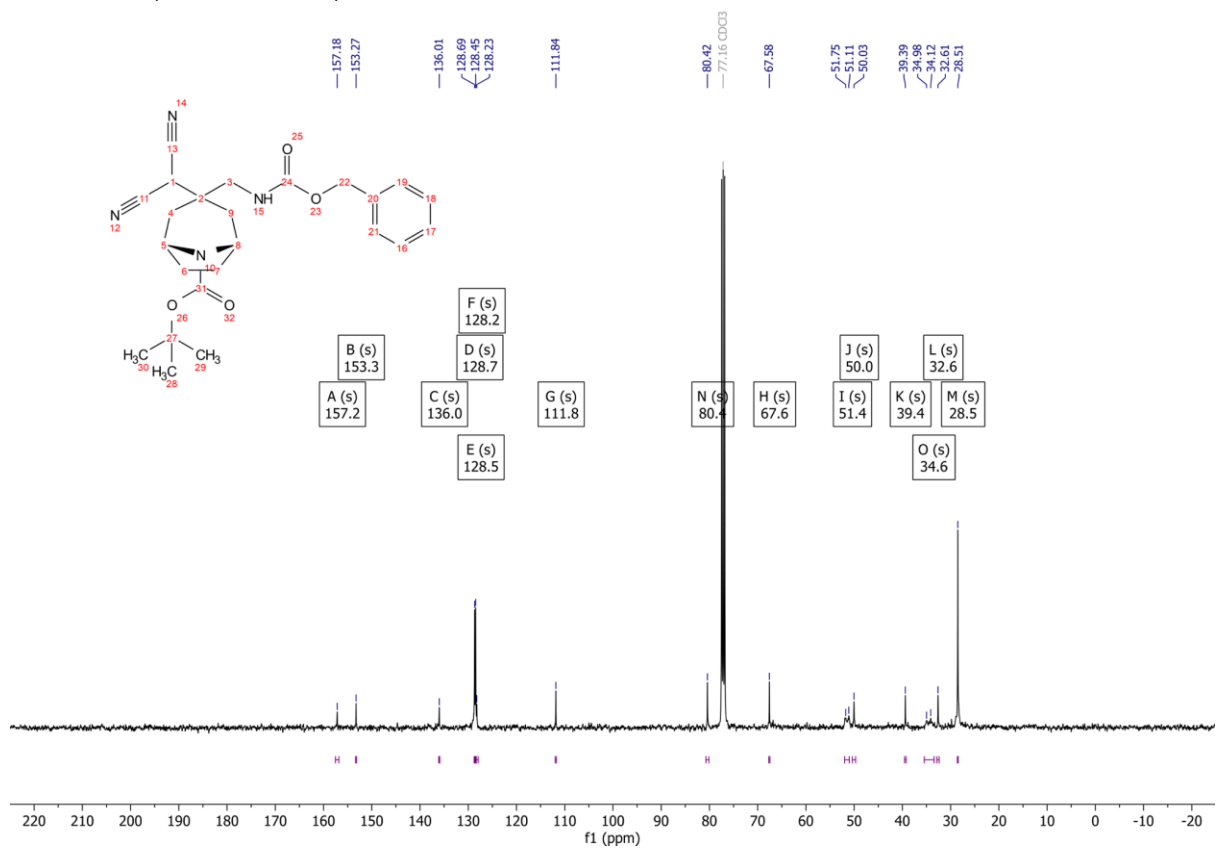
B7 ¹³C NMR (151 MHz, CDCl₃)



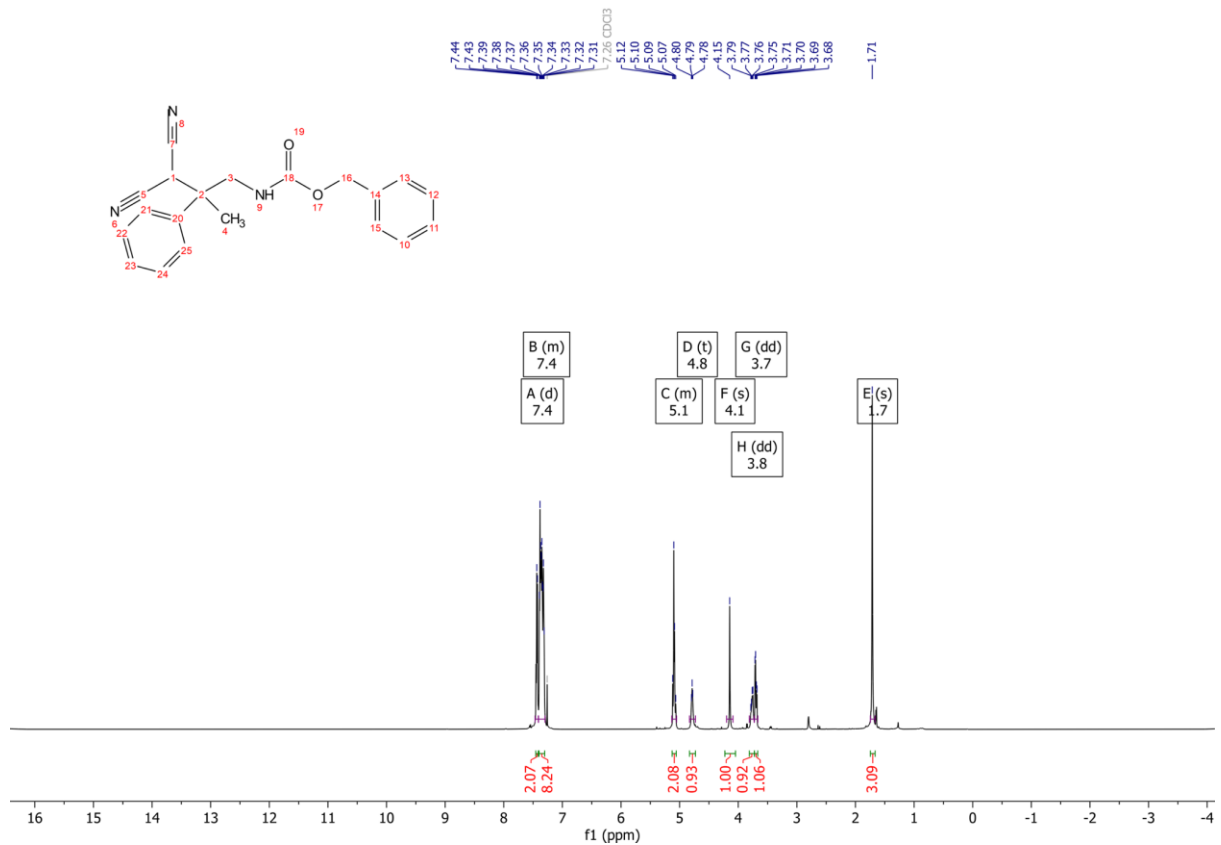
B8 ^1H NMR (400 MHz, CDCl_3)



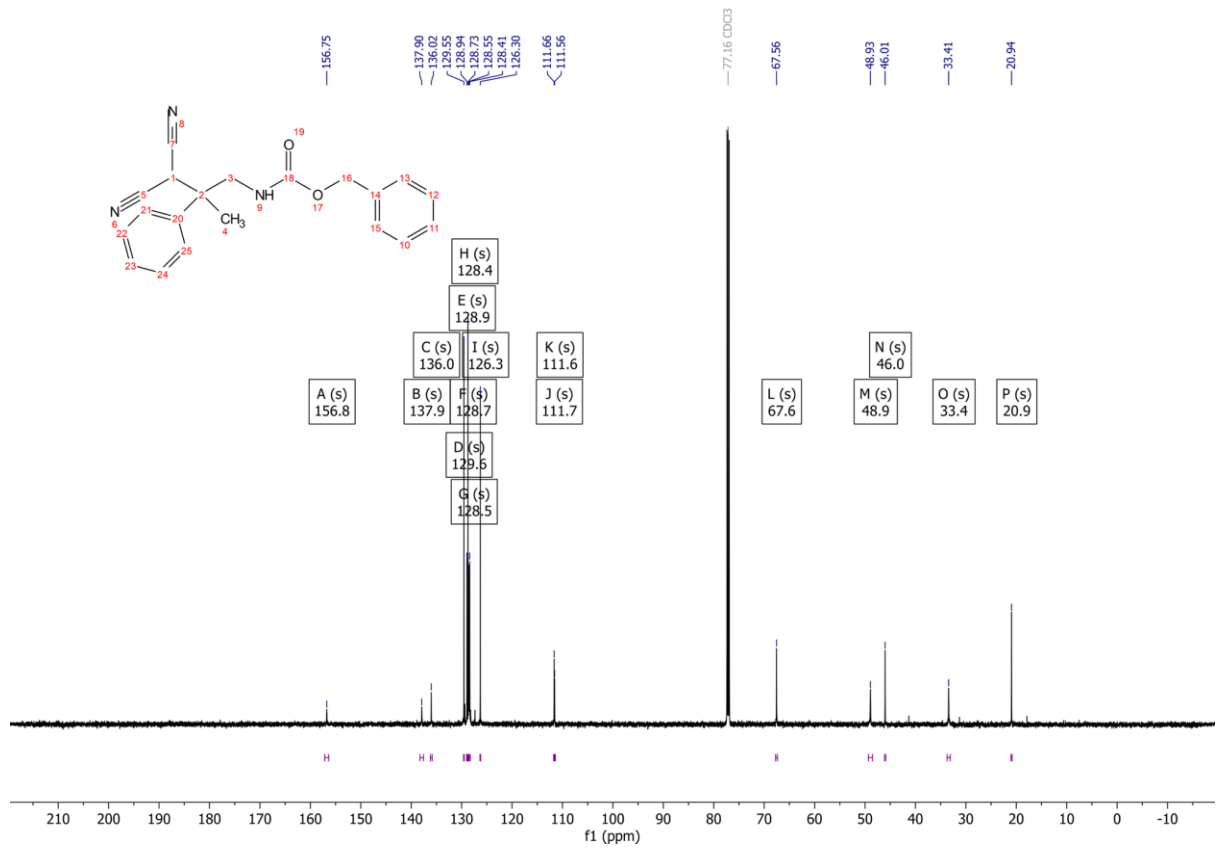
B8 ^{13}C NMR (101 MHz, CDCl_3)



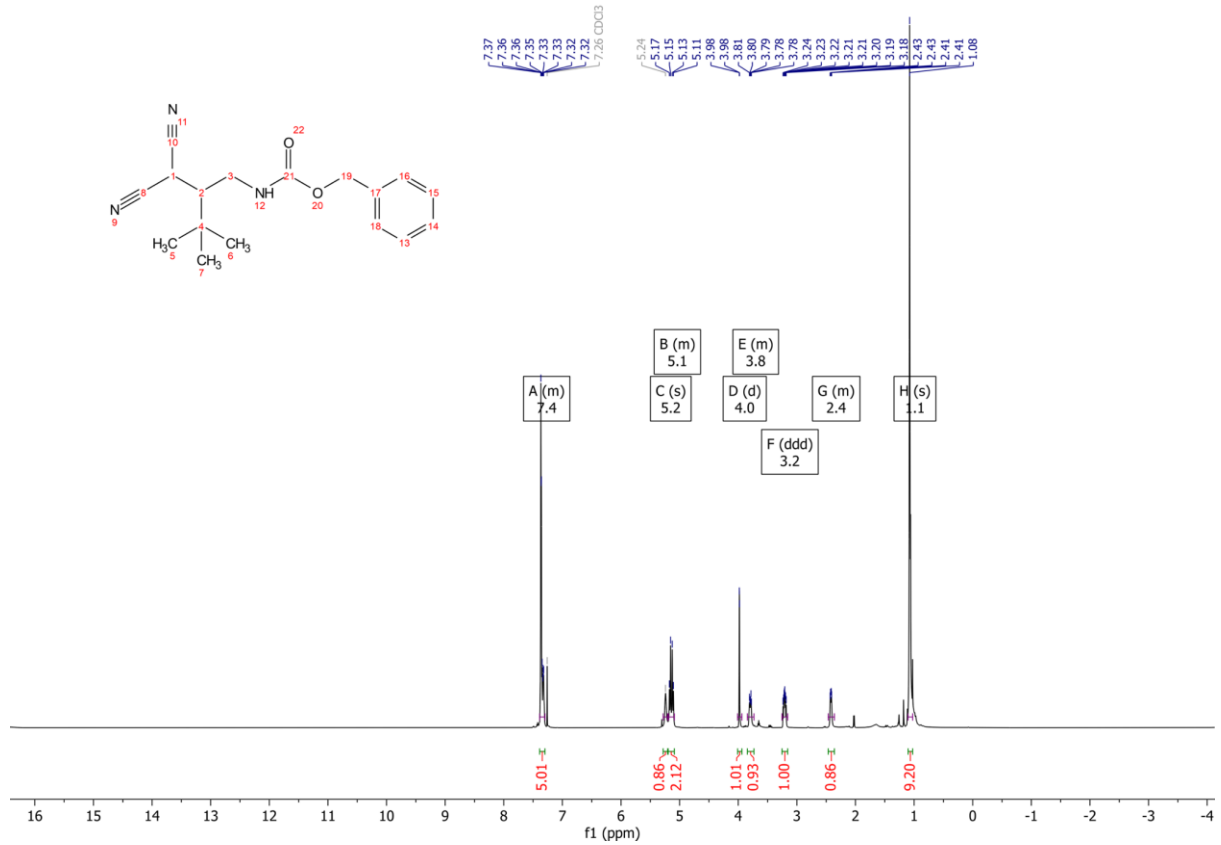
B9 ¹H NMR (600 MHz, CDCl₃)



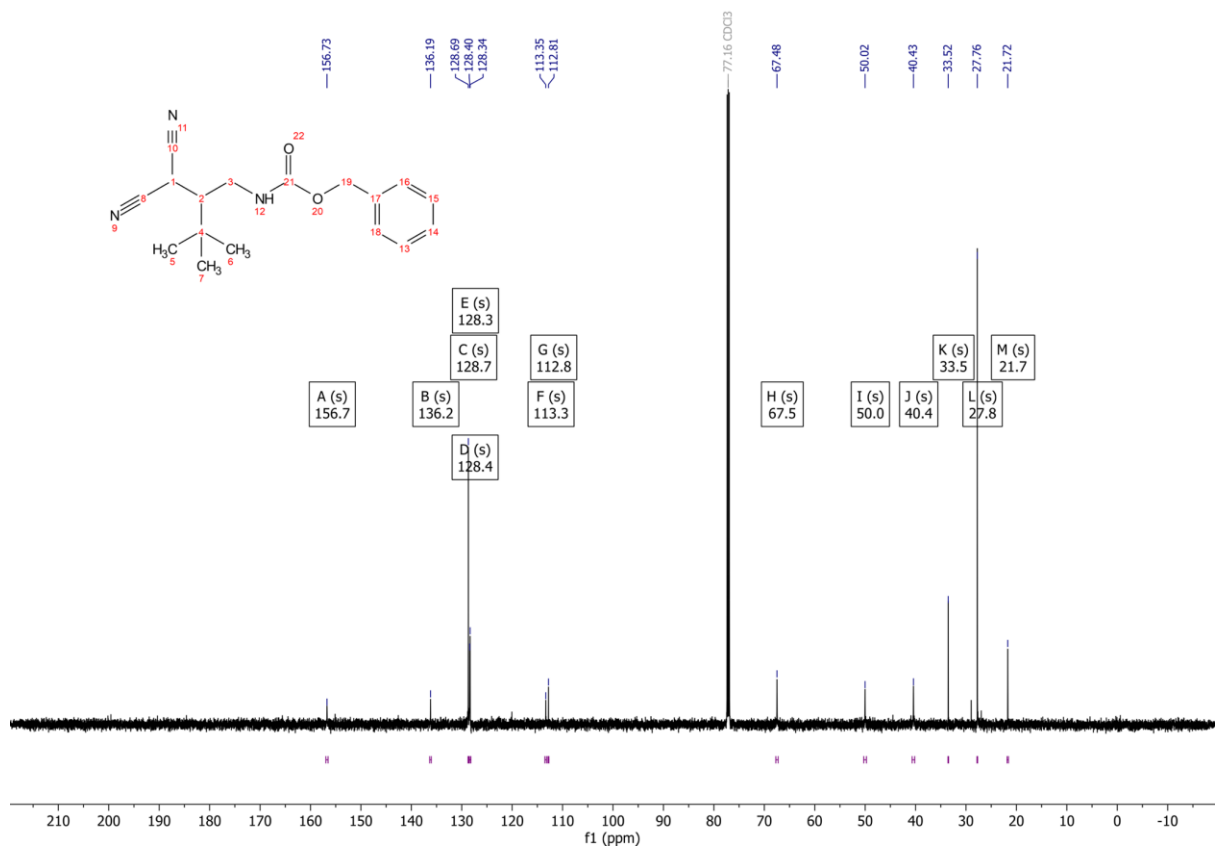
B9 ¹³C NMR (151 MHz, CDCl₃)



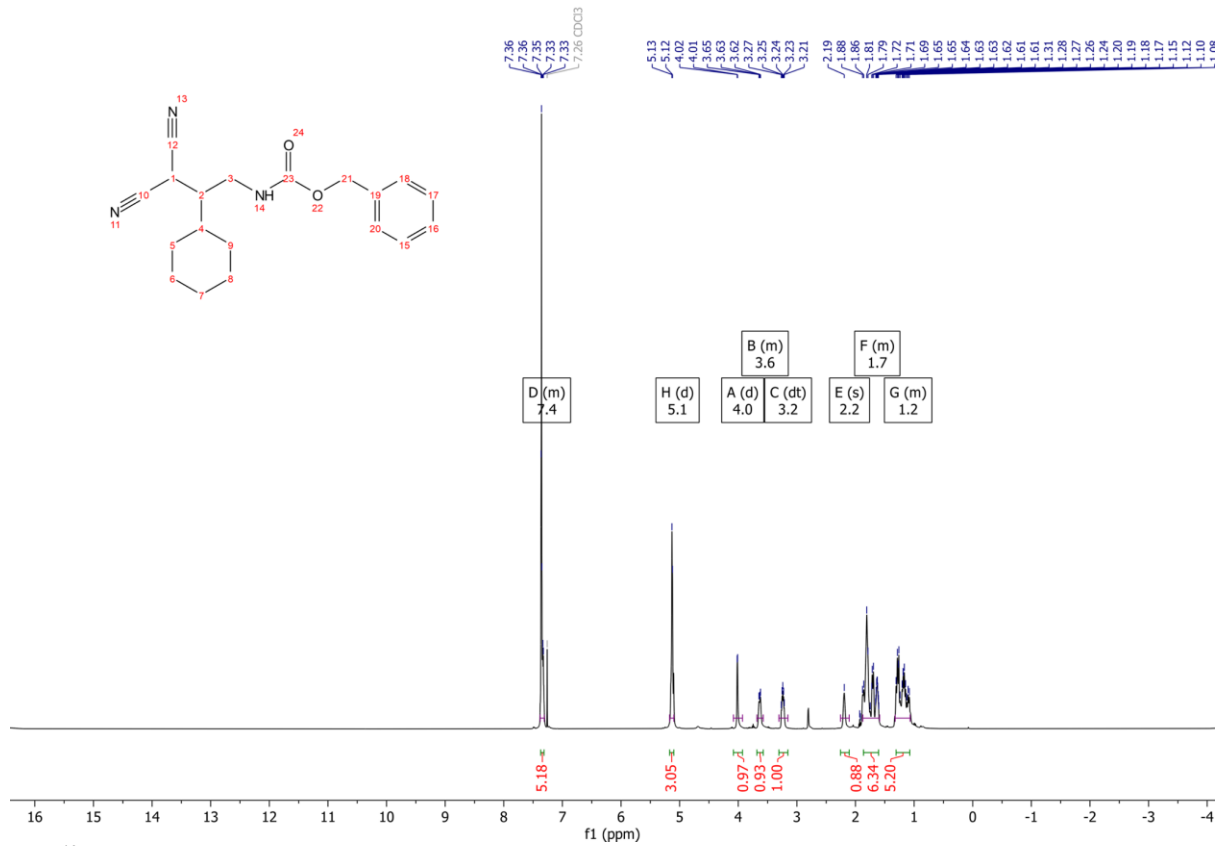
B10 ¹H NMR (600 MHz, CDCl₃)



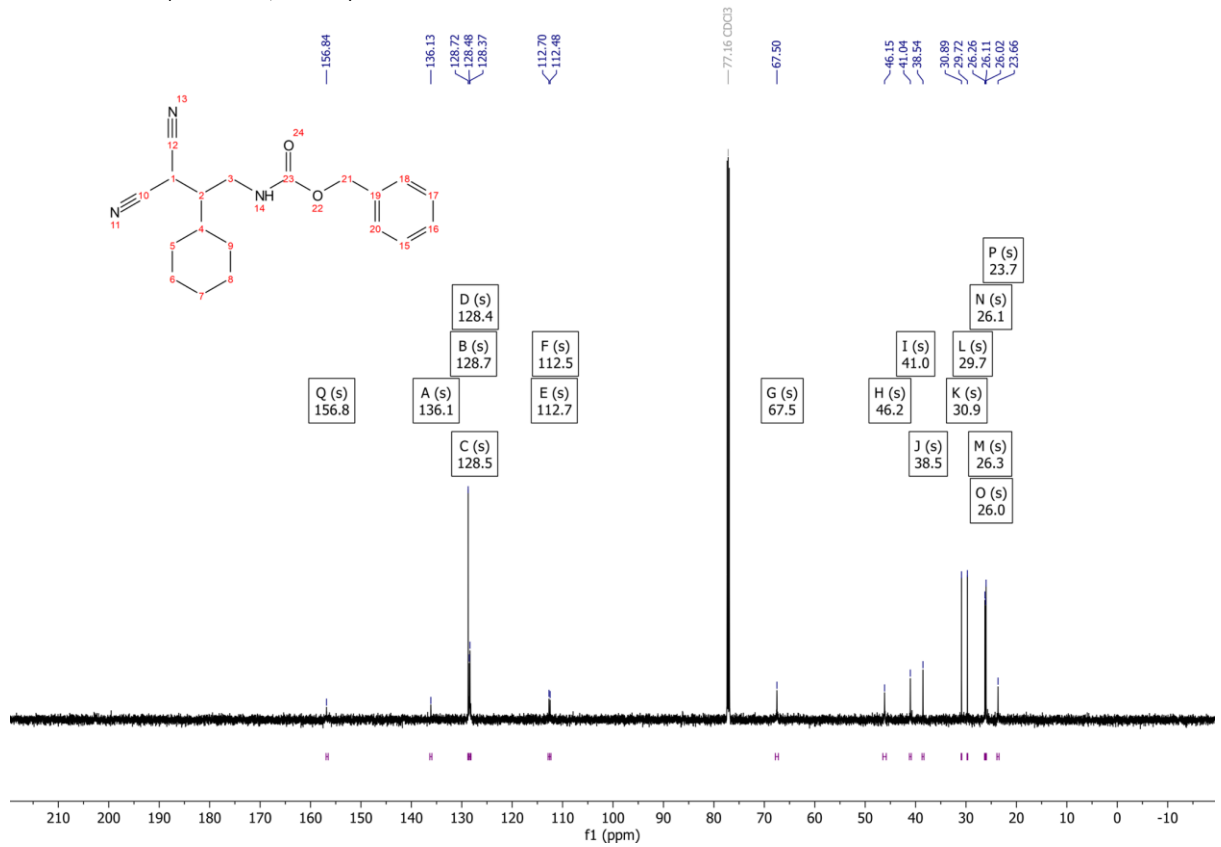
B10 ¹³C NMR (151 MHz, CDCl₃)



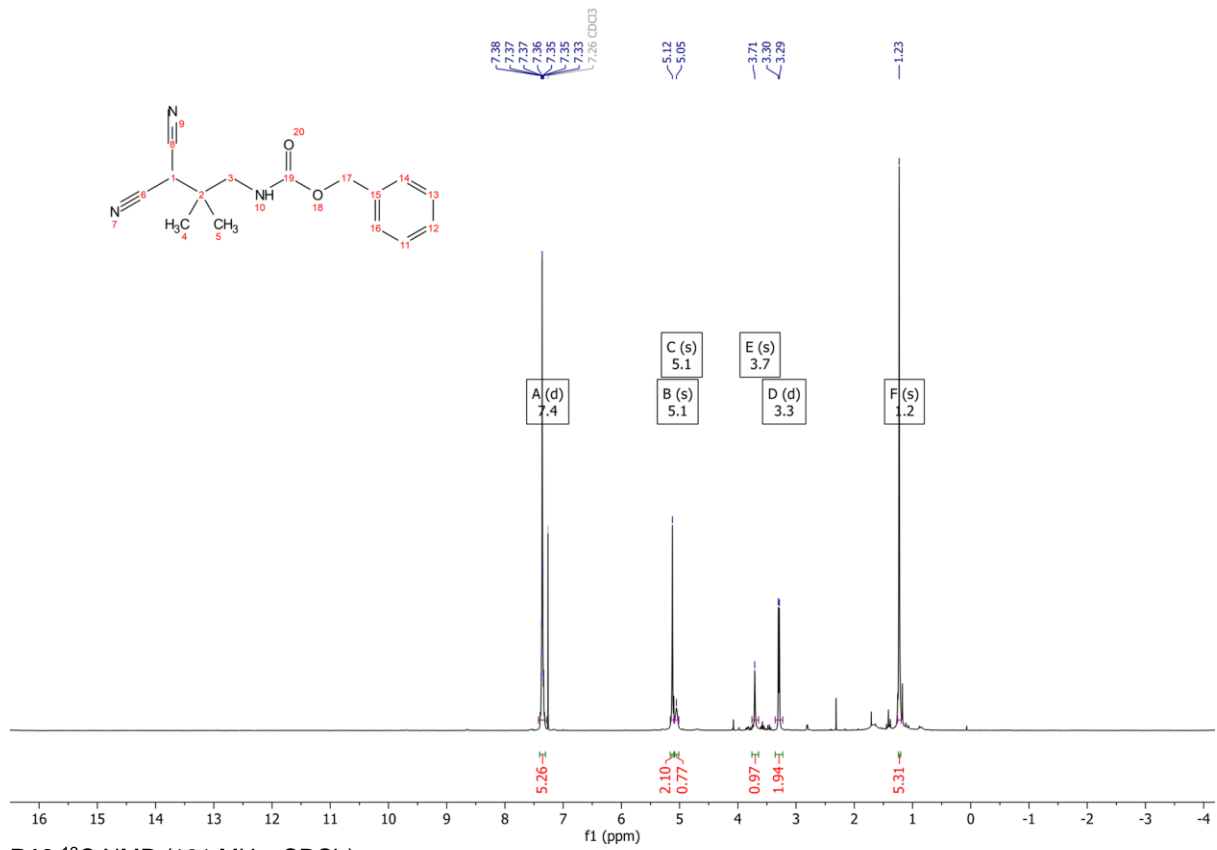
B11 ^1H NMR (600 MHz, CDCl_3)



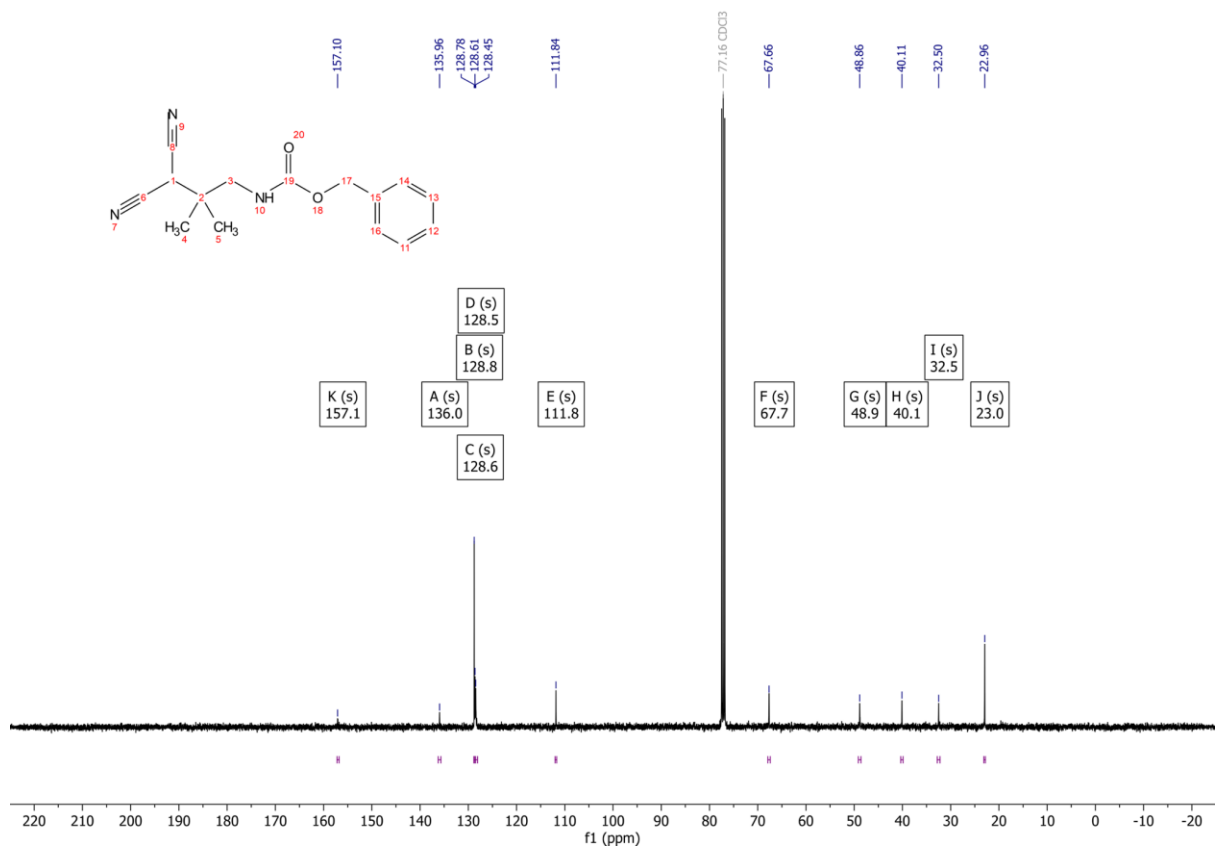
B11 ^{13}C NMR (151 MHz, CDCl_3)



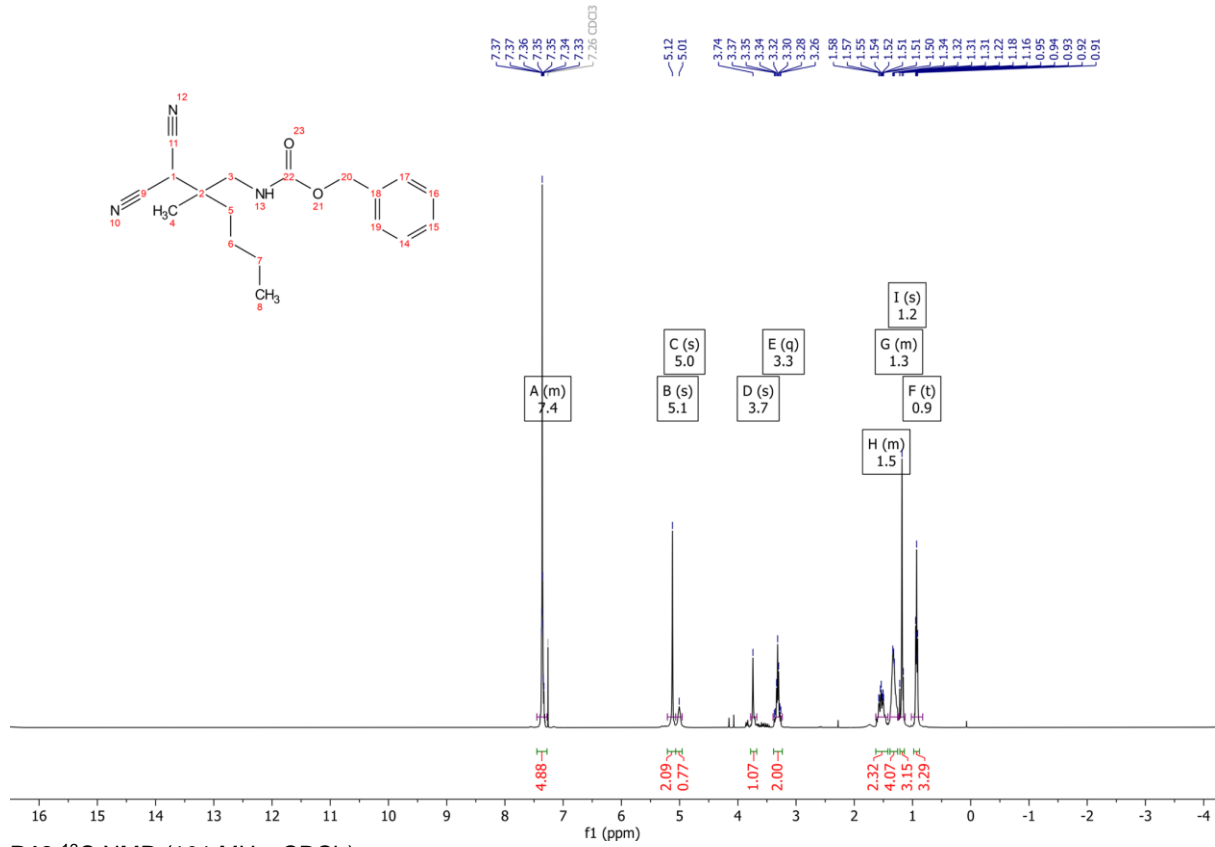
B12 ¹H NMR (400 MHz, CDCl₃)



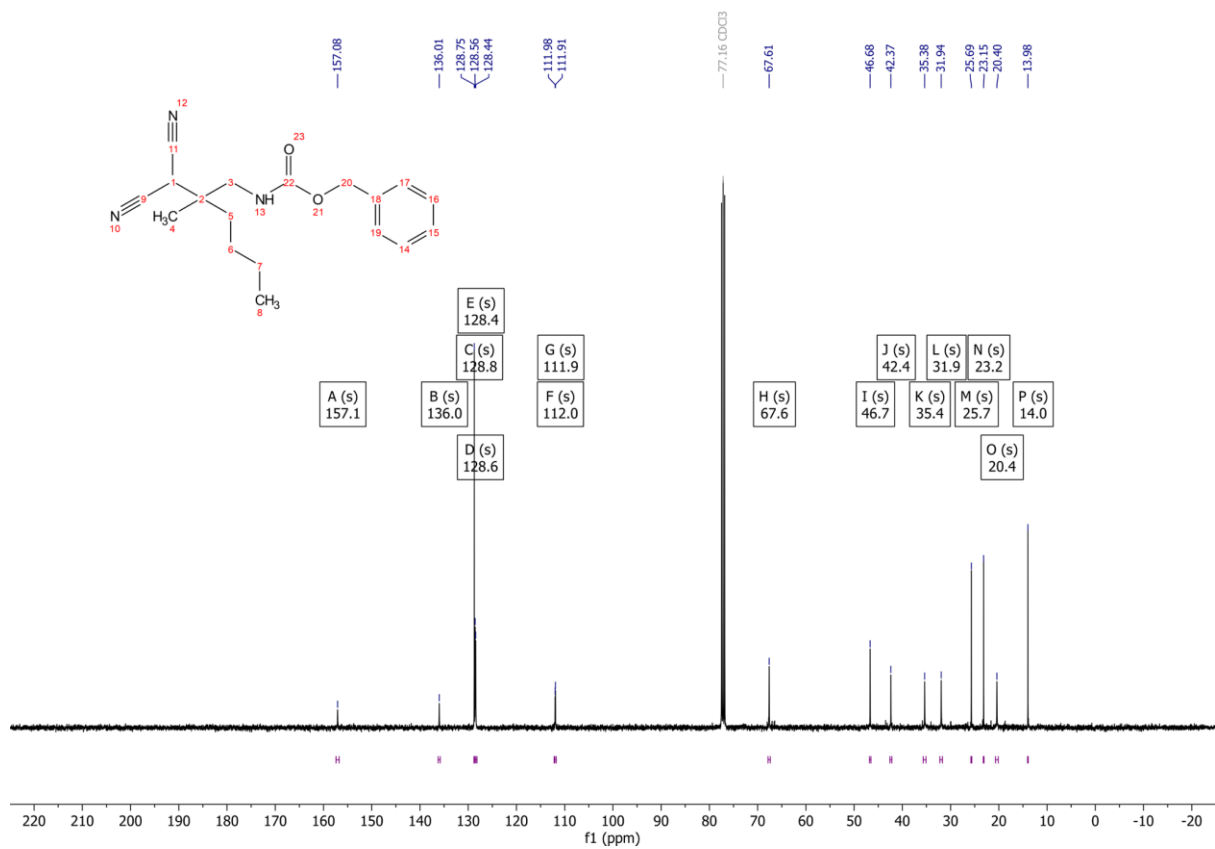
B12 ¹³C NMR (101 MHz, CDCl₃)



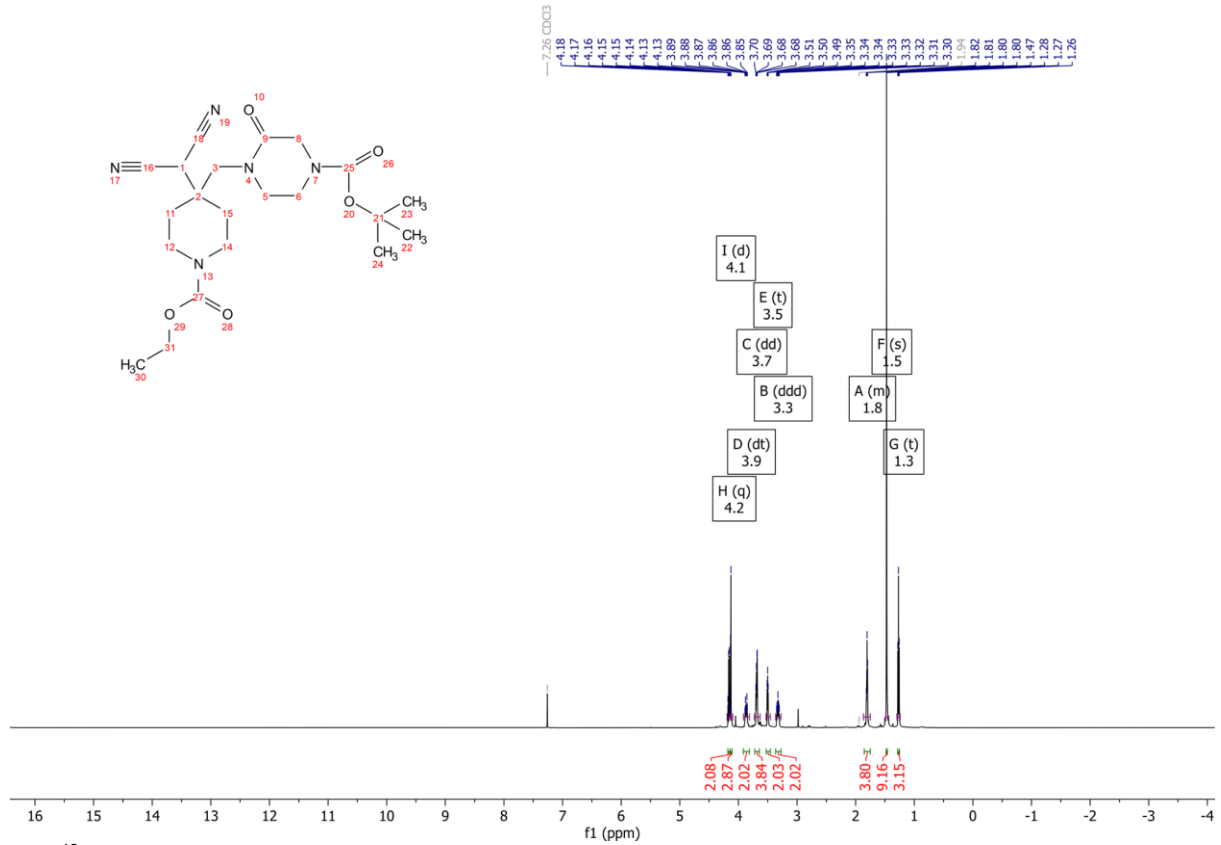
B13 ¹H NMR (400 MHz, CDCl₃)



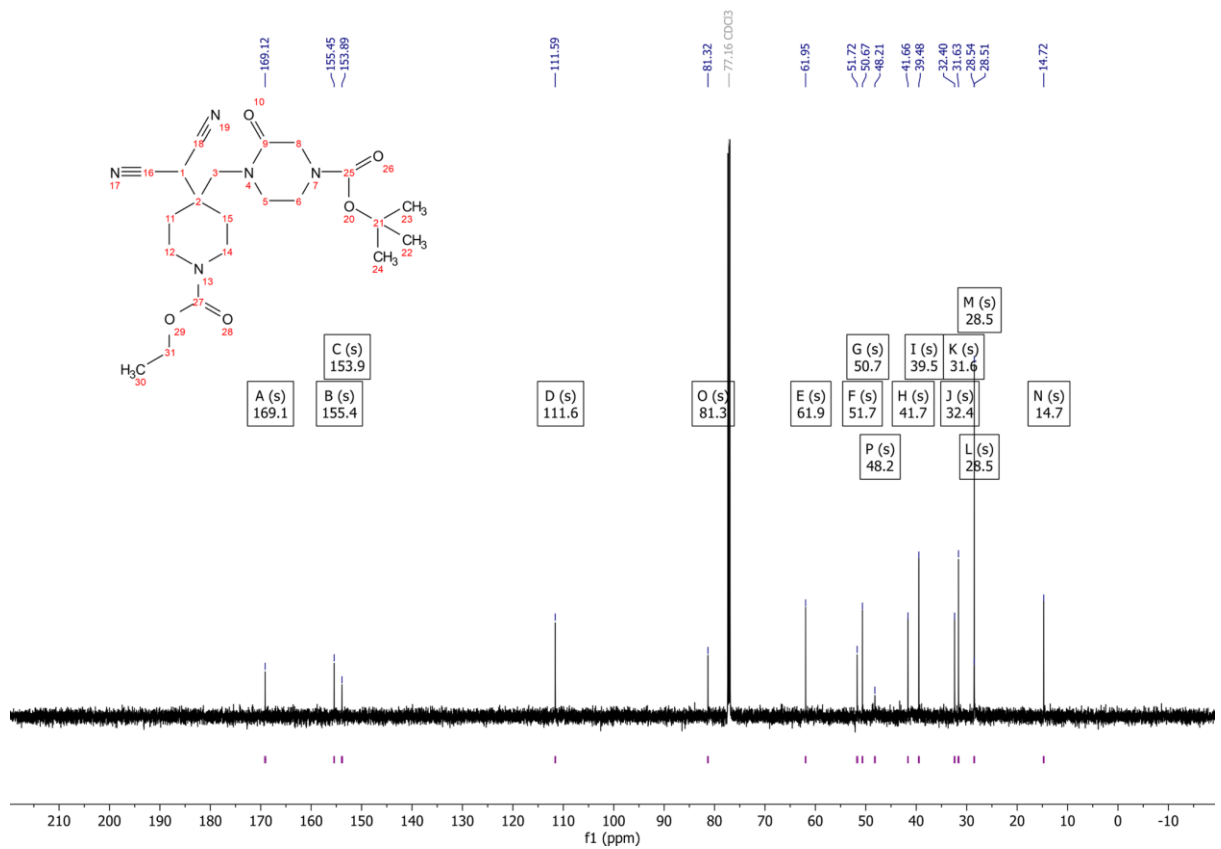
B13 ¹³C NMR (101 MHz, CDCl₃)



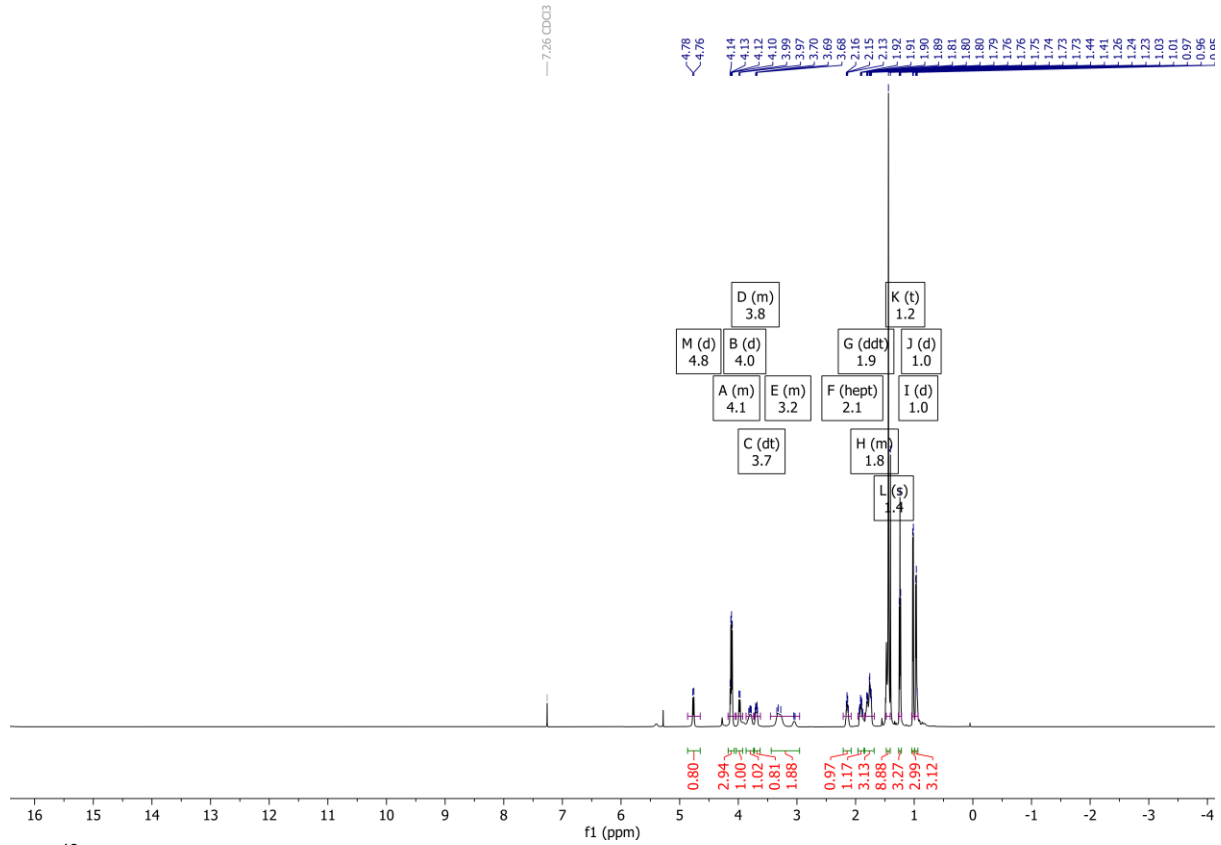
B15 ¹H NMR (600 MHz, CDCl₃)



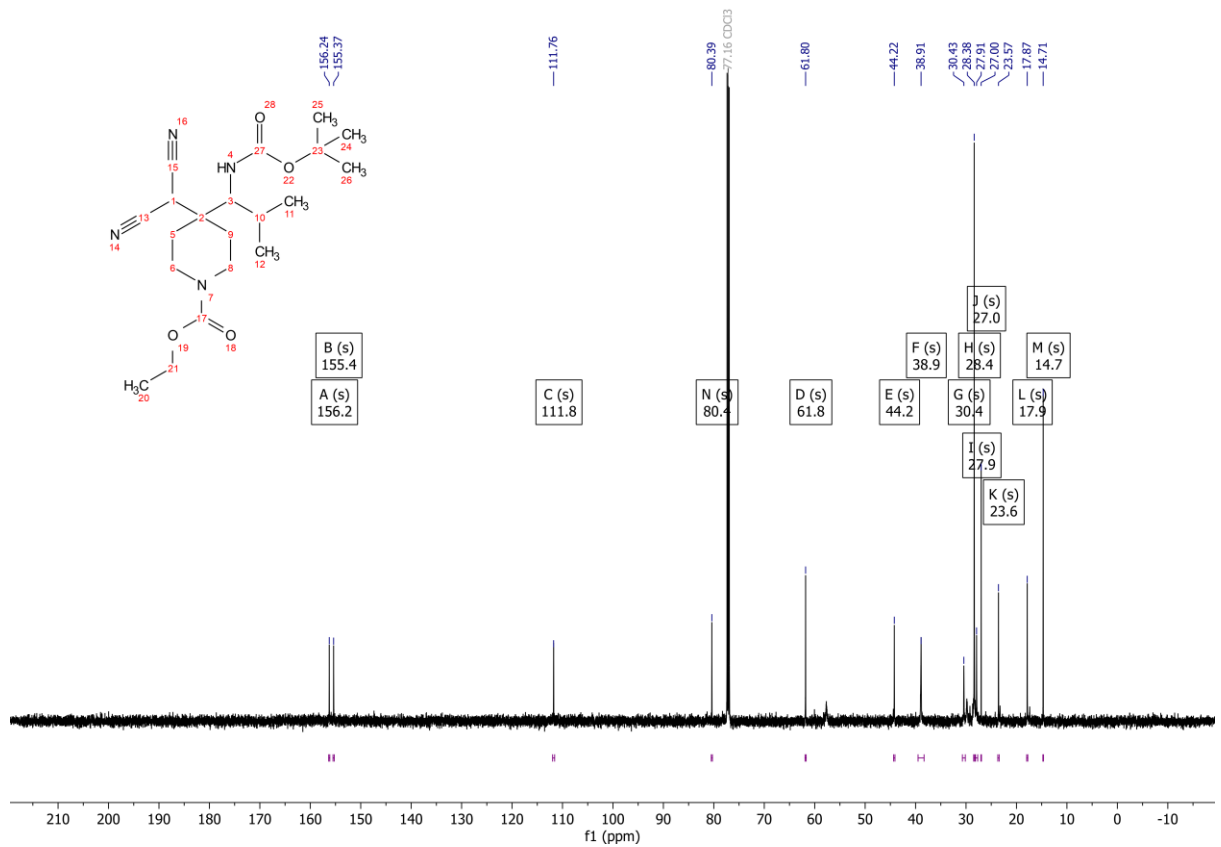
B15 ¹³C NMR (151 MHz, CDCl₃)



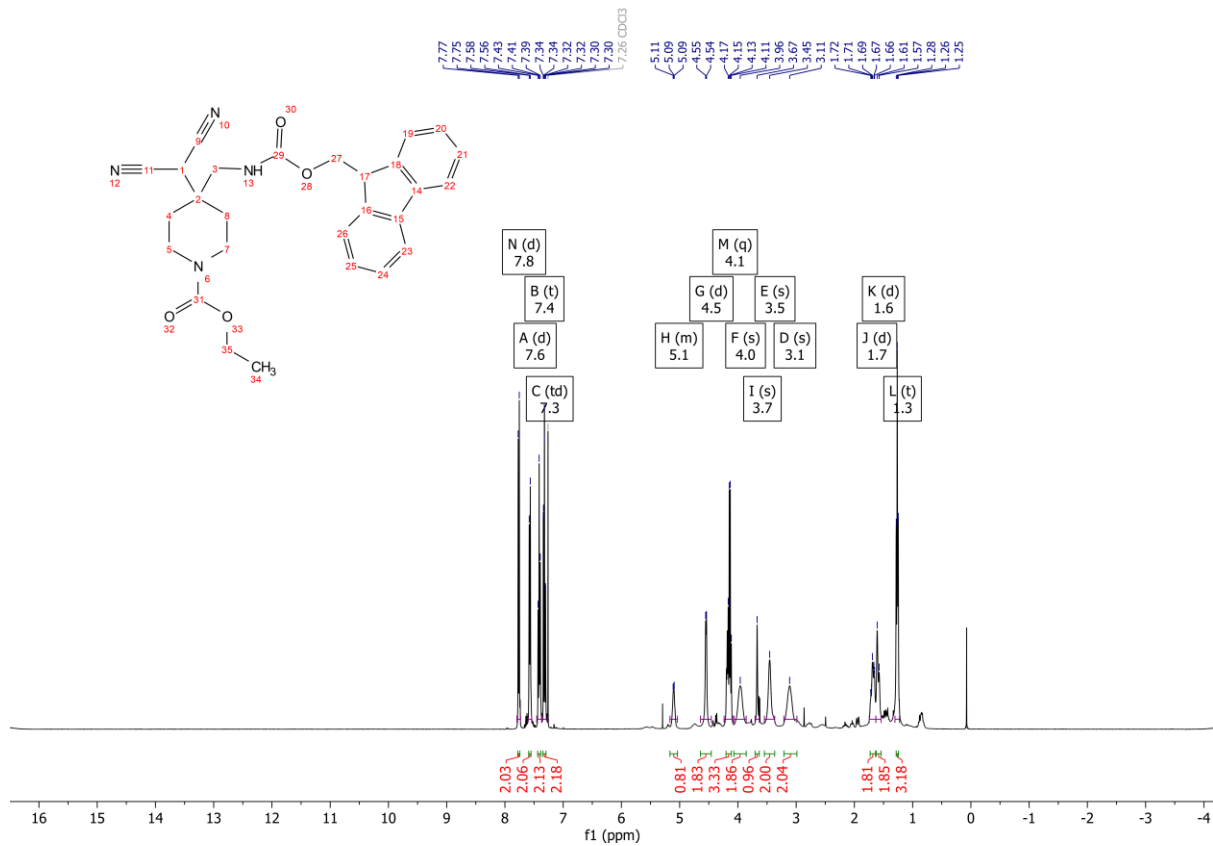
B16 ^1H NMR (600 MHz, CDCl_3)



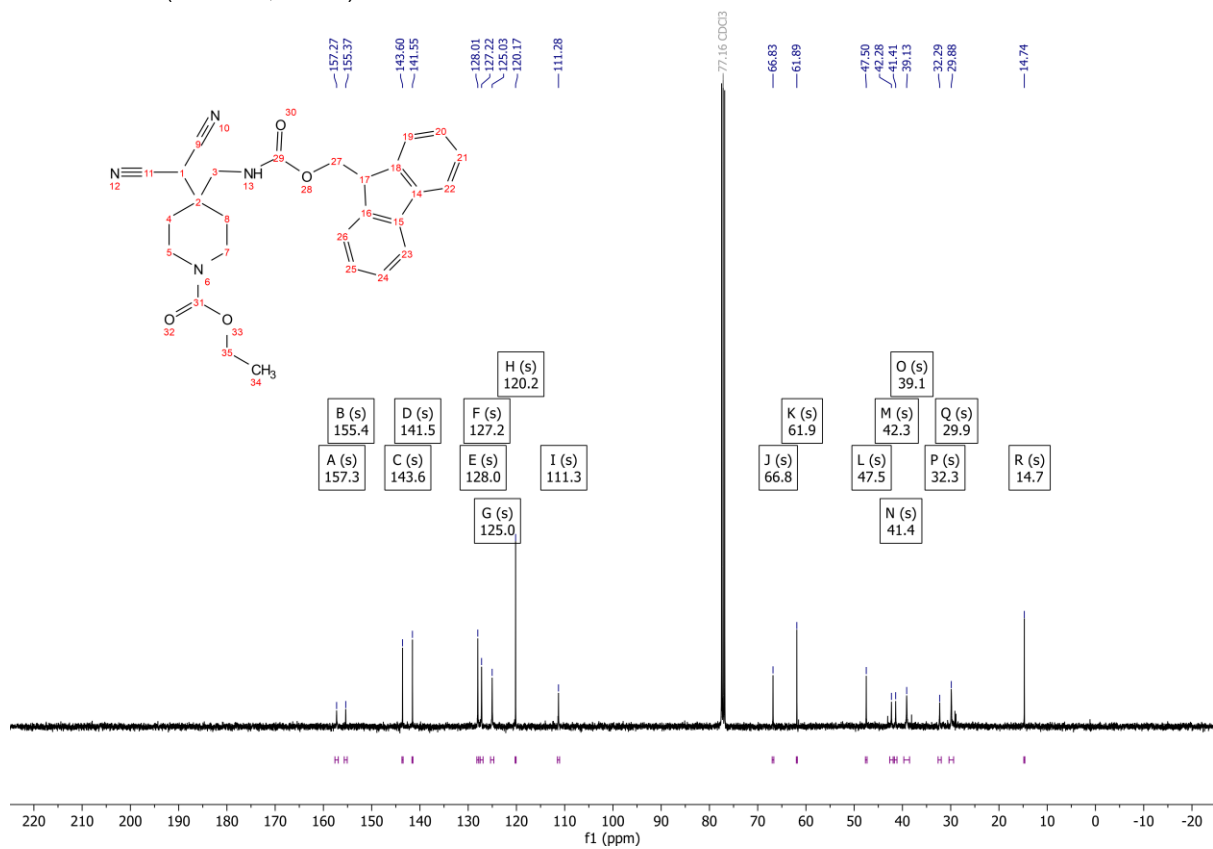
B16 ^{13}C NMR (151 MHz, CDCl_3)



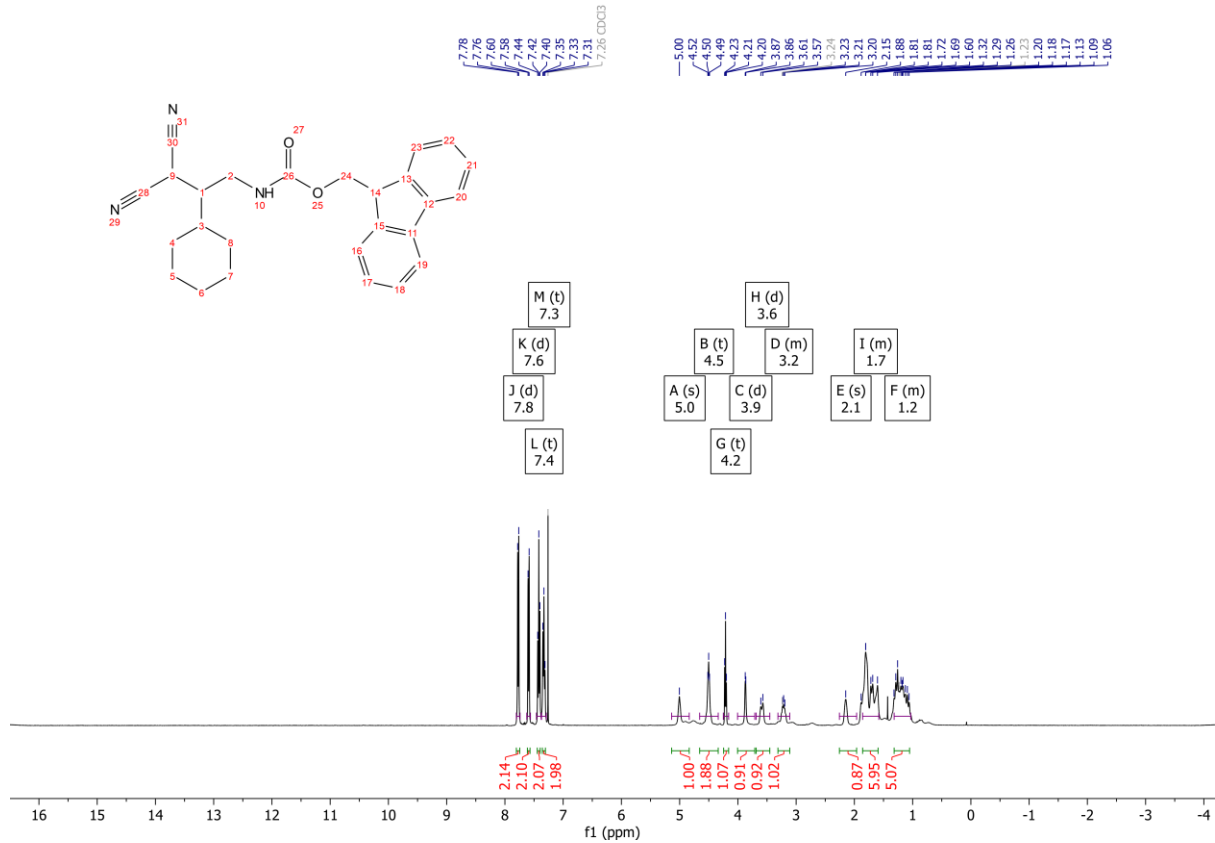
B17 ¹H NMR (600 MHz, CDCl₃)



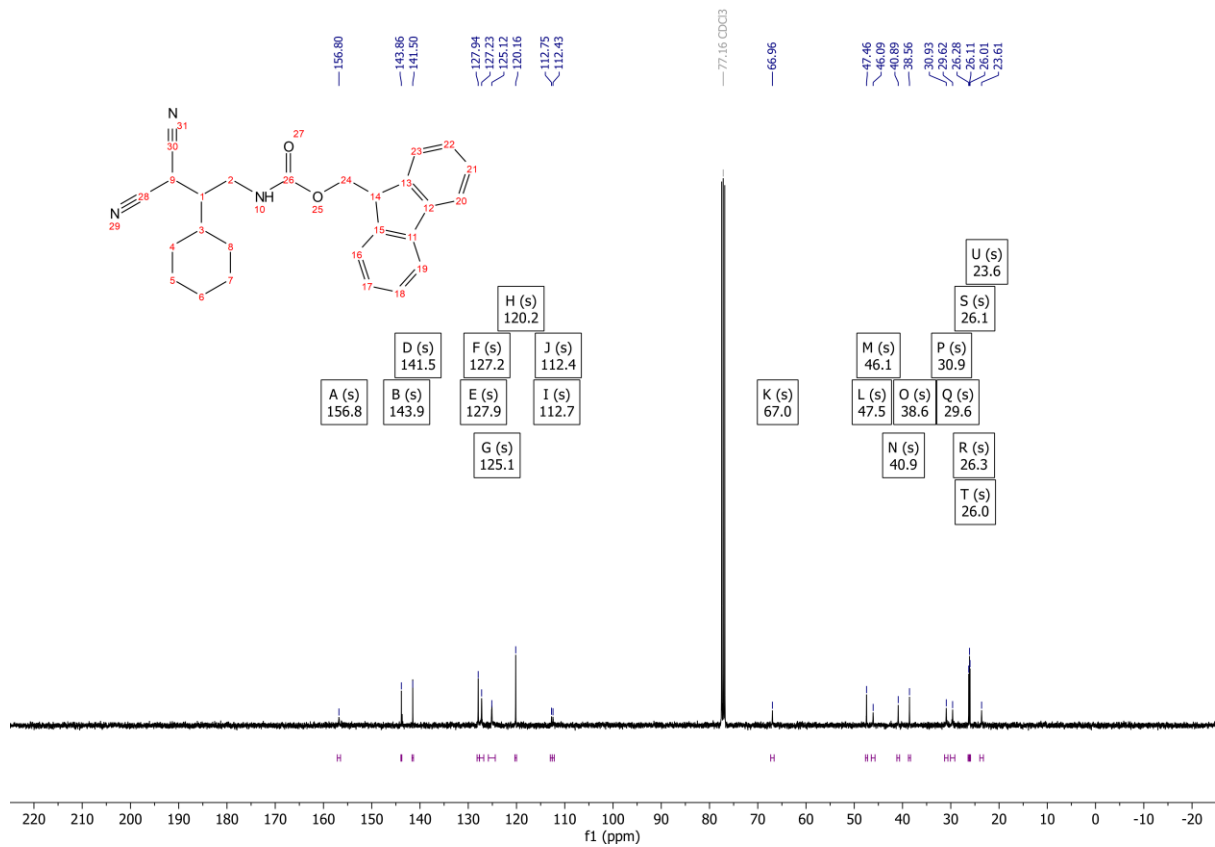
B17 ¹³C NMR (151 MHz, CDCl₃)



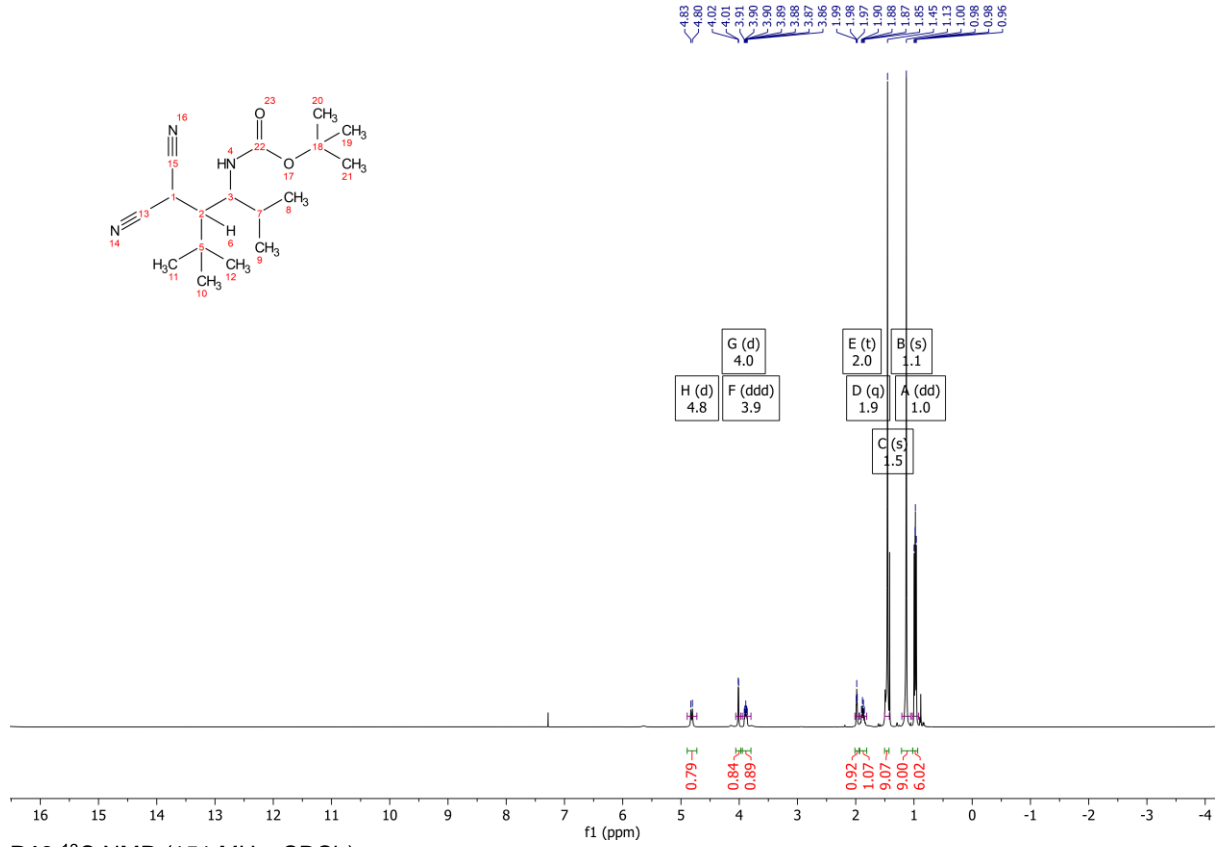
B18 ¹H NMR (600 MHz, CDCl₃)



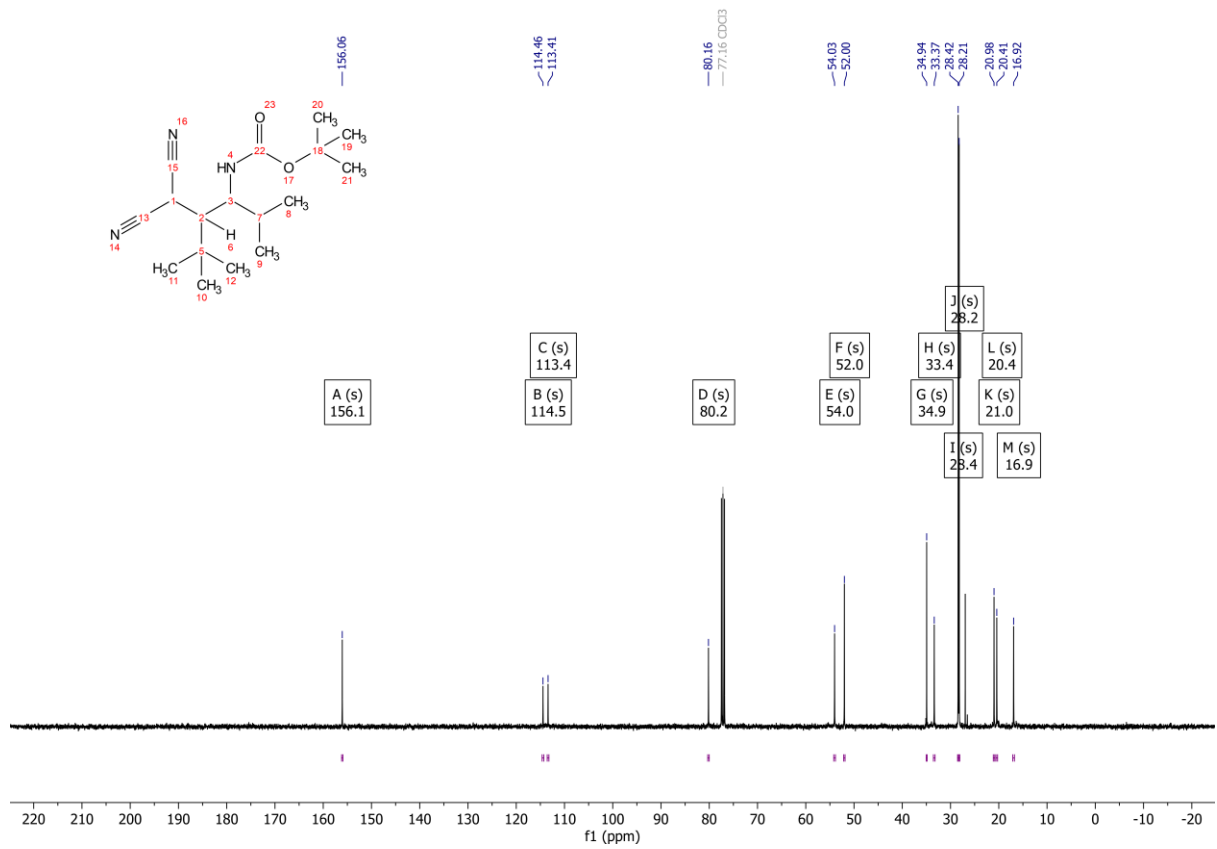
B18 ¹³C NMR (151 MHz, CDCl₃)



B19 ^1H NMR (600 MHz, CDCl_3)

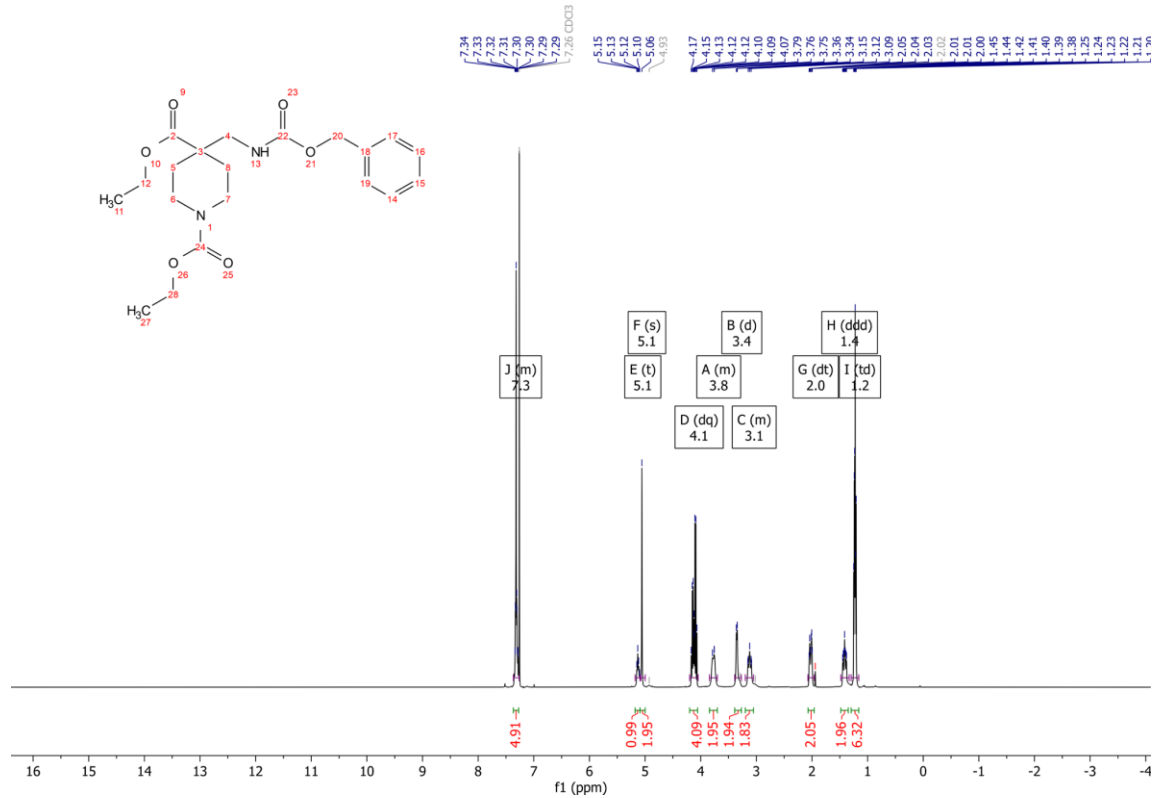


B19 ^{13}C NMR (151 MHz, CDCl_3)

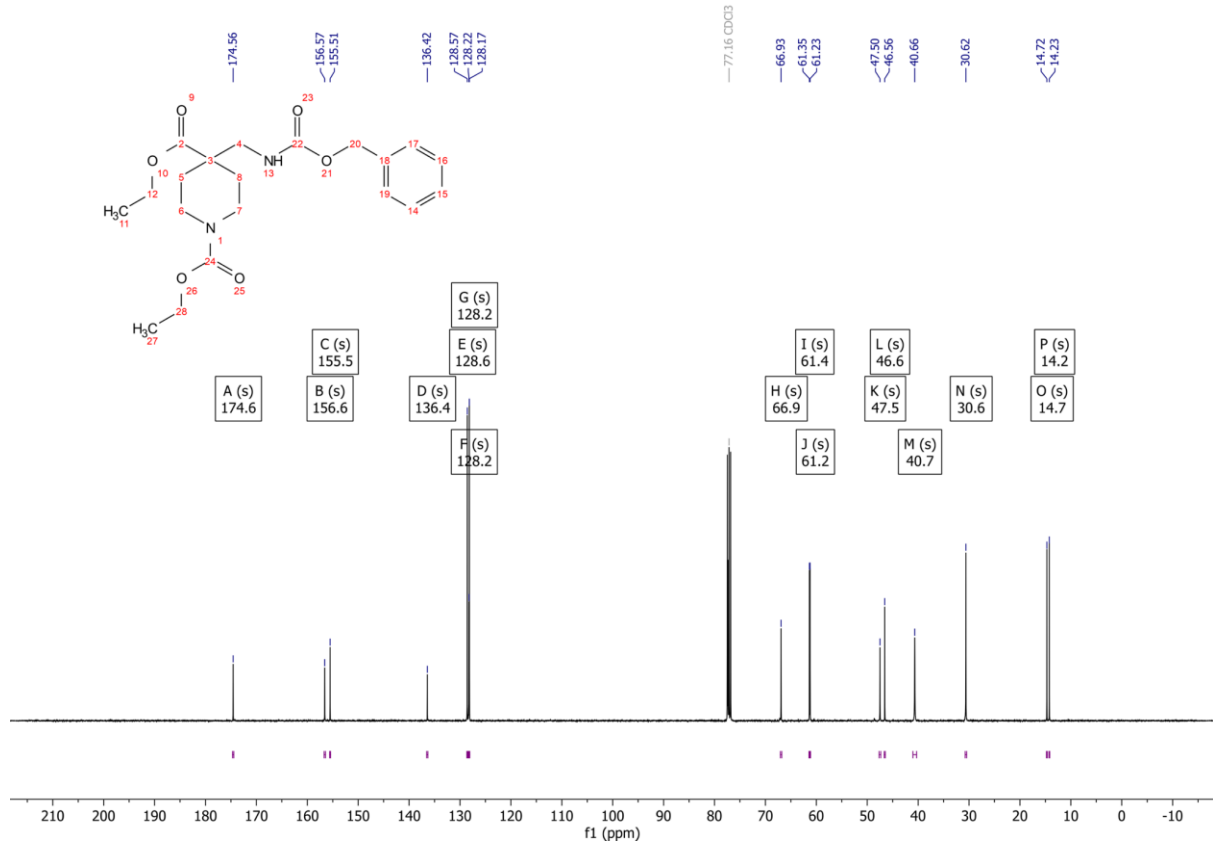


β -Amino Esters/Amides

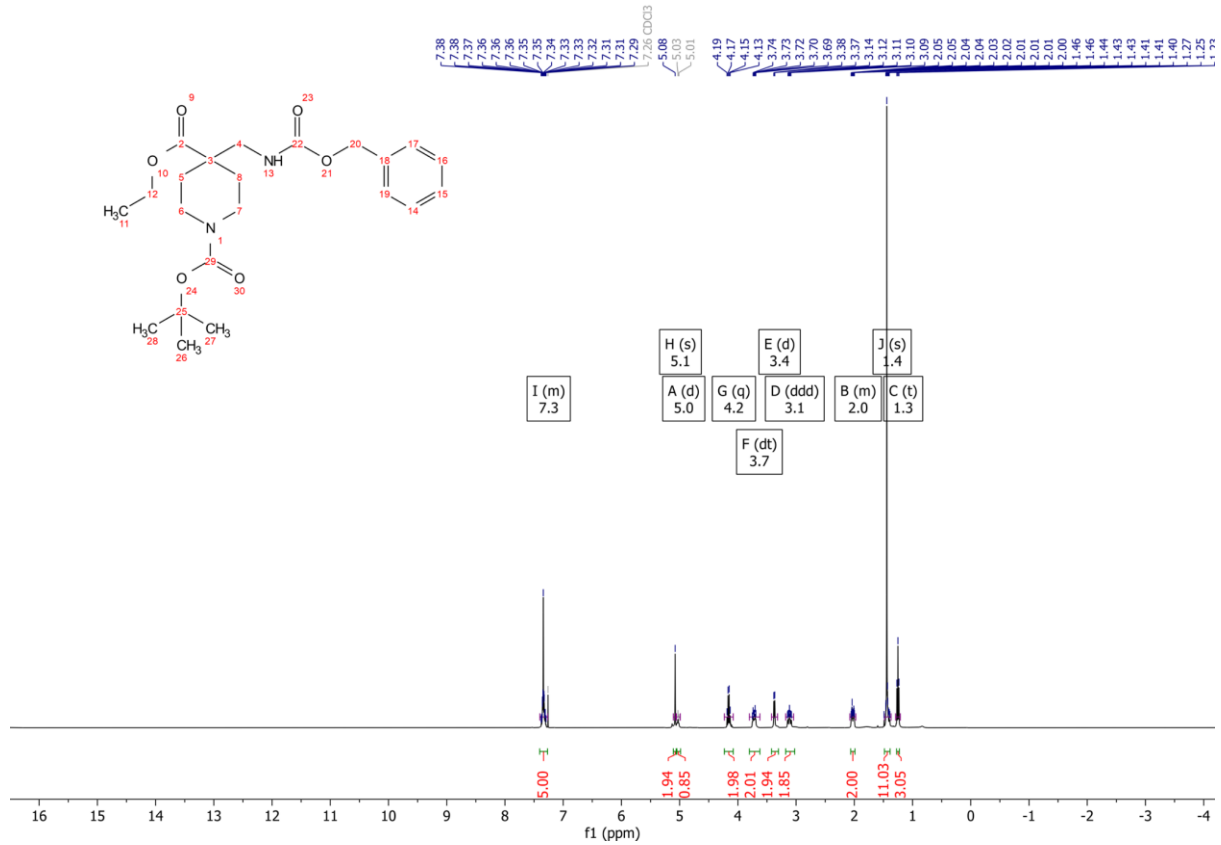
112 ^1H NMR (400 MHz, CDCl_3)



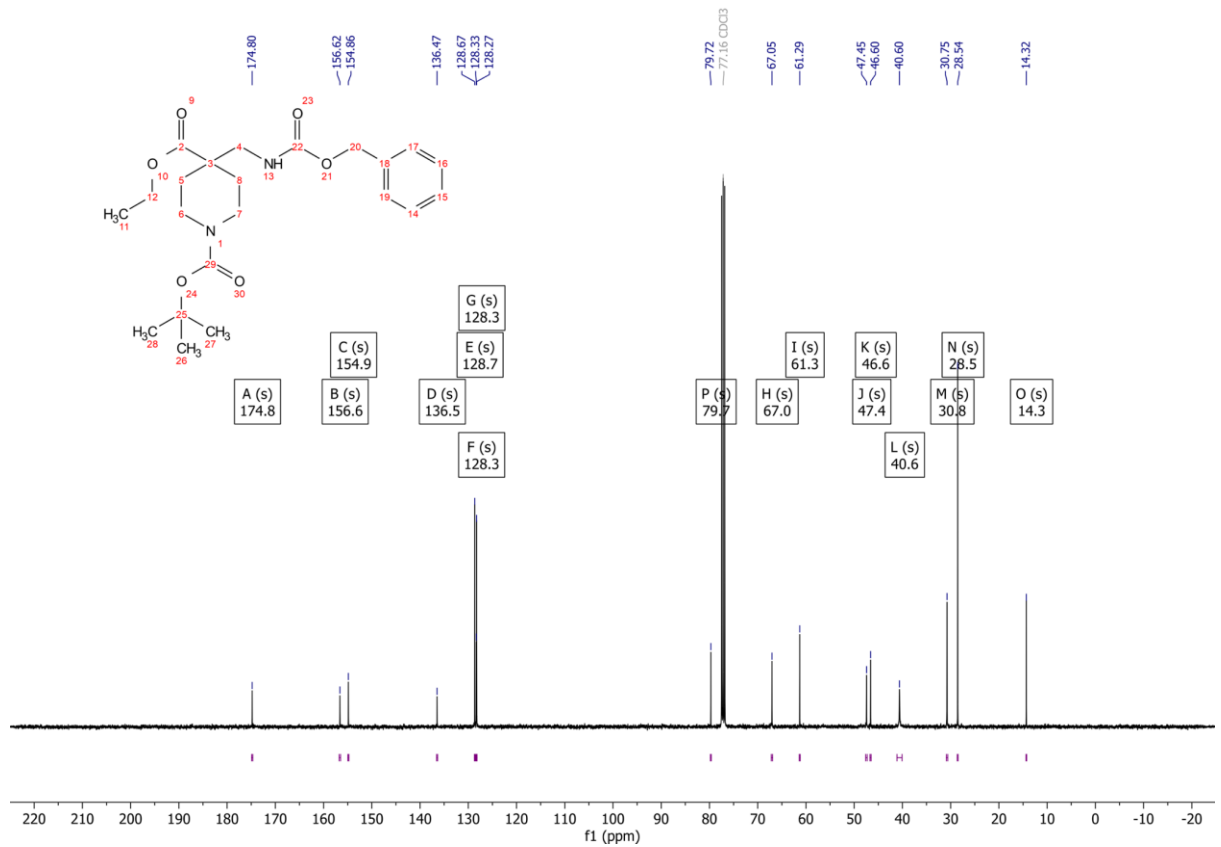
112 ^{13}C NMR (101 MHz, CDCl_3)



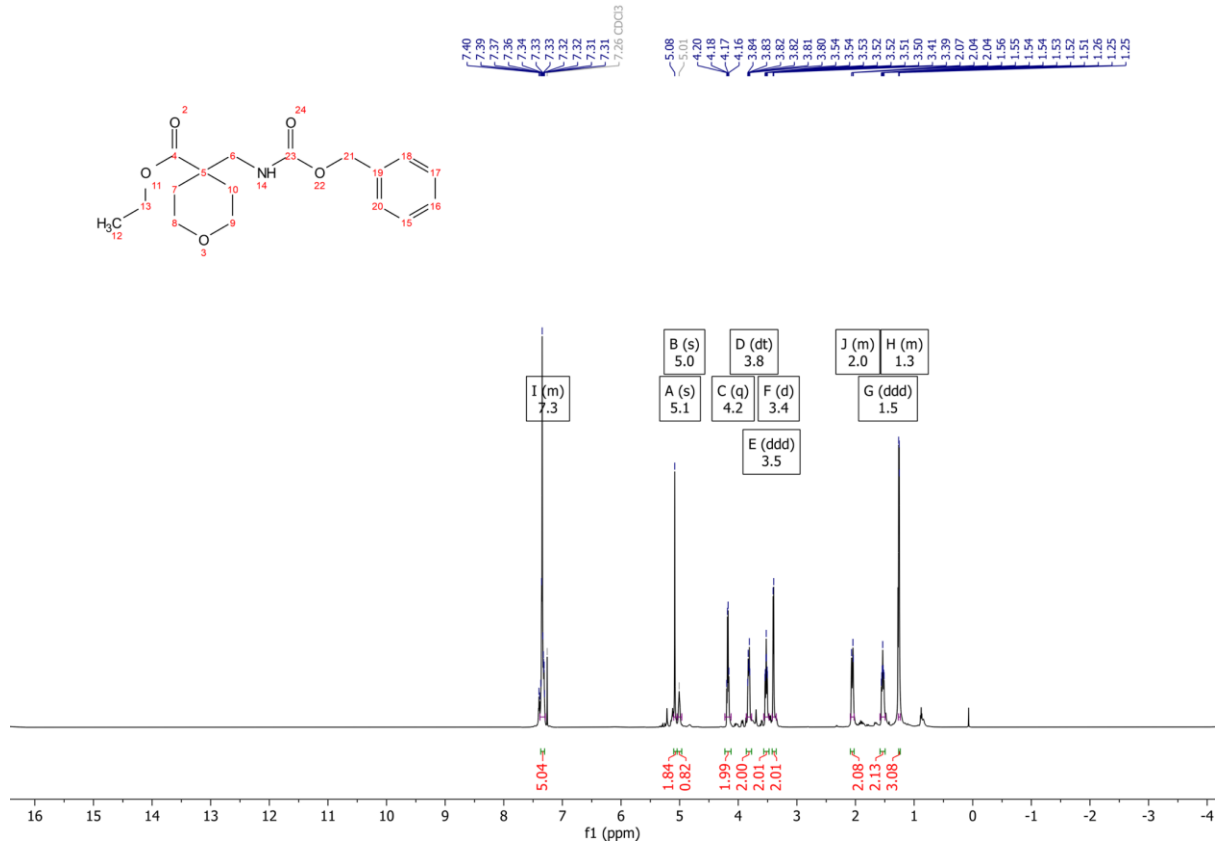
113 ¹H NMR (400 MHz, CDCl₃)



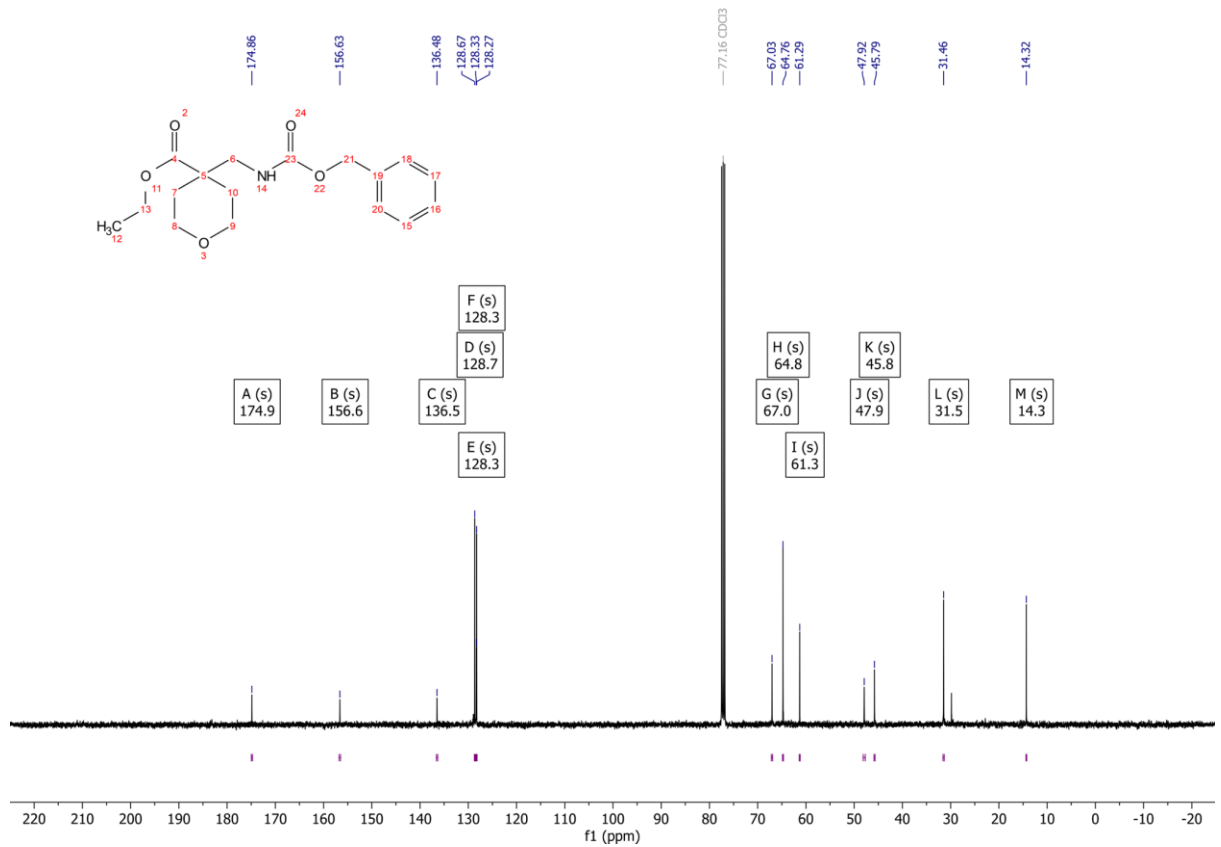
113 ¹³C NMR (101 MHz, CDCl₃)



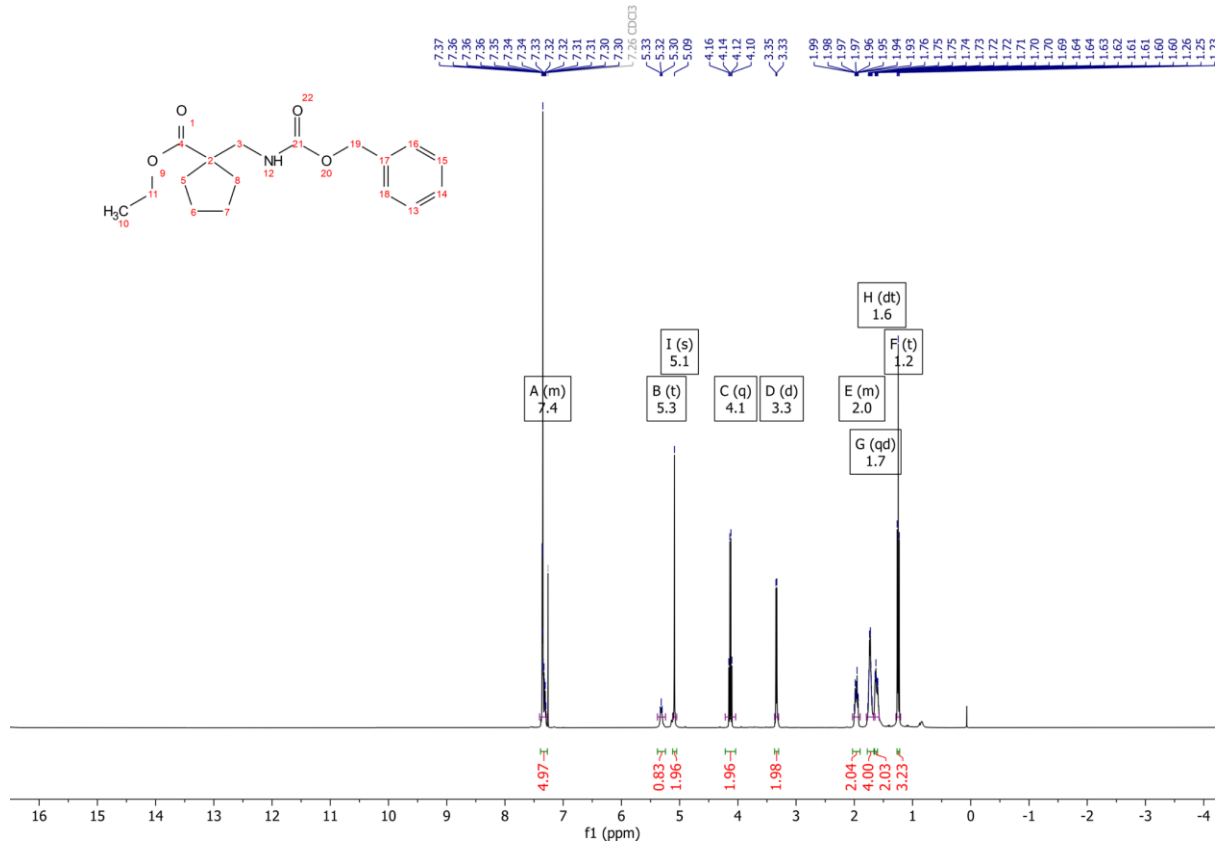
114 ¹H NMR (600 MHz, CDCl₃)



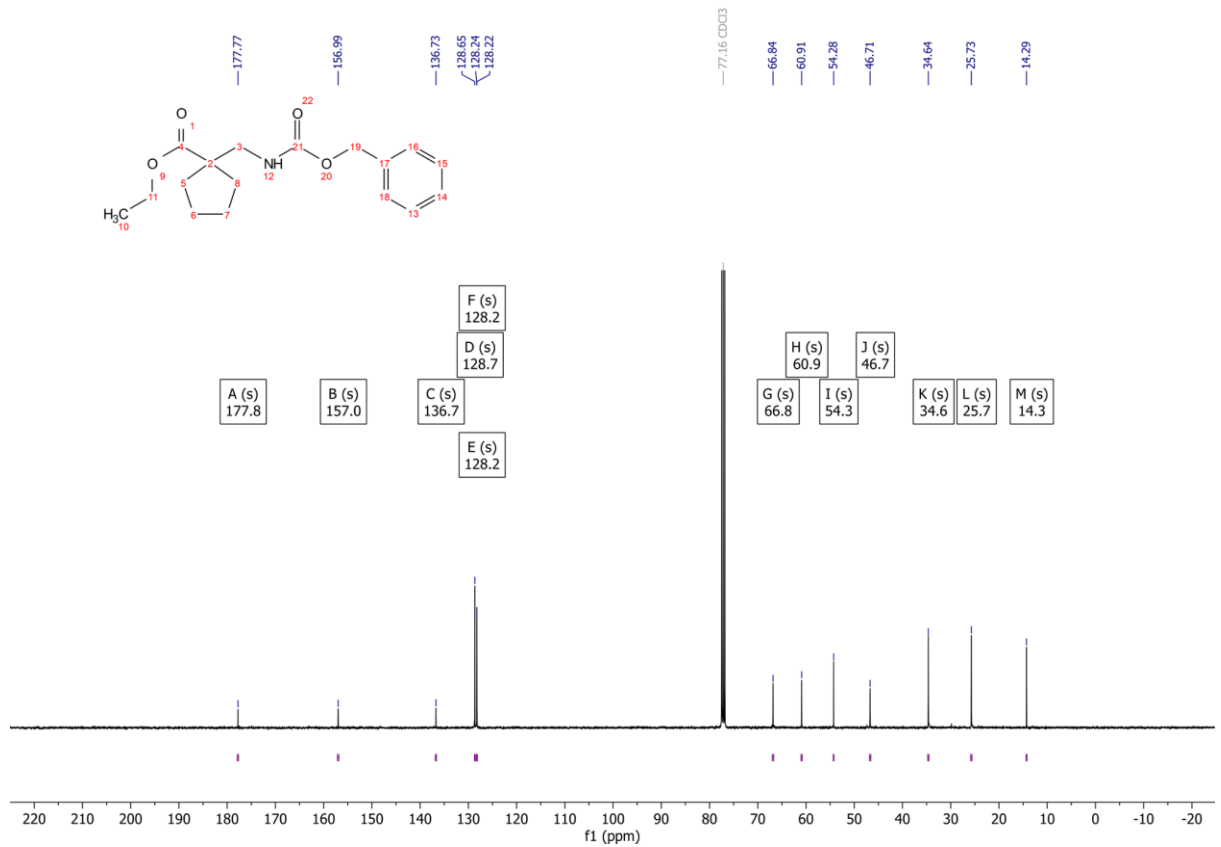
114 ¹³C NMR (101 MHz, CDCl₃)



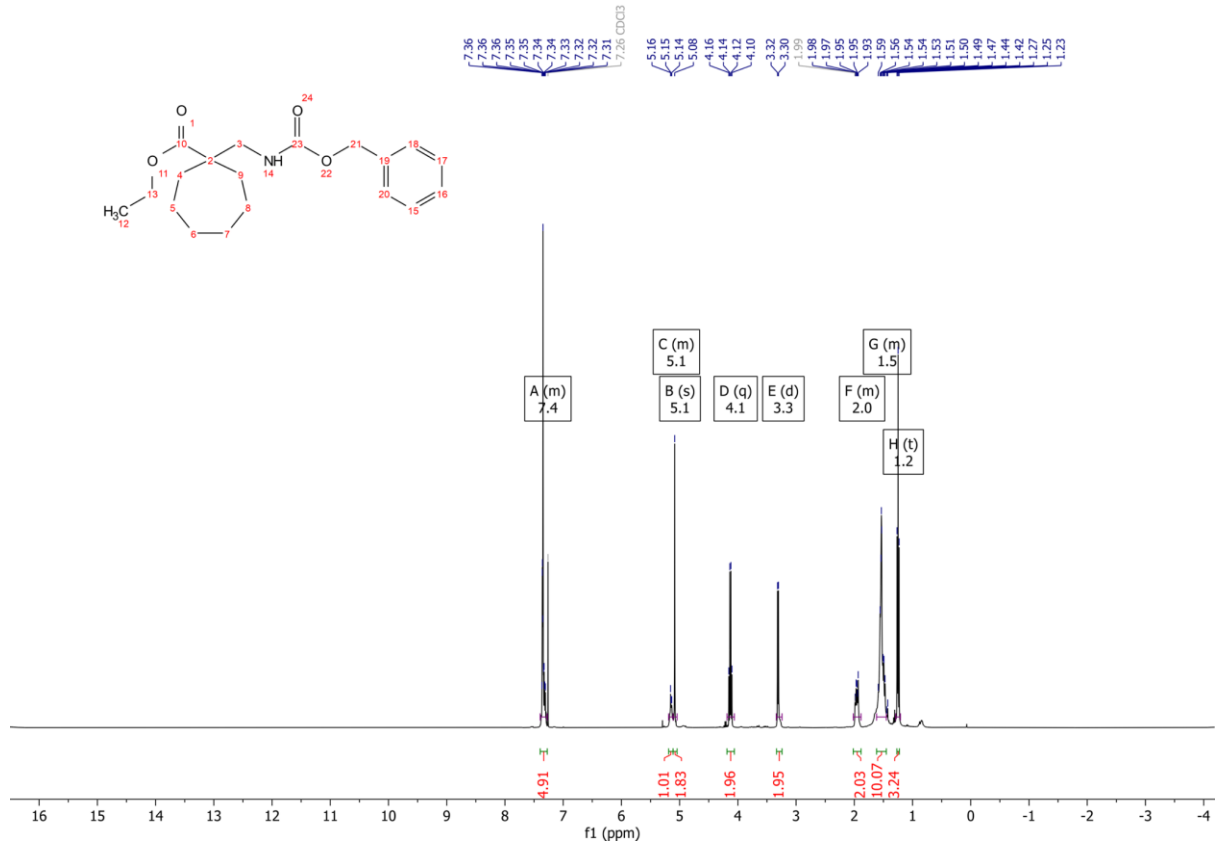
115 ¹H NMR (400 MHz, CDCl₃)



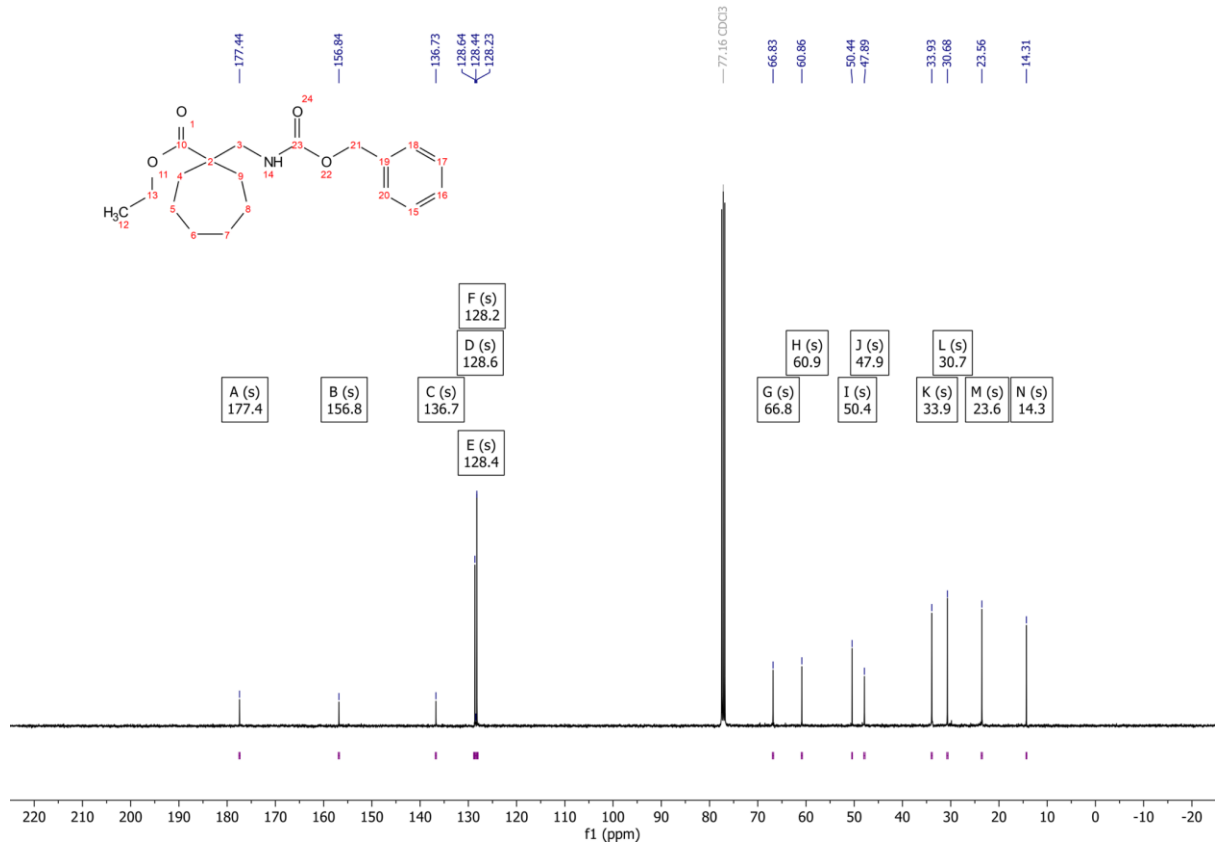
115 ¹³C NMR (101 MHz, CDCl₃)



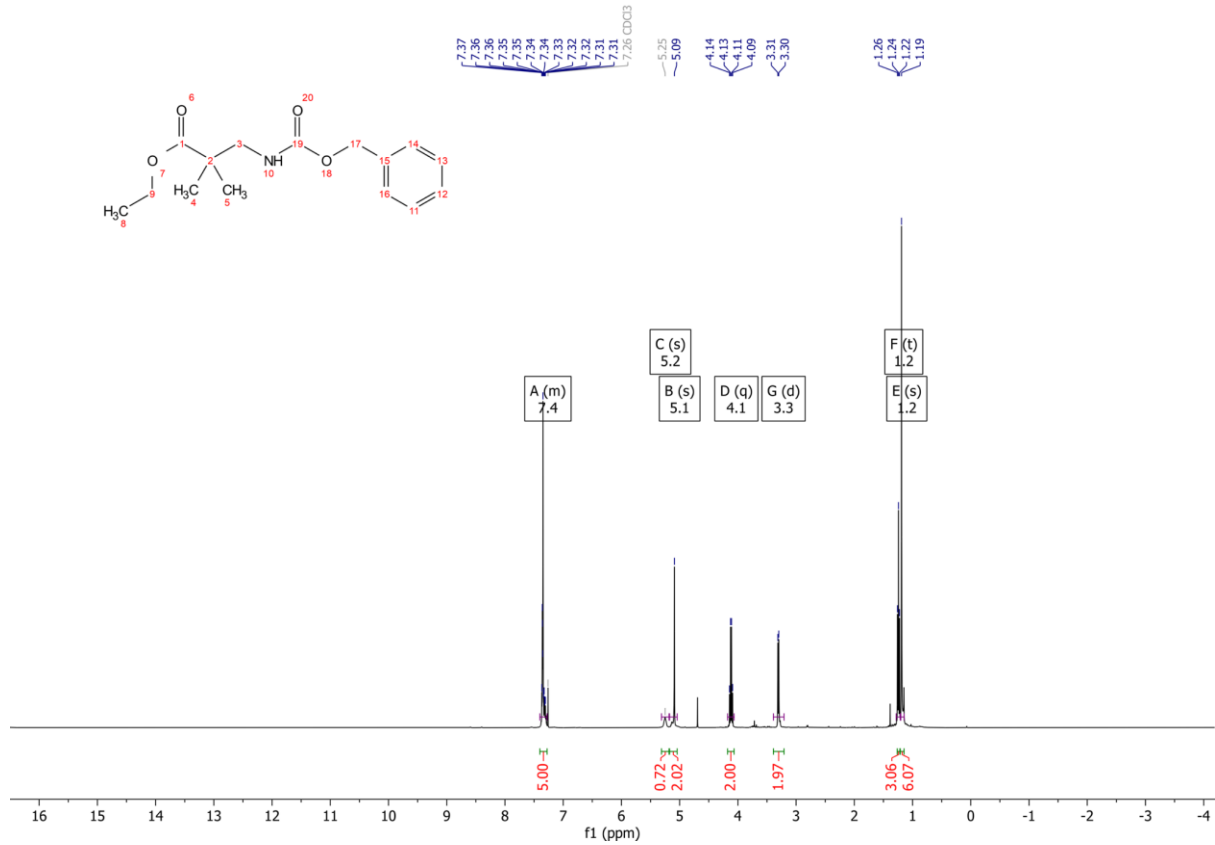
117 ¹H NMR (400 MHz, CDCl₃)



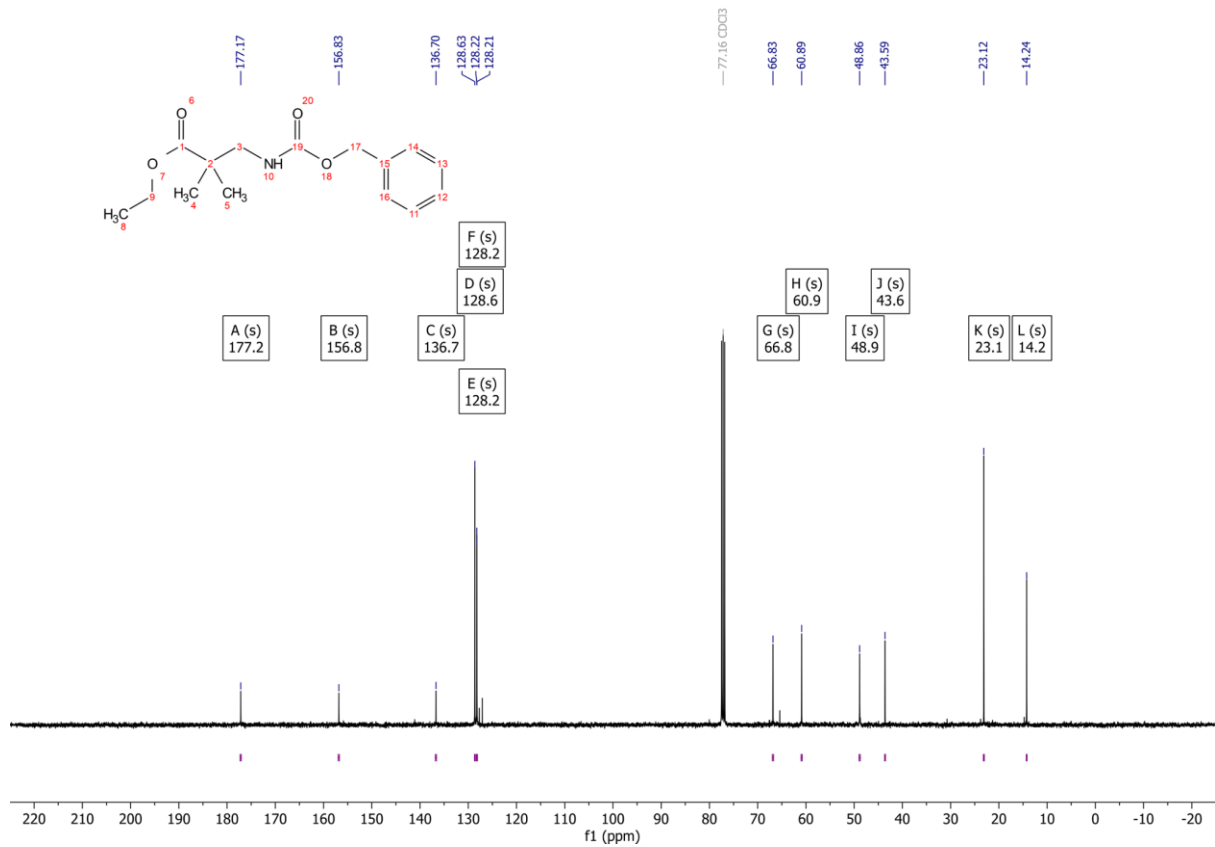
117 ¹³C NMR (101 MHz, CDCl₃)



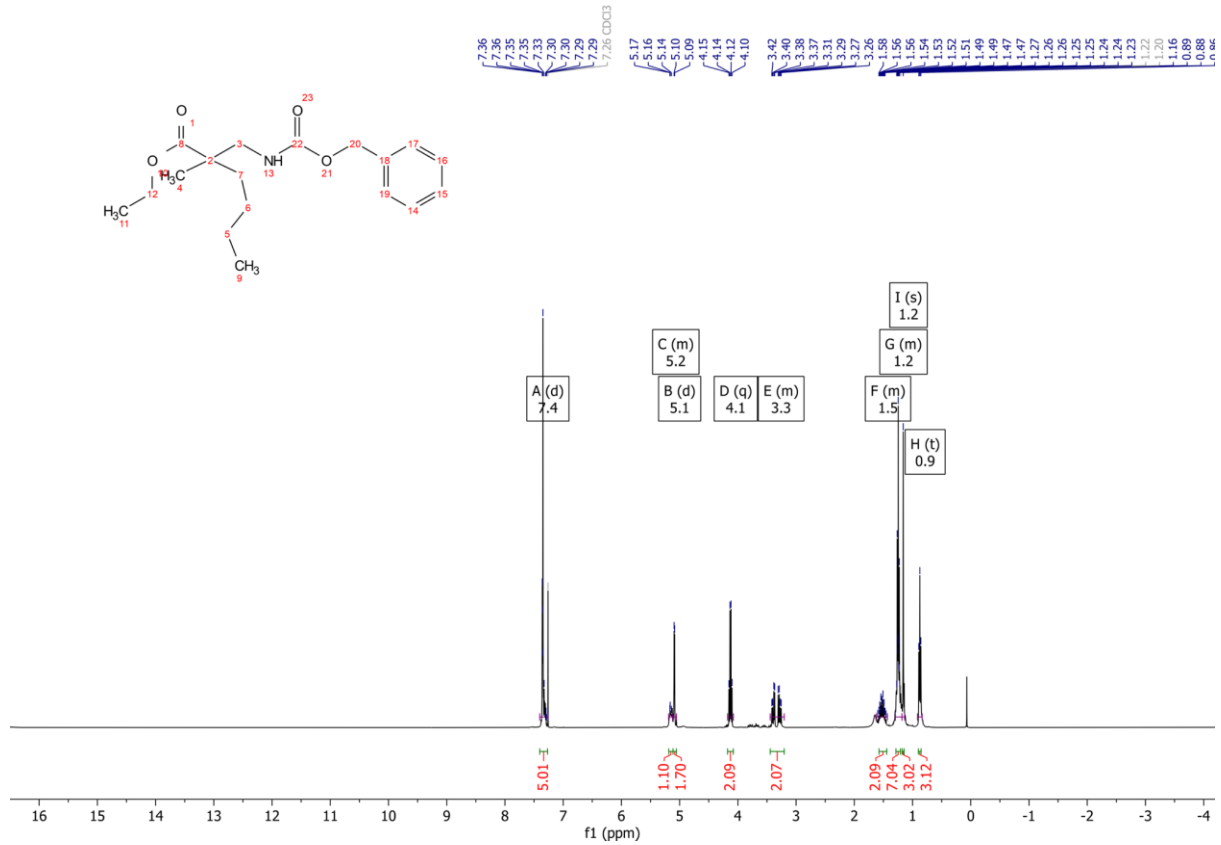
118 ¹H NMR (400 MHz, CDCl₃)



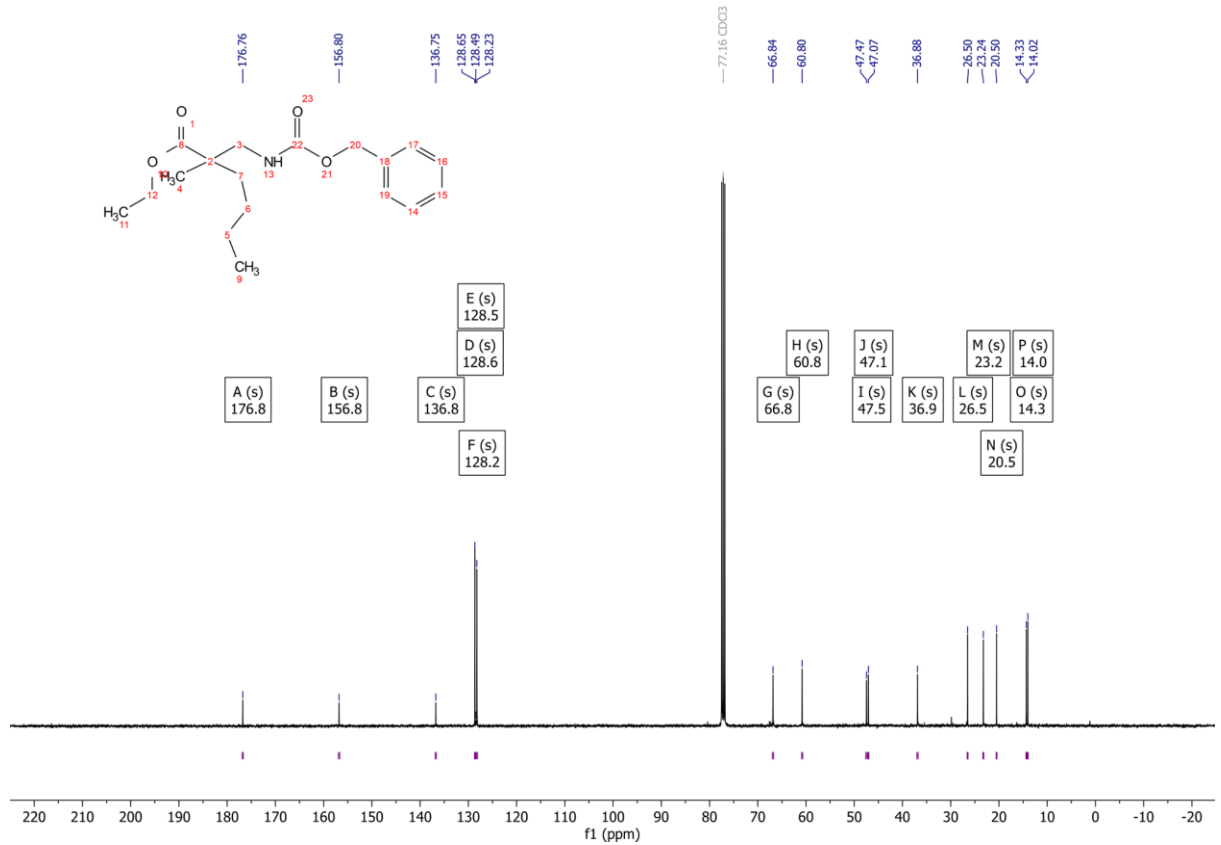
118 ¹³C NMR (101 MHz, CDCl₃)



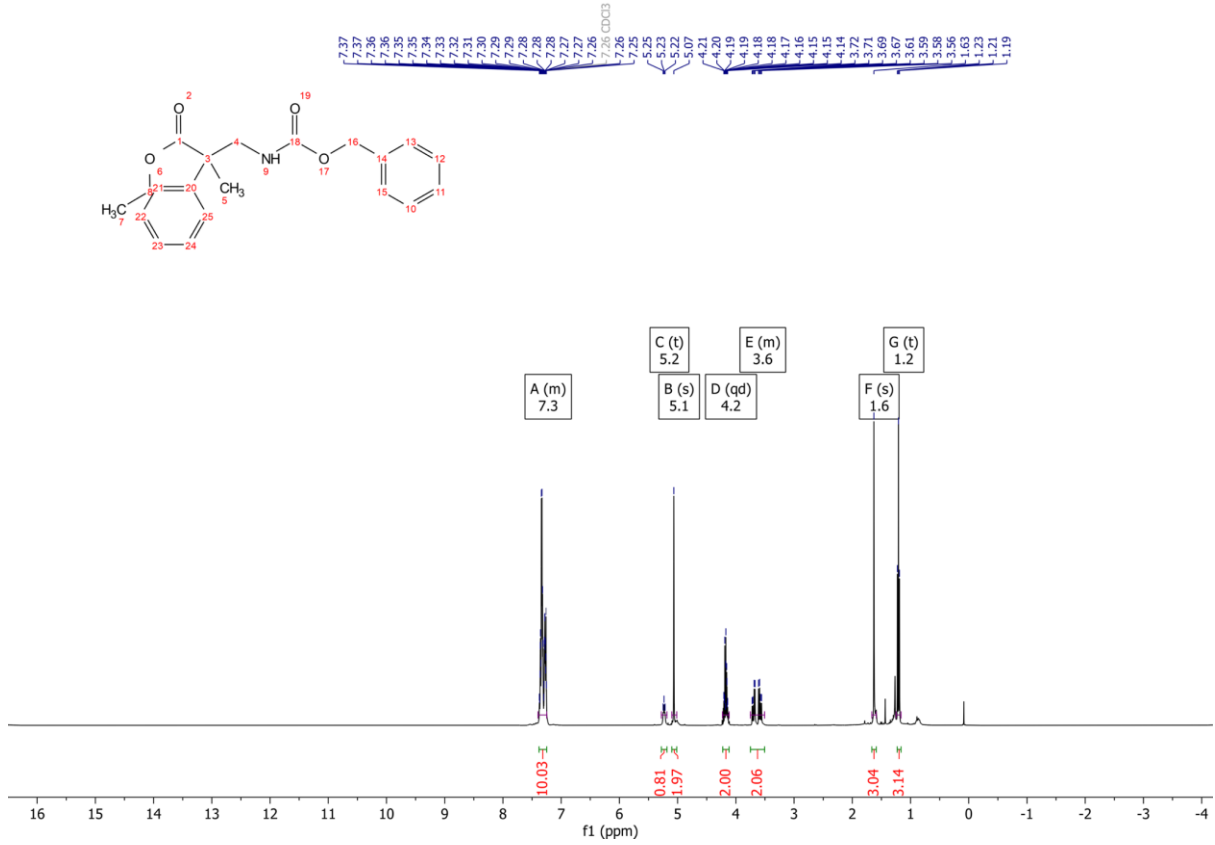
119 ¹H NMR (400 MHz, CDCl₃)



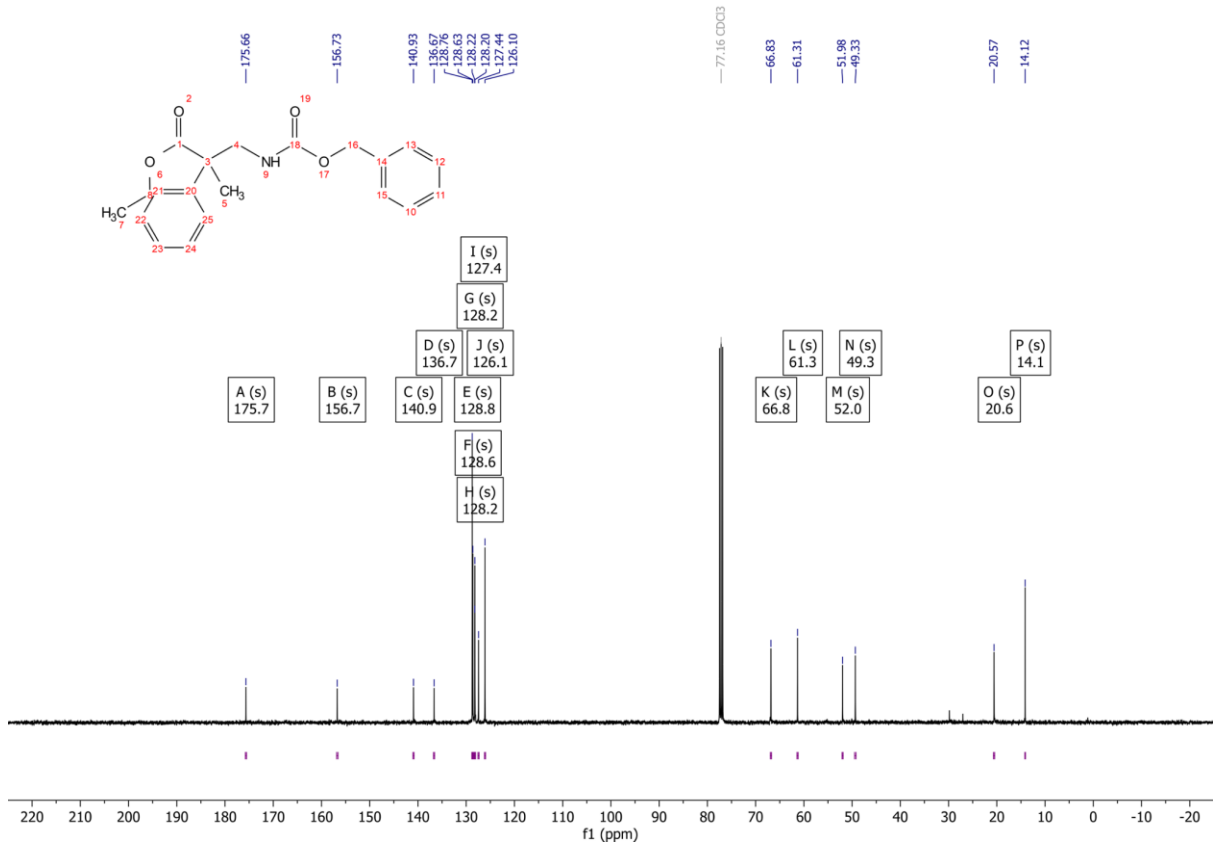
119 ¹³C NMR (101 MHz, CDCl₃)



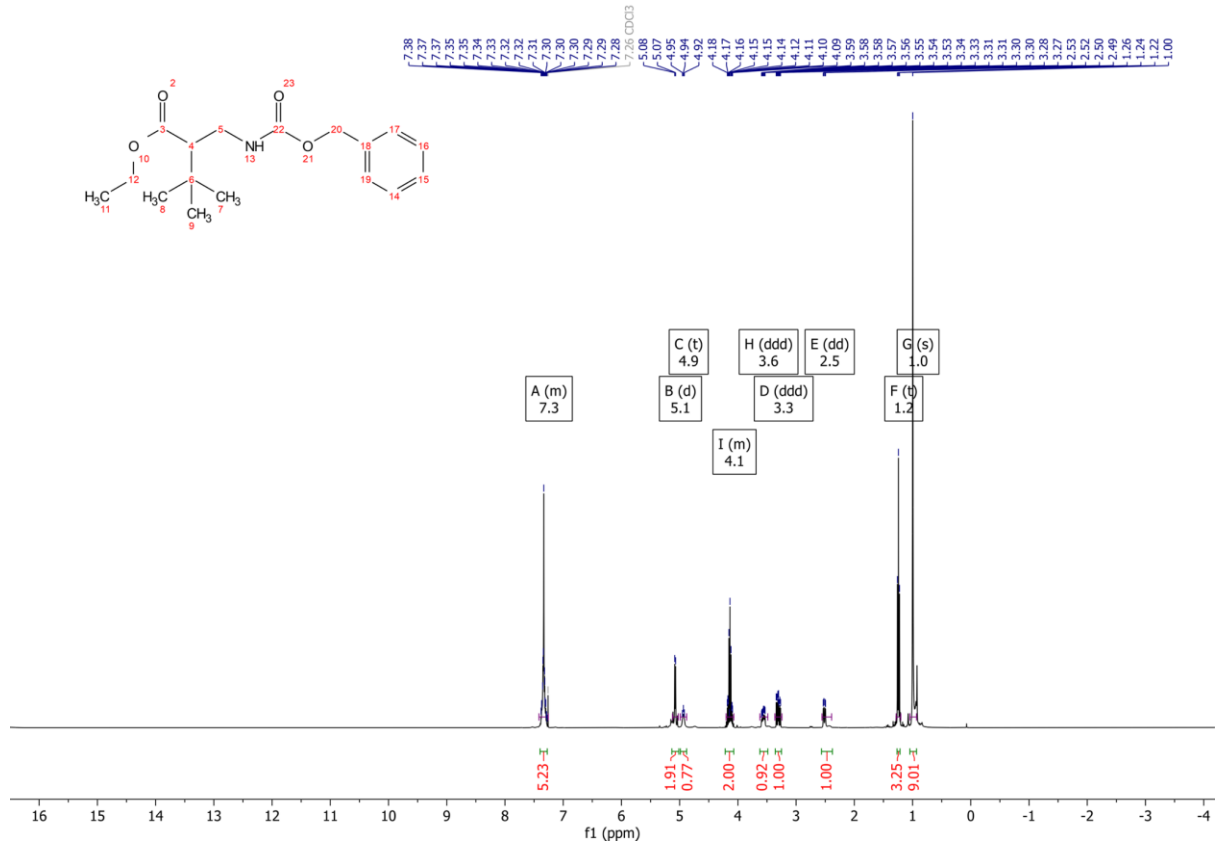
120 ¹H NMR (400 MHz, CDCl₃)



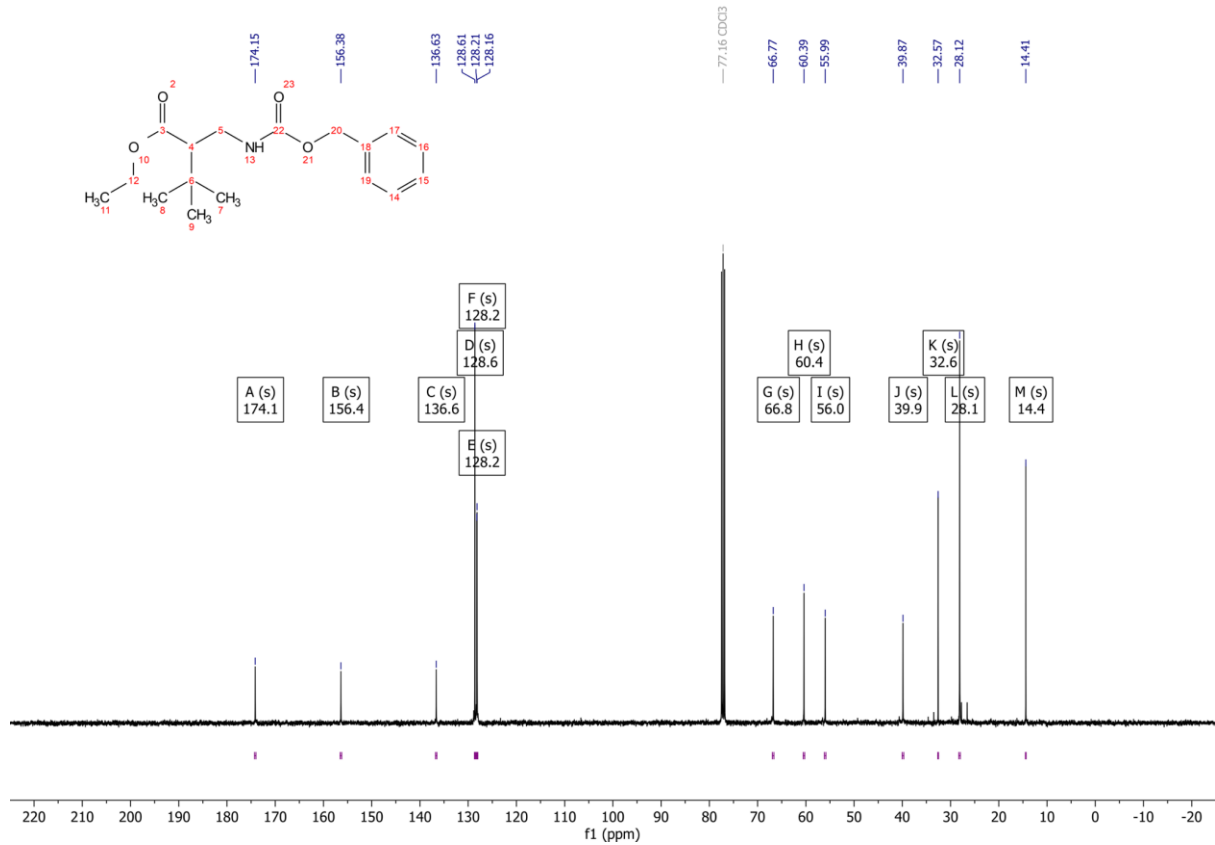
120 ¹³C NMR (101 MHz, CDCl₃)



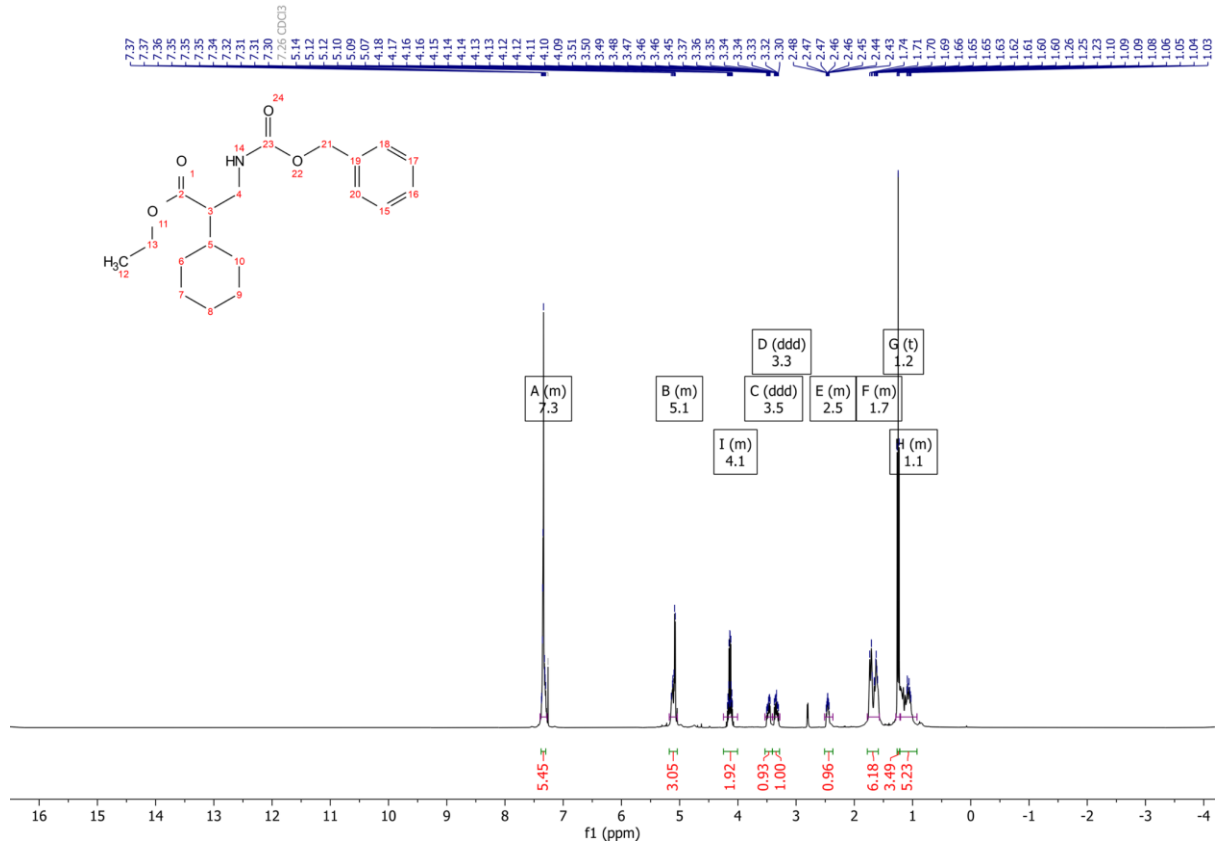
126 ¹H NMR (400 MHz, CDCl₃)



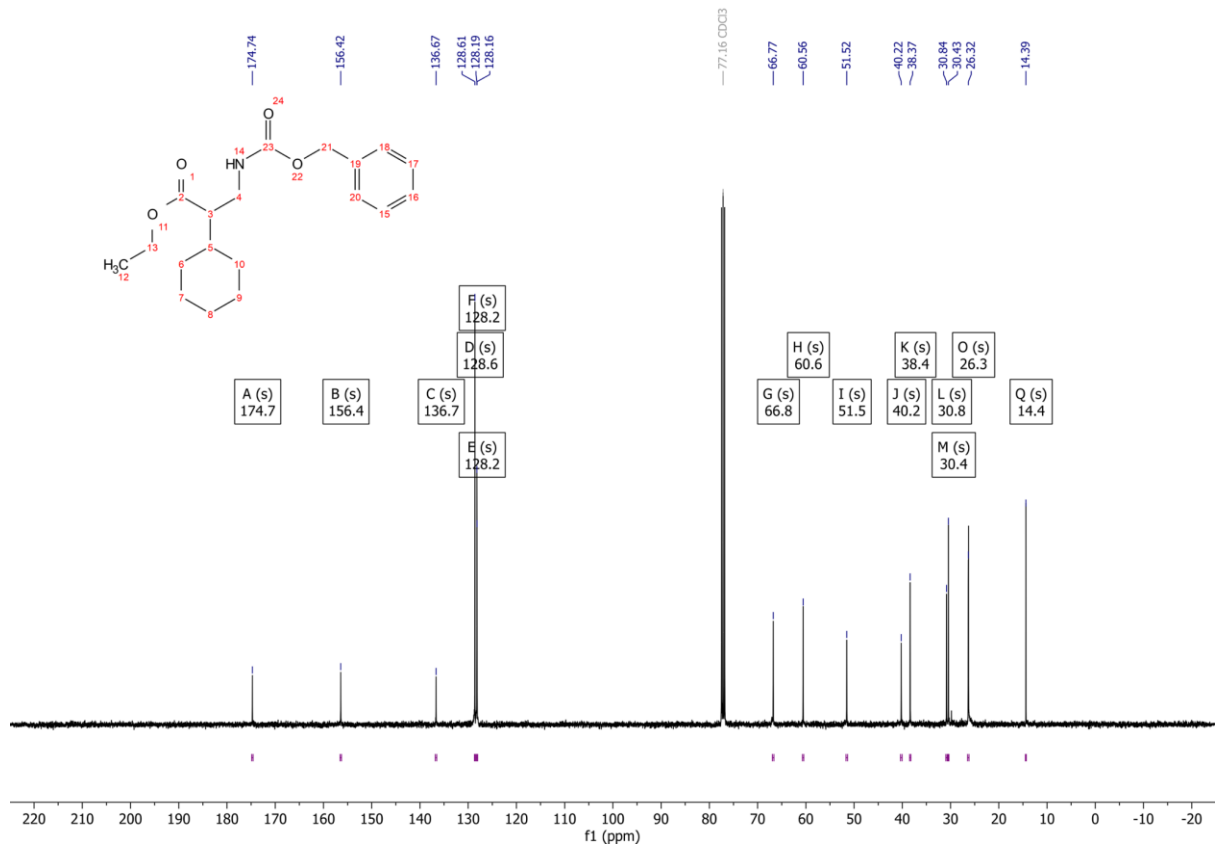
126 ¹³C NMR (101 MHz, CDCl₃)



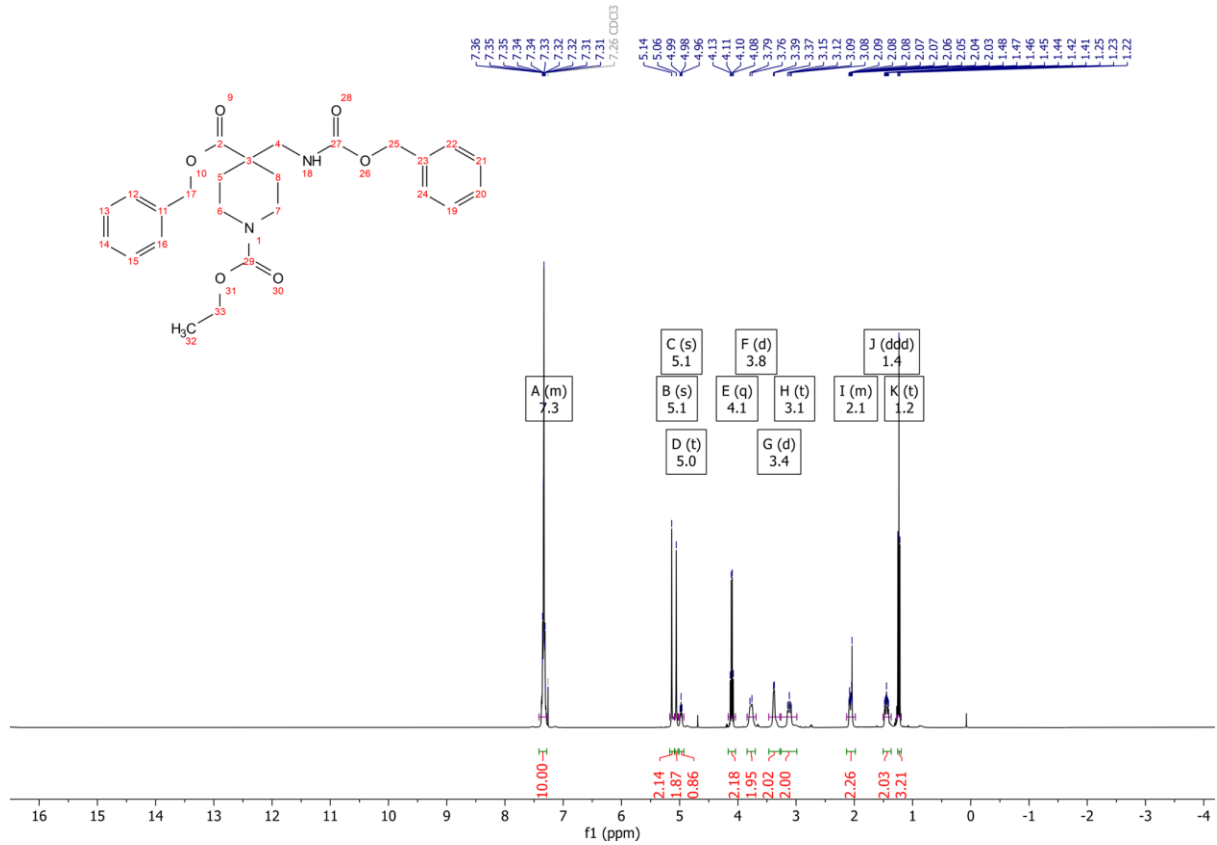
127 ¹H NMR (400 MHz, CDCl₃)



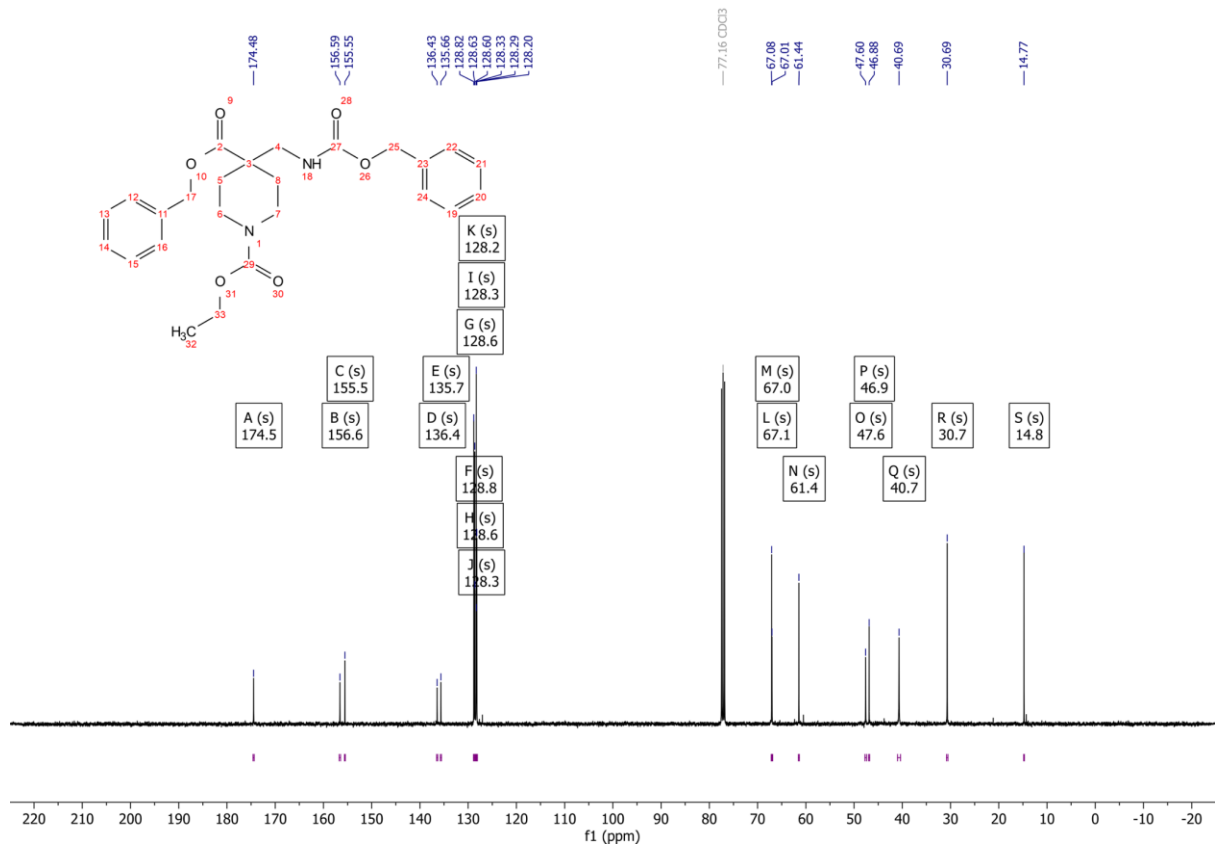
127 ¹³C NMR (101 MHz, CDCl₃)



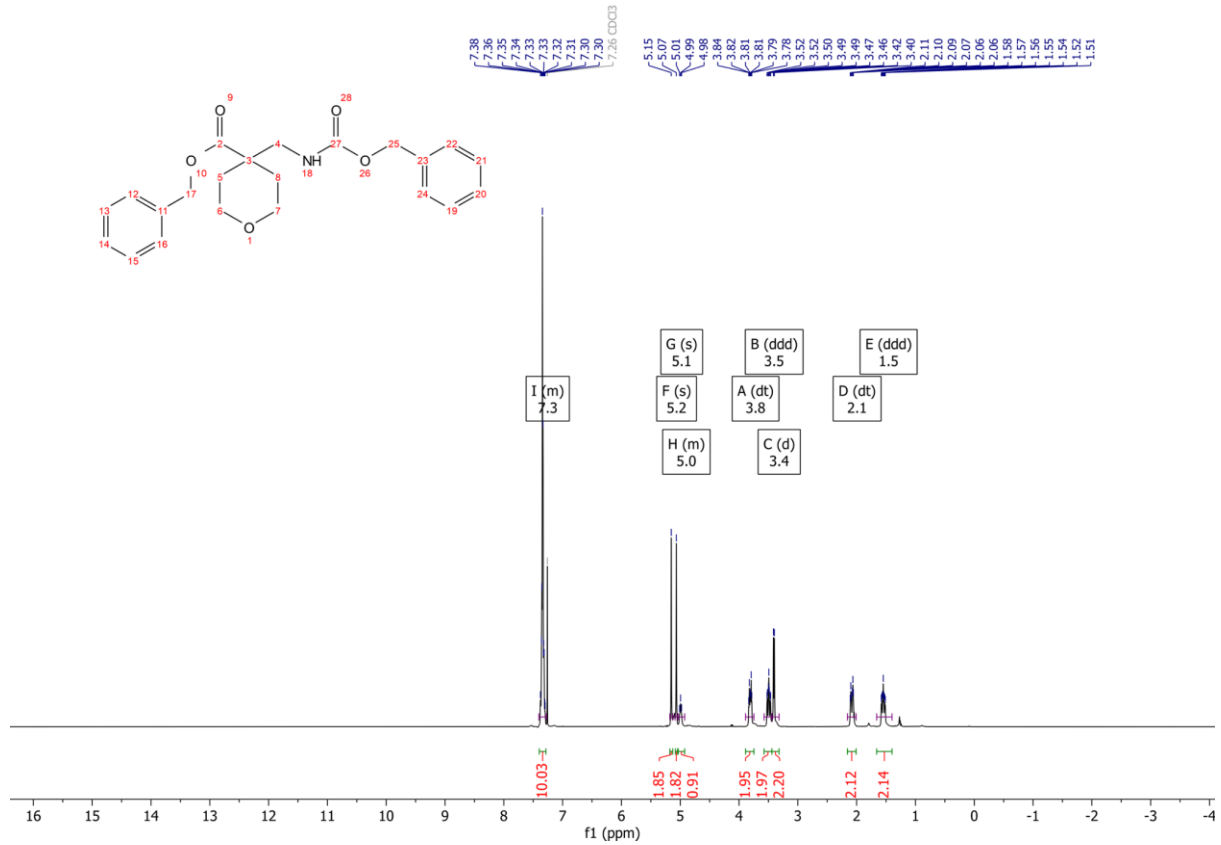
111 ¹H NMR (400 MHz, CDCl₃)



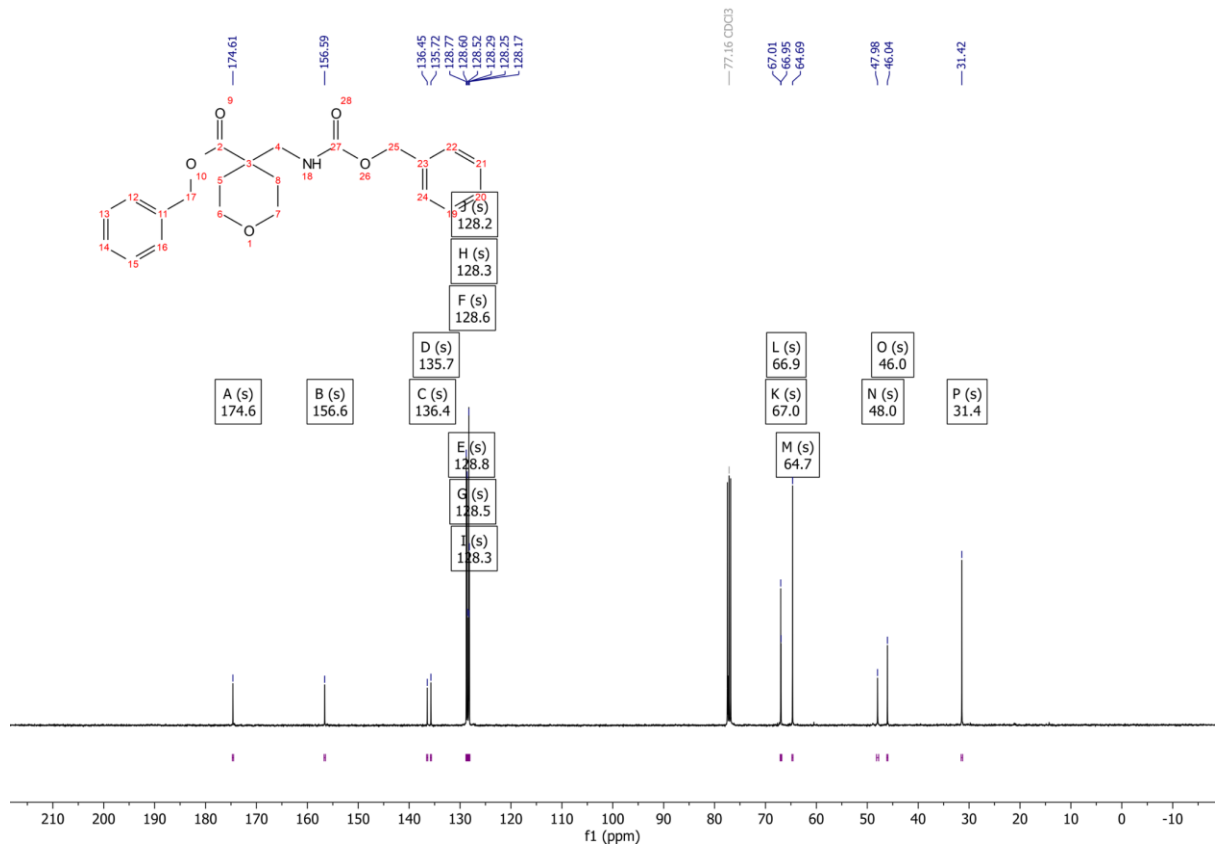
111 ¹³C NMR (101 MHz, CDCl₃)



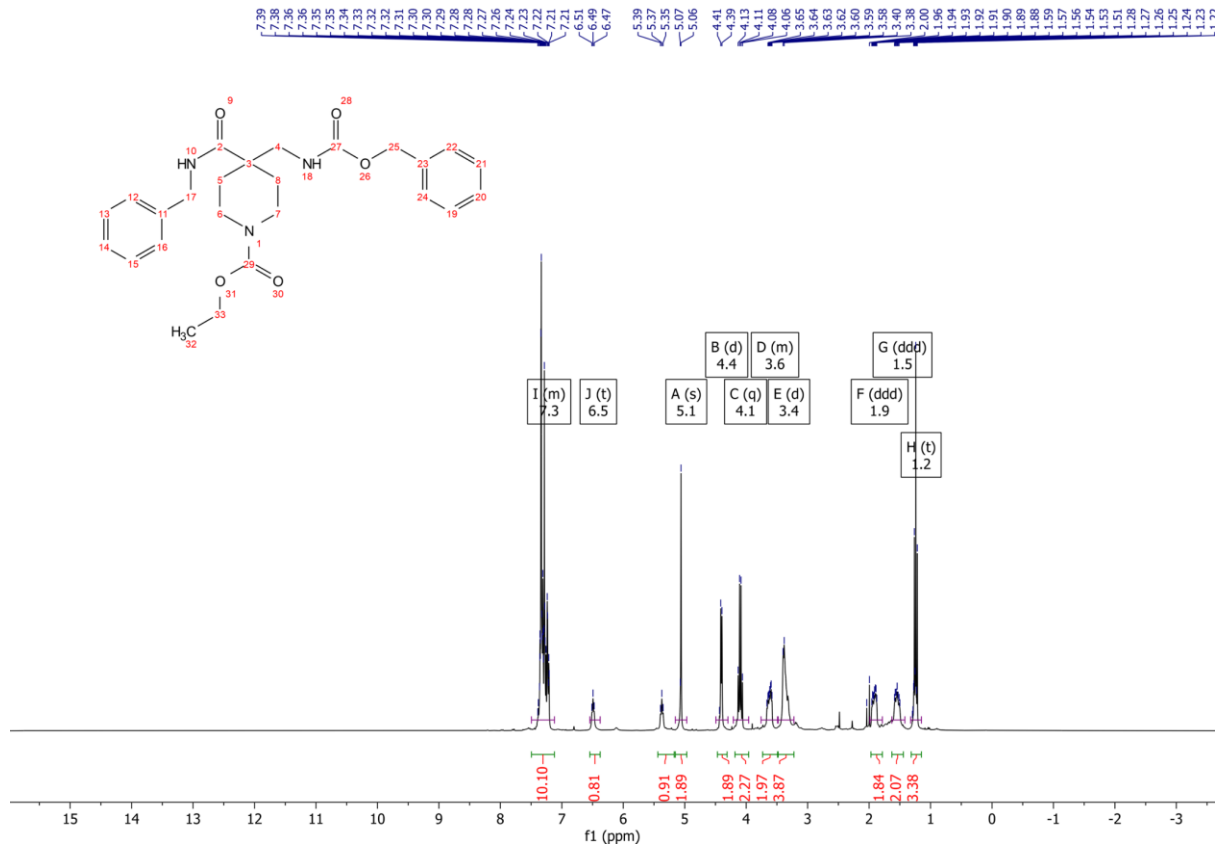
131 ¹H NMR (400 MHz, CDCl₃)



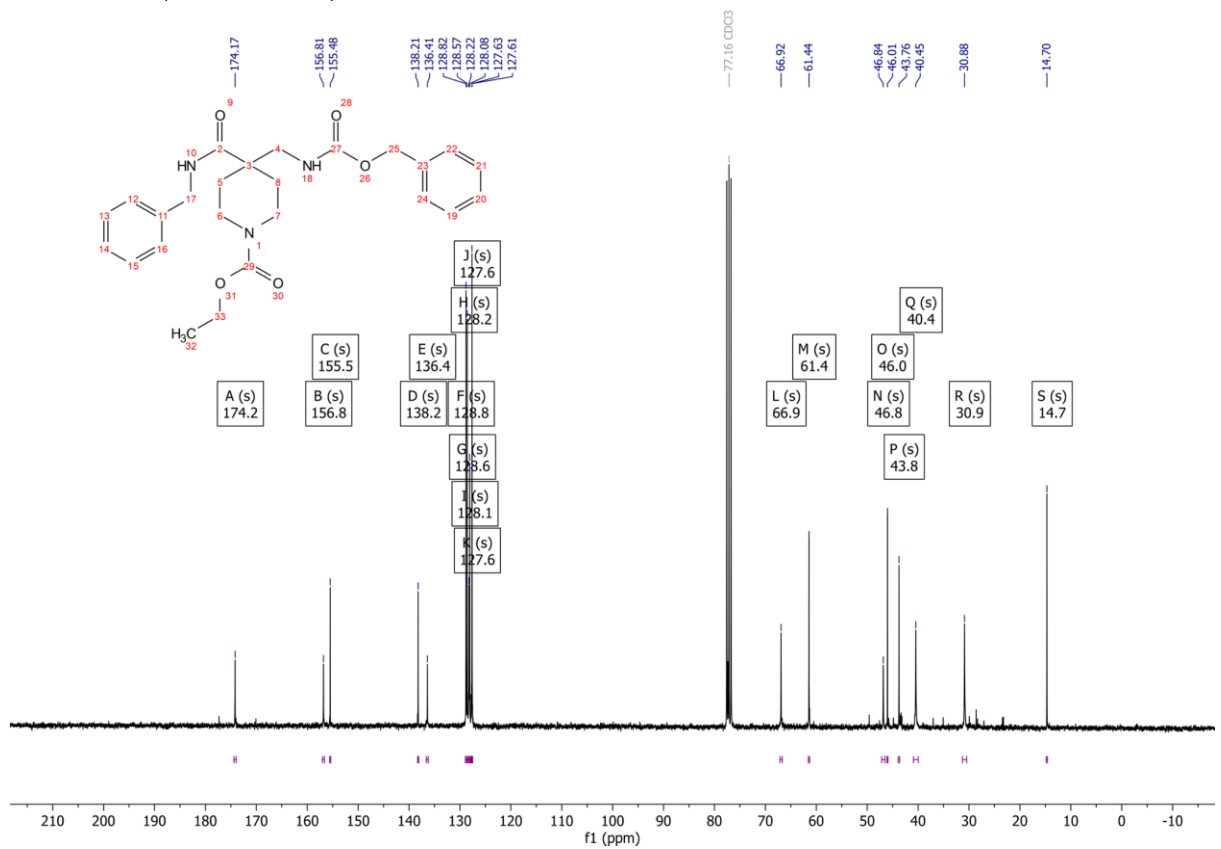
131 ¹³C NMR (101 MHz, CDCl₃)



132 ¹H NMR (300 MHz, CDCl₃)

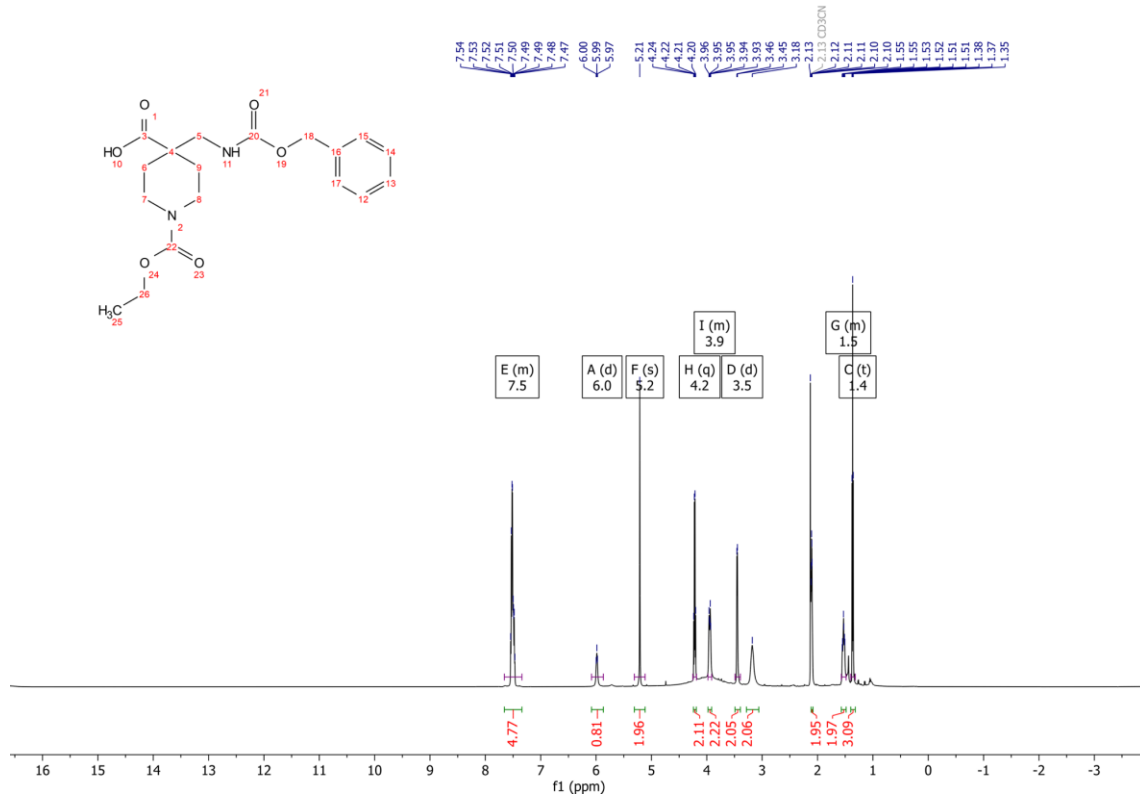


132 ¹³C NMR (75 MHz, CDCl₃)



β-Amino Acids

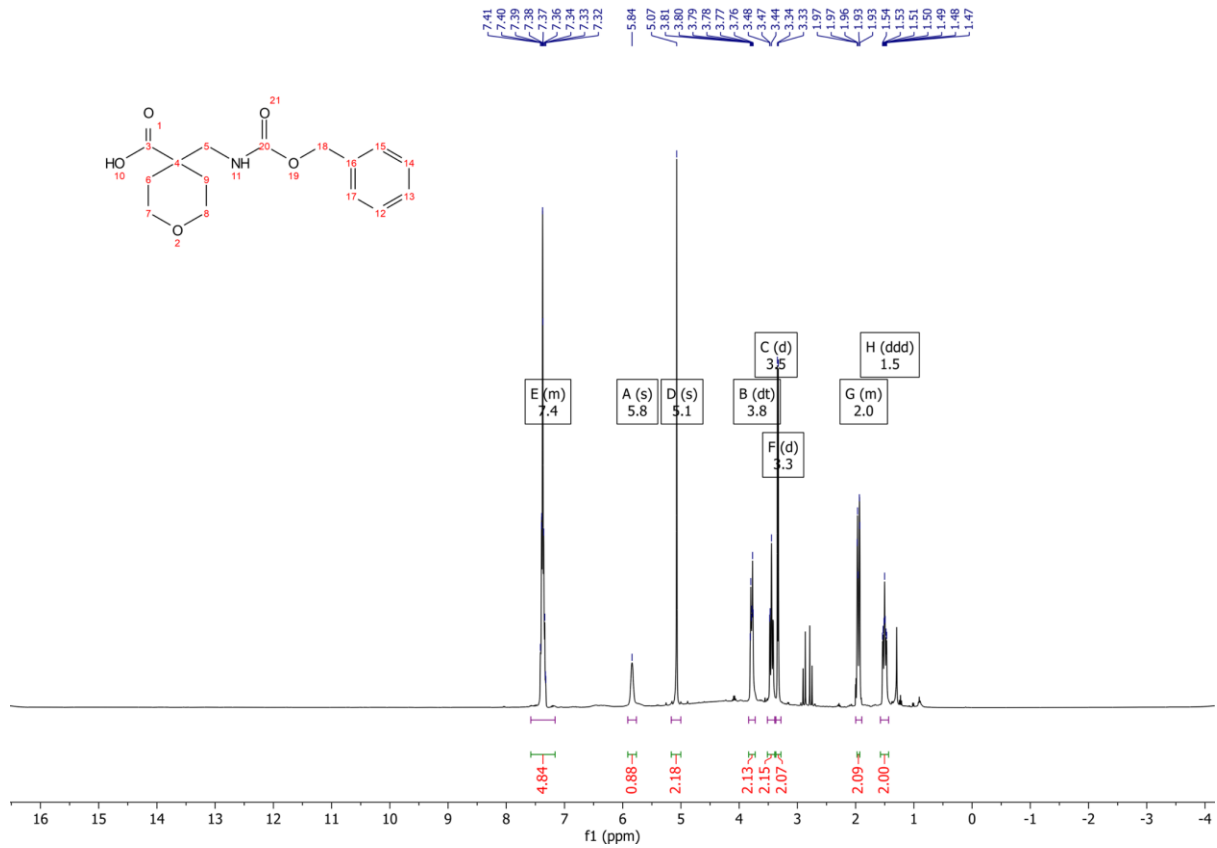
136 ¹H NMR (600 MHz, CD₃CN)



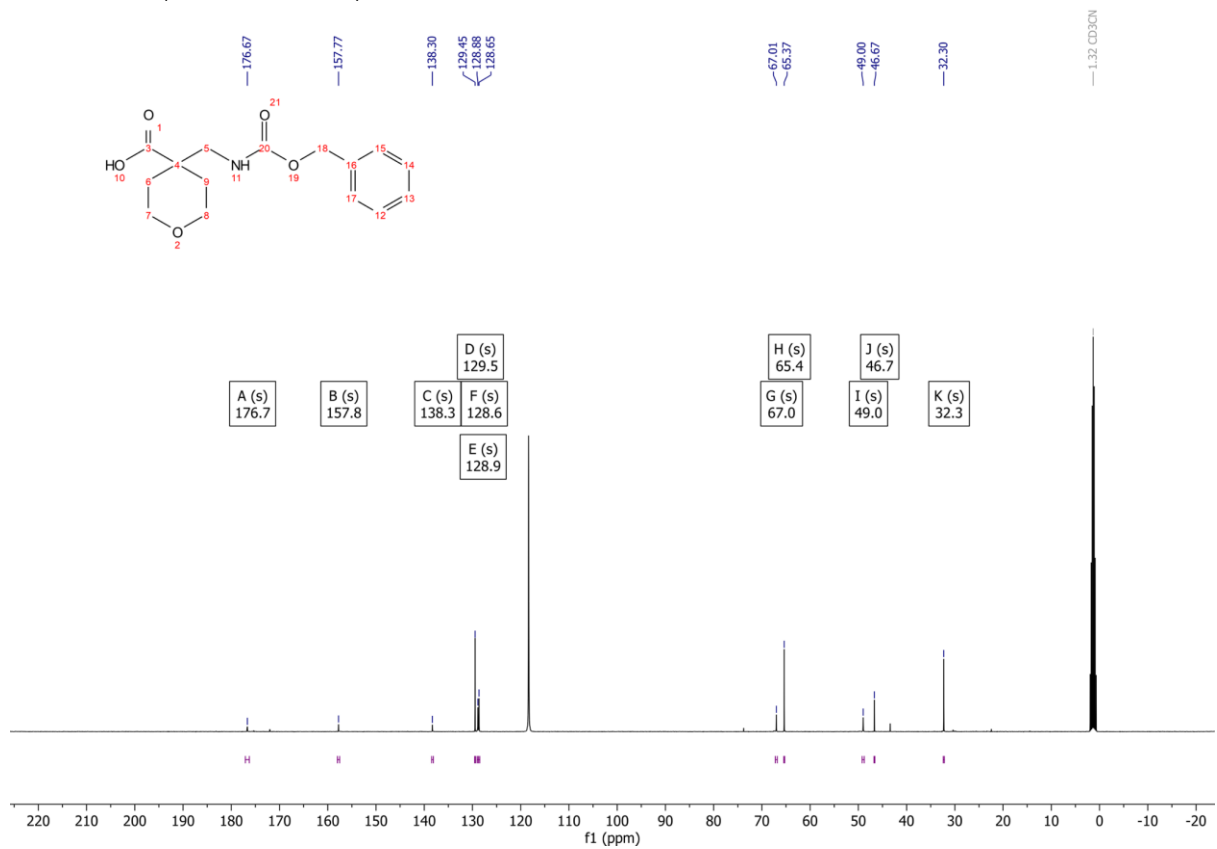
136 ¹³C NMR (101 MHz, CD₃CN)



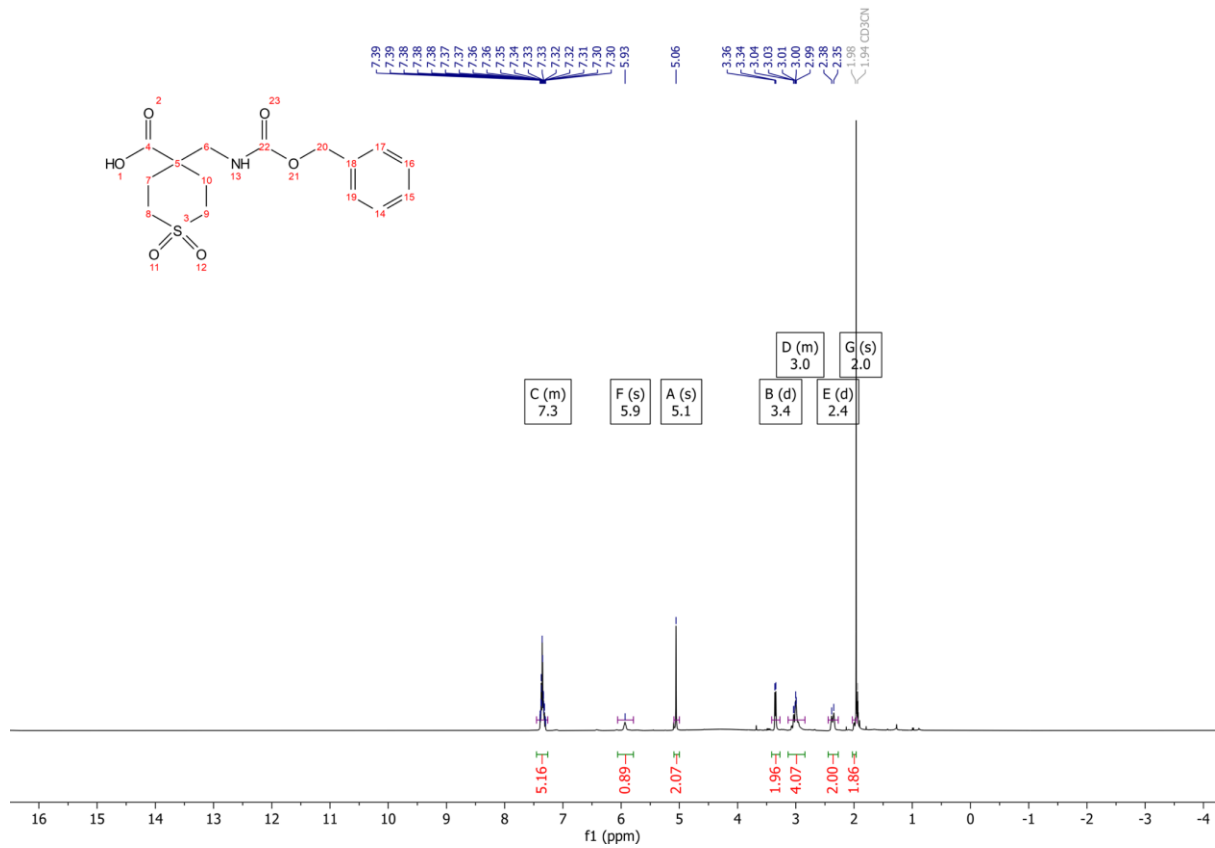
137 ¹H NMR (400 MHz, CD₃CN)



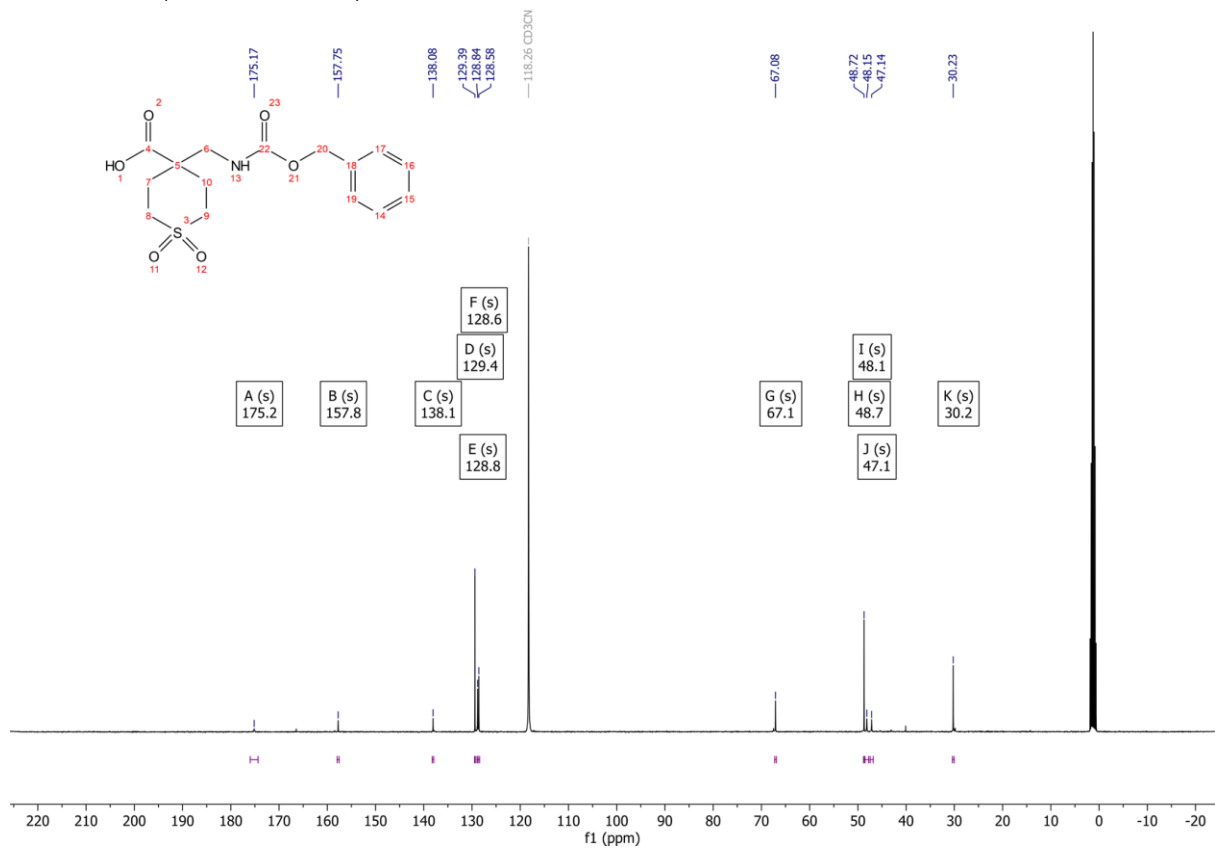
137 ¹³C NMR (101 MHz, CD₃CN)



138 ¹H NMR (400 MHz, CD₃CN)



138 ¹³C NMR (101 MHz, CD₃CN)



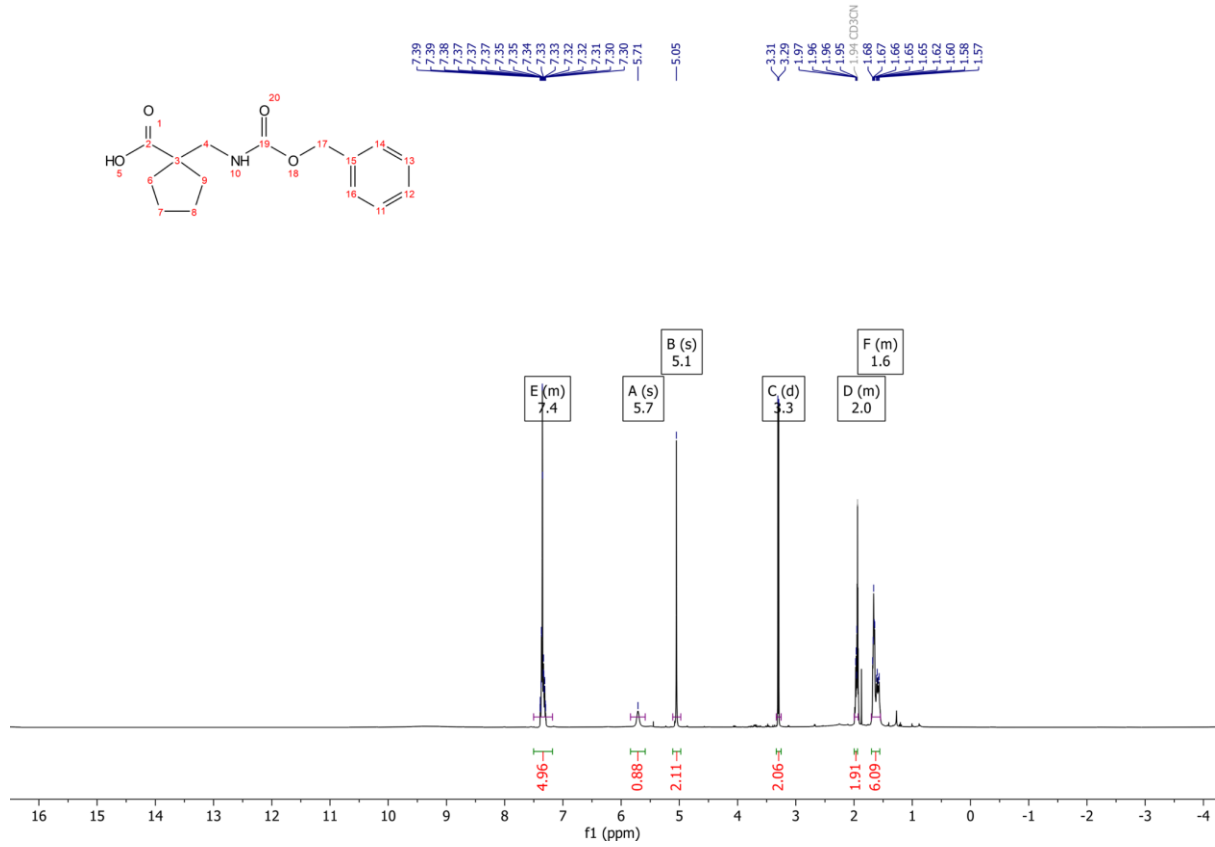
139 ¹H NMR (600 MHz, CD₃CN)



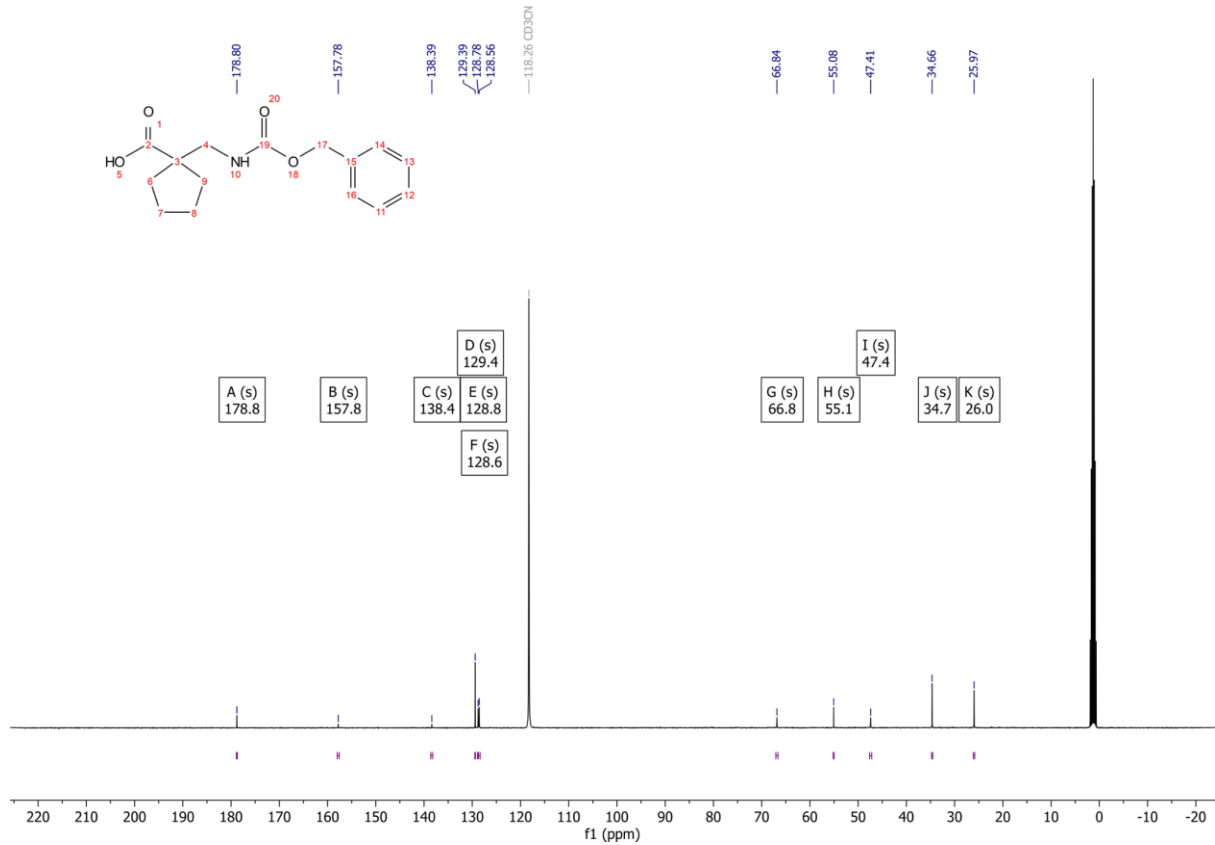
139 ¹³C NMR (101 MHz, CD₃CN)



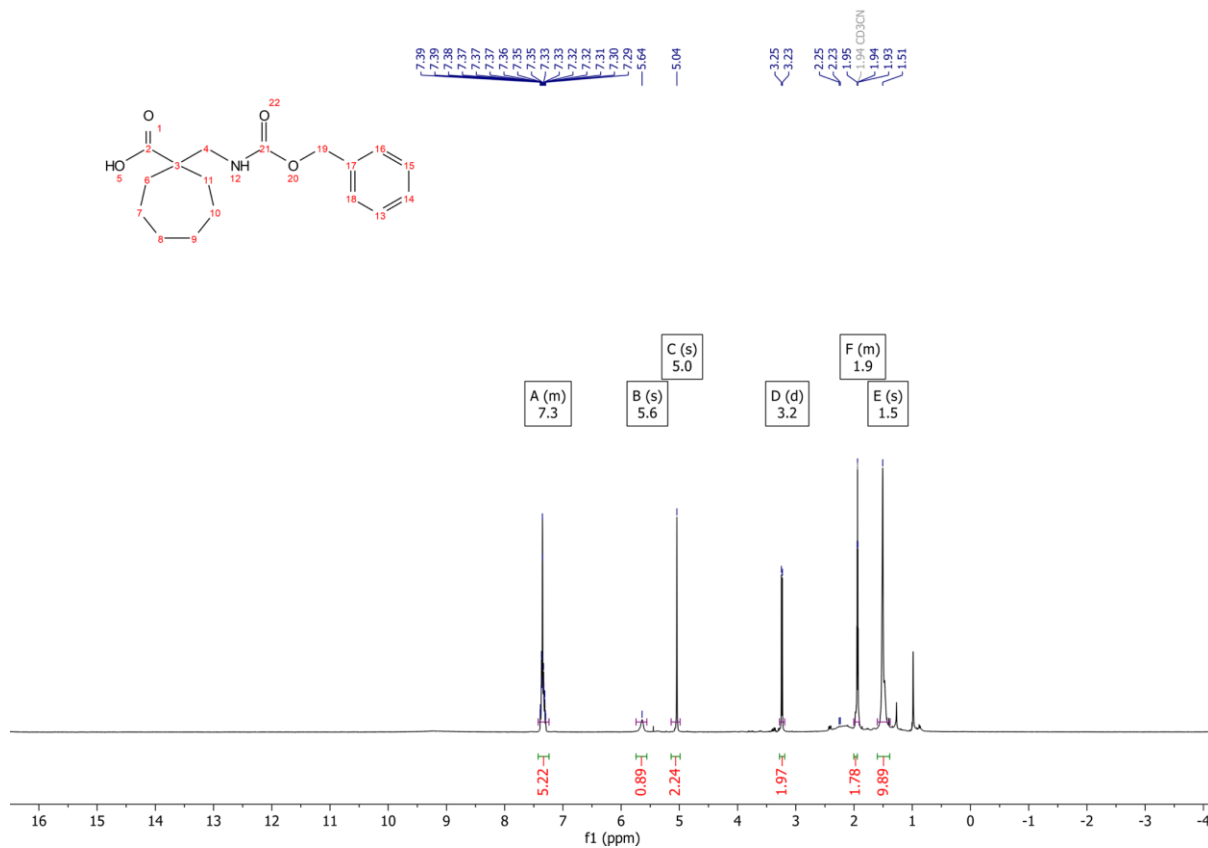
140 ¹H NMR (400 MHz, CD₃CN)



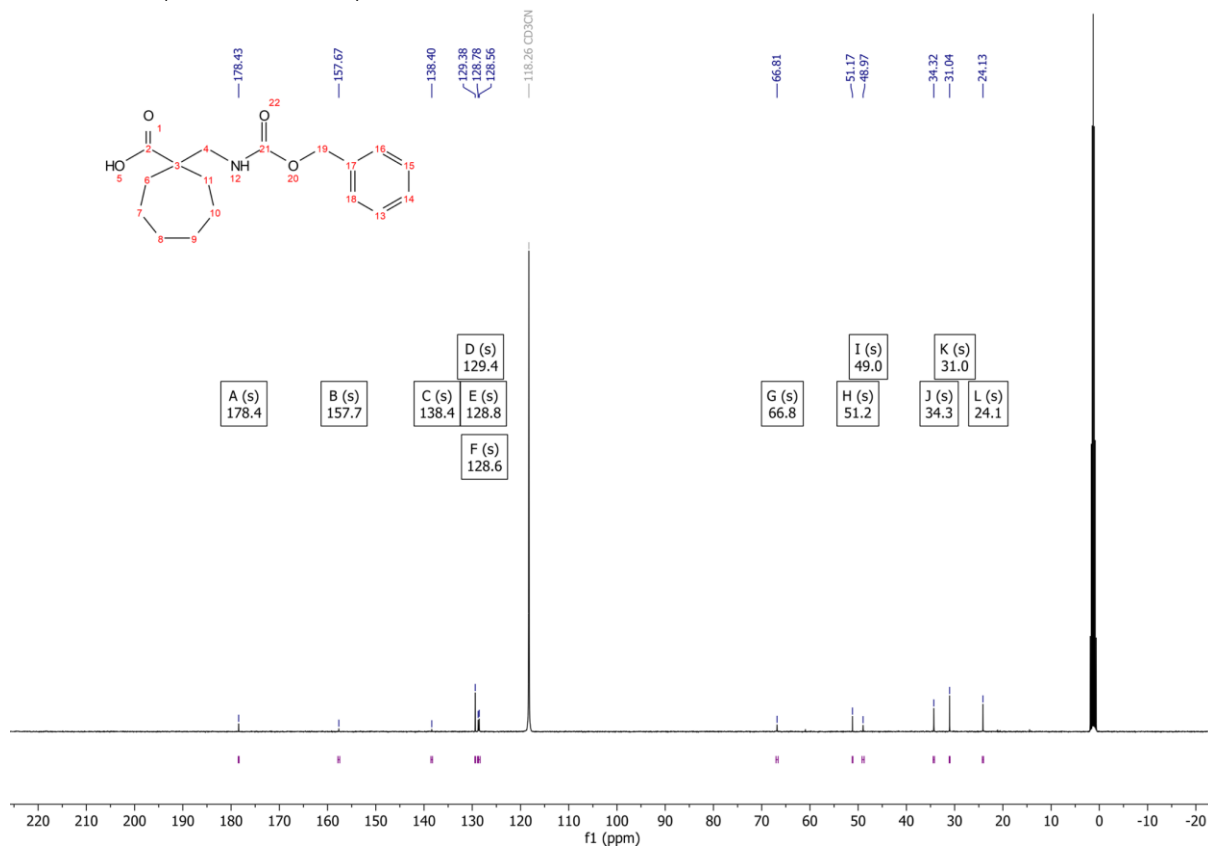
140 ¹³C NMR (101 MHz, CD₃CN)



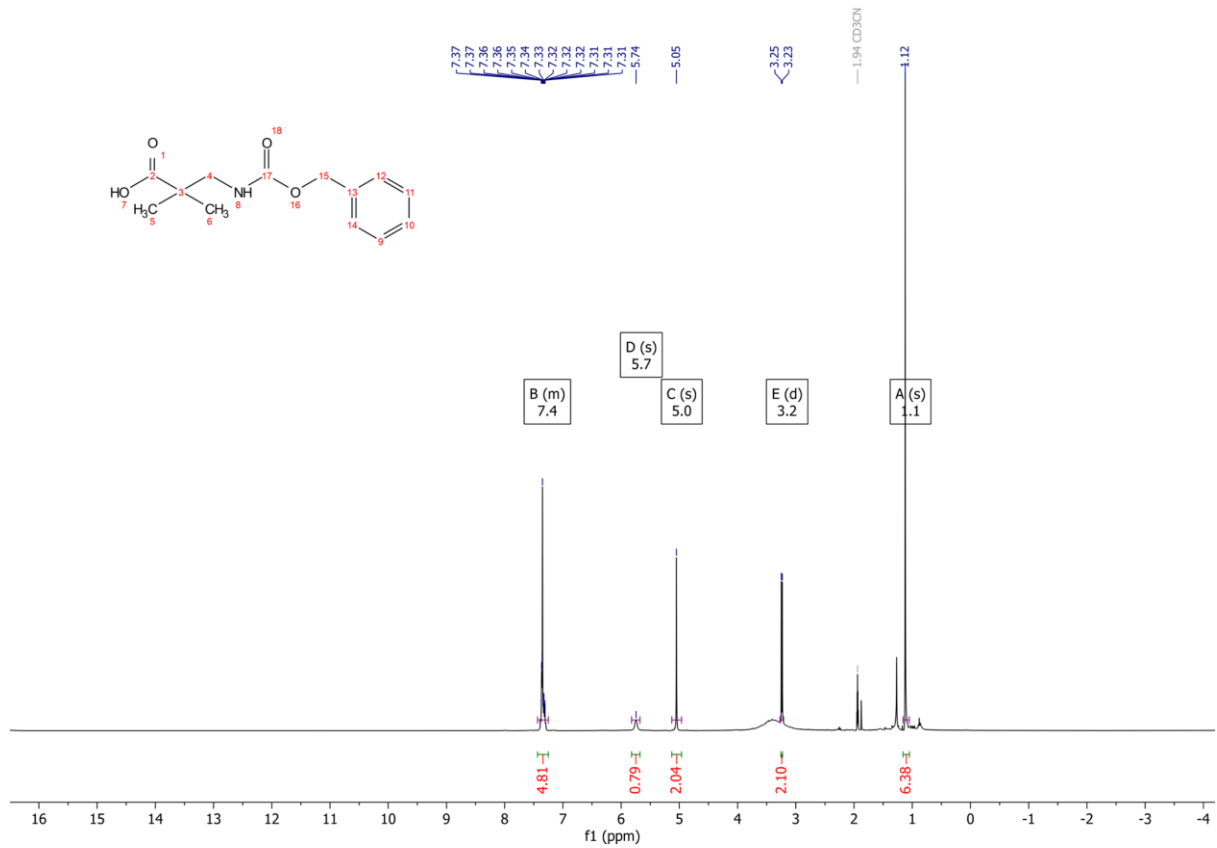
141 ¹H NMR (400 MHz, CD₃CN)



141 ¹³C NMR (101 MHz, CD₃CN)



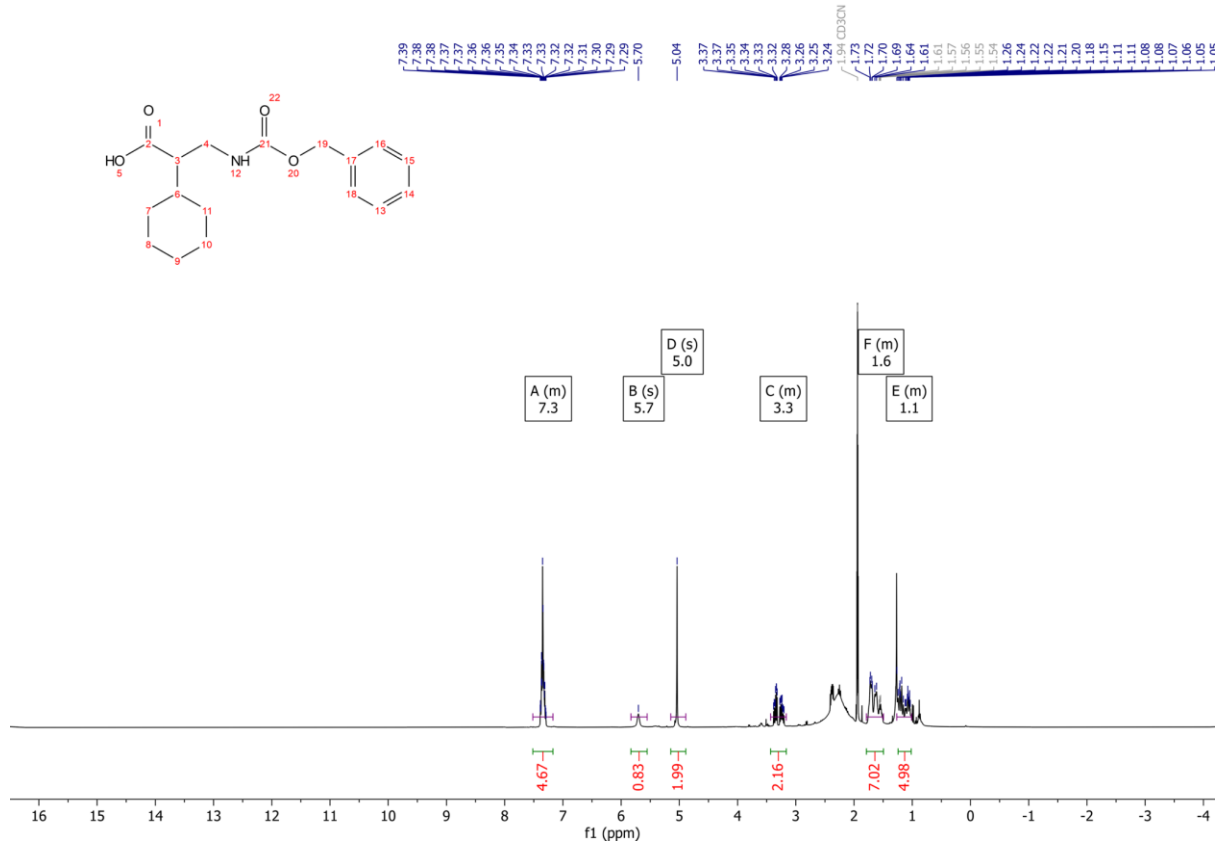
142 ¹H NMR (400 MHz, CD₃CN)



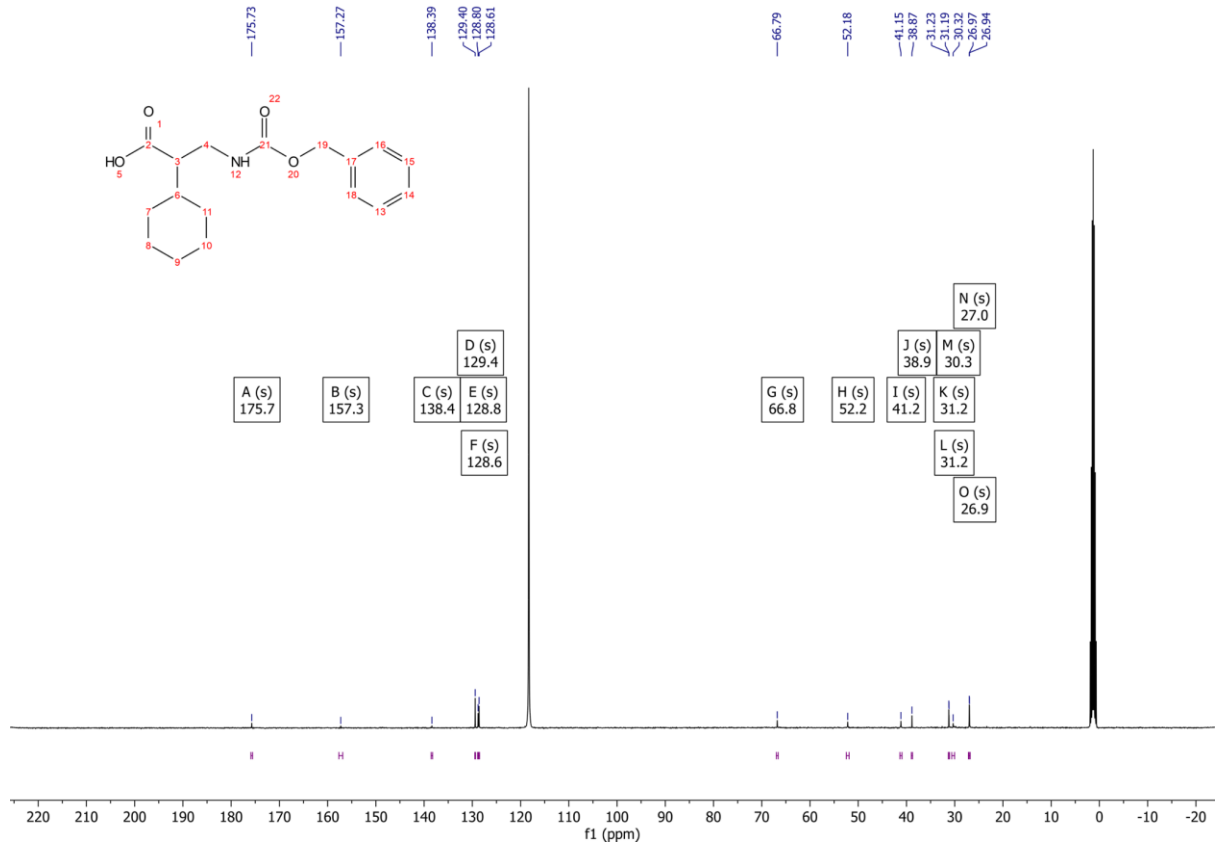
142 ¹³C NMR (101 MHz, CD₃CN)



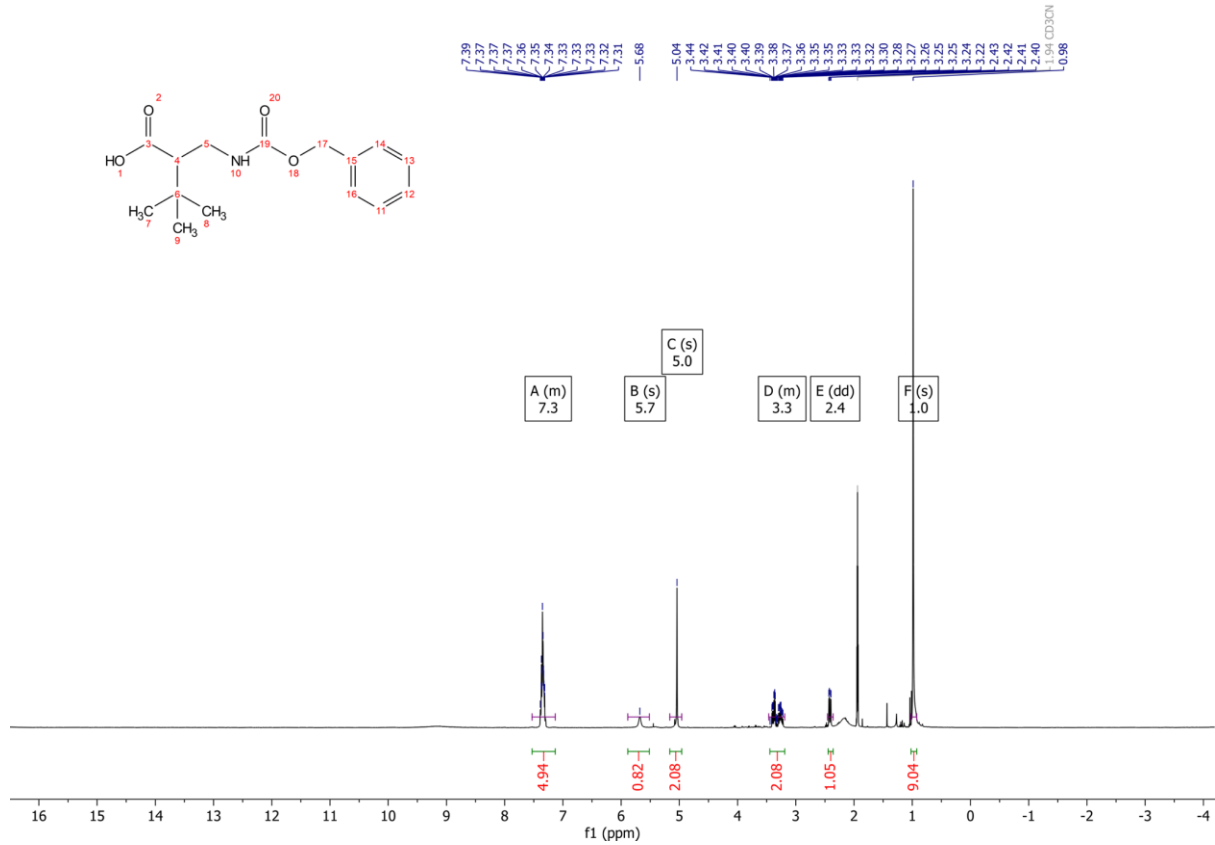
143 ¹H NMR (400 MHz, CD₃CN)



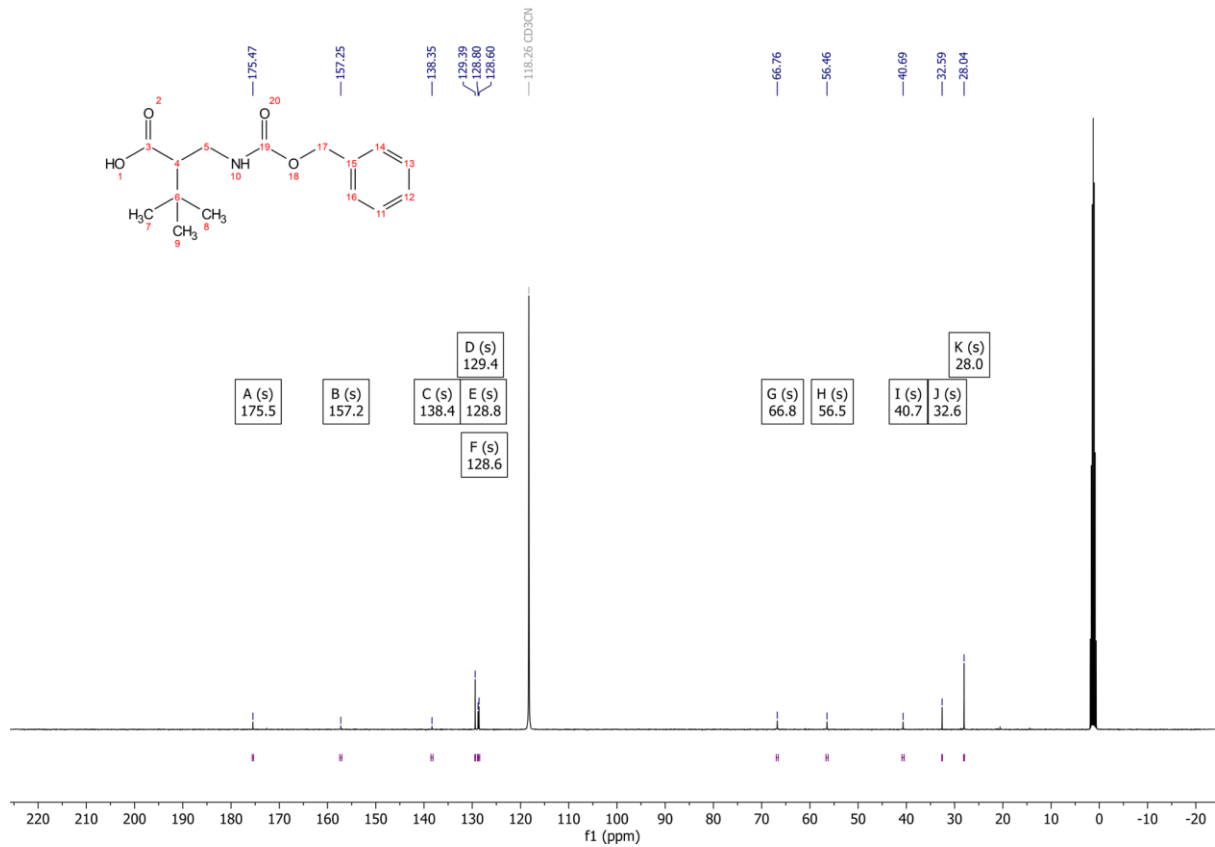
143 ¹³C NMR (101 MHz, CD₃CN)



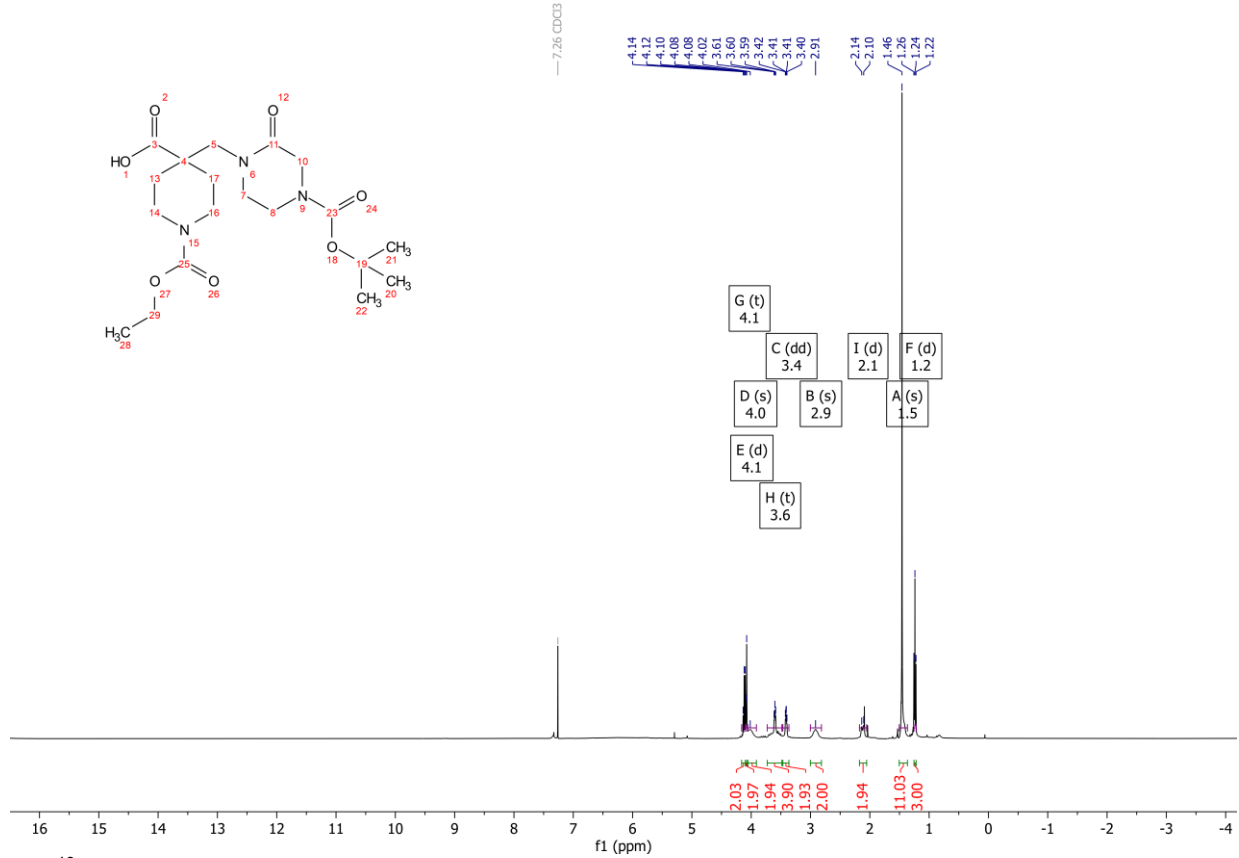
144 ¹H NMR (400 MHz, CD₃CN)



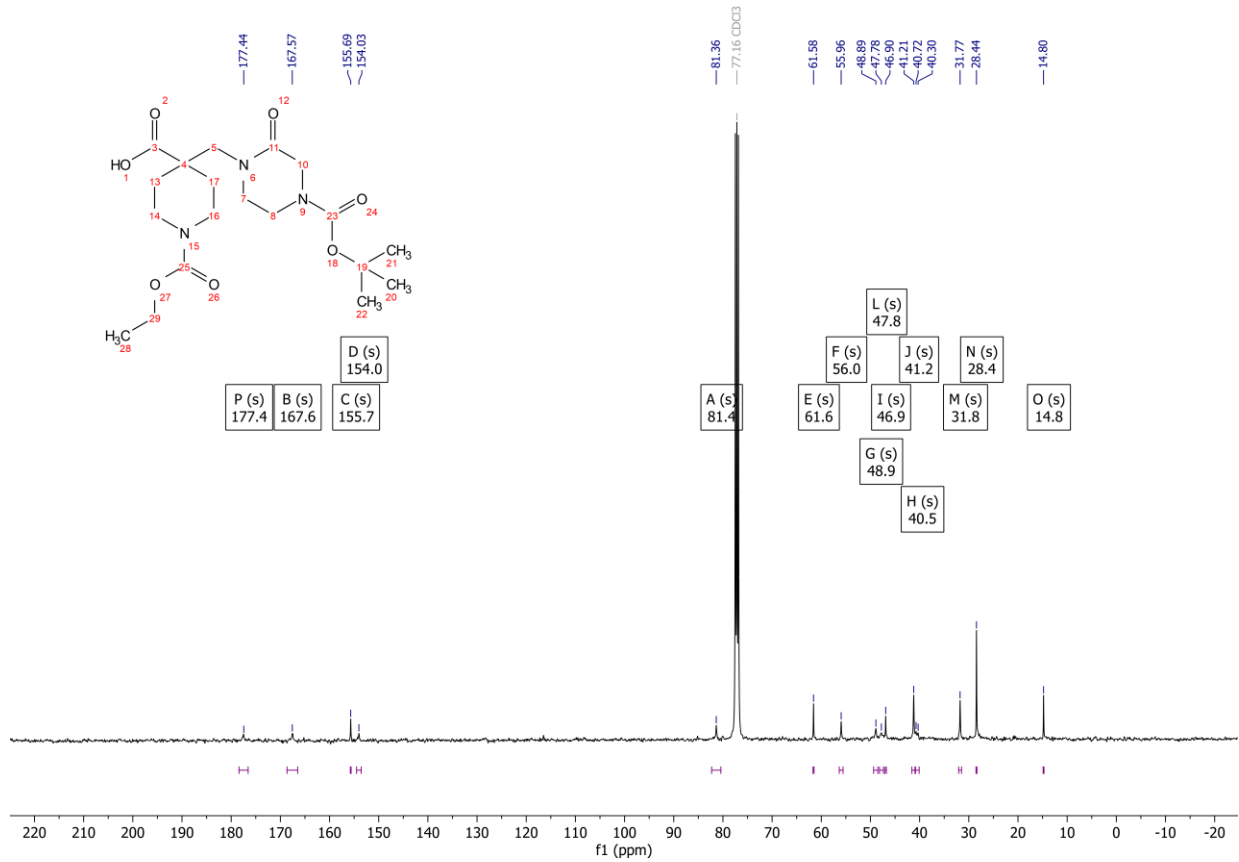
144 ¹³C NMR (101 MHz, CD₃CN)



145 ¹H NMR (400 MHz, CDCl₃)

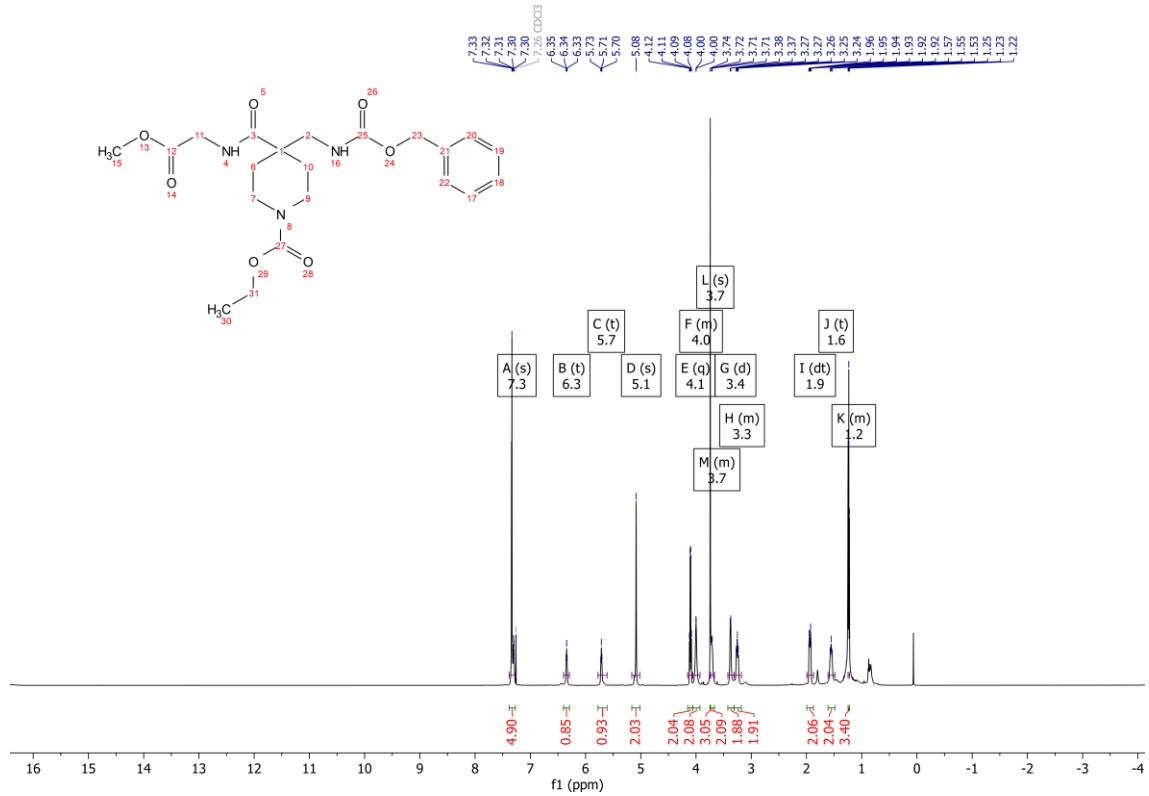


145 ¹³C NMR (101 MHz, CDCl₃)

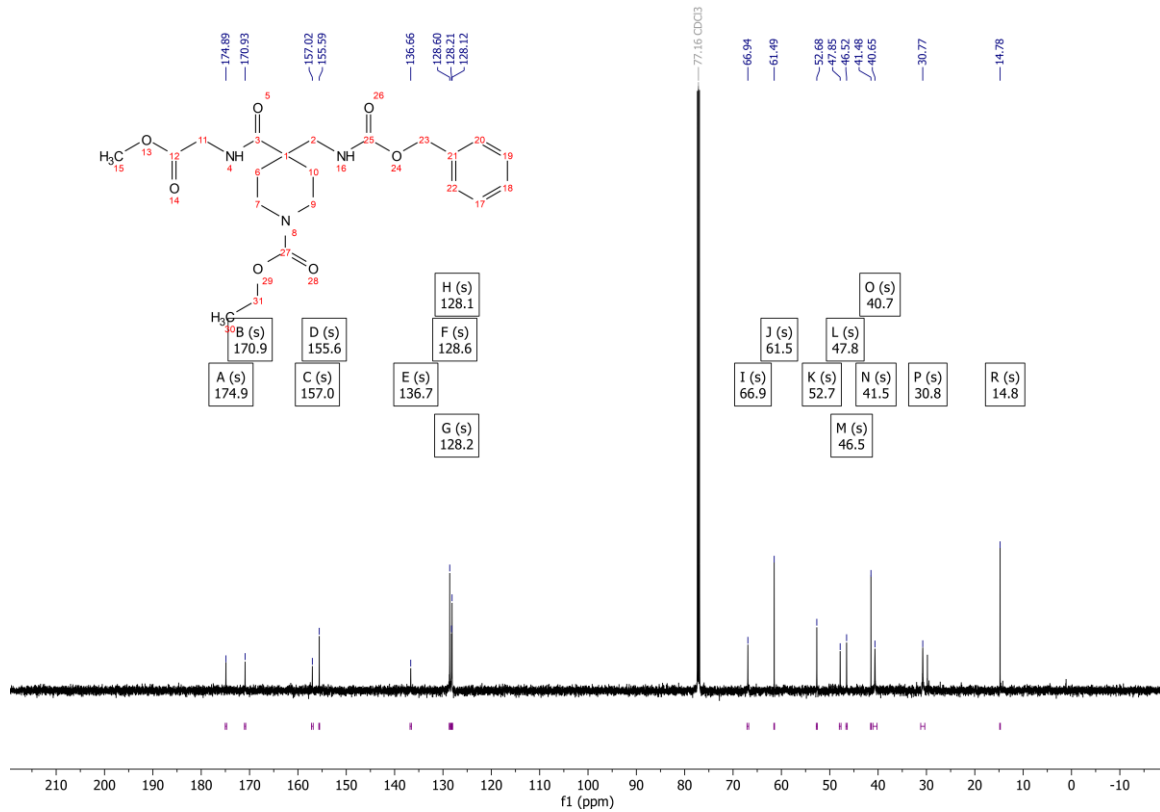


Product Derivatisations

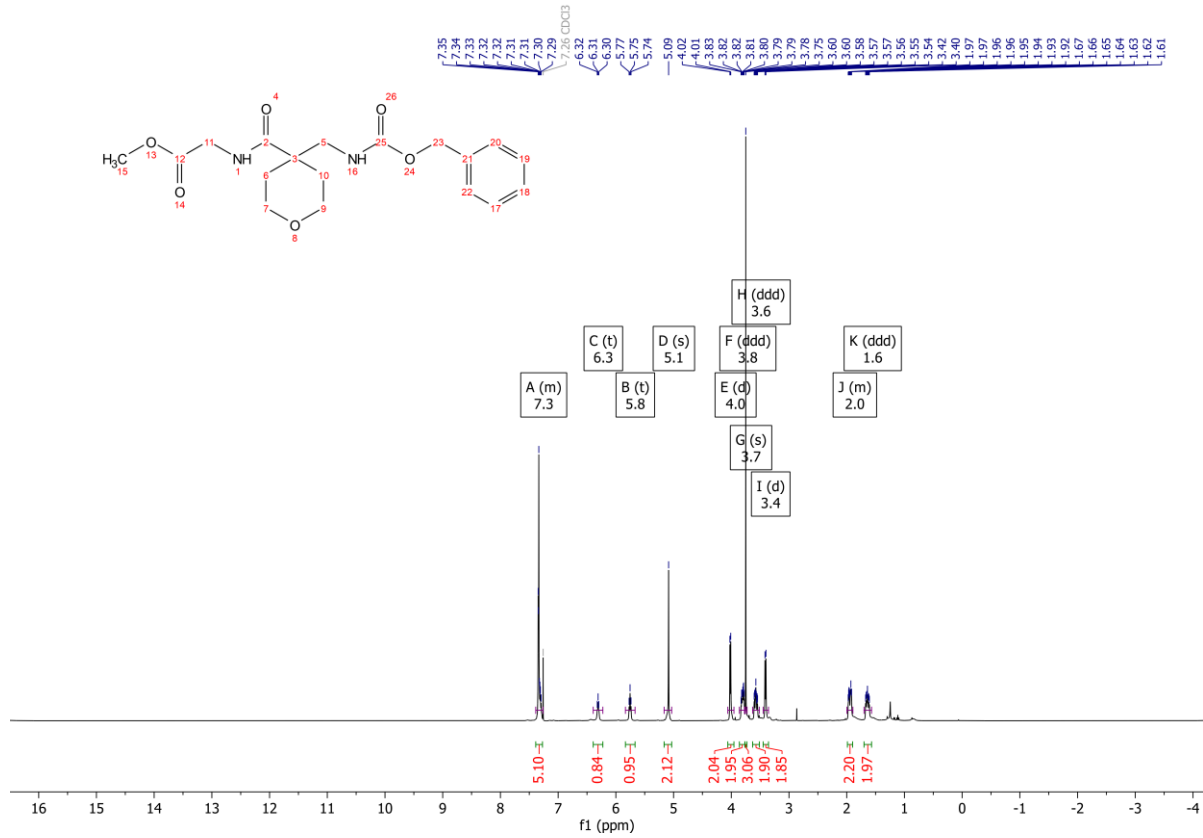
Peptide A ¹H NMR (400 MHz, CDCl₃)



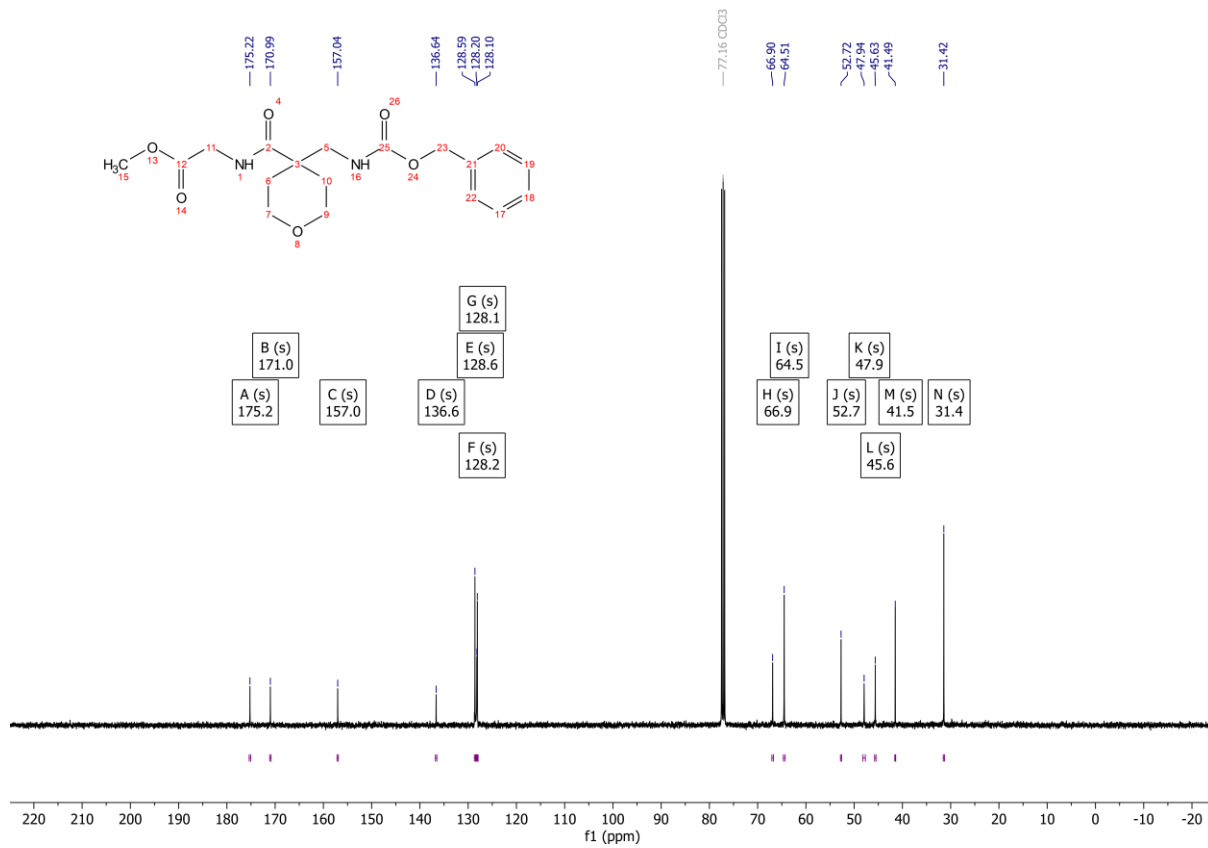
Peptide A ¹³C NMR (101 MHz, CDCl₃)



Peptide B ¹H NMR (400 MHz, CDCl₃)

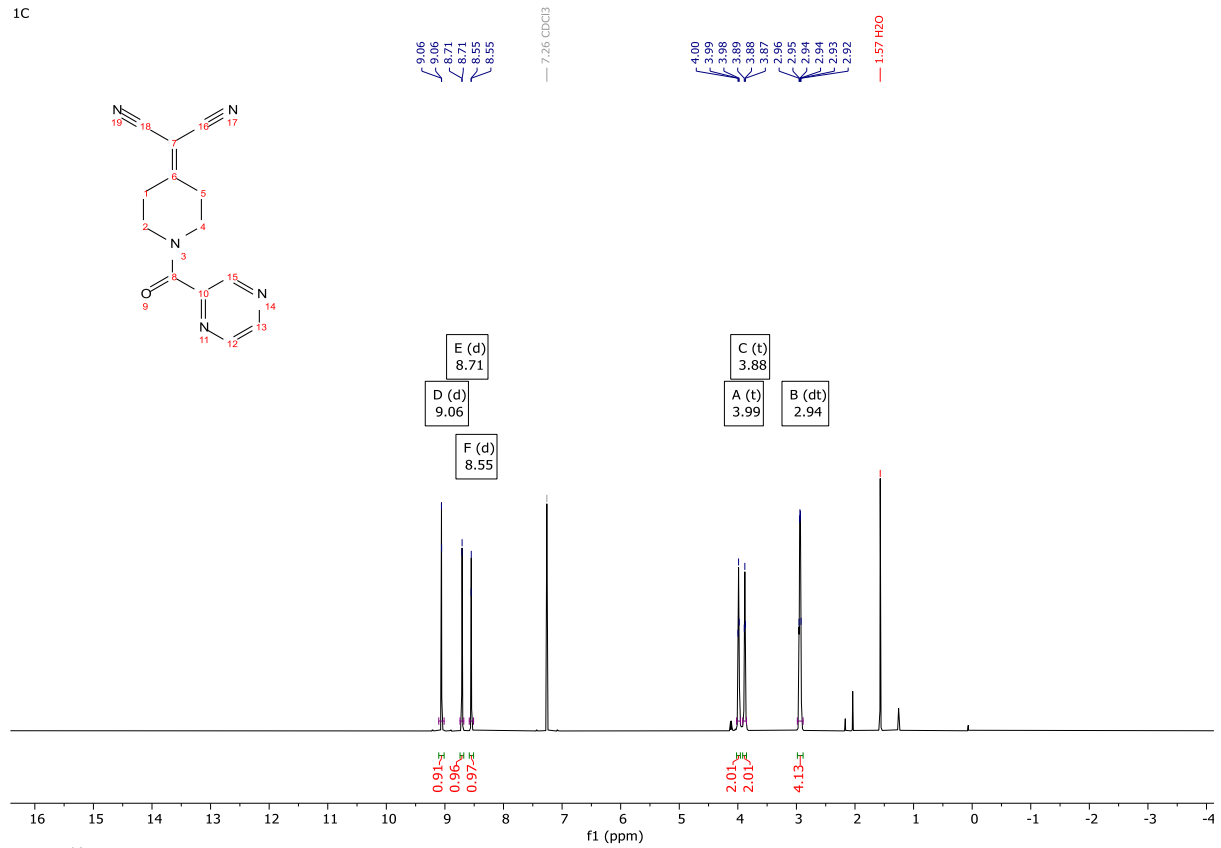


Peptide B ¹³C NMR (101 MHz, CDCl₃)



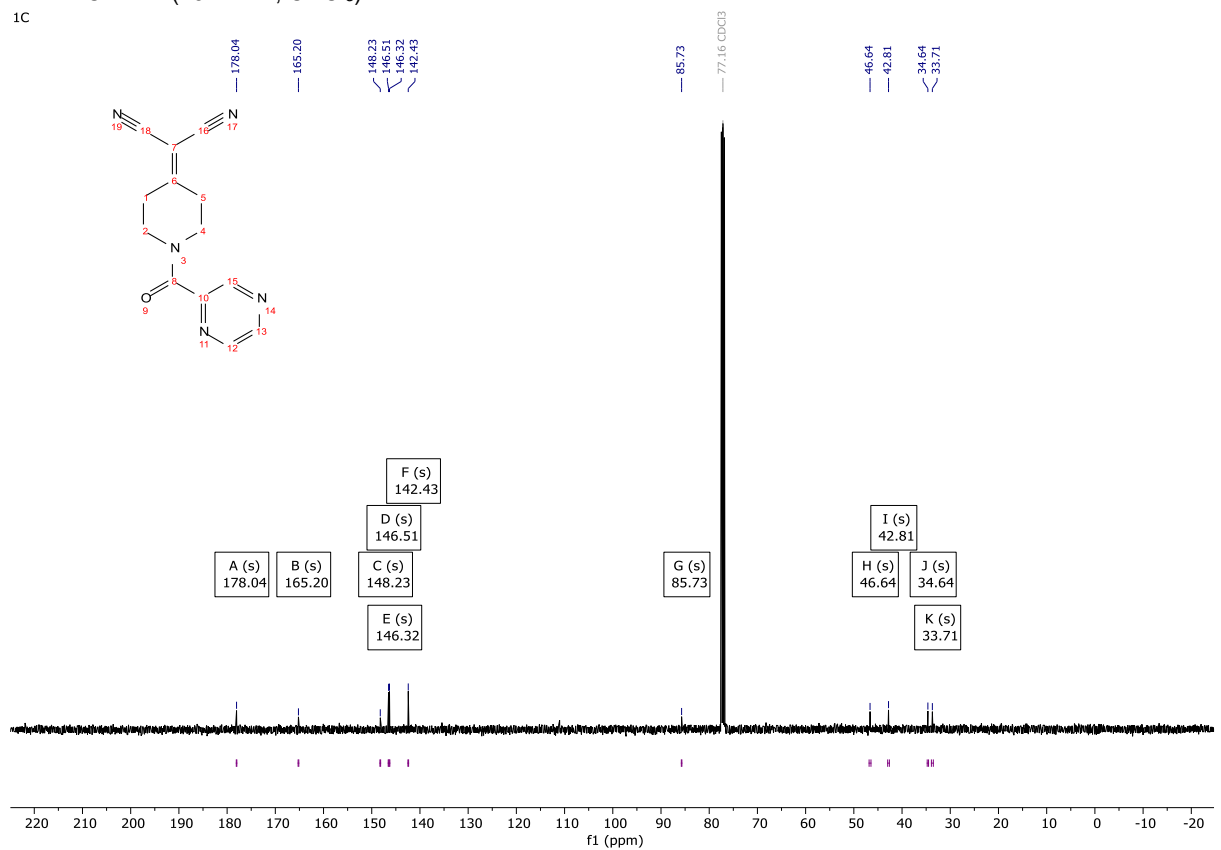
A21 ¹H NMR (400 MHz, CDCl₃)

1C



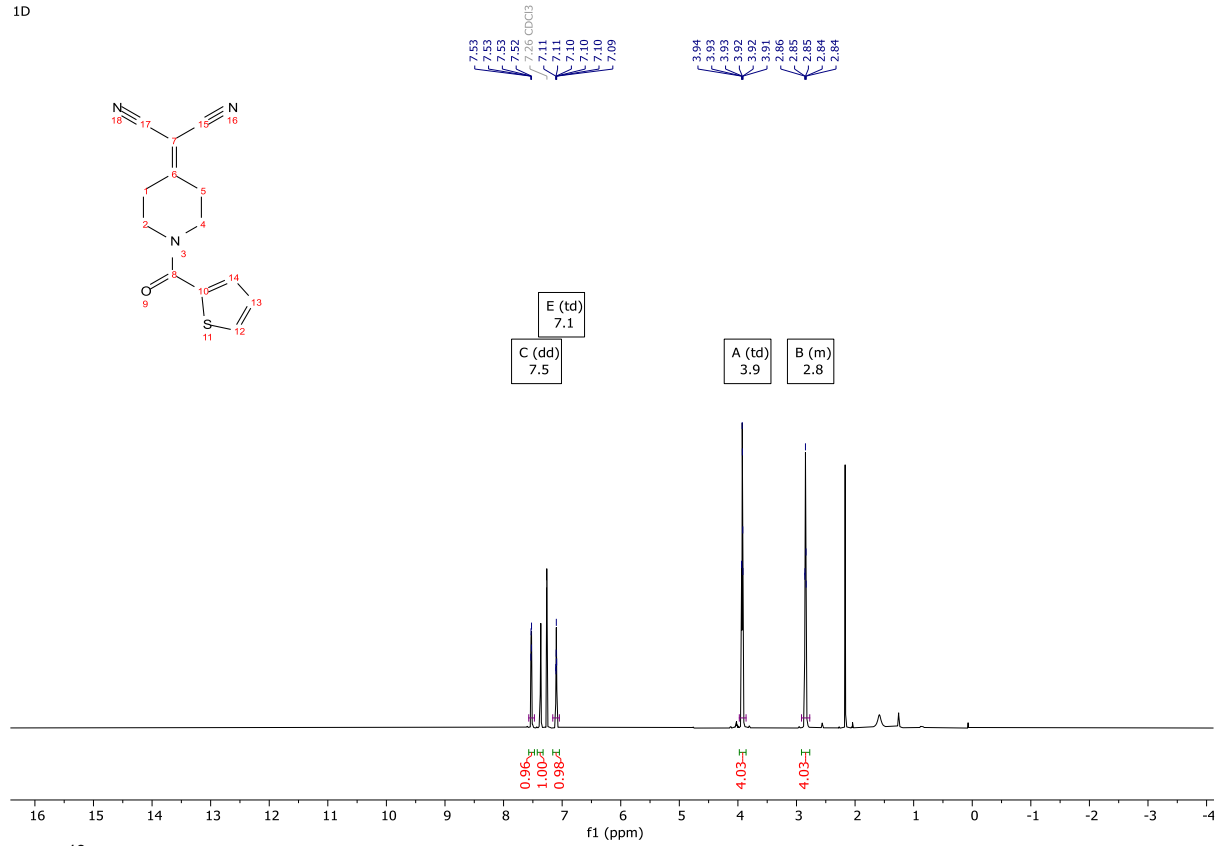
A21 ¹³C NMR (101 MHz, CDCl₃)

1C



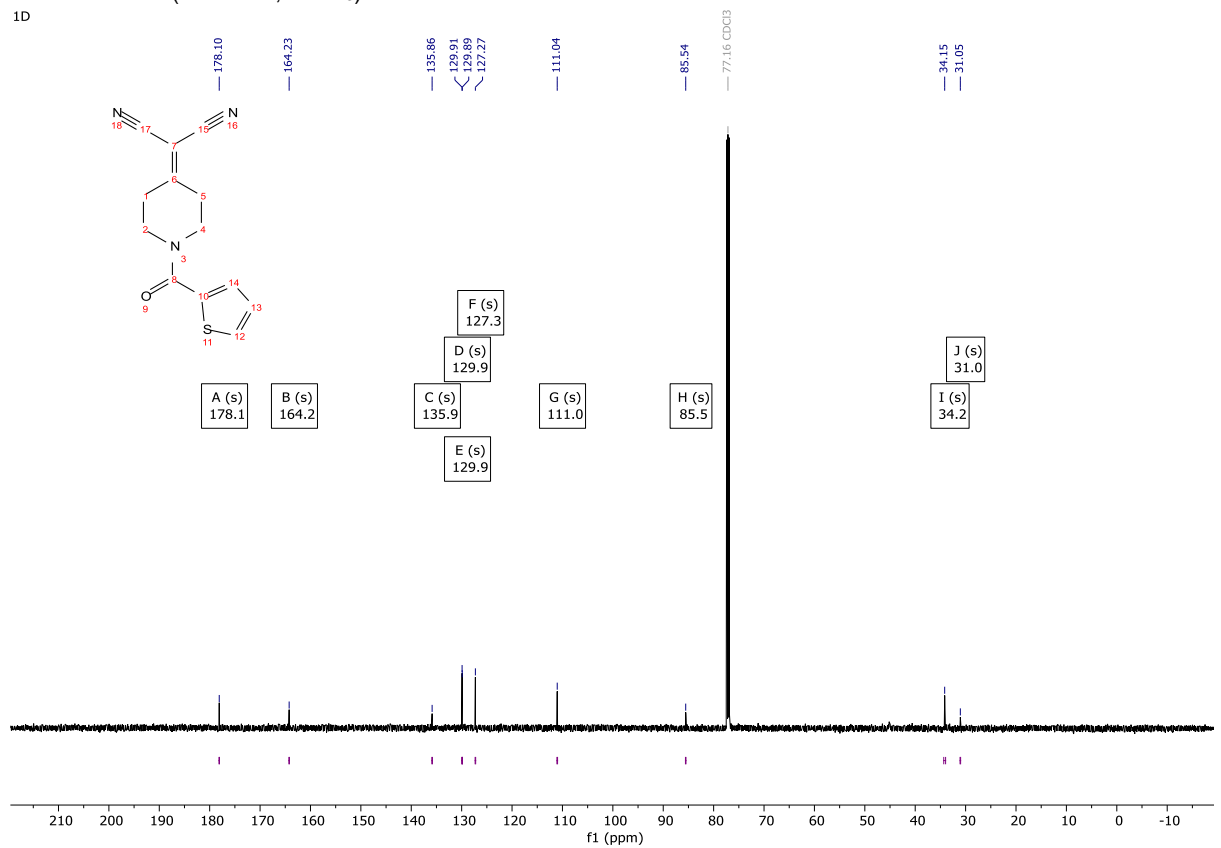
A22 ¹H NMR (400 MHz, CDCl₃)

1D



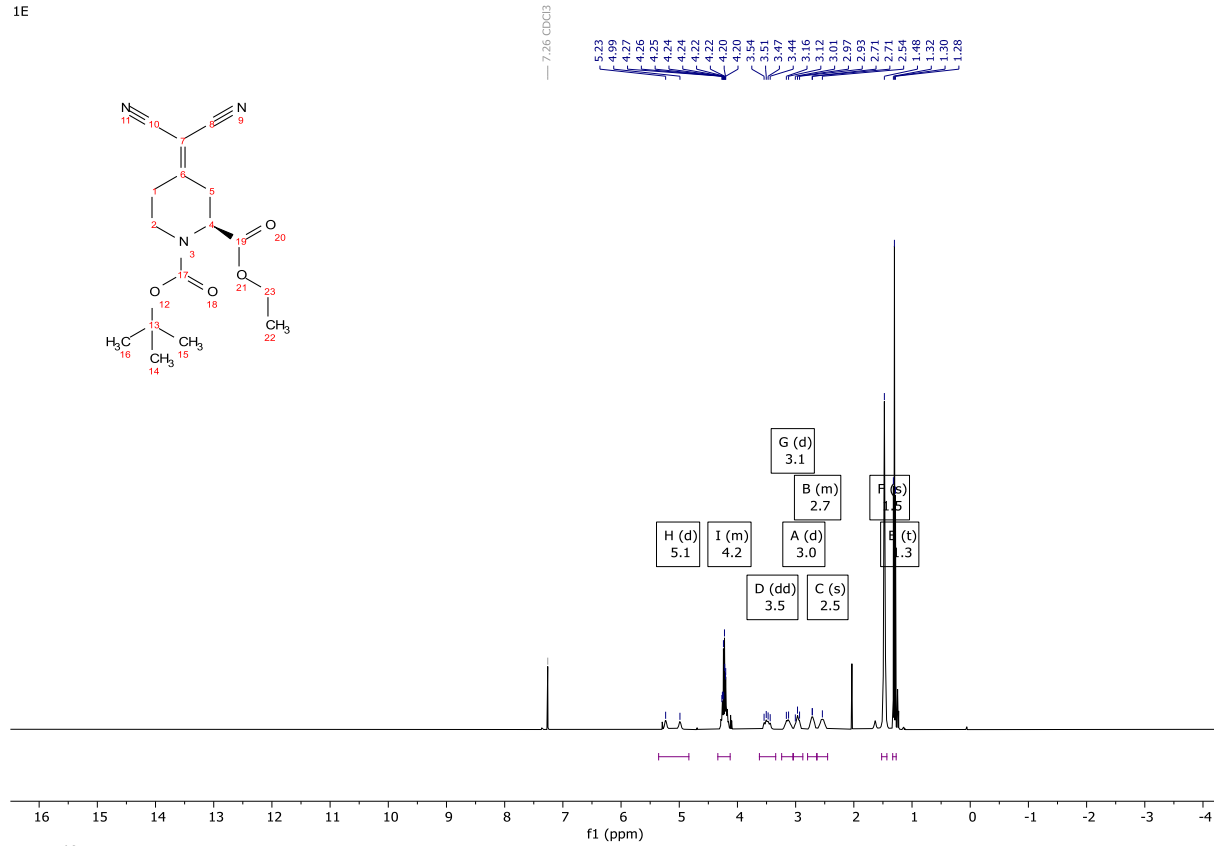
A22 ¹³C NMR (101 MHz, CDCl₃)

1D



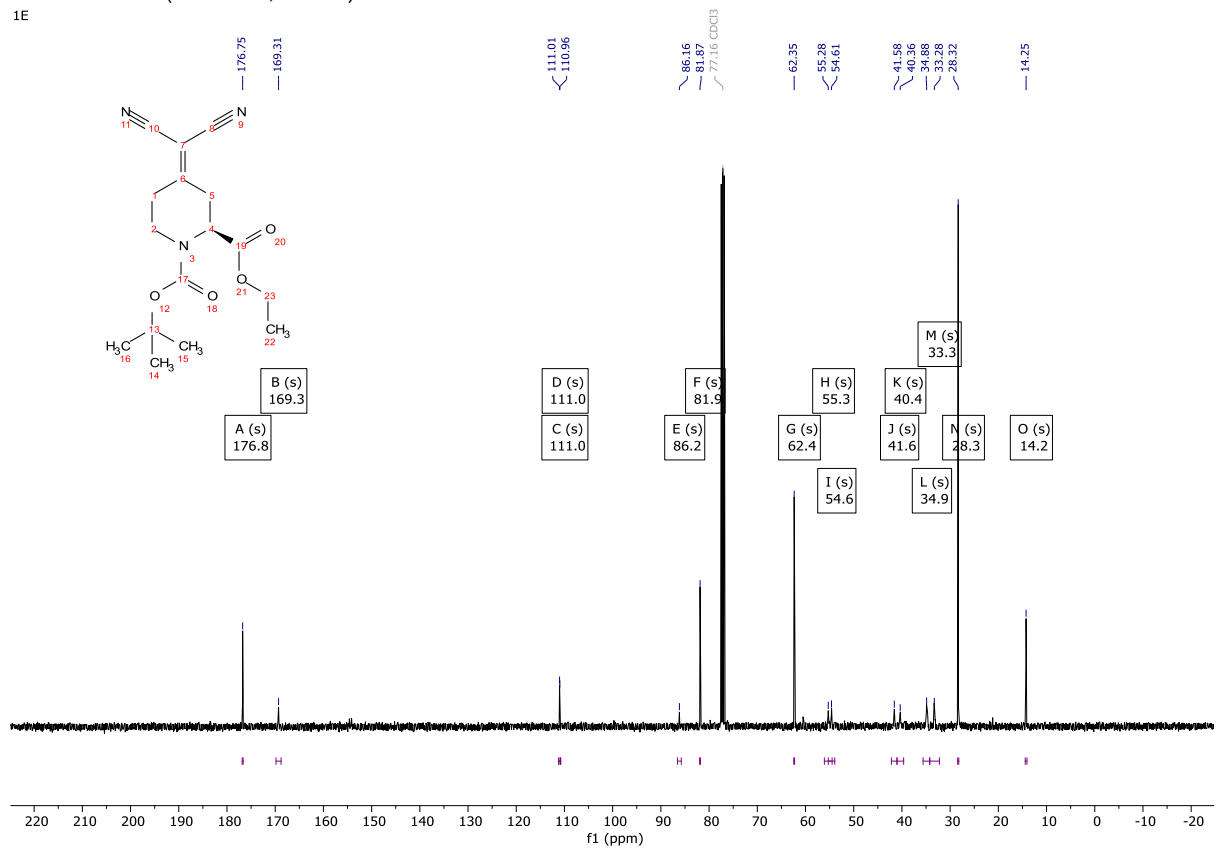
A23 ¹H NMR (400 MHz, CDCl₃)

1E



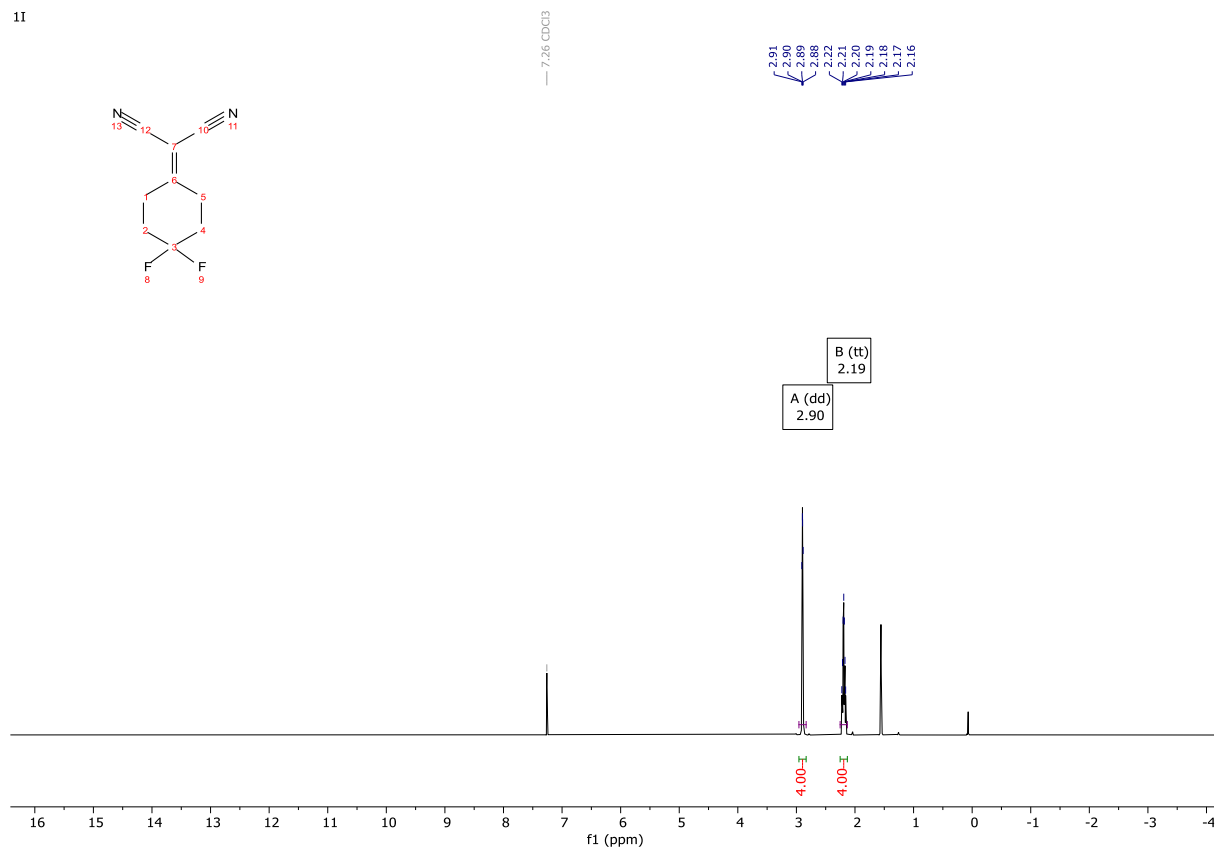
A23 ¹³C NMR (101 MHz, CDCl₃)

1E



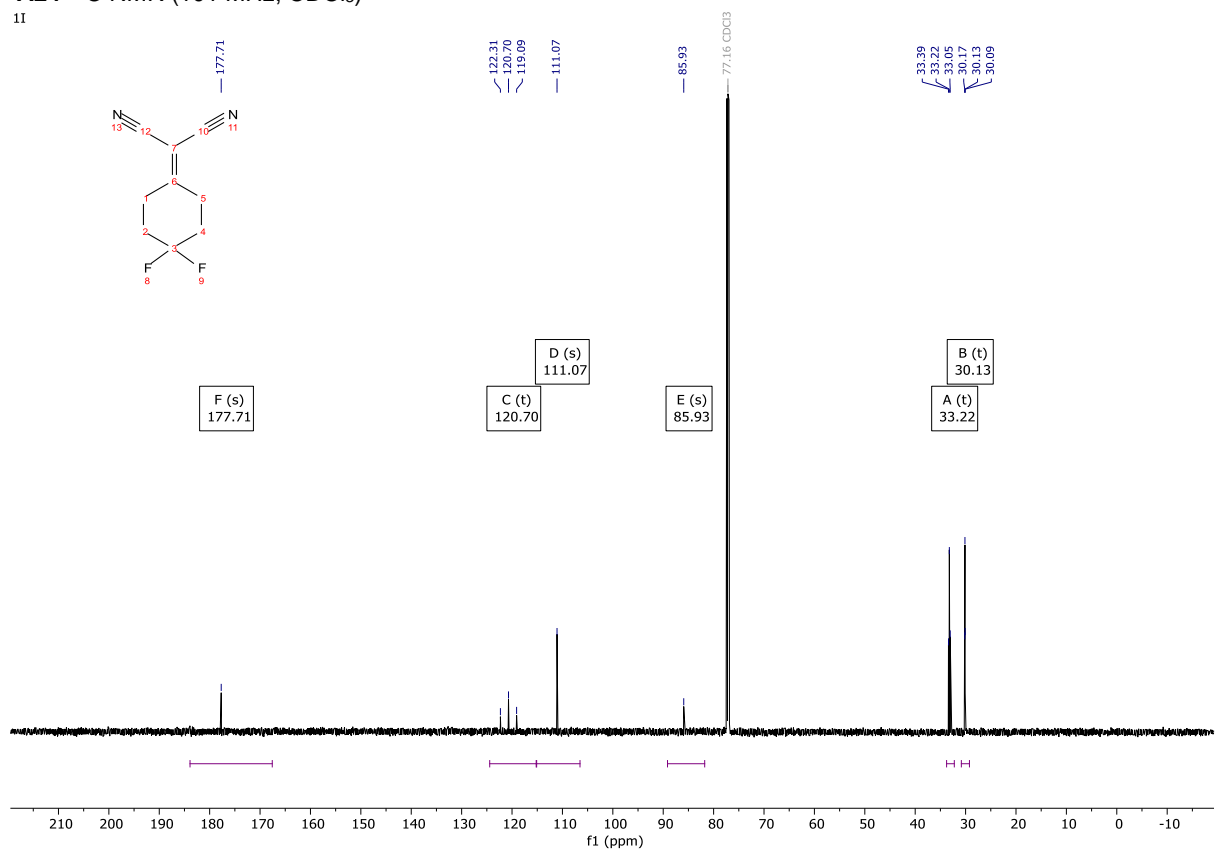
A24 ¹H NMR (400 MHz, CDCl₃)

11



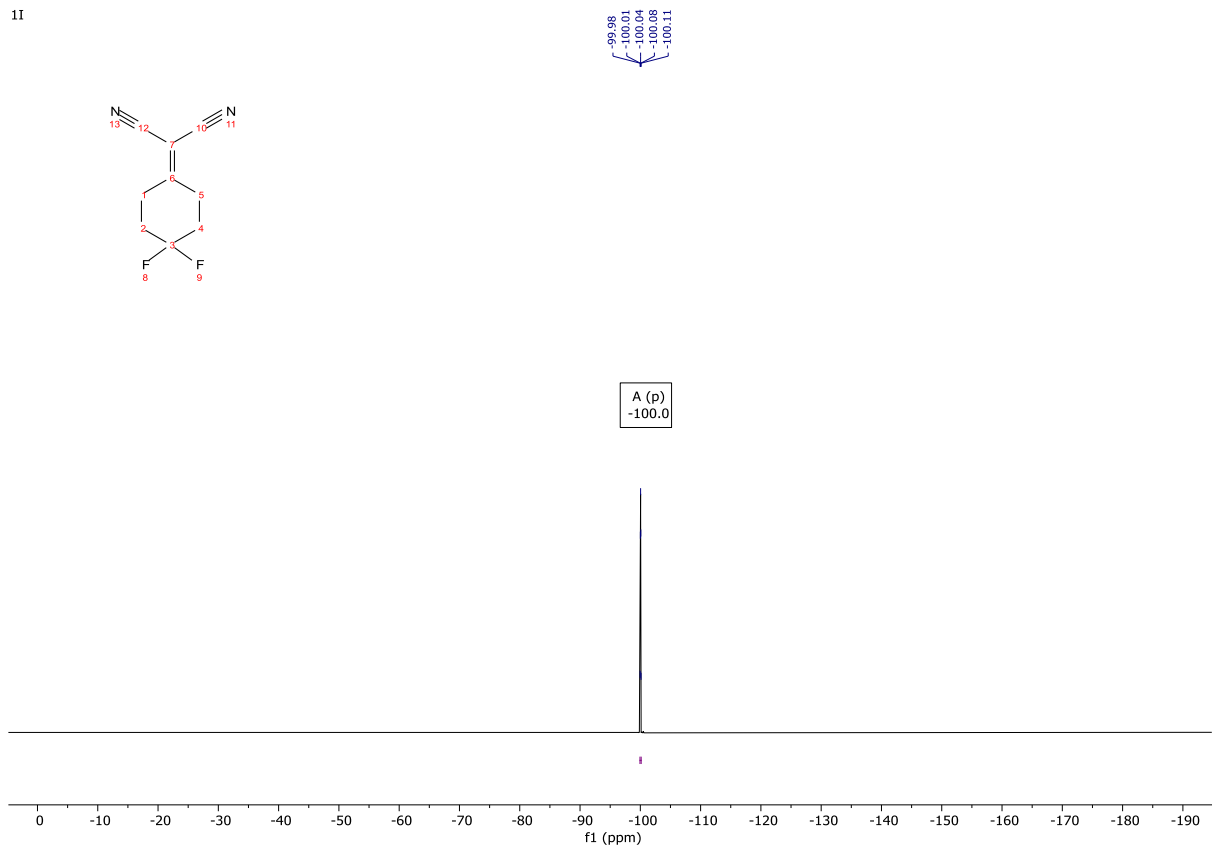
A24 ¹³C NMR (101 MHz, CDCl₃)

11



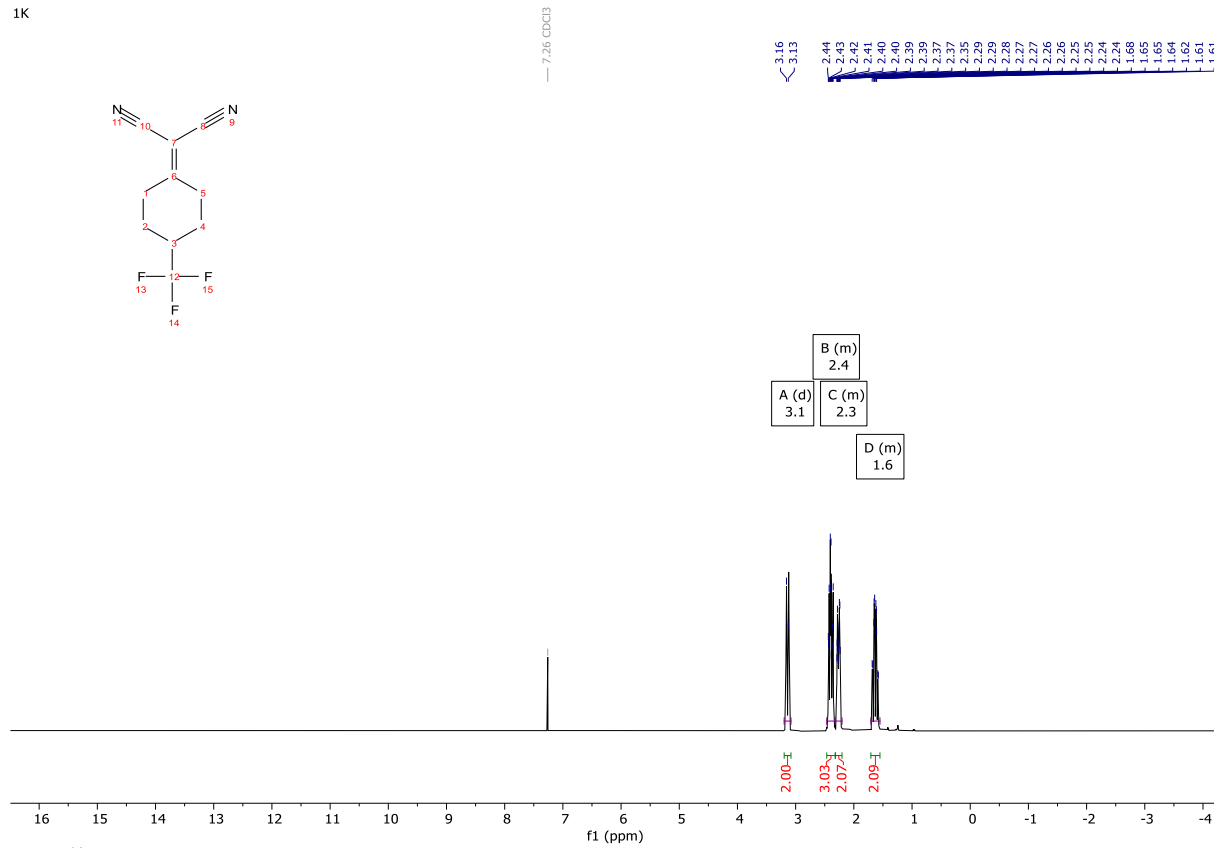
A21¹⁹F{¹H} NMR (376 MHz, CDCl₃)

11



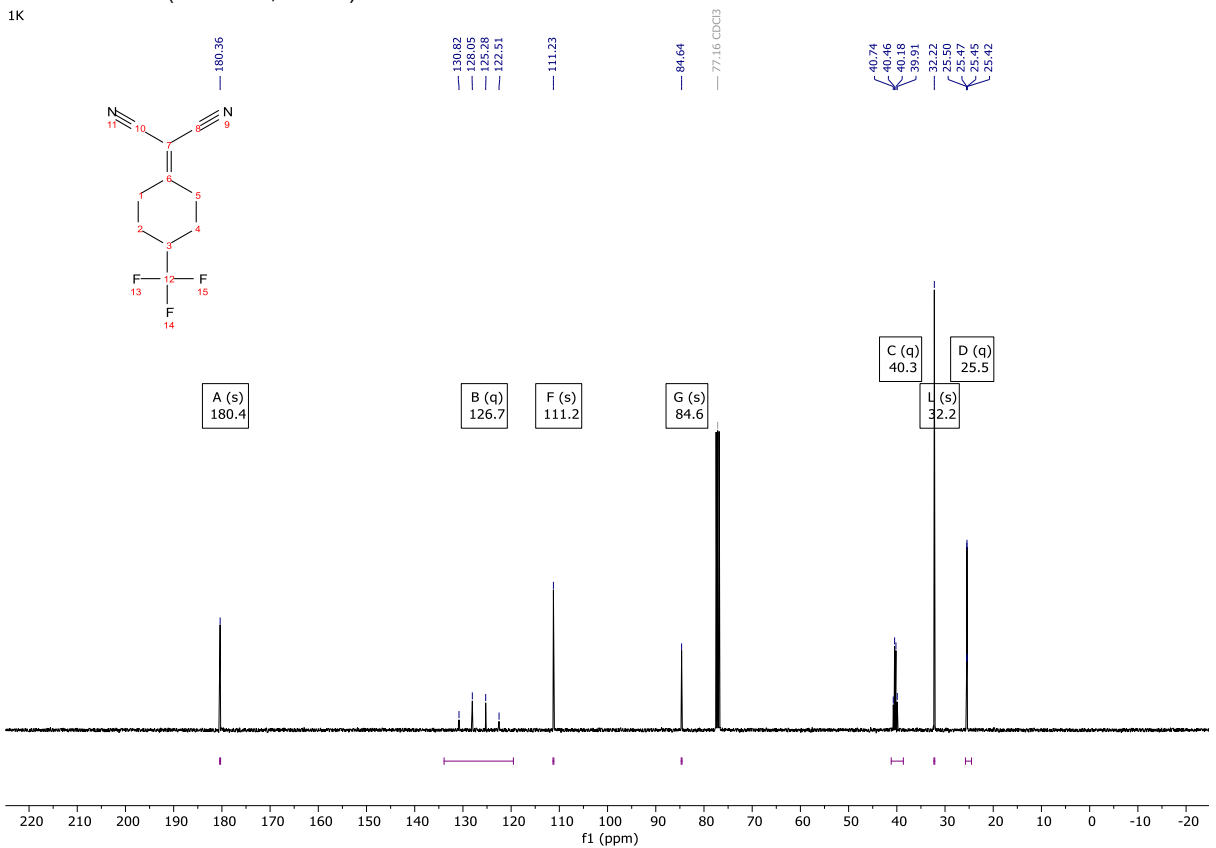
A25 ¹H NMR (400 MHz, CDCl₃)

1K



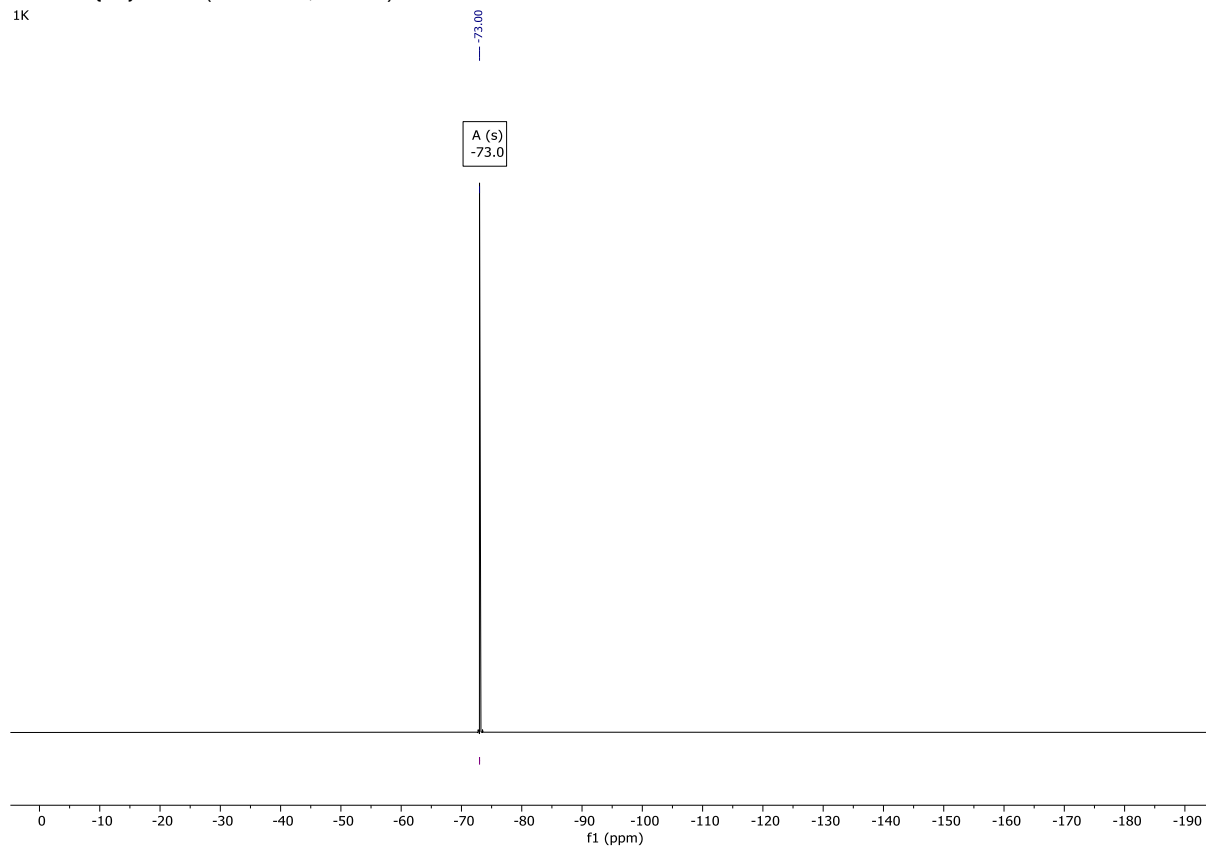
A25 ¹³C NMR (101 MHz, CDCl₃)

1K



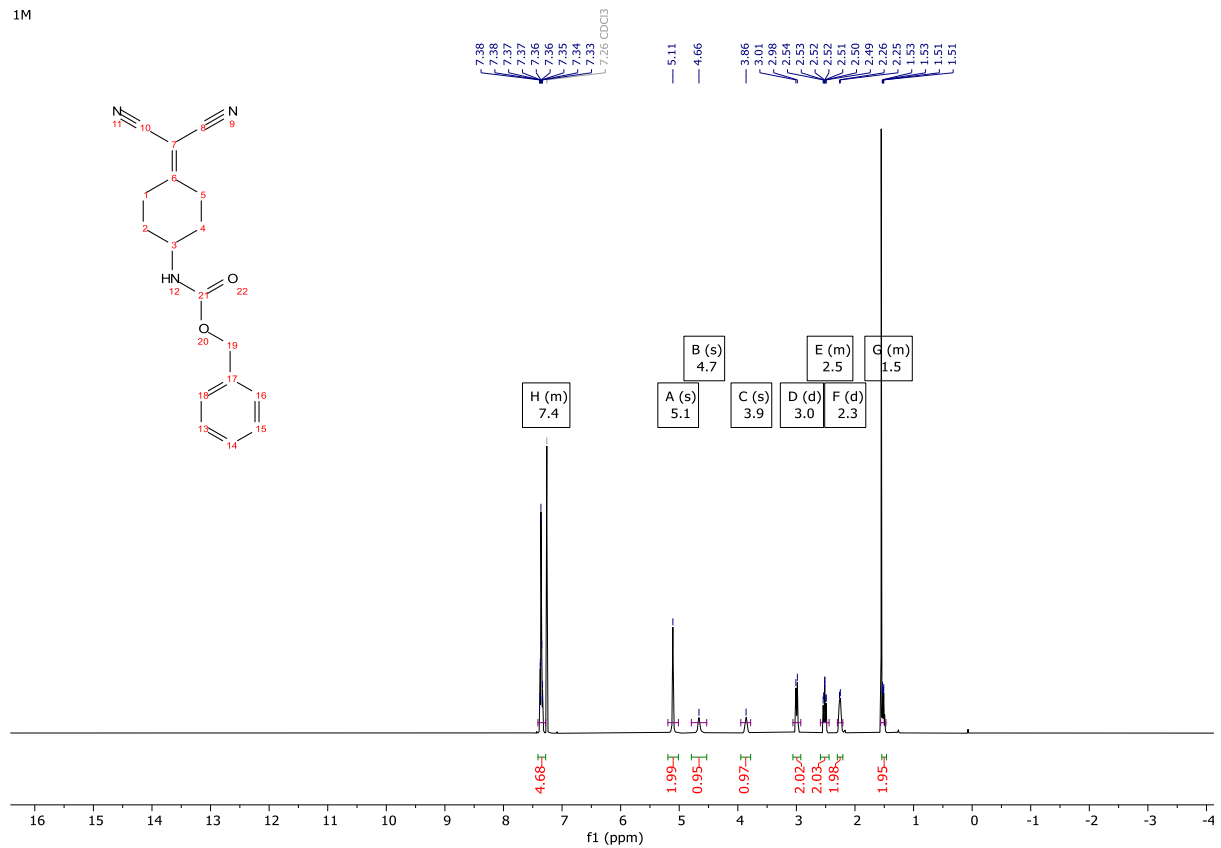
A25 $^{19}\text{F}\{^1\text{H}\}$ NMR (376 MHz, CDCl_3)

1K



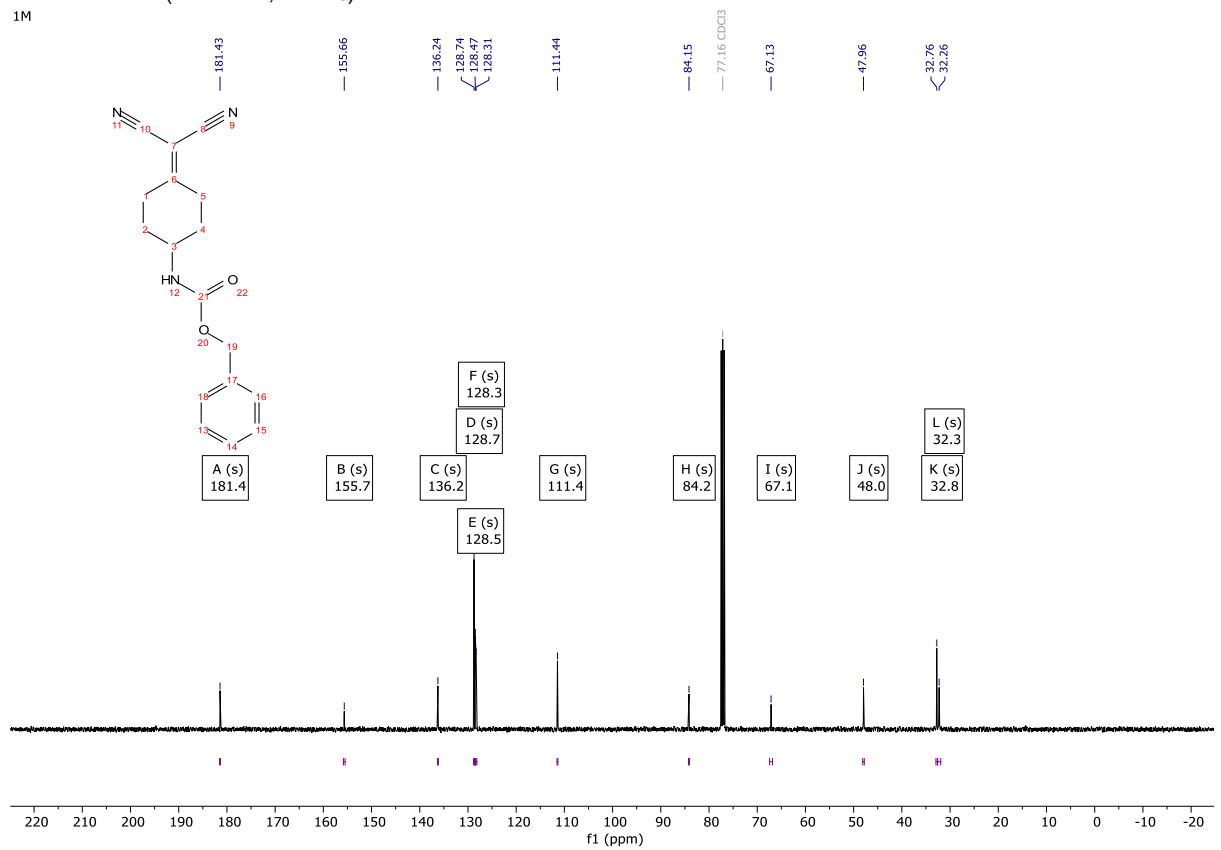
A27 ¹H NMR (400 MHz, CDCl₃)

1M



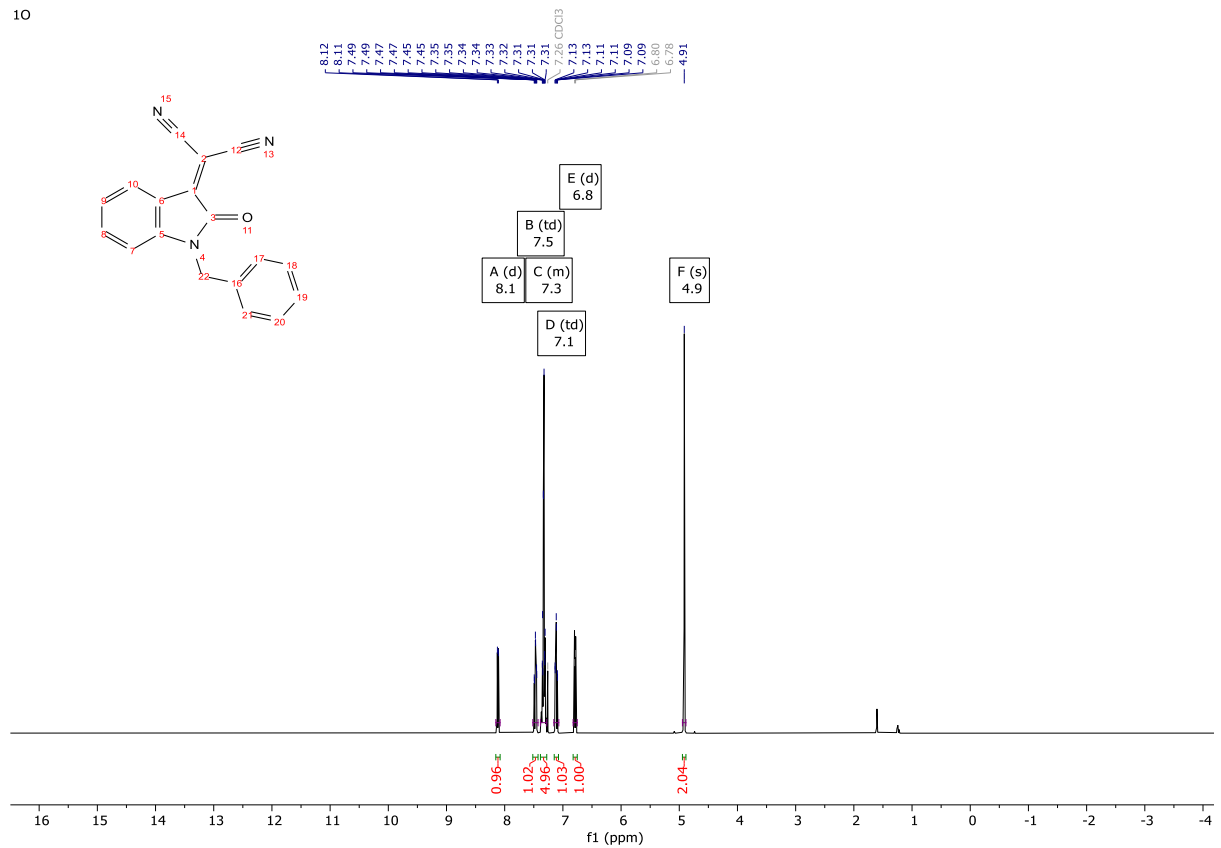
A27 ¹³C NMR (101 MHz, CDCl₃)

1M



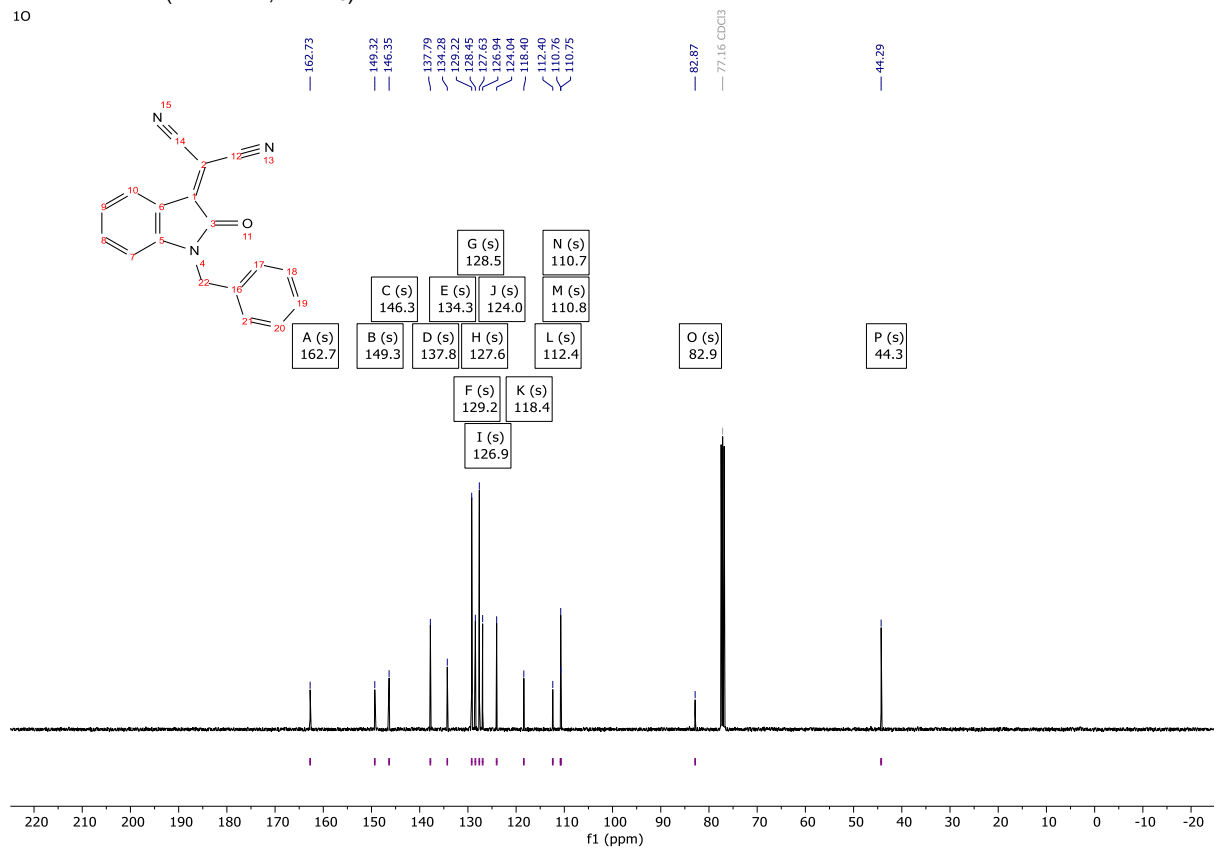
A28 ¹H NMR (400 MHz, CDCl₃)

10



A28 ¹³C NMR (101 MHz, CDCl₃)

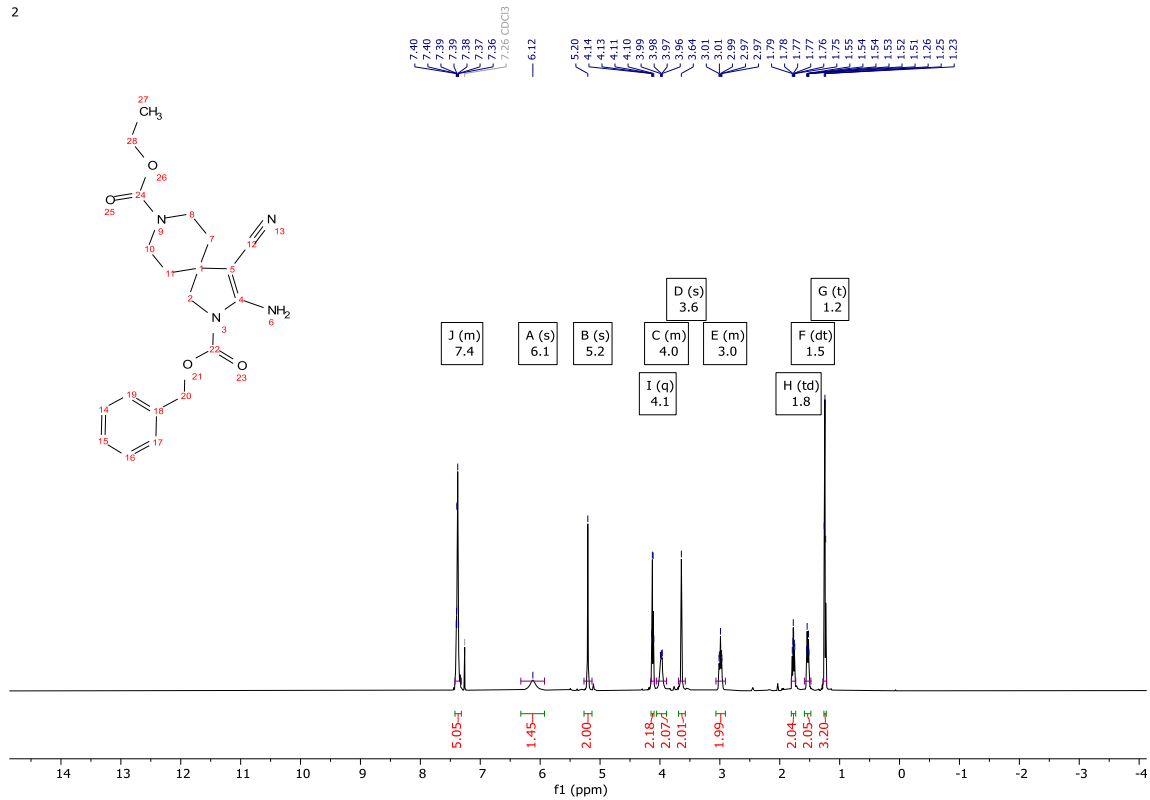
10



Polar Spirocycles

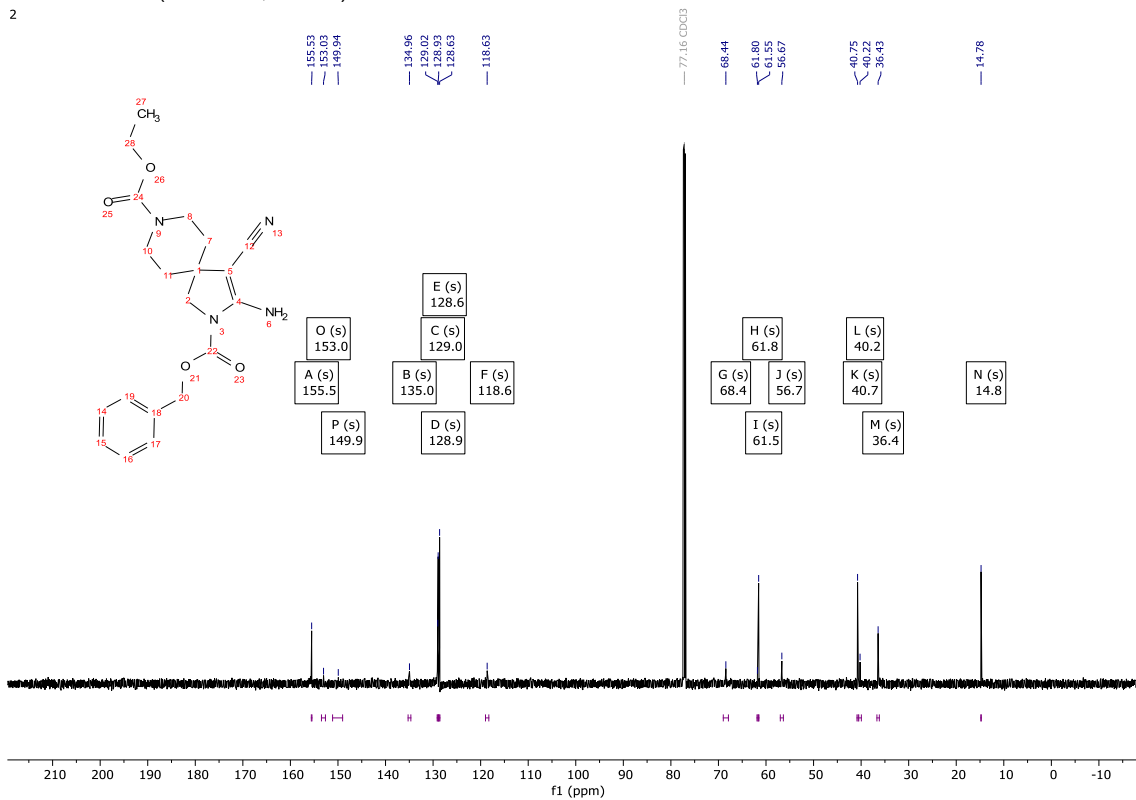
111 ¹H NMR (400 MHz, CDCl₃)

2



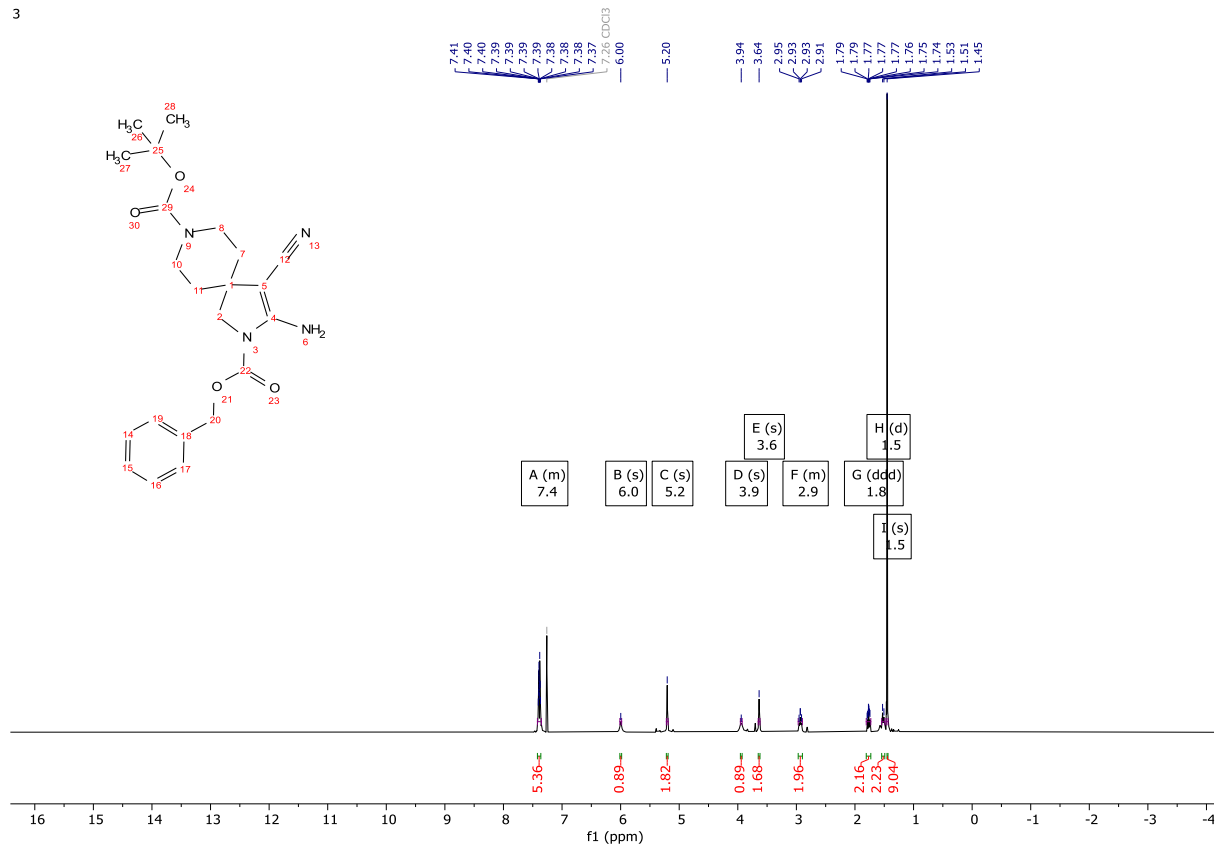
111 ¹³C NMR (101 MHz, CDCl₃)

2



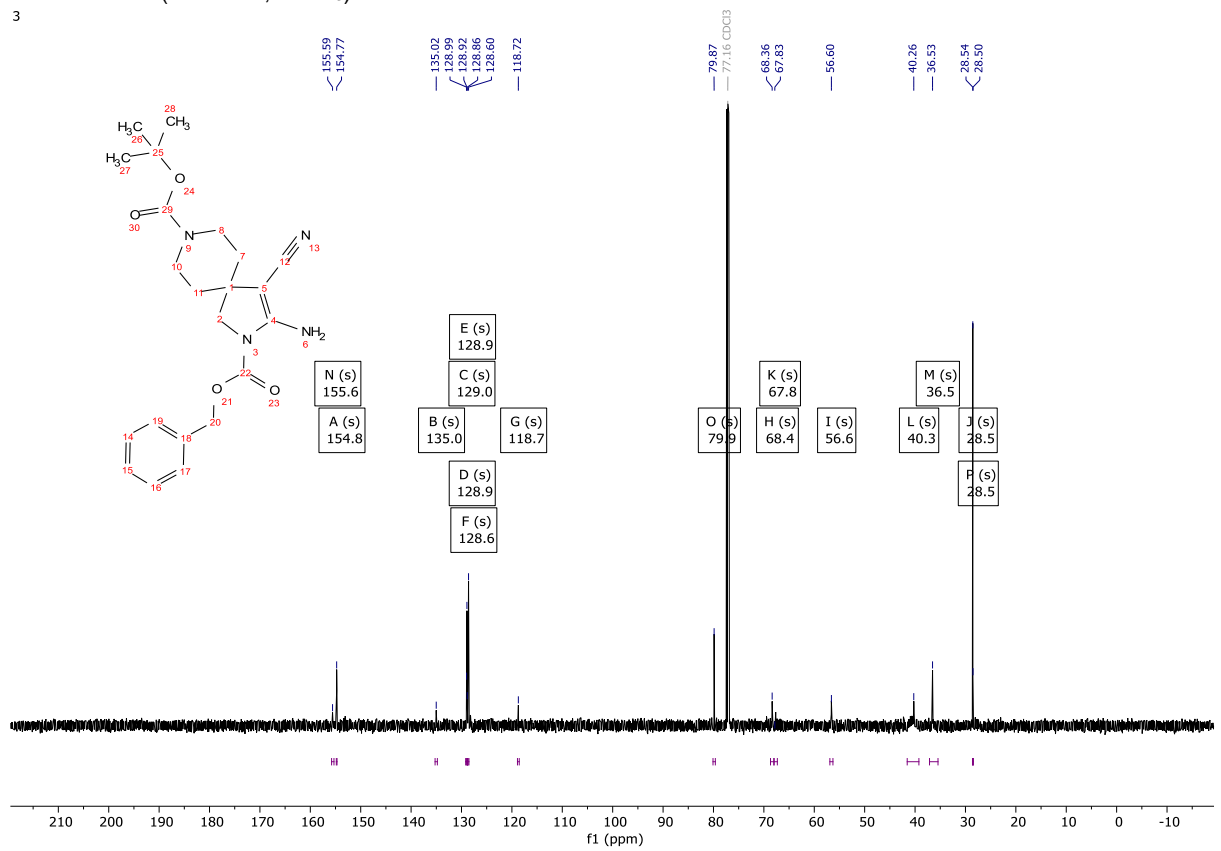
201 ¹H NMR (400 MHz, CDCl₃)

3



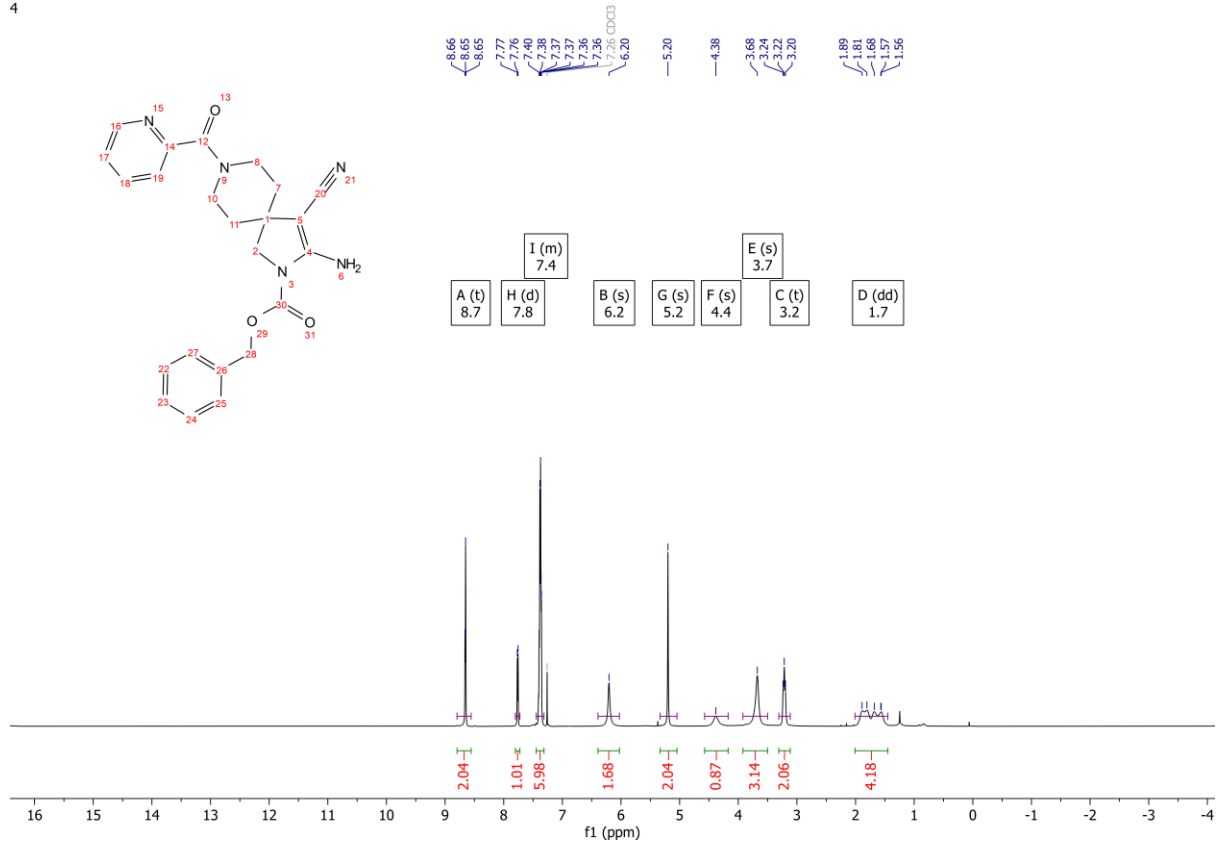
201 ¹³C NMR (101 MHz, CDCl₃)

3



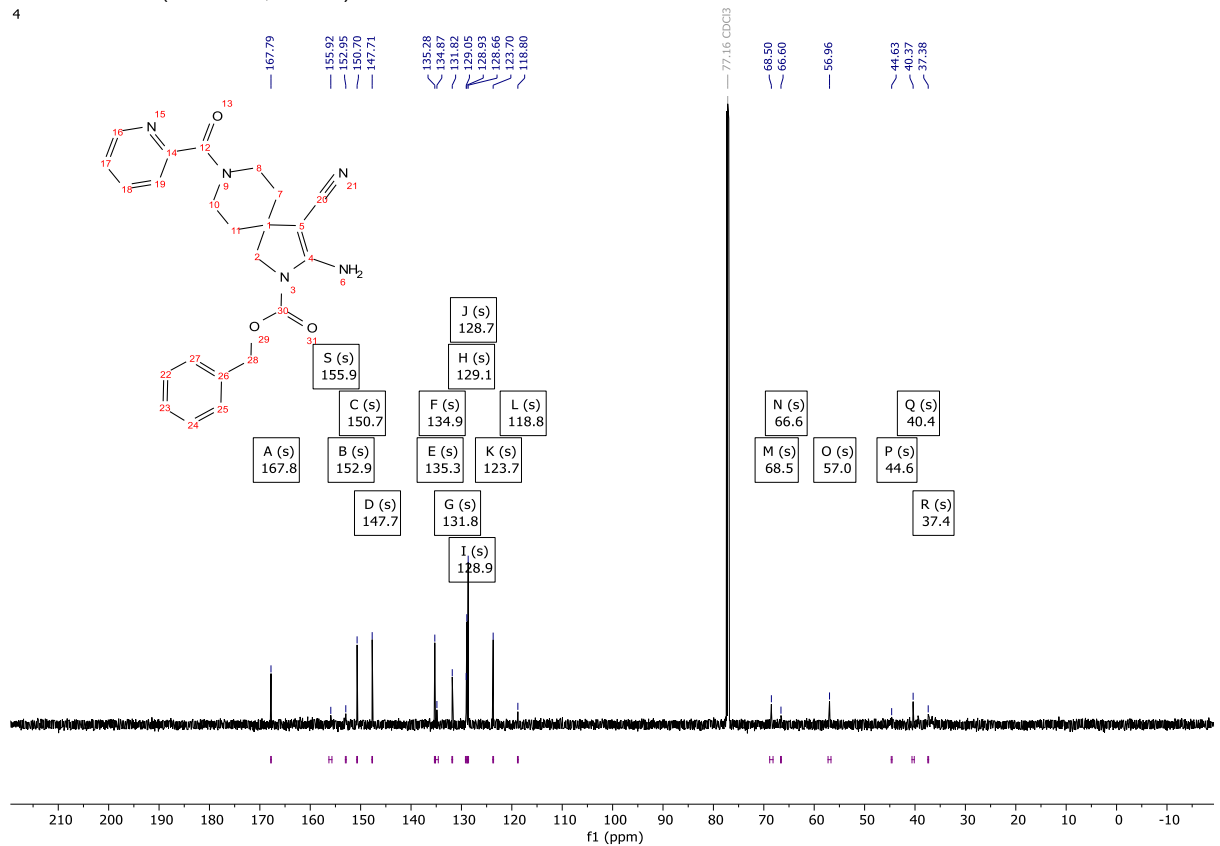
202 ¹H NMR (400 MHz, CDCl₃)

4



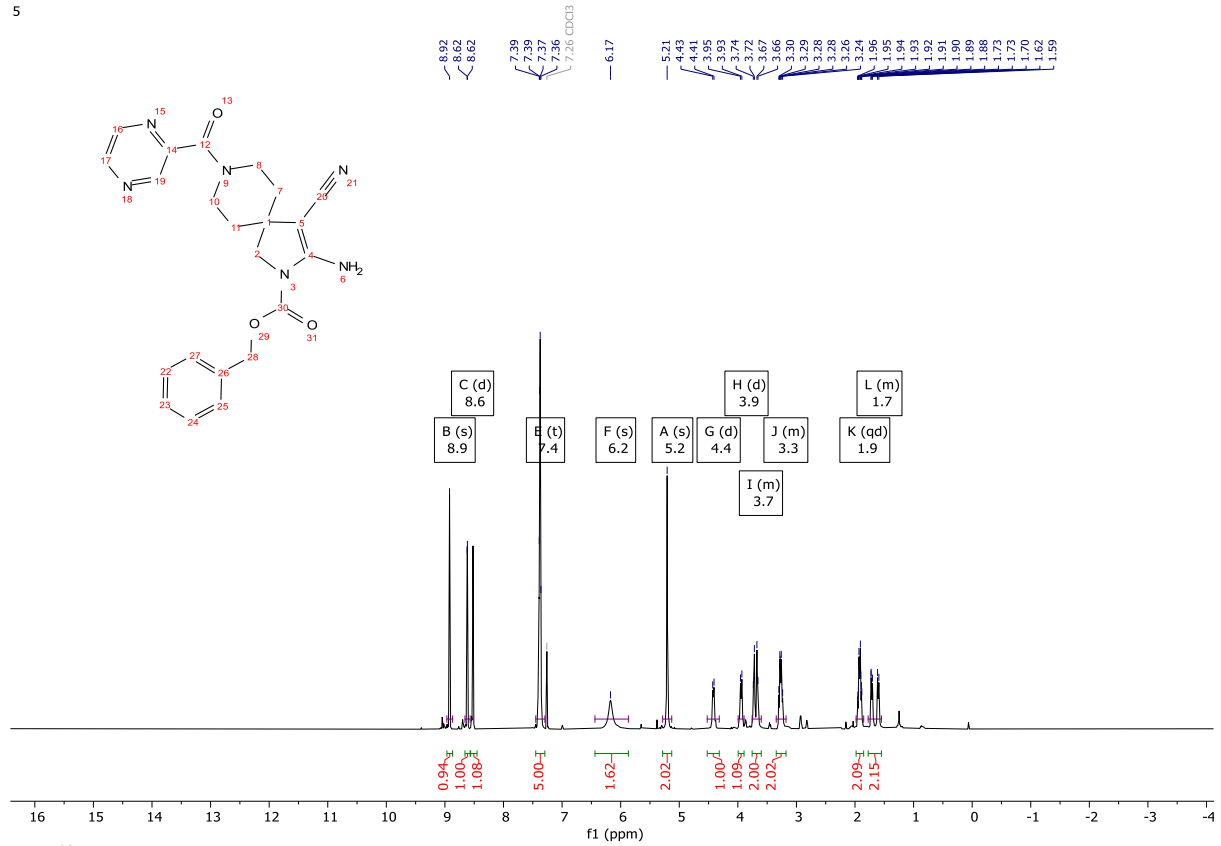
202 ¹³C NMR (101 MHz, CDCl₃)

4



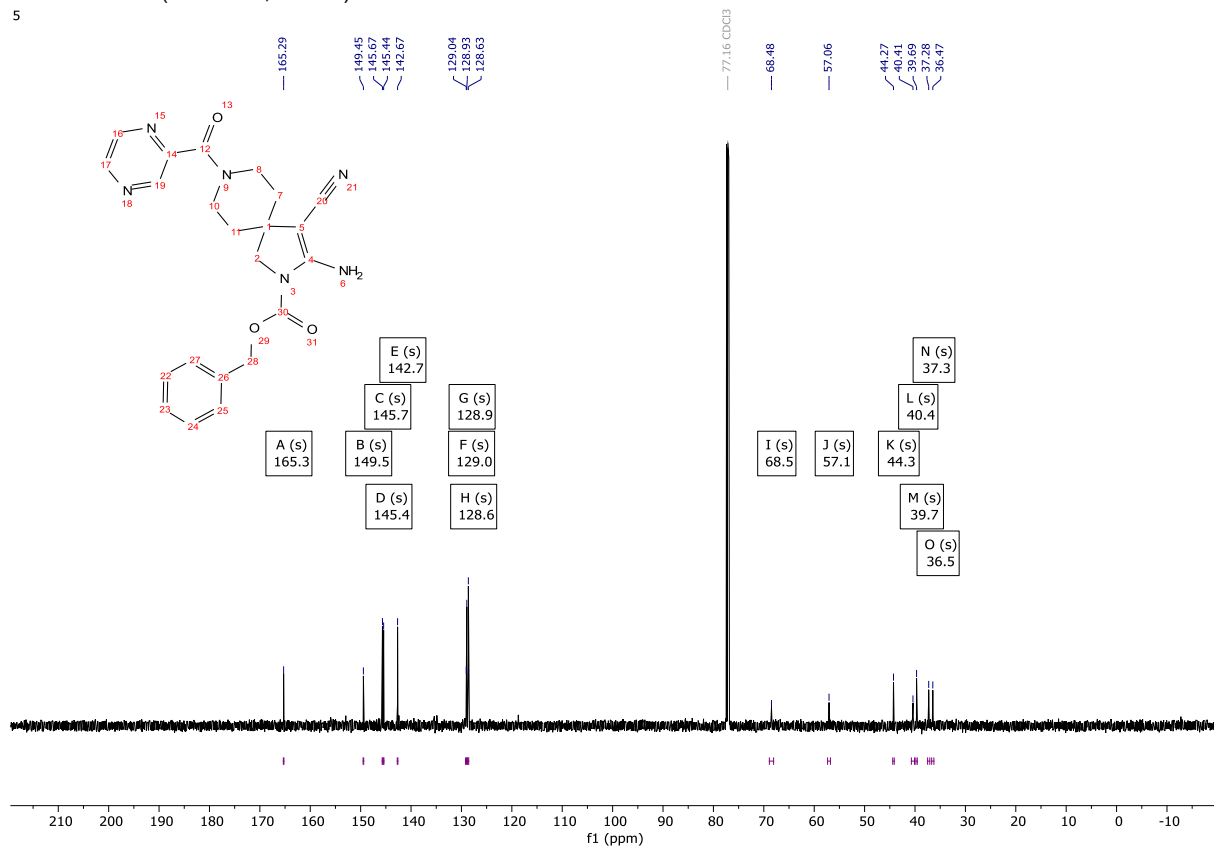
203 ¹H NMR (400 MHz, CDCl₃)

5



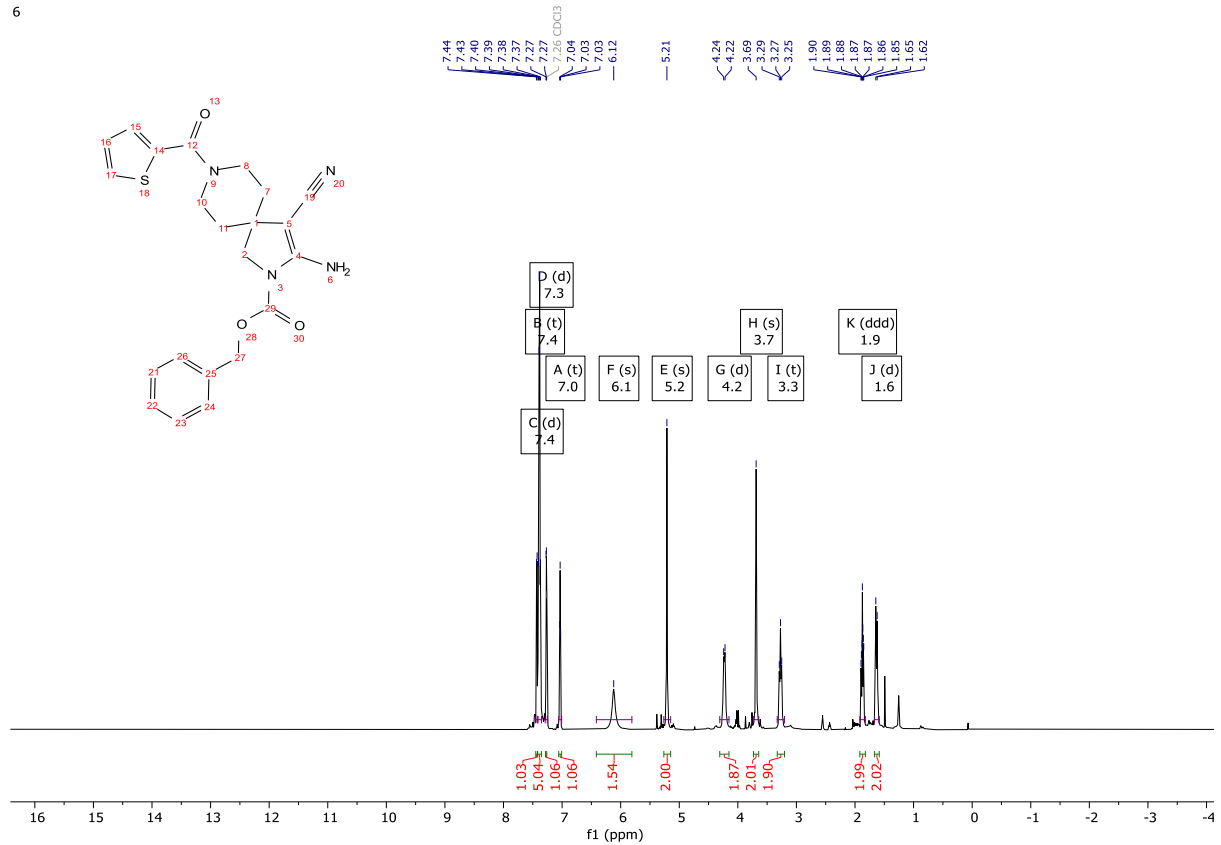
203 ¹³C NMR (101 MHz, CDCl₃)

5



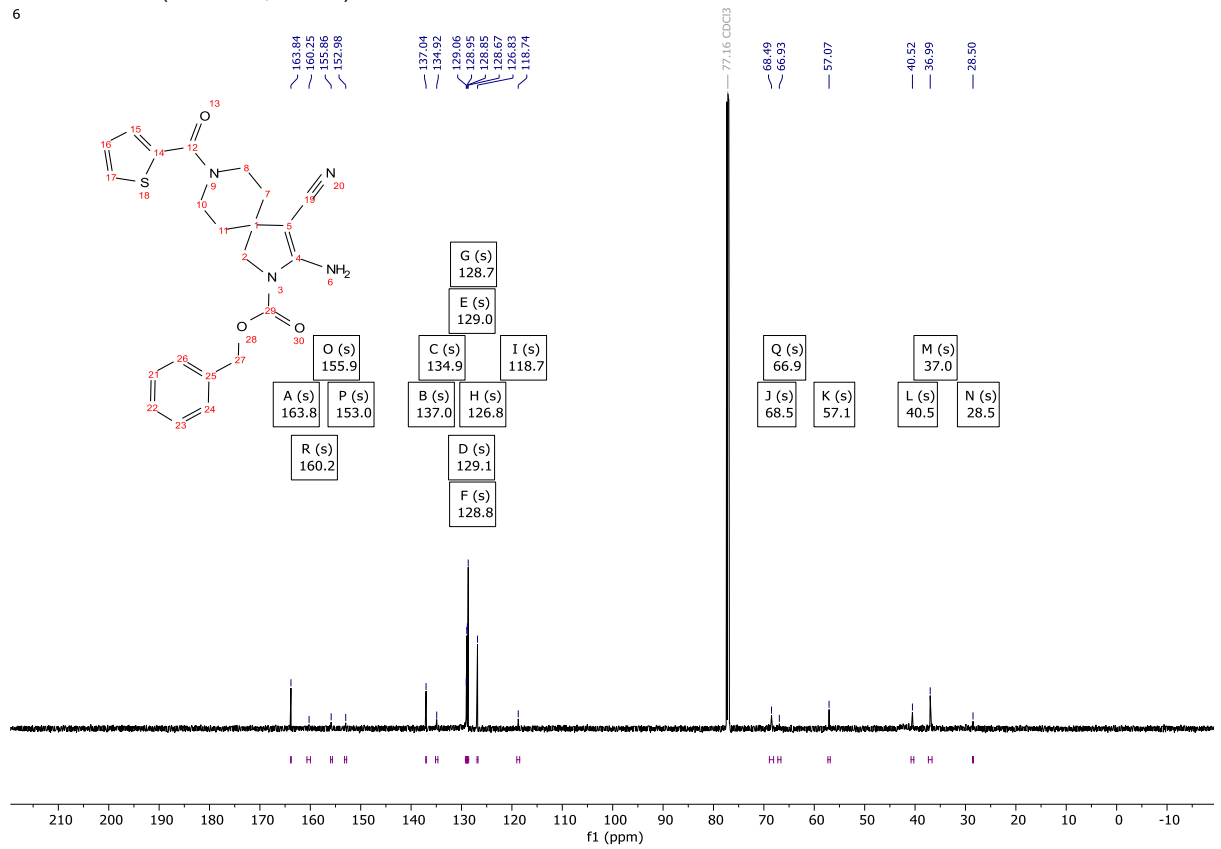
204 ¹H NMR (400 MHz, CDCl₃)

6



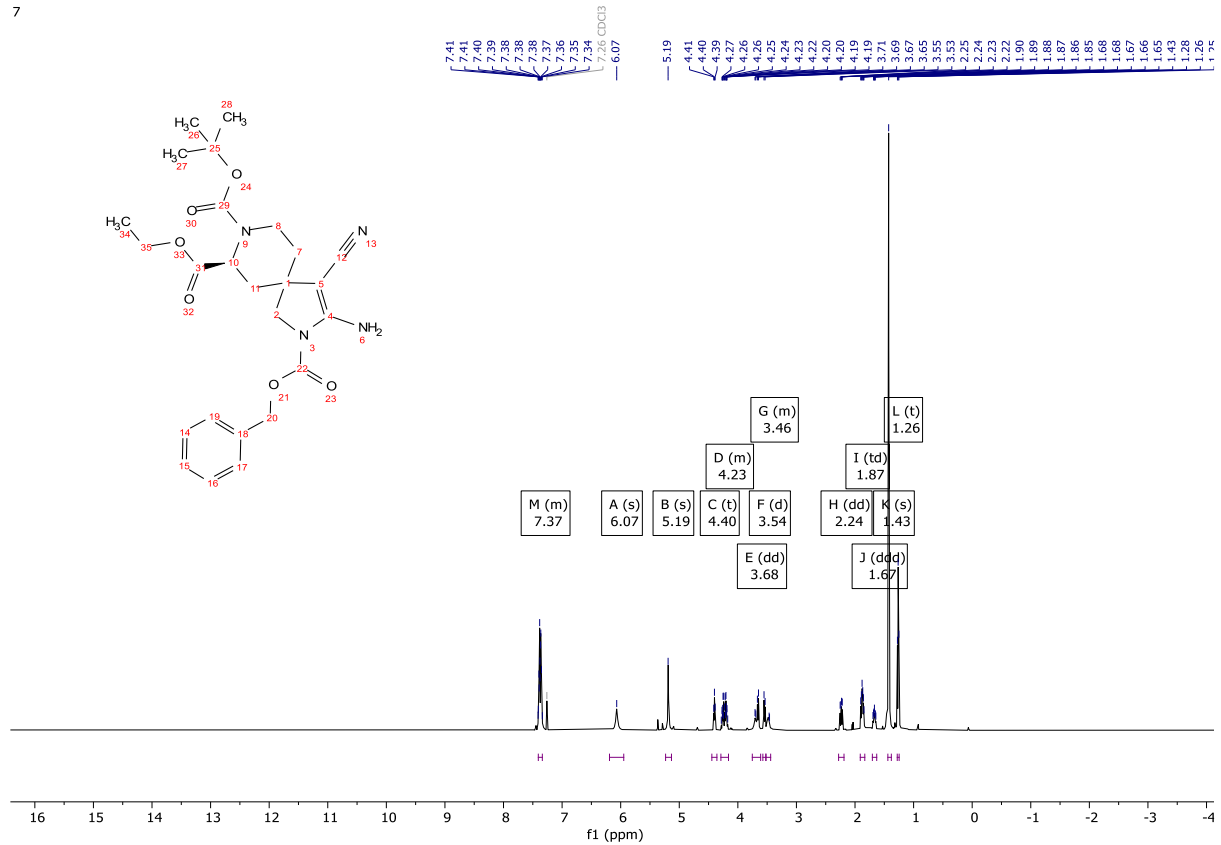
204 ¹³C NMR (101 MHz, CDCl₃)

6



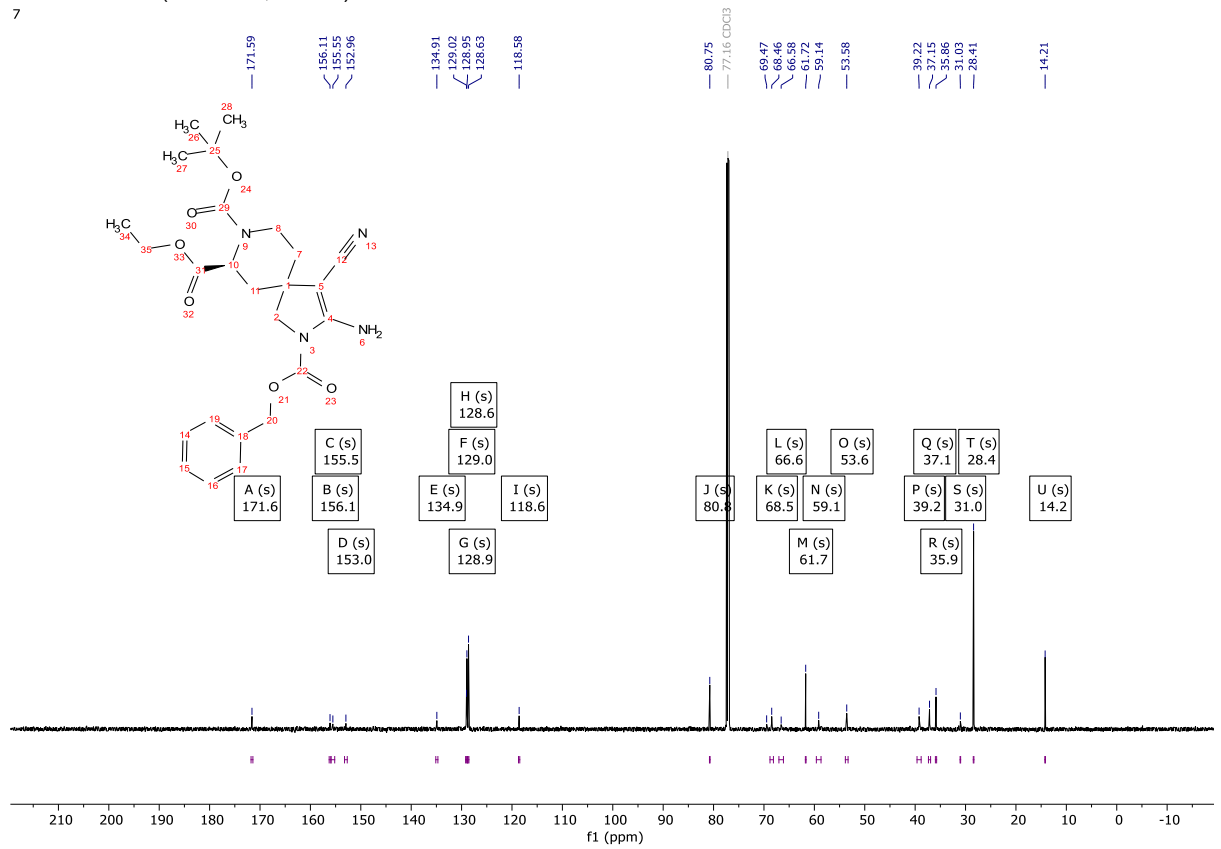
205 ¹H NMR (400 MHz, CDCl₃)

7



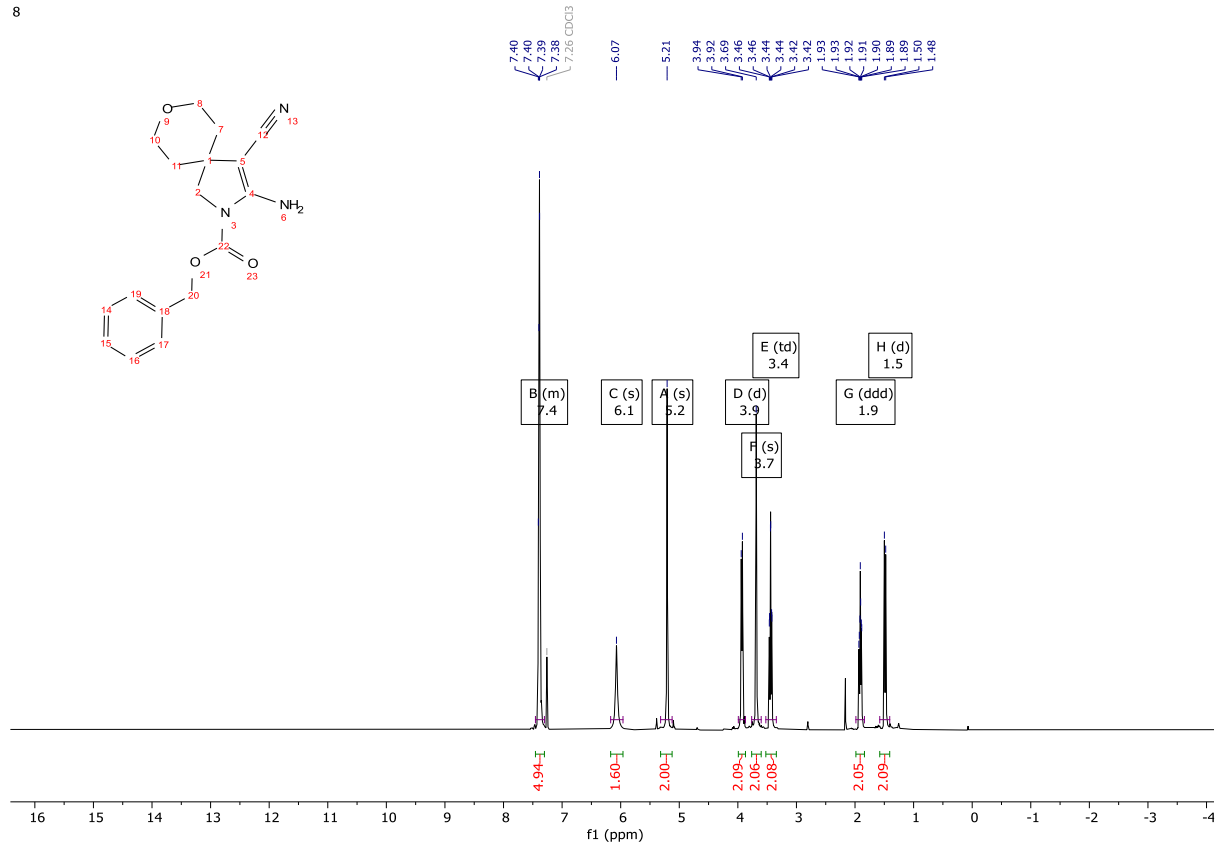
205 ¹³C NMR (101 MHz, CDCl₃)

7



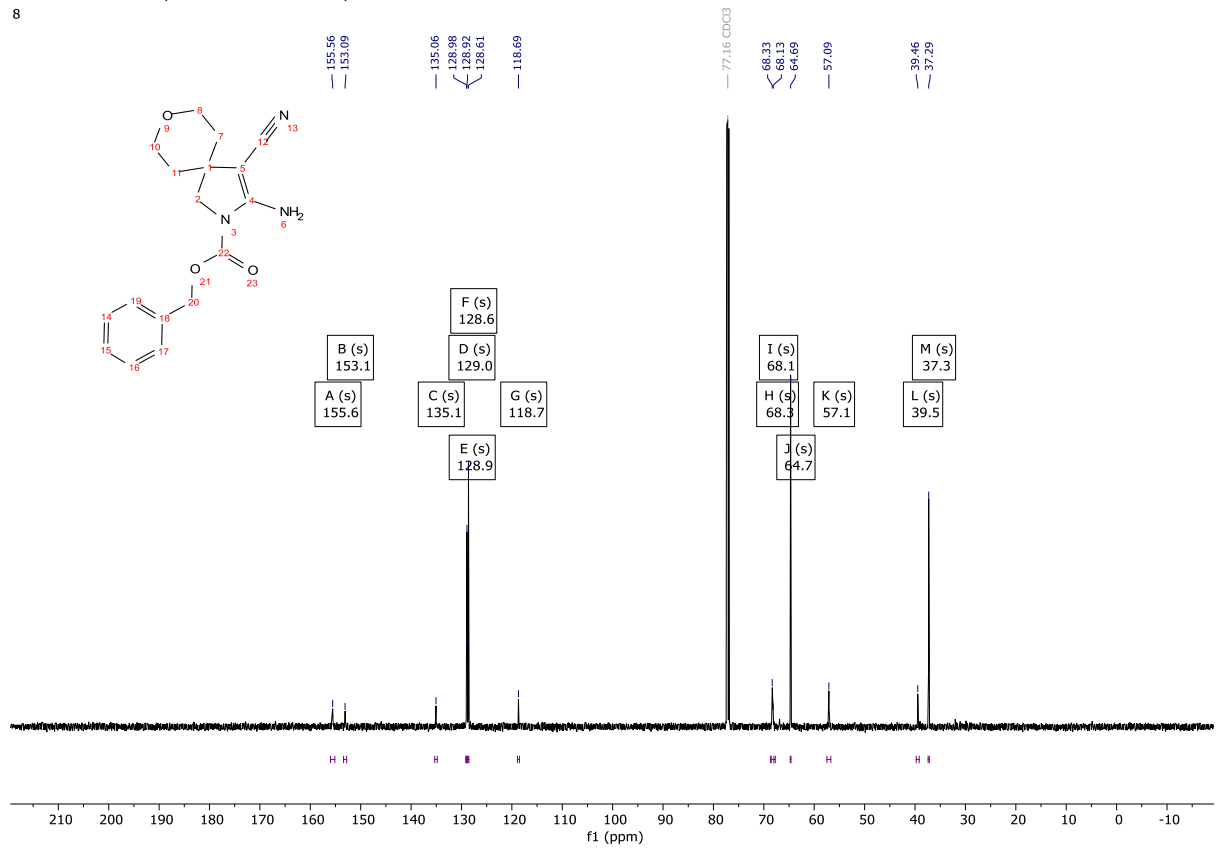
206 ¹H NMR (400 MHz, CDCl₃)

8



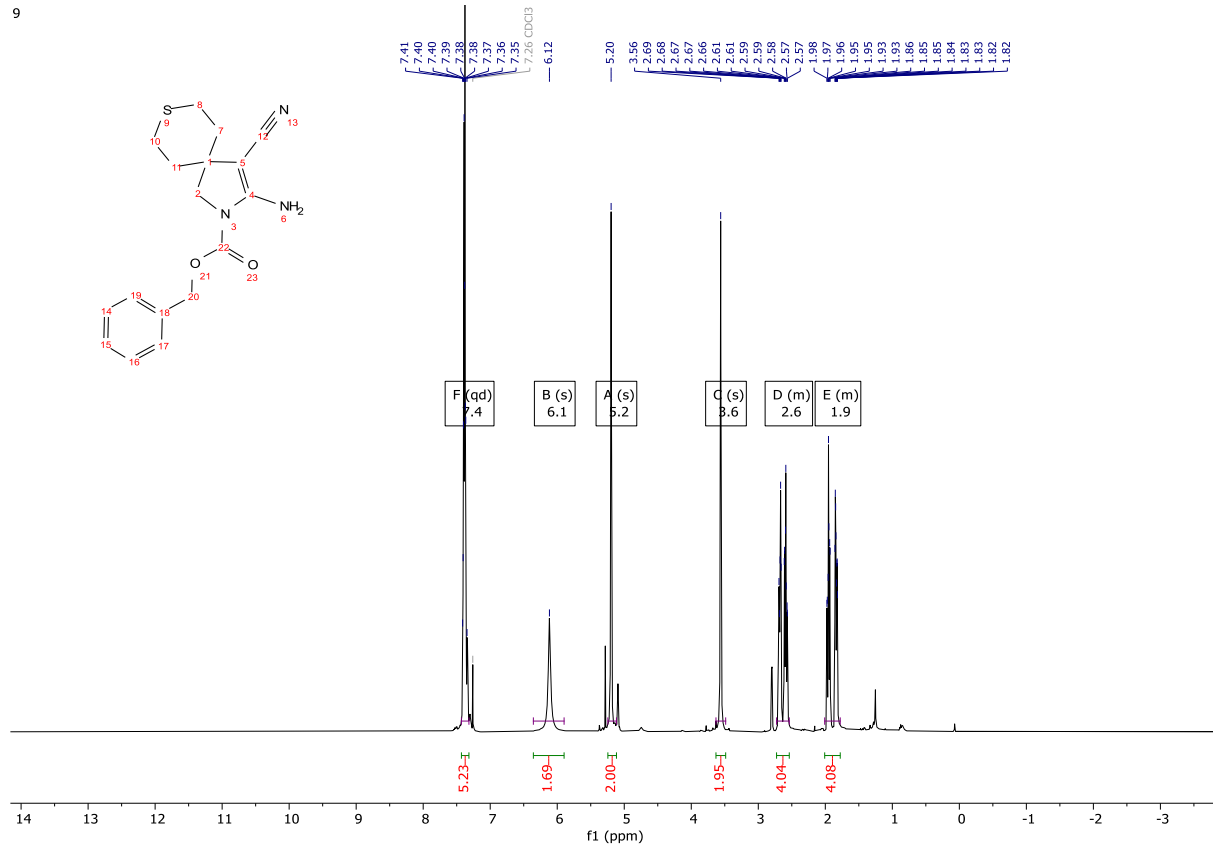
206 ¹³C NMR (101 MHz, CDCl₃)

8



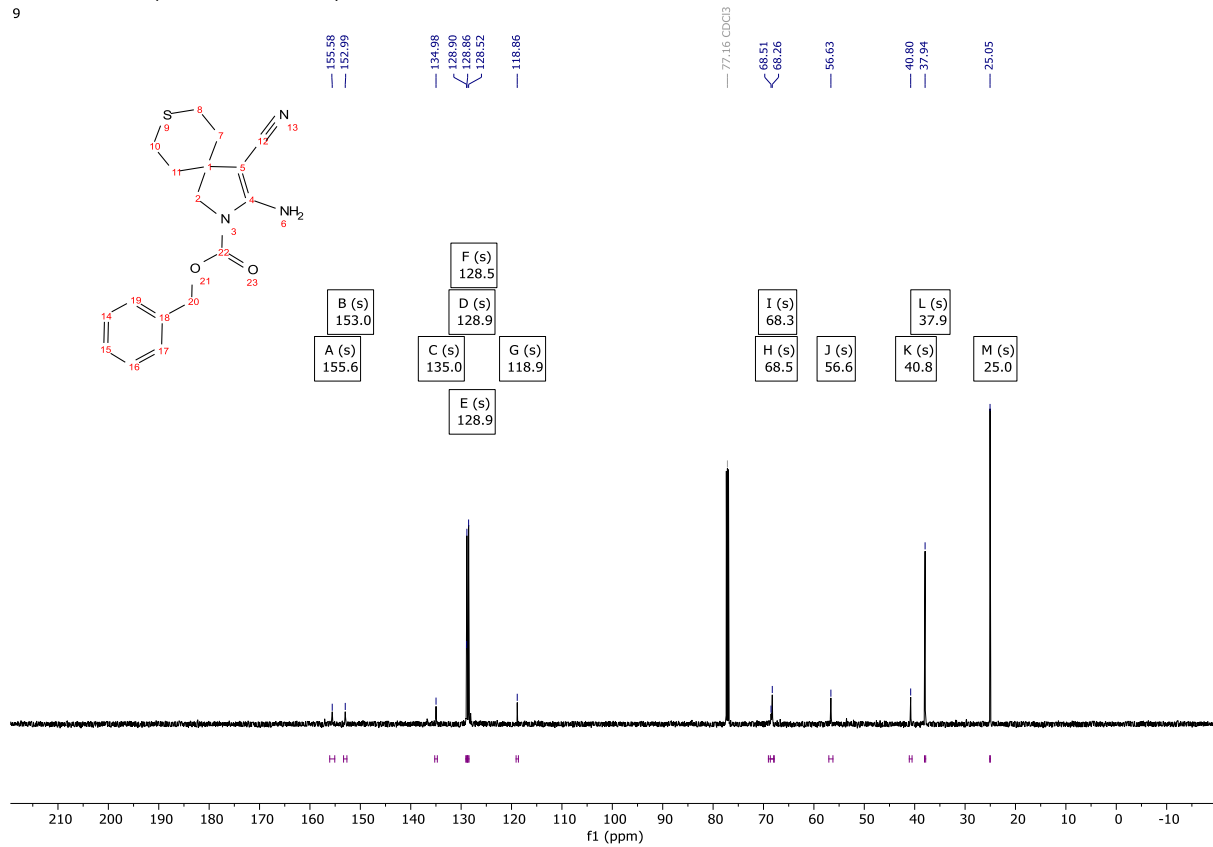
207 ¹³C NMR (101 MHz, CDCl₃)

9



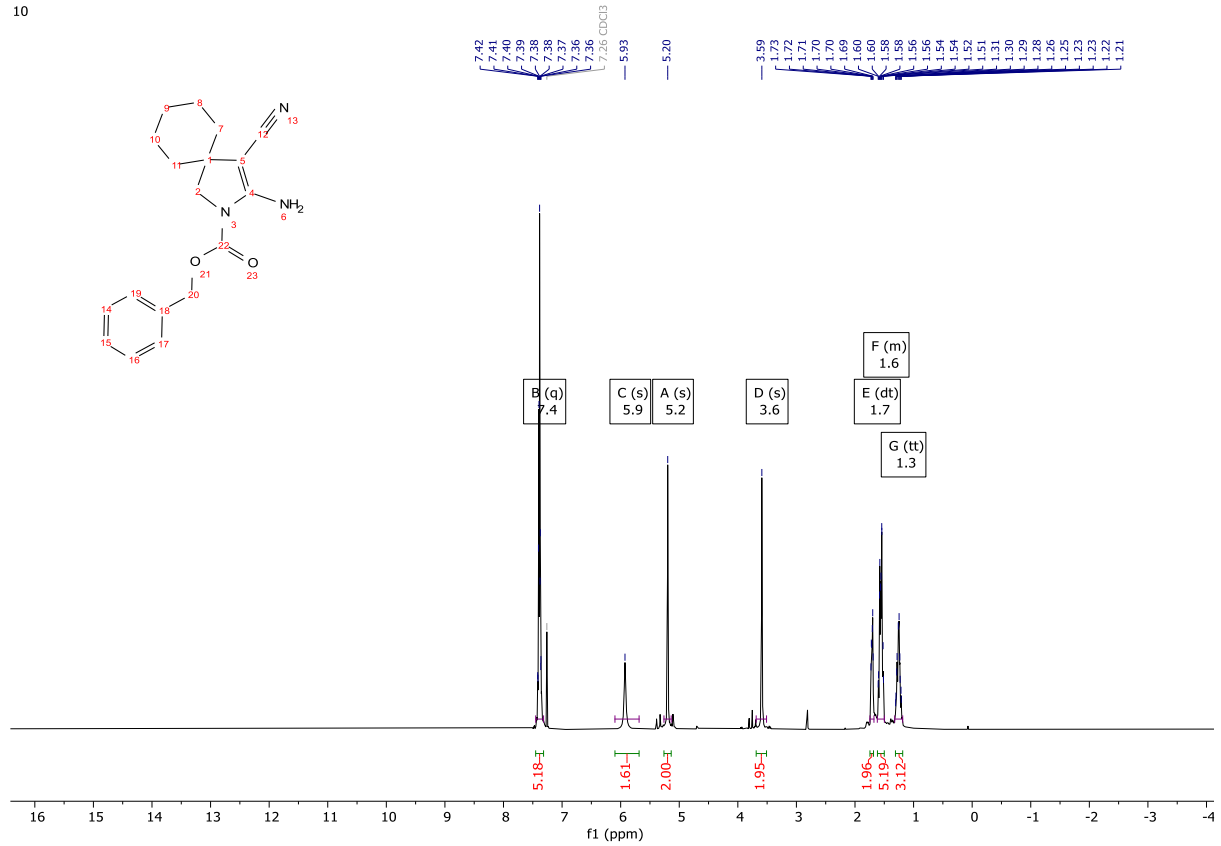
207 ¹H NMR (400 MHz, CDCl₃)

9



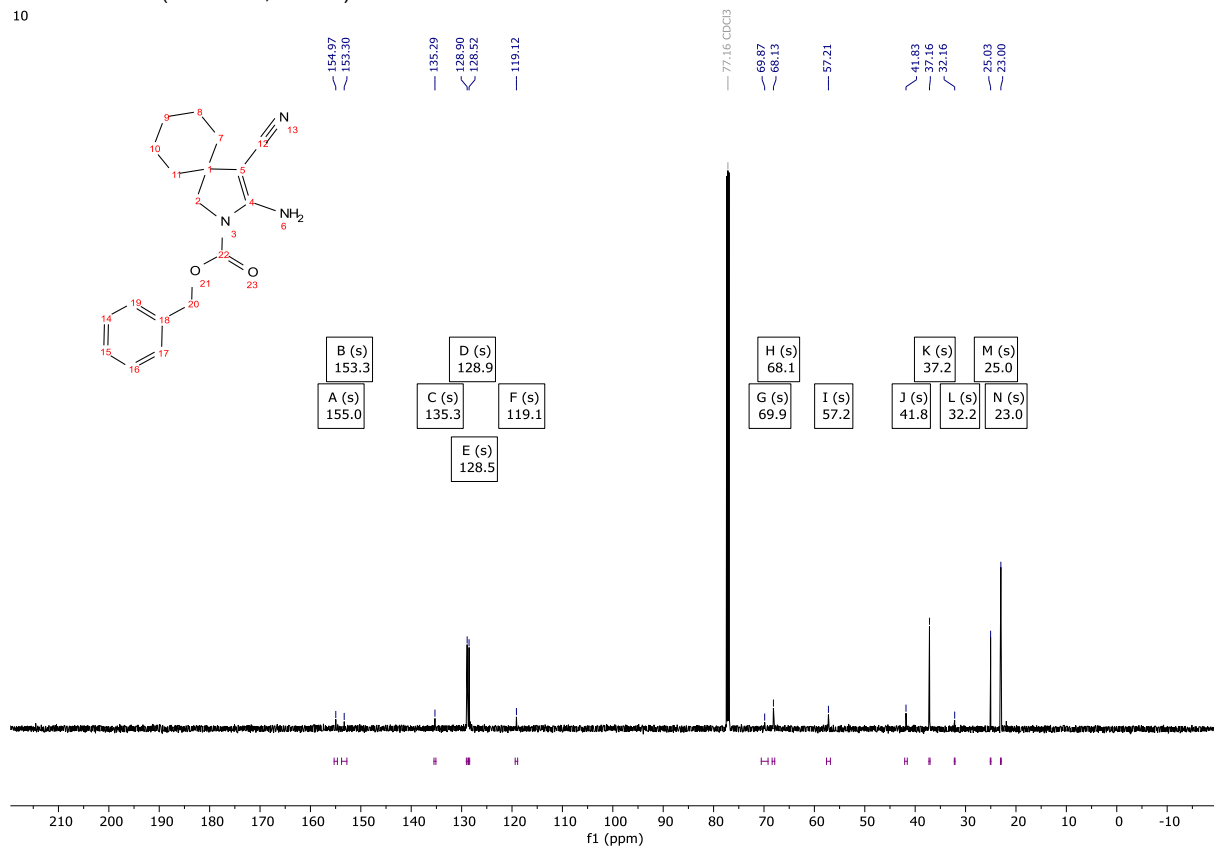
208 ¹H NMR (400 MHz, CDCl₃)

10

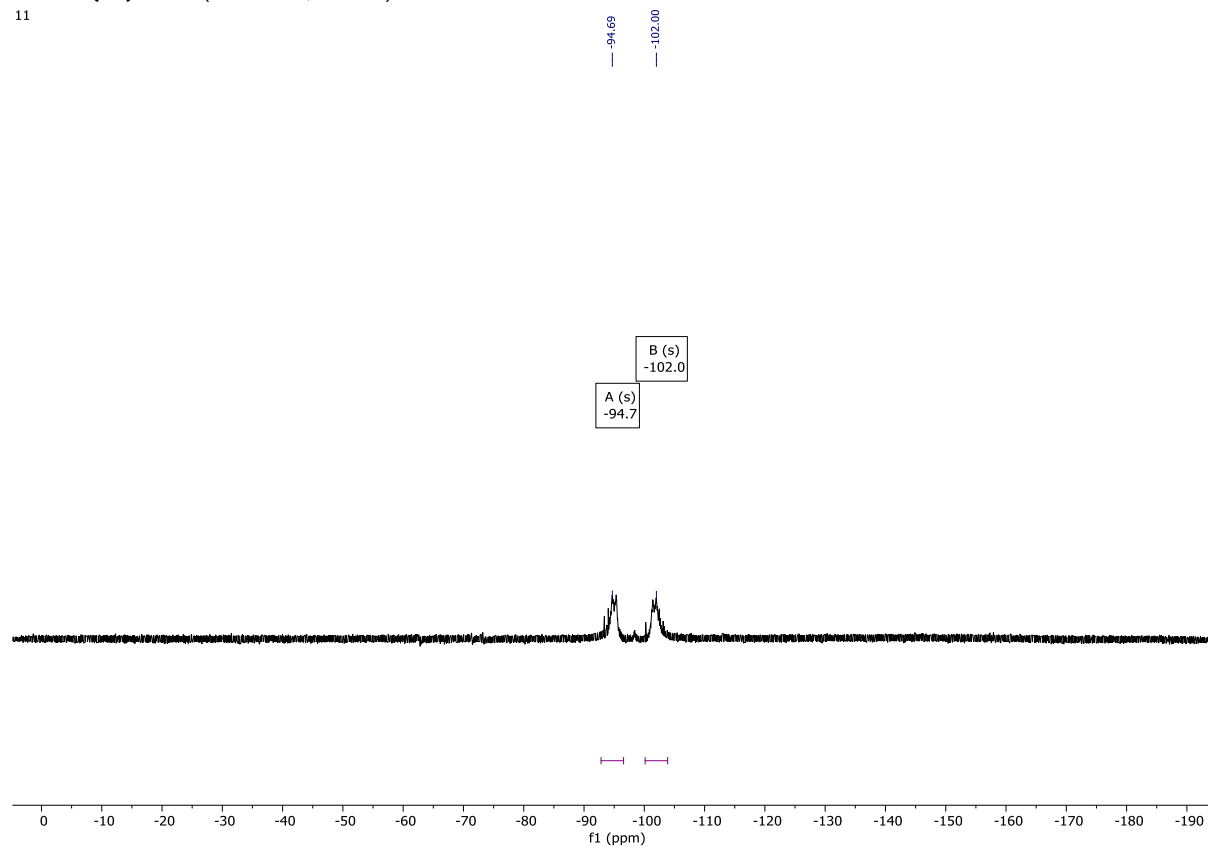


208 ¹³C NMR (101 MHz, CDCl₃)

10

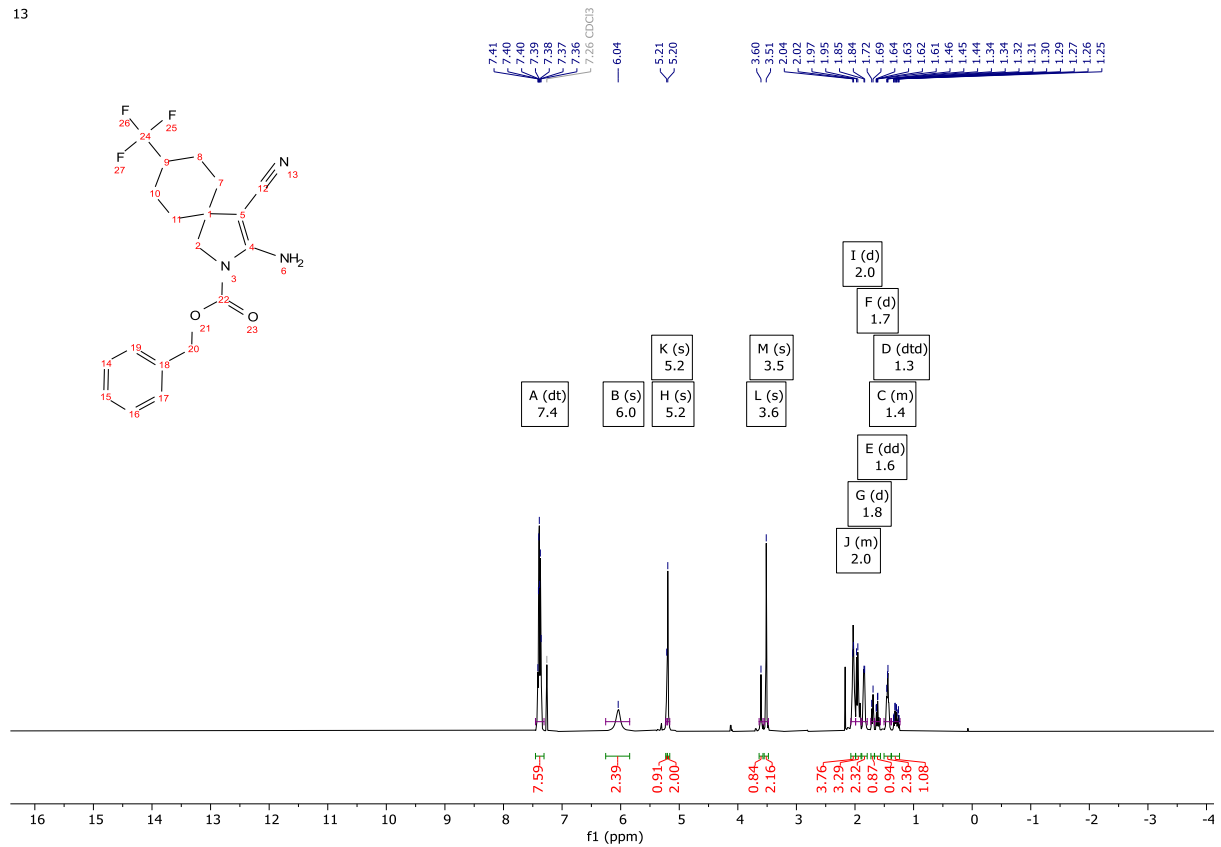


209 $^{19}\text{F}\{^1\text{H}\}$ NMR (376 MHz, CDCl_3)
11



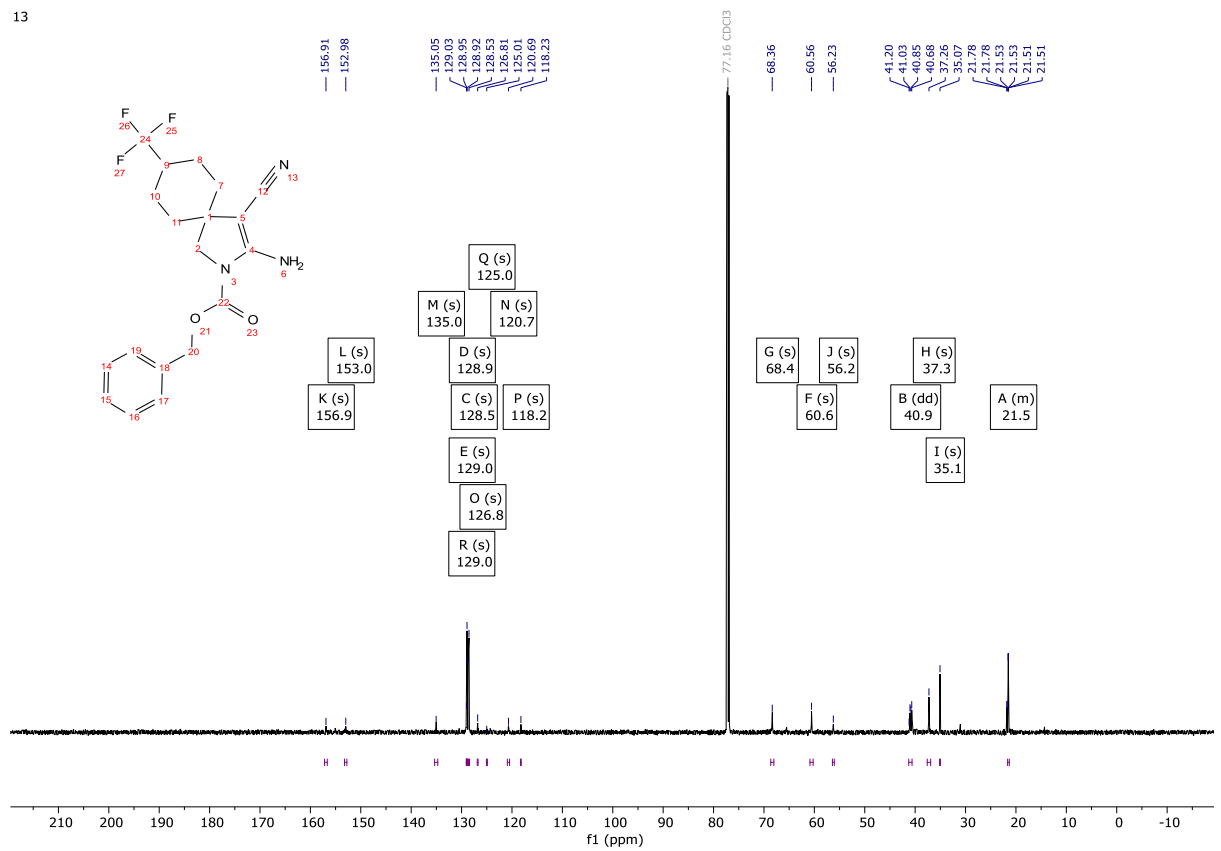
211 ¹H NMR (400 MHz, CDCl₃)

13



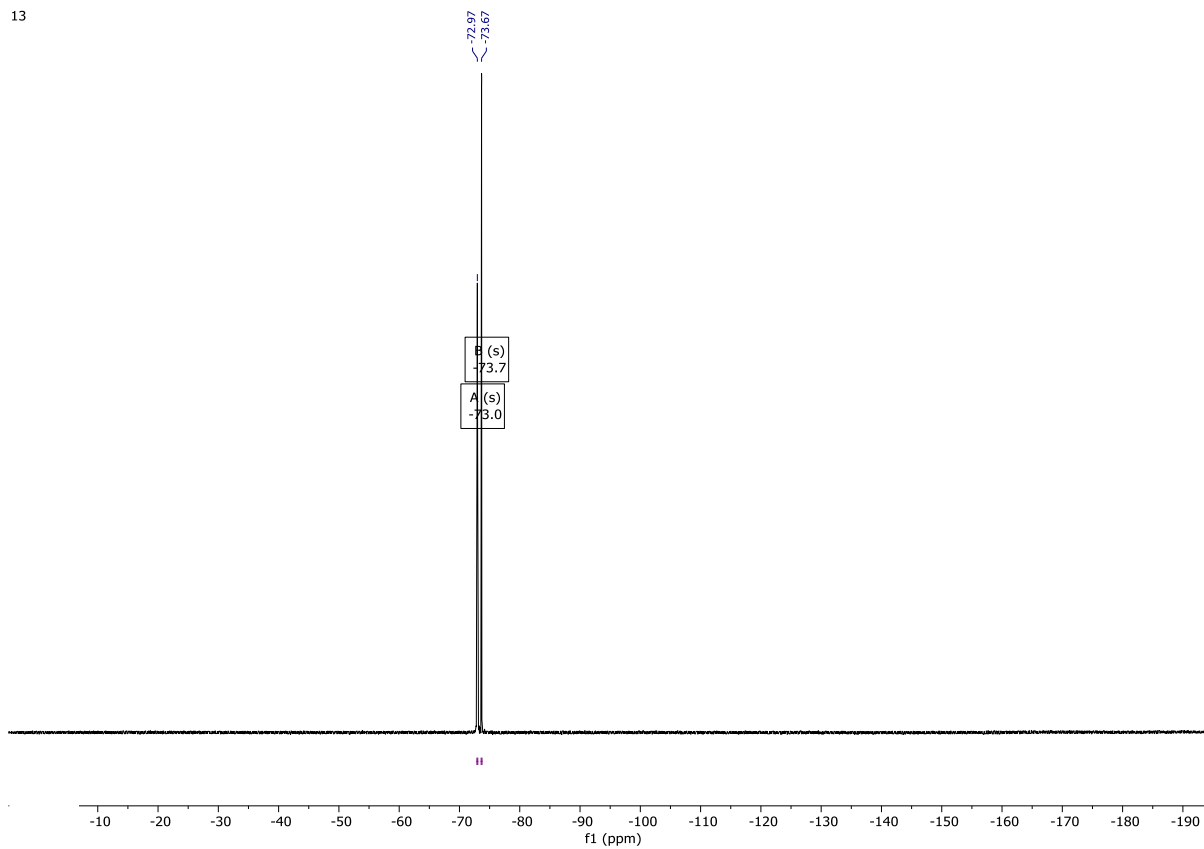
211 ¹³C NMR (101 MHz, CDCl₃)

13

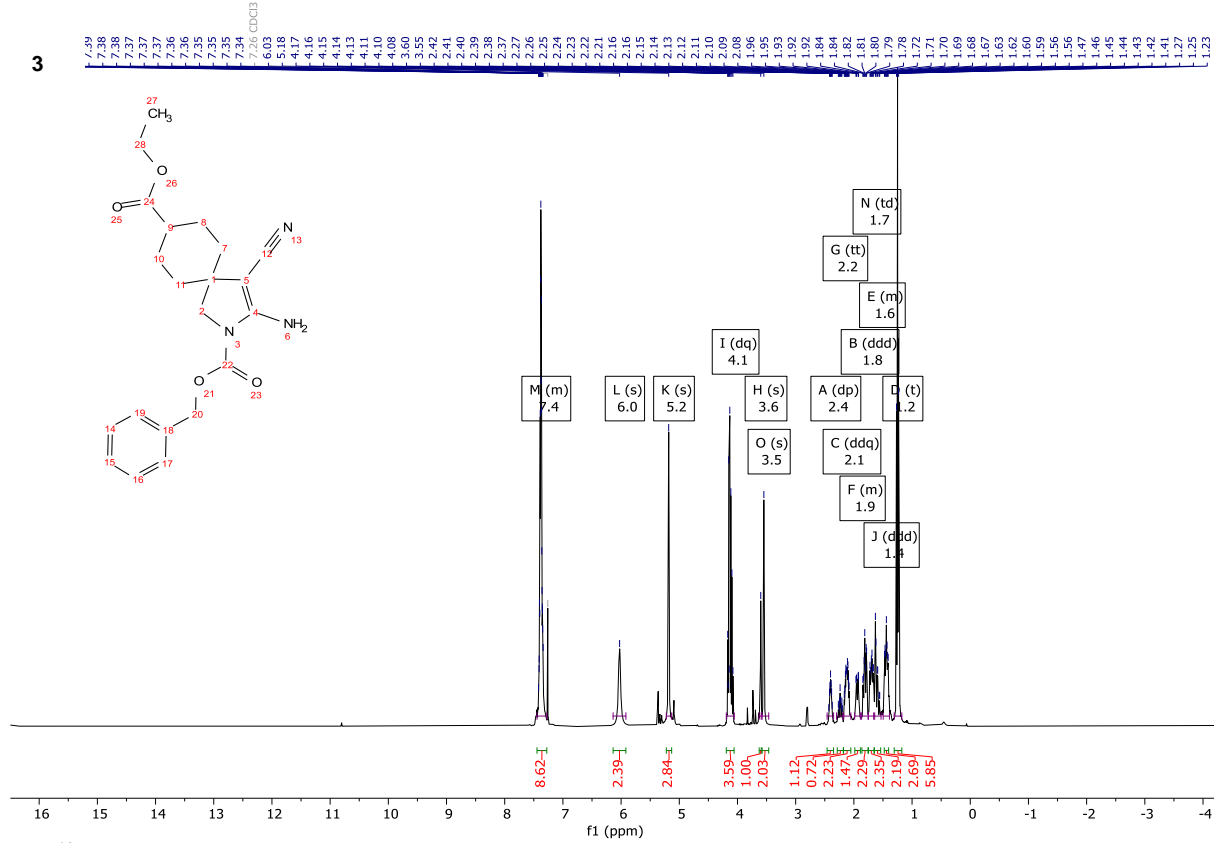


211 $^{19}\text{F}\{^1\text{H}\}$ NMR (376 MHz, CDCl_3)

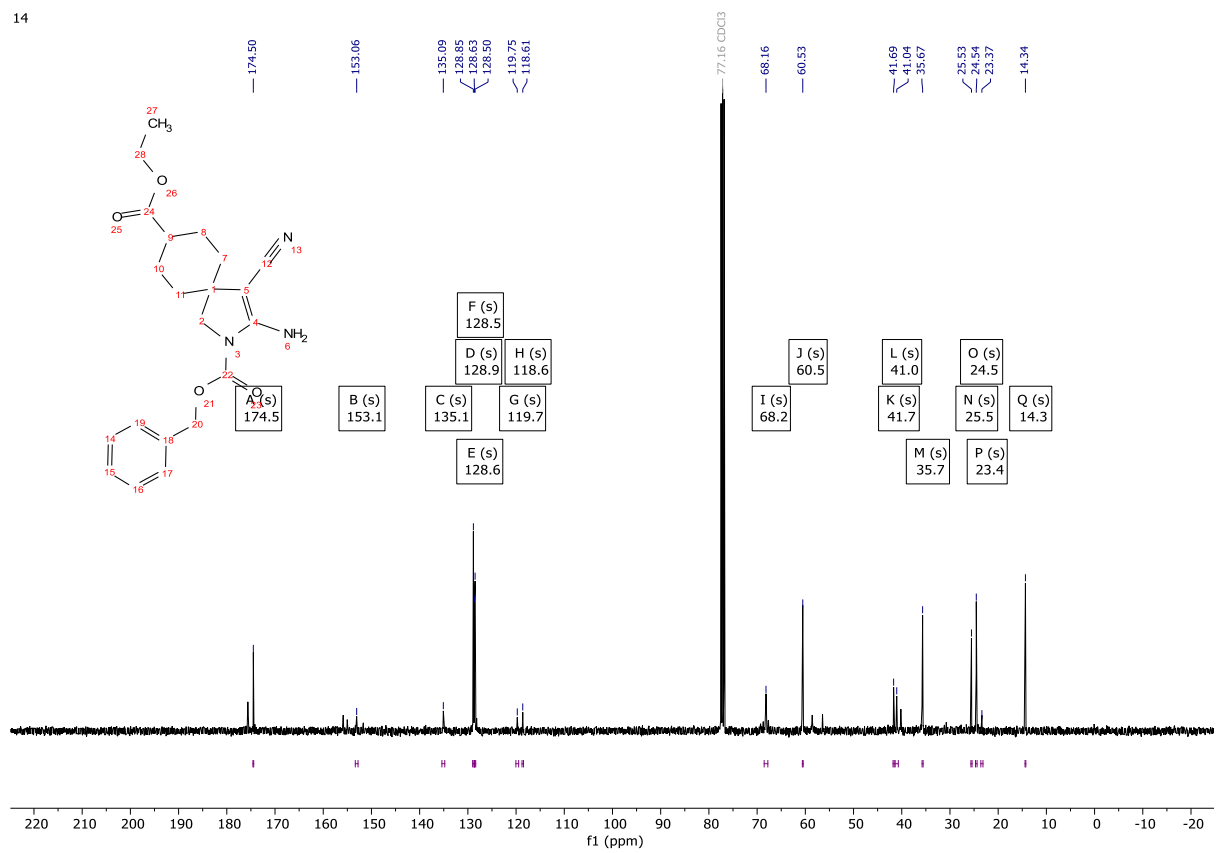
13



212 ¹H NMR (400 MHz, CDCl₃)

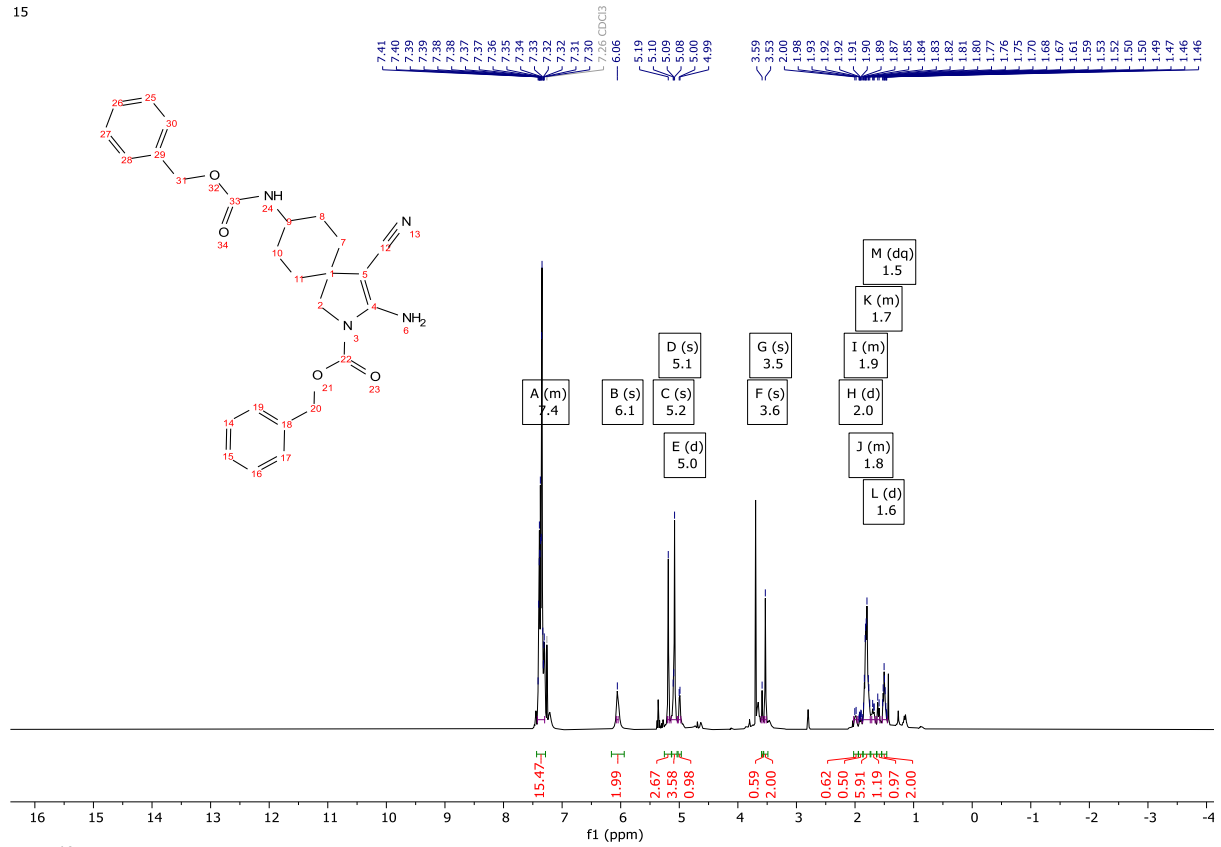


212 ¹³C NMR (101 MHz, CDCl₃)



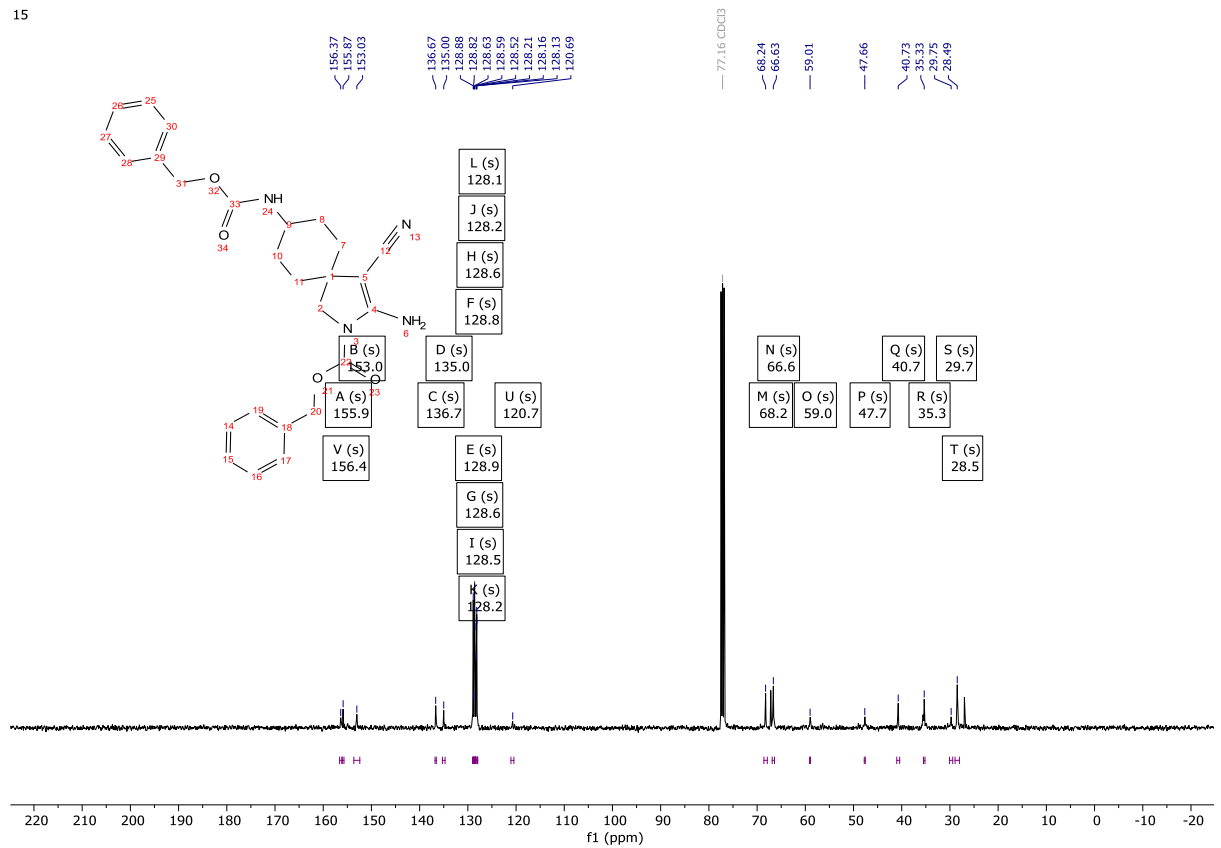
213 ¹H NMR (400 MHz, CDCl₃)

15



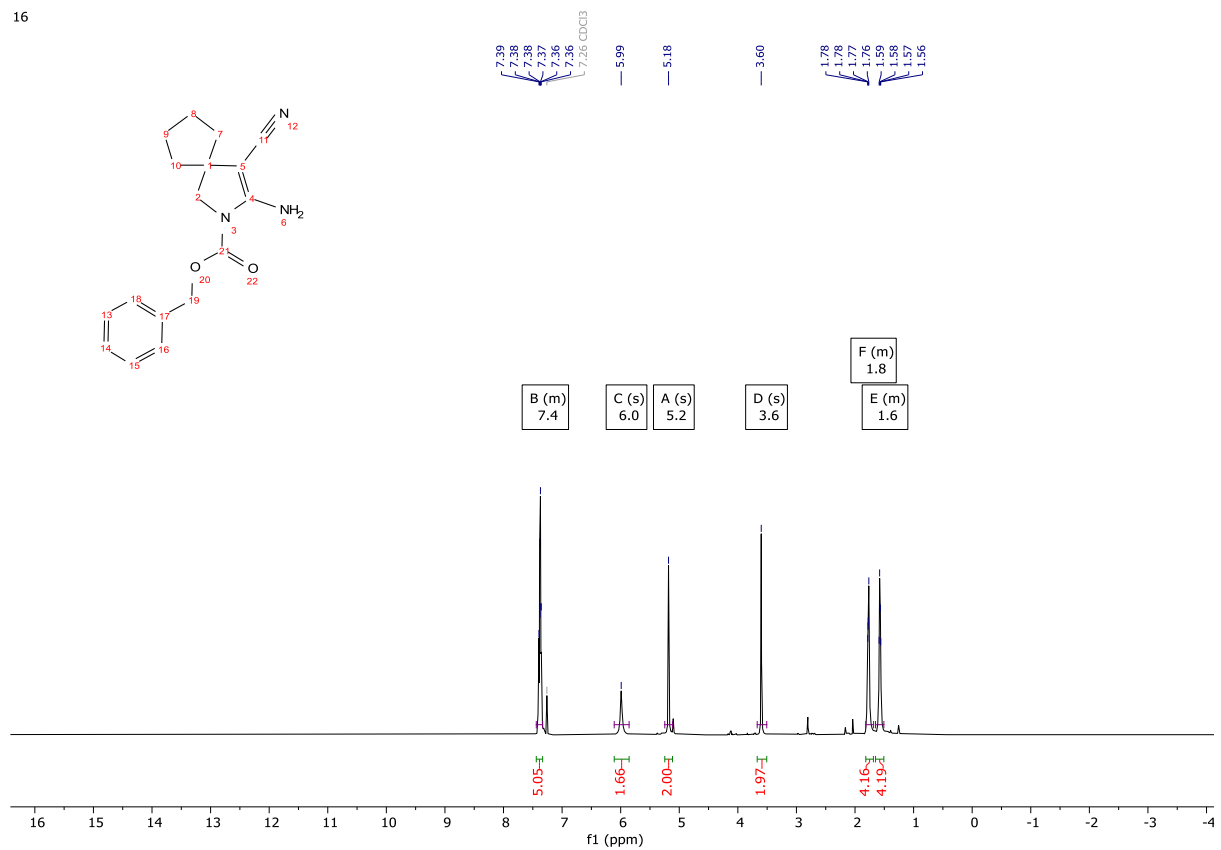
213 ¹³C NMR (101 MHz, CDCl₃)

15



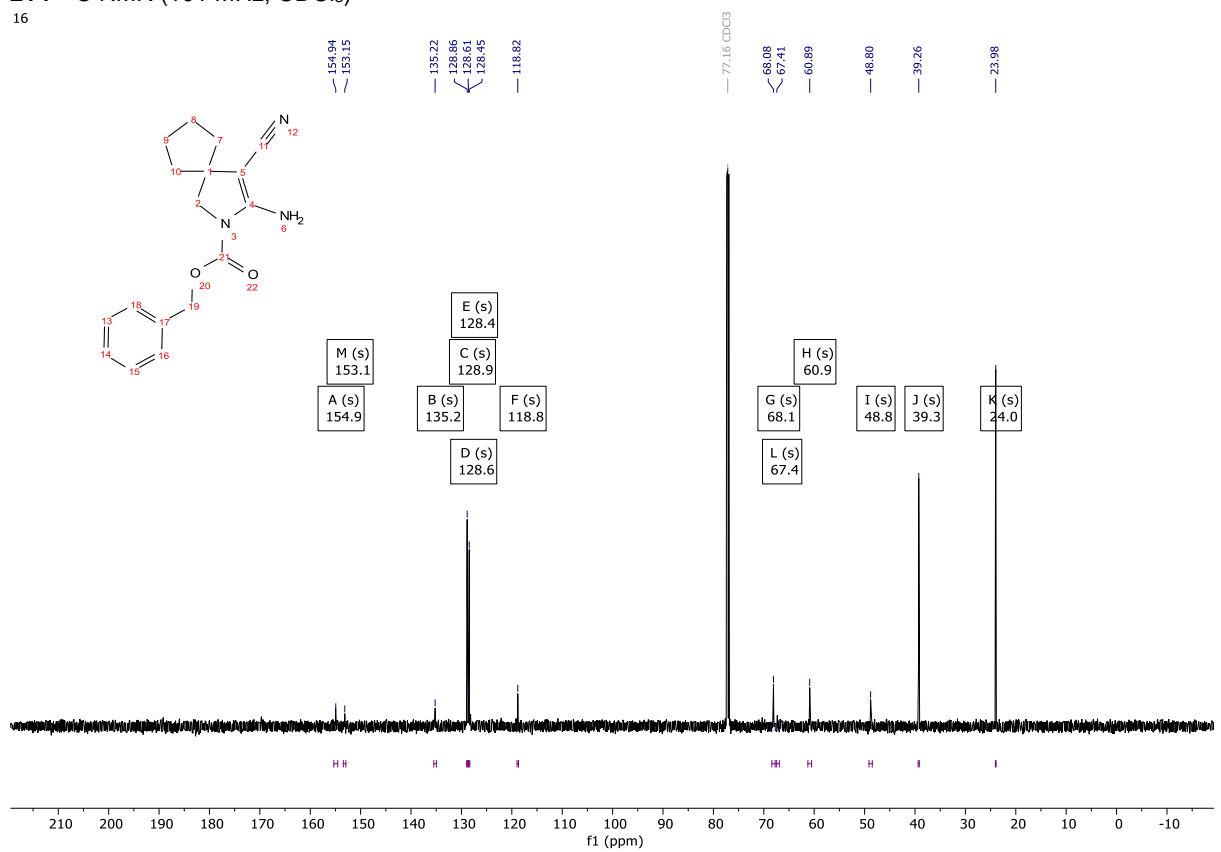
214 ¹H NMR (400 MHz, CDCl₃)

16



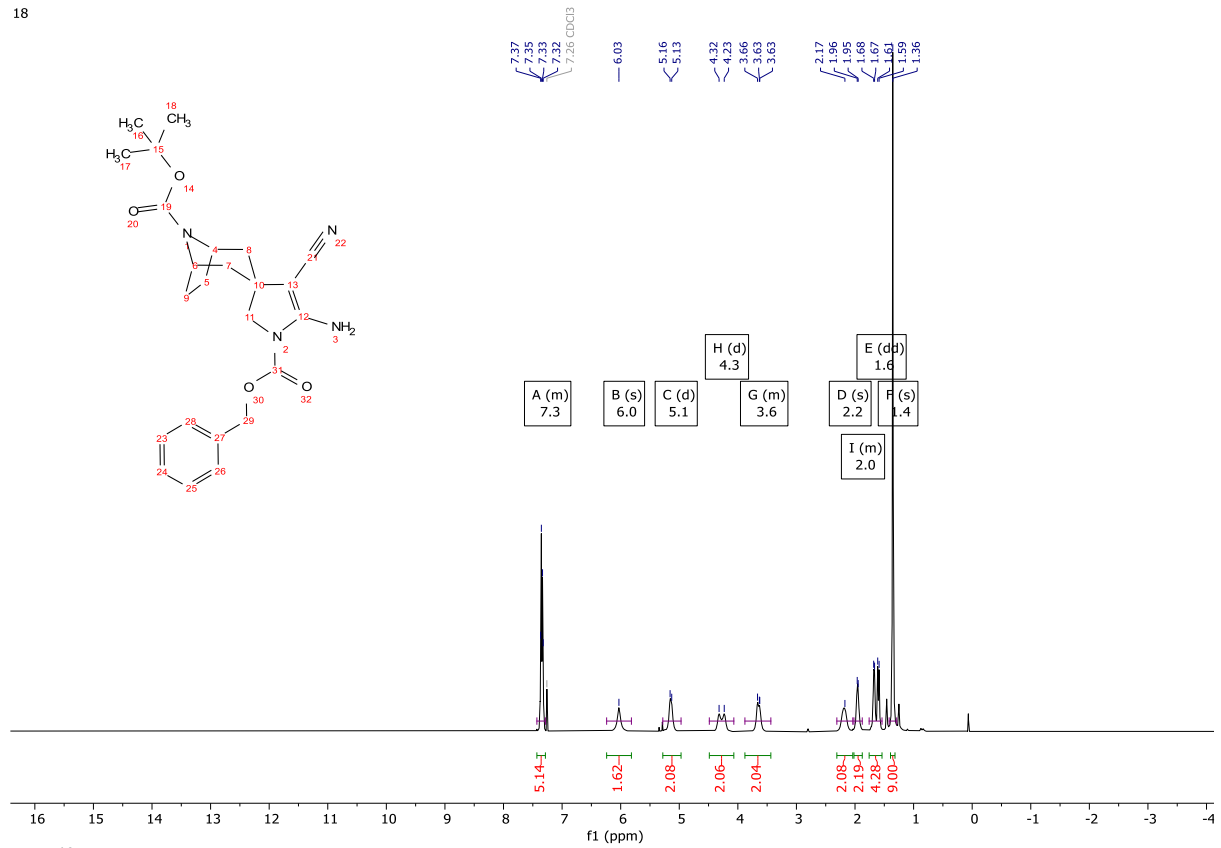
214 ¹³C NMR (101 MHz, CDCl₃)

16



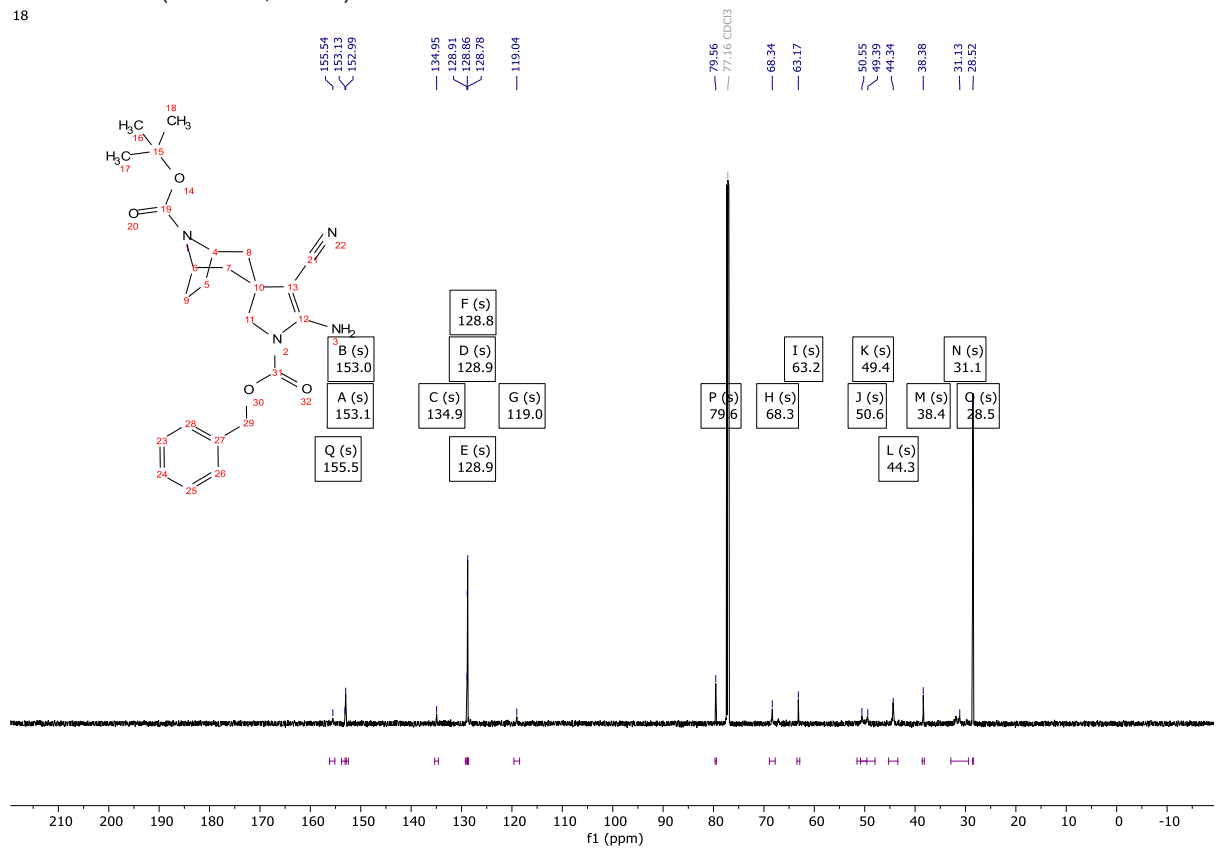
216 ¹H NMR (400 MHz, CDCl₃)

18



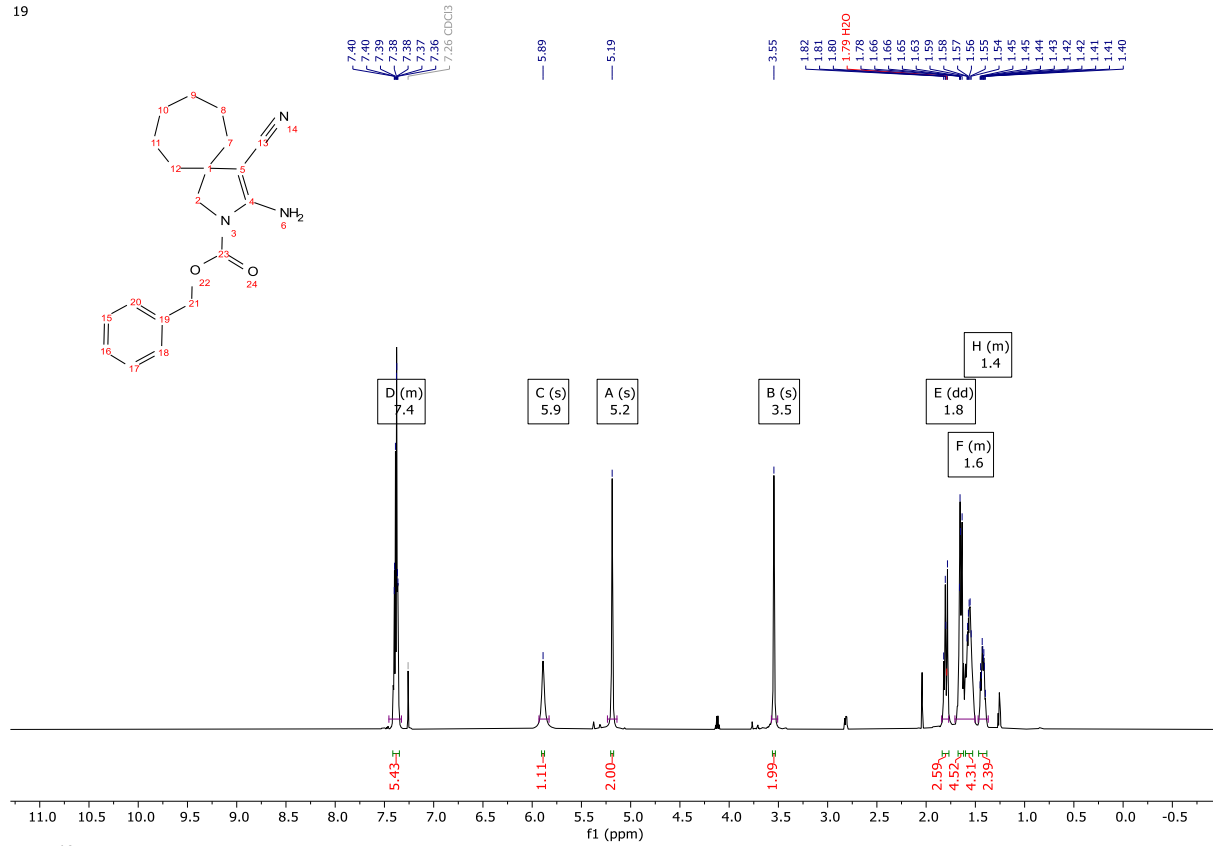
216 ¹³C NMR (101 MHz, CDCl₃)

18



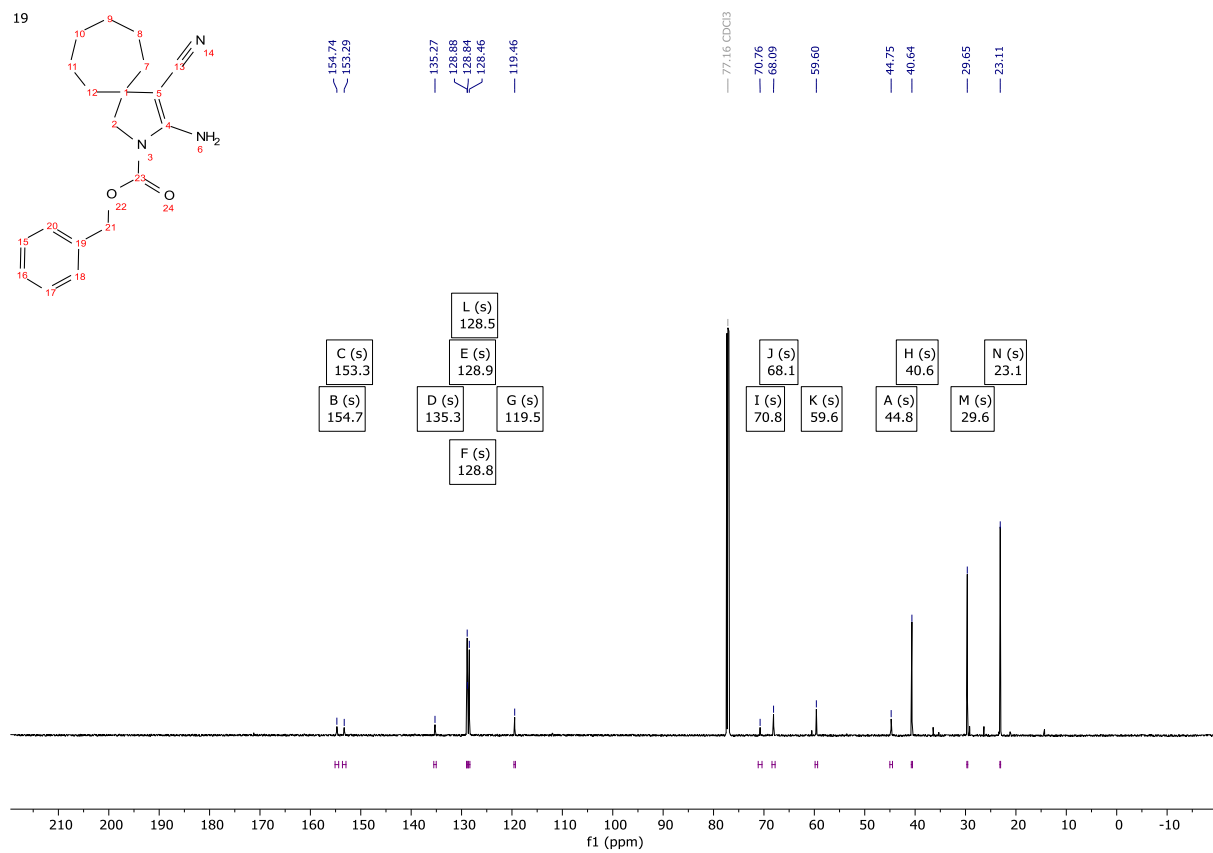
217 ¹H NMR (400 MHz, CDCl₃)

19



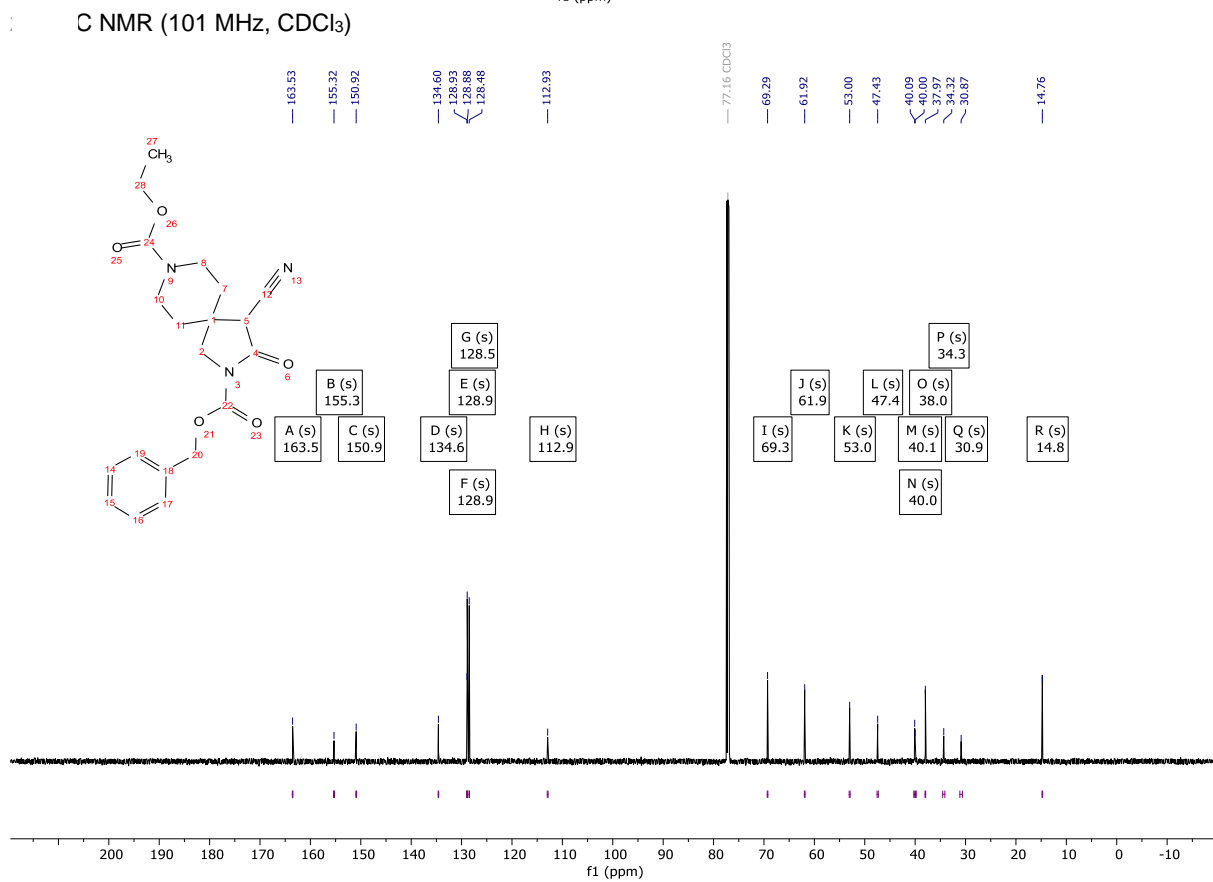
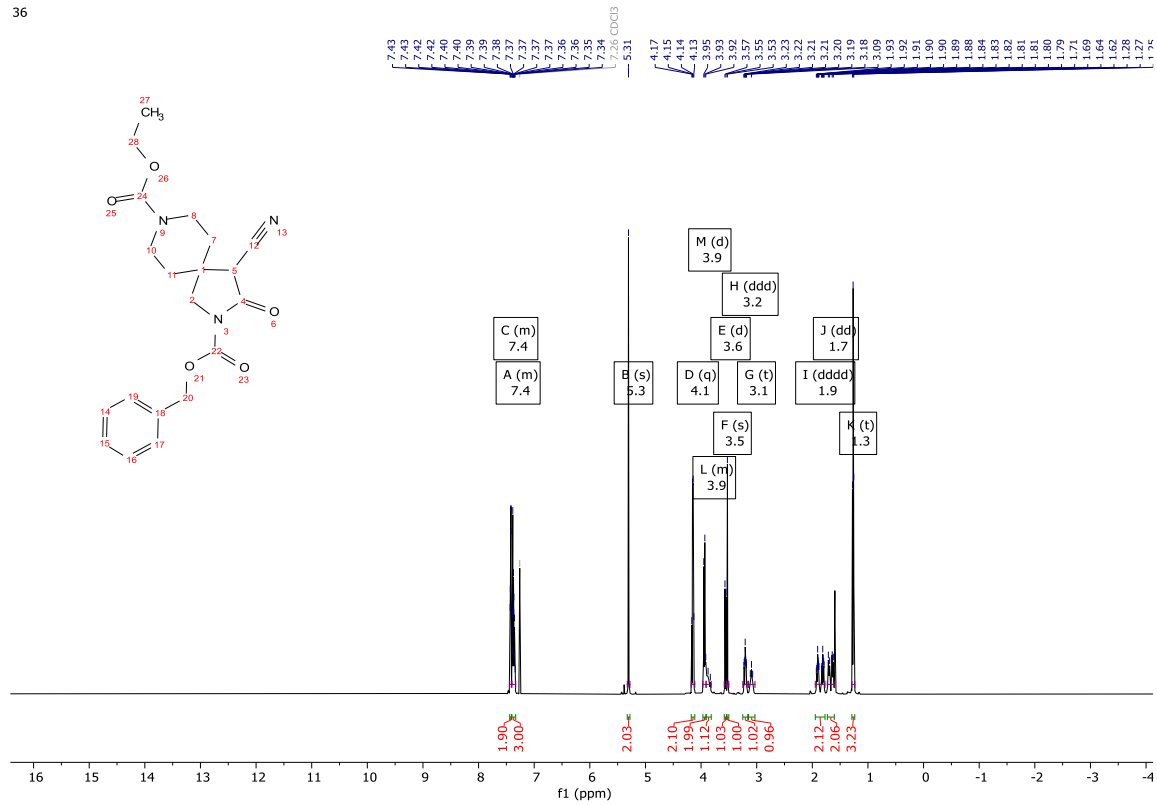
217 ¹³C NMR (101 MHz, CDCl₃)

19



Product Derivatisations

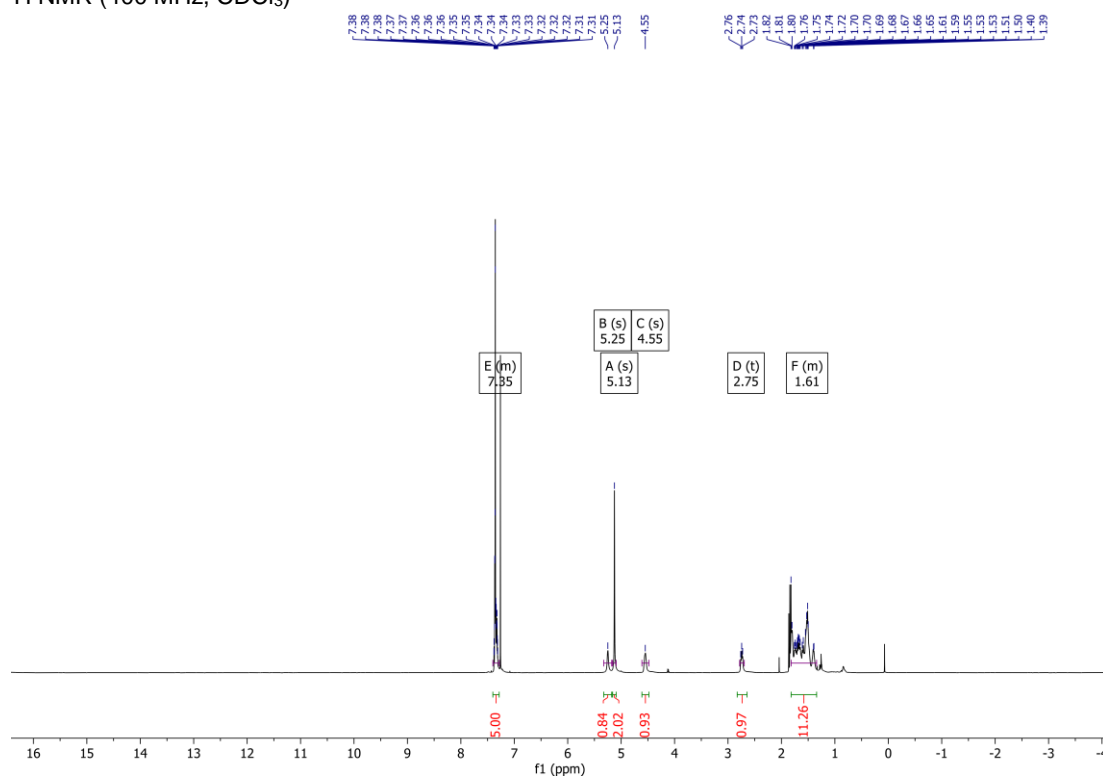
229 ¹H NMR (400 MHz, CDCl₃)



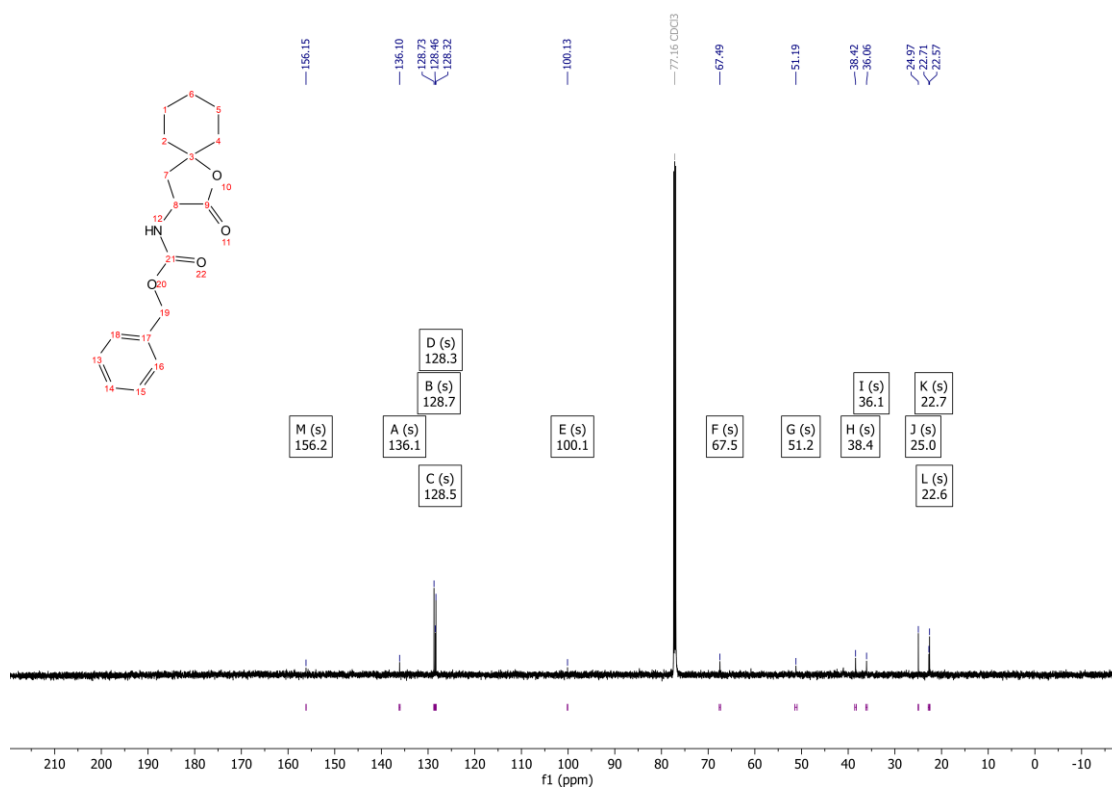
Chapter III: Synthesis of α -Amino Spirocyclic γ -Butyrolactones

Products

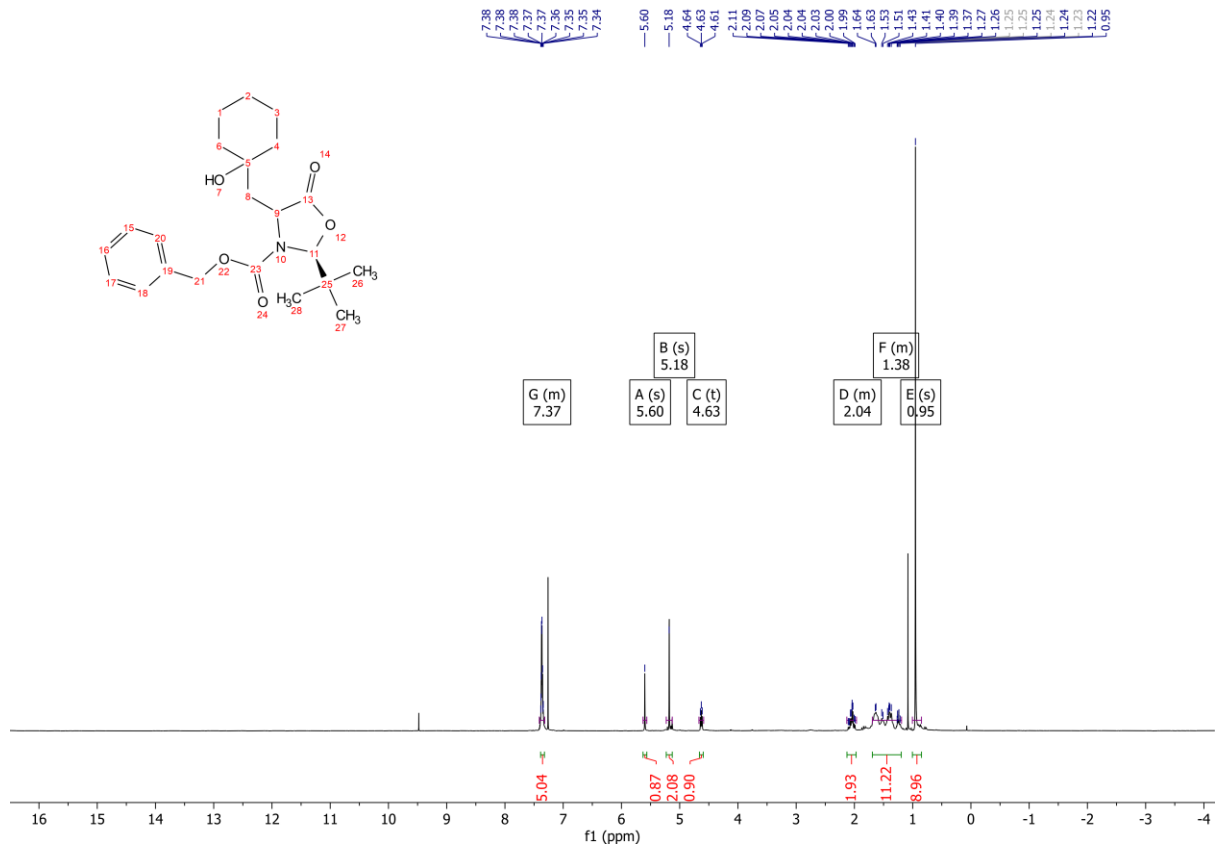
259 ^1H NMR (400 MHz, CDCl_3)



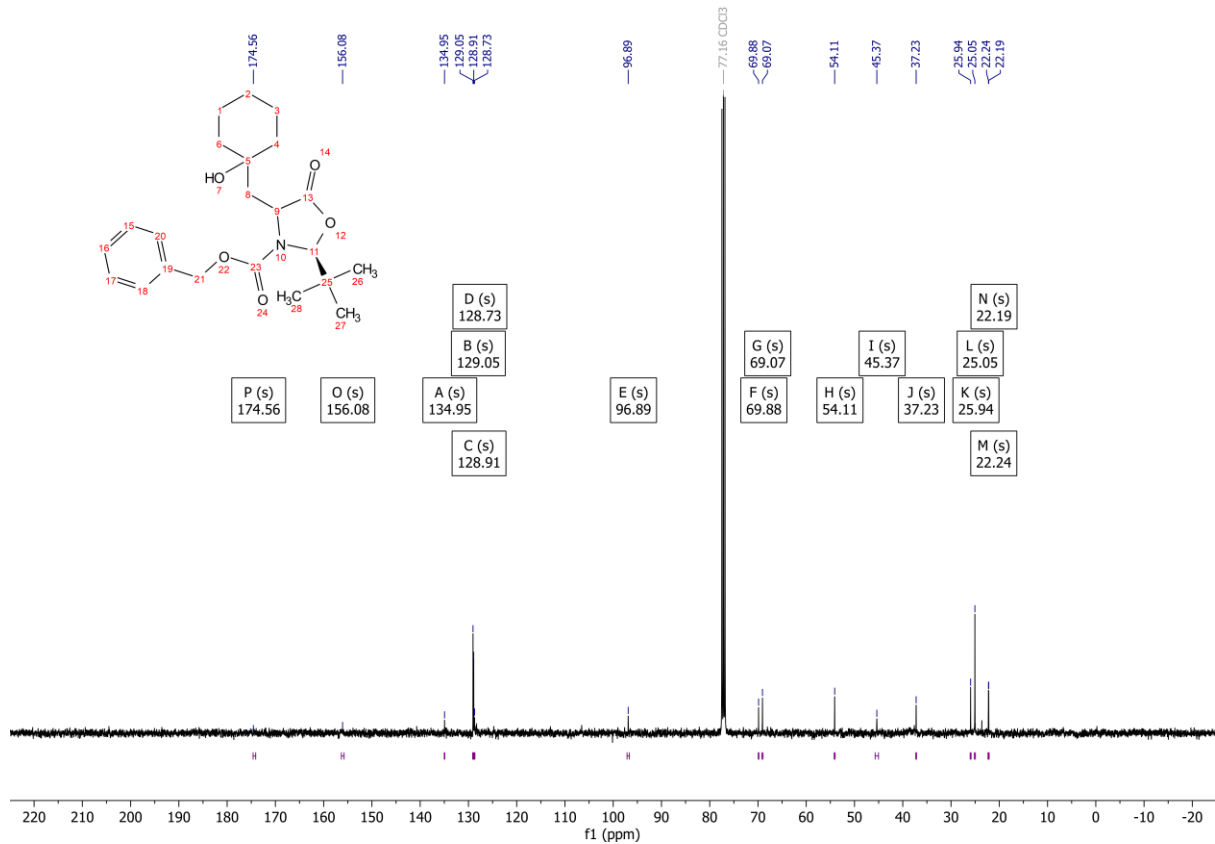
259 ^{13}C NMR (101 MHz, CDCl_3)



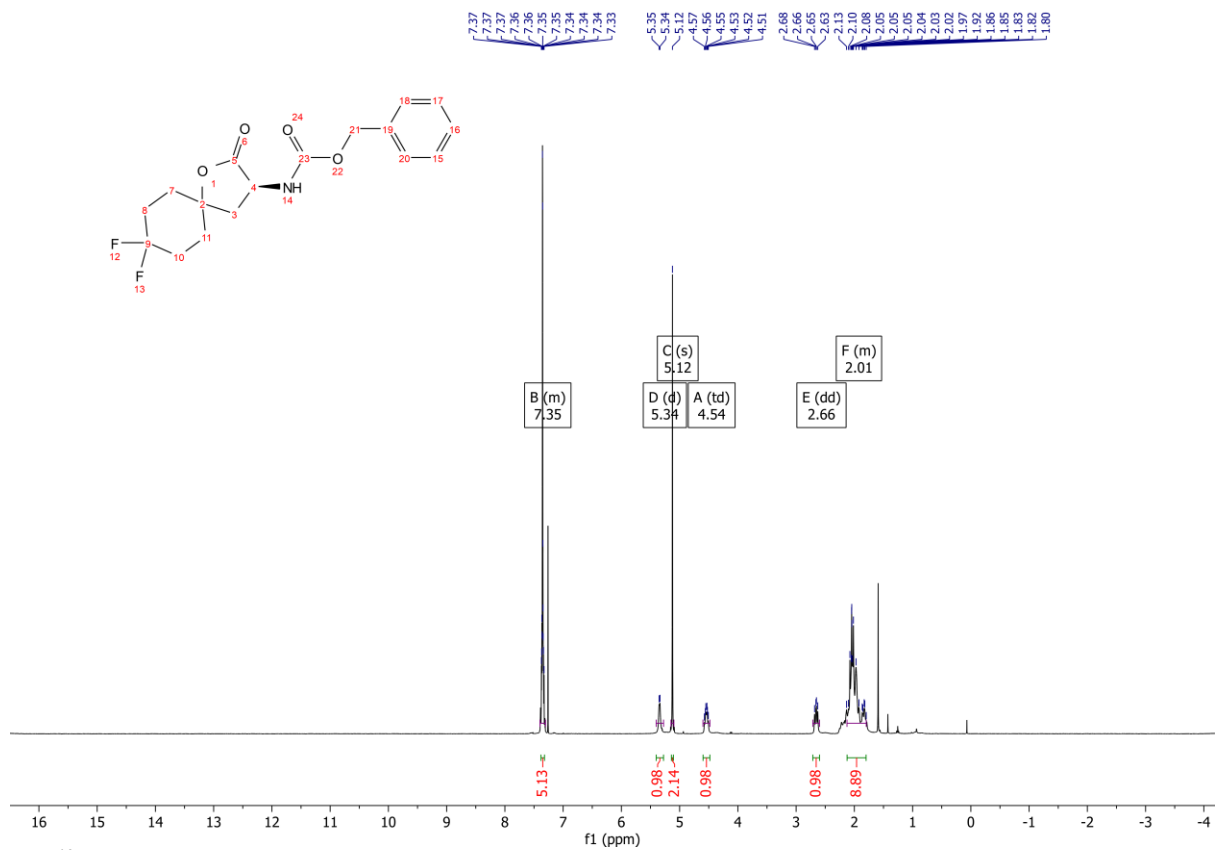
259B ¹H NMR (400 MHz, CDCl₃)



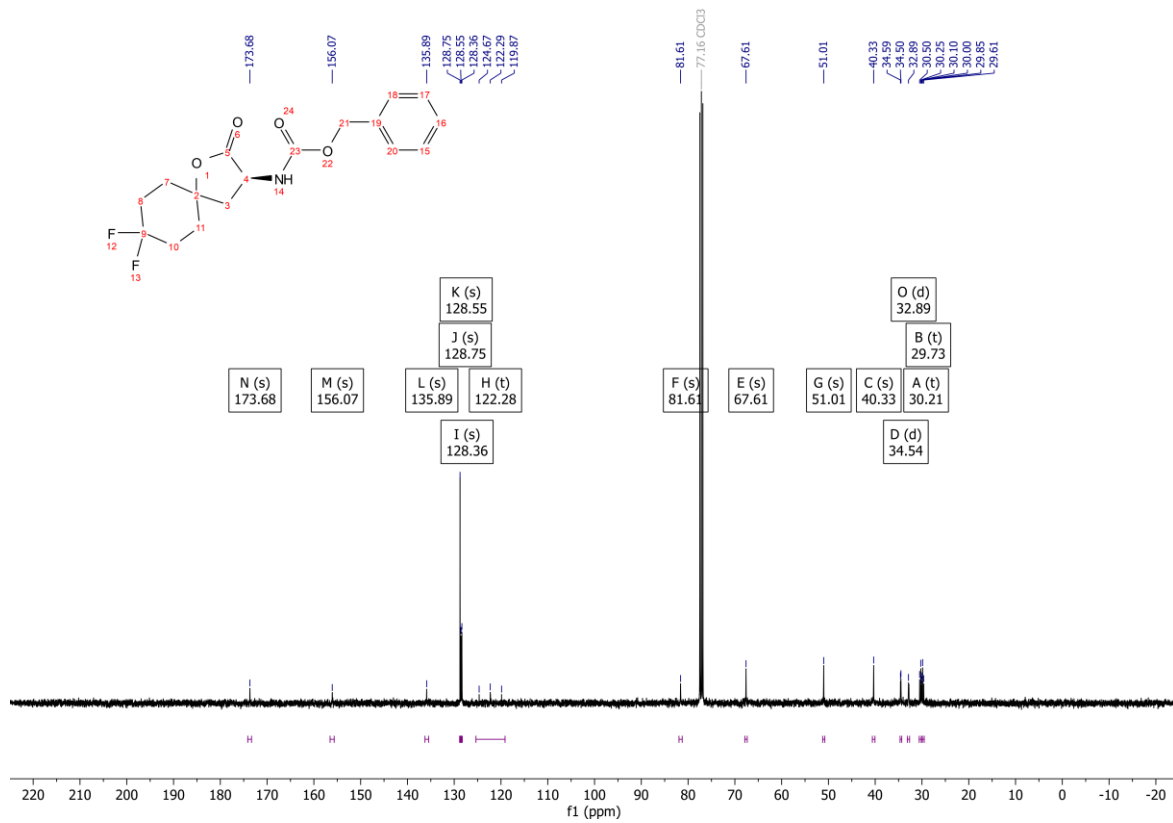
259B ¹³C NMR (101 MHz, CDCl₃)



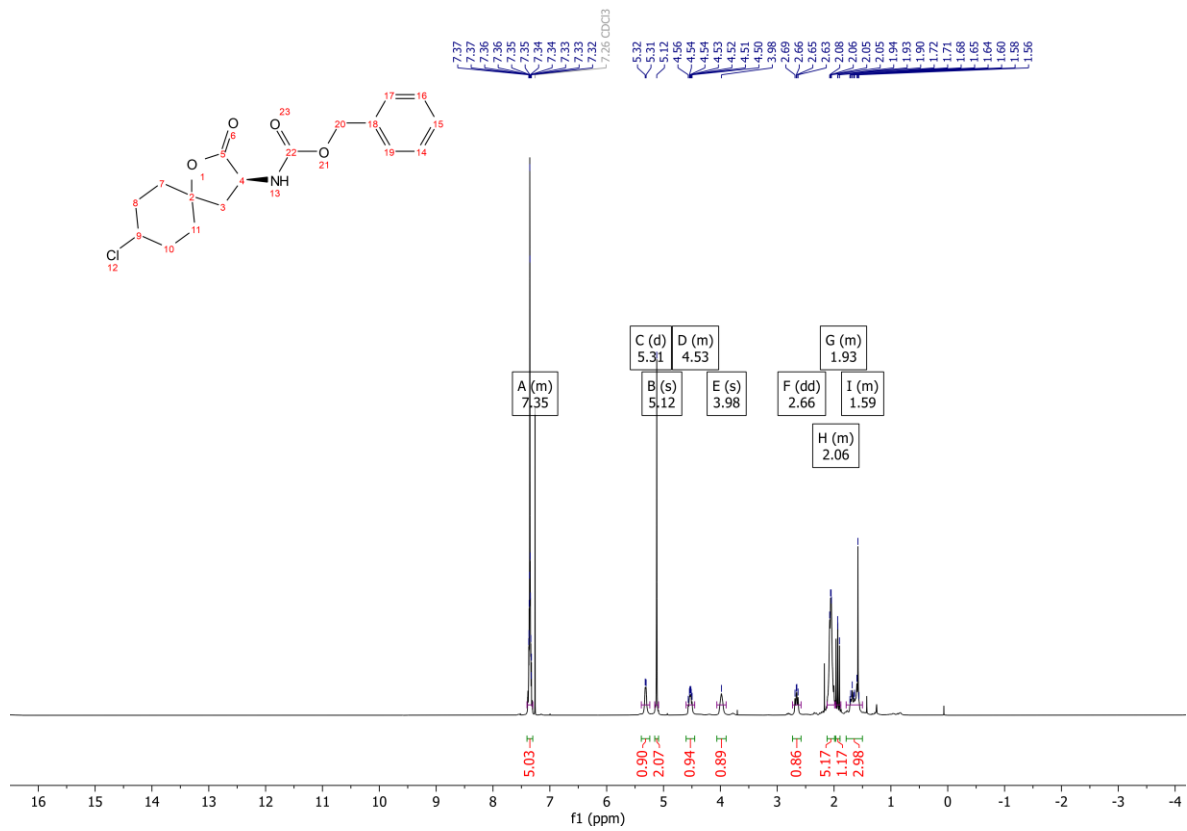
260 ¹H NMR (400 MHz, CDCl₃)



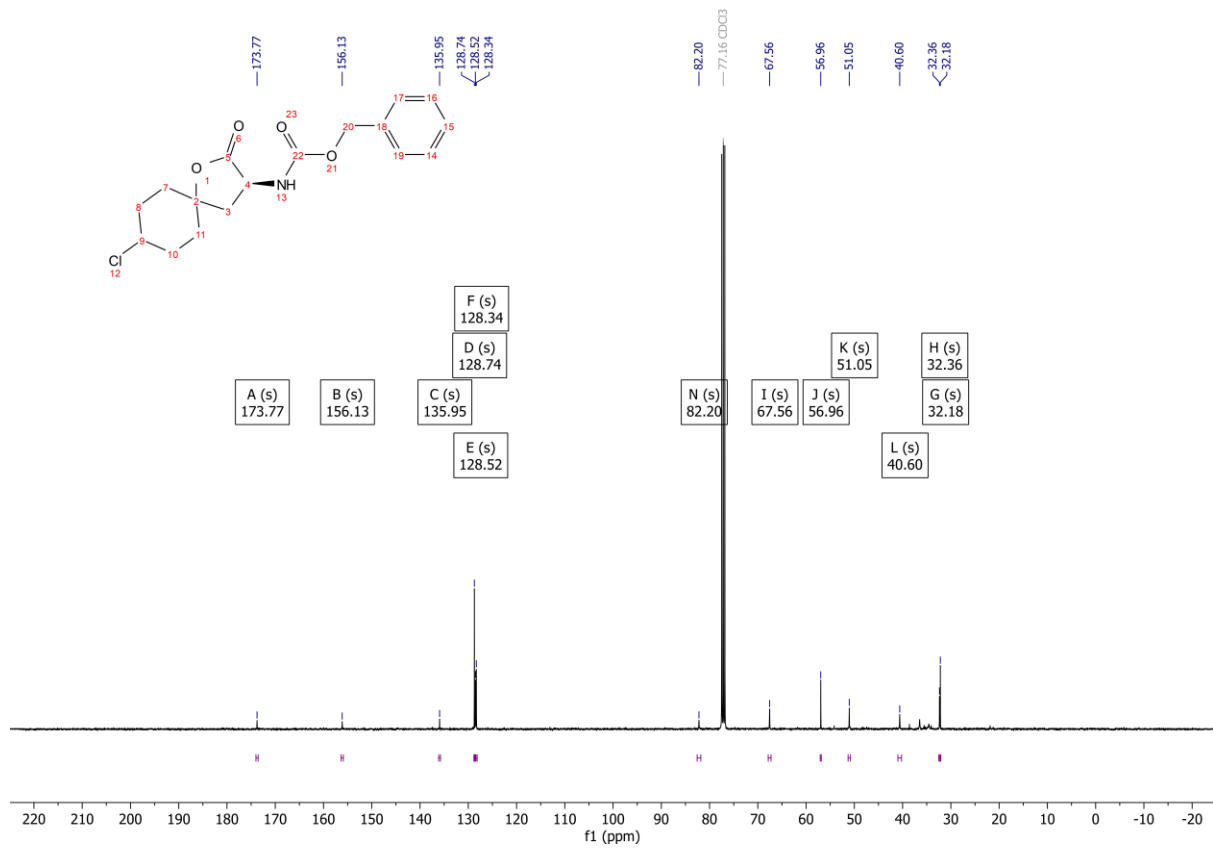
260 ¹³C NMR (101 MHz, CDCl₃)



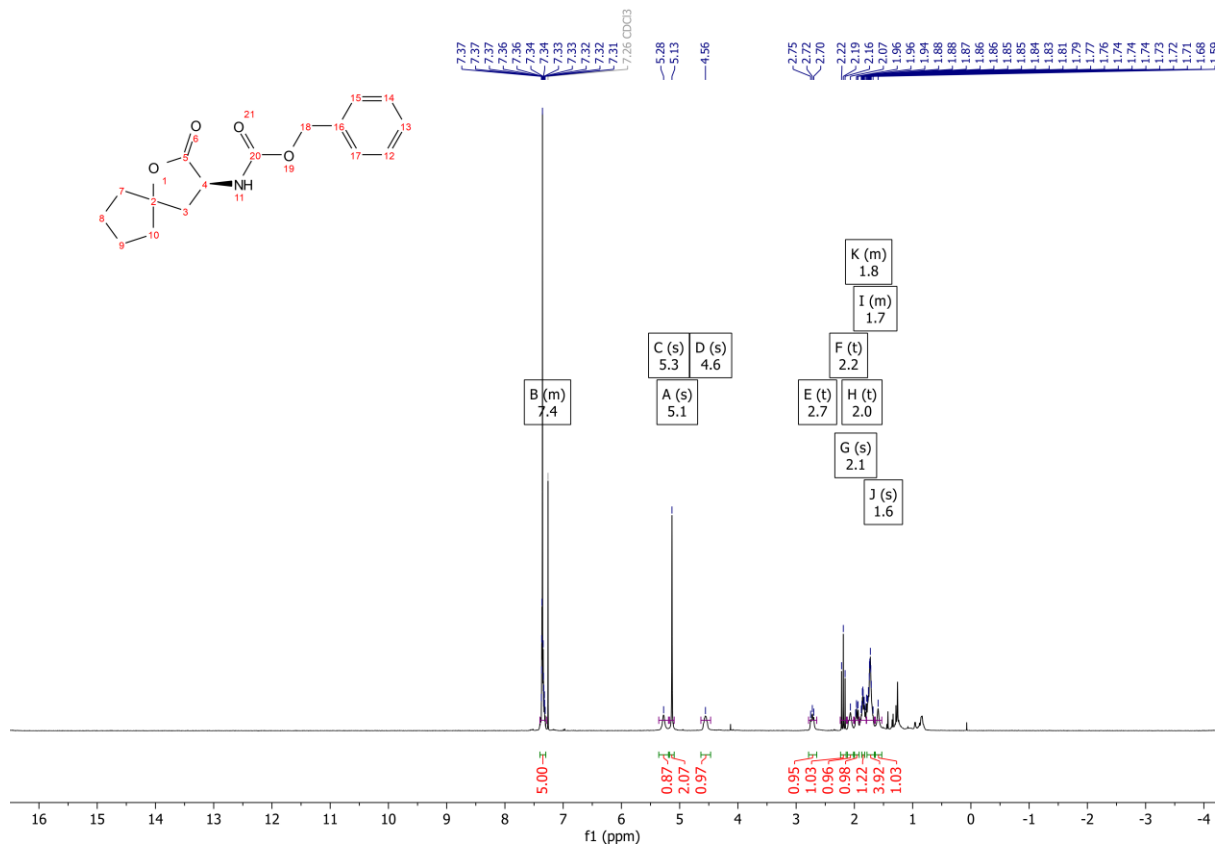
261 ¹H NMR (400 MHz, CDCl₃)



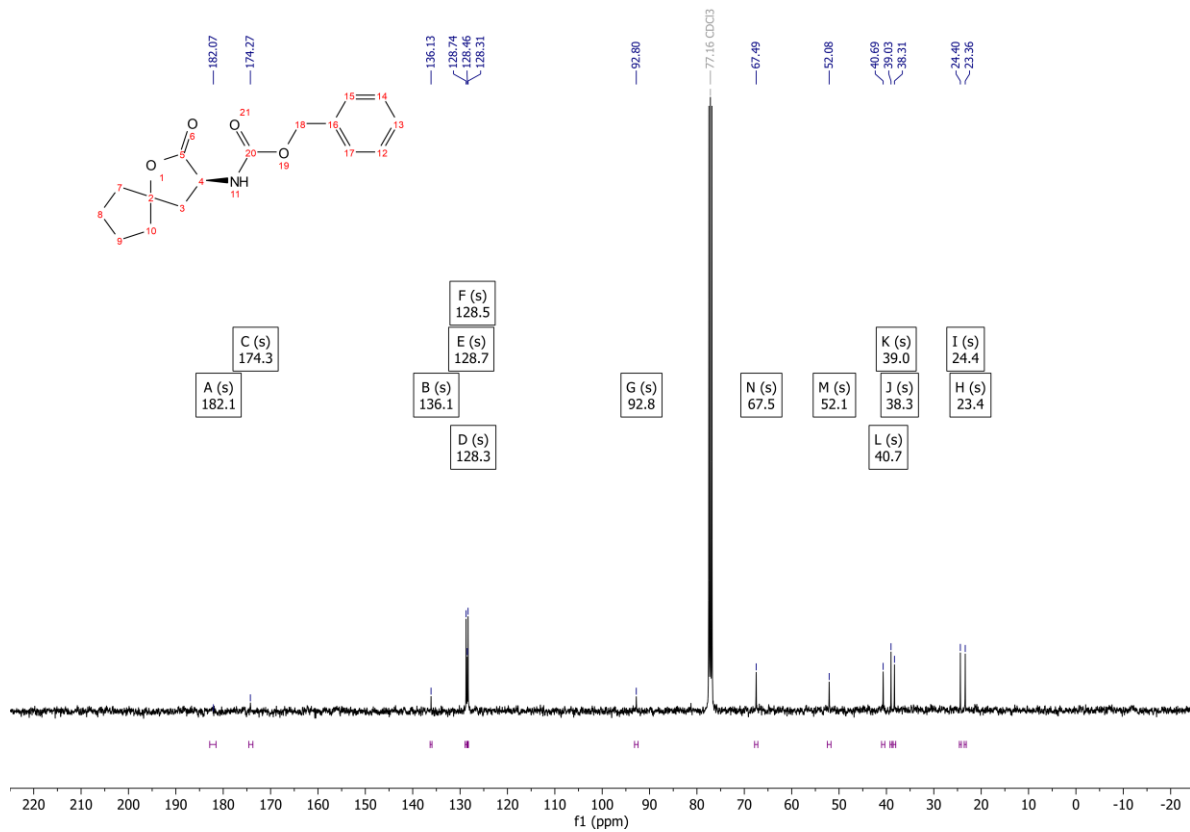
261 ¹³C NMR (101 MHz, CDCl₃)



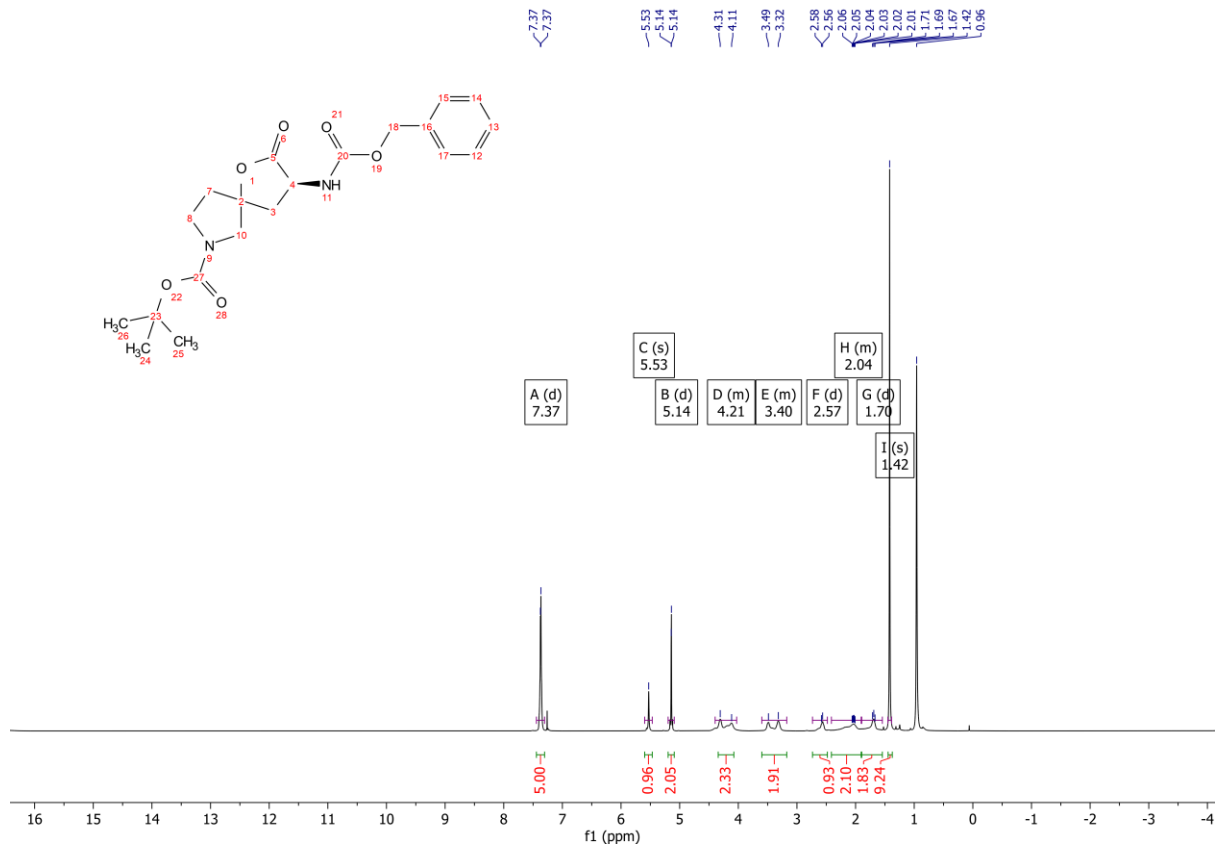
266 ¹H NMR (400 MHz, CDCl₃)



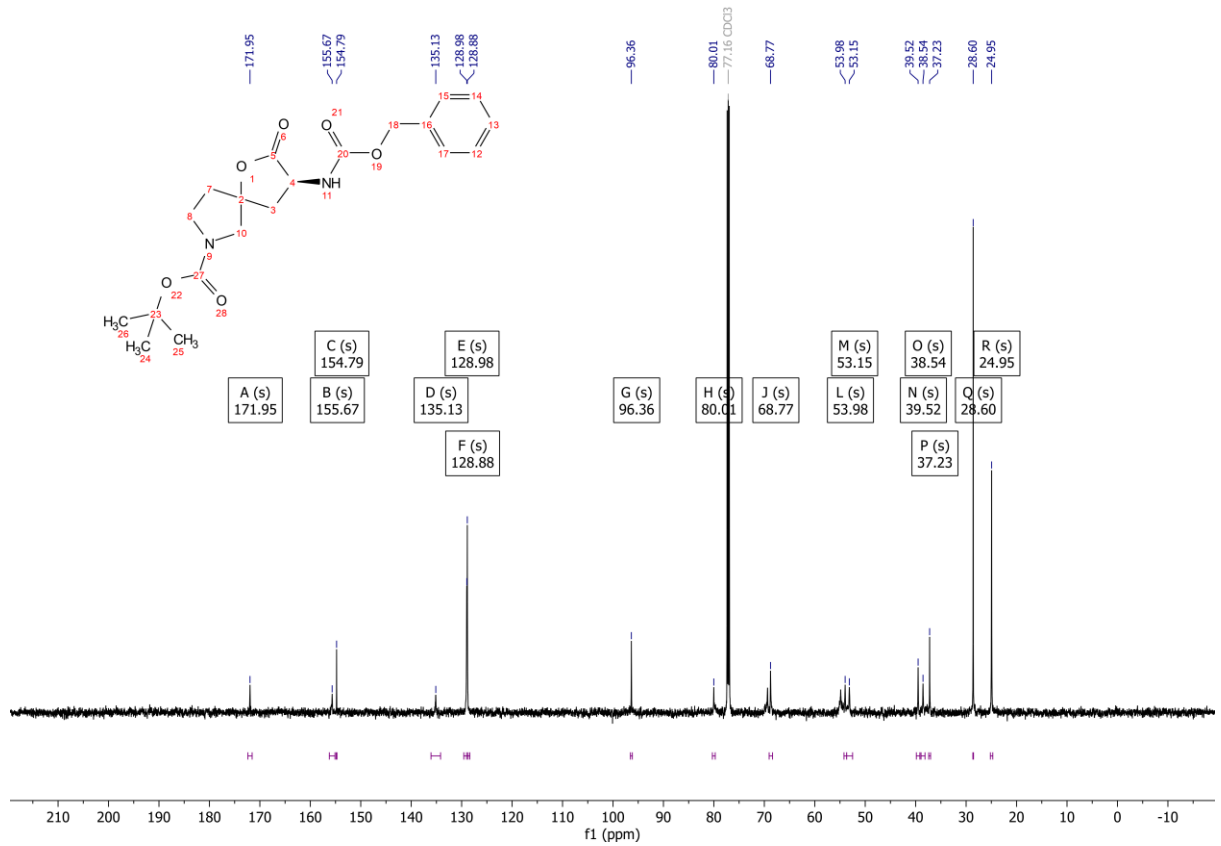
266 ¹³C NMR (101 MHz, CDCl₃)



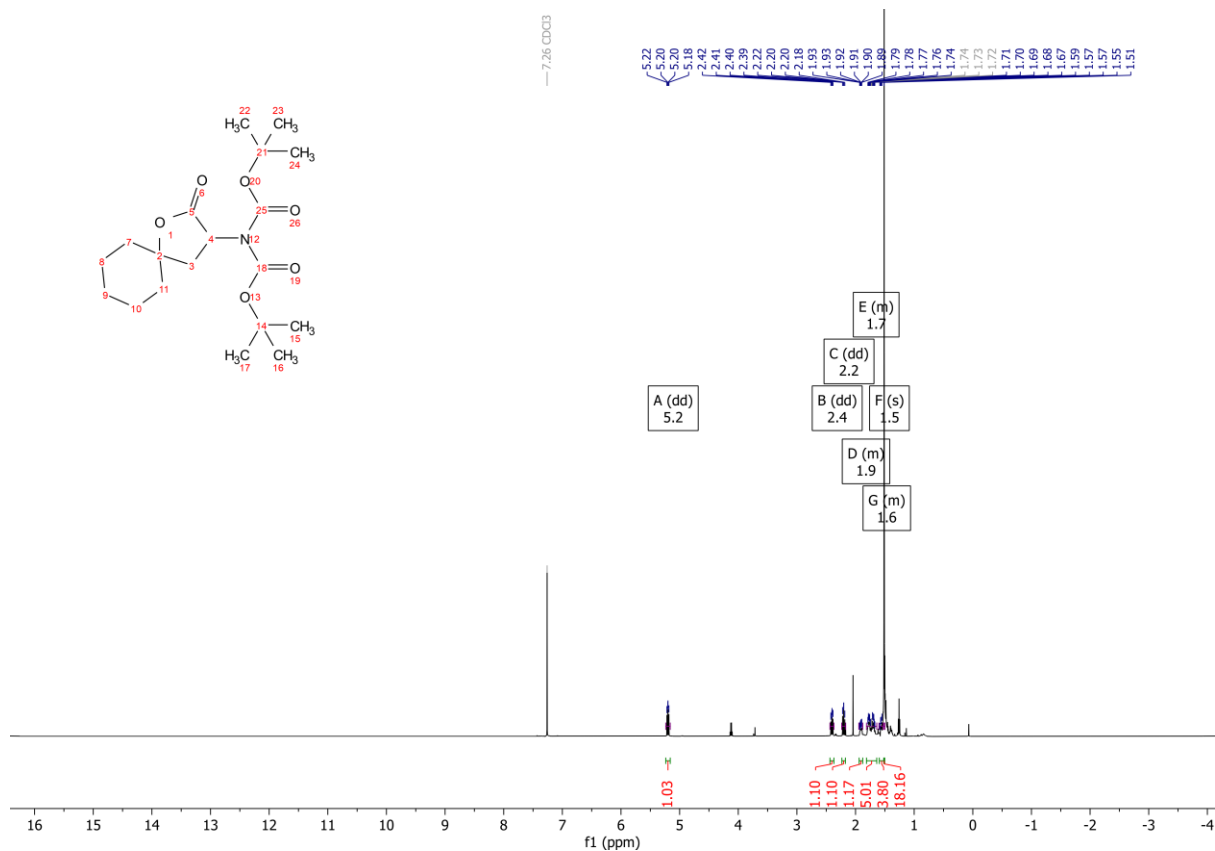
267 ¹H NMR (400 MHz, CDCl₃)



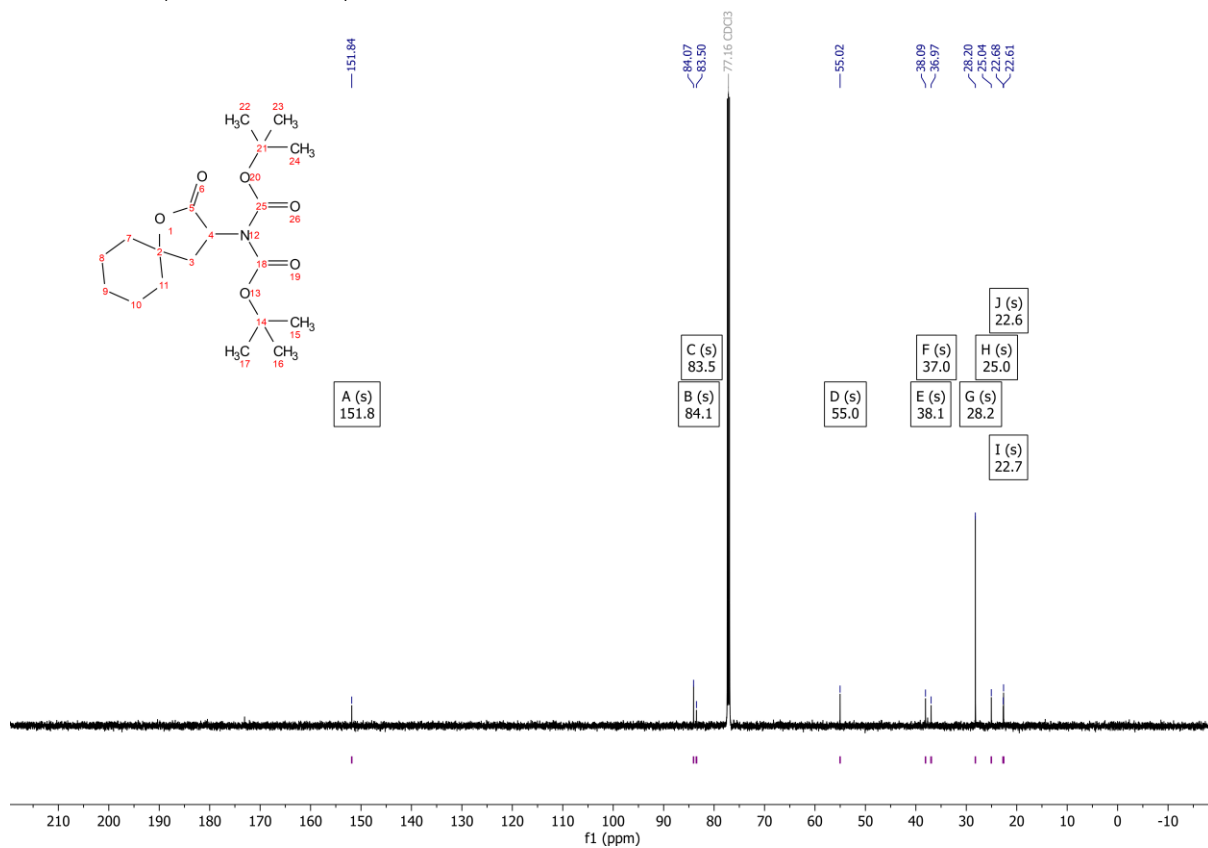
267 ¹³C NMR (101 MHz, CDCl₃)



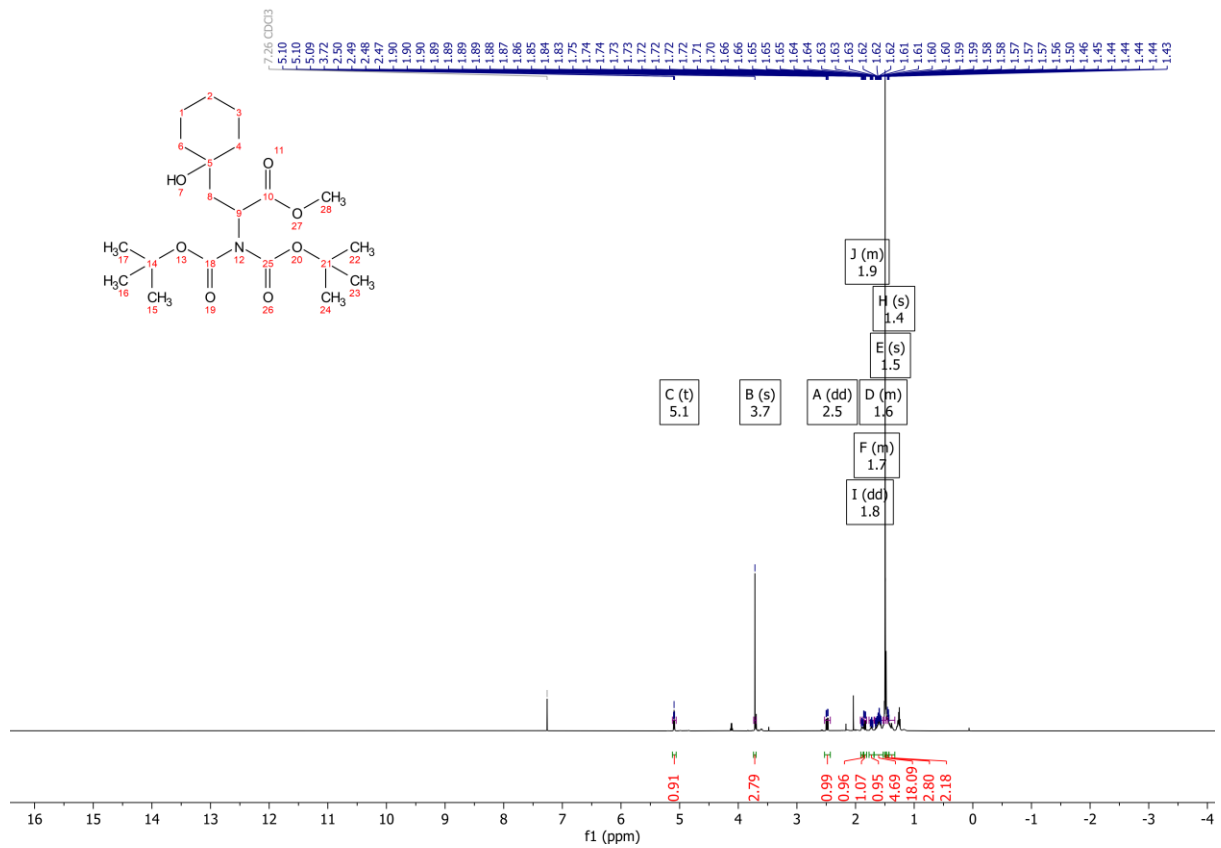
265 ¹H NMR (400 MHz, CDCl₃)



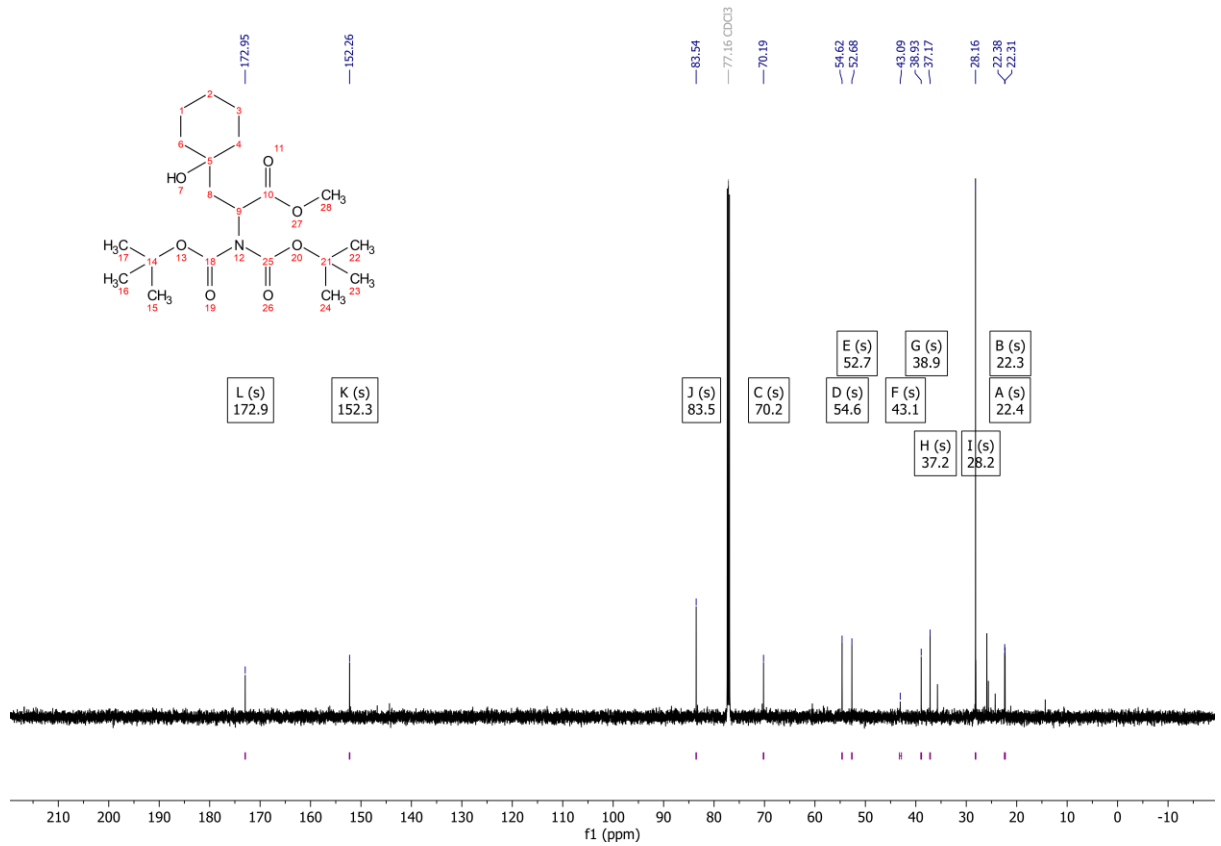
265 ¹³C NMR (101 MHz, CDCl₃)



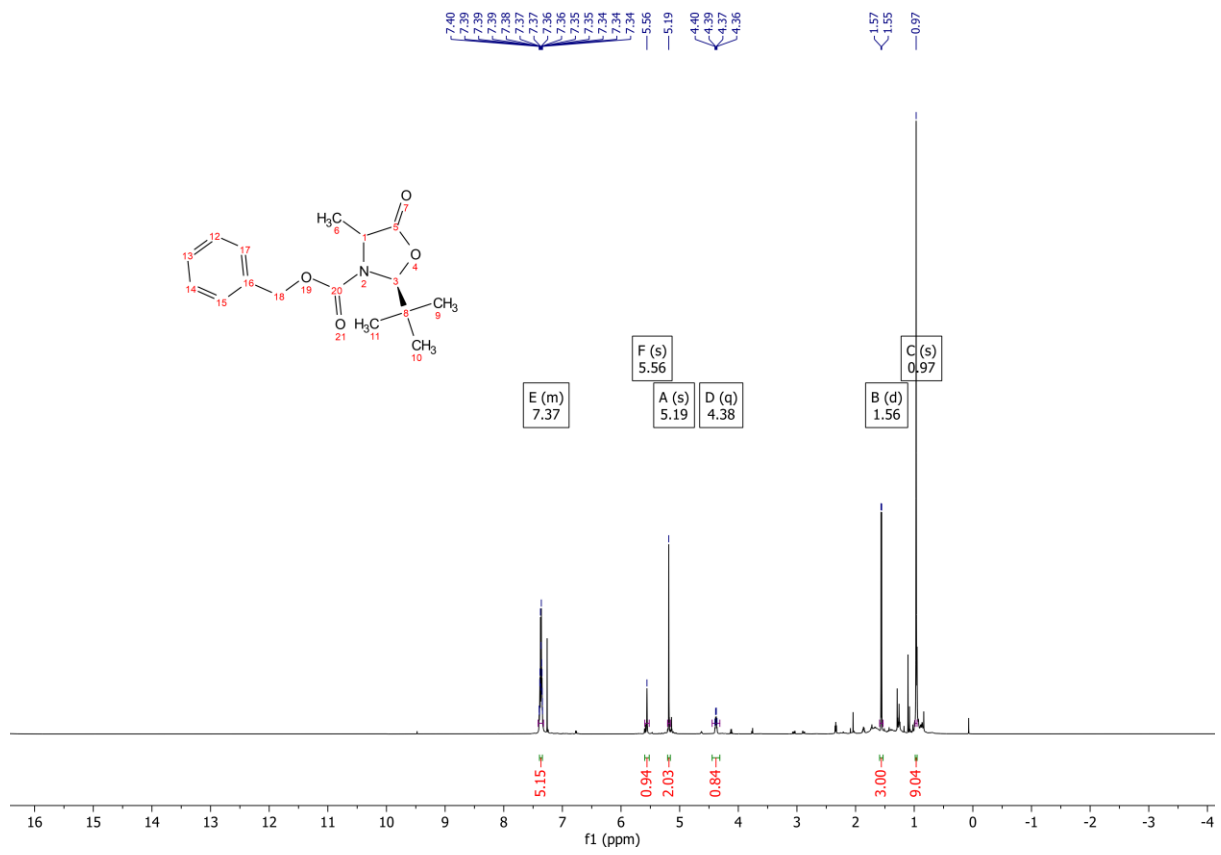
265B ¹H NMR (400 MHz, CDCl₃)



265B ¹³C NMR (101 MHz, CDCl₃)



Decomposition Product



References

- (1) Ambrogelly, A.; Palioura, S.; Söll, D. Natural Expansion of the Genetic Code. *Nat. Chem. Biol.* **2007**, *3* (1), 29–35.
- (2) Hausmann, E.; Neuman, W. F. Conversion of Proline to Hydroxyproline and Its Incorporation into Collagen. *J. Biol. Chem.* **1961**, *236* (1), 149–152.
- (3) Patil, S. T.; Zhang, L.; Martenyi, F.; Lowe, S. L.; Jackson, K. A.; Andreev, B. V.; Avedisova, A. S.; Bardenstein, L. M.; Gurovich, I. Y.; Morozova, M. A.; Mosolov, S. N.; Neznanov, N. G.; Reznik, A. M.; Smulevich, A. B.; Tochilov, V. A.; Johnson, B. G.; Monn, J. A.; Schoepp, D. D. Activation of MGlut2/3 Receptors as a New Approach to Treat Schizophrenia: A Randomized Phase 2 Clinical Trial. *Nat. Med.* **2007**, *13* (9), 1102–1107.
- (4) Monn, J. A.; Valli, M. J.; Massey, S. M.; Hao, J.; Reinhard, M. R.; Bures, M. G.; Heinz, B. A.; Wang, X.; Carter, J. H.; Getman, B. G.; Stephenson, G. A.; Herin, M.; Catlow, J. T.; Swanson, S.; Johnson, B. G.; McKinzie, D. L.; Henry, S. S. Synthesis and Pharmacological Characterization of 4-Substituted-2-Aminobicyclo[3.1.0]Hexane-2,6-Dicarboxylates: Identification of New Potent and Selective Metabotropic Glutamate 2/3 Receptor Agonists. *J. Med. Chem.* **2013**, *56* (11), 4442–4455.
- (5) Monn, J. A.; Prieto, L.; Taboada, L.; Pedregal, C.; Hao, J.; Reinhard, M. R.; Henry, S. S.; Goldsmith, P. J.; Beadle, C. D.; Walton, L.; Man, T.; Rudyk, H.; Clark, B.; Tupper, D.; Baker, S. R.; Lamas, C.; Montero, C.; Marcos, A.; Blanco, J.; Bures, M.; Clawson, D. K.; Atwell, S.; Lu, F.; Wang, J.; Russell, M.; Heinz, B. A.; Wang, X.; Carter, J. H.; Xiang, C.; Catlow, J. T.; Swanson, S.; Sanger, H.; Broad, L. M.; Johnson, M. P.; Knopp, K. L.; Simmons, R. M. A.; Johnson, B. G.; Shaw, D. B.; McKinzie, D. L. Synthesis and Pharmacological Characterization of C4-Disubstituted Analogs of 1S,2S,5R,6S-2-Aminobicyclo[3.1.0]Hexane-2,6-Dicarboxylate: Identification of a Potent, Selective Metabotropic Glutamate Receptor Agonist and Determination of Agonist-Bound Human. *J. Med. Chem.* **2015**, *58* (4), 1776–1794.
- (6) Andersson, E.; Hedman, E.; Enander, J.; Radu Djurfeldt, D.; Ljótsson, B.; Cervenka, S.; Isung, J.; Svanborg, C.; Mataix-Cols, D.; Kalso, V.; Andersson, G.; Lindefors, N.; Rück, C. D-Cycloserine vs Placebo as Adjunct to Cognitive Behavioral Therapy for Obsessive-Compulsive Disorder and Interaction With Antidepressants: A Randomized Clinical Trial. *JAMA Psychiatry* **2015**, *72* (7), 659–667.
- (7) Katagiri, K.; Tori, K.; Kimura, Y.; Yoshida, T.; Nagasaki, T.; Minato, H. A New Antibiotic. Furanomycin, an Isoleucine Antagonist. *J. Med. Chem.* **1967**, *10* (6), 1149–1154.
- (8) Larden, D. W.; Cheung, H. T. A. Synthesis of N- α -Aminoacyl Derivatives of Melphalan for Potential Use in Drug Targeting. *Tetrahedron Lett.* **1996**, *37* (42), 7581–7582.
- (9) Coleman, M. W. Determination of the Enantiomeric Purity of Oxfenicine by High-Performance Liquid Chromatography. *Chromatographia* **1983**, *17* (1), 23–26.
- (10) Lloyd, K. G.; Davidson, L.; Hornykiewicz, O. The Neurochemistry of Parkinson's Disease: Effect of L-Dopa Therapy. *J. Pharmacol. Exp. Ther.* **1975**, *195* (3), 453–464.
- (11) Mandel, S. J.; Brent, G. A.; Larsen, P. R. Levothyroxine Therapy in Patients with Thyroid Disease. *Ann. Intern. Med.* **1993**, *119* (6), 492–502.
- (12) Berkowitz, D. B.; Charette, B. D.; Karukurichi, K. R.; McFadden, J. M. α -Vinyllic Amino Acids: Occurrence, Asymmetric Synthesis and Biochemical Mechanisms. *Tetrahedron Asymmetry*. **2006**, *17* (6), 869–882.
- (13) Nowak, M. G.; Skwarecki, A. S.; Milewska, M. J. Amino Acid Based Antimicrobial Agents – Synthesis and Properties. *ChemMedChem* **2021**, *16* (23), 3513–3544.
- (14) Owen, D. R.; Allerton, C. M. N.; Anderson, A. S.; Aschenbrenner, L.; Avery, M.; Berritt, S.; Boras, B.; Cardin, R. D.; Carlo, A.; Coffman, K. J.; Dantonio, A.; Di, L.; Eng, H.; Ferre, R.; Gajiwala, K. S.; Gibson, S. A.; Greasley, S. E.; Hurst, B. L.; Kadar, E.

- P.; Kalgutkar, A. S.; Lee, J. C.; Lee, J.; Liu, W.; Mason, S. W.; Noell, S.; Novak, J. J.; Obach, R. S.; Ogilvie, K.; Patel, N. C.; Pettersson, M.; Rai, D. K.; Reese, M. R.; Sammons, M. F.; Sathish, J. G.; Singh, R. S. P.; Steppan, C. M.; Stewart, A. E.; Tuttle, J. B.; Updyke, L.; Verhoest, P. R.; Wei, L.; Yang, Q.; Zhu, Y. An Oral SARS-CoV-2 Mpro Inhibitor Clinical Candidate for the Treatment of COVID-19. *Science*. **2021**, *374* (6575), 1586–1593.
- (15) Dhillon, S.; Weber, J. Saxagliptin. *Drugs* **2009**, *69* (15), 2103–2114.
- (16) Kobayashi, J.; Hirasawa, H.; Ozawa, T.; Ozawa, T.; Takeda, H.; Fujimori, Y.; Nakanishi, O.; Kamada, N.; Ikeda, T. Synthesis and Optimization of Novel α -Phenylglycinamides as Selective TRPM8 Antagonists. *Bioorg. Med. Chem.* **2017**, *25* (2), 727–742.
- (17) Bruce, M. A.; St. Laurent, D. R.; Poindexter, G. S.; Monkovic, I.; Huang, S.; Balasubramanian, N. Kinetic Resolution of Piperazine-2-Carboxamide by Leucine Aminopeptidase. An Application in the Synthesis of the Nucleoside Transport Blocker (-) Draflazine. *Synth. Commun.* **1995**, *25* (17), 2673–2684.
- (18) Farmer, L. J.; Ledebor, M. W.; Hooch, T.; Arnost, M. J.; Bethiel, R. S.; Bennani, Y. L.; Black, J. J.; Brummel, C. L.; Chakilam, A.; Dorsch, W. A.; Fan, B.; Cochran, J. E.; Halas, S.; Harrington, E. M.; Hogan, J. K.; Howe, D.; Huang, H.; Jacobs, D. H.; Laitinen, L. M.; Liao, S.; Mahajan, S.; Marone, V.; Martinez-Botella, G.; McCarthy, P.; Messersmith, D.; Namchuk, M.; Oh, L.; Penney, M. S.; Pierce, A. C.; Raybuck, S. A.; Rugg, A.; Salituro, F. G.; Saxena, K.; Shannon, D.; Shlyakter, D.; Swenson, L.; Tian, S.-K.; Town, C.; Wang, J.; Wang, T.; Wannamaker, M. W.; Winqvist, R. J.; Zuccola, H. J. Discovery of VX-509 (Decernotinib): A Potent and Selective Janus Kinase 3 Inhibitor for the Treatment of Autoimmune Diseases. *J. Med. Chem.* **2015**, *58* (18), 7195–7216.
- (19) Hill, T. A.; Shepherd, N. E.; Diness, F.; Fairlie, D. P. Constraining Cyclic Peptides To Mimic Protein Structure Motifs. *Angew. Chemie Int. Ed.* **2014**, *53* (48), 13020–13041.
- (20) Furber, M.; Tiden, A.-K.; Gardiner, P.; Mete, A.; Ford, R.; Millichip, I.; Stein, L.; Mather, A.; Kinchin, E.; Luckhurst, C.; Barber, S.; Cage, P.; Sanganee, H.; Austin, R.; Chohan, K.; Beri, R.; Thong, B.; Wallace, A.; Oreffo, V.; Hutchinson, R.; Harper, S.; Debreczeni, J.; Breed, J.; Wissler, L.; Edman, K. Cathepsin C Inhibitors: Property Optimization and Identification of a Clinical Candidate. *J. Med. Chem.* **2014**, *57* (6), 2357–2367.
- (21) Algera, R. F.; Baldwin, A. F.; Bowles, P.; Clarke, H. J.; Connor, C. G.; Cordi, E. M.; Do, N. M.; Nicholson, L. D.; Georgian, W.; Happe, A.; Herman, M. I.; Hilou, E.; James, C.; Johnson, A. M.; Kalinowski, M.; Kulkarni, S. A.; Launer-Felty, K. D.; Lee, J. W.; Lee, T.; Lopez, J.; McInturff, E. L.; Piper, J. L.; Place, D. W.; Ragan, J. A.; Rauschenberger, B.; Ryder, K.; Stanley, M.; Weisenburger, G. A.; Weekly, R. M.; Allais, C. Synthesis of Nirmatrelvir: Design and Optimization of an Efficient Telescoped Amidation–Dehydration Sequence. *Org. Process Res. Dev.* **2023**, *27* (12), 2250–2259.
- (22) Society, C. A Novel Route to the 4-Anilido-4-(Methoxycarbonyl)Piperidine Class of Analgetics. *J. Org. Chem.* **1990**, No. 55, 4207–4209.
- (23) Coleman Michael D; Latham, David W S; Whitehead, Andrew J, M. J. G. A Convenient Method for the N-Acylation and Esterification of Hindered Amino Acids: Synthesis of Ultra Short Acting Opioid Agonist, Remifentanil. *Synlett* **1999**, 1999 (12), 1923–1924.
- (24) Ji, X.; Nielsen, A. L.; Heinis, C. Cyclic Peptides for Drug Development. *Angew. Chemie Int. Ed.* **2024**, *63* (3), e202308251.
- (25) Agarwala, A.; Asim, R.; Ballantyne, C. M. Oral PCSK9 Inhibitors. *Curr. Atheroscler. Rep.* **2024**, *26* (5), 147–152.
- (26) Release, N. Merck Initiates Phase 3 Clinical Program for Oral PCSK9 Inhibitor Candidate MK-0616. **2023**, 1–5.

- (27) Tanada, M.; Tamiya, M.; Matsuo, A.; Chiyoda, A.; Takano, K.; Ito, T.; Irie, M.; Kotake, T.; Takeyama, R.; Kawada, H.; Hayashi, R.; Ishikawa, S.; Nomura, K.; Furuichi, N.; Morita, Y.; Kage, M.; Hashimoto, S.; Nii, K.; Sase, H.; Ohara, K.; Ohta, A.; Kuramoto, S.; Nishimura, Y.; Iikura, H.; Shiraishi, T. Development of Orally Bioavailable Peptides Targeting an Intracellular Protein: From a Hit to a Clinical KRAS Inhibitor. *J. Am. Chem. Soc.* **2023**, *145* (30), 16610–16620.
- (28) Prior, I. A.; Lewis, P. D.; Mattos, C. A Comprehensive Survey of Ras Mutations in Cancer. *Cancer Res.* **2012**, *72* (10), 2457–2467.
- (29) Miura, T.; Lee, K. J.; Katoh, T.; Suga, H. In Vitro Selection of Macrocyclic L- α /d- α / β / γ -Hybrid Peptides Targeting IFN- γ /IFNGR1 Protein–Protein Interaction. *J. Am. Chem. Soc.* **2024**.
- (30) Kuhl, A.; Hahn, M. G.; Dumić, M.; Mittendorf, J. Alicyclic β -Amino Acids in Medicinal Chemistry. *Amino Acids* **2005**, *29* (2), 89–100.
- (31) Andreja, H.; Tatjana, G.; Gabrijele, E.; Nataša, M.; Mihael, S.; Joachim, M.; Ulrich, G.; Axel, S.; Wolfgang, S. In Vitro Activity and In Vivo Efficacy of Icofungipen (PLD-118), a Novel Oral Antifungal Agent, against the Pathogenic Yeast *Candida Albicans*. *Antimicrob. Agents Chemother.* **2006**, *50* (9), 3011–3018.
- (32) Panikkar, G. P. Cocaine Addiction: Neurobiology and Related Current Research in Pharmacotherapy. *Subst. Abus.* **1999**, *20* (3), 149–166.
- (33) Bajaj, N.; Hauser, R. A.; Grachev, I. D. Clinical Utility of Dopamine Transporter Single Photon Emission CT (DaT-SPECT) with (^{123}I) Ioflupane in Diagnosis of Parkinsonian Syndromes. *J. Neurol. Neurosurg. & Psychiatry* **2013**, *84* (11), 1288 LP – 1295.
- (34) Narancic, T.; Almahboub, S. A.; O'Connor, K. E. Unnatural Amino Acids: Production and Biotechnological Potential. *World J. Microbiol. Biotechnol.* **2019**, *35* (4), 67.
- (35) Avan, I.; Hall, C. D.; Katritzky, A. R. Peptidomimetics via Modifications of Amino Acids and Peptide Bonds. *Chem. Soc. Rev.* **2014**, *43* (10), 3575–3594.
- (36) Knowles, W. S.; Sabacky, M. J. Catalytic Asymmetric Hydrogenation Employing a Soluble, Optically Active, Rhodium Complex. *Chem. Commun.* **1968**, No. 22, 1445–1446.
- (37) Ellis, J. M.; Campbell, M. E.; Kumar, P.; Geunes, E. P.; Bingman, C. A.; Buller, A. R. Biocatalytic Synthesis of Non-Standard Amino Acids by a Decarboxylative Aldol Reaction. *Nat. Catal.* **2022**, *5* (2), 136–143.
- (38) Wang, J.; Liu, X.; Feng, X. Asymmetric Strecker Reactions. *Chem. Rev.* **2011**, *111* (11), 6947–6983.
- (39) Junge, K.; Hagemann, B.; Enthaler, S.; Spannenberg, A.; Michalik, M.; Oehme, G.; Monsees, A.; Riermeier, T.; Beller, M. Synthesis of Chiral Monodentate Binaphthophosphine Ligands and Their Application in Asymmetric Hydrogenations. *Tetrahedron: Asymmetry* **2004**, *15* (17), 2621–2631.
- (40) Strecker, A. Ueber Die Künstliche Bildung Der Milchsäure Und Einen Neuen, Dem Glycocollo Homologen Körper; *Justus Liebigs Ann. Chem.* **1850**, *75* (1), 27–45.
- (41) Zandbergen, P.; Brussee, J.; van der Gen, A.; Kruse, C. G. Stereoselective Synthesis of β -Hydroxy- α -Amino Acids from Chiral Cyanohydrins. *Tetrahedron: Asymmetry* **1992**, *3* (6), 769–774.
- (42) Tan, L.; Yasuda, N.; Yoshikawa, N.; Hartner, F. W.; Eng, K. K.; Leonard, W. R.; Tsay, F.-R.; Volante, R. P.; Tillyer, R. D. Stereoselective Syntheses of Highly Functionalized Bicyclo[3.1.0]Hexanes: A General Methodology for the Synthesis of Potent and Selective MGLuR2/3 Agonists. *J. Org. Chem.* **2005**, *70* (20), 8027–8034.
- (43) Petasis, N. A.; Akritopoulou, I. The Boronic Acid Mannich Reaction: A New Method for the Synthesis of Geometrically Pure Allylamines. *Tetrahedron Lett.* **1993**, *34* (4), 583–586.
- (44) Jiang, B.; Yang, C.-G.; Gu, X.-H. A Highly Stereoselective Synthesis of Indolyl N-Substituted Glycines. *Tetrahedron Lett.* **2001**, *42* (13), 2545–2547.

- (45) Nanda, K. K.; Wesley Trotter, B. Diastereoselective Petasis Mannich Reactions Accelerated by Hexafluoroisopropanol: A Pyrrolidine-Derived Arylglycine Synthesis. *Tetrahedron Lett.* **2005**, *46* (12), 2025–2028.
- (46) Currie, G. S.; Drew, M. G. B.; Harwood, L. M.; Hughes, D. J.; Luke, R. W. A.; Vickers, R. J. Chirally Templated Boronic Acid Mannich Reaction in the Synthesis of Optically Active α -Amino Acids. *J. Chem. Soc. Perkin Trans. 1* **2000**, No. 17, 2982–2990.
- (47) Harwood, L. M.; Currie, G. S.; Drew, M. G. B.; Luke, R. W. A. Asymmetry in the Boronic Acid Mannich Reaction: Diastereocontrolled Addition to Chiral Iminium Species Derived from Aldehydes and (S)-5-Phenylmorpholin-2-One. *Chem. Commun.* **1996**, No. 16, 1953–1954.
- (48) HARADA, K. Asymmetric Synthesis of α -Amino-Acids by the Strecker Synthesis. *Nature* **1963**, *200* (4912), 1201.
- (49) Zuend, S. J.; Coughlin, M. P.; Lalonde, M. P.; Jacobsen, E. N. Scaleable Catalytic Asymmetric Strecker Syntheses of Unnatural α -Amino Acids. *Nature* **2009**, *461* (7266), 968–970.
- (50) Schöllkopf, U.; Groth, U.; Deng, C. Enantioselective Syntheses of (R)-Amino Acids Using L-Valine as Chiral Agent. *Angew. Chemie Int. Ed. English* **1981**, *20* (9), 798–799.
- (51) Seebach, D.; Boes, M.; Naef, R.; Schweizer, W. B. Alkylation of Amino Acids without Loss of the Optical Activity: Preparation of α -Substituted Proline Derivatives. A Case of Self-Reproduction of Chirality. *J. Am. Chem. Soc.* **1983**, *105* (16), 5390–5398.
- (52) Tran, L. D.; Daugulis, O. Nonnatural Amino Acid Synthesis by Using Carbon–Hydrogen Bond Functionalization Methodology. *Angew. Chemie Int. Ed.* **2012**, *51* (21), 5188–5191.
- (53) He, J.; Li, S.; Deng, Y.; Fu, H.; Laforteza, B. N.; Spangler, J. E.; Homs, A.; Yu, J.-Q. Ligand-Controlled C(Sp³)–H Arylation and Olefination in Synthesis of Unnatural Chiral α -Amino Acids. *Science* **2014**, *343* (6176), 1216–1220.
- (54) Noyori, R.; Ohkuma, T.; Kitamura, M.; Takaya, H.; Sayo, N.; Kumobayashi, H.; Akutagawa, S. Asymmetric Hydrogenation of β -Keto Carboxylic Esters. A Practical, Purely Chemical Access to β -Hydroxy Esters in High Enantiomeric Purity. *J. Am. Chem. Soc.* **1987**, *109* (19), 5856–5858.
- (55) Knowles, W. S. Asymmetric Hydrogenations (Nobel Lecture). *Angew. Chemie Int. Ed.* **2002**, *41* (12), 1998–2007.
- (56) Kitamura, M.; Tsukamoto, M.; Bessho, Y.; Yoshimura, M.; Kobs, U.; Widhalm, M.; Noyori, R. Mechanism of Asymmetric Hydrogenation of α -(Acylamino)Acrylic Esters Catalyzed by BINAP–Ruthenium(II) Diacetate. *J. Am. Chem. Soc.* **2002**, *124* (23), 6649–6667.
- (57) Nájera, C.; Sansano, J. M. Catalytic Asymmetric Synthesis of α -Amino Acids. *Chemical Reviews. American Chemical Society* **2007**, 4584–4671.
- (58) Federsel, H.-J. Asymmetry on Large Scale: The Roadmap to Stereoselective Processes. *Nat. Rev. Drug Discov.* **2005**, *4* (8), 685–697.
- (59) Knowles, W. S. Asymmetric Hydrogenation. *Acc. Chem. Res.* **1983**, *16* (3), 106–112.
- (60) Blicke, F. F. The Mannich Reaction. In *Organic Reactions*; **2011**; 303–341.
- (61) Wenzel, A. G.; Jacobsen, E. N. Asymmetric Catalytic Mannich Reactions Catalyzed by Urea Derivatives: Enantioselective Synthesis of β -Aryl- β -Amino Acids. *J. Am. Chem. Soc.* **2002**, *124* (44), 12964–12965.
- (62) Romanens, A.; Bélanger, G. Preparation of Conformationally Restricted B_{2,2}- and B_{2,2,3}-Amino Esters and Derivatives Containing an All-Carbon Quaternary Center. *Org. Lett.* **2015**, *17* (2), 322–325.
- (63) Rulev, A. Y.; Azad, S.; Kotsuki, H.; Maddaluno, J. Direct Access to Cumbersome Aminated Quaternary Centers by Hyperbaric Aza-Michael Additions. *European J. Org. Chem.* **2010**, *2010* (33), 6423–6429.

- (64) Sibi, M. P.; Deshpande, P. K. A New Methodology for the Synthesis of β -Amino Acids. *J. Chem. Soc. Perkin Trans. 1* **2000**, No. 9, 1461–1466.
- (65) Hansen, T.; Alst, T.; Havelkova, M.; Strøm, M. B. Antimicrobial Activity of Small β -Peptidomimetics Based on the Pharmacophore Model of Short Cationic Antimicrobial Peptides. *J. Med. Chem.* **2010**, *53* (2), 595–606.
- (66) Zhang, D.; Chen, X.; Zhang, R.; Yao, P.; Wu, Q.; Zhu, D. Development of β -Amino Acid Dehydrogenase for the Synthesis of β -Amino Acids via Reductive Amination of β -Keto Acids. *ACS Catal.* **2015**, *5* (4), 2220–2224.
- (67) Ye, T.; McKervey, M. A. Organic Synthesis with α -Diazo Carbonyl Compounds. *Chem. Rev.* **1994**, *94* (4), 1091–1160.
- (68) Müller, Annett; Vogt, Carla; Sewald, Norbert, A. V. Synthesis of Fmoc- β -Homoamino Acids by Ultrasound-Promoted Wolff Rearrangement. *Synthesis (Stuttg)*. **1998**, *1998* (06), 837–841.
- (69) Pinho, V. D.; Gutmann, B.; Kappe, C. O. Continuous Flow Synthesis of β -Amino Acids from α -Amino Acids via Arndt–Eistert Homologation. *RSC Adv.* **2014**, *4* (70), 37419–37422.
- (70) Kirmse, W. 100 Years of the Wolff Rearrangement. *European J. Org. Chem.* **2002**, *2002* (14), 2193–2256.
- (71) Eitzinger, A.; Winter, M.; Schörghenheimer, J.; Waser, M. Quaternary B₂,2-Amino Acid Derivatives by Asymmetric Addition of Isoxazolidin-5-Ones to Para-Quinone Methides. *Chem. Commun.* **2020**, *56* (4), 579–582.
- (72) Weiner, B.; Szymański, W.; Janssen, D. B.; Minnaard, A. J.; Feringa, B. L. Recent Advances in the Catalytic Asymmetric Synthesis of β -Amino Acids. *Chem. Soc. Rev.* **2010**, *39* (5), 1656–1691.
- (73) Hsiao, Y.; Rivera, N. R.; Rosner, T.; Krska, S. W.; Njolito, E.; Wang, F.; Sun, Y.; Armstrong, J. D.; Grabowski, E. J. J.; Tillyer, R. D.; Spindler, F.; Malan, C. Highly Efficient Synthesis of β -Amino Acid Derivatives via Asymmetric Hydrogenation of Unprotected Enamines. *J. Am. Chem. Soc.* **2004**, *126* (32), 9918–9919.
- (74) Deng, J.; Hu, X.-P.; Huang, J.-D.; Yu, S.-B.; Wang, D.-Y.; Duan, Z.-C.; Zheng, Z. Enantioselective Synthesis of B₂-Amino Acids via Rh-Catalyzed Asymmetric Hydrogenation with BoPhoz-Type Ligands: Important Influence of an N–H Proton in the Ligand on the Enantioselectivity. *J. Org. Chem.* **2008**, *73* (5), 2015–2017.
- (75) Lin, D.; Deng, G.; Wang, J.; Ding, X.; Jiang, H.; Liu, H. Efficient Synthesis of Symmetrical α,α -Disubstituted β -Amino Acids and α,α -Disubstituted Aldehydes via Dialkylation of Nucleophilic β -Alanine Equivalent. *J. Org. Chem.* **2010**, *75* (5), 1717–1722.
- (76) Davies, J.; Janssen-Müller, D.; Zimin, D. P.; Day, C. S.; Yanagi, T.; Elfert, J.; Martin, R. Ni-Catalyzed Carboxylation of Aziridines En Route to β -Amino Acids. *J. Am. Chem. Soc.* **2021**, *143* (13), 4949–4954.
- (77) Fernández-Suárez, M.; Muñoz, L.; Fernández, R.; Riguera, R. Asymmetric Synthesis of the β -Amino Acid Methyl Ester Derivative of Onchidin: (2S,3S)-Methyl-3-Amino-2-Methyl-7-Octynoate and Its Enantiomer. *Tetrahedron: Asymmetry* **1997**, *8* (11), 1847–1854.
- (78) Buckel, W.; Golding, B. T. Radical Enzymes. In *Encyclopedia of Radicals in Chemistry, Biology and Materials*; 2012.
- (79) Beckwith, A. L. J. Centenary Lecture. The Pursuit of Selectivity in Radical Reactions. *Chem. Soc. Rev.* **1993**, *22* (3), 143–151.
- (80) Binkley, R. W.; Binkley, E. Radical Reactions of Carbohydrates. In *Volume I: Structure and Reactivity of Carbohydrate Radicals*, 2013.
- (81) He, C.; Ke, J.; Liu, W.; Zhu, X.; Tan, X. Akzeptierter Artikel Titel: Electrochemical Radical Silyl-Oxygenation of Activated Alkenes.
- (82) Elgrishi, N.; Rountree, K. J.; McCarthy, B. D.; Rountree, E. S.; Eisenhart, T. T.; Dempsey, J. L. A Practical Beginner's Guide to Cyclic Voltammetry. *J. Chem. Educ.*

- 2018, 95 (2), 197–206.
- (83) Hofmann, A. W. Ueber Die Einwirkung Des Broms in Alkalischer Lösung Auf Die Amine. *Berichte der Dtsch. Chem. Gesellschaft* **1883**, 16 (1), 558–560.
- (84) Minisci, F.; Bernardi, R.; Bertini, F.; Galli, R.; Perchinummo, M. Nucleophilic Character of Alkyl Radicals—VI: A New Convenient Selective Alkylation of Heteroaromatic Bases. *Tetrahedron* **1971**, 27 (15), 3575–3579.
- (85) van der Kerk, G. J. M.; Noltes, J. G.; Luijten, J. G. A. Investigations on Organo-Tin Compounds. VII the Addition of Organo-Tin Hydrides to Olefinic Double Bonds. *J. Appl. Chem.* **1957**, 7 (7), 356–365.
- (86) Kuivila, H. G.; Menapace, L. W. Reduction of Alkyl Halides by Organotin Hydrides¹, 2. *J. Org. Chem.* **1963**, 28 (9), 2165–2167.
- (87) Barton, D. H. R.; McCombie, S. W. A New Method for the Deoxygenation of Secondary Alcohols. *J. Chem. Soc. Perkin Trans. 1* **1975**, No. 16, 1574–1585.
- (88) Crich, D.; Quintero, L. Radical Chemistry Associated with the Thiocarbonyl Group. *Chem. Rev.* **1989**, 89 (7), 1413–1432.
- (89) Barton, D. H. R.; Crich, D.; Motherwell, W. B. New and Improved Methods for the Radical Decarboxylation of Acids. *J. Chem. Soc. Chem. Commun.* **1983**, No. 17, 939–941.
- (90) Barton, D. H. R.; Crich, D.; Motherwell, W. B. A Practical Alternative to the Hunsdiecker Reaction. *Tetrahedron Lett.* **1983**, 24 (45), 4979–4982.
- (91) Fittig, R. Ueber Einige Producte Der Trocken Destillation Essigsaurer Salze. *Justus Liebigs Ann. Chem.* **1859**, 110 (1), 17–23.
- (92) Kronenwetter, H.; Husek, J.; Etz, B.; Jones, A.; Manchanayakage, R. Electrochemical Pinacol Coupling of Aromatic Carbonyl Compounds in a [BMIM][BF₄]-H₂O Mixture. *Green Chem.* **2014**, 16 (3), 1489–1495.
- (93) Mukaiyama, T.; Sato, T.; Hanna, J. REDUCTIVE COUPLING OF CARBONYL COMPOUNDS TO PINACOLS AND OLEFINS BY USING TICl₄ AND Zn. *Chem. Lett.* **1973**, 2 (10), 1041–1044.
- (94) Giese, B.; Juan Antonio, G. G. Carbon-carbon Bond Formation by Addition of σ -Radicals to Alkenes. *Tetrahedron Lett.* **1982**, 23 (27), 2765–2766.
- (95) Giese, B.; Zwick, W. Reactivity of Alkenes in Free-Radical Additions. *Angew. Chemie Int. Ed. English* **1978**, 17 (1), 66–67.
- (96) Kitcatt, D. M.; Nicolle, S.; Lee, A.-L. Direct Decarboxylative Giese Reactions. *Chem. Soc. Rev.* **2022**, 51 (4), 1415–1453.
- (97) Zersetzung Der Valeriansäure Durch Den Elektrischen Strom. *Justus Liebigs Ann. Chem.* **1848**, 64 (3), 339–341.
- (98) Kolbe, H. Untersuchungen Über Die Elektrolyse Organischer Verbindungen. *Justus Liebigs Ann. Chem.* **1849**, 69 (3), 257–294.
- (99) Barton, D. H. R.; Hervé, Y.; Potier, P.; Thierry, J. Reductive Radical Decarboxylation of Amino-Acids and Peptides. *J. Chem. Soc. Chem. Commun.* **1984**, No. 19, 1298–1299.
- (100) Hunsdiecker, H.; Hunsdiecker, C. Über Den Abbau Der Salze Aliphatischer Säuren Durch Brom. *Berichte der Dtsch. Chem. Gesellschaft A B Ser.* **1942**, 75 (3), 291–297.
- (101) Tucker, J. W.; Stephenson, C. R. J. Shining Light on Photoredox Catalysis: Theory and Synthetic Applications. *J. Org. Chem.* **2012**, 77 (4), 1617–1622.
- (102) Ravelli, D.; Protti, S.; Fagnoni, M. Carbon–Carbon Bond Forming Reactions via Photogenerated Intermediates. *Chem. Rev.* **2016**, 116 (17), 9850–9913.
- (103) Yi, H.; Zhang, G.; Wang, H.; Huang, Z.; Wang, J.; Singh, A. K.; Lei, A. Recent Advances in Radical C–H Activation/Radical Cross-Coupling. *Chem. Rev.* **2017**, 117 (13), 9016–9085.
- (104) Griffin, J. D.; Zeller, M. A.; Nicewicz, D. A. Hydrodecarboxylation of Carboxylic and Malonic Acid Derivatives via Organic Photoredox Catalysis: Substrate Scope and Mechanistic Insight. *J. Am. Chem. Soc.* **2015**, 137 (35), 11340–11348.

- (105) Capaldo, L.; Buzzetti, L.; Merli, D.; Fagnoni, M.; Ravelli, D. Smooth Photocatalyzed Benzoylation of Electrophilic Olefins via Decarboxylation of Arylacetic Acids. *J. Org. Chem.* **2016**, *81* (16), 7102–7109.
- (106) P. Roberts, B. Polarity-Reversal Catalysis of Hydrogen-Atom Abstraction Reactions: Concepts and Applications in Organic Chemistry. *Chem. Soc. Rev.* **1999**, *28* (1), 25–35.
- (107) Parr, R. G.; Szentpály, L. v.; Liu, S. Electrophilicity Index. *J. Am. Chem. Soc.* **1999**, *121* (9), 1922–1924.
- (108) Davies, J.; Svejstrup, T. D.; Fernandez Reina, D.; Sheikh, N. S.; Leonori, D. Visible-Light-Mediated Synthesis of Amidyl Radicals: Transition-Metal-Free Hydroamination and N-Arylation Reactions. *J. Am. Chem. Soc.* **2016**, *138* (26), 8092–8095.
- (109) De Vleeschouwer, F.; Van Speybroeck, V.; Waroquier, M.; Geerlings, P.; De Proft, F. Electrophilicity and Nucleophilicity Index for Radicals. *Org. Lett.* **2007**, *9* (14), 2721–2724.
- (110) McCallum, T.; Pitre, S. P.; Morin, M.; Scaiano, J. C.; Barriault, L. The Photochemical Alkylation and Reduction of Heteroarenes. *Chem. Sci.* **2017**, *8* (11), 7412–7418; Fox, M. A.; Whitesell, J. K. *Organic Chemistry*; Jones & Bartlett Learning, 2004.
- (111) Ciamician, G. The Photochemistry of the Future. *Science* **1912**, *36* (926), 385–394.
- (112) Ischay, M. A.; Anzovino, M. E.; Du, J.; Yoon, T. P. Efficient Visible Light Photocatalysis of [2+2] Enone Cycloadditions. *J. Am. Chem. Soc.* **2008**, *130* (39), 12886–12887.
- (113) Nicewicz, D. A.; MacMillan, D. W. C. Merging Photoredox Catalysis with Organocatalysis: The Direct Asymmetric Alkylation of Aldehydes. *Science* **2008**, *322* (5898), 77–80.
- (114) Narayanam, J. M. R.; Tucker, J. W.; Stephenson, C. R. J. Electron-Transfer Photoredox Catalysis: Development of a Tin-Free Reductive Dehalogenation Reaction. *J. Am. Chem. Soc.* **2009**, *131* (25), 8756–8757.
- (115) Nagatomo, M.; Nishiyama, H.; Fujino, H.; Inoue, M. Decarbonylative Radical Coupling of α -Aminoacyl Tellurides: Single-Step Preparation of γ -Amino and α,β -Diamino Acids and Rapid Synthesis of Gabapentin and Manzacidin A. *Angew. Chemie Int. Ed.* **2015**, *54* (5), 1537–1541.
- (116) Chatgililoglu, C.; Crich, D.; Komatsu, M.; Ryu, I. Chemistry of Acyl Radicals. *Chem. Rev.* **1999**, *99* (8).
- (117) Wu, G.; Wang, J.; Liu, C.; Sun, M.; Zhang, L.; Ma, Y.; Cheng, R.; Ye, J. Transition metal-free, visible-light-mediated construction of α,β -diamino esters via decarboxylative radical addition at room temperature. *Org. Chem. Front.*, **2019**, *6*, 2245–2249.
- (118) Zeng, H.; Yang, S.; Li, H.; Lu, D.; Gong, Y.; Zhu, J.-T. Site-Specific Functionalization of 1,3-Dioxolane with Imines: A Radical Chain Approach to Masked α -Amino Aldehydes. *J. Org. Chem.* **2018**, *83* (9), 5256–5266.
- (119) Yang, S.; Zhu, S.; Lu, D.; Gong, Y. Polarity-Reversed Addition of Enol Ethers to Imines under Visible Light: Redox-Neutral Access to Azide-Containing Amino Acids. *Org. Lett.* **2019**, *21* (20), 8464–8468.
- (120) Ni, S.; Garrido-Castro, A. F.; Merchant, R. R.; de Gruyter, J. N.; Schmitt, D. C.; Mousseau, J. J.; Gallego, G. M.; Yang, S.; Collins, M. R.; Qiao, J. X.; Yeung, K.-S.; Langley, D. R.; Poss, M. A.; Scola, P. M.; Qin, T.; Baran, P. S. A General Amino Acid Synthesis Enabled by Innate Radical Cross-Coupling. *Angew. Chemie* **2018**, *130* (44), 14768–14773.
- (121) Matsumoto, Y.; Sawamura, J.; Murata, Y.; Nishikata, T.; Yazaki, R.; Ohshima, T. Amino Acid Schiff Base Bearing Benzophenone Imine As a Platform for Highly Congested Unnatural α -Amino Acid Synthesis. *J. Am. Chem. Soc.* **2020**, *142* (18), 8498–8505.
- (122) Lu, H.; Hu, Y.; Jiang, H.; Wojtas, L.; Zhang, X. P. Stereoselective Radical Amination

- of Electron-Deficient C(Sp³)–H Bonds by Co(II)-Based Metalloradical Catalysis: Direct Synthesis of α -Amino Acid Derivatives via α -C–H Amination. *Org. Lett.* **2012**, *14* (19), 5158–5161.
- (123) Ye, C.-X.; Dansby, D. R.; Chen, S.; Meggers, E. Expedited Synthesis of α -Amino Acids by Single-Step Enantioselective α -Amination of Carboxylic Acids. *Nat. Synth.* **2023**, *2* (7), 645–652.
- (124) Fan, X.; Gong, X.; Ma, M.; Wang, R.; Walsh, P. J. Visible Light-Promoted CO₂ Fixation with Imines to Synthesize Diaryl α -Amino Acids. *Nat. Commun.* **2018**, *9* (1), 4936.
- (125) Ju, T.; Fu, Q.; Ye, J.-H.; Zhang, Z.; Liao, L.-L.; Yan, S.-S.; Tian, X.-Y.; Luo, S.-P.; Li, J.; Yu, D.-G. Selective and Catalytic Hydrocarboxylation of Enamides and Imines with CO₂ to Generate α,α -Disubstituted α -Amino Acids. *Angew. Chemie Int. Ed.* **2018**, *57* (42), 13897–13901.
- (126) Song, L.; Fu, D.-M.; Chen, L.; Jiang, Y.-X.; Ye, J.-H.; Zhu, L.; Lan, Y.; Fu, Q.; Yu, D.-G. Visible-Light Photoredox-Catalyzed Remote Difunctionalizing Carboxylation of Unactivated Alkenes with CO₂. *Angew. Chemie Int. Ed.* **2020**, *59* (47), 21121–21128.
- (127) Seo, H.; Katcher, M. H.; Jamison, T. F. Photoredox Activation of Carbon Dioxide for Amino Acid Synthesis in Continuous Flow. *Nat. Chem.* **2017**, *9* (5), 453–456.
- (128) Steckelberg, A.-L.; Akiyama, B. M.; Costantino, D. A.; Sit, T. L.; Nix, J. C.; Kieft, J. S. A Folded Viral Noncoding RNA Blocks Host Cell Exoribonucleases through a Conformationally Dynamic RNA Structure. *Proc. Natl. Acad. Sci.* **2018**, *115* (25), 6404–6409.
- (129) Shah, A. A.; Kelly, M. J.; Perkins, J. J. Access to Unnatural α -Amino Acids via Visible-Light-Mediated Decarboxylative Conjugate Addition to Dehydroalanine. *Org. Lett.* **2020**, *22* (6), 2196–2200.
- (130) Rossolini, T.; Leitch, J. A.; Grainger, R.; Dixon, D. J. Photocatalytic Three-Component Umpolung Synthesis of 1,3-Diamines. *Org. Lett.* **2018**, *20* (21), 6794–6798.
- (131) Rossolini, T.; Ferko, B.; Dixon, D. J. Photocatalytic Reductive Formation of α -Tertiary Ethers from Ketals. *Org. Lett.* **2019**, *21* (17), 6668–6673.
- (132) de Bruijn, A. D.; Roelfes, G. Chemical Modification of Dehydrated Amino Acids in Natural Antimicrobial Peptides by Photoredox Catalysis. *Chem. – A Eur. J.* **2018**, *24* (44), 11314–11318.
- (133) Brandhofer, T.; Mancheño, O. G. Versatile Ru-Photoredox-Catalyzed Functionalization of Dehydro-Amino Acids and Peptides. *ChemCatChem* **2019**, *11* (16), 3797–3801.
- (134) Petracca, R.; Bowen, K. A.; McSweeney, L.; O’Flaherty, S.; Genna, V.; Twamley, B.; Devocelle, M.; Scanlan, E. M. Chemoselective Synthesis of N-Terminal Cysteinyll Thioesters via β,γ -C,S Thiol-Michael Addition. *Org. Lett.* **2019**, *21* (9), 3281–3285.
- (135) Qin, T.; Malins, L. R.; Edwards, J. T.; Merchant, R. R.; Novak, A. J. E.; Zhong, J. Z.; Mills, R. B.; Yan, M.; Yuan, C.; Eastgate, M. D.; Baran, P. S. Nickel-Catalyzed Barton Decarboxylation and Giese Reactions: A Practical Take on Classic Transforms. *Angew. Chemie Int. Ed.* **2017**, *56* (1), 260–265.
- (136) Sim, J.; Campbell, M. W.; Molander, G. A. Synthesis of α -Fluoro- α -Amino Acid Derivatives via Photoredox-Catalyzed Carbofluorination. *ACS Catal.* **2019**, *9* (2), 1558–1563.
- (137) Wright, T. H.; Bower, B. J.; Chalker, J. M.; Bernardes, G. J. L.; Wiewiora, R.; Ng, W.-L.; Raj, R.; Faulkner, S.; Vallée, M. R. J.; Phanumartwiwath, A.; Coleman, O. D.; Thézénas, M.-L.; Khan, M.; Galan, S. R. G.; Lercher, L.; Schombs, M. W.; Gerstberger, S.; Palm-Espling, M. E.; Baldwin, A. J.; Kessler, B. M.; Claridge, T. D. W.; Mohammed, S.; Davis, B. G. Posttranslational Mutagenesis: A Chemical Strategy for Exploring Protein Side-Chain Diversity. *Science* **2016**, *354* (6312), aag1465.
- (138) Karady, S.; Amto, J. S.; Weinstock, L. M. Enantioretentive Alkylation of Acyclic Amino Acids. *Tetrahedron Lett.* **1984**, *25* (39), 4337–4340.

- (139) Beckwith, A. L. J.; Chai, C. L. L. Diastereoselective Radical Addition to Derivatives of Dehydroalanine and of Dehydrolactic Acid. *J. Chem. Soc. { } Chem. Commun.* **1990**, No. 16, 1087–1088.
- (140) Aycock, R. A.; Vogt, D. B.; Jui, N. T. A Practical and Scalable System for Heteroaryl Amino Acid Synthesis. *Chem. Sci.* **2017**, *8* (12), 7998–8003.
- (141) Aycock, R. A.; Pratt, C. J.; Jui, N. T. Aminoalkyl Radicals as Powerful Intermediates for the Synthesis of Unnatural Amino Acids and Peptides. *ACS Catal.* **2018**, *8* (10), 9115–9119.
- (142) Trowbridge, A.; Reich, D.; Gaunt, M. J. Multicomponent Synthesis of Tertiary Alkylamines by Photocatalytic Olefin-Hydroaminoalkylation. *Nature* **2018**, *561* (7724), 522–527.
- (143) Merkens, K.; Aguilar Troyano, F. J.; Djossou, J.; Gómez-Suárez, A. Synthesis of Unnatural α -Amino Acid Derivatives via Light-Mediated Radical Decarboxylative Processes. *Adv. Synth. Catal.* **2020**, *362* (12), 2354–2359.
- (144) Ji, P.; Zhang, Y.; Dong, Y.; Huang, H.; Wei, Y.; Wang, W. Synthesis of Enantioenriched α -Deuterated α -Amino Acids Enabled by an Organophotocatalytic Radical Approach. *Org. Lett.* **2020**, *22* (4), 1557–1562.
- (145) Zhang, O.; Schubert, J. W. Derivatization of Amino Acids and Peptides via Photoredox-Mediated Conjugate Addition. *J. Org. Chem.* **2020**, *85* (9), 6225–6232.
- (146) Qian, B.; Chen, S.; Wang, T.; Zhang, X.; Bao, H. Iron-Catalyzed Carboamination of Olefins: Synthesis of Amines and Disubstituted β -Amino Acids. *J. Am. Chem. Soc.* **2017**, *139* (37), 13076–13082.
- (147) Hidasová, D.; Janák, M.; Jahn, E.; Císařová, I.; Jones, P. G.; Jahn, U. Diastereoselective Radical Couplings Enable the Asymmetric Synthesis of Anti- β -Amino- α -Hydroxy Carboxylic Acid Derivatives. *European J. Org. Chem.* **2018**, *2018* (37), 5222–5230.
- (148) Chen, X.; Zard, S. Z. Convergent Route to β -Amino Acids and to β -Heteroarylethylamines: An Unexpected Vinylation Reaction. *Org. Lett.* **2020**, *22* (9), 3628–3632.
- (149) Tan, G.; Das, M.; Keum, H.; Bellotti, P.; Daniliuc, C.; Glorius, F. Photochemical Single-Step Synthesis of β -Amino Acid Derivatives from Alkenes and (Hetero)Arenes. *Nat. Chem.* **2022**.
- (150) Abbott, Edwin Abbott. *Flatland: a romance of many dimensions*. Barnes & Noble, 1966.
- (151) Lovering, F.; Bikker, J.; Humblet, C. Escape from Flatland: Increasing Saturation as an Approach to Improving Clinical Success. *J. Med. Chem.* **2009**, *52* (21), 6752–6756.
- (152) Hou, T. J.; Xia, K.; Zhang, W.; Xu, X. J. ADME Evaluation in Drug Discovery. 4. Prediction of Aqueous Solubility Based on Atom Contribution Approach. *J. Chem. Inf. Comput. Sci.* **2004**, *44* (1), 266–275.
- (153) Karthikeyan, M.; Glen, R. C.; Bender, A. General Melting Point Prediction Based on a Diverse Compound Data Set and Artificial Neural Networks. *J. Chem. Inf. Model.* **2005**, *45* (3), 581–590.
- (154) Lipinski, C. A. Chapter 27. Bioisosterism in Drug Design; Bailey, D. M. B. T.-A. R. in M. C., Ed.; Academic Press, 1986; Vol. 21, pp 283–291.
- (155) Subbaiah, M. A. M.; Meanwell, N. A. Bioisosteres of the Phenyl Ring: Recent Strategic Applications in Lead Optimization and Drug Design. *J. Med. Chem.* **2021**, *64* (19), 14046–14128.
- (156) Garthwaite, S. M.; McMahon, E. G. The Evolution of Aldosterone Antagonists. *Mol. Cell. Endocrinol.* **2004**, *217* (1), 27–31.
- (157) Li, D. B.; Rogers-Evans, M.; Carreira, E. M. Synthesis of Novel Azaspiro[3.4]Octanes as Multifunctional Modules in Drug Discovery. *Org. Lett.* **2011**, *13* (22), 6134–6136.
- (158) Epplin, R. C.; Paul, S.; Herter, L.; Salome, C.; Hancock, E. N.; Larrow, J. F.; Baum, E.

- W.; Dunstan, D. R.; Ginsburg-Moraff, C.; Fessard, T. C.; Brown, M. K. [2]-Ladderanes as Isosteres for Meta-Substituted Aromatic Rings and Rigidified Cyclohexanes. *Nat. Commun.* **2022**, *13* (1), 6056.
- (159) Fujiwara, K.; Nagasawa, S.; Maeyama, R.; Segawa, R.; Hirasawa, N.; Iwabuchi, Y. Selective Synthesis of 1,3-Substituted Cuneanes: En Route to Potent Bioisosteres of *m*-Substituted Benzenes. **2023**, 1–7.
- (160) Smith, E.; Jones, K. D.; O'Brien, L.; Argent, S. P.; Salome, C.; Lefebvre, Q.; Valery, A.; Böcö, M.; Newton, G. N.; Lam, H. W. Silver(I)-Catalyzed Synthesis of Cuneanes from Cubanes and Their Investigation as Isosteres. *J. Am. Chem. Soc.* **2023**, *145* (30), 16365–16373.
- (161) Dibchak, D.; Snisarenko, M.; Mishuk, A.; Shablykin, O.; Bortnichuk, L.; Klymenko-Ulianov, O.; Kheylik, Y.; Sadkova, I. V.; Rzepa, H. S.; Mykhailiuk, P. K. General Synthesis of 3-Azabicyclo[3.1.1]Heptanes and Evaluation of Their Properties as Saturated Isosteres**. *Angew. Chemie Int. Ed.* **2023**, *62* (39), e202304246.
- (162) Denisenko, A.; Garbuz, P.; Voloshchuk, N. M.; Holota, Y.; Al-Maali, G.; Borysko, P.; Mykhailiuk, P. K. 2-Oxabicyclo[2.1.1]Hexanes as Saturated Bioisosteres of the Ortho-Substituted Phenyl Ring. *Nat. Chem.* **2023**, *15* (8), 1155–1163.
- (163) Levterov, V. V.; Panasiuk, Y.; Sahun, K.; Stashkevych, O.; Badlo, V.; Shablykin, O.; Sadkova, I.; Bortnichuk, L.; Klymenko-Ulianov, O.; Holota, Y.; Lachmann, L.; Borysko, P.; Horbatok, K.; Bodenchuk, I.; Bas, Y.; Dudenko, D.; Mykhailiuk, P. K. 2-Oxabicyclo[2.2.2]Octane as a New Bioisostere of the Phenyl Ring. *Nat. Commun.* **2023**, *14* (1), 5608.
- (164) Agasti, S.; Beltran, F.; Pye, E.; Kaltsoyannis, N.; Crisenza, G. E. M.; Procter, D. J. A Catalytic Alkene Insertion Approach to Bicyclo[2.1.1]Hexane Bioisosteres. *Nat. Chem.* **2023**, *15* (4), 535–541.
- (165) Vitaku, E.; Smith, D. T.; Njardarson, J. T. Analysis of the Structural Diversity, Substitution Patterns, and Frequency of Nitrogen Heterocycles among U.S. FDA Approved Pharmaceuticals. *J. Med. Chem.* **2014**, *57* (24), 10257–10274.
- (166) Bull, J. A.; Croft, R. A.; Davis, O. A.; Doran, R.; Morgan, K. F. Oxetanes: Recent Advances in Synthesis, Reactivity, and Medicinal Chemistry. *Chem. Rev.* **2016**, *116* (19), 12150–12233.
- (167) Carreira, E. M.; Fessard, T. C. Four-Membered Ring-Containing Spirocycles: Synthetic Strategies and Opportunities. *Chem. Rev.* **2014**, *114* (16), 8257–8322.
- (168) Johansson, A.; Löfberg, C.; Antonsson, M.; von Unge, S.; Hayes, M. A.; Judkins, R.; Ploj, K.; Benthem, L.; Lindén, D.; Brodin, P.; Wennerberg, M.; Fredenwall, M.; Li, L.; Persson, J.; Bergman, R.; Pettersen, A.; Gennemark, P.; Hogner, A. Discovery of (3-(4-(2-Oxa-6-Azaspiro[3.3]Heptan-6-ylmethyl)Phenoxy)Azetidin-1-yl)(5-(4-Methoxyphenyl)-1,3,4-Oxadiazol-2-yl)Methanone (AZD1979), a Melanin Concentrating Hormone Receptor 1 (MCHR1) Antagonist with Favorable Physicochemical Properties. *J. Med. Chem.* **2016**, *59* (6), 2497–2511.
- (169) Wuitschik, G.; Carreira, E. M.; Wagner, B.; Fischer, H.; Parrilla, I.; Schuler, F.; Rogers-Evans, M.; Müller, K. Oxetanes in Drug Discovery: Structural and Synthetic Insights. *J. Med. Chem.* **2010**, *53* (8), 3227–3246.
- (170) Mallinger, A.; Crumpler, S.; Pichowicz, M.; Waalboer, D.; Stubbs, M.; Adeniji-Popoola, O.; Wood, B.; Smith, E.; Thai, C.; Henley, A. T.; Georgi, K.; Court, W.; Hobbs, S.; Box, G.; Ortiz-Ruiz, M.-J.; Valenti, M.; De Haven Brandon, A.; TePoele, R.; Leuthner, B.; Workman, P.; Aherne, W.; Poeschke, O.; Dale, T.; Wienke, D.; Esdar, C.; Rohdich, F.; Raynaud, F.; Clarke, P. A.; Eccles, S. A.; Stieber, F.; Schiemann, K.; Blagg, J. Discovery of Potent, Orally Bioavailable, Small-Molecule Inhibitors of WNT Signaling from a Cell-Based Pathway Screen. *J. Med. Chem.* **2015**, *58* (4), 1717–1735.
- (171) Knoevenagel, E. Condensation von Malonsäure Mit Aromatischen Aldehyden Durch Ammoniak Und Amine. *Berichte der Dtsch. Chem. Gesellschaft* **1898**, *31* (3), 2596–2619.

- (172) van Beurden, K.; de Koning, S.; Molendijk, D.; van Schijndel, J. The Knoevenagel Reaction: A Review of the Unfinished Treasure Map to Forming Carbon–Carbon Bonds. *Green Chem. Lett. Rev.* **2020**, *13* (4), 85–100.
- (173) Puthran, D.; Poojary, B.; Nayak, S. G.; Purushotham, N.; Rasheed, M. S.; Hegde, H. Design, Synthesis, Molecular Docking, and Biological Evaluation of Novel Selenium Containing Lumefantrine Analogues. *J. Heterocycl. Chem.* **2020**, *57* (3), 1319–1329.
- (174) List, B. Emil Knoevenagel and the Roots of Aminocatalysis. *Angew. Chemie Int. Ed.* **2010**, *49* (10), 1730–1734.
- (175) Lee, A.; Michrowska, A.; Sulzer-Mosse, S.; List, B. The Catalytic Asymmetric Knoevenagel Condensation. *Angew. Chemie Int. Ed.* **2011**, *50* (7), 1707–1710.
- (176) Grenning, A. J. Simplifying Complex Scaffold Synthesis: Knoevenagel Adduct Allyl Anions as Easily Generated Multifunctional Reagents. *Synlett* **2017**, *28* (06), 633–639.
- (177) Ramirez, N. P.; Gonzalez-Gomez, J. C. Decarboxylative Giese-Type Reaction of Carboxylic Acids Promoted by Visible Light: A Sustainable and Photoredox-Neutral Protocol. *European J. Org. Chem.* **2017**, *2017* (15), 2154–2163.
- (178) Salaverri, N.; Carli, B.; Gratal, P. B.; Marzo, L.; Alemán, J. Remote Giese Radical Addition by Photocatalytic Ring Opening of Activated Cycloalkanols. *Adv. Synth. Catal.* **2022**, *364* (10), 1689–1694.
- (179) Bell, J. D.; Robb, I.; Murphy, J. A. Highly Selective α -Aryloxyalkyl C–H Functionalisation of Aryl Alkyl Ethers. *Chem. Sci.* **2022**, *13* (43), 12921–12926.
- (180) Chowdhury, R.; Dubey, A. K.; Ghosh, R. Synthesis of Functionalized Organosilicon Compounds/Distal Ketones via Ring-Opening Giese Addition of Cycloalkanols under Organophotocatalytic Conditions. *J. Org. Chem.* **2024**, *89* (10), 7187–7200.
- (181) Zhang, M.; Yuan, X.-A.; Zhu, C.; Xie, J. Deoxygenative Deuteration of Carboxylic Acids with D₂O. *Angew. Chemie* **2019**, *131* (1), 318–322.
- (182) Wang, B.; Ascenzi Pettenuzzo, C.; Singh, J.; McCabe, G. E.; Clark, L.; Young, R.; Pu, J.; Deng, Y. Photoinduced Site-Selective Functionalization of Aliphatic C–H Bonds by Pyridine N-Oxide Based HAT Catalysts. *ACS Catal.* **2022**, *12* (16), 10441–10448.
- (183) Li, L.; Fang, L.; Wu, W.; Zhu, J. Visible-Light-Mediated Intermolecular Radical Conjugate Addition for the Construction of Vicinal Quaternary Carbon Centers. *Org. Lett.* **2020**, *22* (14), 5401–5406.
- (184) Mikata, Y.; Inaba, Y.; Morioka, M.; Yano, S. General Synthesis of Sugar-Pendant 1,3-Propanediamines Containing a C-Glycoside Linkage. *Tetrahedron Lett.* **2004**, *45* (48), 8785–8788.
- (185) Kawamoto, T.; Oritani, K.; Kawabata, A.; Morioka, T.; Matsubara, H.; Kamimura, A. Hydrodeacylation of Secondary Alkyl Nitriles and Malononitriles to Alkanes Using DiMeImd-BH₃. *J. Org. Chem.* **2020**, *85* (9), 6137–6142.
- (186) Nemoto, H.; Kubota, Y.; Yamamoto, Y. Development of a New Acyl Anion Equivalent for the Preparation of Masked Activated Esters, and Their Use to Prepare a Dipeptide. *J. Org. Chem.* **1990**, *55* (15), 4515–4516.
- (187) Yang, K. S.; Nibbs, A. E.; Türkmen, Y. E.; Rawal, V. H. Squaramide-Catalyzed Enantioselective Michael Addition of Masked Acyl Cyanides to Substituted Enones. *J. Am. Chem. Soc.* **2013**, *135* (43), 16050–16053.
- (188) Kagawa, N.; Nibbs, A. E.; Rawal, V. H. One-Carbon Homologation of Primary Alcohols to Carboxylic Acids, Esters, and Amides via Mitsunobu Reactions with MAC Reagents. *Org. Lett.* **2016**, *18* (10), 2363–2366.
- (189) Li, J.; Lear, M. J.; Hayashi, Y. Sterically Demanding Oxidative Amidation of α -Substituted Malononitriles with Amines Using O₂. *Angew. Chemie - Int. Ed.* **2016**, *55* (31), 9060–9064.
- (190) Hayashi, Y.; Li, J.; Asano, H.; Sakamoto, D. Sterically Congested Ester Formation from α -Substituted Malononitrile and Alcohol by an Oxidative Method Using Molecular Oxygen. *European J. Org. Chem.* **2019**, *2019* (4), 675–677.

- (191) Cabrele, C.; Martinek, T. A.; Reiser, O.; Berlicki, Ł. Peptides Containing β -Amino Acid Patterns: Challenges and Successes in Medicinal Chemistry. *J. Med. Chem.* **2014**, *57* (23), 9718–9739.
- (192) Del Borgo, M.; Kulkarni, K.; Aguilar, M.-I. Using β -Amino Acids and β -Peptide Templates to Create Bioactive Ligands and Biomaterials. *Curr. Pharm. Des.* **2017**, *23*.
- (193) Hoffman, J. R.; Stout, J. R.; Harris, R. C.; Moran, D. S. β -Alanine Supplementation and Military Performance. *Amino Acids* **2015**, *47* (12), 2463–2474.
- (194) Schneider, F.; Krämer, R.; Burkovski, A. Identification and Characterization of the Main β -Alanine Uptake System in Escherichia Coli. *Appl. Microbiol. Biotechnol.* **2004**, *65* (5), 576–582.
- (195) Parthasarathy, A.; Savka, M. A.; Hudson, A. O. The Synthesis and Role of β -Alanine in Plants. *Front. Plant Sci.* **2019**, *10*.
- (196) Steunenbergh, P.; Könst, P. M.; Scott, E. L.; Franssen, M. C. R.; Zuilhof, H.; Sanders, J. P. M. Polymerisation of β -Alanine through Catalytic Ester–Amide Exchange. *Eur. Polym. J.* **2013**, *49* (7), 1773–1781.
- (197) Hagen, W. R.; Vanoni, M. A.; Rosenbaum, K.; Schnackerz, K. D. On the Iron–Sulfur Clusters in the Complex Redox Enzyme Dihydropyrimidine Dehydrogenase. *Eur. J. Biochem.* **2000**, *267* (12), 3640–3646.
- (198) Miltenberger, K. Hydroxycarboxylic Acids, Aliphatic. In *Ullmann's Encyclopedia of Industrial Chemistry*, 2000.
- (199) Paulsen, M. H.; Ausbacher, D.; Bayer, A.; Engqvist, M.; Hansen, T.; Haug, T.; Anderssen, T.; Andersen, J. H.; Sollid, J. U. E.; Strøm, M. B. Antimicrobial Activity of Amphipathic α,α -Disubstituted β -Amino Amide Derivatives against ESBL – CARBA Producing Multi-Resistant Bacteria; Effect of Halogenation, Lipophilicity and Cationic Character. *Eur. J. Med. Chem.* **2019**, *183*, 111671.
- (200) Alonso Carlos del; González, Javier, E. P. Synthesis of α,α -Disubstituted β -Amino Esters and Peptide Derivatives. *Synlett* **2002**, *2002* (01), 69–72.
- (201) Büschleb, M.; Dorich, S.; Hanessian, S.; Tao, D.; Schenthal, K. B.; Overman, L. E. Synthetic Strategies toward Natural Products Containing Contiguous Stereogenic Quaternary Carbon Atoms. *Angew. Chemie Int. Ed.* **2016**, *55* (13), 4156–4186.
- (202) Saavedra, C.; Hernández, R.; Boto, A.; Álvarez, E. Catalytic, One-Pot Synthesis of β -Amino Acids from α -Amino Acids. Preparation of α,β -Peptide Derivatives. *J. Org. Chem.* **2009**, *74* (13), 4655–4665.
- (203) Jia, H.; Ritter, T. α -Thianthrenium Carbonyl Species: The Equivalent of an α -Carbonyl Carbocation. *Angew. Chemie Int. Ed.* **2022**, *61* (39), e202208978.
- (204) Tanaka, N.; Zhu, J. L.; Valencia, O. L.; Schull, C. R.; Scheidt, K. A. Cooperative Carbene Photocatalysis for β -Amino Ester Synthesis. *J. Am. Chem. Soc.* **2023**, *145* (45), 24486–24492.
- (205) Cheng, R. P.; Gellman, S. H.; DeGrado, W. F. β -Peptides: From Structure to Function. *Chem. Rev.* **2001**, *101* (10), 3219–3232.
- (206) Wang, L.; Wang, N.; Zhang, W.; Cheng, X.; Yan, Z.; Shao, G.; Wang, X.; Wang, R.; Fu, C. Therapeutic Peptides: Current Applications and Future Directions. *Signal Transduct. Target. Ther.* **2022**, *7* (1), 48.
- (207) Meiresonne, T.; Mangelinckx, S.; De Kimpe, N. Synthesis of Novel β -Aminocyclobutanecarboxylic Acid Derivatives by a Solvent-Free Aza–Michael Addition and Subsequent Ring Closure. *Org. Biomol. Chem.* **2011**, *9* (20), 7085–7091.
- (208) Yu. Rulev, A. Aza-Michael Reaction: A Decade Later – Is the Research Over? *European J. Org. Chem.* **2023**, *26* (26), e202300451.
- (209) Lahtigui, O.; Emmetiere, F.; Zhang, W.; Jirno, L.; Toledo-Roy, S.; Hershberger, J. C.; Macho, J. M.; Grenning, A. J. Assembly of Terpenoid Cores by a Simple, Tunable Strategy. *Angew. Chemie Int. Ed.* **2016**, *55* (51), 15792–15796.
- (210) Cheraghi, S. Aqueous DABCO , an Efficient Medium for Rapid Organocatalyzed Knoevenagel Condensation and the Gewald Reaction. **2014**, *38* (4).

- (211) Beesley, R. M.; Ingold, C. K.; Thorpe, J. F. The Formation and Stability of Spiro-Compounds. Part I. Spiro-Compounds from Cyclohexane. *J. Chem. Soc. Trans.* **1915**, 107 (0), 1080–1106.
- (212) Gavriilidis, A.; Constantinou, A.; Hellgardt, K.; Hii, K. K. (Mimi); Hutchings, G. J.; Brett, G. L.; Kuhn, S.; Marsden, S. P. Aerobic Oxidations in Flow: Opportunities for the Fine Chemicals and Pharmaceuticals Industries. *React. Chem. Eng.* **2016**, 1 (6), 595–612.
- (213) Mallia, C. J.; Baxendale, I. R. The Use of Gases in Flow Synthesis. *Org. Process Res. Dev.* **2016**, 20 (2), 327–360.
- (214) Plutschack, M. B.; Pieber, B.; Gilmore, K.; Seeberger, P. H. The Hitchhiker's Guide to Flow Chemistry. *Chem. Rev.* **2017**, 117 (18), 11796–11893.
- (215) Laudadio, G.; Govaerts, S.; Wang, Y.; Ravelli, D.; Koolman, H. F.; Fagnoni, M.; Djuric, S. W.; Noël, T. Selective C(Sp³)-H Aerobic Oxidation Enabled by Decatungstate Photocatalysis in Flow. *Angew. Chemie Int. Ed.* **2018**, 57 (15), 4078–4082.
- (216) Sun, Y.; Qiao, Z.; Li, D.; Ni, J.; Wang, J.; Wang, P.; Song, N.; Li, M. Access to 6-Deoxy-Heptose Constructs by One Carbon Homologation of Hexoses with Malononitrile: Divergent Synthesis of *Campylobacter* Jejuni Strain 81-176 Capsular Trisaccharide Repeating Unit Derivatives. *Org. Lett.* **2022**, 24 (43), 7944–7949.
- (217) Lowry, M. S.; Goldsmith, J. I.; Slinker, J. D.; Rohl, R.; Pascal, R. A.; Malliaras, G. G.; Bernhard, S. Single-Layer Electroluminescent Devices and Photoinduced Hydrogen Production from an Ionic Iridium(III) Complex. **2005**.
- (218) Zuo, Z.; MacMillan, D. W. C. Decarboxylative Arylation of α -Amino Acids via Photoredox Catalysis: A One-Step Conversion of Biomass to Drug Pharmacophore. *J. Am. Chem. Soc.* **2014**, 136 (14), 5257–5260.
- (219) Kaupmees, K.; Trummal, A.; Leito, I. Basicities of Strong Bases in Water: A Computational Study. *Croat. Chem. Acta* **2014**, 87, 385–395.
- (220) Özkay, Y.; Işıklıdağ, İ.; İncesu, Z.; Akalın, G. Synthesis of 2-Substituted-N-[4-(1-Methyl-4,5-Diphenyl-1H-Imidazole-2-Yl)Phenyl]Acetamide Derivatives and Evaluation of Their Anticancer Activity. *Eur. J. Med. Chem.* **2010**, 45 (8), 3320–3328.
- (221) Hwang, D. J.; Kim, S. N.; Choi, J. H.; Lee, Y. S. Dicafeoyl- or Digalloyl Pyrrolidine and Furan Derivatives as HIV Integrase Inhibitors. *Bioorg. Med. Chem.* **2001**, 9 (6), 1429–1437.
- (222) Melo, P. S.; Justo, G. Z.; de Azevedo, M. B. M.; Durán, N.; Haun, M. Violacein and Its β -Cyclodextrin Complexes Induce Apoptosis and Differentiation in HL60 Cells. *Toxicology* **2003**, 186 (3), 217–225.
- (223) Gupta, P.; Garg, P.; Roy, N. In Silico Screening for Identification of Novel HIV-1 Integrase Inhibitors Using QSAR and Docking Methodologies. *Med. Chem. Res.* **2013**.
- (224) Caruano, J.; Muccioli, G. G.; Robiette, R. Biologically Active γ -Lactams: Synthesis and Natural Sources. *Org. Biomol. Chem.* **2016**, 14 (43), 10134–10156.
- (225) Taylor, E. C.; Hendess, R. W. Synthesis of 4-Amino-5-Cyanopyrrolo [2,3-d]Pyrimidine, the Aglycone of Toyocamcin. *J. Am. Chem. Soc.* **1964**, 86 (5), 951–952.
- (226) Zaware, N.; Kisliuk, R.; Bastian, A.; Ihnat, M. A.; Gangjee, A. Synthesis and Evaluation of 5-(Arylthio)-9H-Pyrimido[4,5-b]Indole-2,4-Diamines as Receptor Tyrosine Kinase and Thymidylate Synthase Inhibitors and as Antitumor Agents. *Bioorg. Med. Chem. Lett.* **2017**, 27 (7), 1602–1607.
- (227) Gangjee, A.; Zaware, N.; Raghavan, S.; Ihnat, M.; Shenoy, S.; Kisliuk, R. L. Single Agents with Designed Combination Chemotherapy Potential: Synthesis and Evaluation of Substituted Pyrimido[4,5-b]Indoles as Receptor Tyrosine Kinase and Thymidylate Synthase Inhibitors and as Antitumor Agents. *J. Med. Chem.* **2010**, 53 (4), 1563–1578.
- (228) Gangjee, A.; Zaware, N.; Raghavan, S.; Disch, B. C.; Thorpe, J. E.; Bastian, A.; Ihnat, M. A. Synthesis and Biological Activity of 5-Chloro-N4-Substituted Phenyl-9H-Pyrimido[4,5-b]Indole-2,4-Diamines as Vascular Endothelial Growth Factor Receptor-

- 2 Inhibitors and Antiangiogenic Agents. *Bioorg. Med. Chem.* **2013**, *21* (7), 1857–1864.
- (229) Ferreira, V. F.; de Souza, M. C. B. V.; Cunha, A. C.; Pereira, L. O. R.; Ferreira, M. L. G. RECENT ADVANCES IN THE SYNTHESIS OF PYRROLES. *Org. Prep. Proced. Int.* **2001**, *33* (5), 411–454.
- (230) Cho, H.; Madden, R.; Nisanci, B.; Török, B. The Paal-Knorr Reaction Revisited. A Catalyst and Solvent-Free Synthesis of Underivatized and N-Substituted Pyrroles. *Green Chem.* **2015**, *17* (2), 1088–1099.
- (231) Knorr, L. Einwirkung Des Diacetbernsteinsäureesters Auf Ammoniak Und Primäre Aminbasen. *Berichte der Dtsch. Chem. Gesellschaft* **2006**, *18*, 299–311.
- (232) Amarnath, V.; Anthony, D. C.; Amarnath, K.; Valentine, W. M.; Wetterau, L. A.; Graham, D. G. Intermediates in the Paal-Knorr Synthesis of Pyrroles. *J. Org. Chem.* **1991**, *56* (24), 6924–6931.
- (233) Danks, T. N. Microwave Assisted Synthesis of Pyrroles. *Tetrahedron Lett.* **1999**, *40* (20), 3957–3960.
- (234) Albrecht Ludwig Harreus; R. Backes; J.-O. Eichler; R. Feuerhake; C. Jäkel; U. Mahn; R. Pinkos; R. Vogelsang (2011). "2-Pyrrolidone". *Ullmann's Encyclopedia of Industrial Chemistry*. Weinheim: Wiley-VCH.
- (235) Ledoux, A.; Sandjong Kuigwa, L.; Framery, E.; Andrioletti, B. A Highly Sustainable Route to Pyrrolidone Derivatives – Direct Access to Biosourced Solvents. *Green Chem.* **2015**, *17* (6), 3251–3254.
- (236) Webers, V. J.; Bruce, W. F. The Leuckart Reaction: A Study of the Mechanism. *J. Am. Chem. Soc.* **1948**, *70* (4), 1422–1424.
- (237) Wang, F.; Zhang, X.; He, Y.; Fan, X. Selective Synthesis of Pyrrolidin-2-Ones and 3-Iodopyrroles via the Ring Contraction and Deformylative Functionalization of Piperidine Derivatives. *Org. Biomol. Chem.* **2019**, *17* (1), 156–164.
- (238) Ong, M.; Arnold, M.; Walz, A. W.; Wahl, J. M. Stereospecific Nitrogen Insertion Using Amino Diphenylphosphinates: An Aza-Baeyer–Villiger Rearrangement. *Org. Lett.* **2022**, *24* (33), 6171–6175.
- (239) Zang, Y.; Sui, Q.; Xu, Q.; Ma, M.; Li, G.; Zhu, F. TiCl₄-Catalyzed Deoxygenative Reduction of Amides to Amines Using Ammonia Borane. *Tetrahedron Lett.* **2023**, *124*, 154598.
- (240) Collins, C. J.; Lanz, M.; Singaram, B. Facile Reduction of Tertiary Lactams to Cyclic Amines with 9-Borabicyclo[3.3.1]Nonane (9-BBN). *Tetrahedron Lett.* **1999**, *40* (19), 3673–3676.
- (241) Yao, W.; Fang, H.; He, Q.; Peng, D.; Liu, G.; Huang, Z. A BEt₃-Base Catalyst for Amide Reduction with Silane. *J. Org. Chem.* **2019**, *84* (10), 6084–6093.
- (242) Ogata, O.; Nara, H.; Matsumura, K.; Kayaki, Y. Formal Deoxygenative Hydrogenation of Lactams Using PNHP-Pincer Ruthenium Complexes under Nonacidic Conditions. *Org. Lett.* **2019**, *21* (24), 9954–9959.
- (243) Del Castillo, E.; Muñiz, K. Enantioselective Synthesis of Nicotine via an Iodine-Mediated Hofmann–Löffler Reaction. *Org. Lett.* **2019**, *21* (3), 705–708.
- (244) Löffler, K.; Freytag, C. Über Eine Neue Bildungsweise von N-Alkylierten Pyrrolidinen. *Berichte der Dtsch. Chem. Gesellschaft* **1909**, *42* (3), 3427–3431.
- (245) Shkunnikova, S.; Zipse, H.; Šakić, D. Role of Substituents in the Hofmann–Löffler–Freytag Reaction. A Quantum-Chemical Case Study on Nicotine Synthesis. *Org. Biomol. Chem.* **2021**, *19* (4), 854–865.
- (246) O'Broin, C. Q.; Fernández, P.; Martínez, C.; Muñiz, K. N-Iodosuccinimide-Promoted Hofmann–Löffler Reactions of Sulfonimides under Visible Light. *Org. Lett.* **2016**, *18* (3), 436–439.
- (247) Arena, G.; Chen, C. C.; Leonori, D.; Aggarwal, V. K. Concise Synthesis of (+)-Allo-Kainic Acid via Mgl₂-Mediated Tandem Aziridine Ring Opening–Formal [3 + 2] Cycloaddition. *Org. Lett.* **2013**, *15* (16), 4250–4253.
- (248) Chavdarian, C. G.; Seeman, J. I.; Wooten, J. B. Bridged Nicotines. Synthesis of Cis-

- 2,3,3a,4,5,9b-Hexahydro-1-Methyl-1H-Pyrrolo[2,3-f]Quinoline. *J. Org. Chem.* **1983**, *48* (4), 492–494.
- (249) Jefford, C. W.; Kubota, T.; Zaslona, A. Intramolecular Carbenoid Reactions of Pyrrole Derivatives. A Total Synthesis of (±)-Ipalbidine. *Helv. Chim. Acta* **1986**, *69* (8), 2048–2061.
- (250) Lovering, F.; Bikker, J.; Humblet, C. Escape from Flatland: Increasing Saturation as an Approach to Improving Clinical Success. *J. Med. Chem.* **2009**, *52* (21), 6752–6756.
- (251) Lovering, F. Escape from Flatland 2: Complexity and Promiscuity. *Medchemcomm* **2013**, *4* (3), 515–519.
- (252) Chalyk, B. A.; Butko, M. V.; Yanshyna, O. O.; Gavrilenko, K. S.; Druzenko, T. V.; Mykhailiuk, P. K. Synthesis of Spirocyclic Pyrrolidines: Advanced Building Blocks for Drug Discovery. *Chem. – A Eur. J.* **2017**, *23* (66), 16782–16786.
- (253) Melnykov, K. P.; Artemenko, A. N.; Ivanenko, B. O.; Sokolenko, Y. M.; Nosik, P. S.; Ostapchuk, E. N.; Grygorenko, O. O.; Volochnyuk, D. M.; Ryabukhin, S. V. Scalable Synthesis of Biologically Relevant Spirocyclic Pyrrolidines. *ACS omega*. Enamine Ltd., Chervonotkatska Street 78, Kyiv 02094, Ukraine. 2019, pp 7498–7515.
- (254) Lazarus, H. M.; Denning, J.; Wring, S.; Palacios, M.; Hoffman, S.; Crizer, K.; Kamau-Kelley, W.; Symonds, W.; Feldman, J. A Trial Design to Maximize Knowledge of the Effects of Rodatristat Ethyl in the Treatment of Pulmonary Arterial Hypertension (ELEVATE 2). *Pulm. Circ.* **2022**, *12* (2), e12088.
- (255) Young, D. The Way of Synthesis. Evolution of Design and Methods for Natural Products (Tomás Hudlicky and Josephine W. Reed). *J. Chem. Educ.* **2008**, *85*, 1626.
- (256) Regnier, G.; Canevari, R.; Douarec, J. Le; Medicale, R. United States Patent Office. **1968**, No. li, 3–6.
- (257) Pramanik, C.; Bapat, K.; Patil, P.; Kotharkar, S.; More, Y.; Gotrane, D.; Chaskar, S. P.; Mahajan, U.; Tripathy, N. K. Nitro-Aldol Approach for Commercial Manufacturing of Fenspiride Hydrochloride. *Org. Process Res. Dev.* **2019**, *23* (6), 1252–1256.
- (258) Moffett, R. B. Antispasmodics. IX. 1-Azaspiro[4.5]Decane and Derivatives1. *J. Am. Chem. Soc.* **1957**, *79* (12), 3186–3190.
- (259) Shi, M.; Liu, L.-P.; Tang, J. Gold(I)-Catalyzed Domino Ring-Opening Ring-Closing Hydroamination of Methylenecyclopropanes (MCPs) with Sulfonamides: Facile Preparation of Pyrrolidine Derivatives. *Org. Lett.* **2006**, *8* (18), 4043–4046.
- (260) Perry, M. A.; Hill, R. R.; Leong, J. J.; Rychnovsky, S. D. Stereochemical Outcomes in Reductive Cyclizations To Form Spirocyclic Heterocycles. *Org. Lett.* **2015**, *17* (13), 3268–3271.
- (261) Espinosa, M.; Noda, H.; Shibasaki, M. Synthesis of Unprotected Spirocyclic β -Prolines and β -Homoprolines by Rh-Catalyzed C–H Insertion. *Org. Lett.* **2019**, *21* (23), 9296–9299.
- (262) Tite, T.; Sabbah, M.; Levacher, V.; Brière, J.-F. Organocatalysed Decarboxylative Protonation Process from Meldrum’s Acid: Enantioselective Synthesis of Isoxazolidinones. *Chem. Commun.* **2013**, *49* (98), 11569–11571.
- (263) Liu, Z.; Hartwig, J. F. Mild, Rhodium-Catalyzed Intramolecular Hydroamination of Unactivated Terminal and Internal Alkenes with Primary and Secondary Amines. *J. Am. Chem. Soc.* **2008**, *130* (5), 1570–1571.
- (264) Maddocks, C. J.; Ermanis, K.; Clarke, P. A. Asymmetric “Clip-Cycle” Synthesis of Pyrrolidines and Spiropyrrolidines. *Org. Lett.* **2020**, *22* (20), 8116–8121.
- (265) Escolano, M.; Gaviña, D.; Díaz-Oltra, S.; Sánchez-Roselló, M.; del Pozo, C. Enantioselective Synthesis of Fluorinated Indolizidinone Derivatives. *Org. Lett.* **2023**, *25* (18), 3222–3227.
- (266) Flodén, N. J.; Trowbridge, A.; Willcox, D.; Walton, S. M.; Kim, Y.; Gaunt, M. J. Streamlined Synthesis of C(Sp³)-Rich N-Heterospirocycles Enabled by Visible-Light-Mediated Photocatalysis. *J. Am. Chem. Soc.* **2019**, *141* (21), 8426–8430.

- (267) Ryder, A. S. H.; Cunningham, W. B.; Ballantyne, G.; Mules, T.; Kinsella, A. G.; Turner-Dore, J.; Alder, C. M.; Edwards, L. J.; McKay, B. S. J.; Grayson, M. N.; Cresswell, A. J. Photocatalytic α -Tertiary Amine Synthesis via C–H Alkylation of Unmasked Primary Amines. *Angew. Chemie Int. Ed.* **2020**, *59* (35), 14986–14991.
- (268) Ye, J.; Kalvet, I.; Schoenebeck, F.; Rovis, T. Direct α -Alkylation of Primary Aliphatic Amines Enabled by CO₂ and Electrostatics. *Nat. Chem.* **2018**, *10* (10), 1037–1041.
- (269) Hashimoto, T.; Takino, K.; Hato, K.; Maruoka, K. A Bulky Thiyl-Radical Catalyst for the [3+2] Cyclization of N-Tosyl Vinylaziridines and Alkenes. *Angew. Chemie Int. Ed.* **2016**, *55* (28), 8081–8085.
- (270) Ohno, H. Synthesis and Applications of Vinylaziridines and Ethynylaziridines. *Chem. Rev.* **2014**, *114* (16), 7784–7814.
- (271) Lindner, H.; Amberg, W. M.; Martini, T.; Fischer, D. M.; Moore, E.; Carreira, E. M. Photo- and Cobalt-Catalyzed Synthesis of Heterocycles via Cycloisomerization of Unactivated Olefins. *Angew. Chemie Int. Ed.* **2024**, *63* (19), e202319515.
- (272) Zombeck, A.; Hamilton, D. E.; Drago, R. S. Novel Catalytic Oxidations of Terminal Olefins by Cobalt(II)-Schiff Base Complexes. *J. Am. Chem. Soc.* **1982**, *104* (24), 6782–6784.
- (273) Hamilton, D. E.; Drago, R. S.; Zombeck, A. Mechanistic Studies on the Cobalt(II) Schiff Base Catalyzed Oxidation of Olefins by O₂. *J. Am. Chem. Soc.* **1987**, *109* (2), 374–379.
- (274) Inoki, S.; Kato, K.; Takai, T.; Isayama, S.; Yamada, T.; Mukaiyama, T. Bis(Trifluoroacetylacetonato)Cobalt(II) Catalyzed Oxidation-Reduction Hydration of Olefins Selective Formation of Alcohols from Olefins. *Chem. Lett.* **1989**, *18* (3), 515–518.
- (275) Jiang, P.; Hu, B.; Yuan, X.; Yang, J.; Yang, X.; Lin, J.; Jin, Y. Synthesis of 2-Aminofurans and 2-Aminothiophenes through Elemental Sulfur-Promoted Switchable Redox Condensation Reaction of Enaminones with Methylene Nitriles. *J. Org. Chem.* **2022**, *87* (22), 15312–15326.
- (276) Maxwell, R.; Roth, R. H. Conversion of 1,4-Butanediol to γ -Hydroxybutyric Acid in Rat Brain and in Peripheral Tissue. *Biochem. Pharmacol.* **1972**, *21* (11), 1521–1533.
- (277) Goodwin, A. K.; Brown, P. R.; Jansen, E. E. W.; Jakobs, C.; Gibson, K. M.; Weerts, E. M. Behavioral Effects and Pharmacokinetics of Gamma-Hydroxybutyrate (GHB) Precursors Gamma-Butyrolactone (GBL) and 1,4-Butanediol (1,4-BD) in Baboons. *Psychopharmacology (Berl.)* **2009**, *204* (3), 465–476.
- (278) Poldrugo, F.; Snead, O. C. 1,4 Butanediol, γ -Hydroxybutyric Acid and Ethanol: Relationships and Interactions. *Neuropharmacology* **1984**, *23* (1), 109–113.
- (279) Kawashiro, T.; Yamashita, K.; Zhao, X.-J.; Koyama, E.; Tani, M.; Chiba, K.; Ishizaki, T. A Study on the Metabolism of Etoposide and Possible Interactions with Antitumor or Supporting Agents by Human Liver Microsomes. *J. Pharmacol. Exp. Ther.* **1998**, *286* (3), 1294 LP – 1300.
- (280) Schultz, B. J.; Kim, S. Y.; Lau, W.; Sattely, E. S. Total Biosynthesis for Milligram-Scale Production of Etoposide Intermediates in a Plant Chassis. *J. Am. Chem. Soc.* **2019**, *141* (49), 19231–19235.
- (281) Hur, J.; Jang, J. *A Review of the Pharmacological Activities and Recent Synthetic Advances of γ -Butyrolactones*; 2021.
- (282) Baker, N. C.; Lipinski, M. J.; Lhermusier, T.; Waksman, R. Overview of the 2014 Food and Drug Administration Cardiovascular and Renal Drugs Advisory Committee Meeting About Vorapaxar. *Circulation* **2014**, *130* (15), 1287–1294.
- (283) Pavlović, D.; Mutak, S.; Andreotti, D.; Biondi, S.; Cardullo, F.; Paio, A.; Piga, E.; Donati, D.; Lociuro, S. Synthesis and Structure–Activity Relationships of α -Amino- γ -Lactone Ketolides: A Novel Class of Macrolide Antibiotics. *ACS Med. Chem. Lett.* **2014**, *5* (10), 1133–1137.
- (284) Ablaza, S. L.; Pai, N. N.; Le Quesne, P. W. Quararibea Metabolites. 2.1 Efficient

- Synthetic Approaches to (±)-(2S, 3S, 4R)- γ -Hydroxyisoleucine, the Characteristic Quararibea Amino Acid. *Nat. Prod. Lett.* **1995**, 6 (1), 77–80.
- (285) Dong, Y.; Niranjan; Ablaza, S. L.; Yu, S.-X.; Bolvig, S.; Forsyth, D. A.; Le Quesne, P. W. Quararibea Metabolites. 4.1 Total Synthesis and Conformational Studies of (±)-Funebrine and (±)-Funebral. *J. Org. Chem.* **1999**, 64 (8), 2657–2666.
- (286) Yu, S.-X.; Le Quesne, P. W. Quararibea Metabolites. 3. Total Synthesis of (±) -Funebral, a Rotationally Restricted Pyrrole Alkaloid, Using a Novel Paal-Knorr Reaction. *Tetrahedron Lett.* **1995**, 36 (35), 6205–6208.
- (287) Tamura, O.; Iyama, N.; Ishibashi, H. Syntheses of (-)-Funebrine and (-)-Funebral, Using Sequential Transesterification and Intramolecular Cycloaddition of a Chiral Nitron. *J. Org. Chem.* **2004**, 69 (5), 1475–1480.
- (288) Smith, A. B.; Liu, H.; Hirschmann, R. A Second-Generation Synthesis of Polypyrrolinone Nonpeptidomimetics: Prelude to the Synthesis of Polypyrrolinones on Solid Support. *Org. Lett.* **2000**, 2 (14), 2037–2040.
- (289) Graham, S. L.; deSolms, S. J.; Giuliani, E. A.; Kohl, N. E.; Mosser, S. D.; Oliff, A. I.; Pompliano, D. L.; Rands, E.; Breslin, M. J. Pseudopeptide Inhibitors of Ras Farnesyl-Protein Transferase. *J. Med. Chem.* **1994**, 37 (6), 725–732.
- (290) Wei, Z.; Li, T.; Gu, Y.; Zhang, Q.; Wang, E.; Li, W.; Wang, X.; Li, Y.; Li, H. Design, Synthesis, and Biological Evaluation of N-Acyl-Homoserine Lactone Analogs of Quorum Sensing in *Pseudomonas Aeruginosa*. *Front. Chem.* **2022**, 10.
- (291) Hu, X.; Li, S.; McMahon, G. E.; Lala, S. D.; Rudolph, E. A. Molecular Mechanisms of Mineralocorticoid Receptor Antagonism by Eplerenone. *Mini-Reviews in Medicinal Chemistry*. 2005, pp 709–718.
- (292) Larik, F. A.; Saeed, A.; Shahzad, D.; Faisal, M.; El-Seedi, H.; Mehfooz, H.; Channar, P. A. Synthetic Approaches towards the Multi Target Drug Spironolactone and Its Potent Analogues/Derivatives. *Steroids* **2017**, 118, 76–92.
- (293) Cella, J. A.; Kagawa, C. M. STEROIDAL LACTONES. *J. Am. Chem. Soc.* **1957**, 79 (17), 4808–4809.
- (294) Neises, B.; Steglich, W. Simple Method for the Esterification of Carboxylic Acids. *Angew. Chemie Int. Ed. English* **1978**, 17 (7), 522–524.
- (295) Gosselin, P.; Perrotin, A.; Mille, S. New Preparation of (3aR*,6S*,7aR*)-6,7,7-Trimethylhexahydro-2-Benzofuran- 1(3H)-One: Formal Synthesis of (±)- γ -Irone. *Tetrahedron* **2001**, 57, 733–738.
- (296) Kitahara, T.; Mori, K. The Synthesis of (±)- γ -Ironest. **1983**, 47 (3), 1980–1982.
- (297) Inanaga, J.; Hirata, K.; Saeki, H.; Katsuki, T.; Yamaguchi, M. A Rapid Esterification by Means of Mixed Anhydride and Its Application to Large-Ring Lactonization. *Bull. Chem. Soc. Jpn.* **1979**, 52 (7), 1989–1993.
- (298) Li, F.; Renata, H. A Chiral-Pool-Based Strategy to Access Trans-Syn-Fused Drimane Meroterpenoids: Chemoenzymatic Total Syntheses of Polysin, N-Acetyl-Polyveoline and the Chrodrimanins. *J. Am. Chem. Soc.* **2021**, 143 (43), 18280–18286.
- (299) Baeyer, A.; Villiger, V. Einwirkung Des Caro'schen Reagens Auf Ketone. *Berichte der Dtsch. Chem. Gesellschaft* **1899**, 32 (3), 3625–3633.
- (300) Zhou, L.; Liu, X.; Ji, J.; Zhang, Y.; Hu, X.; Lin, L.; Feng, X. Enantioselective Baeyer–Villiger Oxidation: Desymmetrization of Meso Cyclic Ketones and Kinetic Resolution of Racemic 2-Arylcyclohexanones. *J. Am. Chem. Soc.* **2012**, 134 (41), 17023–17026.
- (301) Leisch, H.; Morley, K.; Lau, P. C. K. Baeyer–Villiger Monooxygenases: More Than Just Green Chemistry. *Chem. Rev.* **2011**, 111 (7), 4165–4222.
- (302) Murahashi, S.-I.; Ono, S.; Imada, Y. Asymmetric Baeyer–Villiger Reaction with Hydrogen Peroxide Catalyzed by a Novel Planar-Chiral Bisflavin. *Angew. Chemie Int. Ed.* **2002**, 41 (13), 2366–2368.
- (303) Dowle, M. D.; Davies, D. I. Synthesis and Synthetic Utility of Halolactones. *Chem. Soc. Rev.* **1979**, 8 (2), 171–197.
- (304) Huang, T.; Li, C.-J. Synthesis of α -Amino γ -Lactone via a Novel Tandem Three-

- Component Reaction of Alkenes, Glyoxylates and Amines. *Tetrahedron Lett.* **2000**, *41* (50), 9747–9751.
- (305) Curran, D. P.; Chen, M. H.; Spletzer, E.; Seong, C. M.; Chang, C. T. Atom-Transfer Addition and Annulation Reactions of Iodomalonates. *J. Am. Chem. Soc.* **1989**, *111* (24), 8872–8878.
- (306) Triandafillidi, I.; Kokotou, M. G.; Kokotos, C. G. Photocatalytic Synthesis of γ -Lactones from Alkenes: High-Resolution Mass Spectrometry as a Tool To Study Photoredox Reactions. *Org. Lett.* **2018**, *20* (1), 36–39.
- (307) Iwasaki, M.; Miki, N.; Ikemoto, Y.; Ura, Y.; Nishihara, Y. Regioselective Synthesis of γ -Lactones by Iron-Catalyzed Radical Annulation of Alkenes with α -Halocarboxylic Acids and Their Derivatives. *Org. Lett.* **2018**, *20* (13), 3848–3852.
- (308) Duhamel, T.; Muñiz, K. Cooperative Iodine and Photoredox Catalysis for Direct Oxidative Lactonization of Carboxylic Acids. *Chem. Commun.* **2019**, *55* (7), 933–936.
- (309) Zeller, M. A.; Riener, M.; Nicewicz, D. A. Butyrolactone Synthesis via Polar Radical Crossover Cycloaddition Reactions: Diastereoselective Syntheses of Methylene lactocin and Protolichesterinic Acid. *Org. Lett.* **2014**, *16* (18), 4810–4813.
- (310) Rafiee, M.; Miles, K. C.; Stahl, S. S. Electrocatalytic Alcohol Oxidation with TEMPO and Bicyclic Nitroxyl Derivatives: Driving Force Trumps Steric Effects. *J. Am. Chem. Soc.* **2015**, *137* (46), 14751–14757.
- (311) Jeffrey, J. L.; Terrett, J. A.; MacMillan, D. W. O–H Hydrogen Bonding Promotes H-Atom Transfer from a C–H Bonds for C-Alkylation of Alcohols. *Science* **2015**, *349* (6255), 1532–1536.
- (312) Merkens, K.; Sanosa, N.; Funes-Ardoiz, I.; Gómez-Suárez, A. Accessing α -Amino Ketyl Radicals from β -Amino Alcohols via Chemoselective Hydrogen Atom Transfer Catalysis. *ACS Catal.* **2022**, 13186–13192.
- (313) Scott, S. K.; Grenning, A. J. An Enyne Cope Rearrangement Enables Polycycloalkane Synthesis from Readily Available Starting Materials. *Angew. Chemie Int. Ed.* **2017**, *56* (28), 8125–8129.
- (314) Hyatt, J. A. Convenient Monoketalization of Methides Calcd for Preferable to the Higher Yielding Route to 1 Reported By. **1983**, *131*, 129–131.
- (315) Yamashita, K.; Tanaka, T.; Hayashi, M. Use of Isopropyl Alcohol as a Solvent in Ti(O-*i*-Pr)₄-Catalyzed Knoevenagel Reactions. *Tetrahedron* **2005**, *61* (33), 7981–7985.
- (316) Sun, Y.; Qiao, Z.; Li, D.; Ni, J.; Wang, J.; Wang, P.; Song, N.; Li, M. Access to 6-Deoxy-Heptose Constructs by One Carbon Homologation of Hexoses with Malononitrile: Divergent Synthesis of Campylobacter Jejuni Strain 81-176 Capsular Trisaccharide Repeating Unit Derivatives. *Org. Lett.* **2022**, *24* (43), 7944–7949.
- (317) Cismesia, M. A.; Yoon, T. P. Characterizing Chain Processes in Visible Light Photoredox Catalysis. *Chem. Sci.* **2015**, *6* (10), 5426–5434.
- (318) Yu, Y.-Q.; Wang, Z.-L. A Simple, Efficient and Green Procedure for Knoevenagel Condensation in Water or under Solvent-Free Conditions. *J. Chinese Chem. Soc.* **2013**, *60* (3), 288–292.
- (319) Huang, L.-S.; Lai, Y.-H.; Yang, C.; Xu, D.-Z. Iron-Catalyzed One-Pot Oxidation/Knoevenagel Condensation Reaction Using Air as an Oxidant. *Appl. Organomet. Chem.* **2019**, *33* (6), e4910.